

**Massachusetts Institute of Technology
Woods Hole Oceanographic Institution**



**Joint Program
in Oceanography/
Applied Ocean Science
and Engineering**



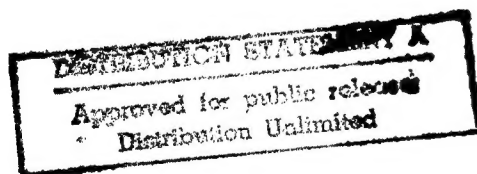
DOCTORAL DISSERTATION

*Compositional Heterogeneity Within Oceanic POM:
A Study Using Flow Cytometry and Mass Spectrometry*

by

Elizabeth C. Minor

June 1998



MIT/WHOI

98-08

**Compositional Heterogeneity Within Oceanic POM:
A Study Using Flow Cytometry and Mass Spectrometry**

by

Elizabeth C. Minor

Massachusetts Institute of Technology
Cambridge, Massachusetts 02139

and

Woods Hole Oceanographic Institution
Woods Hole, Massachusetts 02543

June 1998

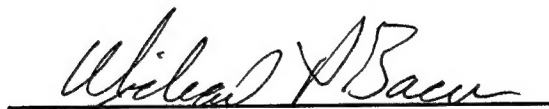
DOCTORAL DISSERTATION

Funding was provided by the National Science Foundation (OCE-9503455), the Department of Energy-Ocean Margins Project (DE-FG02-92ER61428), and the Foundation of Fundamental Research on Matter (FOM) financed by the Dutch Organization of Scientific Research.

Reproduction in whole or in part is permitted for any purpose of the United States Government. This thesis should be cited as: Elizabeth C. Minor, 1998. Compositional Heterogeneity Within Oceanic POM: A Study Using Flow Cytometry and Mass Spectrometry. Ph.D. Thesis. MIT/WHOI, 98-08.

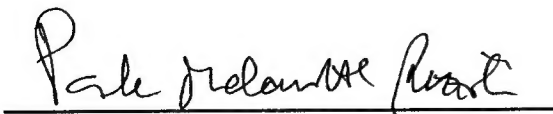
Approved for publication; distribution unlimited.

Approved for Distribution:

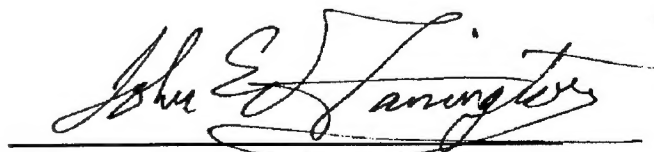


Michael P. Bacon, Chair

Department of Marine Chemistry and Geochemistry



Paola Malanotte-Rizzoli
MIT Director of Joint Program



John W. Farrington
WHOI Dean of Graduate Studies

COMPOSITIONAL HETEROGENEITY WITHIN OCEANIC POM:
A STUDY USING FLOW CYTOMETRY AND MASS SPECTROMETRY

by

Elizabeth C. Minor

B.A., The College of William and Mary
(1992)

submitted in partial fulfillment of the requirements for the degree of

Doctor of Philosophy

at the

Massachusetts Institute of Technology

and the

Woods Hole Oceanographic Institution

March 1998

© Elizabeth C. Minor 1998
All rights reserved

The author hereby grants MIT and WHOI permission to reproduce and to distribute copies of this thesis in whole or in part.

Signature of author Elizabeth C. Minor
Joint Program in Oceanography,
Massachusetts Institute of Technology/Woods Hole Oceanographic Institution

Certified by T. Eglinton
Timothy I. Eglinton
Thesis Supervisor

Accepted by Ed Boyle
Edward A. Boyle
Chair, Joint Committee for Chemical Oceanography
Massachusetts Institute of Technology/Woods Hole Oceanographic Institution

Compositional heterogeneity within oceanic POM: A study using flow cytometry and mass spectrometry

Elizabeth C. Minor

Submitted in March 1998 in partial fulfillment of the requirements for the degree of Doctor of Philosophy
at the Massachusetts Institute of Technology and the Woods Hole Oceanographic Institution

Abstract

This thesis applied direct temperature-resolved mass spectrometry (DT-MS), flow cytometry, and multivariate statistics to the study of marine particulate organic matter (POM) collected from the North Atlantic.

DT-MS is an important asset to marine organic geochemistry as a single two minute analysis (with 16 eV, EI⁺ ionization) provides information on polysaccharides, proteins, and lipids within concentrated and desalted samples. Although the molecular-level information obtained with DT-MS is less detailed than traditional analyses of specific compound classes, DT-MS can act as a useful molecular-level screening technique (as illustrated in this thesis), indicating what samples and compound classes to investigate more thoroughly.

In addition to its rapidity, DT-MS only requires microgram quantities of sample. This sensitivity permits the coupling of DT-MS and preparative flow cytometry. In this thesis, preparative flow cytometry was used to isolate "phytoplankton" and "detritus" (i.e., non-phytoplankton particles) in 2→53 μm POM. The molecular-level differences between and within small-particle POM (<53 μm), large-particle POM (>53 μm), "phytoplankton" and "detritus" were explored using DT-MS and discriminant analysis. For POM collected from the Mid-Atlantic Bight and from Great Harbor, Woods Hole, MA, small-particle POM contained more phytoplankton chemical characteristics than large-particle POM. In Great Harbor, the molecular-level characteristics of large-particle POM indicated a significant grazer biomass component. On the MAB (in March 1996), the large-particle POM appeared more phytodetrital. "Phytoplankton" was enriched in protein, chlorophyll and lipids as compared to "detritus," which was enriched in selected polysaccharides.

As the polysaccharide composition of POM subclasses was a major source of variation, polysaccharides in selected samples were further studied using ammonia and deuterated ammonia CI⁺ DT-MS. Principal component analysis of the resulting NH₃-CI⁺ spectra indicated that the majority of polysaccharide variation in the selected samples could be explained by a component that appeared related to the degree of degradation of the organic matter.

The results from this thesis, coupled with existing work on particulate and dissolved organic matter, were used to support a modified "size-reactivity continuum model" of organic matter cycling.

Thesis Supervisor: Timothy Eglinton

To my parents, "Uncle Ben," and the old Venture

Aknowledgements

This thesis would never have been finished without the help of a great many people. I would like to thank my advisor Tim Eglinton for introducing me to the field, giving me free reign with lots of instruments, and convincing me to do more than I thought I could. Thanks to my committe members are also in order. Without Rob Olson's expertise, the flow cytometer might be in even more pieces today than it was when I started. Jaap Boon's perspective as a mass spectrometrlist helped greatly in the interpretation of DT-MS data. Phil Gschwend's inciteful questions have given the thesis more coherence, comprehensibility, and depth, though Phil probably still wishes for more "oceanography." Thanks also to Jean Whelan and John Hayes for their suggestions and encouragement. Thanks to Carl Johnson for his mass spectrometry guidance and his patience with questions, frustration, and my choice of lab music. The following current and former Fye, Redfield, and Clark folks should also be recognized for their helpfulness and patience: William Little, Bob Nelson, Nelson Frew, Lorraine Eglinton, Dan Repeta, Kathy Barbeau, Ann Pearson, Liz Kujawinski, Lihini Aluwihare, Jim Moffett, Bryan Benitez-Nelson, Joyce Irvine, Diana Franks, Fredrica Valois, John Waterbury, Alexi Shalapyonok, Luda Shalapyonok, Michele Durand, Erik Zettler, and Dave Kulis.

A large portion of this thesis work took place away from the WHOI campus. Therefore, thanks are also in order for the FOM-Amolf folks including: Jos Pureveen, Gert Eijkel, Jerre van der Horst, Ron Herren, Peter Arisz, Oscar van den Brink, Gisela, and Sophie Peulve. The captains and crews of the *R/V Columbus Iselin*, the *R/V Cape Henlopen*, and the *R/V Endeavor* should be acknowledged for sampling assistance. The following people also lent a hand when sampling got difficult: Ken Buesseler, John Andrews, Melissa Bowen, Penny Chisholm, Bob Chen, Maureen Conte, ...

Special thanks are due to the Houses of Angst and Good Food: Kathy Barbeau, Sue Bello, Lisa Max, Laura Magde, Jay Austin, Kelsey Jordahl, Jamie Pringle, Tad Snow. They provided support and encouragement, cared for Jack the Iguana when necessary, and listened to me "when I needed to vent." Jay, in particular, should be thanked for listening, lab assistance, graphics and computer assistance, proof reading, good cooking, bad puns, and more.

This acknowledgements section would not be complete without a mention of my parents, who, when I was growing up, were willing to find space in the house for enough books, a trunkful of rocks, a carload of fossils, a microscope, a stray cat, and a lizard. I know I would never have made it this far without their help.

Finally, this work was funded by the following agencies: the U.S. National Science Foundation (OCE-9503455), the U.S. Department of Energy-Ocean Margins Project (DE-FG02-92ER61428), and the Foundation of Fundamental Research on Matter (FOM) financed by the Dutch Organization of Scientific Research.

Table of Contents

Abstract.....	3
Acknowledgements.....	5
Table of Contents.....	7
List of Tables.....	10
List of Figures.....	11
 Chapter 1: Introduction	
General.....	15
Chemical characteristics of phytoplankton.....	17
Attenuation and modification of the primary producer signal.....	19
Analytical techniques.....	24
Cross-flow filtration.....	25
Flow cytometry.....	26
Direct temperature-resolved mass spectrometry.....	28
Multivariate analysis.....	33
References.....	39
 Chapter 2: Methods	
Introduction.....	45
Experimental	
Analytical method.....	46
Evaluation of filtration effects.....	49
Evaluation of particle populations via flow cytometry vs microscopy.....	50
Analysis of the desalting procedure.....	51
Determination and application of DT-MS response factors.....	52
The comparison of DT-MS and HPLC measurements of POC/chlorophyll ratios.....	53
Procedural blanks.....	54
Results and discussion.....	55
Sample handling: Contamination.....	55
Sample handling: Filtration effects.....	57
Sample handling: Flow cytometric separation of “phytoplankton” and “detritus”.....	61
Sample handling: The salt issue.....	63
DT-MS considerations.....	72
The comparison of DT-MS and HPLC measurements of POC/chlorophyll ratios.....	79
Procedural blanks.....	82

Conclusions.....	82
References.....	86
Chapter 3: DT-MS of North Atlantic suspended POM: An investigation of diglycerides, triglycerides, and phospholipids	
Abstract.....	89
Introduction.....	89
Experimental.....	91
Results and Discussion	
Discriminant analysis (of spectra from DT-MS, 16 eV, EI ⁺).....	94
The “diglyceride signal”.....	101
Analysis of standards (EI ⁺ , NH ₃ -CI ⁺ , ND ₃ -CI ⁺ DT-MS).....	101
Analysis of selected samples (EI ⁺ , NH ₃ -CI ⁺ , ND ₃ -CI ⁺ DT-MS).....	106
Discussion of the “diglyceride signal”	110
Summary and Conclusions.....	116
References.....	118
Chapter 4: The compositional heterogeneity of particulate organic matter from the surface ocean: An investigation using flow cytometry and DT-MS	
Abstract.....	121
Introduction.....	122
Experimental.....	123
Results.....	134
Large-particle and small-particle POM: Average spectra.....	134
Large-particle vs small-particle POM: Discriminant analysis.....	140
“Phytoplankton” and “detritus”: Average spectra.....	141
“Phytoplankton” vs “detritus”: Discriminant analysis.....	150
Discussion.....	150
Summary and Conclusions.....	160
References.....	163
Chapter 5: Polysaccharides in oceanic POM as determined by chemical ionization DT-MS	
Abstract.....	167
Introduction.....	168
Experimental.....	169
Results	
Polysaccharides of POM subclasses.....	174
Principal component analysis (PCA).....	181

Discussion.....	187
Conclusions.....	195
References.....	197
Chapter 6: Molecular-level variations in POM subclasses along the Mid-Atlantic Bight	
Abstract.....	201
Introduction.....	202
Experimental.....	203
Region of interest.....	206
Sampling method for molecular-level analyses.....	207
Flow cytometry.....	209
DT-MS and multivariate analysis.....	209
Ancillary data.....	210
Results	
Chlorophyll <i>a</i> concentrations and phytoplankton/ (phytoplankton + detritus) ratios.....	211
Large-particle POM.....	214
Small-particle POM.....	218
“Phytoplankton”.....	224
“Detritus”.....	228
Discussion.....	228
Conclusions.....	235
References.....	238
Chapter 7: Synthesis, conclusions, and future work	
General.....	241
A modified size-reactivity continuum model.....	244
Future work	
Organic matter cycling: Unresolved issues from this thesis.....	251
Additional areas for further research.....	253
References.....	256
Appendix 1: Characteristic ions in DT-MS.....	259
Appendix 2: GC-MS of selected samples.....	265
Extraction procedure.....	265
Results.....	268
Appendix 3: Ancillary data and EI ⁺ DT-MS spectra from the MAB and WHTS data sets.....	269

List of Tables

Chapter 1:

Table 1.1: The major fatty acids in phytoplankton.....	18
Table 1.2: Phytoplankton cultures used in the example of discriminant analysis.....	34

Chapter 2:

Table 2.1. Characteristic ions (16 eV, EI ⁺) for common laboratory/ shipboard contaminants.....	55
Table 2.2. Characteristic ions chosen from DT-MS (16 eV, EI ⁺) of selected standards.....	72

Chapter 4:

Table 4.1. Relative intensities of DT-MS signatures for lipid and biopolymer components in the average spectra of MAB POM.....	158
Table 4.2. Same as Table 3.1, but for the WHTS POM subclasses.....	158

Chapter 5:

Table 5.1. Characteristic carbohydrate m/z values.....	173
Table 5.2. [POC]/[chlorophyll <i>a</i>] and (C/N) _a ratios for POM samples.....	186

Chapter 6:

Table 6.1. Ancillary data for MAB samples.....	212
Table 6.2. Variables used in correlation matrices.....	213

Appendix 1

Table A1.1. Characteristic ions in DT-MS.....	259
---	-----

Appendix 2:

Table A2.1. Compounds identified in GC-MS analysis of WHTS#5.....	266
---	-----

Appendix 3:

Table A3.1. MAB ancillary data.....	271
Table A3.2. WHTS ancillary data.....	272
Table A3.3. Pigment results from HPLC analysis of WHTS and MAB samples.....	273
Table A3.4a. List of EI ⁺ DT-MS spectra from the MAB included in Appendix 3.....	275
A3.4b. List of EI ⁺ DT-MS spectra from the WHTS included in Appendix 3.....	276

List of Figures

Chapter 1:

Fig. 1.1. The major compound classes found in oceanic organic matter.....	16
Fig. 1.2. Schematic of flow cytometric sorting.....	27
Fig. 1.3. Schematic of DT-MS.....	29
Fig. 1.4. DT-MS (low voltage EI) analysis of <i>Pavlova lutheri</i>	31
Fig. 1.5. DT-MS spectra from analysis of (a) whole cells and (b) a solvent extract of <i>Isochrysis galbana</i>	32
Fig. 1.6. Score plot from discriminant analysis of algal culture DT-MS spectra.....	36
Fig. 1.7. Spectra illustrating the loadings of variables in DF1 and DF2 from Fig. 1.6.....	37

Chapter 2:

Fig. 2.1. Analytical scheme for oceanic large-particle and small-particle POM.....	47
Fig. 2.2. DT-MS spectrum of a strongly contaminated Sargasso Sea sample.....	56
Fig. 2.3. Flow cytometry "windows" used for determining filtration effects.....	58
Fig. 2.4. FCM analysis of unfiltered and filtered aliquots of two seawater samples reported as (a) counts/mL seawater and (b) the ratio of phytoplankton counts to total phytoplankton plus detritus counts.....	59
Fig. 2.5. (a) A comparison of phytoplankton counts/mL seawater as determined by flow cytometry and by microscopy and image analysis. (b). A comparison of the detritus counts/mL seawater as determined by flow cytometry and the detrital carbon content/mL seawater as determined by microscopy and image analysis.....	62
Fig. 2.6a. Score plot for principal component analysis of algal samples with and without salt.....	64
2.6b. Loadings plot for Principal Component 1.....	65
Fig. 2.7a. DT-MS (16 eV, EI ⁺) of an <i>Emiliana huxleyi</i> culture suspended in a small amount of salt-water culture media b&c. Replicate DT-MS analyses of the same culture after desalting.....	67
Fig. 2.8. Elemental carbon analysis of each step of the desalting procedure for small-particle POM.....	70
Fig. 2.9. Elemental carbon analysis of the grinding and desalting procedure for >53 μ m particles.....	71
Fig. 2.10a. DT-MS (16 eV, EI ⁺) response factors for selected standards in terms of TIC area/ng of standard.....	74
2.10b. For selected standards, the amount of TIC intensity that can be accounted for by characteristic ions or ion series.....	75

2.10c. Response factors for characteristic ions of standards analyzed via DT-MS.....	77
Fig. 2.11a. DT-MS response factors of selected fatty acids and sterols in standards with and without a particle (Al_2O_3) matrix.	
2.11b. The intensity of a constant concentration of caffeine standard in various concentrations of POM.....	78
Fig. 2.12. The comparison of POC/chlorophyll as determined by elemental analysis/HPLC and by DT-MS.....	80
Fig. 2.13a. DT-MS of a flow cytometry blank and a “phytoplankton” sample.....	83
2.13b. DT-MS of a homogenization/desalting procedure blank and a large-particle POM sample.....	84
Chapter 3:	
Fig. 3.1. <i>R/V Cape Henlopen</i> #9512 POM sampling stations.....	92
Fig. 3.2. Score plot from discriminant analysis of suspended POM samples.....	95
Fig. 3.3. Reconstructed difference spectra for Discriminant Function 1.....	96
Fig. 3.4. Reconstructed difference spectra for Discriminant Function 2.....	97
Fig. 3.5a. Seawater temperature vs Discriminant Function1 scores	
3.5b. Seawater salinity vs Discriminant Function 2 scores.....	99
Fig. 3.6. DT-MS analyses of the triglyceride trilinolein.....	102
Fig. 3.7. DT-MS analyses of the diglyceride glyceryl-1-palmitin-3-olein.....	103
Fig. 3.8. DT-MS analyses of the phospholipid L- α -phosphatidylcholine, β -oleoyl, γ -palmitoyl.....	104
Fig. 3.9a, b, & c. EI^+ , $\text{NH}_3\text{-CI}^+$, and $\text{ND}_3\text{-CI}^+$ DT-MS analyses of suspended POM sample 7B.....	107
Fig. 3.10a, b, & c. EI^+ , $\text{NH}_3\text{-CI}^+$, and $\text{ND}_3\text{-CI}^+$ DT-MS analyses of suspended POM sample 11A-CM.....	108
Fig. 3.11a & b. EI^+ and $\text{NH}_3\text{-CI}^+$ DT-MS analyses of suspended POM sample 5C-S.....	109
Fig. 3.12. Seawater fluorescence vs seawater temperature.....	113
Chapter 4:	
Fig. 4.1. EN279 and WHTS sampling stations.....	124
Fig. 4.2. The analytical scheme used for the MAB and WHTS samples.....	126
Fig. 4.3a. The average spectrum for large-particle POM from the MAB.....	130
4.3b. The average spectrum for large-particle POM from the WHTS.....	131
Fig. 4.4a. The average spectrum for small-particle POM from the MAB.....	132
4.4b. The average spectrum for small-particle POM from the WHTS.....	133
Fig. 4.5a. The score plot from discriminant analysis of large-particle and small-particle POM from the MAB.....	136
4.5b. The reconstructed spectrum for Discriminant Funtion 1.....	137

Fig. 4.6a. The score plot from discriminant analysis of large-particle and small-particle POM from the WHTS.....	138
4.6b. The reconstructed spectrum for Discriminant Function 1.....	139
Fig. 4.7. The flow cytometry sort windows for sample WHTS13.....	142
Fig. 4.8a. Flow cytometric analyses of total >2 μm POM, "phytoplankton," and "detritus" from the MAB.....	143
4.8b. Same as Fig 4.8a, but for the WHTS sample set.....	144
Fig. 4.9a. The average spectrum for "phytoplankton" from the MAB.....	146
4.9b. The average spectrum for "phytoplankton" from the WHTS.....	147
Fig. 4.10a. The average spectrum for "detritus" from the MAB.....	148
4.10b. The average spectrum for "detritus" from the WHTS.....	149
Fig. 4.11. The total ion current and mass chromatograms for m/z 76, 64, 96, 152 from DT-MS analysis of a "detritus" sample from the MAB.....	151
Fig. 4.12a. The score plot from discriminant analysis of MAB "phytoplankton" and "detritus".....	152
4.12b. The reconstructed spectrum for Discriminant Function 1.....	153
Fig. 4.13a. The score plot for discriminant analysis of WHTS "phytoplankton" and "detritus".....	154
4.13b. The reconstructed spectrum for Discriminant Function 1.....	155
Chapter 5:	
Fig. 5.1. MAB and WHTS sampling stations.....	170
Fig. 5.2. Schematic of the three major forms of polysaccharide dissociation during DT-MS.....	175
Fig. 5.3a. $\text{NH}_3\text{-Cl}^+$ mass spectrum for sample 8-S	
5.3b. $\text{NH}_3\text{-Cl}^+$ mass spectrum for sample 8-G.....	177
Fig. 5.4a. $\text{NH}_3\text{-Cl}^+$ mass spectrum for sample WHTS13-S	
5.4b. $\text{NH}_3\text{-Cl}^+$ mass spectrum for sample WHTS13-G.....	178
Fig. 5.5a. $\text{NH}_3\text{-Cl}^+$ mass spectrum for sample WHTS13-P	
5.5b. $\text{NH}_3\text{-Cl}^+$ mass spectrum for sample WHTS13-D.....	180
Fig. 5.6. Score plot for principal component analysis of $\text{NH}_3\text{-Cl}^+$ mass spectra.....	182
Fig. 5.7a. Reconstructed spectrum for Principal Component +1.....	183
5.7b. Reconstructed spectrum for Principal Component -1.....	184
Fig. 5.8a. $\text{NH}_3\text{-Cl}^+$ DT-MS of UDOM from Georges Bank	
5.8b. $\text{NH}_3\text{-Cl}^+$ spectrum of DPP72.....	193
Chapter 6:	
Fig. 6.1. MAB sampling stations.....	204
Fig. 6.2. AVHRR image (March 4, 1996, 12:08:49 GMT) illustrating the shelf/slope front in the MAB.....	205
Fig. 6.3. Analytical scheme for large-volume POM samples.....	208
Fig. 6.4. Score plot of Discriminant Function 1 from analysis of	

	MAB large-particle POM.....	215
Fig. 6.5.	Reconstructed spectrum of DF1 from analysis of MAB large-particle POM.....	216
Fig. 6.6a.	Plot of DF1 score (from Fig. 6.4) vs seawater temperature	
6.6b.	Plot of DF1 score vs the unfiltered seawater ratio of phytoplankton/total analyzed particles	
6.6c.	Plot of DF1 score vs phytoplankton/total analyzed particles in 2.0→53 μ m POM.....	217
Fig. 6.7.	Score plot of Discriminant Function 1 vs Discriminant Function 2 from analysis of MAB small-particle POM.....	220
Fig. 6.8.	Reconstructed spectrum for DF1 from Fig. 6.7.....	221
Fig. 6.9.	Reconstructed spectrum for DF2 from Fig. 6.7.....	222
Fig. 6.10a.	Plot of DF1 score from analysis of small-particle POM vs PO ₄ concentration	
6.10b.	Plot of DF2 score vs. [POC]/[chlorophyll <i>a</i>].....	223
Fig. 6.11.	Score plot for discriminant analysis of MAB “phytoplankton”.....	225
Fig. 6.12.	Reconstructed spectrum for DF1 from Fig. 6.11.....	226
Fig. 6.13a.	Plot of DF1 score from analysis of MAB “phytoplankton” vs [POC]/[chlorophyll <i>a</i>]	
6.13b.	Plot of DF1 vs the ratio of phytoplankton/total analyzed particles in 2.0→53 μ m samples.....	227
Fig. 6.14.	Score plot showing DF1 vs DF2 from analysis of MAB “detritus”.....	229
Fig. 6.15.	Reconstructed spectrum from DF1 in Fig. 6.14.....	230
Chapter 7:		
Fig. 7.1.	Score plot of discriminant analysis of large-particle POM and “phytoplankton” from the MAB.....	246
Fig. 7.2.	Reconstructed mass spectrum for DF1 from Fig. 7.1.....	247
Fig. 7.3.	The modified size-reactivity continuum model.....	250
Appendix 2:		
Fig. A2.1	GC-MS of WHTS#5.....	267
Appendix 3:		
	Plots of total ion chromatograms and mass spectra for the samples in the WHTS and MAB data sets.....	278-337

Chapter 1

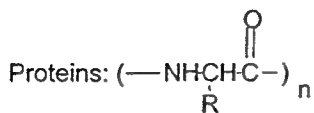
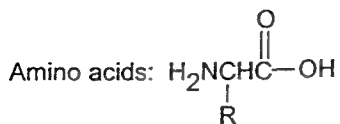
Introduction

General

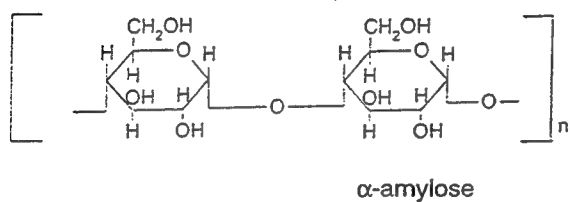
The major compound classes found in oceanic organic matter include proteins, carbohydrates, nucleic acids, aminosugars, and lipids (Fig. 1.1). These compounds perform different functions in living organisms, and the common functions (as discussed in Voet and Voet, 1990; and Chester, 1990) will be mentioned here. Proteins, biopolymers of amino acids, are involved in the transport of molecules through cell membranes. As enzymes, proteins also catalyze reactions both within and outside a cell. Carbohydrates serve energy storage and structural functions, as illustrated by the respective roles of starch in plants and cellulose in trees. Aminosugars, compounds in which a sugar -OH group has been replaced by an amine, are found (as chitin) in the exoskeletons of copepods and crabs and (as peptidoglycan) in bacterial cell walls. Nucleic acids (as DNA) carry the genetic information of a cell and (as RNA) provide this information to sites of protein synthesis. Lipids, operationally defined as insoluble in water but soluble in organic solvents, perform fairly diverse functions. Triglycerides and wax esters are energy storage compounds. Triglycerides can also act as buoyancy controls for a cell. Sterols are hormonal regulators and are also involved in determining membrane fluidity. Lipids are particularly important to the marine geochemist because, in their extractable form, they can be used as biomarkers indicating sources and transformations of organic matter.

Reduced (organic) carbon enters the world ocean through two main sources: export from terrestrial ecosystems and autochthonous primary production. Autochthonous primary production forms the base for food chains in the ocean and is generally the primary source of reduced carbon in surface oceans. Therefore, it is necessary to briefly describe the chemical characteristics of the main primary producers,

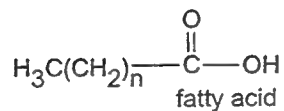
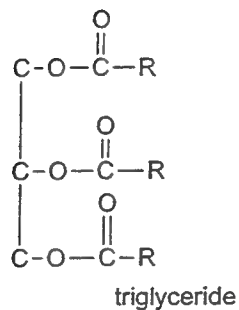
The major organic compound classes found in oceanic OM:



Carbohydrates: $\text{C}_6\text{H}_{12}\text{O}_6$



Lipids:

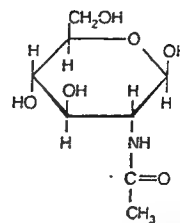


$\text{C}_{14:0}$ FA= myristic acid

$\text{C}_{16:0}$ FA= palmitic acid

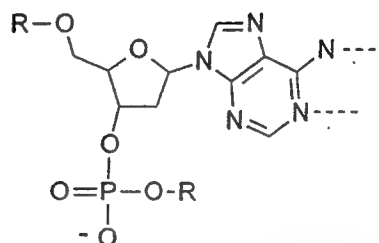
$\text{C}_{18:0}$ FA= stearic acid

Aminosugars:



N-acetylglucosamine

Nucleic acids:



segment of a single DNA chain
(the base is adenine)

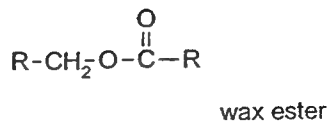
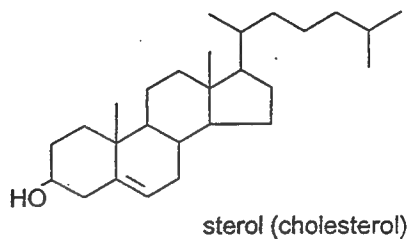


Fig. 1.1. The major compound classes found in oceanic organic matter.

phytoplankton, as reported in the literature, before discussing the reactivity and fate of oceanic organic matter.

Chemical characteristics of phytoplankton

The relative abundance of lipids, protein, and carbohydrates in phytoplankton is relatively similar across species and class lines. Parsons et al. (1984) reported that the ash-free dry weight composition of phytoplankton (collected during logarithmic growth phase) ranges between 35 to 68% protein, 20 to 42% carbohydrate, and 4 to 16% lipid. Later work by Brown et al. (1996) found the composition of the diatom *Thalassiosira pseudonana* (during logarithmic growth phase) to be consistent with these values, though lipid percentages were slightly higher (23-31%, organic weight %) and carbohydrates to be slightly less prevalent (10-27%, organic weight %). These values are strongly dependent upon growth phase, however, and may also vary with light regime or other factors (e.g., Brown et al., 1996). For example, as phytoplankton cultures shifted from logarithmic to stationary phase, the composition of *T. pseudonana* became depleted in protein and enriched in lipids and carbohydrate.

The lipid composition of phytoplankton has received considerable attention due to the use of cultured phytoplankton as feedstock in aquatic farming (e.g., Chu and Depuy, 1980; Volkman, 1989; Brown et al., 1996) and the use of lipids as biomarkers in the marine environment (e.g., Volkman, 1986; Prahl et al., 1988; and many others). A very brief sampling of this work will be discussed here. The principle lipids in three species of diatoms (determined by Lee et al., 1971, and reported in Parsons et al., 1984) are as follows (in terms of percentage of total lipids): phospholipids (50 to 57%), triglycerides (12 to 16%), sterols (10 to 17%) free fatty acids (5 to 16%) and hydrocarbons (2 to 11%). These percentages are also affected by phytoplankton growth stage and other factors. Brown et al. (1996) reported a decrease in polar lipids (from 79-89% of total lipids to 48-

Table 1.1. The major fatty acids in phytoplankton (from Volkman, 1989).

Phytoplankton class	Major fatty acids
Bacillariophyceae	16:1(n-7), 16:0, 14:0, 20:5(n-3)
Cryptophyceae	18:4(n-3), 16:0, 18:3(n-3), 18:2 (n-6), 20:5 (n-3)
Chlorophyceae (analysis of <i>Dunaliella</i>)	16:0, 16:4(n-3), 18:2(n-6), 18:3(n-3)
Prymnesiophyceae	16:0, 16:1(n-7), 18:1(n-9), 18:4(n-3), 20:5(n-3), 22:6(n-3)
Dinophyceae	16:0, 18:4(n-3), 20:5(n-3), 22:6(n-3) and often 18:5(n-3)

57%) and an increase in triglycerides (from $\leq 10\%$ to 22-45% of total lipids) as *T. pseudonana* moved from logarithmic to stationary phase.

Fatty acids form a large proportion of the total lipid in phytoplankton as, in addition to existing as free fatty acids, they are major constituents of phospholipids and triglycerides. Their distribution in particulate organic matter (POM) has been used to indicate phytoplankton, zooplankton, and bacterial biomass contributions (as in Wakeham and Canuel, 1988; Conte, 1989; Columbo et al., 1996). The total fatty acid composition of phytoplankton classes has been reviewed by Volkman (1989), and the major fatty acids found in each class are shown in Table 1.1. In addition to the ubiquitous $C_{16:0}$ fatty acid, other major phytoplankton fatty acids typically include $C_{16:1}$, $C_{16:4}$, $C_{14:0}$, C_{18} (with various levels of unsaturation) and $C_{20:5}$.

Sterols, like fatty acids, are also used as biomarkers in the marine environment. While a review of the literature on phytoplankton sterols is beyond the scope of this introduction (see Volkman, 1986), it is worth mentioning three sterols that, while not unambiguous, can provide information on organic matter sources. 24-methylcholesta-5,22E-dien-3 β -ol is often used as a diatom biomarker, while the presence of 4 α ,23,24 trimethyl-cholest-22-en-3 β -ol, or dinosterol, is generally attributed to dinoflagellates. While cholesterol is synthesized by phytoplankton, it is a primary zooplankton sterol

(Volkman 1986), and is generally interpreted as an indicator of zooplankton biomass (as in Wakeham and Canuel, 1988).

Attenuation and modification of the primary producer organic matter signal

The organic matter produced during photosynthesis by phytoplankton in the surface ocean undergoes many reactions and physical transformations including incorporation into grazer biomass or egestion in fecal pellets (e.g., Harvey et al., 1987, Cowie and Hedges, 1996), incorporation into marine snow (e.g., Alldredge and Silver, 1988) and/or the dissolved organic matter pool, remineralization (the most likely eventual fate for organic carbon in the ocean, Hedges, 1992), and for a very small percentage (<0.2% of marine primary production), burial in ocean sediments (Hedges, 1992). These chemical, biological, and physical processes not only affect the concentration of organic matter in the water column (or sediments) but substantially change the composition of the organic matter as well.

The attenuation and modification of the primary production organic matter signal within the oceanic water column has been explored in several ways. Vertical profiles of organic matter composition and flux have been used to obtain estimates of diagenetic reactivity (e.g., Wakeham et al., 1984; Hedges et al., 1988; Wakeham, 1997). Laboratory degradation experiments using phytoplankton cultures and various combinations of bacteria and heterotrophs have been used to monitor remineralization of organic matter (Westrich and Berner, 1984), the conversion of phytoplankton organic material into bacterial and/or grazer biomass (e.g., Harvey et al., 1987; Harvey and Macko, 1997) and the chemical composition of the remaining "detritus." Various size fractions of organic matter at field sites and within culture experiments have been analyzed to examine relationships among "sinking" particulate organic matter (POM), "suspended" POM, colloidal (or ultrafiltered) dissolved organic matter (UDOM), and/or dissolved organic matter (DOM) (e.g., Skoog and Benner, 1997, Biddanda and Benner, 1997).

Depth has been considered a proxy for extent of diagenesis, allowing the effects of diagenesis to be monitored by sediment trap deployments and/or filtration of particles at different depths (e.g., Wakeham et al., 1984; Hedges et al., 1988; Wakeham and Canuel, 1988; Wakeham and Lee, 1993; Hernes et al., 1996; Wakeham et al., 1997). Such work has led to a general measure of the reactivity of different components of POM. For example, comparison of the fluxes of organic material intercepted by sediment traps over different depths at sites in the Sargasso Sea, the equatorial Atlantic, the north Pacific, the California current, and the Peruvian upwelling region has led to the following diagenetic sequence (from most to least reactive): “hydrolyzable amino acids>total fatty acids>lipids>POC>total particulate matter” (Wakeham et al., 1984). However, a somewhat different diagenetic sequence emerges from recent work in the equatorial Pacific: “pigments>>lipids>amino acids>carbohydrates” (Wakeham et al., 1997). Studies of sediment trap and sediment samples from a coastal site (Dabob Bay in Puget Sound, Washington) also indicate that plant pigments are more reactive than plankton lipids and that both of these are more reactive than carbohydrates (Hedges et al., 1988). Fluxes within compound classes have also been determined (e.g., for aldoses, Hernes et al., 1996; for lignin-derived phenols and for neutral sugars, Hedges et al., 1988; for lipids, Wakeham et al., 1984; Wakeham and Canuel, 1988; for amino acids, Lee and Cronin, 1984).

Laboratory degradation experiments use time rather than depth as a measure of the degree of diagenesis. From such experiments, rate constants for degradation of algal organic matter have been determined (Emerson and Hedges, 1988, and references therein). These constants appear dependent upon the experimental time scale, which is probably due, at least in part, to the fact that the particulate organic carbon consists of many compound classes with varying levels of reactivity (Westrich and Berner, 1984; Emerson and Hedges, 1988, and references therein). Such varying reactivity levels have led to the “multiple-G” model of organic matter degradation (Westrich and Berner, 1984; Boudreau and Ruddick, 1991 and references therein) and its refinement into “reactive

continuum" models (Middelburg, 1989; and Boudreau and Ruddick, 1991). In addition to the monitoring of bulk organic matter degradation, laboratory degradation studies have also monitored the preferential degradation of various compound classes. For example, Harvey et al. (1995) monitored the decay of *Thalassiosira weissflogii* (a diatom) and *Synechococcus* sp. (a coccoid cyanobacterium) under oxic and anoxic conditions in a flow-through system in which macrozooplankton grazers were excluded. They found that, under oxic degradation, carbohydrates are most reactive, followed by protein and then lipid. Under anoxic conditions, however, protein has higher degradation rates than carbohydrates.

The attenuation of the primary producer organic matter signal by zooplankton grazing has also been studied in laboratory experiments. These have varied widely in emphasis, from evaluations of the effects of grazing on phytoplankton lipid biomarkers (e.g., Harvey et al., 1987) to studies of the assimilation of total organic matter and quantitatively important substituents (proteins and carbohydrates, e.g., Cowie and Hedges, 1996). In feeding experiments with the dinoflagellate *Scrippsiella trochoidea* and the copepod *Calanus helgolandicus*, Harvey et al. (1987) found that polyunsaturated fatty acids (PUFA) are preferentially assimilated, and proposed that zooplankton grazing may be responsible for the lack of PUFA in sediment trap material. Harvey et al. (1987) also found that sterols were assimilated by copepods while stanols were not. Cowie and Hedges (1996) monitored the ingestion of ¹⁴C-labelled diatoms (*T. weissflogii*) by the copepod *Calanus pacificus*. They found the following sequence of digestion efficiencies (from highest to lowest): "total N>organic C>total chlorophyll-type pigments." Amino acid and neutral aldose analyses also indicated that diatom intracellular material was preferentially assimilated.

Investigations of different size classes of organic material have also been undertaken in an attempt to further understand relationships between "sinking" POM, responsible for most of the vertical flux of organic matter in the oceans, "suspended" organic matter, responsible for most of the particulate organic mass in the ocean (McCave

et al., 1975 and Bishop et al., 1977), ultrafiltered or colloidal dissolved organic matter (UDOM), the largest “concentratable” pool of dissolved organic matter at the present time (Benner et al., 1992), and bulk DOM, the largest reactive reduced carbon pool in the oceans.

Studies of the lipid contents of suspended and sinking POM (Wakeham and Canuel, 1988; Conte, 1989) indicate that these two pools of organic matter are chemically distinct but that suspended organic matter is more labile than the sinking pool over the entire depth range studied (the euphotic zone to 1000-1500 m). These results contradict two previously existing views concerning the relationship between these pools. It has been proposed that suspended POM should be either more refractory than sinking POM, due to a longer residence time in the water column (Tanoue and Handa, 1980), or chemically similar to sinking POM, due to exchange between the two particle pools (Bacon et al., 1985). Results from such work on lipids (e.g., Wakeham and Canuel, 1988; Conte, 1989) indicate that the distinction of POM based solely on whether it is sinking or suspended cannot fully resolve issues concerning the organic matter cycle in the ocean. Both Wakeham and Canuel (1988) and Conte (1989) suggest that the sinking particle pool contains a subset that behaves relatively conservatively (the measured sinking pool) and a subset (previously unmeasured or incorporated into other measurements) which contributes labile organic matter to the suspended pool (Conte, 1989; Wakeham and Canuel, 1988).

The lipid studies of sinking and suspended POM also appear to contradict the “size reactivity continuum model” proposed by Amon and Benner (1996) based on results from bacterial degradation experiments using different size classes of DOM, and extended to oceanic POM in Skoog and Benner (1997). In this model, as in the Tanoue and Handa (1980) hypothesis mentioned in the previous paragraph, particles become less bioreactive and more diagenetically altered as their size decreases.

The complexity of organic matter cycling in the water column evident from the above discussion indicates the following needs: (i) to understand the composition of

organic matter particles at a level beyond the simple definitions inherent in present isolation techniques, and (ii) to encompass as broad a range of biochemicals as possible.

In this thesis the relationships among and within size classes of organic matter are further explored using direct temperature-resolved mass spectrometry (DT-MS). With low voltage electron impact ionization (EI^+ , 16 eV), DT-MS provides molecular-level information over a wide range of compound classes. As only microgram quantities of material are needed, larger data sets can be screened for molecular-level variations, which can be further explored by additional mass spectrometry techniques (as in Chapters 3 and 5) or by other more traditional approaches (see Appendix 2). DT-MS with ammonia chemical ionization provides polysaccharide oligomer information (also on microgram quantities of sample) and should therefore prove a useful complement to traditional neutral aldose analyses. It is used in Chapter 5 to explore polysaccharide variations in $>53\ \mu\text{M}$ and $>2\ \mu\text{m}$, $<53\ \mu\text{m}$ POM.

The sensitivity of DT-MS also opens an additional avenue for exploring the attenuation of the primary production organic matter signal in the oceans. DT-MS can be coupled with flow cytometric sorting to provide molecular-level characterization of morphologically (or optically) discrete particle types such as phytoplankton in natural suspended POM samples (as in Chapters 4 and 6). This allows the direct comparison between primary producer organic matter and that of bulk small-particle ($>2\ \mu\text{m}$, $<53\ \mu\text{m}$) POM, bulk large-particle ($>53\ \mu\text{m}$) POM, and "detritus," defined here as the non-chlorophyll fluorescing pool of small-particle POM. The variations in chemical composition among these POM subclasses are discussed in Chapter 4. Variations within these subclasses as a function of location along the Mid-Atlantic Bight are included in Chapter 6. Chapter 7 includes discussion of the attenuation of the primary production organic matter signal along with general conclusions and suggestions for future work.

Analytical techniques

As mentioned above, direct temperature-resolved mass spectrometry (DT-MS) using low-voltage electron impact ionization (16 eV EI⁺) is used to provide rapid broad-band molecular-level characterization of POM samples. It is used here in conjunction with multivariate analysis techniques (principal component analysis and discriminant analysis) to explore chemical variations among and within POM subclasses. Since DT-MS requires only microgram quantities of sample, it is a logical counterpart to flow cytometric separation of “phytoplankton” and “detritus” from >2 µm, <53 µm POM.

Initial 16 eV EI⁺ characterization of POM data sets and multivariate exploration of this data indicates chemical variations worthy of further, more detailed characterization. While detailed chemical assays are beyond the scope of the present study, different modes of MS analysis are used to provide further insights into the chemical characteristics of POM and its subclasses. In Chapter 3 initial EI⁺ DT-MS of the Henlopen small-particle POM data set leads to more detailed analysis of triglyceride, diglyceride, and phospholipid components via ammonia and deuterated-ammonia chemical ionization (CI⁺) DT-MS. Polysaccharide variations among POM subclasses indicated by 16 eV EI⁺ DT-MS in Chapter 4 are further explored CI⁺ DT-MS in Chapter 5.

Flow cytometric sorting is coupled with DT-MS in order to obtain molecular-level characteristics of subclasses (“phytoplankton” and “detritus”) within small-particle POM. The “phytoplankton” and “detrital” subclasses isolated from this POM are chemically distinct in both spatially varying and temporally varying data sets (Chapter 4 of this thesis).

As both flow cytometry and DT-MS require samples suspended in liquid, samples for this study were obtained using cross-flow filtration as well as conventional (gravity and/or mild vacuum) filtration methods. The following sections introduce cross-flow

filtration, flow cytometry and the various MS techniques applied in this study. The actual method development is discussed in Chapter 2.

Cross-flow Filtration

In the past decade, cross-flow filtration (CFF, also called tangential-flow filtration) has become increasingly popular in marine chemistry studies for the processing of colloids and particles from large volume (10-1000 L) samples of seawater. It has been of particular value in investigations of the organic and trace metal constituents of marine colloids (e.g., Amon and Benner, 1994, 1996, McCarthy et al., 1996, Aluwihare et al., 1997, Guo et al., 1996, Moran and Moore, 1989, Buesseler et al., 1996 and references therein). In this study CFF was chosen for the concentration of particulate ($>0.8 \mu\text{m}$) organic matter for the following two reasons. First, large amounts of sample were desirable for method development, flow cytometry, and ancillary measurements. Second, and perhaps more importantly, the fact that CFF retentate remains suspended in liquid (as opposed to becoming embedded in a filter) was considered a desirable feature because both DT-MS and flow cytometry require particle suspensions.

In all filtration techniques a concentration gradient forms between membrane and bulk sample as particles larger than the pore size are preferentially retained by the membrane. CFF increases possible flow rates and hence sample volumes for these samples by reducing the concentration gradient that forms between membrane and bulk sample. It does this by driving the sample parallel to the membrane and filtering due to hydrostatic pressure, rather than the conventional gravity or vacuum pressure. The sample is driven past this membrane multiple times, decreasing in volume each time and concurrently increasing in the concentration of particles of interest (as described in Buesseler et al., 1996; Klap, 1997).

The ability to easily process large volume samples by CFF has been mainly responsible for its popularity in marine chemistry, however, the user must be aware that

CFF is not an easily characterized technique. Size cutoff characteristics for a particular membrane may vary with operating conditions, particle shape, and varying physicochemical interactions between the particle and the membrane surface (Buessler et al, 1996; Gustafsson et al., 1996). Particle adsorption and particle breakthrough at high concentration factors are also very real concerns.

As this study is qualitative in nature, concentrating on molecular-level variations in chemical composition among and within POM subclasses, CFF performance was monitored in terms of potential fractionation of particle populations rather than absolute recoveries or mass balances (see Chapter 4).

Flow Cytometry

In flow cytometry individual particles in a stream of water are directed through a focused laser beam and are characterized on the basis of light scattering and fluorescent properties. Two properties commonly analyzed in oceanographic samples (and used in this thesis to discriminate “phytoplankton” and “detritus”) are forward angle light scatter (a function of size) and red fluorescence (a function of chlorophyll content). Other properties can be used to determine phytoplankton cell type: depolarization of forward light scatter indicates the presence of a calcium carbonate shell; a high ratio of right angle light scatter to forward angle light scatter indicates that a cell is long and narrow (such as a pennate diatom); and orange fluorescence results from phycoerythrin within the cell (Olson et al., 1989, 1990). Fluorescent probes may also be used to gain additional information; for example, Dorsey et al. (1989) illustrate the usefulness of fluorescein diacetate (FDA) as a measure of cell viability for phytoplankton populations.

Flow cytometric sorting allows the physical separation of particles according to a preselected combination of the above properties. Vibration of a bimorph crystal separates the sample stream into microdroplets; those droplets containing the described particles are electrostatically charged and are then separated from the main stream of droplets as

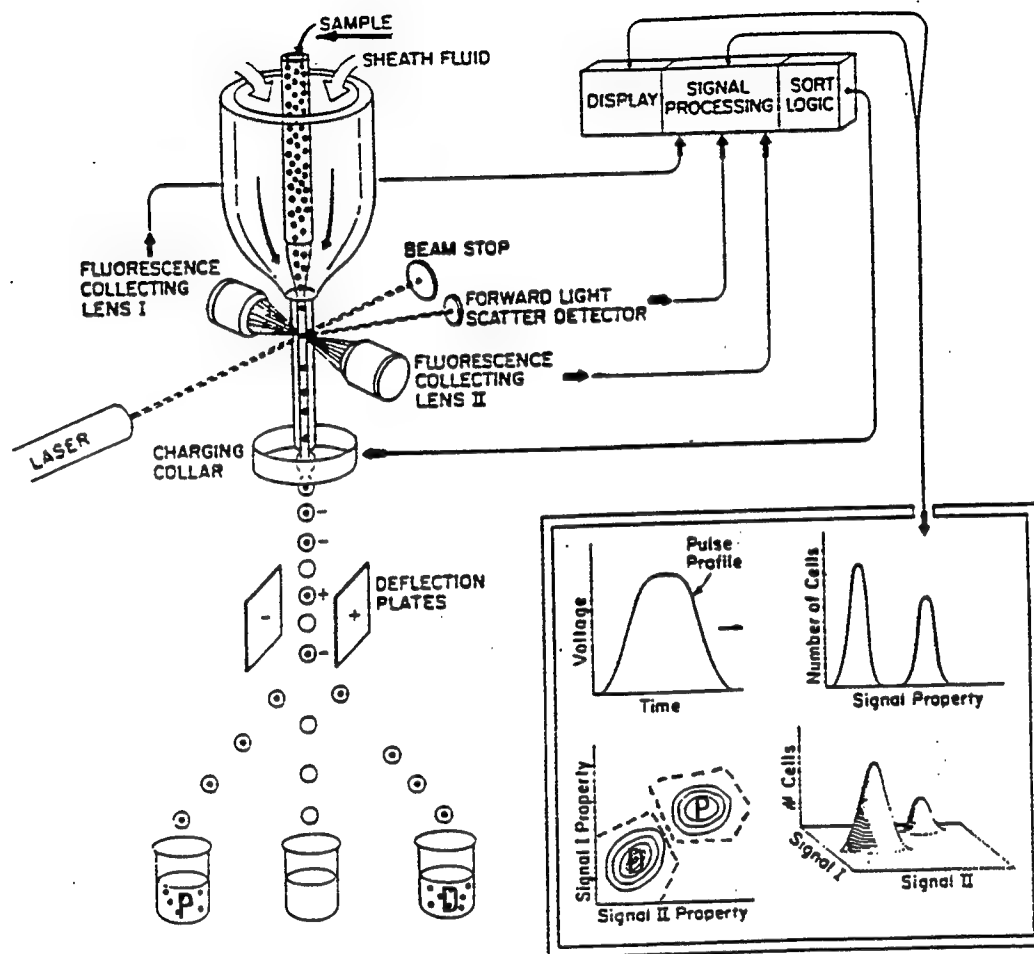


Fig. 1.2. Schematic of flow cytometric sorting.

they pass through an electric field (Fig. 1.2). Sorting rate depends upon the ratio of desired and non-desired particles in a sample as each particle must pass through the laser beam individually. The biomass yield rate resulting from this sorting rate depends upon the size (or more specifically, the biomass) of the particles being sorted. For $>2\text{ }\mu\text{m}$, $<53\text{ }\mu\text{m}$ POM, an EPICS V flow cytometer (Redfield Building, WHOI), under the best conditions, yields 1-10 μg of particulate matter in three to five hours of sorting. Therefore, chemical characterization of flow cytometrically sorted particles requires techniques with sufficient sensitivity to be performed on microgram quantities of material.

Direct Temperature-resolved Mass Spectrometry

Past studies of the chemical composition of POM have been hindered by two analytical limitations. Large sample sizes were required and the existing analytical procedures were time-consuming and generally compound class specific (e.g. Repeta and Gagosian, 1983; Wakeham et al., 1984; Wakeham and Ertel, 1988; Lee and Cronin, 1984). Recently, however, DT-MS, a technique coupling thermal evaporation/pyrolysis and mass spectrometry, has been shown to provide molecular-level characterization on microgram quantities of material from both marine phytoplankton cultures and field samples of POM (Eglinton et al., 1996).

In DT-MS a sample is placed on a resistively heated probe which is inserted into the ionization chamber of the mass spectrometer. The temperature of the probe is increased at a preprogrammed rate and desorption of volatile material and subsequent thermal dissociation (pyrolysis) of polymeric material occur within the ion chamber itself (Fig. 1.3). This technique offers several advantages over the pyrolysis-mass spectrometry methods previously applied to the study of aquatic POM (see, for example, Saliot et al, 1984; Meuzelaar et al., 1982; and references therein). In previous studies, Curie-point pyrolysis was implemented outside the ion source of the mass spectrometer and the

Schematic Diagram of Direct Temperature-resolved Mass Spectrometry (DT-MS)

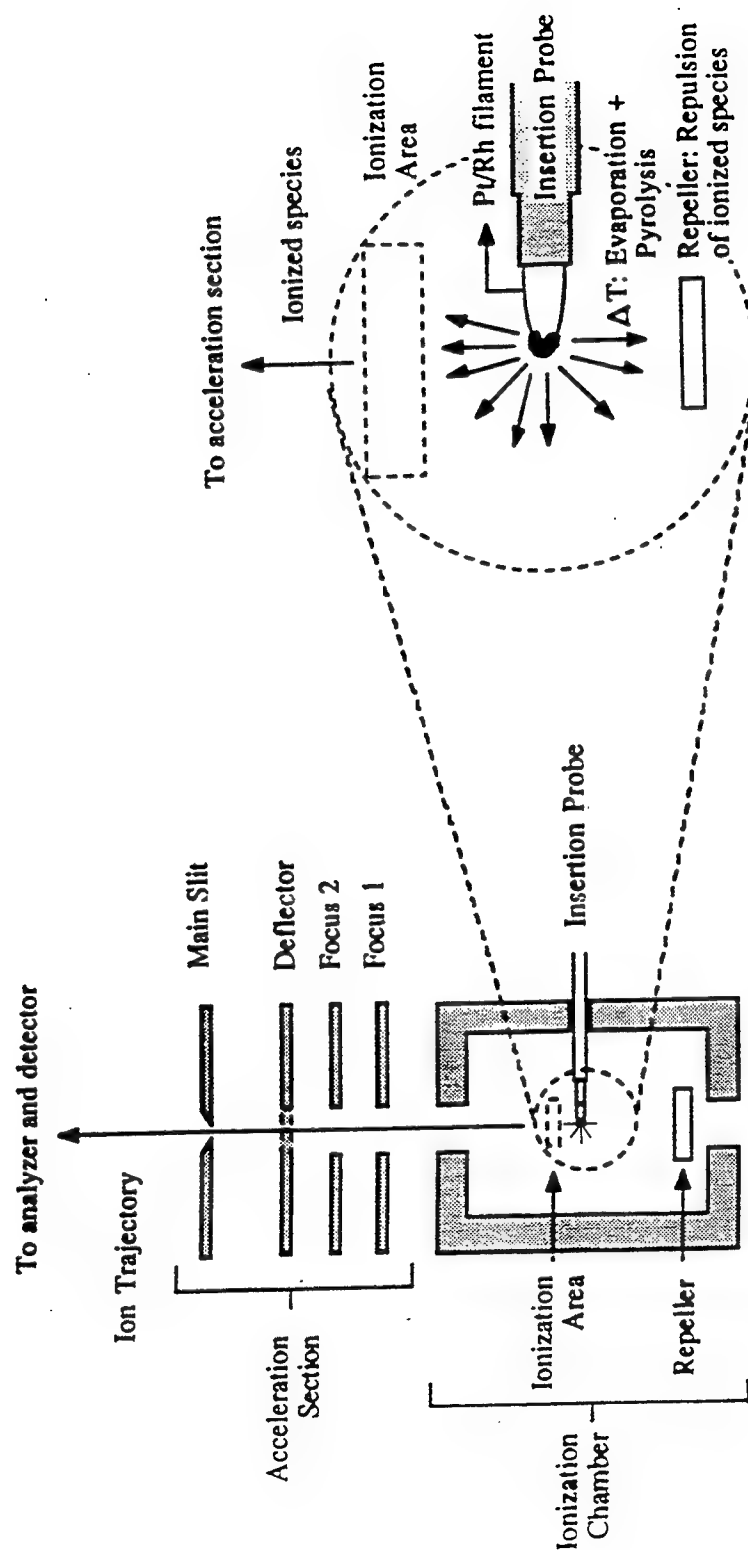


Fig. 1.3. Schematic of DT-MS.

resulting pyrolysates entered the ion source through an expansion chamber. This geometry limited analysis to lower molecular-weight products (<250 amu); both heavier and more polar fragments condensed before reaching the ion chamber. In DT-MS this fractionation is virtually eliminated as pyrolysis and ionization occur in essentially the same location. In contrast to the near instantaneous heating of a sample in Curie point pyrolysis, in DT-MS the probe temperature is increased at a predetermined rate (~20°C/s). This allows the sequential evolution and monitoring of volatile (primarily lipid) and biopolymeric material during a single measurement as shown in Fig. 1.4 (Eglinton et al., 1996). The scans for each region can be summed to yield composite desorption and pyrolysis mass spectra. As van der Heijden et al. (1990) and Eglinton et al. (1996) have shown, such composite desorption mass spectra appear to contain the same information as mass spectra obtained from solvent extractions of the same sample (Fig. 1.5). This implies that data obtained from DT-MS of whole cells during the course of a two minute analysis are comparable to conventional lipid measurements, although, of course, the conventional measurements provide additional structural information.

Curie-point pyrolysis-MS and DT-MS share other distinct advantages over traditional methods of characterizing POM. Both have rapid analysis times (2-5 min/sample) and can be used with relatively little pre-run sample manipulation. In addition, the data obtained is in numeric form; therefore, it can be incorporated directly into the matrix equations used in multivariate analysis. This ease in applying multivariate analysis makes DT-MS a useful technique for exploring molecular-level variations among POM subclasses, whose DT-MS mass spectra might otherwise prove too complicated for rigorous interpretation.

DT-MS does have its limitations, too. It is not yet a quantitative technique, though the response factors of various compound classes have been determined (for 16 eV EI⁺ conditions, see Chapter 2). It offers no isomer information. Indeed, the nature of its measurements even precludes absolute identification of the compounds contributing to a particular m/z value. Categorical compound assignments can be obtained through more

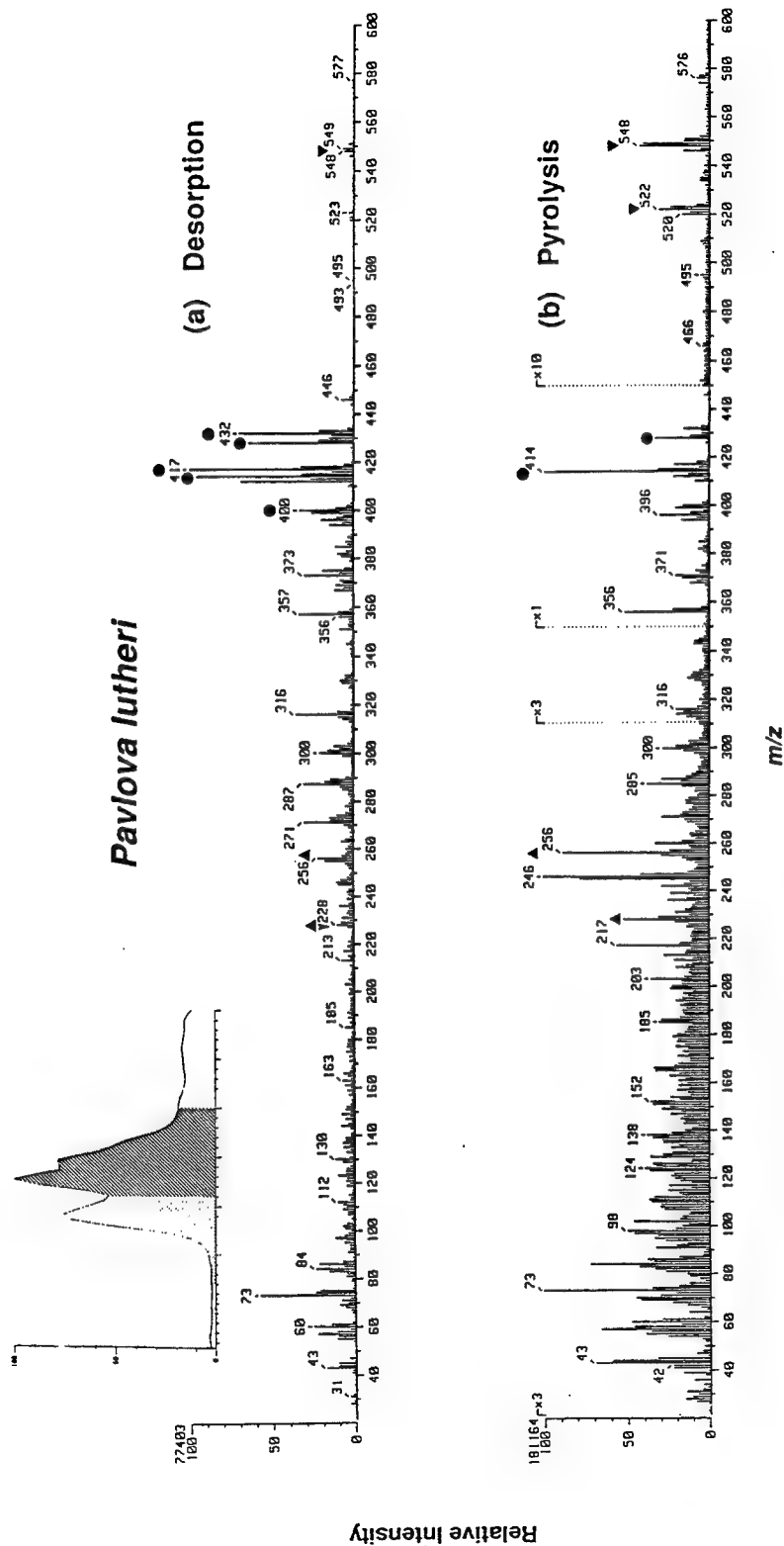


Fig. 1.4. DT-MS (low voltage EI) data from analysis of the prymnesiophyte *Pavlova lutheri*. The inset is a plot of the TIC (Total Ion Chromatograph). Fig. 1.4(a) is the mass spectrum resulting from summation over the desorption region (indicated by light shading in the inset) Fig. 1.4(b) results from summation over the pyrolysis region (indicated by darker shading in the TIC). Symbols denote: ● sterols, ▲ fatty acids, ▼ glycerides. Based on a figure from Eglinton et al., 1996.

Isochrysis galbana

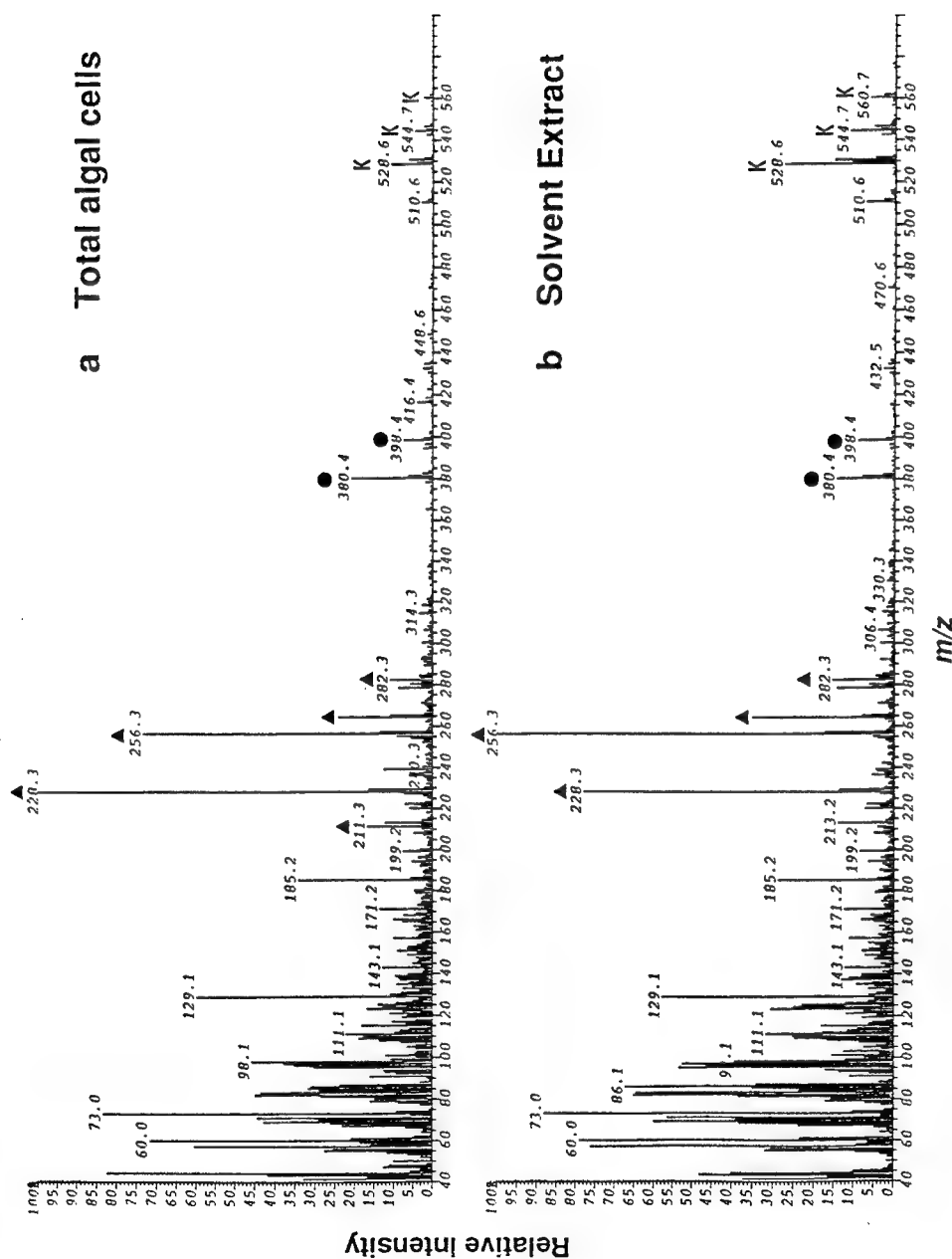


Fig. 1.5. DT-MS spectra for *Isochrysis galbana*: (a) mass spectra summed over the desorption section of the TIC profile; (b) mass spectra summed over the TIC peak from the measurement of a solvent (lipid) extract. Symbols denote: ● sterols, ▲ fatty acids, K alkenones. Based on a figure from Eglinton et al., 1996.

sophisticated MS techniques (high resolution MS, MS/MS), however, there is a trade-off as the techniques yielding more structural information can only be applied to reduced mass unit ranges. Pyrolysis mass spectrometry (the analytical category in which DT-MS falls) of POM results in complex spectra as POM contains nonpolar and polar organic constituents intimately associated with inorganic matrices. Although both desorption and pyrolysis yield mass spectra following certain known reaction rules, data processing techniques such as principle component analysis/discriminant analysis and analysis through neural networks are necessary for separating important patterns from the vast array of information obtained (as illustrated by Saliot et al., 1984; de Waart et al., 1991; Eglinton et al., 1992; Smiley et al., 1994; and others). Finally, DT-MS, even with its least selective ionization mode (low-voltage EI^+) does not provide an equal amount of information on all compound classes; therefore, there is a distinct possibility that important details of the chemical composition of certain samples can be obscured.

Despite these limitations, DT-MS fills an important gap in the study of POM. EI^+ DT-MS gives rapid molecular-level information on a broad array of biochemicals (see Appendix 1) while traditional techniques tend to be limited to one or a couple of compound classes. It also requires little or no sample workup and can be performed on microgram quantities of material. Therefore, it allows the rapid analysis of large sample sets (over a hundred samples can be analyzed per week), thus providing a statistically significant framework in which to place the more laborious and more detailed molecular-level studies. It can also, perhaps, supply information as to the molecular level variations responsible for changes in bulk measurements of POM (e.g., $\delta^{13}C$, C/N, etc.).

Multivariate Analysis

The two multivariate analysis techniques used in this study are principal component analysis (PCA) and discriminant analysis (DA), in this case a two-stage principal component analysis (Hoogerbrugge et al., 1983). PCA is a technique for

reducing the dimensionality of a data set by creating linear combinations of the measured variables. A limited number of these linear combinations or principal components should explain most of the variance in the original data set. PCA is similar to factor analysis but where factor analysis begins with a particular model for the data, PCA places no restrictions upon the covariance matrix which undergoes eigenanalysis (Meglen, 1992; for further description of PCA see Davis, 1986; Meglen, 1992). Discriminant analysis (DA), as used here, maximizes variance among samples and minimizes variance among replicate mass spectrometric analyses of the samples. This treatment, therefore, serves to reduce interference associated with sample inhomogeneity and instrument variability.

Table 1.2. Phytoplankton cultures used in the example of discriminant analysis.

Genus and species (strain)	Class	Code
<i>Hymenomonas carterae</i>	Prymnesiophyceae	Hym
<i>Emiliana huxleyi</i> (12-1)	Prymnesiophyceae	Emil1
<i>Emiliana huxleyi</i> (BT-6)	Prymnesiophyceae	Emil2
<i>Pleurochrysis carterae</i>	Prymnesiophyceae	Pleur
<i>Syracosphaera</i>	Prymnesiophyceae	Syr
<i>Phaeodactylum tricornutum</i>	Bacillariophyceae	Pheo
<i>Cylindrotheca fusiformis</i>	Bacillariophyceae	Cyl
<i>Thalassiosira weissflogii</i>	Bacillariophyceae	Thal
<i>Minutocellus polymorphus</i>	Bacillariophyceae	Min
<i>Amphidinium carterae</i>	Dinophyceae	Amph
<i>Dunelliella tertiolecta</i>	Chlorophyceae	Dun
<i>Pycnococcus provasoli</i>	Chlorophyceae	Pycn
<i>Nannochloris</i>	Chlorophyceae	Nan
<i>Porphyridium cruentum</i>	Rhodophyceae	Porph

Score plots resulting from PCA or DA indicate relationships among samples. Reconstructed spectra from the principal components (or discriminant functions) indicate the relationships among variables, i.e., m/z values, responsible for the relationships among the samples. These m/z values can be tentatively identified by comparison with literature values (Meuzelaar et al., 1982; Boon and de Leeuw, 1987; Saiz-Jiminez et al.,

1987; Lomax et al., 1991; Eglinton et al., 1996; and others) and values from additional analyses of standards, and the spectra can be considered illustrations of molecular-level differences among samples in the data set. It should be emphasized that the spectra resulting from PCA or DA are **difference** spectra; chemical characteristics shared by all samples in the data set will not appear. It should also be emphasized that DT-MS linked to PCA or DA is not a quantitative technique; with DT-MS, compound classes vary in response factor and sensitivity to matrix effects. Therefore, care must be taken in considering relative intensities of two m/z values within a difference spectrum as indicative of the relative amounts of enrichment of the precursor compounds.

A study of marine algal cultures (see Table 1.2 for cultures and their abbreviations) is presented here to illustrate the coupling of DT-MS and multivariate analysis as a technique for determining molecular-level variance in chemically complex samples. Duplicate measurements of the 14 algal cultures were performed on a Jeol SX-102A mass spectrometer using Electron Impact (EI^+) ionization (16 eV). For each measurement mass spectra summed over the peak in the Total Ion Current (TIC) curve were exported to a SUN Unix workstation for principal component and discriminant analyses using the program FOMpyroMAP (FOM Institute, the Netherlands).

Examples of the kind of information obtained are shown in Fig. 1.6 and Fig. 1.7. In Fig. 1.6, relationships among the algal samples are illustrated by plotting sample scores in two-dimensional space with Discriminant Function 1 (DF1) and DF2, responsible for 39% and 30% of the external variance, respectively, as the x- and y-axes. The more chemically similar the samples (in DF1 and DF2), the closer together they fall in the score plot (Fig. 1.6). Abridged information on variable loadings is superimposed on this score plot, and Fig. 1.7 contains complete loading information, in the form of reconstructed mass spectra, for DF+1, DF-1, DF+2, and DF-2. As shown in Fig. 1.6, DF1 separates *Nannochloris* sp. from *Emiliana huxleyi*, while DF2 strongly separates *Dunalliella tertiolecta* from *Minutocellus polymorphus* and *Cylindrotheca fusiformis*. As Fig. 1.7 illustrates, DF1 is primarily a function of desorbable (lipid) components. DF+1 contains

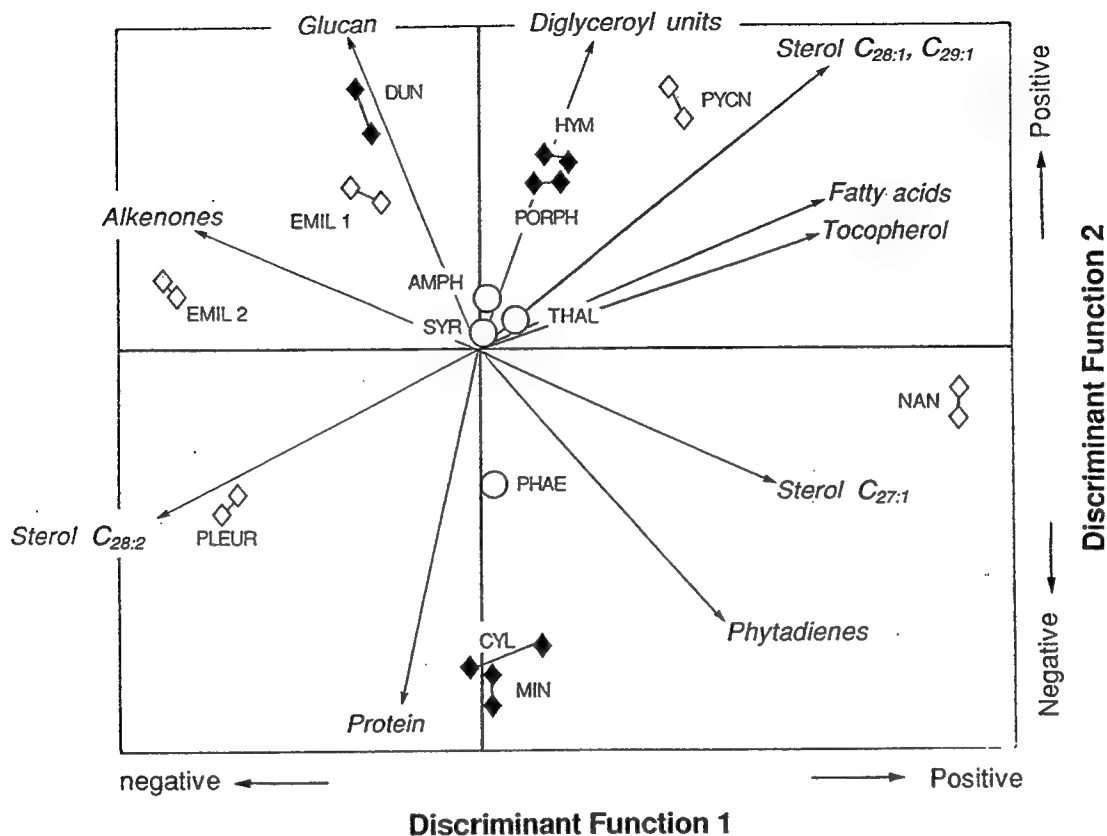


Fig. 1.6. Score plot from discriminant analysis of algal culture DT-MS spectra (summed over the entire TIC peak). Solid symbols indicate samples that plot above the DF1/DF2 plane (i.e., in the DF+3 region). Open symbols indicate samples falling in the DF-3 region. Loadings of the major variables (mass unit values) separating the samples are superimposed on the score plot. All data was acquired on a Jeol SX-102 instrument under EI⁺, 16 eV conditions. See Table 1.2 for explanation of the algal culture abbreviations. Modified from Eglinton et al., 1996.

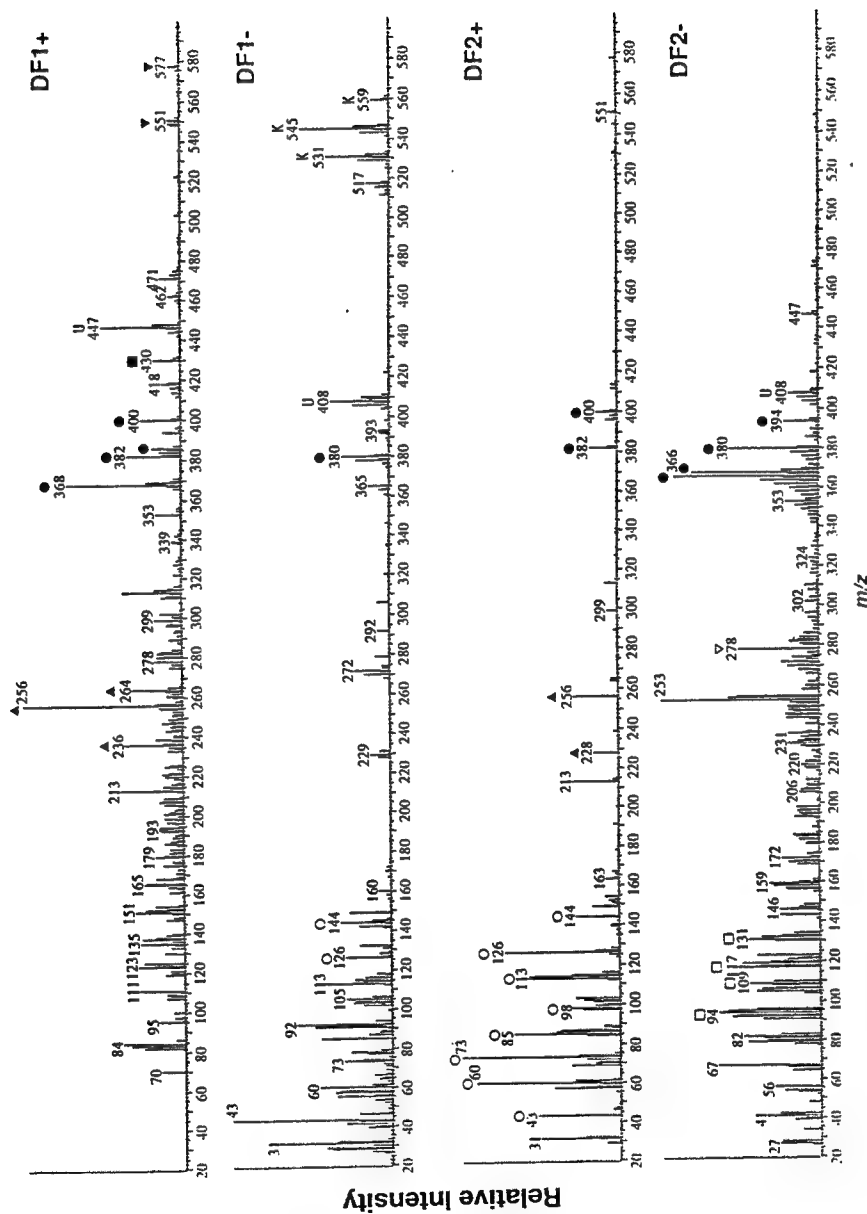


Fig. 1.7. Spectra illustrating the loadings of variables (m/z values) in DF1 and DF2 from Fig. 1.6. Symbols denote: ● sterols, Δ fatty acids, ▽ glycerides, ■ tocopherols, O polysaccharide fragments, ▽ phytadienes, □ protein fragments, K alkenones, U unknowns. Note: these spectra are not corrected for mass defect. Modified from Eglinton et al., 1996.

strong fatty acid (m/z 236, 256, 264) and sterol (m/z 368, 382, 386, 400) signatures as well as tocopherol (m/z 430) and diglyceride (m/z 551, 577) peaks and an unknown peak at m/z 477. DF-1 contains a strong signature from C_{37-39} alkenones (m/z 531, 545, 559), a $C_{28:2}$ sterol peak (m/z 380), and an unknown peak at m/z 408. DF+2 is a function of polysaccharide pyrolysis products (m/z 144, 126, 114, 98, 85, 73, 60, 43) but also includes $C_{16:0}$ and $C_{14:0}$ fatty acids and $C_{28:1}$ sterol (m/z 400, from the molecular ion, and m/z 382, from $M-H_2O$). DF-2 contains protein fragments (m/z 94, 117, 131) phytadiene (from chlorophyll, m/z 278) and $C_{27:2}$ and $C_{28:2}$ sterols.

This algal study illustrates that it is possible to determine significant molecular-level variations within a data set consisting of chemically complex samples. In this thesis both principal component analysis and discriminant analysis are applied to natural oceanic POM samples.

References:

- Allredge and Silver (1988). Characteristics, dynamics, and significance of marine snow. *Prog. Oceanogr.*, **20**, 41-82.
- Aluwihari L. I, Repeta D. J., and Chen R. F. (1997). A major biopolymeric component to dissolved organic carbon in surface seawater. *Nature* **387**, 166-169.
- Amon R.M.W. and Benner R. (1996) Bacterial utilization of different size classes of dissolved organic matter. *Limnol. Oceanogr.*, **41**(1), 41-51.
- Bacon M. P., Hun C. A., Fleer A. P. and Deuser W. G. (1985). Seasonality in the flux of natural radionuclides and plutonium in the deep Sargasso Sea. *Deep-Sea Res.*, **32**, 273-286.
- Biddanda B and Benner R. (1997). Carbon, nitrogen, and carbohydrate fluxes during the production of particulate and dissolved organic matter by marine phytoplankton. *Limnol. Oceanogr.*, **42**(3), 506-518.
- Bishop J. K. B., Edmond J. M., Ketten D. R., Bacon M. P., and Silker W. B. (1977). The chemistry, biology, and vertical flux of particulate matter from the upper 400 m of the Equatorial Atlantic Ocean. *Deep-Sea Res.*, **24**, 511-548.
- Boon J.J. (1992). Analytical pyrolysis mass spectrometry: new vistas opened by temperature-resolved in-source PYMS. *Int.J.Mass.Spec and Ion Process.*, **118/119**, 755-787.
- Boon, J. J. and de Leeuw J. W. (1987). Amino acid sequence information in proteins and complex proteinaceous material revealed by pyrolysis-capillary gas chromatography-low and high resolution mass spectrometry. *J. Anal. and Appl. Pyr.*, **11**, 313-327.
- Boudreau B. P. and Ruddick B. R. (1991). On a reactive continuum representation of organic matter diagenesis. *Am. J. of Science*, **291**, 507-538.
- Brown M. R., Dunstan G. A., Norwood S. J., and Miller K. A. (1996). Effects of harvest stage and light on the biochemical composition of the diatom *Thalassiosira pseudonana*. *J. Phycol.* **32**, 64-73.
- Buesseler K. O., Bauer J. E., Chen R. F., Eglinton T. I., Gustafsson O., Landing W., Mopper K., Moran S. B., Santschi P. H., VernonClark R., Wells M. L. (1996). An intercomparison of cross-flow filtration techniques used for sampling marine colloids: Overview and organic carbon results. *Mar. Chem.*, **55**, 1-31.

- Chester R. (1990). *Marine Geochemistry*. Unwin Hyman Ltd, London, 698 pp.
- Chu F. E. and Dupuy J. L. (1980). The fatty acid composition of three unicellular algal species used as food sources for larvae of the American oyster (*Crassostrea virginica*). *Lipids*, **15**, 356-364.
- Columbo J. C., Silverberg N., and Gearing J. N. (1996). Lipid biogeochemistry in the Laurentian Trough: I-fatty acids, sterols and aliphatic hydrocarbons in rapidly settling particles. *Org. Geochem.*, **25**(3/4), 211-225.
- Conte M.H. (1989). The biogeochemistry of particulate lipids in warm-core Gulf Stream ring systems, Ph.D. Thesis, 584 pp.
- Cowie G. L. and Hedges J. I. (1996). Digestion and alteration of the biochemical constituents of a diatom (*Thalassiosira weissflogii*) ingested by an herbivorous zooplankton (*Calanus pacificus*). *Limnol. Oceanogr.*, **41**(4), 581-594.
- Davis J. C. (1986). *Statistics and data analysis in geology*. New York, John Wiley and Sons, 646 pp.
- Dorsey J., Yentsch C. M., Mayo S., and McKenna C. (1989). Rapid analytical technique for the assessment of cell metabolic activity in marine microalgae. *Cytometry*, **10**, 622-628.
- Eglinton T. I., Boon J. J., Minor E. C., and Olson R. J. (1996). Microscale characterization of algal and related particulate organic matter by direct temperature-resolved mass spectrometry. *Mar. Chem.*, **52**, 27-54.
- Eglinton T. I., Sinninghe Damste J. S., Pool W., de Leeuw J. W., Eijkel G., Boon J. J. (1992). Organic sulfur in macromolecular sedimentary organic matter-II: Analysis of distributions of organic sulfur pyrolysis products using multivariate techniques. *Geochim. Cosmochim. Acta*, **56**, 1545-1560.
- Emerson S. and Hedges J. I. (1988). Processes controlling the organic content of open ocean sediments. *Paleoceanography*, **3**(5), 621-634.
- Guo L., Santschi P. H., Cifuentes L. A., Trumbore S. E., Southon J. (1996). Cycling of high-molecular-weight dissolved organic matter in the Middle Atlantic Bight as revealed by carbon isotopic (^{13}C and ^{14}C) signatures. *Limnol. Oceanogr.*, **41**(6), 1242-1252.
- Gustafsson O., Buesseler K. O., Gschwend P. M. (1996). On the integrity of cross-flow filtration for collecting marine organic colloids. *Mar. Chem.*, **55**(1/2), 93-111.

Harvey H. R. and Macko S. A. (1997). Catalysts or contributors? Tracking the bacterial mediation of early diagenesis in the marine water column. *Org. Geochem.*, **26**(9/10), 531-544.

Harvey H. R., Tuttle J. H., and Bell J. T. (1995). Kinetics of phytoplankton decay during simulated sedimentation: Changes in biochemical composition and microbial activity under oxic and anoxic conditions. *Geochim. Cosmochim. Acta*, **59**(16), 3367-3377.

Harvey H. R., Eglinton G., O'Hara S. C. M. and Corner E. D. S. (1987). Biotransformation and assimilation of dietary lipids by *Calanus* feeding on a dinoflagellate. *Geochim. Cosmochim. Acta*, **51**, 3031-3040.

Hedges J. I. (1992). Global biogeochemical cycles: progress and problems. *Mar. Chem.*, **39**, 67-93.

Hedges J. I., Clark W. A., and Cowie G. L. (1988). Fluxes and reactivities of organic matter in a coastal marine bay. *Limnol. Oceanogr.*, **33**(5), 1137-1152.

van der Heijden E., Boon J. J., Scheijen M. A. (1990). Pyrolysis mass spectrometric mapping of selected peats and peatified plant tissues. In: Sopo R. (Ed.) *Peat 90--Versatile Peat*, the Association of Finnish Peat Industries, Jyskae, Finland, pp. 148-163.

Hernes P.J., Hedges J.I., Peterson M.L., Wakeham S.G., and Lee C. (1996) Neutral carbohydrate geochemistry of particulate material in the central Equatorial Pacific. *Deep Sea Res. II*, **43**, 1181-1204.

Hoogerbrugge R., Willig S. J., and Kistemaker P.G., (1983). Discriminant analysis by double stage principle component analysis. *Anal. Chem.* **55**, 1710-1712.

Lee C. and Cronin C. (1984). Particulate amino acids in the sea: Effects of primary productivity and biological decomposition. *J. Mar. Res.*, **42**, 1075-1097.

Lee R. F., Nevenzel J. C., and Paffenhoffer G. A. (1971). Importance of wax esters and other lipids in the marine food chain: Phytoplankton and copepods. *Mar. Biol.*, **9**, 99-108.

Lomax J. A, Boon J. J., and Hoffmann R. A. (1991) Characterisation of polysaccharides by in-source pyrolysis positive- and negative-ion direct chemical ionisation-mass spectrometry. *Carbohydrate Research*, **221**, 219-233.

McCarthy, M., J. Hedges, R. Benner (1996). Major biochemical composition of dissolved high molecular weight organic matter in seawater. *Mar. Chem.* **55**: 281-297.

McCave I. N. (1975). Vertical flux of particles in the ocean. *Deep-Sea Res.*, **22**, 491-502.

- Meglen R. R. (1992). Examining large data bases: a chemometric approach using principle component analysis. *Mar. Chem.*, **39**, 217-237.
- Meuzelaar H. L. C., Haverkamp J., and Hileman F. D. (1982). *Pyrolysis Mass Spectrometry of Recent and Fossil Biomaterials: Compendium and Atlas*. Elsevier Press, New York, 293 pp.
- Middelburg J. J. (1989). A simple rate model for organic matter decomposition in marine sediments. *Geochim. Cosmochim. Acta*, **53**, 1577-1581.
- Moran S. B. and Moore R. M. (1989). The distribution of colloidal aluminum and organic carbon in coastal and open ocean waters off Nova Scotia. *Geochim. Cosmochim. Acta*, **53**, 2519-2527.
- Olson R. J., Chisholm S. W., Zettler E. R., Altabet M. A., and Dusenberry J. A. (1990). Spatial and temporal distributions of prochlorophyte picoplankton in the North Atlantic Ocean. *Deep-Sea Res.*, **37**, 1033-1051.
- Olson R. J., Zettler E. R., and Anderson O. K. (1989). Discrimination of eukaryotic phytoplankton cell types from light scatter and autofluorescence properties measured by flow cytometry. *Cytometry*, **10**, 636-643.
- Parsons T. R., Takahashi M., Hargrave B. (1984). *Biological Oceanographic Processes*, 3rd Ed., New York, Pergamon Press, 330 p.
- Prahl F. G., Muehlhausen L. A., and Zahnle D. L. (1988). Further evaluation of long-chain alkenones as indicators of paleoceanographic conditions. *Geochim. Cosmochim. Acta*, **52**, 2303-2310.
- Repeta D. J. and Gagosian R. B. (1983). Carotenoid transformation products in the upwelling waters off the Peruvian coast: suspended particulate matter, sediment trap material and zooplankton fecal pellet analyses. In: Bjoroy M. (Ed.) *Advances in Organic Geochemistry, 1981*, Wiley and Sons, pp. 380-388.
- Saiz-Jiminez C., Boon J. J., Hedges J. I., Hessels J. K. C. and de Leeuw J. W. (1987). Chemical characterization of recent and buried woods by analytical pyrolysis: Comparison of pyrolysis data with ¹³C NMR and wet chemical data. *J. Anal. Appl. Pyr.*, **11**, 437-450.
- Saliot A., Ulloa-Guevara A., Viets T. C., de Leeuw J. W., Schenk P. A., Boon J. J. (1984). The application of pyrolysis-mass spectrometry and pyrolysis-gas

chromatography-mass spectrometry to the chemical characterization of suspended matter in the ocean. *Org. Geochem.*, **6**, 295-304.

Skoog A. and Benner R. (1997). Aldoses in various size fractions of marine organic matter: Implications for carbon cycling. *Limnol. Oceanogr.*, in press.

Smiley G. D., Aplin A. C., Larter S. R. (1994). Characterization and quantification of DOM by analysis of Py-MS spectra using artificial neural networks. Presentation at the 1994 ACS Meeting in San Diego.

Tanoue E. and Handa N. (1980). Vertical transport of organic materials in the Northern Pacific as determined by sediment trap experiment. 1. Fatty acid composition. *J. Ocean. Soc. Japan*, **36**, 231-245.

Voet D. and Voet J. G. (1990). *Biochemistry*. John Wiley & Sons, New York, 1223 pp.

deWaart J., Tas A. C., la Vos G. F., van der Greef J. (1991). Characterization of algae by pyrolysis-direct chemical ionization (tandem) mass spectrometry. *J. Anal. Appl. Pyr.*, **18**, 245-260.

Wakeham S. G. and Lee C. (1993). Production, transport, and alteration of particulate organic matter in the marine water column. In: Engel M. H. and Macko S. A. (Ed.) *Organic Geochemistry*, Plenum Press, New York, pp. 145-169.

Wakeham S. G. and Canuel E. A. (1988). Organic geochemistry of particulate matter in the eastern tropical North Pacific Ocean: Implications for particle dynamics. *J. Mar. Res.*, **46**, 183-213.

Wakeham S. G. and Ertel J. R. (1988). Diagenesis of organic matter in suspended particles and sediments in the Cariaco Trench. *Org. Geochem.*, **13**, 815-822.

Wakeham S.G., Lee C., and Hedges J. I. (1997). Fluxes of major biochemicals in the equatorial Pacific Ocean. *Biogeochemistry of Marine Organic Matter*, submitted.

Wakeham, S.G., Lee C., Farrington J. W., and Gagosian R. B. (1984). Biogeochemistry of particulate organic matter in the oceans: results from sediment trap experiments. *Deep-Sea Res.*, **31**(5), 509-528.

Westrich J. T. and Berner R. A. (1984). The role of sedimentary organic matter in bacterial sulfate reduction: The G model tested. *Limnol. Oceanogr.*, **29**, 236-249.

Volkman J. K. (1989). Fatty acids of microalgae used as feedstocks in aquaculture. In: Cambie R. C. (Ed.), *Fats for the Future*, Ellis Horwood, Chichester, pp. 263-283.

Volkman J. K. (1986). A review of sterol markers for marine and terrigenous organic matter. *Org. Geochem.* **9**(2), 83-99.

Chapter 2 Methods

Introduction

The thesis work in the following chapters relies strongly on two techniques: direct temperature-resolved mass spectrometry (DT-MS), a form of pyrolysis mass spectrometry or Py-MS (e.g. Boon et al., 1992), and flow cytometry (described in Herzenburg and Sweet, 1976, for examples of oceanographic applications see Chisholm et al., 1988; Sosik et al., 1989; Olson et al., 1990a; Olson et al., 1990b). DT-MS (16eV EI⁺) fills the unique role of providing first-order broad-band molecular-level characterization of microgram quantities of organic matter. It is used here, coupled with principle component and discriminant analyses, as an initial screening technique for understanding variations in oceanic particulate organic matter (POM) composition. In addition, its sensitivity and its non-specificity over many compound classes make it suitable for coupling with preparative flow cytometry in order to explore heterogeneity within small-particle (<53 μm) POM. Flow cytometric sorting is used in this thesis to separate suspended particles on the basis of red fluorescence in addition to size, thereby enabling the chemical characterization of “phytoplankton” and “detritus” (everything not phytoplankton) separated from field samples of small-particle (>2 μm , <53 μm) POM.

The application of these techniques to the study of oceanic organic matter imposes certain non-traditional sample-handling procedures as samples must be suspended in liquid for introduction to the flow cytometry flow cell and for application to the DT-MS sample probe. The non-selectivity of EI⁺ (the most widely-used ionization mode) DT-MS leads to responses over a wide range of compound classes, which includes a wide variety of contaminants as well. In addition, the small sample size requirements in DT-MS can make it difficult to analyze representative portions of heterogeneous samples such as large-particle (> 53 μm) POM. Finally, the presence of salt interferes with the mass spectrometry, often swamping the detector with inorganic species (e.g., HCl, m/z 36, and

SO₂, m/z 64) and stabilizing organic molecules so that when they finally fragment, they yield small uninformative ions.

Although flow cytometry and DT-MS are not yet widely used as analytical tools in marine chemistry, it is likely that these techniques will see increasing application as the instrumentation improves in flexibility, availability, and ease of use. Therefore, this chapter offers a protocol for sample collection, processing, and measurement which yields reproducible, informative results. The flow cytometric approach is tested by comparing FCM analyses of oceanic POM samples with analyses of the same samples via microscope techniques (staining and image analysis, Williams et al., 1995 and Verity and Sieracki, 1993). The relative response of common compound classes under EI⁺ DT-MS conditions is determined by analysis of selected standards. These factors are then used to quantify the relative contribution of various compound classes in two natural POM samples. The potential of DT-MS as a quantitative technique is further explored by comparing DT-MS determinations of particulate organic carbon to chlorophyll ratios (POC/chl) in natural POM samples with the same ratios determined by elemental analysis and liquid chromatography (HPLC).

Experimental

Analytical method

The analytical method is outlined in Fig. 2.1. Seawater is collected via Niskin bottle, diaphragm pump, or peristaltic pump and prefiltered through a nylon 53 µm screen to separate large-particle POM from small-particle POM (the 53 µm cut-off has been used in previous studies to separate an approximation of sinking POM from an approximation of suspended POM, see Bishop and Edmond, 1976). Tangential flow filtration or TFF (0.8 µm Fluoro centrasette and ultrasette, Filtron, driven by Masterflex peristaltic pumps) concentrates the smaller particles while keeping them suspended in seawater. Typically,

ANALYTICAL SCHEME

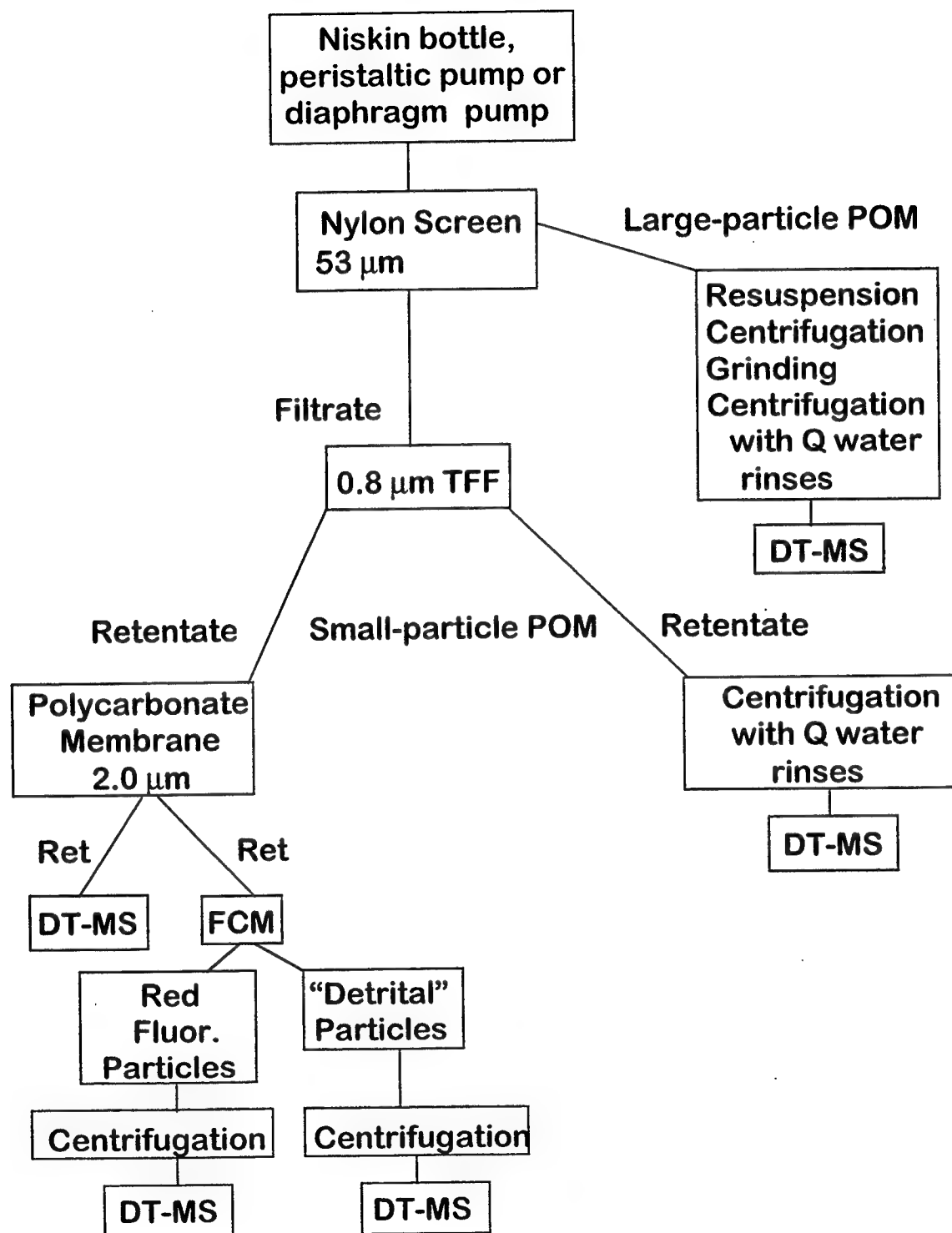


Fig. 2.1. Analytical scheme for oceanic large-particle and small-particle POM.

4 L to 100 L of seawater are concentrated to approximately 100 mL. The larger volume samples are initially processed via Filtron centrasette (inlet pressure < 20 psi, filtrate flow rate 0.5 L to 1.5 L per minute) to 4 L. The 4 L samples (both original seawater samples and centrasette retentate) are concentrated to approximately 100 mL on a Filtron ultrasette system (inlet pressure < 20 psi). The larger volume samples are not necessary for DT-MS but are taken in order to obtain enough material for ancillary analytical techniques. For DT-MS analysis 3-15 mL aliquots of such a sample are concentrated by centrifugation (4 minutes at 10,500xG on a Fisher Micro-Centrifuge, Model 59A). The resulting pellet of small-particle POM is desalted in the following manner: the pellet is resuspended in 1 mL of deionized water or Milli-Q™ water and centrifuged as above, the supernatant is discarded, and the rinsing step is repeated twice. Large-particle POM is resuspended off the nylon screen, concentrated by centrifugation (10 minutes at ~1800xG on an IEC HN-SII centrifuge, Damon/IEC Division), homogenized via Teflon tissue grinder, and then desalted as above. Samples are stored in liquid nitrogen after tangential flow filtration and/or after centrifugation as necessary.

For flow cytometric sorting of small-particle POM, there are two further filtration steps. The >0.8 µm retentate is filtered onto a 2 µm polycarbonate membrane filter (Poretics) using a slight vacuum (<5 psi); the sample is rinsed with and resuspended in <0.2 µm syringe-filtered seawater and then placed in liquid nitrogen to await flow cytometry. Just prior to sorting, the sample is thawed and syringe-filtered through a 53 µm nylon screen to remove any aggregates that may clog the flow cell tip. Desalting of sorted samples is done by using Milli-Q™ water sheath fluid during flow cytometry and by centrifuging the resulting samples. These desalted samples are then analyzed via DT-MS.

The sample pellets, resuspended in a small quantity of Milli-Q™ water, are analyzed in triplicate via DT-MS. The mass spectrometers used are either a JEOL SX-102 (16 eV EI⁺, acceleration voltage 8.0 kV, direct inlet, mass range 20-1000, scan

speed 1s, resolution 3000) with the sample probe resistively heated from 0 to 1.1 A at 0.5 A/min or a VG AutoSpecQ (16 eV EI⁺, acceleration voltage 8.0 kV, direct inlet, mass range 41-795, scan speed 2 s, resolution 1000) with the sample probe (a platinum/rhodium (87/13) wire (0.125 mm diam.)) resistively heated to just below the melting point of the wire over 1.5 minutes. To reduce the resulting information to a manageable level, spectra (in integer form, mass defect=0.7 or 0.75) are then exported to a multivariate statistics program (FOMPyroMAP or Chemometricks) and molecular-level differences among the spectra are investigated using principal component and discriminant analyses (as in Saliot et al., 1984; Eglinton et al., 1992; and others; for a description of PCA see Windig et al., 1981/1982; and Meglen, 1992; and for further discussion of DT-MS applications in marine organic geochemistry, see Eglinton et al., 1996; and Klap et al., 1996).

Evaluation of filtration effects

The potential fractionation of particle populations by tangential flow filtration was explored by comparing the "phytoplankton" and "detrital" windows of flow cytometric analyses of unfiltered and filtered (>0.8 µm, <53 µm and >2.0µm, <53 µm) aliquots of the same samples ("wh" collected from Great Harbor, Woods Hole, MA in February 1997 and "s" collected in June 1995 off the shelf of the US East Coast at 37°15'N, 73°3'W). Both unfiltered and filtered aliquots were frozen in liquid nitrogen between sampling and flow cytometric analysis. Subsamples of the filtered samples were rediluted (after thawing) to their initial concentration using <0.22 µm Great Harbor water (which was syringe filtered that day using a Millex-GV™, 0.22 µm filter unit). The filtered and unfiltered samples plus an aliquot of the <0.2 µm Great Harbor water used for dilution were then analyzed on an EPICS V flow cytometer (Coulter, Inc) using a Cicero data acquisition system (Cytomation, Inc.), a standard lens assembly, a 100 µm jet-in-air flow

cell, excitation at 488 nm with a 130 mW laser beam and detector settings optimized for eukaryotic phytoplankton.

Evaluation of particle populations via flow cytometry vs microscopy

The same flow cytometry conditions were used in a comparison of flow cytometry particle determinations and microscopy determinations using color image analysis (performed in Peter Verity's laboratory at SKIO, see Verity and Sieracki, 1993 for a description of the technique). For this comparison unfiltered seawater samples were collected via diaphragm pump from surface waters on the continental shelf of the U.S. east coast. Two samples were taken from each sampling station. One was placed into liquid nitrogen for preservation until flow cytometric analysis. The second was split into two aliquots which were preserved with glutaraldehyde. Propidium iodide was added to the first aliquot (staining time, 5 minutes). The sample was then filtered onto a 0.8 μm black Poretics polycarbonate filter and resuspended to 7 mL with Milli-Q™ water; when the volume reached 5 mL, 150 μL of 4',6-diamidino-2-phenylindole (DAPI) was added (staining time, 5 minutes). The sample was then reconcentrated onto the black membrane filter which was placed on a slide; low-fluorescence immersion oil was added along with a cover slip and the slide was frozen. The second aliquot was stained with proflavin, filtered immediately, resuspended in milli-Q water, stained with DAPI as above and prepared as a slide (staining protocols from Williams et al., 1995 and Verity and Williams, personal communication). The combination of propidium iodide and DAPI was used to distinguish plankton and detritus. Proflavin was used to identify autotrophic vs heterotrophic cells. Proflavin staining can affect the PI/DAPI identification of detritus (Williams et al., 1995) and was therefore performed on the second aliquot of sample.

Analysis of the desalting procedure

The necessity of the desalting step in the analytical method (Fig. 2.1) was tested on three cultures of marine phytoplankton. *Emiliana huxleyi*, *Phaeodactylum tricornutum*, and *Pycnococcus provasolii* were grown in 20 L batch cultures in modified F/2 medium (made using filtered Vineyard Sound seawater) kept at 19°C on a 14:10 light:dark cycle and bubbled with air. The cultures were harvested via centrifugation (20 minutes at 1500 rpm, IEC Model K Centrifuge) when cell densities reached 290,000 cells/mL, 2,900,000 cells/mL, and 2,500,000 cells/mL, respectively. Two aliquots from each resulting pellet, resuspended in approximately 1 mL of supernatant, were removed and placed in liquid nitrogen until DT-MS analysis. Subsamples of all three cultures were combined and two aliquots were taken from this sample as well and stored in liquid nitrogen. Just prior to DT-MS analysis, the aliquots were thawed and one from each sample was desalted following the protocol for small-particle POM samples. The aliquots with salt were further concentrated by centrifugation (4 minutes at 10,500xG on a Fisher Micro-Centrifuge, Model 59A) and resuspended into 0.5 mL total volume of supernatant and pellet. The aliquots with salt and without salt were then analyzed via DT-MS on a VG AutospecQ mass spectrometer (same conditions as described above). The resulting spectra for each culture were initially compared visually. In addition, the spectra, in integer mode (mass defect=0.7 or 0.75), were summed over the entire TIC (total ion chromatogram), and exported to a multivariate statistics program (Chemometrics, developed at FOM-AMOLF and modified at WHOI). They were then analyzed by principle component analysis (after removal of the inorganic and contaminant peaks m/z 64, from SO_2 , 81, probably from Na_2Cl^+ , and 100, perhaps from tetrafluoroethylene).

Two TFF (>0.8 μm , <53 μm) samples ("a" from Great Harbor, Woods Hole, and "b" from the continental shelf of the U.S. east coast, 35°26.7'N, 74°47.29'W) were used to evaluate the potential loss of dissolved and colloidal carbon released from POM during

the desalting procedure. These samples were thawed, further concentrated via centrifugation as above, resuspended in Milli-Q™ water and respun (3 times), with the supernatant removed after each rinse. Aliquots were removed from the initial sample, the supernatant after the first centrifugation, the supernatant from each rinse with Milli-Q™ water, and the resuspended pellets. These aliquots and a Milli-Q™ water blank were placed in tin cups and dried at low heat in a dry bath. The total carbon content of these samples was then determined using a Fisons EA 1108 Elemental Analyzer.

The homogenization and desalting procedure for large-particle POM was also tested by taking aliquots from each step for elemental analysis. Two >53 µm samples from the continental shelf of the U.S. east coast were used.

Determination and application of DT-MS response factors

DT-MS (16 eV EI⁺) response factors were determined for a selected suite of lipid and biopolymer standards. Each standard was analyzed three to six times and response factors were determined for the TIC (total ion chromatogram), characteristic ion series, the molecular ion where possible, and selected fragment ions. For better comparison with multivariate statistics results, mass spectra were processed in integer mode (mass defect=0.7 or 0.75). The response factors and their standard deviations were calculated using the concentration of the standard, the volume added to the sample wire, and the area under the curve of the mass chromatogram for the selected m/z value or values.

Mixed lipid standards with and without a particle matrix (Al₂O₃) were analyzed to determine matrix effects on fatty acid and sterol response factors. The effect of a natural matrix, POM from the Peruvian upwelling region, was studied by adding various concentrations of POM and determining the response factor for a constant concentration of caffeine.

The response factors discussed above were used to calculate the relative contribution of various compound classes from the DT-MS spectra of two >0.8 µm, <53

μm samples from Great Harbor, Woods Hole, MA. Both standards and samples were analyzed on a VG Autospec-Q mass spectrometer with the same conditions as described in the Analytical Method section. In order to evaluate day-to-day variations in instrument sensitivity, caffeine was used as an external standard.

The comparison of DT-MS and HPLC measurements of POC/chlorophyll ratios

In an attempt to further determine the potential of DT-MS as a quantitative method, small particle POM samples (either $>0.8 \mu\text{m}$, $<53 \mu\text{m}$ or $>2 \mu\text{m}$, $<53 \mu\text{m}$), [POC] samples and pigment samples were collected from the same stations along the Mid-Atlantic Bight and in Great Harbor, Woods Hole, MA. The small-particle POM samples and the pigment filters were kept in liquid nitrogen until analysis; the [POC] samples were stored in a conventional freezer. The POM samples were processed as described in Fig.1, and analyzed in triplicate via DT-MS (16 eV EI^+ , VG AutospecQ). The [POC] and pigment samples, consisting of 1 to 2 L of seawater, were collected by either peristaltic or diaphragm pump and filtered onto GF/F filters using a pressure cannister and N_2 gas ($<5 \text{ psi}$). Prior to analysis on a Fisons EA 1108 Elemental Analyzer, the [POC] filters were placed over fuming HCl for 24-48 hours and dried overnight in an oven at approximately 60°C . The filters were then weighed and cut into pieces, replicates of which were analyzed on the elemental analyzer. The pigment samples were extracted in acetone; an internal standard (zinc pyropheophorbide octadecyl ester collection 26-31, Fraction 6, from D. Repeta, WHOI) was used for quantification. Pigment extracts were injected onto a C-8 column (Rainin "Microsorb 'short-one,'" particle size $3 \mu\text{m}$, pore size 100 angstroms, column size $4.6 \times 100 \text{ mm}$) in a Waters 600E HPLC system with a photodiode array detector. Solvent A was $\text{MeOH}: 0.5 \text{ N NH}_4\text{Ac}$ (75:25); Solvent B, MeOH ; solvent program (minutes, % Solvent A, % Solvent B); (0;100,0), (20;35,65); (30; 25,75); (35;0,100); flow rate 1.0 mL/min (Goericke and Repeta, 1993).

DT-MS total ion chromatographs and mass chromatograms for phytadiene (a chlorophyll pyrolysis product, m/z 278) were integrated in order to determine the [TIC]/[phytadiene] (area/area) ratio for each sample. A comparable ratio, [POC]/[chl a], was determined from the elemental analysis and HPLC data.

Procedural blanks

DT-MS (16 eV, EI^+ , VG AutospecQ) analysis was performed on blanks from both the flow cytometric sorting procedure and from the homogenization and desalting procedure for large-particle POM samples in order to determine if these procedures introduced organic contaminants. Unfortunately, a true blank for the cross-flow filtration step was not feasible as it would require 100 L of organic-free water with the same ionic strength as seawater. Constraints on the filtration step were limited to flow cytometric analyses of POM from filtered and unfiltered aliquots of seawater samples, and to DT-MS analyses of methanol and dichloromethane extractions of the peristaltic tubing used in the pump driving the cross-flow filtration.

The flow cytometry blanks were collected by using 3.8% NaCl solution as a sample (in order to provide the ionic strength necessary for charging water droplets for sorting, see Chapter 1) and Milli-Q™ water as sheath fluid. The flow cytometer was set in Sort Test mode, in which droplets are charged regardless of whether or not they contain particles of interest, and the resulting blanks were collected from both the left and right streams. For comparison with the blanks, a POM sample ($>3\ \mu\text{m}$, $<53\ \mu\text{m}$) collected from surface waters in the Peruvian upwelling region was sorted via flow cytometer and the resulting “detrital” and “phytoplankton” samples were also analyzed by DT-MS.

The blank for the homogenization and desalting of large-particle POM consisted of 4.8 mL of deionized water which was centrifuged, ground with a Teflon tissue grinder and “desalted” by centrifugation with deionized water rinses. It, like field POM samples,

was stored in liquid nitrogen prior to analysis by DT-MS. For comparison, a >53 μm POM sample from Great Harbor, Woods Hole, MA was also analyzed by DT-MS.

Results and discussion

It was necessary to examine the applicability of the method illustrated in Fig. 2.1. Areas of concern in sample handling included filtration effects, desalting issues, and the identification of phytoplankton for flow cytometric sorting. In order to determine how representative DT-MS mass spectra were, response factor variations and matrix effects also needed to be explored.

Sample handling: Contamination

The typical shipboard environment (and the land laboratory environment as well) contains many contaminants (see Table 2.1) that are measured readily by DT-MS and can obscure important information on the chemical characteristics of natural particles. Phthalates (often from gloves and air circulation systems), silicone (from peristaltic pump tubing and mass spectrometer pump oil), and polystyrene (which can come from Styrofoam packing used to protect delicate laboratory set-ups at sea) all yield strong DT-MS signals. Fig. 2.2, the DT-MS spectrum of a dilute particle sample (>0.3

Table 2.1. Characteristic ions (16 eV, EI^+) for common laboratory/shipboard contaminants.

Common contaminants	characteristic ions (DT-MS, 16eV EI^+)
salt	
HCl	36
SO_2	64
?	81
phthalate	149, 167, 187, 279
polystyrene	104, 206, 207, 208, 312
silicone	207, 208, 209, 267, 281, 282, 283, 341, 355, 356, 357, 415, 429, 430, 431, 489, 503, 504, 505,...

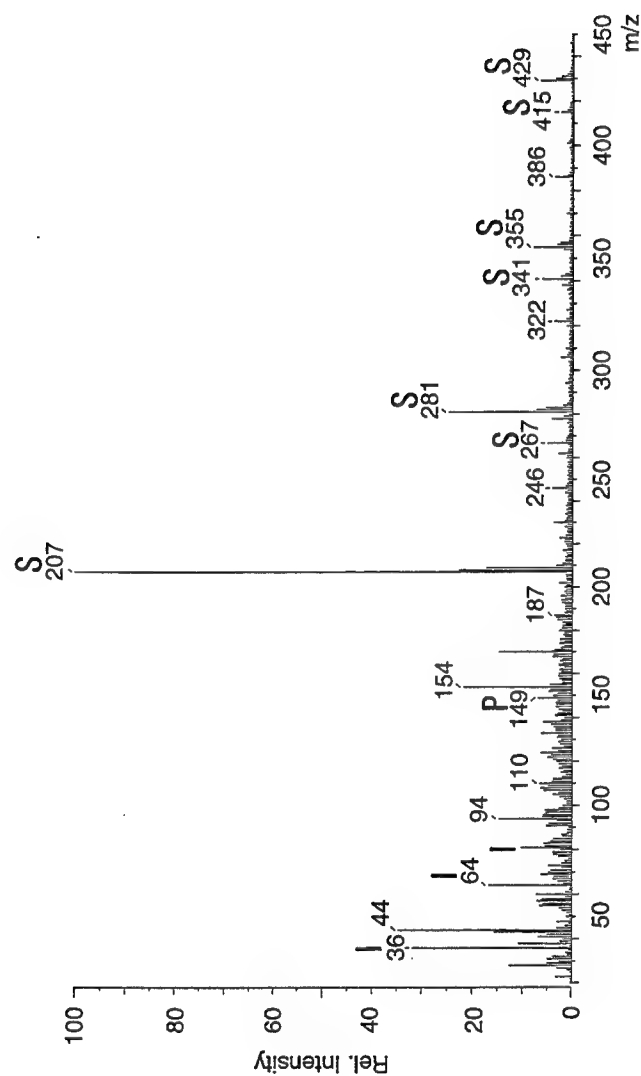


Fig. 2.2. DT-MS (16 eV, EI⁺) analysis of a strongly contaminated Sargasso Sea (34°31.68'N, 66°41.65'W) suspended POM (>0.3, <53 μm) sample from 2000 m. Note the silicone (S) and phthalate (P) signals and the inorganic signals (I) resulting from incomplete desalting of the sample.

μm , $<53 \mu\text{m}$) from 2000 m depth in the Sargasso Sea ($34^{\circ} 31.68'\text{N}$, $66^{\circ}41.65'\text{W}$), illustrates the sensitivity of this analysis to phthalates (m/z 149, 279) and silicone (m/z 207, 208, 209, 281, 282, 283, repeating every 74 mass units). Silicone is an especially bad contaminant as its fragments cover so many mass units and can easily obscure compounds of interest such as tocopherol (m/z 430). We have found it necessary to use a tougher peristaltic tubing than silicone (e.g., Pharmed Masterflex) and while this minimizes the contamination from tubing material, the use of another pump style, such as a diaphragm pump or an impeller pump (e.g., Gustafsson et al., 1996) would probably be optimal, provided the pressure pulses are sufficiently gentle. As for the other major source of silicone contamination, analyzing sufficient organic material (several μg) swamps the silicone signal from mass spectrometer pump oil. In addition, the following common sense practices prove important: minimize sample contact with the open air; avoid the use of Styrofoam packing materials in the lab and use judiciously in packing for cruises; and avoid glove-sample contact as much as possible.

Sample handling: filtration effects

The issue of possible fractionation of particle populations by tangential flow filtration was addressed using flow cytometric analysis of unfiltered and filtered (and rediluted, see experimental section) aliquots of a coastal sample (“wh”) and an open ocean sample (“s”). For each aliquot the number of counts falling in the “phytoplankton” and “detrital” regions (based on forward light scatter and red fluorescence; the forward light scatter parameters were those used for sorting $>2 \mu\text{m}$ samples) were determined (see Fig. 2.3a). Fig. 2.4a depicts the “detritus” and “phytoplankton” counts per mL seawater for the unfiltered and filtered samples and the $<0.2 \mu\text{m}$ seawater used to dilute the filtered samples back to their original concentrations. The total suspended particle counts in the $>0.8 \mu\text{m}$ samples are one to two orders of magnitude lower than literature values (i.e., counts of surface ocean suspended particles with a diameter $>1 \mu\text{m}$ obtained from Coulter

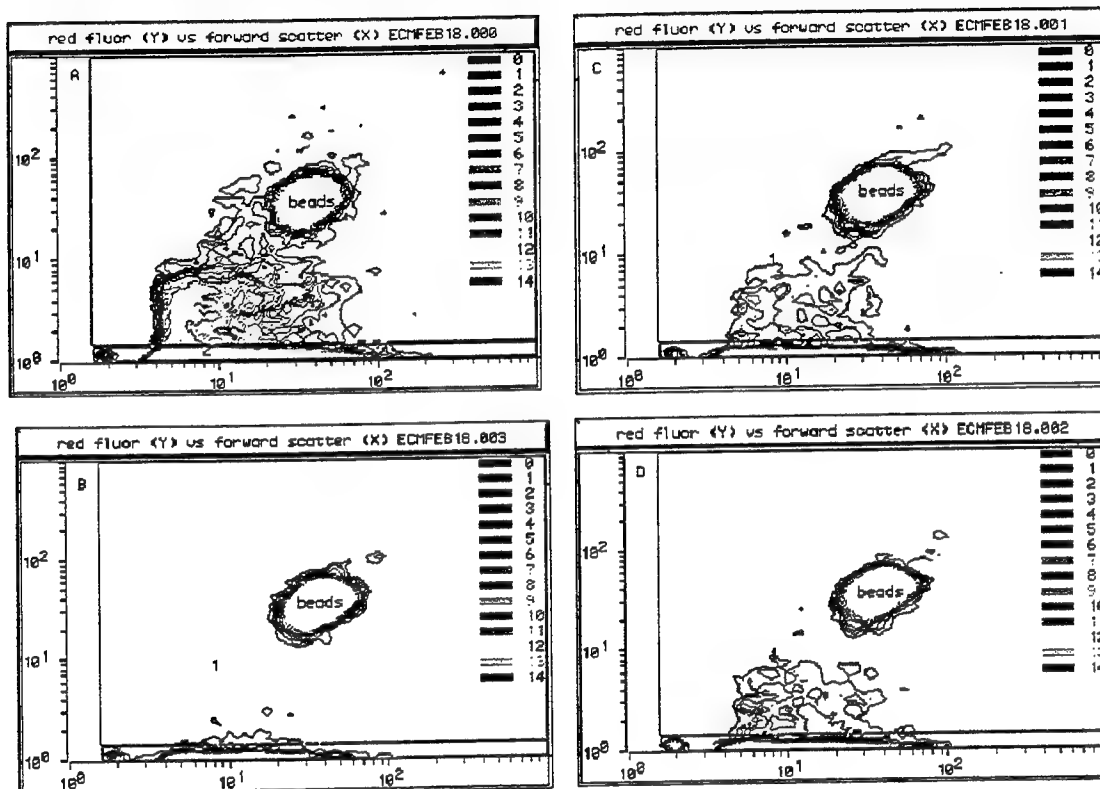


Fig. 2.3. Flow cytometry “windows” used for determining filtration effects. Region 1 includes phytoplankton and fluorescent beads (used as an internal standard); region 2 includes “detritus.” Figure (A) shows flow cytometric analysis of unfiltered sample **wh**. Figure (B) shows the $<0.2\ \mu\text{m}$ seawater used to dilute filtered samples back to their original concentrations and can be considered a flow cytometric blank. Figure (C) is **wh** after TFF filtration ($>0.8\ \mu\text{m}$, $<53\ \mu\text{m}$). Figure (D) is **wh** after both TFF and gravity/slight vacuum filtration ($>2\ \mu\text{m}$, $<53\ \mu\text{m}$).

FCM analysis of filtration step

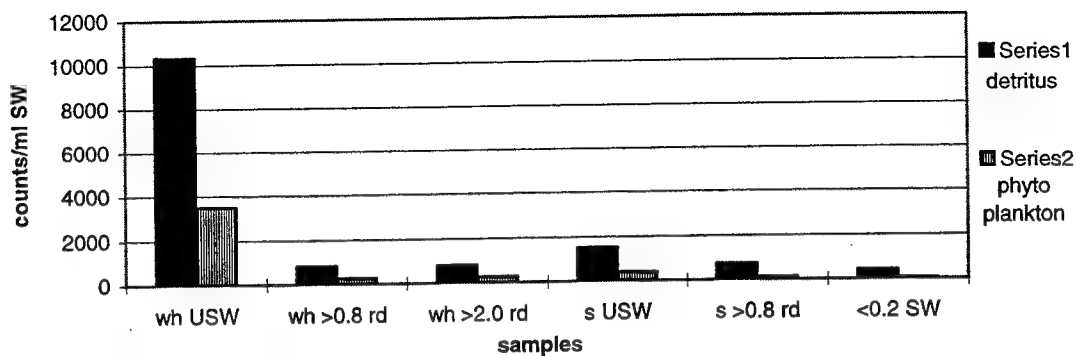
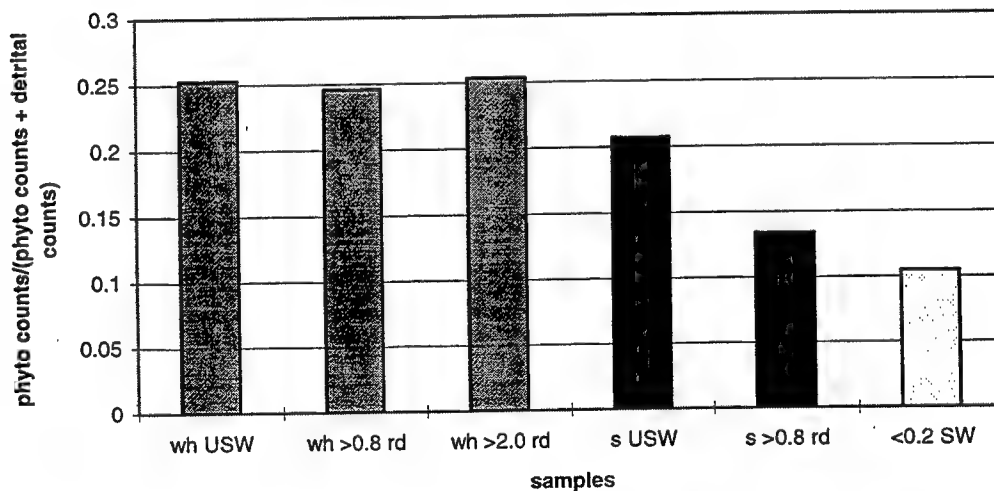


Fig. 2.4 a. FCM analysis, reported as counts/mL seawater of unfiltered and filtered aliquots of two seawater samples (**wh** from Great Harbor, Woods Hole, MA and **s** from the northwest Atlantic Ocean (37°15.03'N, 73°3.03'W) and <0.2 μ m Great Harbor, MA water used to redilute the filtered samples back to their original concentrations). "USW" indicates unfiltered seawater, ">0.8 rd" and ">2.0 rd" indicate, respectively, >0.8 μ m, <53 μ m and >2.0 μ m, <53 μ m filtered seawater rediluted to their original concentrations.

FCM analysis of filtration step



b. The same FCM analyses as in Fig 2.4a, but reported as a ratio of phytoplankton counts to total phytoplankton plus detritus counts.

Counter determinations, reported in McCave, 1975). While this discrepancy may result from filtration effects, it must be remembered that the flow cytometry counts were made on samples from a different location at a different time and that only a few mLs of seawater (or their equivalent) were actually analyzed. The $>0.8\ \mu\text{m}$, $<53\ \mu\text{m}$ coastal (**wh**) sample shows a 13-fold reduction in both detritus counts/mL seawater and phytoplankton counts/mL seawater when compared to unfiltered **wh**. The $>2.0\ \mu\text{m}$, $<53\ \mu\text{m}$ aliquot of **wh** differs little from the $>0.8\ \mu\text{m}$, $<53\ \mu\text{m}$ aliquot in either phytoplankton or detrital counts/mL seawater. The open ocean sample (**s**) detrital counts decrease twofold after tangential flow filtration, while the phytoplankton counts decrease fourfold. These decreases in phytoplankton and detritus counts after filtration could result from flow cytometry sensitivity to particles that would flow through our $0.8\ \mu\text{m}$ filters. Forward angle light scatter is merely a proxy for particle size and is affected by particle composition. In addition, the forward angle light scatter detector was optimized for viewing phytoplankton populations rather than for limiting detection to fluorescent bead standards in size ranges greater than $0.8\ \mu\text{m}$. Therefore, we could merely be seeing the effect of imposing a size distinction. The other possible explanations for our decrease in particle counts are, of course, particle break-up during filtration or particle absorption to our filtration system. Most likely, we are seeing a combination of the flow cytometry and filtration effects.

While the recovery/mL seawater decreases with filtration, flow cytometry does not indicate significant fractionation (in terms of the relative amounts of phytoplankton and detritus) of the samples. This is perhaps more strongly illustrated in Fig. 2.4b, where the ratio of phytoplankton to total phytoplankton plus detritus counts is plotted for the unfiltered and filtered samples. This ratio does not change with either tangential flow filtration or tangential flow filtration plus gravity filtration for the **wh** sample and changes from roughly 0.2 to approximately 0.1 with tangential flow filtration of the open ocean sample (**s**). However, it must be mentioned that particular types of detrital or

phytoplankton particles might be removed without changing the overall flow cytometry determinations. This is more likely for detritus particles, which are measured by only one flow cytometry parameter (forward angle light scatter), than for phytoplankton, which are measured by both forward angle light scatter and red fluorescence.

Sample handling: Flow cytometric separation of "phytoplankton" and "detritus"

Red (chlorophyll) fluorescence after excitation at 488 nm provides the basis for flow cytometric separation of phytoplankton and detritus. However, this criterion is not absolutely defined; dimly fluorescing phytoplankton cells may appear detrital and heterotrophs that have just ingested phytoplankton may exhibit red fluorescence themselves. In addition, the fluorescence measured by flow cytometry is dependent upon the position of the particle within the sample stream relative to the laser beam and relative to the detecting lens. Therefore, it becomes necessary to calibrate and monitor the flow cytometer via light and epifluorescence microscopy. Prior to performing flow cytometric sorting, sort "windows" (i.e., regions of interest on one or two-dimensional plots of detector outputs) are chosen. The initial sort output from these windows is visually scanned through a microscope to ensure that the particles being sorted are actually the particles of interest. Further sort output is scanned intermittently to ensure that the expected level of purity in the "phytoplankton" and "detritus" sorts is maintained throughout the procedure. However, it is also beneficial to check flow cytometry counts of "phytoplankton" and "detritus" against completely independent determinations performed on the same samples.

In Fig. 2.5a the phytoplankton counts/mL seawater determined by flow cytometry are plotted against those determined by microscopy and image analysis (Verity and Sieracki, 1993). They agree fairly well (reduced major axis: $r=0.99$, $m=0.90$, $\sigma_m=0.04$, $b=300$, $\sigma_b=200$) for count ranges of 3000 to 12,000 phytoplankton particles. The fact that the slope (m) deviates from the expected value of 1 and the y-intercept (b) is significantly

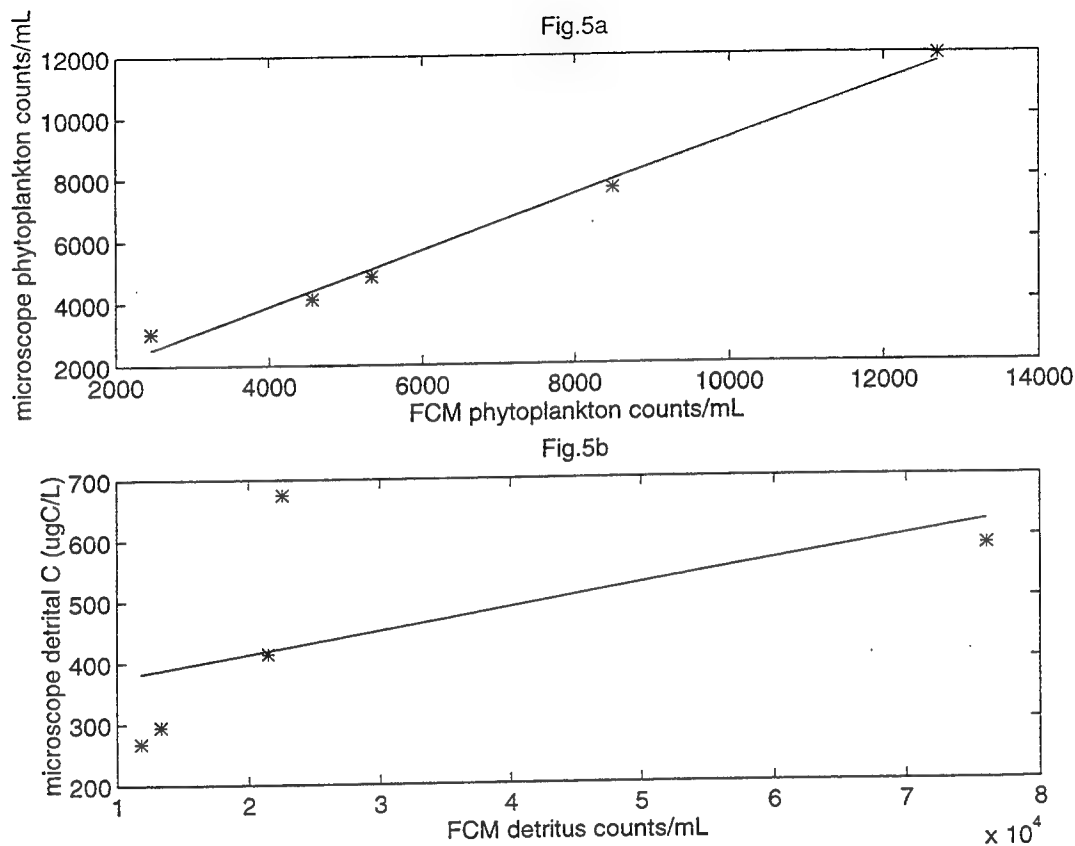


Fig 2.5 a. A comparison of phytoplankton counts/mL seawater as determined by flow cytometry and by microscopy and image analysis. The line is a reduced major axis ($y=mx + b$) with $r=0.99$, $m=0.90$, $\sigma_m=0.04$, $b=300$, $\sigma_b=200$).

b. A comparison of the detritus counts/mL seawater as determined by flow cytometry and the detrital carbon content/mL seawater as determined by microscopy and image analysis. The line is again a major reduced axis ($y=mx+b$) with $r=0.57$, $m=0.004$, $\sigma_m=0.0025$, $b=340$, and $\sigma_b=70$.

different from 0 may result from the inclusion of electronic noise as counts in the flow cytometry data.

Unfortunately, it is not possible to directly compare the flow cytometry “detritus” counts and the microscope “detritus” counts as only the zooplankton component of the FCM “detritus” is directly counted via microscopy. The non-living detritus component is quantified by microscopy as biomass rather than number of counts. Therefore, in an attempt to compare FCM and microscopy “detritus” determinations, the flow cytometry “detritus” counts were plotted against the microscopy biomass determinations for the analogous “detrital” subclass (Fig. 2.5b). Little relationship was found between these “detritus” determinations ($r=0.57$, $m=0.004$, $\sigma_m=0.0025$, $b=340$, $\sigma_b=70$). This could be due to differences between the techniques for identifying “detrital” particles. It may also be due, however, to the fact that biomass is not directly related to particle count; especially for heterogeneous particle populations. Moreira-Turq et al. (1993), while studying particles in Krka estuary in Croatia, find a similar lack of correlation between phytoplankton counts obtained via flow cytometry and concentration measurements (in this case, chlorophyll a concentration). They explain this absence of a relationship as the result of phytoplankton heterogeneity in natural samples and point out that significant correlations between phytoplankton count and chlorophyll a concentration have been found in monospecific cultures (Partensky, 1989).

The comparison of flow cytometry and microscopy indicates that the phytoplankton component of POM can be well identified and separated by our method. Unfortunately, the comparison yields no conclusions as to our ability to identify and separate detritus.

Sample handling: The salt issue

The presence of salts in oceanic samples can adversely affect mass spectrometry. As mentioned above, inorganic signals from seawater can saturate the detector. However,

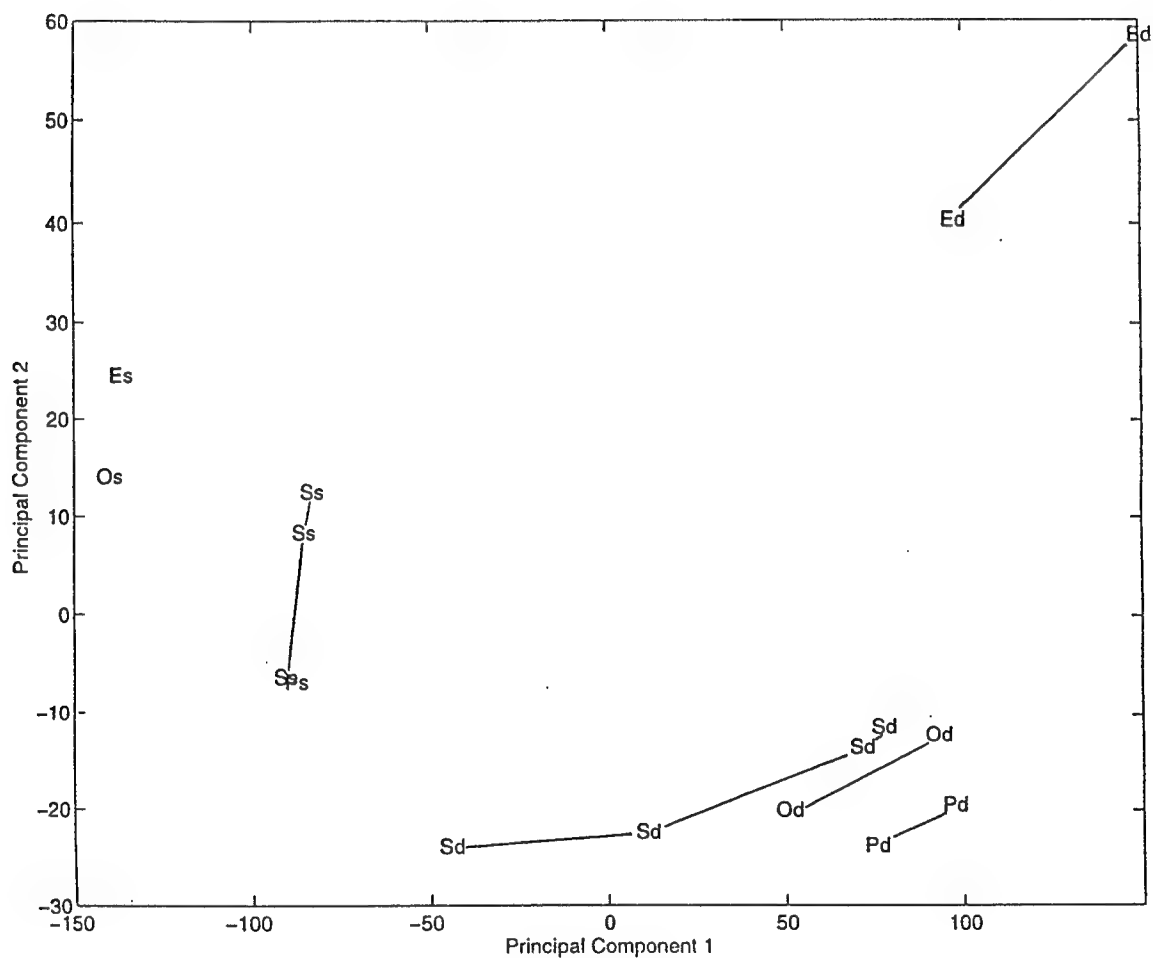


Fig. 2.6a. Score plot for principal component analysis of algal samples with and without salt. E=*Emiliana huxleyi* (Eh BT6), O=*Pycnococcus provasolii* (Ω48-23), P=*Phaeodactylum tricornutum*, S=mixed algal sample containing all three cultures. The subscript "s" indicates that the algae are in seawater; the subscript "d" indicates desalted samples. Each point represents a DT-MS analysis; lines connect replicate analyses. Note that Principal Component 1 separates samples suspended in seawater from those suspended in Milli-Q water.

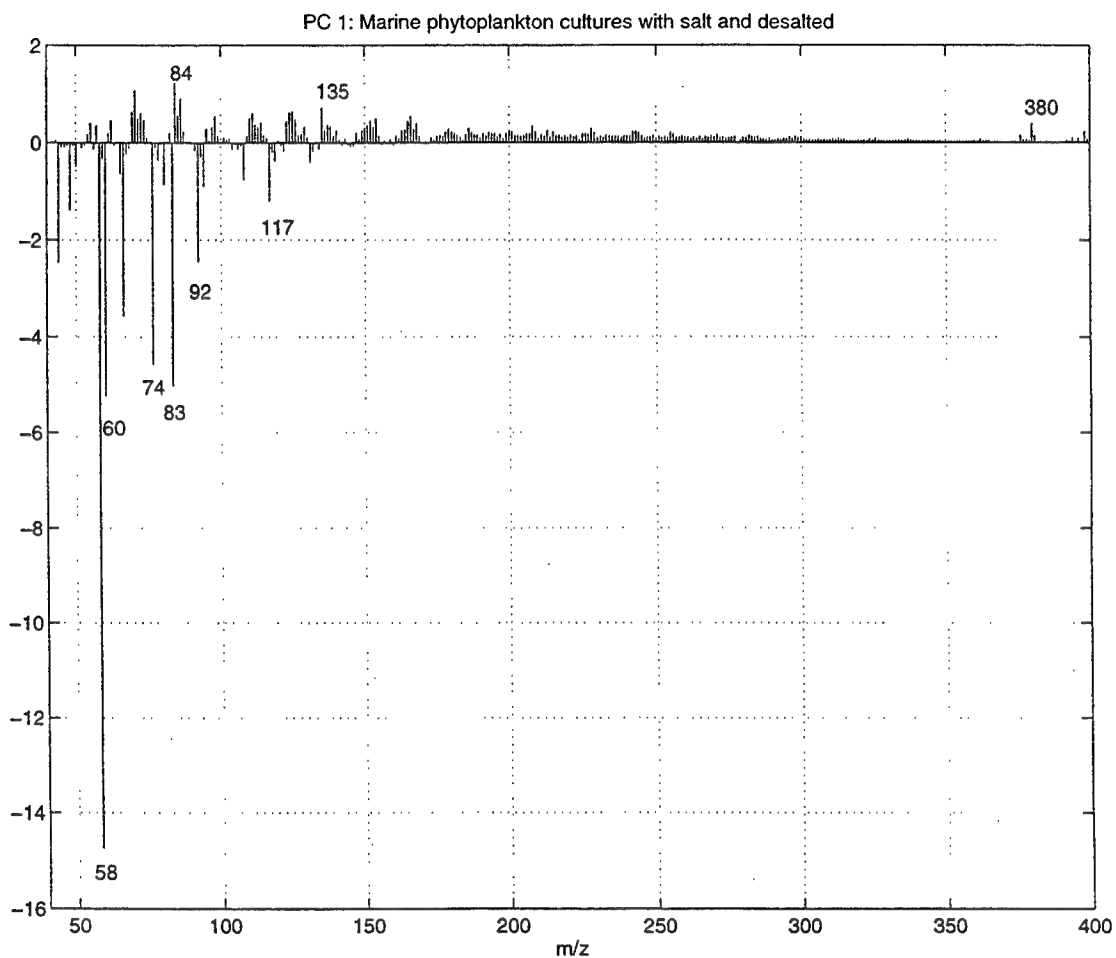


Fig. 2.6b. Loadings plot for Principal Component 1. Note that the negative region, where the seawater samples fall, is characterized by stronger signals in the lower molecular weight region. The desalted samples fall in the positive region and appear enriched in higher molecular-weight ions.

salt remains a problem even if the ratio of organic matter to salt is relatively high, as in algal cultures concentrated via centrifugation and resuspended in a small quantity of seawater. In this case, it appears that the presence of volatile organic molecules as their corresponding sodium salts increases their thermal stability so that, instead of desorbing, they begin to decompose only at high probe temperatures. As a result, they yield fragments that give little structural information about the parent molecules. In addition, the presence of salt appears to affect pyrolysis reactions so that there is a decrease in the prevalence of recognizable ion series from biopolymers (this is particularly noticeable for polysaccharides and nucleic acids).

This problem is illustrated in the following experiment. Replicate aliquots of both individual algal cultures and a mixed algal sample were taken; one aliquot was desalted using the procedure for small-particle POM described above and the other aliquot was left suspended in a small volume of the culture medium. Both sets of aliquots were analyzed via DT-MS, and the resulting spectra, summed over the entire TIC, were then analyzed by principal component analysis. Fig. 2.6a, the score plot of the first two principal components, illustrates that the aliquots containing salt and those that were desalted are clearly separated in the first principal component (which accounts for the largest amount of variance in the data set). The reconstructed spectrum for the first principal component (Fig. 2.6b), which can be thought of as a difference spectrum, shows that the algal samples with salt are enriched in the smaller molecular weight compounds, while the desalted samples show a stronger higher molecular weight signal (including fatty acids and sterols).

One could argue that the separation of samples along Principal Component 1 (Fig. 2.6a) and the relationship among m/z values explaining the separation (Fig. 2.6b) are dominated by the intensity of inorganic signals in the samples containing salt. Therefore, the organic matter signals of the salt-containing samples may still be acceptable. That this is not the case is illustrated by a comparison of the actual DT-MS spectra (rather than the difference spectra) from aliquots of *Emiliana huxleyi* (BT6) culture containing salt

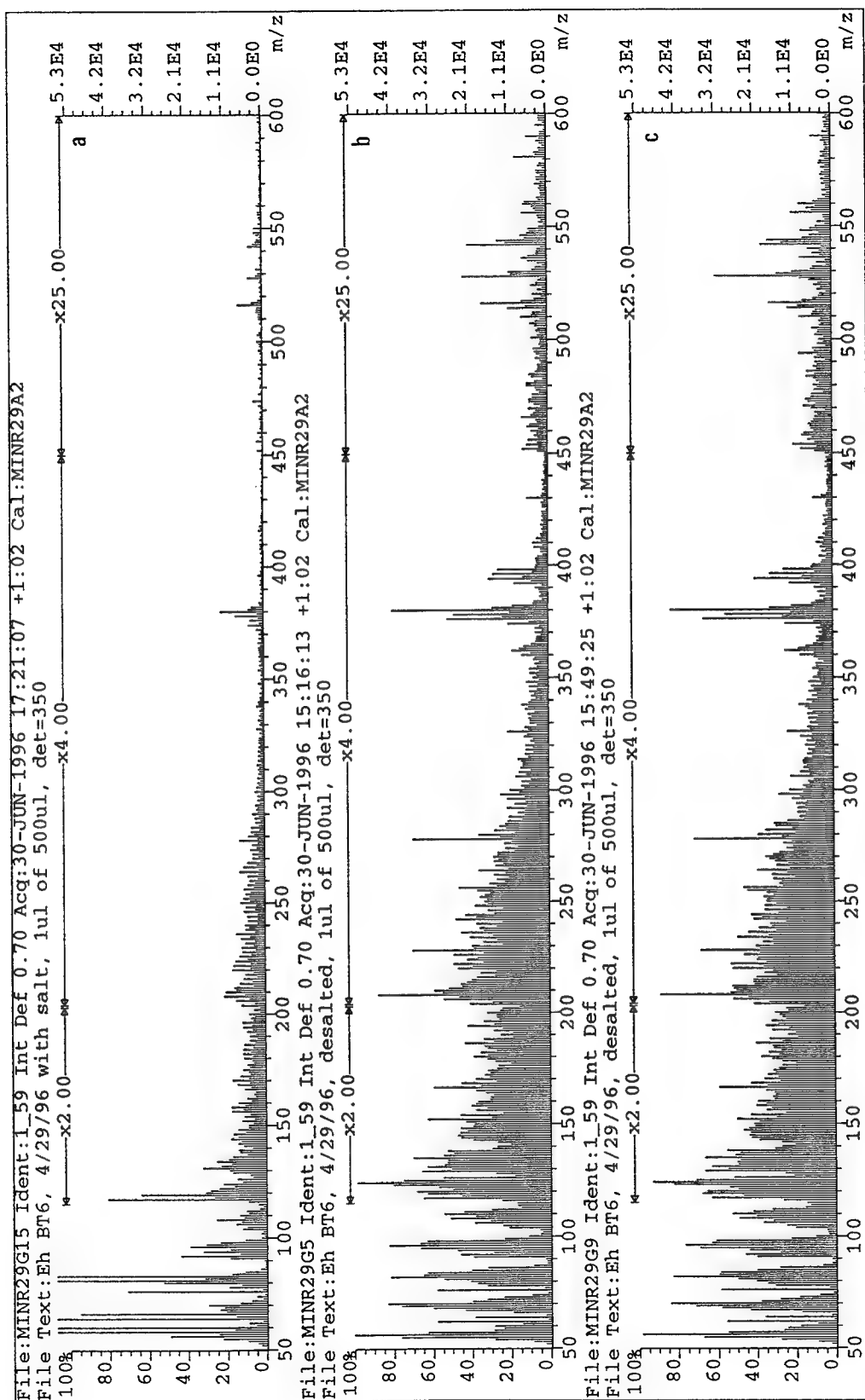


Fig. 2.7a. DT-MS (16 eV, EI⁺) of an *Emiliana huxleyi* culture suspended in a small amount of salt-water culture media.

b & c. Replicate DT-MS analyses of the same culture after desalting.

and after desalting (Fig. 2.7). It should be mentioned that the inorganic mass unit values are offscale in Fig. 2.7a so that the organic information can be highlighted. DT-MS of the aliquot containing salt (Fig. 2.7a) results in a degraded spectrum in which both lipid and biopolymer information has been lost. The comparison of spectra from replicate analyses of the desalted aliquot (Fig. 2.7b & c) indicates that instrument variation cannot be held accountable for the differences between the spectra from the salt-containing and desalted aliquots. It should be noted, however, that there is some indication that samples with an extremely high ratio of organic matter to salt do not have to be desalted. The spectra from the mixed culture aliquots with and without salt (not shown) appeared quite similar (although there was twice the TIC intensity for the sample with salt). Unfortunately, these aliquots were so viscous that it was difficult to load them onto the sample wire. They also coated the sample wire and the ion source to such a degree that there was significant bleed-through into subsequent DT-MS analyses. In general, running samples of this concentration should be avoided.

Although Milli-Q™ rinsed samples appear to yield more informative mass spectra, there was concern that the desalting process could lead to significant release and loss of dissolved and colloidal organic material due to cell lysis. In order to test this possibility, the desalting procedure was applied to two POM samples (>0.8 µm, <53 µm), "a" and "b" (see Experimental). In addition to a Milli-Q™ water blank, the following subsamples were taken during desalting:

- aliquots of the original POM samples ("sa" and "sb", respectively);
- the supernatant from the first centrifugation, which would contain ambient DOC as well as any carbon liberated from POM in the first step ("sup1a," "sup1b");
- the supernatant from each rinse with Milli-Q™ water ("qr1a," "qr2a," and "qr3a" for sample a; "qr1b," "qr2b," and "qr3b" for sample b);
- aliquots of the resulting desalted pellets ("pa" and "pb").

Fig. 2.8 illustrates the results of total carbon analysis on each of these subsamples; the carbon numbers have been multiplied where needed to represent the total pellet and

supernatant carbon levels. Surprisingly little carbon appears to be lost in the Milli-Q™ rinsing steps and the mass balance (i.e., $pa + sup1a + qr1a + qr2a + qr3a = sa$) appears to hold; the sum of parts is 68% of the original sample for **a** and 95% of the original sample for **b**. Assuming that the chemical signature for **sa** is the same as that for **pa**, these desalted samples can be used to characterize the chemical composition of suspended POM.

In the case of large-particle POM, sample heterogeneity becomes a particularly important problem as DT-MS spectra vary considerably in replicate analyses of the same sample. This results from the difficulty in loading a representative set of large particles on the wire. Therefore, after resuspension of sample off the Nylon screen (see Fig. 2.1) and initial concentration by centrifugation, large particle samples were homogenized before further concentration and desalting. The grinding and desalting procedure was also tested via elemental analysis. In this case aliquots of supernatant before grinding (which contain ambient DOC), supernatant from particle concentration after grinding, supernatant from each of the three Milli-Q™ rinses, and the final resuspended pellets were taken (aliquots of the original samples were not taken due to their heterogeneity). Carbon levels in the supernatant collected after grinding (Fig. 2.9, sup2) and during desalting (Fig. 2.9, qr1, qr2, and qr3) were again small, indicating low losses of carbon as a result of these procedures.

Therefore, it appears that the desalting procedure is an acceptable and necessary step when preparing oceanic samples for DT-MS analysis. However, the method is most appropriate for particle-reactive species such as lipids, phospholipids, and structural polysaccharides and proteins, i.e., those compounds least likely to be lost during the desalting procedure.

Elemental analysis of desalting procedure for small-particle POM

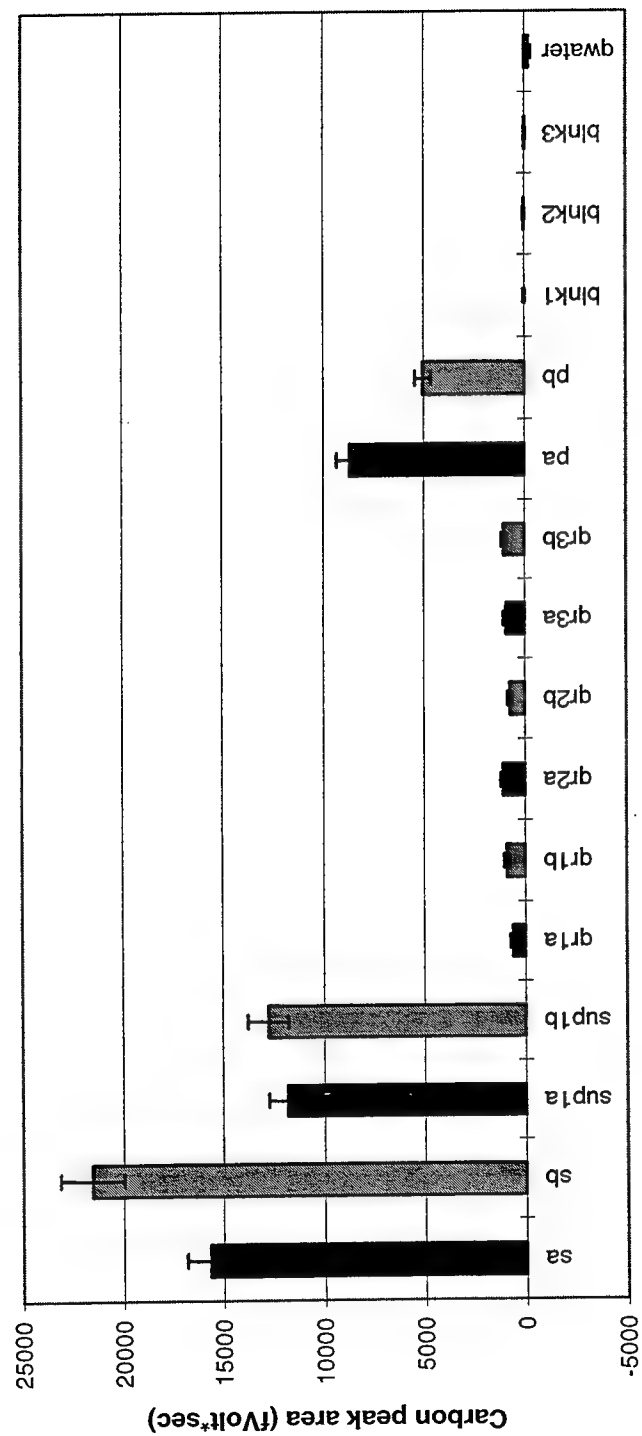


Fig 2.8. Elemental carbon analysis of each step of the desalting procedure for small-particle POM. The Woods Hole dock sample is indicated by "a"; the shelf sample by "b." s=initial sample; sup1=initial supernatant; qr1 (2, 3)=supernatant from the first (second, third) Milli-Q™ water rinse; p=pellet; blk=tin cup blank; qwater=Milli-Q™ water blank (see text for details).

Elemental analysis of grinding and desalting procedure for large-particle POM (carbon mass/total sample)

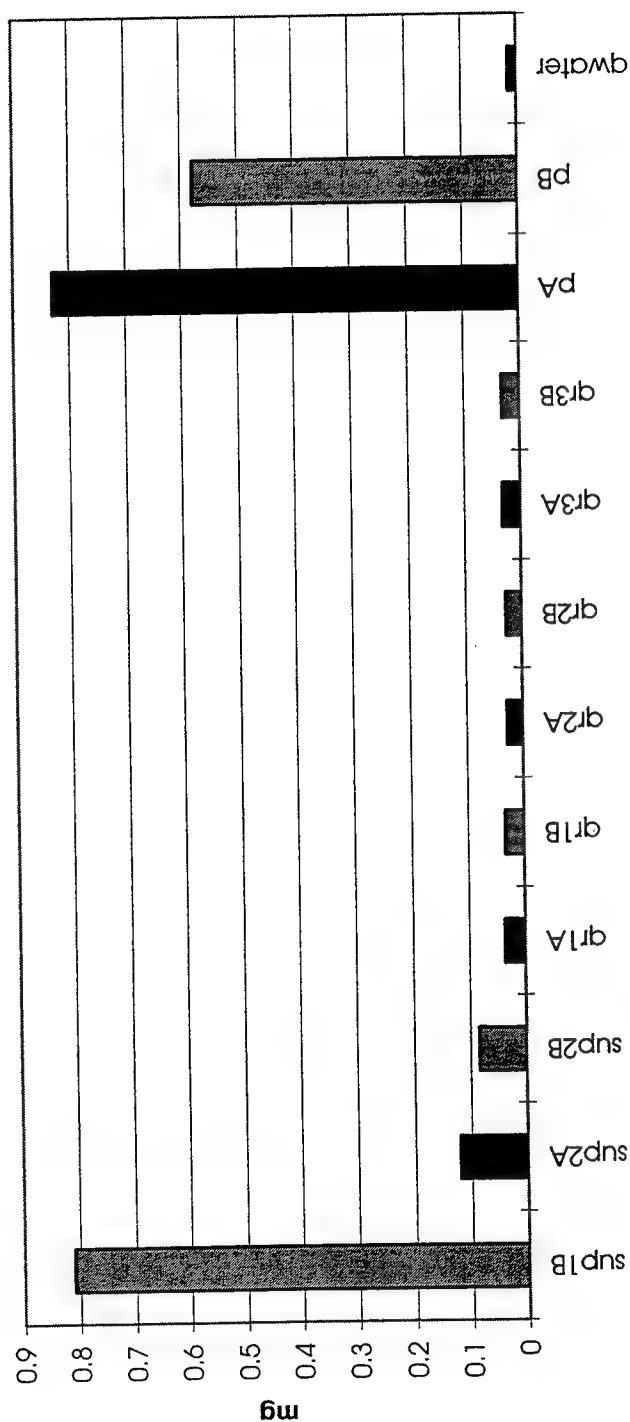


Fig. 2.9. Elemental carbon analysis of the grinding and desalting procedure for >53 μm particles. Samples A and B, from the continental shelf of the U.S. east coast, were ground and desalted as described in the text. Sup1=initial supernatant before grinding; sup2=supernatant after grinding; qr1, qr2, and qr3 are the supernatant from Milli-QTM water rinses 1, 2, and 3; p=pellet; qwater=Milli-QTM water blank.

DT-MS considerations

To date, DT-MS has only been used as a semi-quantitative method. There are two important considerations for the interpretation of the mass spectra generated: response factors for different compound classes can vary strongly, and matrix effects may be important. As both considerations also differ with ionization conditions, the following discussion is limited to low-voltage (16 eV) EI^+ , the form of DT-MS that provides the most general overview of the compound classes present in oceanic POM.

The response factors for characteristic ions or ion series generated during DT-MS are a function of two sets of processes: the formation of a volatile species by either desorption or pyrolysis, and the ionization of this molecule or fragment once it is present in the gas state. In an attempt to probe the relationship between volatilization and ionization, the intensity of the total ion current (or total ion chromatogram, TIC) per ng standard and the intensity of characteristic ions (or ion series) per ng standard were determined from the concentration of the standard, the volume added to the sample wire, and the area under the curve in both the TIC and selected mass chromatograms (intensity vs time plots for specific m/z values).

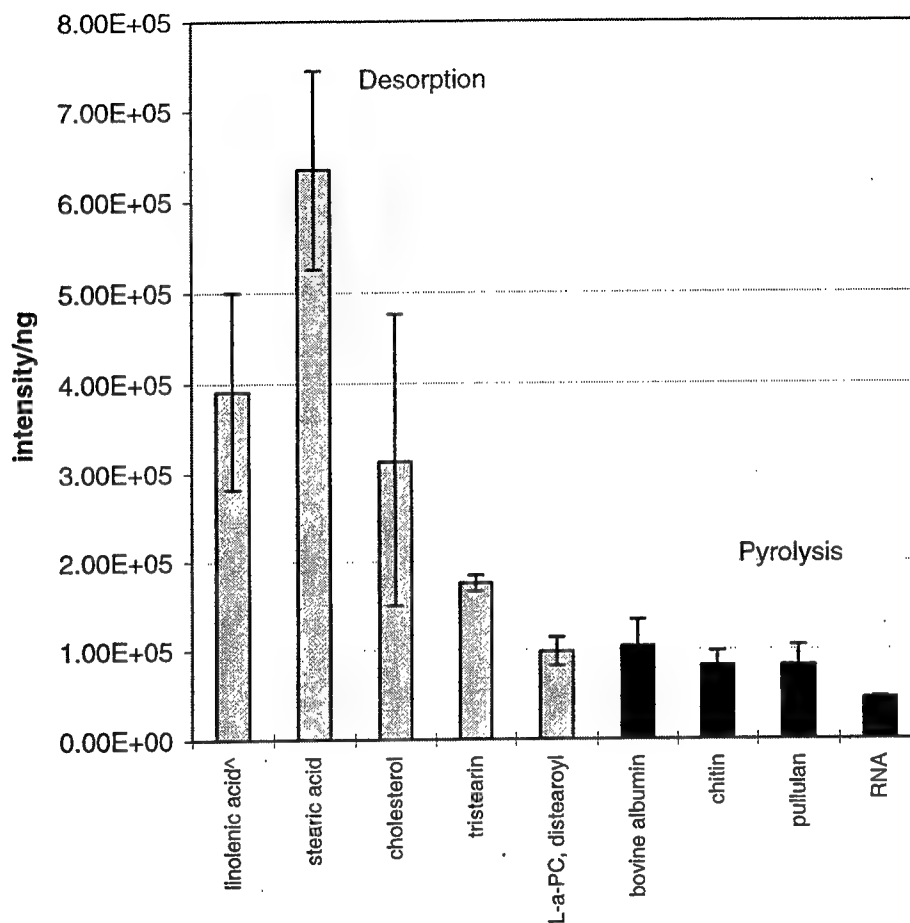
Table 2.2. Characteristic ions chosen from DT-MS (16 eV, EI^+) of selected standards. See Fig. 2.10b.

Compound	m/z values
cholesterol	386, 371, 368, 353, 301, 275, 255
stearic acid	284
linolenic acid	278, 222, 209
tristearin	607, 382, 341, 267
L- α -phosphatidylcholine, distearoyl	607, 606, 395, 341
chitin	139, 125, 114, 84, 59
pullulan	144, 126, 110, 98, 85
RNA	135, 112, 95, 69
bovine albumin	166, 151, 138, 135, 124, 117, 94, 92, 91

Comparison of the TIC intensity/ng for selected standards indicates that compounds undergoing desorption generally yield a higher overall signal than pyrolyzed compounds (Fig. 2.10a). L- α -phosphatidylcholine, distearoyl appears to be an exception to this; however, it must be pointed out that this compound appears considerably later in the course of a DT-MS analysis than the other desorbed standards. While the TIC intensity appears related to the volatilization step, the amount of the TIC accounted for by characteristic ions or ion series (Table 2.2) shows a less interpretable pattern (Fig. 2.10b). However, the two standards whose characteristic ions are responsible for the largest proportion of the TIC are also the two standards that yield strong molecular ions. This may indicate an additional problem not related to ionization efficiency; with compounds that fragment extensively, generic ions and/or characteristic ions that are not easily identifiable can be responsible for a large proportion of the total signal.

The combination of volatilization and ionization processes leads to the relationship among response factors (ratios of the mass chromatogram peak area per ng standard as determined for characteristic ions) shown in Fig. 2.10c. Note that pyrolyzed standards have considerably lower response factors than the majority of the desorbed standards. Response factors (shown in Fig. 2.10c) are highest for the molecular ions of steranes, low molecular weight saturated fatty acids (e.g., C_{18:0}), sterols, tocopherol, and wax esters, and fragment ions from stearyl alcohol (M-H₂O) and the wax esters. Mid-level response factors were found for the molecular ions of unsaturated fatty acids, β -carotene, and stanols, the diglyceride fragment of trimyristin, m/z 224 from stearyl alcohol, m/z 165 from α -tocopherol, m/z 353 from cholestadiene, and m/z 368 from cholesterol (M-H₂O). The lowest response factors were from fragment ions of tristearin, distearin, AMP, phosphatidylcholines, and biopolymers such as bovine albumin, RNA, pullulan, chitin, and alginic acid. While machine sensitivity varied by a factor of two to four, the response factors varied by 3 orders of magnitude, from 2.4E5 for the molecular ion of cholesta-3,5-diene to 3.1E2 for m/z 96 from alginic acid and 2.1E2 for the

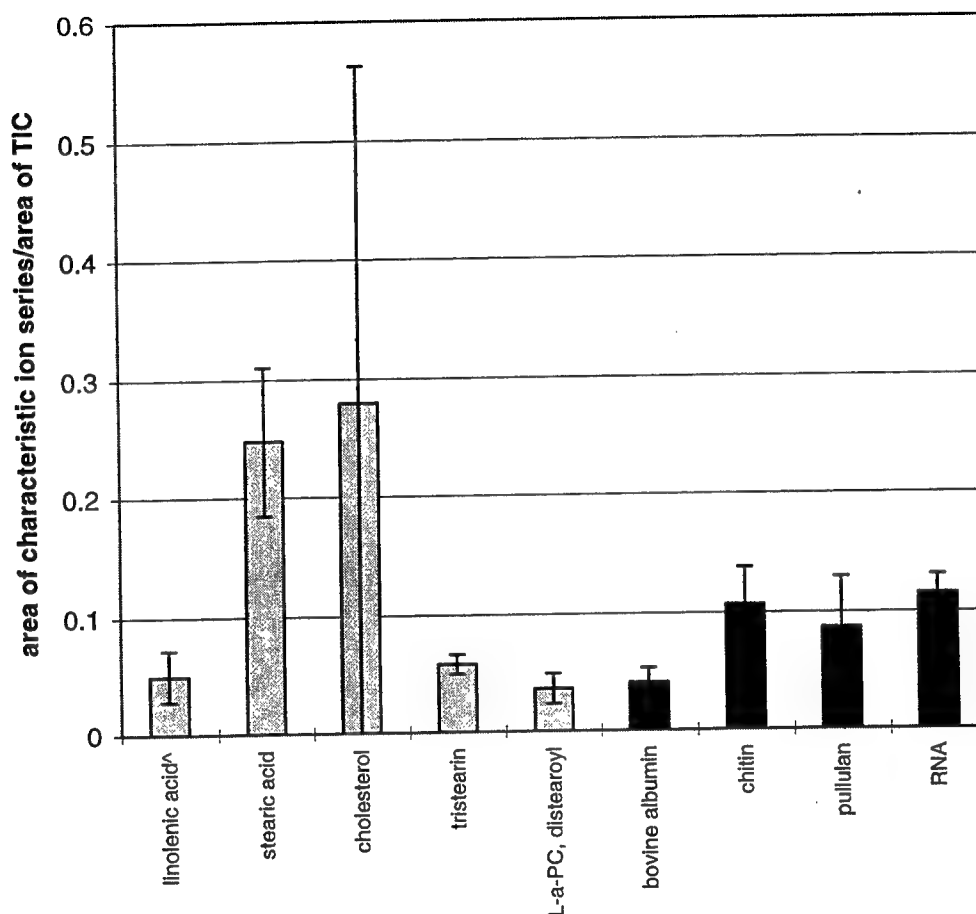
Average TIC (area) per ng of standard



[^]The mass spectrometer was more sensitive the day several linolenic acid replicate analyses were made. Exclusive of this day, sensitivity varied by a factor of 2 or less; inclusive of this day, by a factor of 4.

Fig. 2.10a. DT-MS (16 eV, EI⁺) response factors for selected standards in terms of TIC area/ng of standard. The standards that desorb off the sample wire (grey bars) are listed in order of earliest to latest elution time. The standards that pyrolyze off the wire (black bars) have similar elution times and are, therefore, simply listed in alphabetical order. Note that desorbed standards generally have higher TICs than pyrolyzed standards.

Amount of TIC area accounted for by characteristic ions



^Instrument sensitivity varied by a factor of two or less exclusive of the day several linolenic acid analyses were made. That day sensitivity was higher by an additional factor of two.

Fig. 2.10b. For selected standards (see also Fig. 2.10a), the amount of TIC intensity that can be accounted for by characteristic ions or ion series (see Table 2.2). Grey bars indicate standards that desorb off the sample wire; black bars indicate standards that pyrolyze off the wire. Note that in all the standards, the characteristic ions are responsible for less than half (and in most cases considerably less than half) the area of the TIC.

molecular ion of trimyristin. One other trend that deserves notice is that of fatty acid molecular ion response factors: $C_{18:0} > C_{20:0} > C_{22:0} > C_{24:0} > C_{18:2} > C_{18:3} > C_{18:4} > C_{18:1}$.

It must be emphasized, however, that matrix effects seriously affect response factors (e.g., van der Kaaden et al., 1983). Fig. 2.11a shows the response factors of selected fatty acids and sterols in mixed lipid standards with and without a particle matrix. All the lipids in these standards exhibited a significant decrease in response factor in the presence of Al_2O_3 despite the use of dichloromethane, a non-polar solvent. However, by treating all oceanic POM samples in a consistent manner, we hope to standardize matrix effects. The experiment shown in Fig. 2.11b indicates the potential for this approach. In this case the same amount of caffeine standard was added to different concentrations of natural seawater POM samples diluted in $KMnO_4$ -distilled water. Over a range of 0 to 0.9 mg of POM/mL, the intensity of the mass chromatogram for the molecular ion of caffeine varies by a factor of two or less.

As matrix effects appear manageable, the response factors determined above were used in an initial attempt to apply DT-MS to the quantification of various compound classes within POM samples. Two small-particle POM samples (WHTS9S, and WHTS15S) were collected and analyzed using the protocol in Fig. 2.1. Using the ratio of characteristic ion (or ion series intensity) to TIC intensity in selected standards (Fig. 2.10b) and the characteristic ion (or ion series) intensity in the sample, a calculated TIC for each sample was determined. For both samples, this calculated TIC as compared to the actual TIC is well within the factor of two to four variability in day-to-day instrument sensitivity; for WHTS9S, the calculated TIC is $1.4E9$ while the actual TIC is $6.25E8$; for WHTS15S, the calculated TIC is $8.8E8$ while the actual TIC is $4.1E8$. Using the ratio between characteristic ion intensity and TIC intensity for each standard (in Fig. 2.10b) and the relationship between TIC and ng standard (Fig. 2.10a), the relative contribution of compound classes (as weight % of organic matter) in the samples was determined. WHTS9S was 56% protein, 27% carbohydrate, 18% chitin and <1% lipid. WHTS 15S

Fig. 2.10c. Response factors for characteristic ions of standards analyzed via DT-MS (16 eV, EI⁺) on a VG AutospecQ double focussing mass spectrometer (conditions reported in Experimental). Chitin, alginic acid, L- α -PC, distearoyl, and L- α -PC, dioleoyl were suspended and/or dissolved in methanol. Bovine albumin, RNA, and pullulan were suspended/dissolved in water. Adenosine 3'-monophosphate was suspended/dissolved in methanol:water (1:1); adenosine 5'-monophosphate was suspended/dissolved in methanol:water (1:3). For all other standards, dichloromethane was used as solvent. Peaks labelled only with an m/z value are fragment ions of the labelled peak to their left, * indicates molecular ion, **cis-6,9,12,15-octadecatetraenoic acid. Bold lettering indicates pyrolysis products; regular lettering, desorption products

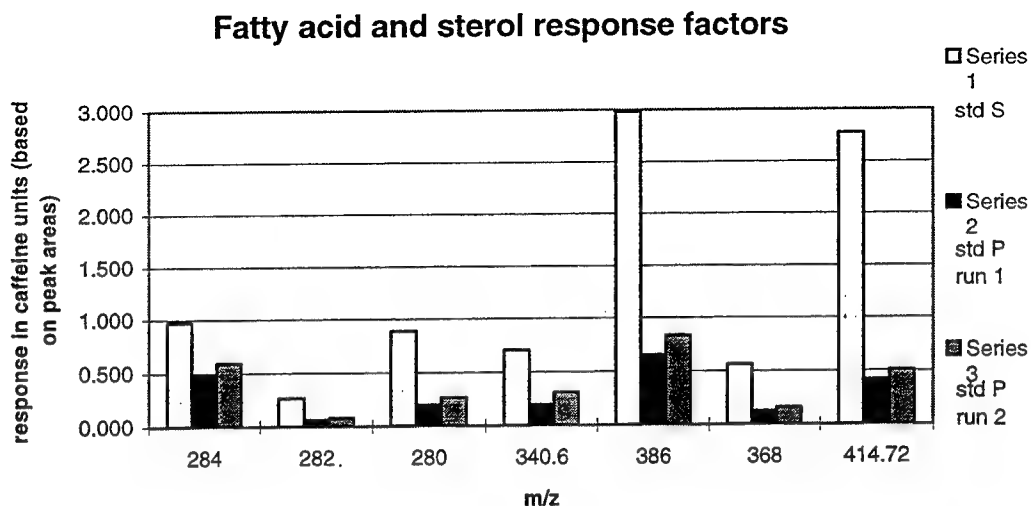
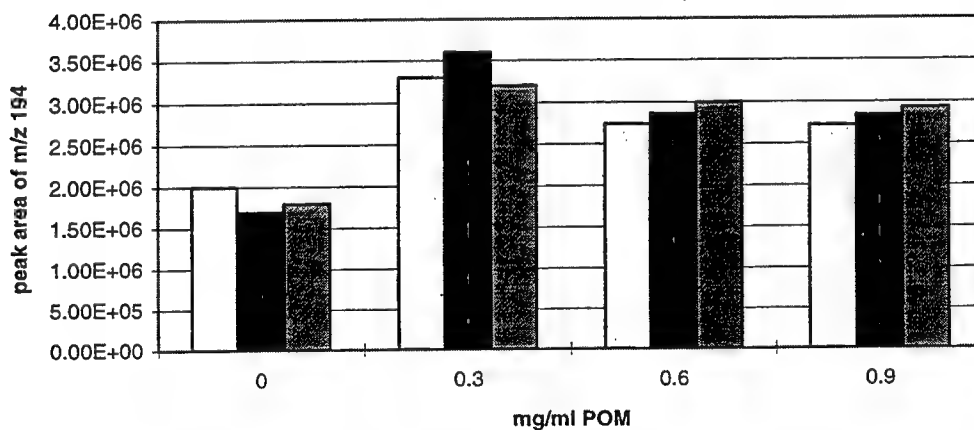


Fig. 2.11a. DT-MS (16eV, EI⁺) response factors relative to intensity/ μ g caffeine (based on peak area of characteristic ions) of C_{18:0}, C_{18:1}, C_{18:2} and C_{22:0} fatty acids (m/z 284, 282, 280, 340.6) and two sterols (cholesterol, m/z 386, 368; β -sitosterol, 414.7) in mixed lipid standards dissolved in dichloromethane. Std S contains no particle matrix; std P contains an Al₂O₃ particle matrix (4.5 mg/mL).

100ug/ml caffeine in various concentrations of an oceanic POM sample



b. The intensity of a constant concentration of caffeine (100 μ g/mL) standard in various concentrations of POM from the Peruvian upwelling region as measured via DT-MS (16 eV, EI⁺). Note that the amount of matrix does not strongly affect caffeine intensity.

was 52% protein, 29% carbohydrate, 19% aminosugar, and <1% lipid. In order to determine if the results were reasonable, these percentages were compared with literature values for the composition (reported as ash-free dry weight %) of phytoplankton (Parsons et al., 1984). While the lipid values are lower than those reported for phytoplankton, the protein and polysaccharide contributions are within the reported range of 35 to 68% (ash free dry weight %) protein and 20 to 42% carbohydrate. As the POM samples, collected from surface waters in Great Harbor, Woods Hole, MA, contain a strong phytoplankton and phytodetritus component, the similarity of the POM and literature phytoplankton values indicates that DT-MS yields reasonable quantitative results.

It should be mentioned that compound identification via DT-MS is tentative; several different ions may contribute to the same integer m/z value. Therefore, for greater confidence in identification of characteristic ions, representative samples should be investigated more thoroughly through ancillary measurements such as high resolution MS, MS-MS, and solvent extraction, derivitization where necessary, and GC-MS.

The comparison of DT-MS and HPLC measurements of POC/chlorophyll ratios

In the previous section, DT-MS was shown to yield reasonable quantitative information. However, in an attempt to further evaluate the potential of DT-MS as a quantitative technique, small-particle POM samples were analyzed in triplicate. For each sample, the [TIC]/[phytadiene] ratio, in other words, the ratio of the total signal intensity over time to the intensity over time resulting from a chlorophyll pyrolysis product (phytadiene, m/z 278), was determined. This ratio can be compared to the [POC]/[chl a] ratio obtained via elemental analysis and HPLC. The [POC]/[chl a] ratio has been used to constrain terrestrial inputs of organic matter in field POM samples or to indicate reworking of organic matter (Cifuentes et al., 1996, and references therein). DT-MS could potentially provide a more rapid method for determining a comparable ratio, as DT-

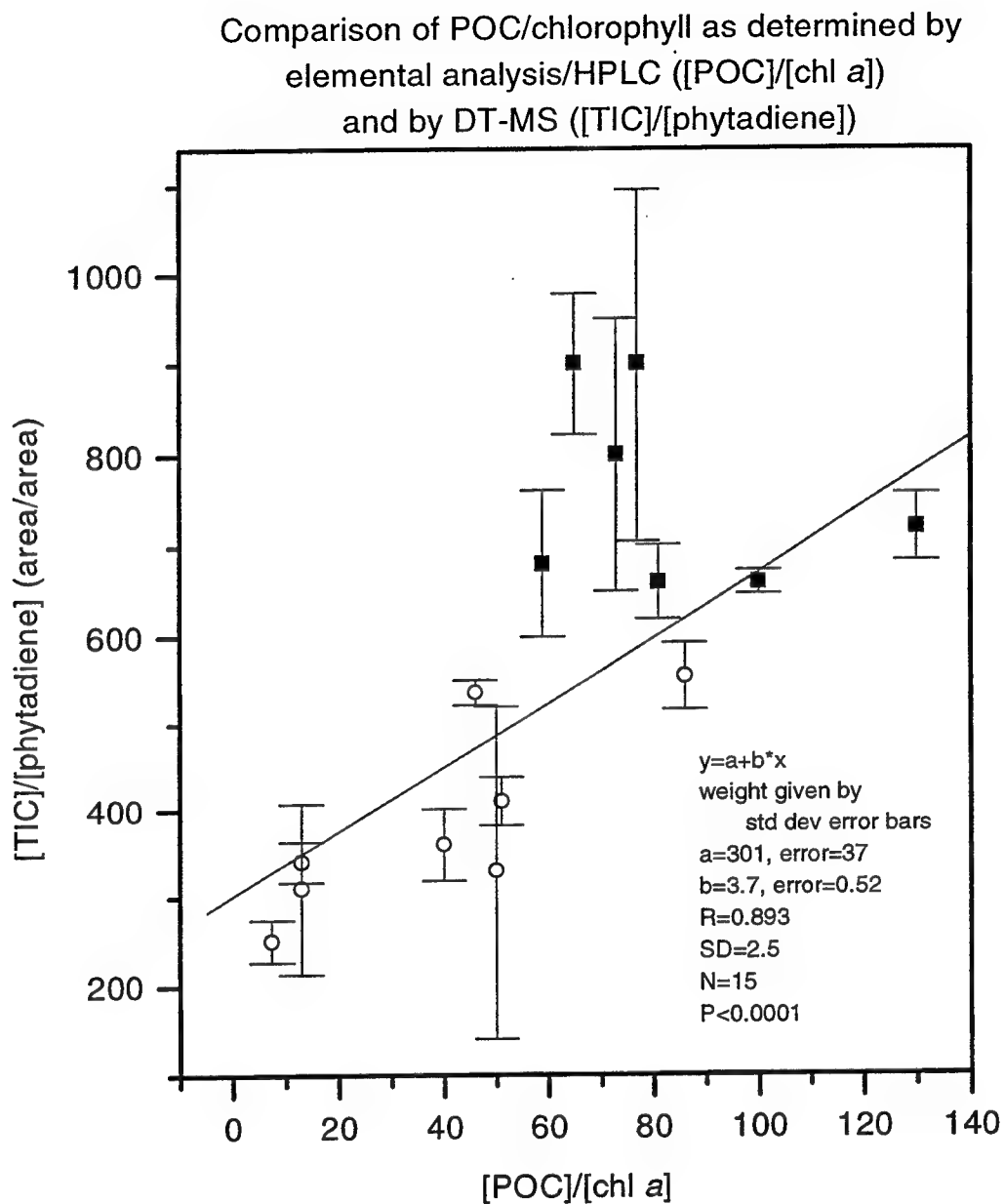


Fig. 2.12. POC/chlorophyll ratios as determined by HPLC and elemental analysis ([POC]/[chl a]) vs the analogous ratios determined by DT-MS ([TIC]/[phytadiene]). See text for details.

MS analyses last two minutes and require little sample preparation (i.e., no solvent extraction or fuming with HCl).

The comparison of [POC]/[chl *a*] ratios and [TIC]/[phytadiene] ratios (Fig. 2.12) indicates that DT-MS can be used to obtain rough estimates of POC/chlorophyll. The two sets of measurements show a linear correlation ($R = 0.713$) significant at $\alpha = 0.05$ when the average y-values are used for a simple linear regression; they exhibit an even better correlation when the standard deviations in the y-measurements are used to provide a weighting factor ($R = 0.893$). It is true that these correlations, while significant, are not stunning. However, it must be remembered that there are multiple potential sources of variation between the two sets of measurements. The samples are collected using different filtration techniques (tangential flow filtration vs. collection on a GF/F filter) as well as different analytical techniques. In addition, some of the DT-MS samples are $>2 \mu\text{m}$, $<53 \mu\text{m}$, while others are $>0.8 \mu\text{m}$, $<53 \mu\text{m}$; the nominal molecular weight cut-off for GF/F filters is $0.8 \mu\text{m}$ (with no corresponding upper size limit). It appears that the difference in particle size in the DT-MS samples may be significant. The $>2 \mu\text{m}$ particles generally appear to fall on the line or below it while the $>0.8 \mu\text{m}$ samples generally fall on the line or above it. This variation could be due to natural differences in particle populations as most of the $>2 \mu\text{m}$ samples are from the Mid-Atlantic Bight and all of the $>0.8 \mu\text{m}$ samples are from Great Harbor, Woods Hole, MA (collected on a monthly basis). It is also quite possible that filtration effects are involved. If a significant proportion of the chlorophyll *a* at a sample site exists in phytoplankton $>0.8 \mu\text{m}$ and $<53 \mu\text{m}$, the $>2 \mu\text{m}$ DT-MS samples would under-represent the amount of chlorophyll present (consistent with the position of these samples on or below the line). The apparent over-representation of chlorophyll by the $>0.8 \mu\text{m}$ DT-MS samples could result from the fact that the regression is based on both size classes of DT-MS samples; it could also result from differences in the retention characteristics of tangential flow filtration systems and glass fiber filters. The relative importance of such potential sources of variation needs to be further explored.

Procedural Blanks

In order to evaluate potential organic contamination, blanks from flow cytometric sorting and from the homogenization and desalting of large-particle POM were analyzed by DT-MS. The most intense mass unit values in the flow cytometry blank (Fig. 2.13a, m/z 58 and 81) appear inorganic and related to NaCl. Any organic contaminants appear insignificant when compared to mass unit intensities in "phytoplankton" isolated (via flow cytometry) from a field POM sample. Comparison of the mass spectra from the homogenization/desalting procedure blank and a large-particle POM sample (Fig. 2.13b) indicates that contamination from the procedure is also insignificant. It should be mentioned that the spectra in Fig. 2.13b were acquired on different days. However, the sensitivity of the mass spectrometer (as determined using a caffeine standard applied to the sample probe) varied by less than a factor of 2 and was actually higher on the day the blank was analyzed.

Conclusions

The sample collection and processing scheme described in the experimental section (Fig. 1) appears valid. With care, sample contamination during shipboard (or laboratory) processing can be reduced to acceptable levels. Relatively unfractionated POM samples suspended in a liquid can be collected by tangential flow filtration (TFF) and TFF combined with slight-vacuum membrane filtration (<5 psi) and subsequent resuspension. Flow cytometric identification of phytoplankton appears consistent with identification via microscopy and image analysis. Desalting samples by centrifugation with Milli-Q™ water rinses leads to little carbon loss, though there may be some loss of hydrophilic constituents of POM. Grinding large particle samples appears to solve sample heterogeneity problems (in other words, making it less likely that a copepod

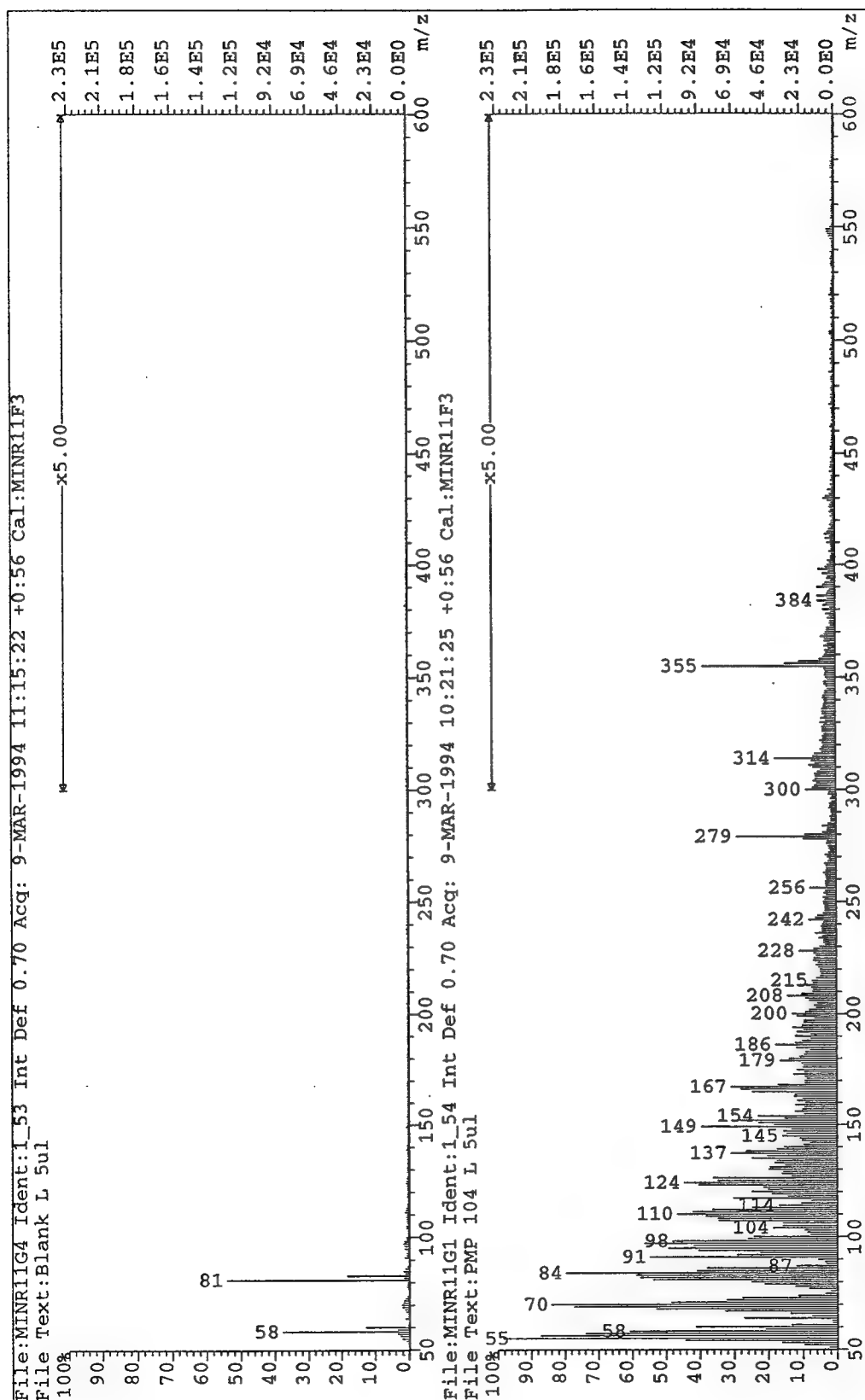


Fig. 2.13a. DT-MS (16 eV, EI⁺) of a flow cytometry blank and a "phytoplankton" sample isolated from field POM (see text for details).

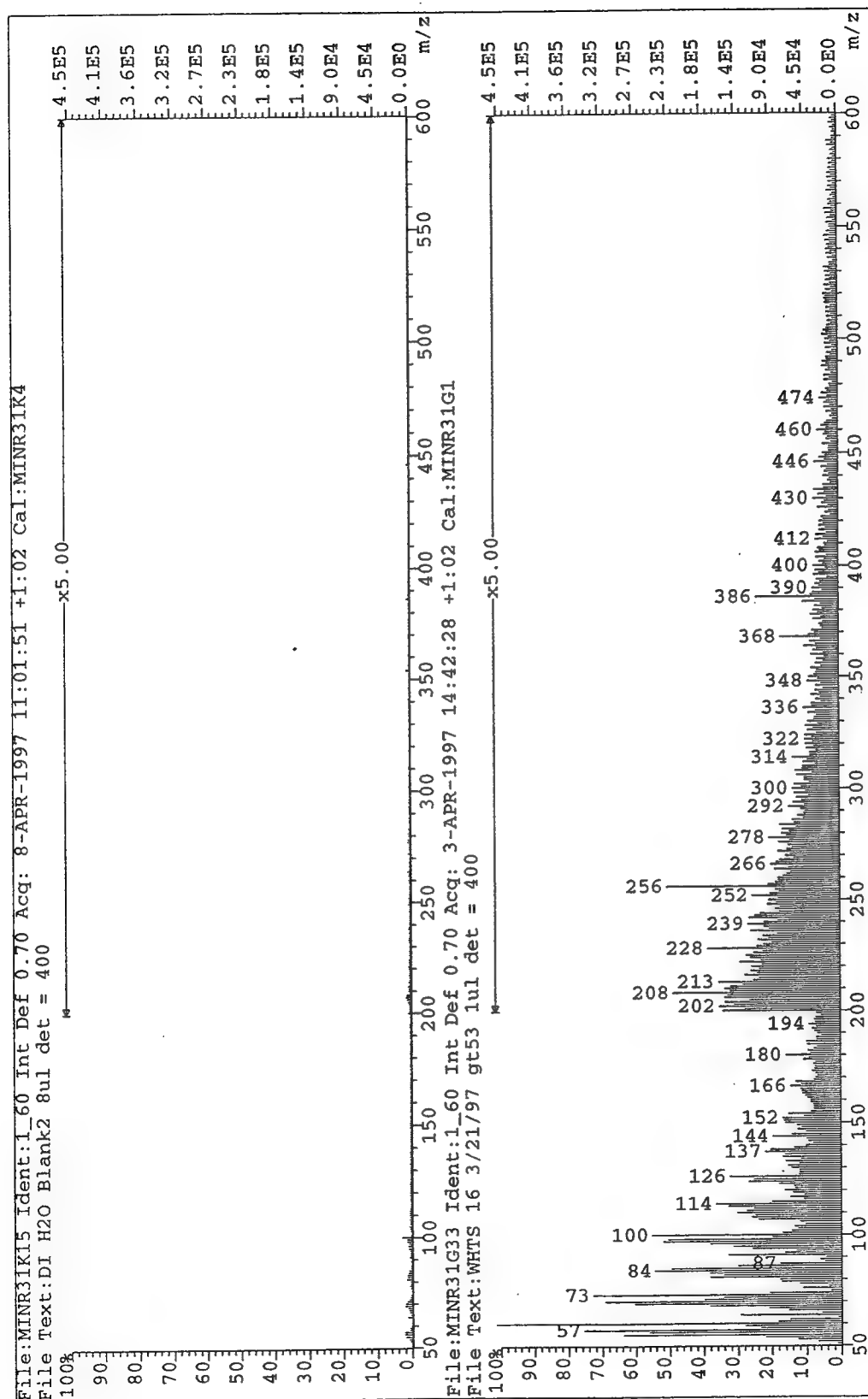


Fig. 2.13b. DT-MS (16 eV, EI^+) of a homogenization/desalting procedure blank and a large-particle POM sample that has undergone the same procedure (see text).

would dominate one measurement while an algal chain dominates the next). DT-MS analysis of blanks indicates that there is little organic carbon contamination from flow cytometric sorting, the desalting of small-particle POM samples, and the homogenization and desalting of large-particle POM samples.

DT-MS appears to yield useful molecular-level information. Although care must be taken in interpreting DT-MS results due to potential matrix effects, the determination of relative response factors of selected standards provides a first step in the interpretation of DT-MS analyses of POM samples. The comparison of POC/chlorophyll *a* ratios determined by DT-MS and by the more traditional elemental analyzer/HPLC approach indicates that DT-MS may potentially be used in a quantitative fashion. The correlation between these two sets of measurements also indicates the validity of using DT-MS in a semi-quantitative fashion (as in the following chapters of this thesis) for the analysis of marine organic matter samples.

References:

- Bishop J. K. B. and Edmond J. M. (1976). A new large-volume *in situ* filtration system for sampling oceanic particulate matter. *J. Mar. Res.*, **32**, 181-198.
- Boon J.J. (1992). Analytical pyrolysis mass spectrometry: new vistas opened by temperature-resolved in-source PYMS. *Int.J.Mass.Spec and Ion Process.*, **118/119**, 755-787.
- Chisholm S. W., Olson R. J., Zettler E. R., Goericke R. Waterbury J. B., and Welshmeyer N. A. (1988). a novel free-living prochlorophyte abundant in the oceanic euphotic zone. *Nature*, **334**(6180), 340-343.
- Cifuentes L.A., Coffin R. B., Solorzano L., Cardenas W., Espinoza J., and Twilley R.R. (1996) Isotopic and elemental variations of carbon and nitrogen in a mangrove estuary. *Estuarine, Coastal and Shelf Science*, **43**, 781-800.
- Eglinton T. I., Boon J. J., Minor E. C., and Olson R. J. (1996). Microscale characterization of algal and related particulate organic matter by direct temperature-resolved mass spectrometry. *Mar.Chem.*, **52**, 27-54.
- Eglinton T. I., Sinninghe Damste J. S., Pool W., de Leeuw J. W., Eijkel G., Boon J. J. (1992). Organic sulfur in macromolecular sedimentary organic matter-II: Analysis of distributions of organic sulfur pyrolysis products using multivariate techniques. *Geochim. Cosmochim. Acta*, **56**, 1545-1560.
- Goericke R. and Repeta D.J. (1993). Chlorophylls *a* and *b* and divinyl chlorophylls *a* and *b* in the open subtropical North Atlantic Ocean. *Mar. Ecol. Prog. Ser.*, **101**, 307-313.
- Gustafsson O., Buesseler K. O., Gschwend P. M. (1996). On the integrity of cross-flow filtration for collecting marine organic colloids. *Mar. Chem.*, **55**(1/2), 93-111.
- Herzenberg L. A. and Sweet R. G. (1976). Fluorescence activated cell sorting. *Sci. American*, **243**, 108-112.
- van der Kaaden A., Haverkamp J., Boon J. J., de Leeuw J. W. (1983). Analytical pyrolysis of carbohydrates: I. Chemical interpretation of matrix influences on pyrolysis-mass spectra of amylose using pyrolysis-gas chromatography-mass spectrometry. *J. An. Appl. Pyrol.*, **5**, 199-220.
- Klap V. A., Boon J. J., Hemminga M. A., van Soelen J. (1996). Assessment of the molecular composition of particulate organic matter exchanged between the Saeftinghe

salt marsh (southwestern Netherlands) and the adjacent water system. *Mar. Chem.* **54**, 221-243.

McCave I. N. (1975). Vertical flux of particles in the ocean. *Deep-Sea Research*, **22**, 491-502.

Meglen R. R. (1992). Examining large data bases: a chemometric approach using principle component analysis. *Mar. Chem.*, **39**, 217-237.

Moreira-Turcq P., Martin J. M., Feury A. (1993). Chemical and biological characterization of particles by flow cytometry in the Krka estuary, Croatia. *Mar. Chem.*, **43**, 115-126.

Olson R. J., Chisholm S. W., Zettler E. R., Altabet M.A., and Dusenberry J. A. (1990a). Spatial and temporal distributions of prochlorophyte picoplankton in the North Atlantic. *Deep-Sea Res.*, **37**(6), 1033-1051.

Olson R. J., Chisholm S. W., Zettler E. R. and Armbrust E. V. (1990b). Pigments, size, and distribution of *Synechococcus* in the North Atlantic and Pacific Oceans. *Limnol. Oceanogr.*, **35**(1), 45-58.

Parsons T. R., Takahashi M., Hargrave B. (1984). *Biological Oceanographic Processes*, 3rd Ed., New York, Pergamon Press, 330 p.

Partensky F. (1989). Strategies de croissance et toxicite de deux dinoflagelles responsables d'eaux colorees: *Gyrodinium aureolum* et *Gyrodinium nagasakiense*. Ph.D. Thesis., Universite de Paris, 165 p.

Salot A., Ulloa-Guevara A., Viets T. C., de Leeuw J. W., Schenk P. A., Boon J. J. (1984). The application of pyrolysis-mass spectrometry and pyrolysis-gas chromatography-mass spectrometry to the chemical characterization of suspended matter in the ocean. *Org. Geochem.*, **6**, 295-304.

Sosik H. M., Chisholm S. W., and Olson R. J. (1989). Chlorophyll fluorescence from single cells: Interpretation of flow cytometric signals. *Limnol. Oceanogr.*, **34**(8), 1749-1761.

Verity P. G. and Sieracki M. E. (1993). Use of color image analysis and epifluorescence microscopy to measure plankton biomass, in Kemp P. F., Sherr B. F., Sherr E. B., and Cole J. J. (Ed) *Handbook of Methods in Aquatic Microbial Ecology*, Lewis Publishers, Boca Raton, pp. 327-338.

Williams S. C., Verity P. G., Beatty T. (1995). A new technique for dual identification of plankton and detritus in seawater. *J. of Plankton Research*, **17**(11), 2037-2047.

Windig W., Kistemaker P. G., and Haverkamp J. (1981/1982). Chemical interpretation of differences in pyrolysis-mass spectra of simulated mixtures of biopolymers by factor analysis with graphical rotation. *J. Anal. Appl. Pyrol*, **3**, 199-212.

Chapter 3
DT-MS of North Atlantic suspended POM:
An investigation of diglycerides, triglycerides, and phospholipids

Abstract

Direct temperature-resolved mass spectrometry (16 eV EI⁺), coupled with statistical (discriminant) analysis, was applied to determine broad-band (i.e., multiple compound class) molecular-level variations in suspended particulate organic matter (POM) collected in May/June 1995 on a transect from the mouth of the Delaware Bay to the Sargasso Sea. The first two discriminant functions resulting from this analysis indicated that ions due to diglyceride moieties were key variables distinguishing POM samples. Selected samples and standards were then further analyzed by chemical ionization techniques (ammonia and deuterated-ammonia CI⁺) in order to determine the origin of this "diglyceride signal." POM from the chlorophyll maximum on the continental shelf was richest in diglycerides, surface-water Sargasso Sea POM contained both triglycerides and diglycerides, and surface-water glycerides from the mouth of the Delaware Bay were primarily triglycerides.

Introduction

The study of organic matter in the oceans is complicated by its heterogeneous chemical composition. Traditional analytical techniques for studying particulate organic matter (POM) and dissolved organic matter (DOM) are generally compound-class specific and often quite labor intensive (e.g., extraction and derivatization followed by GC or GC-MS for analysis of fatty acids and fatty alcohols). As a result, it is difficult to obtain representative data sets of molecular-level differences across multiple compound classes.

Direct temperature-resolved mass spectrometry (DT-MS), a form of pyrolysis mass spectrometry or PYMS (e.g., Boon, 1992), coupled with discriminant analysis (DA)

has been proposed as a useful method for screening large numbers of POM or DOM samples for molecular-level variations (Eglinton et al., 1996). In this study, DT-MS (low voltage EI⁺) and DA were used to explore chemical variations among suspended POM samples collected from the euphotic zone on a transect from the mouth of the Delaware Bay to the Sargasso Sea. The resulting discriminant functions indicated that the presence or absence of certain diglyceride fragments was one of the main chemical variations in the particle populations on this transect.

This "diglyceride signal" could have resulted from differences in the triglyceride, diglyceride or polar membrane lipid (phospholipid or glycolipid) concentrations in the POM samples. It becomes important to determine the origin of this mass spectrometric feature as each of the possible precursors would lead to a different oceanographic interpretation. Variations in the triglyceride composition could indicate different populations of phytoplankton and zooplankton (and/or a difference in the ratio of phytoplankton to zooplankton) or a difference in environmental stress on the phytoplankton population. Triglyceride concentrations in phytoplankton often increase significantly when the cells are stressed by nutrient inavailability, high toxin levels, extreme pH, or other factors (Roessler, 1990, and references therein). Zooplankton may increase their storage lipid (wax ester or triglyceride) load for overwintering purposes and reproduction, as is discussed for herbivorous polar copepods in Albers et al. (1996). Phospholipids are the most significant components of most cellular membranes (Erwin, 1973). Therefore, a variation in the phospholipid contribution to the POM pool could indicate a change in the size of the cells making up the bulk of the POM. In other words, if smaller cells dominated, the ratio of phospholipid to organic carbon (analogous to a surface area to volume ratio) would increase. Finally, diglycerides are not significant components of most cells; therefore, high levels in POM would indicate initial degradation (Parrish, 1988) of triglycerides or phospholipids.

In view of the various precursors that could have given rise to the "diglyceride signature," direct temperature-resolved mass spectrometry with chemical ionization

($\text{NH}_3\text{-Cl}^+$ and $\text{ND}_3\text{-Cl}^+$) was applied to standards and selected samples. As a result, molecular ion information on triglycerides, diglycerides, and (possibly) phospholipids was obtained from unextracted, underivatized samples. This minimizes complications in interpretation as compared to the more traditional GC and GC/MS analyses of esterified fatty acids from these compound classes. The esterification procedure eliminates any linkage information and requires an initial preseparation step in order to distinguish the fatty acid components of each precursor compound class. The two techniques are complimentary, however, as ammonia-Cl DT-MS is not quantitative and cannot provide detailed conformational information on the fatty acid components.

Experimental

Suspended POM ($>0.8\ \mu\text{m}$, $<53\ \mu\text{m}$) was collected between May 29 and June 11, 1995 (*R/V Cape Henlopen*) from nine stations on a transect from the mouth of the Delaware Bay (on the United States east coast) to the Sargasso Sea (Fig. 3.1). Seawater samples were taken via Niskin bottle from the surface (approximately 3 m depth) and occasionally from the chlorophyll maximum. After filtration through a $53\ \mu\text{m}$ Nylon screen (in a stainless steel filter holder), suspended POM from up to 95 L of seawater was concentrated to $\leq 120\ \text{mL}$ via cross-flow filtration ($0.8\ \mu\text{m}$ Fluoro centrasette and ultrasette, Filtron, driven by Masterflex peristaltic pumps using silicone and TeflonTM tubing). Aliquots of this retentate were stored in liquid nitrogen. In the laboratory, these aliquots were thawed and 3 to 15 mL of retentate from each was further concentrated via centrifugation (4 minutes $10,500\times G$ on a Fisher MicroCentrifuge, Model 59A). The resulting pellet was desalted in the following manner: the pellet was resuspended in 1 mL of Milli-QTM water and centrifuged as above, the supernatant was discarded, and the rinsing step was repeated twice.

The sample pellets, resuspended in a small quantity of Milli-Q water, were analyzed in triplicate via DT-MS on a JEOL SX-102 mass spectrometer ($16\ \text{eV EI}^+$,

R/V Cape Henlopen #9512 POM Sampling Stations

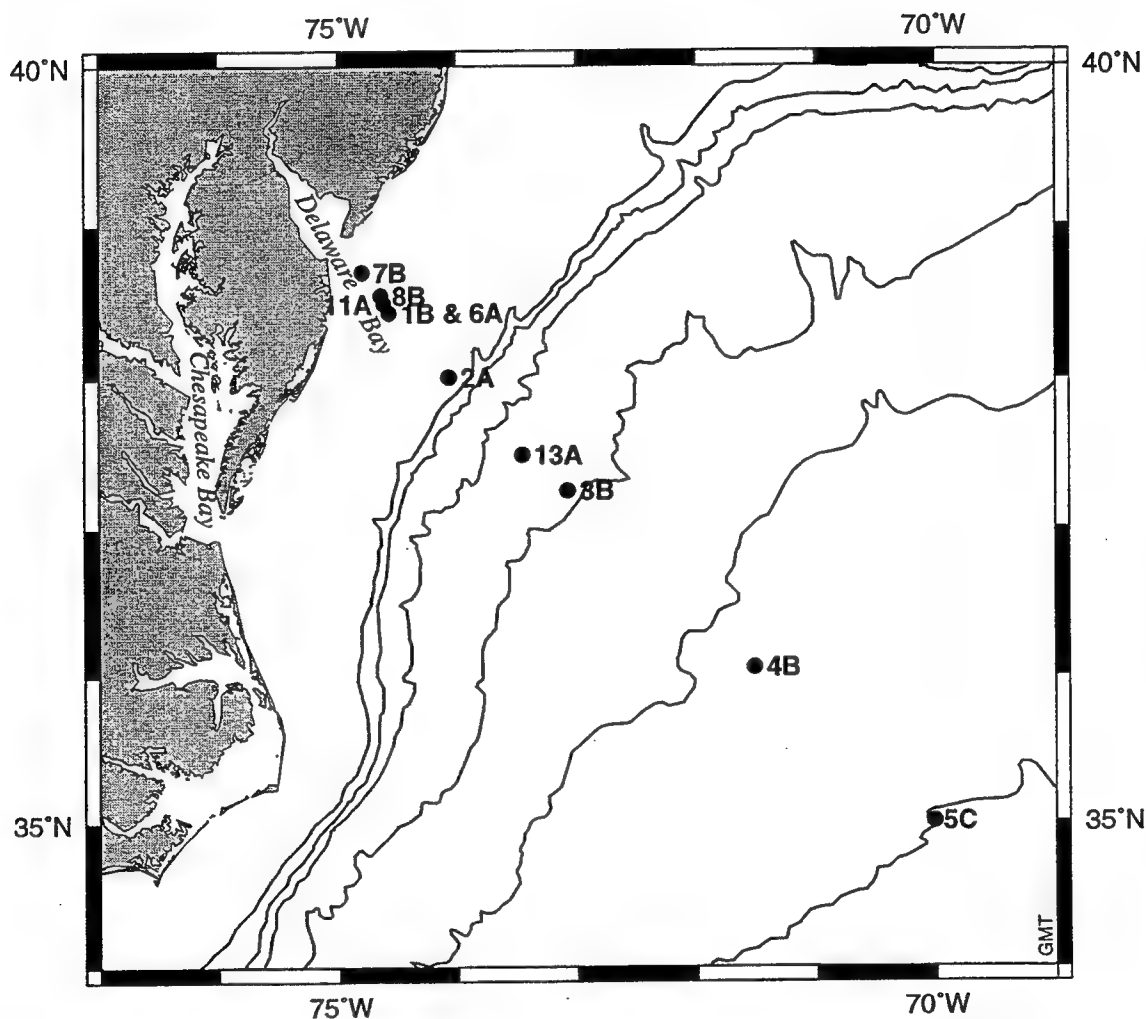


Fig. 3.1. Station locations for collection of suspended POM, *R/V Cape Henlopen*, May 29 - June 11, 1995. Contour lines represent water depths (200 m, 1000 m, 2000 m, 3000 m, 4000 m, and 5000 m).

acceleration voltage 8.0 kV, direct inlet, mass range 20-1000, cycle time 1 s, resolution 3000, source temperature 180°C with the platinum-rhodium sample probe resistively heated from 0 to 1.1 A at 0.5 A/min). To reduce the resulting information to a manageable level, spectra from mass range 20-700 (integer mode, mass correction 0.7) were summed over scans 20-75, normalized with respect to the total ion chromatogram, and exported to a multivariate statistics program (FOMPyroMAP). Scans 20 to 75 were chosen to minimize the contribution of silicone, probably a contaminant from tubing used in the peristaltic pump in the cross-flow filtration system, which appears in later scans. Molecular-level differences among the spectra were investigated using discriminant analysis (in this case, a double-stage principal component analysis as described in Hoogerbrugge et al., 1983).

Representative samples, chosen by analysis of the score plots of the first two discriminant functions, were further analyzed by DT-MS using chemical ionization. For these samples, an additional aliquot of retentate was concentrated and desalted as above. These aliquots were analyzed by $\text{NH}_3\text{-CI}^+$ and $\text{ND}_3\text{-CI}^+$ on a JEOL SX-102 mass spectrometer (direct inlet, mass range 60 to 1000 for $\text{NH}_3\text{-CI}$ (65 to 1000 for ND_3), resolution 3000, sample probe heating ramp 0.5 A/min, source temperature 160 to 175°C).

In order to understand the fragmentation patterns of triglycerides, diglycerides, and phospholipids under the above EI and CI conditions, the following standards (in dichloromethane, Merck, reagent grade) were run by EI^+ (source temperature=190°C), $\text{NH}_3\text{-CI}^+$ and $\text{ND}_3\text{-CI}^+$: glyceryl-1-palmitin-3-olein (Larodan (Malmo)); L- α -phosphatidylcholine, β -oleoyl, γ -palmitoyl; and trilinolein (Sigma). In addition, tristearin and L- α -phosphatidylcholine, dimyristoyl (Sigma) were analyzed via $\text{NH}_3\text{-CI}^+$.

All EI^+ and CI^+ spectra included in this chapter have had a mass correction of 0.7 applied.

Results and Discussion

Discriminant analysis (of spectra from DT-MS, 16 eV, EI⁺)

As mentioned above, discriminant analysis was used to explore molecular-level variations among the POM samples as measured by 16 eV EI⁺ DT-MS. In an initial multivariate analysis where all samples were included, the sample from station 2A was found to be an outlier; we believe this is a sampling artifact from a mistake during cross-flow filtration. Therefore, 2A was used as a test case rather than a training case in subsequent analyses. In other words, 2A was not included in the set of data defining the sample space but was superimposed upon this space after it was defined.

For the analysis described here, surface samples and chlorophyll maximum samples (whose depth varied between 17 m (on the shelf) and 88 m (in the Sargasso Sea), as determined by CTD fluorometer) were included in the data set. Discriminant analysis was run in an essentially unsupervised mode in which replicate runs were grouped together, but the program was given no further information. Therefore, variance among replicates (due to sample heterogeneity or instrument variability) was minimized and variance between samples was maximized. The first two discriminant functions explained the most and next most variance between samples and accounted for 16.5 and 8.8% of the total variance (with between sample to within sample variance ratios of 115 and 37, respectively) in the data set. The reconstructed spectra for DF1 and DF2 (Fig. 3.3, 3.4) indicate chemical differences between samples falling in the negative and positive regions of the functions (shown in the score plot of DF1 vs DF2, Fig. 3.2). It is important to emphasize that these plots should be thought of as difference spectra; the average spectrum for all the samples in the data set is removed in one of the first steps (z-scoring) of the multivariate analysis.

Those samples found in the negative region of DF1, suspended POM from the two nearshore stations and the Sargasso Sea, show stronger sterol and diglyceride signals (Fig.

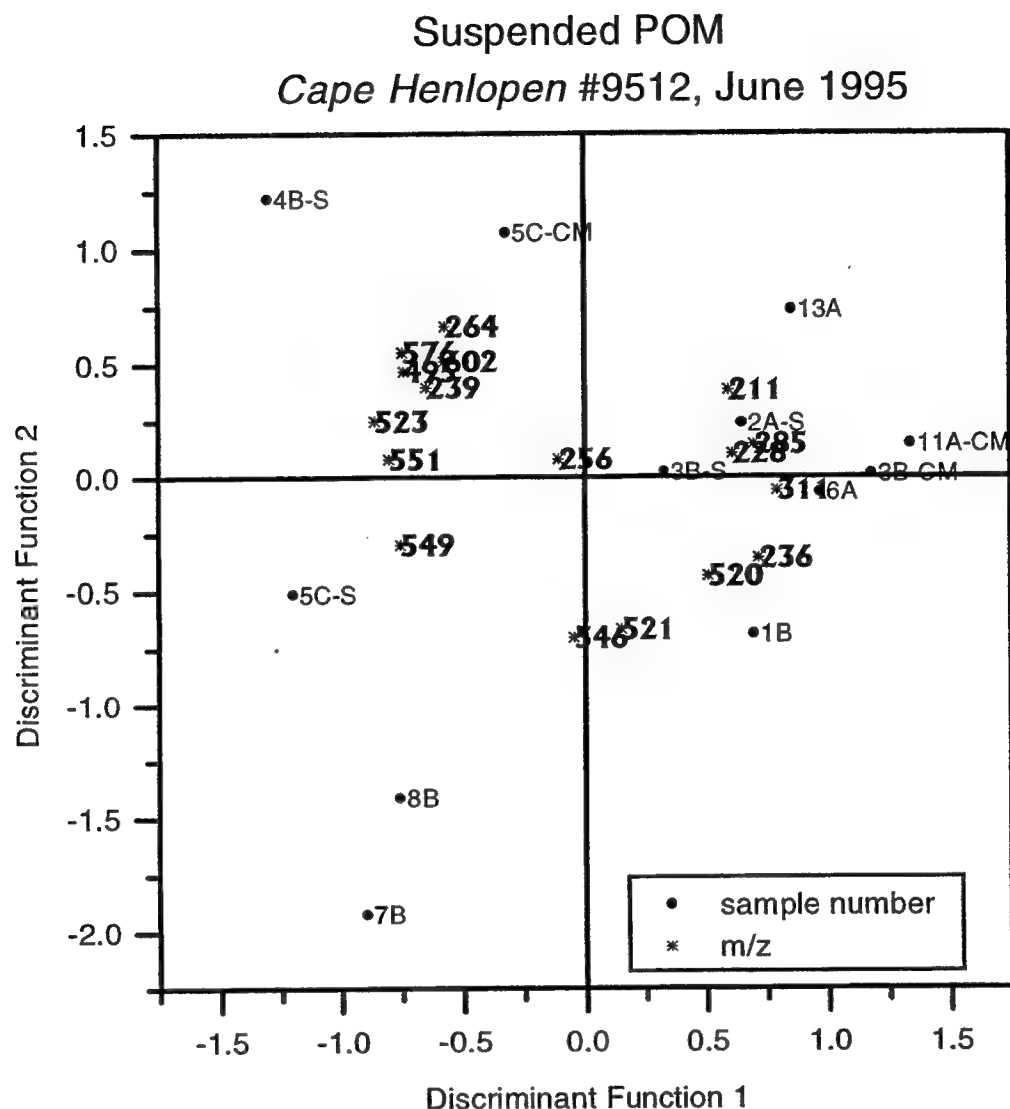


Fig. 3.2. Score plot of Discriminant Function 1 vs. Discriminant Function 2 showing the chemical similarities among suspended POM samples. Superimposed on this plot are loadings of diglyceride, monoglyceride, and fatty acid m/z values (see text for further details).

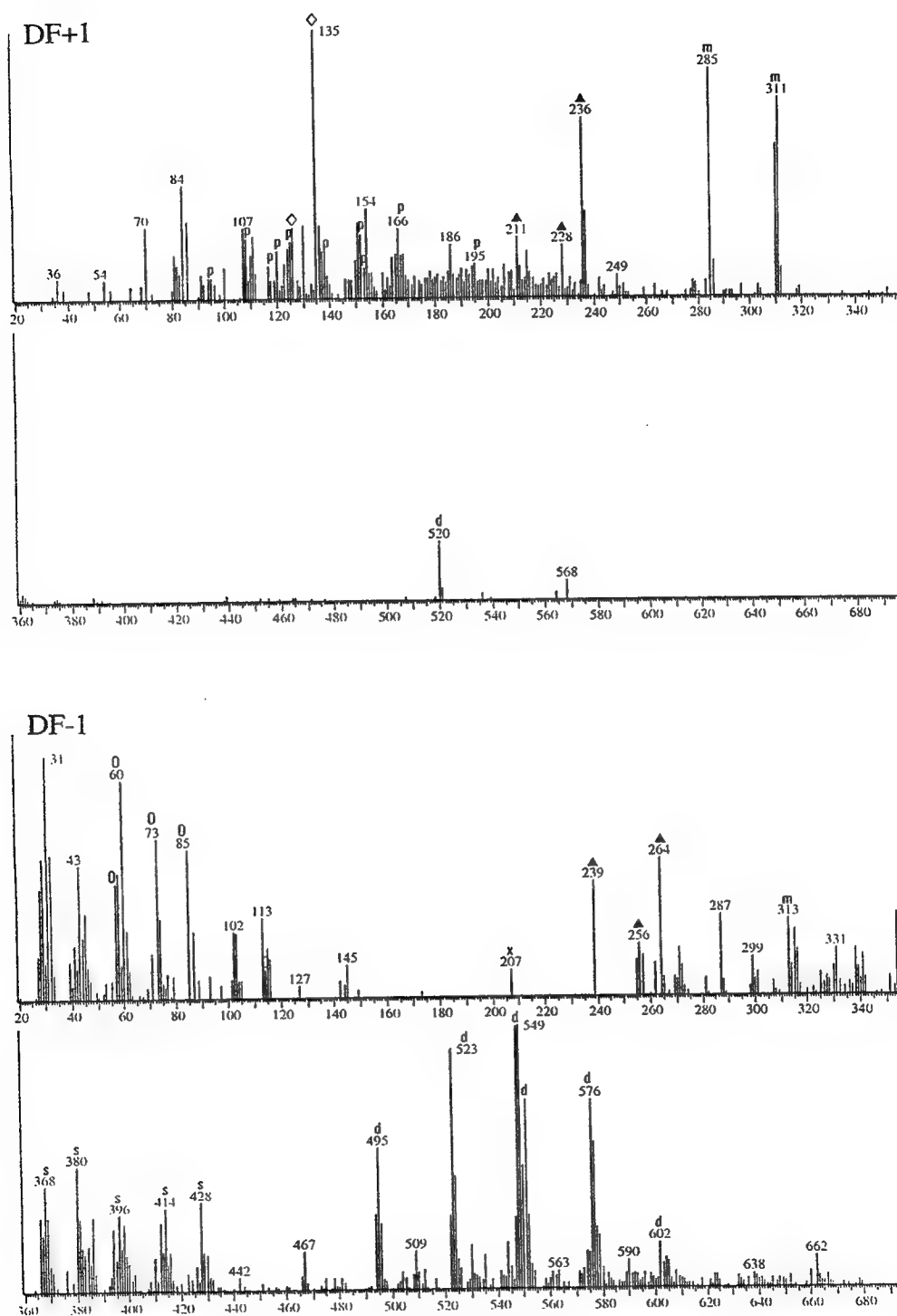


Fig. 3.3. Reconstructed difference spectra for Discriminant Function 1. Symbols: p = protein, \diamond = nucleic acid, Δ = fatty acid, S = sterol, d = diglyceride, m=monoglyceride; x = contaminant.

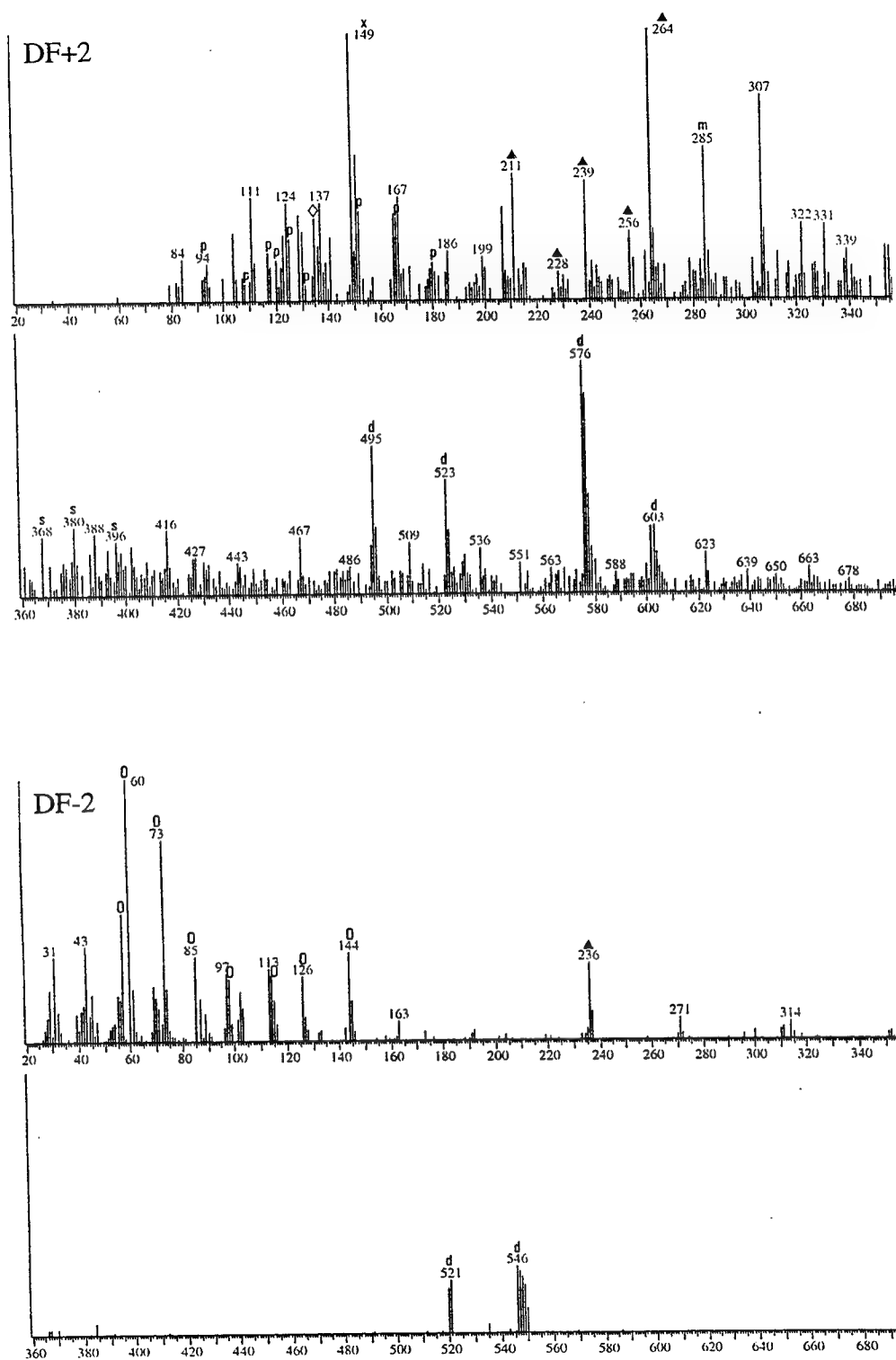


Fig. 3.4. Reconstructed difference spectra for Discriminant Function 2. Symbols as in Fig. 3.3.

3.3, see Appendix 1 for identification of characteristic m/z values). The samples found in the positive region show enhanced nucleic acid, monoglyceride, and protein signatures and are from the continental shelf and slope.

In the reconstructed spectrum for DF2 (Fig. 3.4), the negative region, which contains the nearshore stations, is mainly a polysaccharide signature and the positive region, containing two Sargasso Sea samples and a slope sample, indicates enhancement of lipid (fatty acid, sterol, and diglyceride) and protein signatures.

Weak but significant correlations were found between DF1 and seawater temperature and DF2 and salinity (see Fig. 3.5); these were significant at $\alpha=5\%$; i.e. there is a 5% chance that the variables are actually independent (for a further description of the test of correlation, see Davis, 1986). These correlations might be improved by rotation (e.g., Windig et al., 1981/1982) to maximize the relationship between the external variables of seawater temperature and salinity and the linear combinations of mass spectra variables. Nevertheless, even in this essentially unsupervised form of analysis, DF1 and DF2 clearly exhibit significant correlations with temperature and salinity, respectively.

The enrichment in polysaccharides exhibited by lower salinity samples (DF2-) could indicate a different phytoplankton composition or a land plant signature. There are no concurrent lignin or long-chain n -alkene, n -alkane signatures, so it appears unlikely that the polysaccharides are allochthonous. This is not conclusive evidence, though, as lignin fragments and n -alkene, n -alkane ion series may be buried beneath the ion series from compounds with larger response factors. The hypothesis that the polysaccharide enrichment is due to a shift in the phytoplankton population is consistent with the results of Eglinton et al. (1996). In applying DT-MS to algal cultures, these workers find wide variations in the intensity of the polysaccharide signal both within and between algal classes. In the characterization of 15 algal species (including 2 strains of the prymnesiophyte *Emiliana huxleyi*), the most intense polysaccharide signals are found in the chlorophyte *Dunelliella tertiolecta*, the prymnesiophyte *Syracosphaera*, and the rhodophyte *Porphyridium cruentum*. Although it is possible that these species or similar

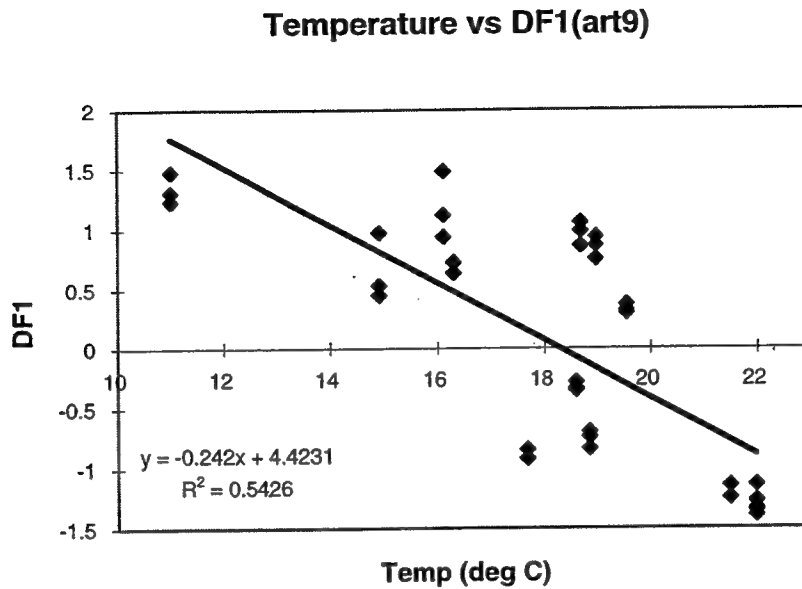
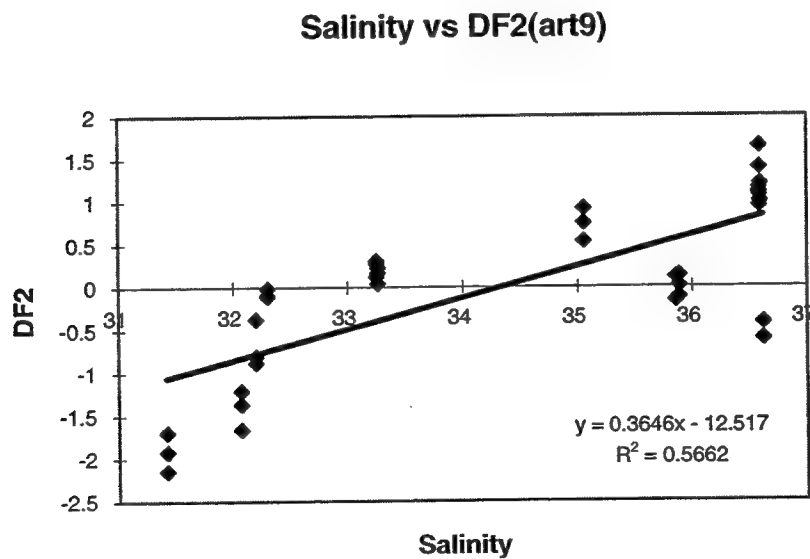


Fig. 3.5.a. Seawater temperature vs Discriminant Function 1 scores.



3.5.b. Seawater salinity vs Discriminant Function 2 scores.

ones are responsible for the polysaccharide signal in DF2-, it is more likely that the signal comes from the enrichment in polysaccharides exhibited by diatoms or dinoflagellates when compared with more oligotrophic phytoplankton such as the prymnesiophyte *Emiliana huxleyi*. The fact that C_{16:1} fatty acid also appears in the negative region of DF2 indicates that the signal may result from diatoms; in contrast, a dinoflagellate signature should contain C_{18:4} and C_{22:6} fatty acids and, probably C_{18:5} (Volkman, 1989; Wakeham and Lee, 1989; Columbo et al., 1996; and references therein).

DF2+, correlated with higher salinity, is richer in lipids and proteins. This could indicate a different phytoplankton community or an increase in the zooplankton contribution to the suspended POM, as zooplankton have high protein and low carbohydrate contents and may contain fairly high lipid contents as compared to phytoplankton (Parsons et al., 1984). The fatty acid signal in DF2+ contains both C_{14:0} fatty acid (bound, m/z 211, and free, m/z 228), generally considered to be phytoplanktonic (Wakeham and Lee, 1989, and sources therein) and a monounsaturated (probably C_{16:0}/C_{18:1}) diglyceride, which, if resulting from a triglyceride precursor, would appear zooplanktonic (Wakeham and Canuel, 1988). Therefore, both an increase in zooplankton contribution and a change in the phytoplankton population appear responsible. Phthalates (m/z 149, 279), believed to be contaminants, also plot within that part of DF2 correlated with higher salinity; the higher salinity samples come from waters with lower POC concentrations and are thus, logically, the samples that should be most susceptible to shipboard and laboratory contamination.

Both the higher salinity (DF2+) and the higher temperature samples (DF1-) appear enriched in diglyceride moieties, though the higher temperature samples are enriched in a more complete suite of diglycerides. These diglycerides could result from mass spectrometric fragmentation of triglycerides or phospholipids or they could indicate actual diglycerides within the sample. Therefore the "diglyceride signal" bears further exploration.

The "diglyceride signal"

A clearer view of the separation of samples by DF1 and DF2 and the contribution of the "diglyceride signal" and fatty acid signal to this separation can be obtained in Fig. 3.2. The samples are plotted in a score plot of DF1 and DF2 with the relative position of key m/z values in this space superimposed on the figure. Similarities among samples are indicated by their nearness in the score plot. The relative contribution of a particular m/z value to each sample is indicated by the direction and distance of the value from the origin. In other words, if the mass unit plots in the same direction from the origin as a sample it is characteristic of that sample; the distance of the m/z value from the origin is an indication of the relative intensity of its contribution to that sample.

In this case it becomes obvious that 7B and 8B, the two nearshore stations, have little contribution from diglyceride or fatty acid fragments. The cluster of shelf and slope samples (1B, 2A-S, 3B-S, 3B-CM, 6A, 11A-CM, 13A) is characterized by m/z 211, 228, 236 (indicative of fatty acids), 285 and 311 (monoglycerides), and 520 (diglyceride). The Sargasso Sea samples (4B-S, 5C-CM, 5C-S) are richer in 239 and 264 (indicative of fatty acids) and 549, 551, 523, 495, 576, and 602 (diglycerides).

In order to determine the chemical compounds responsible for these m/z value variations, selected samples (5C-surf, 7B, and 11A-CM) were analyzed by ammonia-CI and deuterated-ammonia CI. In addition, selected standards were analyzed under identical conditions in order to clarify fragmentation patterns of potential precursors for the "diglyceride signal."

Analysis of standards (EI^+ , NH_3-CI^+ , and ND_3-CI^+ DT-MS)

Fig. 3.6 shows EI^+ , NH_3-CI^+ and ND_3-CI^+ spectra for trilinolein (accurate mass for the molecular ion (MW) is 878.7). In the 16 eV EI^+ spectrum (Fig. 3.6a, mass correction=0.7), the molecular ion, m/z 878, is the base peak, with important

Figure 6

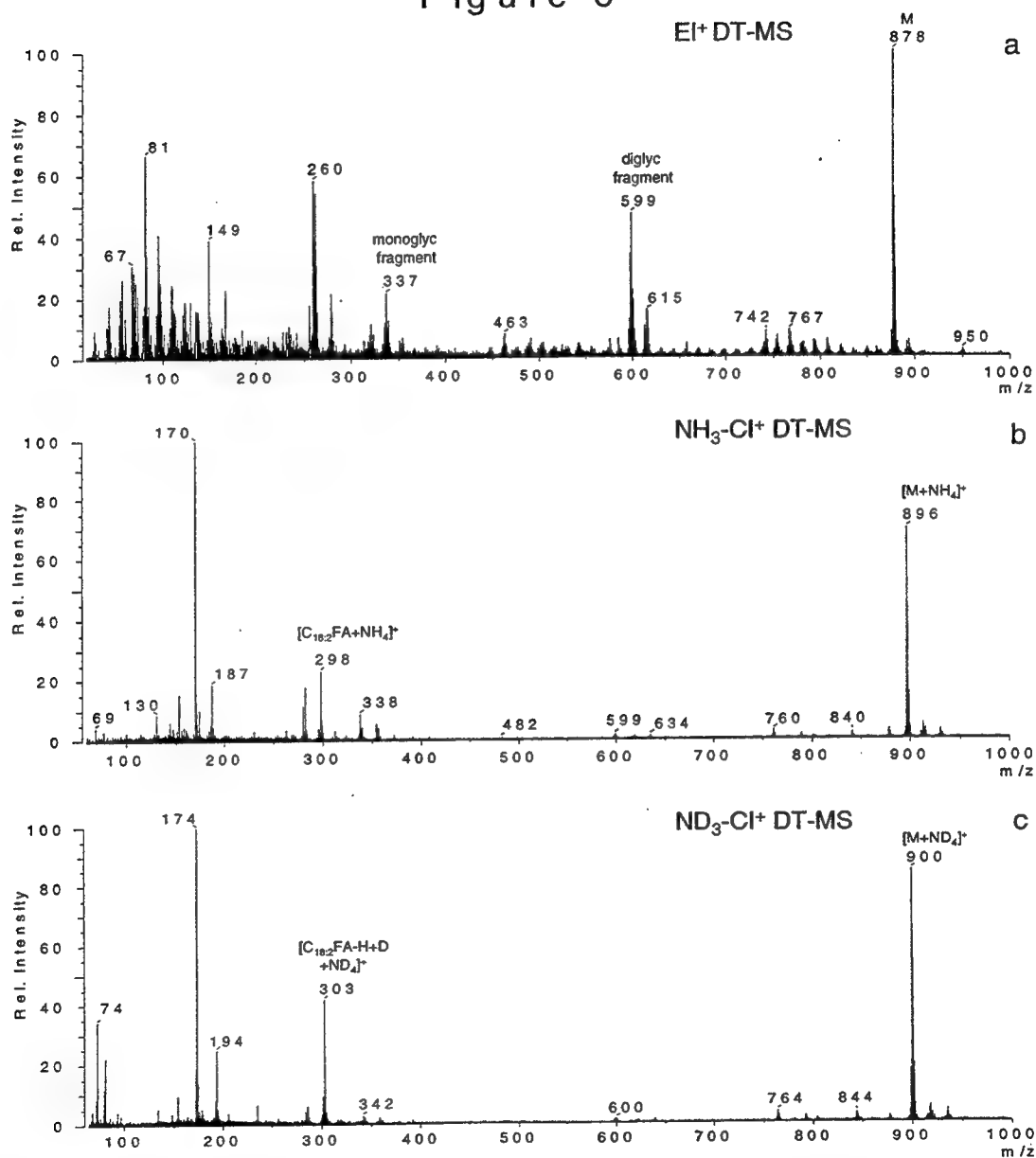


Fig. 3.6. DT-MS analyses of the triglyceride trilinolein in dichloromethane (DCM). All spectra in Figures 3.6 through 3.8 are summed over the peak in the total ion chromatogram (TIC).

For Figures 3.6 through 3.8 “M” indicates molecular ion; “FA,” fatty acid.

Figure 7

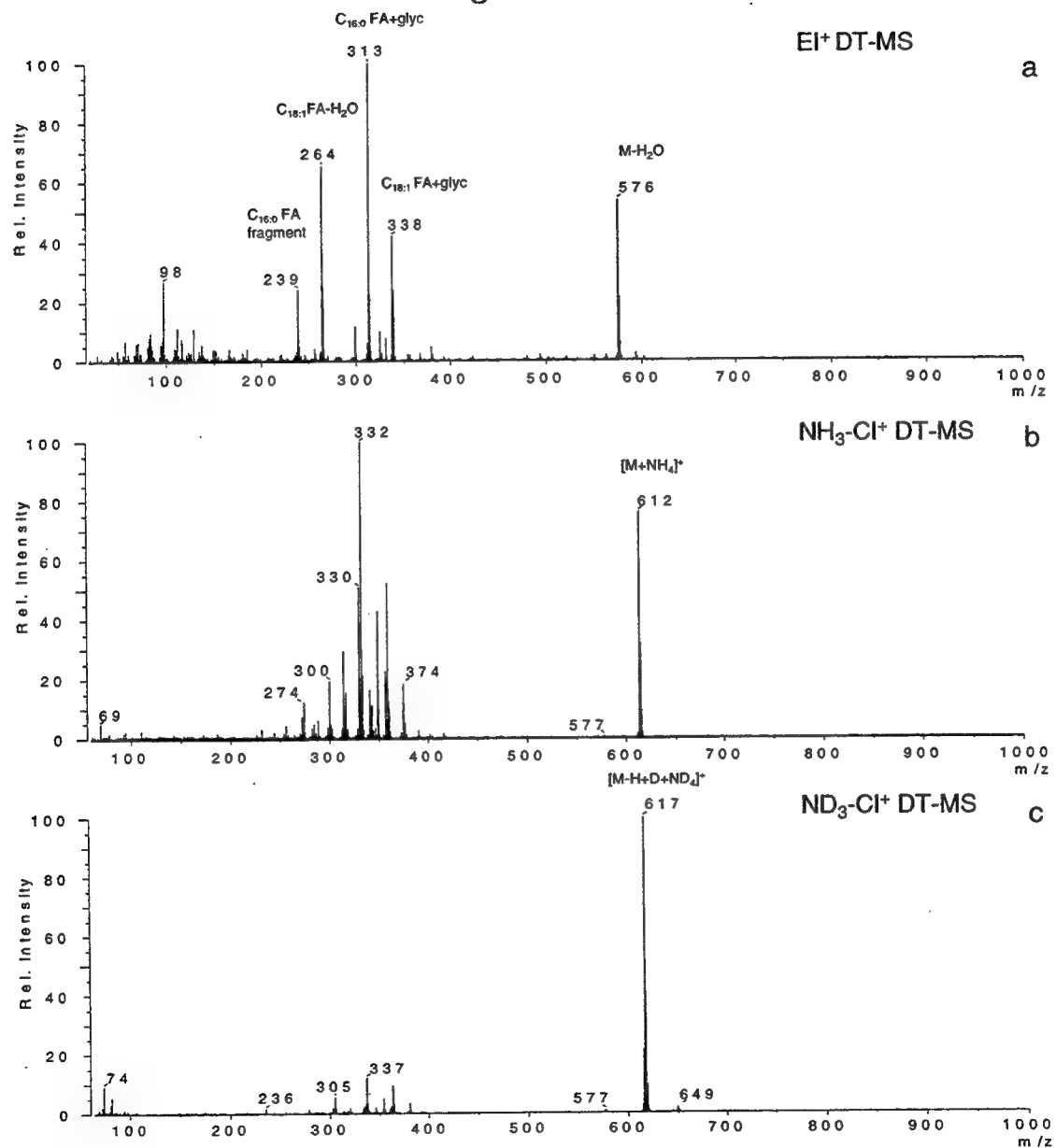


Fig. 3.7. DT-MS analyses of the diglyceride glyceryl-1-palmitin-3-olein (rac).

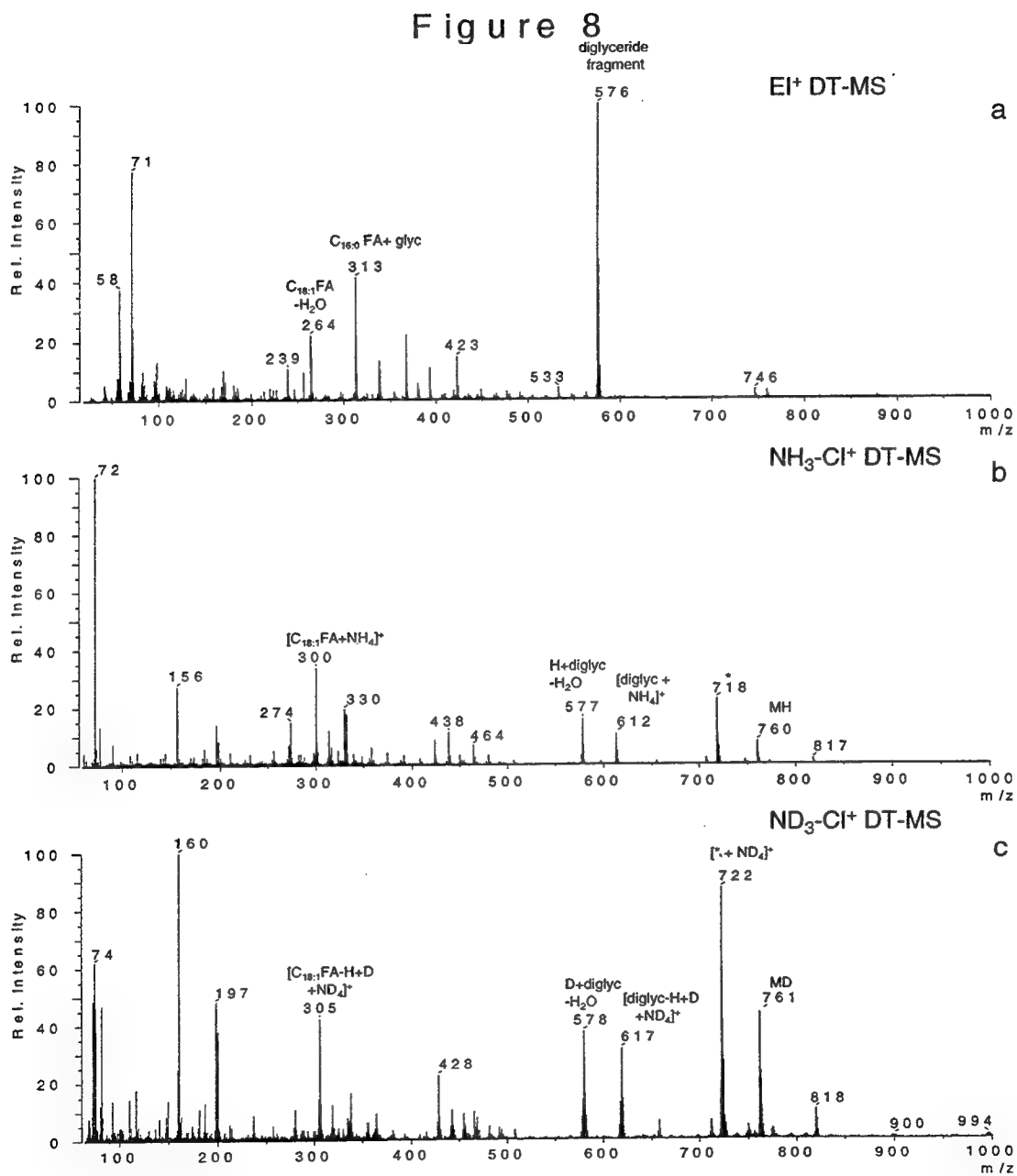


Fig. 3.8. DT-MS analyses of the phospholipid L- α -phosphatidylcholine, β -oleoyl, γ -palmitoyl.

contributions to the spectra from the diglyceride (m/z 599, $[M-279]^+$) fragment (47% of base peak), the monoglyceride fragment (m/z 337, $[M-541]^+$, 23%), m/z 262 (54%), m/z 260 (58%), and m/z 81 (66%). Under ammonia- CI^+ (Fig. 3.6b), trilinolein yields the quasi-molecular ion (m/z 896, $[M+18]^+$, 70%), m/z 170 (base peak), and the ammonium adduct of linoleic acid ($C_{18:2}$ fatty acid, m/z 298, 23%). The ND_3 - CI^+ spectrum (Fig. 3.6c) confirms the assignments from the ammonia- CI spectrum with peaks at m/z 900 and 303, identified as the ND_4 -adducts of the molecular ion and the fatty acid fragment (after replacement of its hydroxyl hydrogen by a deuterium), respectively. The ion corresponding to m/z 170 in the ammonia- CI spectrum is found at m/z 174. These CI findings are consistent with the literature although Waller and Dermer (1980) report that direct inlet ammonia- CI of triglycerides led to a base peak at $[M+NH_4]^+$. We find this to be the case for ammonia- CI of tristearin and suggest that the unsaturation of trilinolein may be responsible for its lower $[M+NH_4]^+$ peak.

The EI^+ and CI^+ spectra for the diglyceride, glyceryl-1-palmitin-3-olein (MW 594.5), are shown in Fig. 3.7. The EI spectrum (Fig. 3.7a) shows peaks at m/z 576 (54% of base peak), resulting from a loss of H_2O from the molecular ion, m/z 338 (42%), a $C_{18:1}$ fatty acid + glycerol fragment, and m/z 313 (base peak) from a $C_{16:0}$ + glycerol fragment. The fatty acid fragments themselves are also found: m/z 264 (65%) corresponding to $C_{18:1}$ fatty acid - H_2O and m/z 239 (25%) corresponding to a $C_{16:0}$ fatty acid fragment. Ammonia- CI in positive ion mode yields a strong mass unit value (m/z 612, 76%) corresponding to the molecular ion $[M+NH_4]^+$. The identification of 612 as the $[M + NH_4]^+$ ion is strengthened by comparison with the ND_3 - CI spectrum, which contains a corresponding peak 5 mass units higher (m/z 617, resulting from exchange of the hydroxyl hydrogen with deuterium and formation of an ND_4 adduct). It is puzzling, however, that the m/z values tentatively identified as ammonium adducts of monoglyceride fragments (m/z 332, base peak, and m/z 358, 50%) are one to two units higher than they should be, yet ND_3 - CI gives the expected additional 5 mass units. It is

also interesting to note the variation in this region between the ammonia and deuterated-ammonia spectra.

Fig. 3.8 shows the spectra for the phospholipid, L- α -phosphatidylcholine, β -oleoyl, γ -palmitoyl (MW 759.6). In the EI spectrum (Fig. 3.8a) the molecular ion intensity is only 3% of the base peak. The dominant fragment ions are m/z 576 (base peak, from the diglyceride fragment), m/z 313 (42%, from the $C_{16:0}$ fatty acid + glycerol fragment), and m/z 71 (77%). Ammonia-CI (Fig. 8b) yields a base peak at m/z 72. The protonated molecular ion (MH) is small (8% of the base peak) and the following fragments are important: m/z 718 (22%), 612 (11%), 577 (16%), 330 (20%) and 300 (34%). The peak at m/z 718 corresponds to a replacement of trimethylamine + H with NH_4^+ ; this interpretation is strengthened by the presence of m/z 722 in the ND_3 -CI spectrum. In previous studies of phosphocholine fragmentation patterns under ammonia-CI conditions, a prominent $[MH-42]^+$ peak has been reported and subsequent examination with deuterated ammonia and $^{15}NH_3$ reagent gases has been used to support this identification (Kuksis and Myher, 1989 and sources therein). The peak at m/z 612 corresponds to the diglyceride ammonium adduct and m/z 577 appears to be the protonated diglyceride- H_2O fragment; these identifications are further supported by the presence of ions with m/z values of 617 and 578 in the ND_3 -CI spectrum. The m/z 330 appears to represent a $C_{16:0}$ fatty acid + glycerol fragment and the m/z 300 is the ammonium adduct of oleic acid.

Analysis of selected samples (EI^+ , NH_3 -CI $^+$, and ND_3 -CI $^+$ DT-MS)

With such information it becomes possible to identify the precursors for the "diglyceride signal" in the EI^+ spectra. The samples 5C-S, 7B, and 11A-CM, from Sargasso Sea surface water, near-shore surface water, and shelf chlorophyll maximum water, respectively, were chosen as representative of different regions in the score plot in Fig. 3.2. 7B and 11A-CM were analyzed by both NH_3 -CI and ND_3 -CI. Due to a scarcity

Figure 9

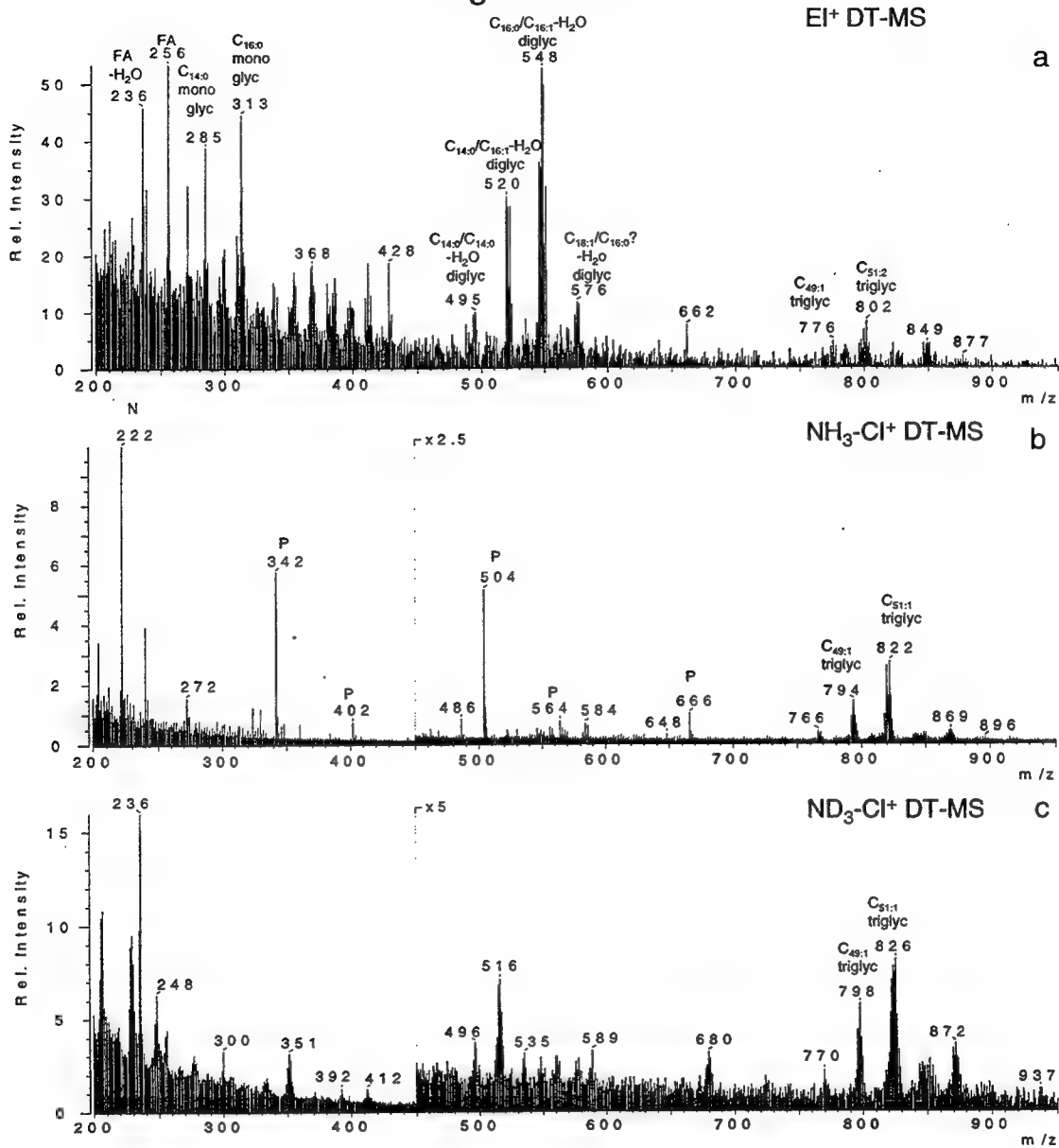


Fig. 3.9. EI⁺ DT-MS mass spectrum of suspended POM sample 7B summed over the TIC scan range used in discriminant analysis.

3.9b. NH₃-Cl⁺ DT-MS mass spectrum of 7B summed over the peak in the TIC.

3.9c. ND₃-Cl⁺ DT-MS mass spectrum of 7B summed over the peak in the TIC.

Symbols used in Fig. 3.9, 3.10, 3.11: P, polyhexose; N, aminosugar; FA, fatty acid.

Figure 10

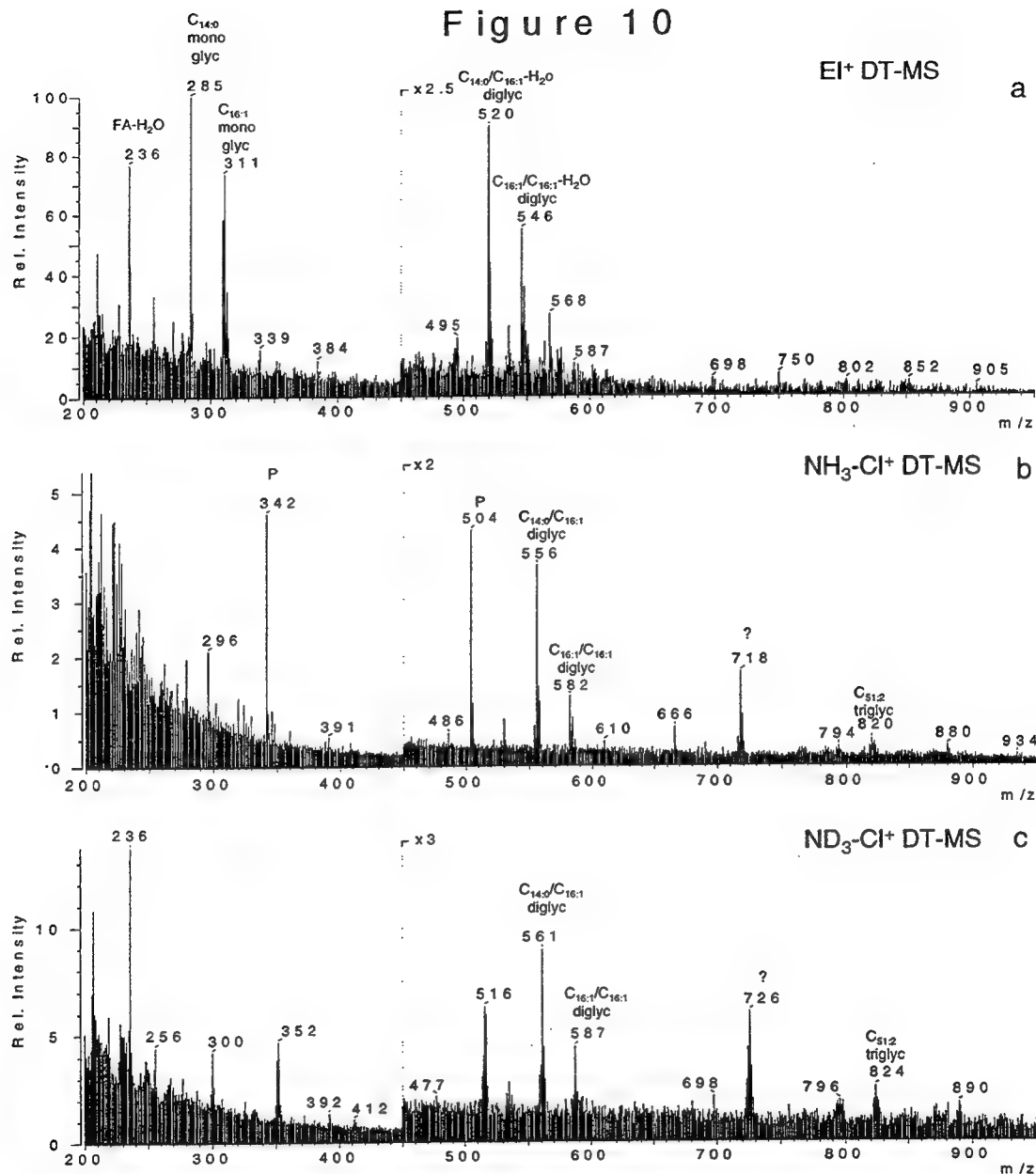


Fig. 3.10a. 16eV, EI⁺ DT-MS mass spectrum of suspended POM sample 11A-CM summed over the TIC scan range used in discriminant analysis.

10b. NH₃-CI⁺ DT-MS mass spectrum of 11A-CM summed over the peak in the TIC.

10c. ND₃-CI⁺ DT-MS mass spectrum of 11A-CM summed over the peak in the TIC.

Figure 11

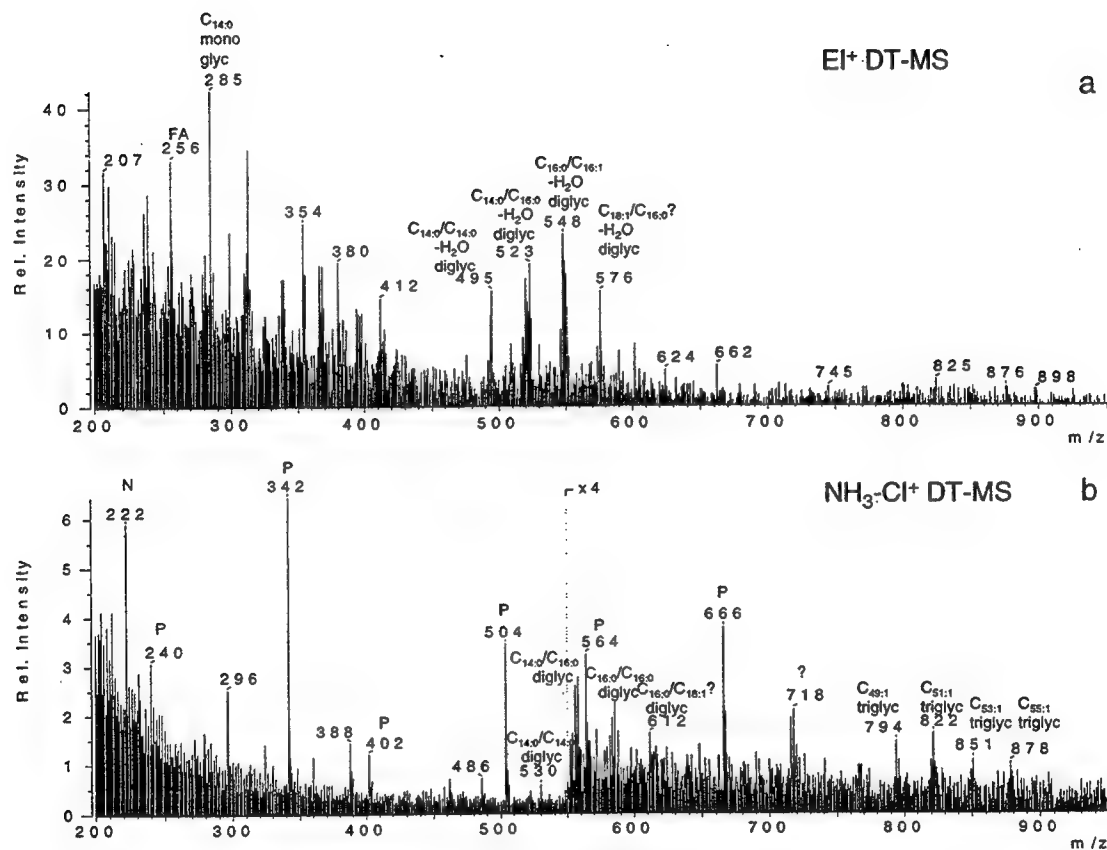


Fig. 3.11a. 16eV, EI⁺ DT-MS mass spectrum of suspended POM sample 5C-S summed over the TIC scan range used in discriminant analysis.

3.11b. NH₃⁺Cl⁻ DT-MS mass spectrum of 5C-S summed over the peak in the TIC.

in sample, 5C-S only underwent NH_3 -CI analysis. Sample 7B (Fig. 3.9) appears to contain mainly triglycerides ($\text{C}_{49:1}$, $\text{C}_{51:1}$ and $\text{C}_{51:2}$) as identified by the two CI spectra. These triglycerides contain $\text{C}_{14:0}$, $\text{C}_{16:0}$, and $\text{C}_{16:1}$ fatty acids as indicated by the following mass unit values in the EI^+ spectrum: m/z 211, 236, and 256 ($\text{C}_{14:0}$ fatty acid fragment, $\text{C}_{16:1}$ fatty acid - H_2O , $\text{C}_{16:0}$ fatty acid), m/z 285 and 313 ($\text{C}_{14:0}$ and $\text{C}_{16:0}$ monoglycerides) and m/z 495, 520, and 548 (tentatively identified as $\text{C}_{14:0}/\text{C}_{14:0}$, $\text{C}_{14:0}/\text{C}_{16:1}$, and $\text{C}_{16:1}/\text{C}_{16:0}$ diglycerides).

11A-CM (Fig. 3.10) contains primarily diglyceride fragments as indicated by the dominant m/z 556 and 582 in the NH_3 -CI spectrum and the presence of related m/z values 5 mass units higher in the ND_3 -CI spectrum. Comparison of the EI and CI spectra suggests that the strongest signals are from $\text{C}_{14:0}/\text{C}_{16:1}$ and $\text{C}_{16:1}/\text{C}_{16:1}$ diglycerides. In addition to diglycerides, there are some triglycerides in the sample, as indicated by the following m/z values in the ammonia-CI spectrum: 794 ($\text{C}_{49:1}$), 820 ($\text{C}_{51:2}$), and 880 ($\text{C}_{55:0}$). The peak occurring at m/z 718 in the NH_3 -CI spectrum is also worth mentioning. Although such a peak was found in the ammonia CI spectrum of L- α -phosphatidylcholine, β -oleoyl, γ -palmitoyl, the peak in 11A-CM does not behave in the same manner. The sample peak does not show an addition of 4 mass units in the ND_3 -CI spectrum, nor does it show other fragments related to a phosphocholine. Therefore, it remains unidentified but could potentially be related to some other membrane component.

The NH_3 -CI spectrum of 5C-S (unlike those of 7B and 11A-CM) contains diglyceride and triglyceride signals of relatively equal intensity. Comparison of the EI and CI spectra (Fig. 3.11) lead to the tentative identification of $\text{C}_{14:0}/\text{C}_{14:0}$, $\text{C}_{16:0}/\text{C}_{14:0}$, $\text{C}_{16:1}/\text{C}_{14:0}$, $\text{C}_{16:0}/\text{C}_{16:0}$, $\text{C}_{16:0}/\text{C}_{16:1}$, $\text{C}_{16:0}/\text{C}_{18:0}$, and mono-unsaturated $\text{C}_{16}/\text{C}_{18}$ diglycerides. The triglycerides in 5C-S are $\text{C}_{49:1}$, $\text{C}_{51:1}$, $\text{C}_{53:1}$, and $\text{C}_{55:1}$. The unidentified m/z 718 peak appears in the NH_3 -CI analysis of 5C-S as well, but is considerably less prominent.

Discussion of the "diglyceride signal"

The results from DT-MS of selected samples under both EI and CI conditions indicate that the "diglyceride signature" in the continental-shelf chlorophyll maximum sample (11A-CM, Fig. 3.10) is due primarily to diglycerides, while in the nearshore surface sample (7B) triglycerides are mainly responsible, and the signature in the Sargasso Sea sample (5C-S) results from diglycerides and triglycerides. It is interesting to incorporate this data with the score plot from discriminant analysis of EI-MS spectra of the entire data set. 7B and 8B, the two most nearshore surface samples are probably triglyceride-rich, as indicated by the CI spectra of 7B, the proximity of the two sampling stations, and the lack of fragment ions in the discriminant function space shared by 7B and 8B (molecular ions of triglycerides were not included in the m/z range of the multivariate analysis). The Sargasso Sea surface samples (4B-S and 5B-S) span the space of many diglyceride ions, as is consistent with the relative intensity of the CI-MS diglyceride and triglyceride signals as compared to intensities in 7B. The shelf and slope surface samples (1B, 2A-S, 3B-S, 6A, 13A) and chlorophyll maximum samples (3B-CM and 11A-CM) are in the region of enrichment in fatty acid and monoglyceride fragments, indicating, perhaps increased lipid degradation as compared to the other samples; this would be consistent with the strong diglyceride signal in found in CI-MS of 11A-CM. Such an interpretation is supported by Parrish (1988), in which the presence of free fatty acids, monoglycerides, and diglycerides are suggested as lipid degradation indicators.

It is necessary to point out that the presence of diglycerides could have resulted from degradation during sample handling and/or storage. However, sample preparation for DT-MS minimizes sample handling considerably over traditional extraction and derivatization techniques, and should therefore have minimized such a release of diglycerides from precursor molecules. Samples for this study were stored in liquid nitrogen (-196°C), which should also minimize lipase activity. For example, although Hazelwood and Dawson (1976) found that active bacterial enzymes from *Butyrivibrio fibrosolvens* degraded phospholipids in cultures kept at -16°C (Hazelwood and Dawson,

1976), they found no evidence of hydrolysis at -70°C . Therefore, while it is impossible to discount the effects of sample handling on the concentration of diglycerides in the sample, it is believed that these effects have been reduced as much as possible at the present time.

The variation in triglyceride content seen in the selected samples could result from species differences among phytoplankton or zooplankton (bacteria are generally considered poor in triglycerides (Goldfine, 1982)). The triglyceride variation could also result from a change in the ratio of phytoplankton and zooplankton as zooplankton may be richer in lipid contents as compared to phytoplankton (Parsons et al., 1984). In the case of an increase in the contribution of zooplankton biomass to suspended POM, one might expect an increase in wax esters, reported by many authors as zooplankton storage lipids. We do not find a significant wax ester component in our mass spectra; however, certain zooplankton species use predominantly triglyceride storage components (e.g., Albers et al., 1996). Finally, the variation in triglycerides could indicate a response to ambient conditions. Zooplankton often increase in lipid concentration prior to overwintering and reproduction (Albers et al., 1996 and references therein). Much work has been done showing that phytoplankton triglyceride concentrations increase significantly as a response to nutrient stress, extreme pH, high toxin levels, increased light intensity, etc. (reviewed by Roessler, 1990). As Roessler (1990) states, triglycerides appear to be an early response mechanism for coping with excess energy inputs in situations in which growth is inhibited by environmental factors. This is consistent with the observation (e.g., Brown et al., 1996; Dunstan et al., 1993) that cell concentrations of triglycerides increase once algal cultures reach stationary phase.

The trend in the "diglyceride signal" with seawater temperature (from discriminant analysis of EI^+ data) can be compared with the plot of seawater fluorescence (obtained via CTD) vs. temperature (Fig. 3.12) in an attempt to constrain the possible reasons for the variation in di- and triglyceride content in the POM samples. The increase in "the diglyceride signature" with temperature does not appear to result from an increase

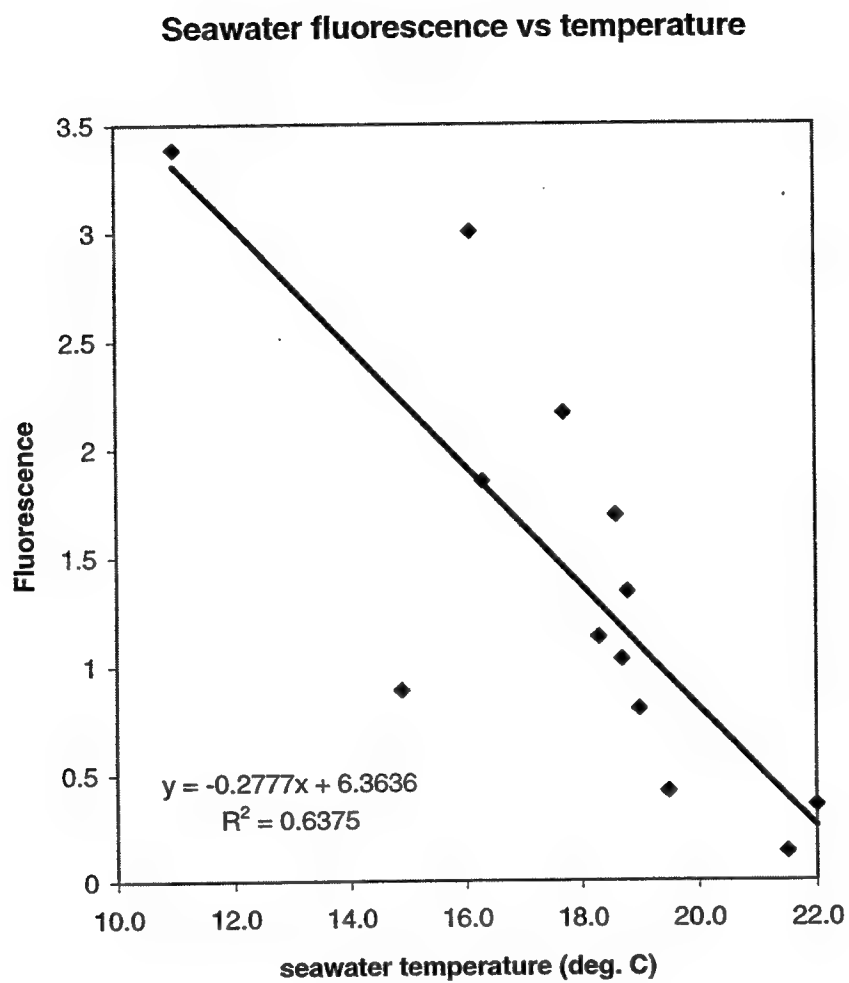


Fig. 3.12. Seawater fluorescence vs. seawater temperature (obtained via CTD, *R/V Cape Henlopen*, cruise #9512).

in phytoplankton biomass as seawater fluorescence levels drop with increasing temperature. Since the POM samples were collected between May 29 and June 11, 1995, the increase in the "diglyceride signal" in the nearshore samples (7B and 8B) could be explained by the presence of a stressed or senescent phytoplankton population remaining after the spring bloom on the shelf, which is documented as occurring during from March to May (Wirick, 1994; Flagg et al., 1994). The spring bloom at the Bermuda Atlantic Time-series Study site has been found to occur slightly earlier (Michaels et al., 1994) but it is conceivable that a similar argument can be used to explain the "diglyceride signal" in the Sargasso Sea samples.

The fatty acid composition of the glycerides can indicate potential variations in the contribution of phytoplankton and zooplankton to the suspended POM pool. While variations in triglycerides with respect to environment make it difficult to use them as source biomarkers, trends among phytoplankton and zooplankton triglycerides have been noted. Phytoplankton triglycerides generally contain C_{14:0}, C_{16:0}, and C_{16:1} fatty acids; zooplankton triglycerides are generally characterized by C_{16:0}, C_{18:1}, C_{18:0} fatty acids, with varying contributions from monounsaturated or polyunsaturated C₂₀ and C₂₂ fatty acids as well (Wakeham and Canuel, 1988). Therefore, in our samples, the glycerides appear to be mainly phytoplanktonic, which is consistent with the lack of a strong cholesterol signal in the sterol region of the EI⁺ spectra. There is, however, some indication (from the presence of m/z 576 in the EI⁺ spectra of Fig. 3.9 & 3.11, for example) that zooplankton contributions cannot be discounted.

It is known that phytoplankton populations on continental shelves are considerably different from those in oligotrophic regions such as the Sargasso Sea (Chisholm et al., 1992, and references therein). It has also been found that phytoplankton populations vary from shelf to slope waters in the Mid-Atlantic Bight (Falkowski et al., 1988, Verity et al., 1996). While not discussed here due to the difficulties in using triglycerides for taxonomic purposes (especially in field POM samples where multiple

triglyceride sources may be present), it is quite likely that phytoplankton species variations also play a role in the triglyceride signals in this data set.

To summarize, the results from DT-MS (EI^+ and CI^+) indicate that the triglycerides and diglycerides in suspended POM appear to be mainly phytoplanktonic in origin. However, the potential role of the phytoplankton-to-zooplankton-to-detritus biomass ratio in determining changes in the glyceride content of POM cannot be discounted. The comparison of seawater fluorescence data, literature data concerning the timing of phytoplankton blooms in this region, the fatty acid composition of the glycerides, and the trend in the EI^+ DT-MS spectra with temperature indicate that the health of the phytoplankton population plays a significant role in determining the glyceride signal. Due to the inability to further constrain the contribution of phytoplankton to the molecular-level composition of suspended POM, it is difficult to determine with any degree of certainty the relative importance of these two possibilities. It is also difficult to constrain the effect of changes in phytoplankton species composition on the diglyceride and triglyceride content of the suspended POM pool.

Finally, it is necessary to mention the surprising lack of phospholipid information in the CI^+ DT-MS spectra of selected samples. Phospholipids are found in plants, animals, and microorganisms (Christie, 1973) and have been reported as representing $\geq 50\%$ of the lipid composition in diatoms (Lee et al., 1971, as reported in Parsons et al., 1984). Therefore, they should appear as components of oceanic suspended POM. It is possible that fragments of phospholipids are being overlooked or overwhelmed in the complex spectra generated by CI^+ DT-MS of total suspended POM. As these lipids are large and complex, they require a considerable amount of energy prior to desorption in DT-MS (Boon, personal comm.). In natural samples they may not occur in sufficient quantities to ensure desorption and ionization at levels above background. An additional and more disturbing possibility is that the phospholipids were preferentially degraded in our samples during sample manipulation or, though less likely, during storage in liquid nitrogen (Conte, 1989). However, in such a case it would appear likely that diglycerides,

monoglycerides, and fatty acids would be prevalent in all samples in which phospholipids appeared absent (including the three samples analyzed by ammonia CI^+ DT-MS).

Summary and Conclusions

DT-MS (16 eV EI^+) and discriminant analysis were used to screen for molecular-level variations among suspended POM samples from a transect in the North Atlantic. Considerable heterogeneity was found within the suspended POM pool. Discriminant Function 1, responsible for the largest amount of between-sample variance, is correlated with seawater temperature. The cooler temperature samples are enriched in nucleic acids, protein, and selected fatty acids; the warmer temperature samples are enriched in lipids, especially sterol and diglyceride ions. Discriminant Function 2, correlated with salinity, indicates that suspended POM from more saline waters is enriched in protein, selected fatty acids, sterols, selected diglycerides, and phthalates. The lower salinity samples (DF-2) are enriched in polysaccharides and $\text{C}_{16:1}$ fatty acid.

One of the major sources of variation in the EI^+ spectra, a "diglyceride signal," was further explored by chemical ionization DT-MS. This "diglyceride signal" appears to result from different levels of precursor triglycerides and diglycerides in the samples. These variations could be explained by changes in the composition of the phytoplankton population, changes in the relative contribution of phytoplankton and zooplankton to suspended POM, differences in growth environment (i.e., the stressing of the phytoplankton population due to a lack of nutrients, increase in light levels, etc.) and/or varying levels of *in situ* degradation. The inability to further determine whether the variability in glycerides is due to changes within the phytoplankton population or to changes in the contribution of phytoplankton, zooplankton, and detritus to suspended POM illustrates the need for the molecular-level characterization of selected subclasses of suspended POM. The isolation of phytoplankton from these suspended POM samples via

flow cytometry (which was applied to later sample sets, Chapters 4 and 6) could perhaps have shed further light upon the "diglyceride signal" and its variations.

Low voltage EI^+ DT-MS coupled with discriminant analysis appears to be a useful technique for the initial screening of complex samples such as oceanic POM. Such a screening can then be followed by more detailed work, such as the CI-MS in this study or the GC-MS work in Appendix 2, in order to further explore important variations identified by discriminant analysis. CI^+ DT-MS, as shown here, can provide more detailed molecular-structure information in situations where sample size is limited.

References

- Albers C. S., Kattner G., and Hagen W. (1996). The compositions of wax esters, triacylglycerols and phospholipids in Arctic and Antarctic copepods: evidence of energetic adaptations. *Mar. Chem.* **55**, 347-358.
- Boon J. J. (1992). Analytical pyrolysis mass spectrometry: new vistas opened by temperature-resolved in-source PYMS. *Int. J. Mass. Spec. and Ion Process.* **118/119**, 755-787.
- Brown M. R., Dunstan G. A., Norwood S. J., and Miller K. A. (1996). Effects of harvest stage and light on the biochemical composition of the diatom *Thalassiosira pseudonana*. *J. Phycol.* **32**, 64-73.
- Chisholm S. W. (1992). Phytoplankton size. In Falkowski P. G. and Woodhead A. D. (Ed.) *Primary Productivity and Biogeochemical Cycles in the Sea*, Plenum Press.
- Christie W. W. (1973). *Lipid Analysis*, New York, Pergamon Press, 338 pp.
- Columbo J. C., Silverberg N., and Gearing J. N. (1996). Lipid biogeochemistry in the Laurentian Trough: I-fatty acids, sterols and aliphatic hydrocarbons in rapidly settling particles. *Org. Geochem.*, **25**(3/4), 211-225.
- Conte M.H. (1989). The biogeochemistry of particulate lipids in warm-core Gulf Stream ring systems, Ph.D. Thesis, 584 pp.
- Davis J.C. (1986). *Statistics and Data Analysis in Geology*, 2nd Ed. New York, John Wiley and Sons, 646 p.
- Dunstan G. A., Volkman J. K., Barrett S. M., and Garland C. D., (1993). Changes in the lipid composition and maximization of the polyunsaturated fatty acid content of three microalgae grown in mass culture. *J. Appl. Phycol.* **5**, 71-83.
- Eglinton T. I., Boon J. J., Minor E. C., and Olson R. J. (1996). Microscale characterization of algal and related particulate organic matter by direct temperature-resolved mass spectrometry. *Mar. Chem.* **52**, 27-54.
- Erwin J. A. (1973). Comparative biochemistry of fatty acids in eukaryotic microorganisms. In Erwin, J.A. (Ed.), *Lipids and Biomembranes of Eukaryotic Microorganisms*, New York, Academic Press, pp 42-143.

- Falkowski P.G., Flagg C.N., Rowe G.T., Smith S.L., Whittedge T.E., and Wirick C.D. (1988). The fate of a spring phytoplankton bloom: export or oxidation? *Continental Shelf Res.* **8**(5-7), 457-484.
- Flagg C. N., Wirick C. D., and Smith S. L. (1994). The interaction of phytoplankton, zooplankton and currents from 15 months of continuous data in the Mid-Atlantic Bight. *Deep-Sea Res. II*, **41**(2/3), 411-435.
- Goldfine H. (1982). *Curr. Top. Membr. Transp.* **17**, 1-43.
- Hazelwood G. P. and Dawson R. M. C. (1976). A phospholipid-deacylating system of bacteria active in a frozen medium. *Biochem. J.* **153**, 49-53.
- Hoogerbrugge R., Willig S. J., and Kistemaker P. G. (1983). Discriminant analysis by double stage principle component analysis. *Anal. Chem.* **55**, 1710-1712.
- Kuksis A. and Myher J. J. (1989). Lipids. In Lawson, A.M. (Ed.) *Mass Spectrometry*, New York, Walter de Gruyter, p. 267-354.
- Lee R. F., Nevenzel J. C., and Paffenhoffer G. A. (1971). Importance of wax esters and other lipids in the marine food chain: Phytoplankton and copepods. *Mar. Biol.*, **9**, 99-108.
- Michaels A. F., Knap A. H., Dow R. L., Gunderson K., Johnson R. J., Sorenson J., Close A., Knauer G. A., Lohrenz S. E., Asper V. A., Tuel M., and Bidigare R. (1994). Seasonal patterns of ocean biogeochemistry at the U.S. JGOFS Bermuda Atlantic Time-series Study site. *Deep-Sea Res. I*, **41**(7): 1013-1038.
- Parrish C. C. (1988). Dissolved and particulate marine lipid classes: A review. *Mar.Chem.* **23**, 17-40.
- Parsons T. R., Takahashi M., Hargrave B. (1984). *Biological Oceanographic Processes*, 3rd Ed., New York, Pergamon Press, 330 p.
- Roessler P. G. (1990). Environmental control of glycerolipid metabolism in microalgae: Commercial implications and future research directions. *J. Phycol.* **26**, 393-399.
- Verity P. G., Paffenhofer G.-A., Wallace D., Sherr E. and Sherr B. (1996). Composition and biomass of plankton in spring on the Cape Hatteras shelf, with implications for carbon flux. *Continental Shelf Research*, **16**(8), 1087-1116.
- Volkman J. K. (1989). Fatty acids of microalgae used as feedstocks in aquaculture. In: Cambie R. C. (Ed.), *Fats for the Future*, Ellis Horwood, Cichester, pp. 263-283.

Waller G. R. and Dermer (1980). *Biochemical Applications of Mass spectrometry, 1st Supplementary Volume*, New York, Wiley and Sons, 1279 pp.

Wakeham S. G. and Lee C. (1989). Organic geochemistry of particulate organic matter in the ocean: The role of particles in oceanic sedimentary cycles. *Org. Geochem.* **14**(1), 83-96.

Wakeham S. G. and Canuel E. A. (1988). Organic geochemistry of particulate matter in the eastern tropical North Pacific Ocean: Implications for particle dynamics. *J. Mar. Res.* **46**, 183-213.

Windig W., Kistemaker P. G., and Haverkamp J. (1981/1982). Chemical interpretation of differences in pyrolysis-mass spectra of simulated mixtures of biopolymers by factor analysis with graphical rotaion. *J. Anal. Appl. Pyrol* **3**, 199-212.

Wirick C. D. (1994). Exchange of phytoplankton across the continental shelf-slope boundary of the Middle Atlantic Bight during spring 1988. *Deep-Sea Res. II*, **41**(2/3), 391-410.

Chapter 4

The compositional heterogeneity of particulate organic matter from the surface ocean: An investigation using flow cytometry and DT-MS

Abstract

The chemical composition of particulate organic matter (POM) in the surface ocean was investigated by collecting two size classes of POM (large-particle, $>53\ \mu\text{m}$, and small-particle, $<53\ \mu\text{m}$, samples) from a station in Great Harbor, Woods Hole, MA, USA (on a monthly basis) and on transects across the Mid-Atlantic Bight (in March 1996). Broad-band molecular-level characteristics of these POM size classes were obtained via direct temperature-resolved mass spectrometry (DT-MS) coupled with multivariate statistics (principal component analysis and discriminant analysis). The small-particle POM pool was further investigated by using flow cytometric sorting to separate it into "phytoplankton" and "detritus" subclasses, which were then characterized by DT-MS and investigated by multivariate statistics as well. For both the Woods Hole (WHTS) and the Mid-Atlantic Bight (MAB) data sets, the statistical treatments separated POM samples primarily according to their class and subclass distinctions, therefore this paper focuses on the molecular-level differences among large-particle and small-particle POM, "phytoplankton" and "detritus." Small-particle POM is found to be more enriched in protein, phytosterols, diglycerides, and chlorophyll than large-particle POM, which is more enriched in pentose polysaccharide fragments, $\text{C}_{16:0}$ fatty acid, and cholesterol. At the WHTS site, large-particle POM is also enriched in chitin and appears to contain a significant grazer biomass component. In the MAB, large-particle POM appears more phytodetrital. "Phytoplankton" is enriched in protein, chlorophyll, and lipids as compared to "detritus." "Detritus" is enriched in selected polysaccharides and appears to be composed of phytodetritus and /or fecal material.

Introduction

Particulate organic matter (POM) in the surface ocean is a heterogeneous mixture of living and senescent phytoplankton, zooplankton, bacteria, transparent exopolymer particles (TEP, Passow et al., 1994) exuded by diatoms and other cells, fecal pellets, aeolian dust, etc. Such heterogeneity within POM has led to several challenges for marine biologists, chemists, and ecologists who have attempted to study and model aspects of the upper ocean carbon cycle. In phytoplankton research it is difficult to obtain the necessary numbers of pure phytoplankton from natural POM samples for chemical analyses. Analyses of cultured phytoplankton do yield chemical information; but as the molecular-level composition of cultures has been shown to change with culture conditions (e.g., Brown et al., 1996), extrapolation of these results to natural populations is not necessarily straightforward. In studies of organic matter cycling, POM has traditionally been separated by size (i.e., separation on filters) or by "sinking rates" (i.e., filtered material vs. sediment trap material), and chemical analyses have been performed on these subclasses. However, fatty acid and sterol distributions within suspended and sinking POM indicate that there are distinct pools within these size classes (Wakeham and Canuel, 1988; Conte, 1989) which exhibit different source and sink functions. In ecological studies, the role of detrital material in food webs is unclear. However, as estimates of the biomass ratio of non-living to living POM in the surface ocean are often greater than one and can approach 10 (Caron et al., 1995; Gassman and Gillbricht, 1982; Pomeroy, 1980), understanding the chemical composition of detritus could prove very important (Verity et al., 1996).

Direct temperature-resolved mass spectrometry (DT-MS) allows rapid broad-band molecular-level characterization of microgram quantities of organic matter (Boon, 1992; Eglinton et al., 1996). Coupled with multivariate analytical techniques, it is a useful screening technique for probing molecular-level variations in POM data sets too large to be easily sampled or measured by traditional techniques. In addition, the sensitivity of

DT-MS facilitates its coupling with techniques for micro-manipulation of samples. Flow cytometric sorting is one such technique which can separate particles on the basis of morphological and chemical characteristics, such as shape or presence of calcium carbonate liths (Olson et al., 1989), in addition to size. While such particle class distinctions are somewhat arbitrary, flow cytometry (FCM) can provide an initial step in exploring POM heterogeneity.

This chapter describes initial results from the study of oceanic POM by flow cytometry and DT-MS. Temporal (seasonal) variability in surface-ocean POM was investigated using samples collected from Great Harbor, Woods Hole over a three year period, and spatial variability in POM was studied in samples obtained in early spring on transects along the Mid-Atlantic Bight (MAB). The POM samples were separated into large-particle ($>53\text{ }\mu\text{m}$) and small-particle pools ($<53\text{ }\mu\text{m}$) with the small-particle pool further separated into "phytoplankton" and "detritus." The molecular-level variations among and within these pools were then explored via DT-MS and multivariate analyses. The result of these statistical treatments was a separation of POM samples based primarily on their class distinctions (large-particle POM, small-particle POM, "phytoplankton" and "detritus") rather than location or season. Therefore, this chapter will focus on the molecular-level differences among these classes and subclasses of surface-ocean POM.

Experimental

To study potential seasonal variations in POM, surface-water ($\sim 1\text{ m}$ depth) samples were collected on a monthly basis from a site in Great Harbor, Woods Hole, MA (station WH, Fig. 4.1) from November 1994 to February 1997. The site is very close to that used by Wainright and Fry (1994) and its background information, described there, will be briefly summarized here. The WHTS (Woods Hole Time Series) site has semi-diurnal tides ($<1\text{ m}$ amplitude), experiences strong mixing due to tidal currents, and, due

EN279 and WHTS Sampling Stations

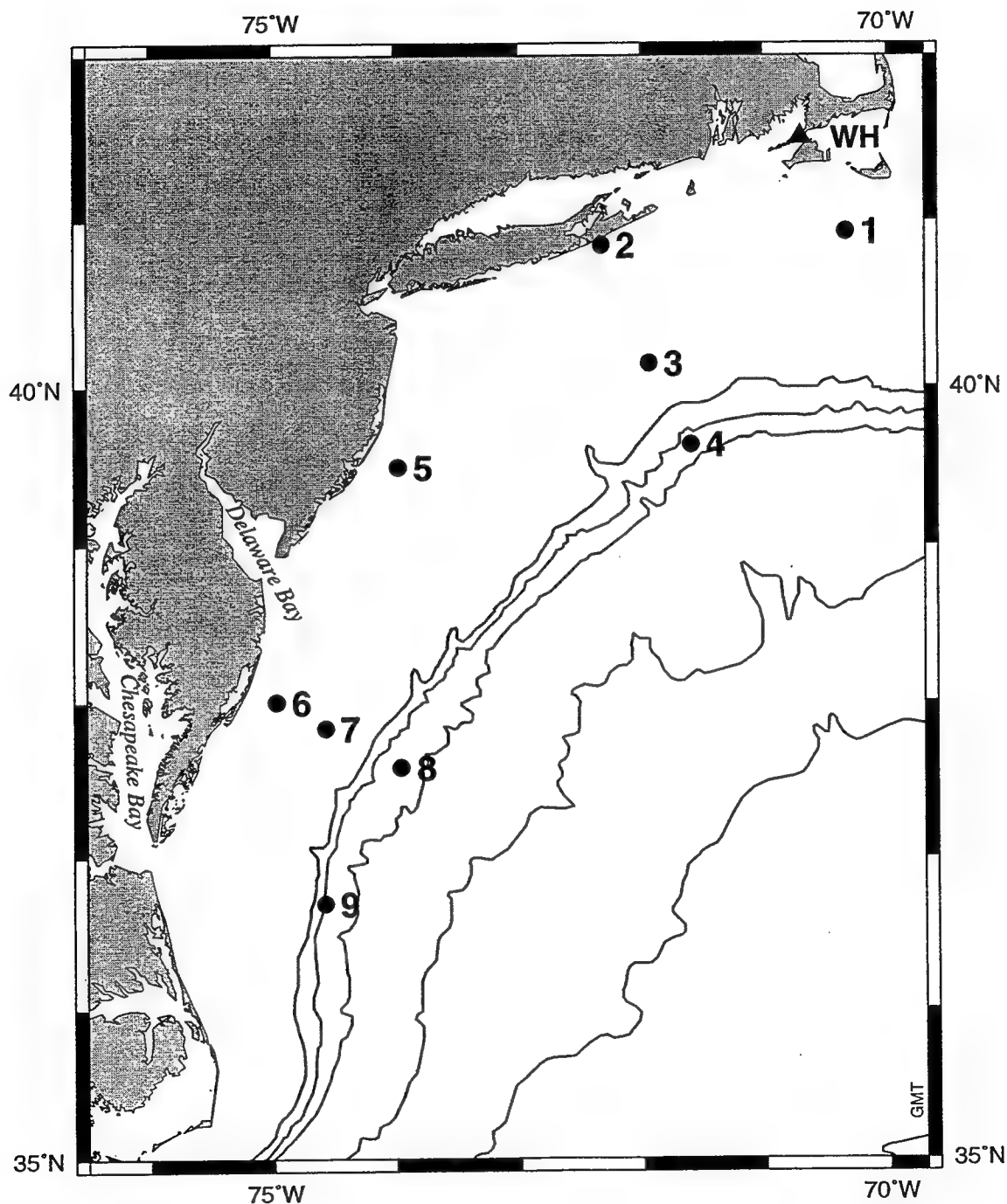


Fig. 4.1. Map showing the monthly sampling station in Great Harbor, Woods Hole, MA (WH) and the sampling stations for cruise EN279 (March 1996). Contour levels represent water depths (200 m, 1000 m, 2000 m, 3000 m, 4000 m, and 5000 m).

to its location, is exposed to water from both Buzzards Bay and Vineyard Sound. It has a fairly constant salinity of 32 psu and a depth of 3 m (for all but two samples, see experimental section). Benthic algae and *Zostera marina* (a seagrass) are present in addition to phytoplankton, zooplankton, bacteria, and detritus in the water column. Nitrate and phosphate concentrations peak in December (at approximately 1 μM as opposed to ≤ 0.2 μM in other months). Great Harbor POC/chlorophyll, C/N and planktonic $\delta^{13}\text{C}$ values are very similar to those on Georges Bank, indicating that Great Harbor can be considered a marine system with primarily autochthonous organic matter (Wainright and Fry, 1994).

For an initial view of spatial variation in POM, surface water (from approximately 3 m depth) was collected from the MAB on multiple transects across the shelf (Cruise EN279, March 1996, see Fig. 4.1). The MAB is a region characterized by a permanent thermohaline front between shelf and slope waters and a general southwestward drift of its shelf waters. To the south it is influenced by freshwater discharges from the Delaware and Chesapeake Bays. Throughout its length it interacts with the Gulf Stream and its eddies (Biscaye et al., 1994). During the EN279 transects, nitrate varied from less than 0.1 μM to 5.3 μM ; phosphate from 0.15 to 0.56 μM . Salinity and temperature (as determined by an on-board SAIL system) varied between 32.27 and 35.25 psu and 2.67 and 9.68°C, respectively, and were comparable to literature values for early spring in the SEEP-II study region of the MAB. As in Biscaye et al. (1994), the inner shelf waters were colder and fresher (2.67 to 4.5°C and 32.27 to 32.59 psu), while those stations off the shelf break were warmer and more saline (8.03 to 9.68°C and 33.24 to 35.25 psu).

The analytical method used for both the WHTS and MAB data sets is outlined in Fig. 4.2 (see also Chapter 2). Seawater was collected via diaphragm or peristaltic pump and prefiltered through a nylon 53 μm screen to separate large-particle from small-particle POM (as in Bishop and Edmond, 1976). Tangential flow filtration or TFF (0.8

ANALYTICAL SCHEME

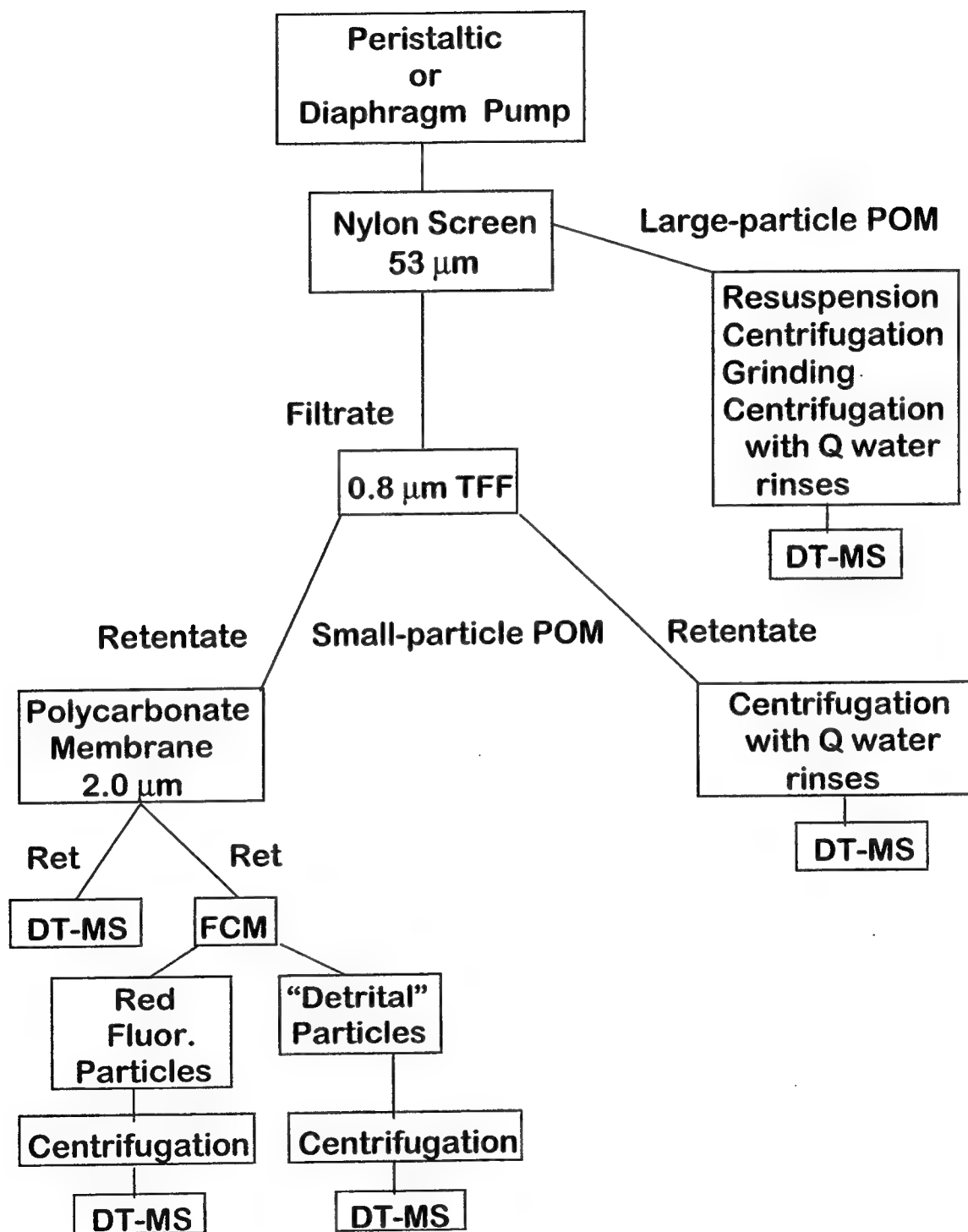


Fig. 4.2. The analytical scheme used for the MAB and WHTS samples.

μm Fluoro centasette and ultrasette, Filtron, driven by Masterflex peristaltic pumps using Pharmed tubing) concentrated the smaller particles while keeping them suspended in seawater. Typically, 4 L to 100 L were concentrated to approximately 100 mL; the larger initial volumes were necessary in order to obtain enough material for measurement by ancillary analytical techniques. For the WHTS samples, 3-15 mL aliquots of this TFF retentate were concentrated by centrifugation (4 minutes at 10,500xG on a Fisher Micro-Centrifuge, Model 59A using polypropylene Eppendorf Safe-Twist Screw Cap Micro Centrifuge Tubes with polyethylene copolymer caps; the centrifuge tubes and caps were solvent-rinsed with methanol and dichloromethane prior to use). The resulting pellet of small-particle POM was desalted in the following manner: the pellet was resuspended in 1 mL of deionized water or Milli-Q™ water and centrifuged as above, the supernatant was discarded, and the rinsing step was repeated twice. Large-particle POM was resuspended off the nylon screen, concentrated by centrifugation (10 minutes at ~1800xG on an IEC HN-SII centrifuge, Damon/IEC Division), homogenized via Teflon tissue grinder, and then desalted as above. Samples were stored in liquid nitrogen after tangential flow filtration and/or after centrifugation as necessary.

For flow cytometric sorting of small-particle POM, two further filtration steps were necessary. The $>0.8 \mu\text{m}$ retentate was filtered onto a $2 \mu\text{m}$ polycarbonate membrane filter (Poretics) using a slight vacuum ($<5 \text{ psi}$); the sample was rinsed with and resuspended in $<0.2 \mu\text{m}$ syringe-filtered seawater and then placed in liquid nitrogen to await flow cytometry. Just prior to sorting the sample was thawed and syringe-filtered through a $53 \mu\text{m}$ nylon screen to remove any aggregates that might have clogged the flow cell tip. To facilitate comparison with flow cytometrically sorted samples, additional $>2 \mu\text{m}$ POM from the MAB was concentrated and desalted by centrifugation as above. This constituted small-particle POM in the MAB data set. Therefore, in this chapter, small-particle POM for WHTS samples was $>0.8 \mu\text{m}$, $<53 \mu\text{m}$, while for the MAB data set the analogous POM pool was $>2 \mu\text{m}$, $<53 \mu\text{m}$. "Phytoplankton" and "detritus" from both the WHTS and the MAB data sets were $>2 \mu\text{m}$, $<53 \mu\text{m}$.

Flow cytometry was performed on an EPICS V flow cytometer (Coulter, Inc.) using a Cicero data acquisition system (Cytomation, Inc.), a standard lens assembly, a 100 μm jet-in-air flow cell, excitation at 488 nm with a 130 mW laser beam and detector settings optimized for eukaryotic phytoplankton. Small-particle POM ($>2\ \mu\text{m}$, $<53\ \mu\text{m}$) was separated into "phytoplankton" and "detritus" based on forward angle light scatter and red fluorescence measurements. Sort purities were assessed by taking aliquots of original sample and the two sorted samples, adding a fluorescent bead internal standard and re-running the aliquots. Desalting of sorted samples was performed by using Milli-QTM water sheath fluid during flow cytometry and by centrifuging the resulting samples.

Sample pellets, resuspended in a small quantity of Milli-QTM water, were analyzed in triplicate via DT-MS on a VG AutospecQ magnetic sector instrument (16 eV EI^+ , acceleration voltage 8.0 kV, direct inlet, mass range 41-795, scan speed 2 s, resolution 1000) with the sample probe (a platinum/rhodium (87/13) wire, 0.125 mm diam.) resistively heated to just below the melting point of the wire. To reduce the resulting information to a manageable level, spectra were then exported to a multivariate statistics program and molecular-level differences among the spectra were investigated using principal component and discriminant analyses (as in Saliot et al., 1984; Eglinton et al., 1992, and others; for further discussion of DT-MS applications in marine organic geochemistry, see Eglinton et al., 1996). In the present study, mass spectra for each run were summed over the entire region of the total ion chromatogram (TIC), averaged to the nearest integer value (with a mass defect of 0.7 or 0.75 applied), and exported to Chemometricks (a MATLAB-based program developed at FOM-AMOLF and further modified at WHOI). Overloaded spectra, m/z values related to salt contamination and one outlier sample (in the EN279 data set) resulting from poor sample preparation were removed from the data sets prior to analysis.

For comparison with DT-MS spectra of natural POM samples, a mixed algal standard was made by combining aliquots of concentrated cultures of *Emiliana huxleyi*, *Phaeodactylum tricornutum*, and *Pycnococcus provasolii*. Each of these phytoplankton

was grown in 10 L batch cultures in modified F/2 medium (made using <0.2 μ m filtered Vineyard Sound seawater) kept at 19°C on a 14:10 light:dark cycle and bubbled with air. The cultures were harvested via centrifugation (20 minutes at 1500 rpm, IEC Model K Centrifuge) when the cell densities reached 290,000 cells/mL, 2,900,000 cells/mL, and 2,500,000 cells/mL respectively. Just prior to DT-MS, the mixed algal standard was desalted via the procedure used for suspended POM samples.

Chitin fragments in DT-MS analyses of natural particles were identified by comparison with analyses of a chitin standard (poly-[1 \rightarrow 4]- β -N-acetyl-D-glucosamine, purified powder from crab shells, Sigma).

Discriminant analysis, in this case a two-stage principal component analysis (Hoogerbrugge et al., 1983) was used to maximize variance between samples and to minimize variance among replicate mass spectrometric analyses of the samples. Score plots resulting from this statistical technique reflect relationships among the samples and reconstructed spectra from the discriminant functions indicate the relationships among variables, i.e. m/z values, causing the relationships among samples. These m/z values can be tentatively identified (in this case based mainly on literature values reported in Eglinton et al., 1996, and Meuzelaar et al., 1982) and the spectra can be interpreted as showing broad-band molecular-level differences among the samples in the data set. It should be emphasized that the reconstructed discriminant spectra are difference spectra; those chemical characteristics shared by all the samples in the discriminant analysis will not appear. Therefore the average or zero-point spectrum for each class or subclass of POM (in other words, the spectrum removed in the z-scoring step of multivariate analysis of that class or subclass) is also provided for both the WHTS and MAB data sets. It should also be emphasized that DT-MS linked to discriminant analysis is not a quantitative technique. Compound classes vary in response factor and sensitivity to matrix effects; therefore, the contribution of a particular ion to a mass spectrum is not necessarily a simple function of the concentration of the precursor compound in the sample. Finally, it should be mentioned that discriminant analysis results are sensitive to

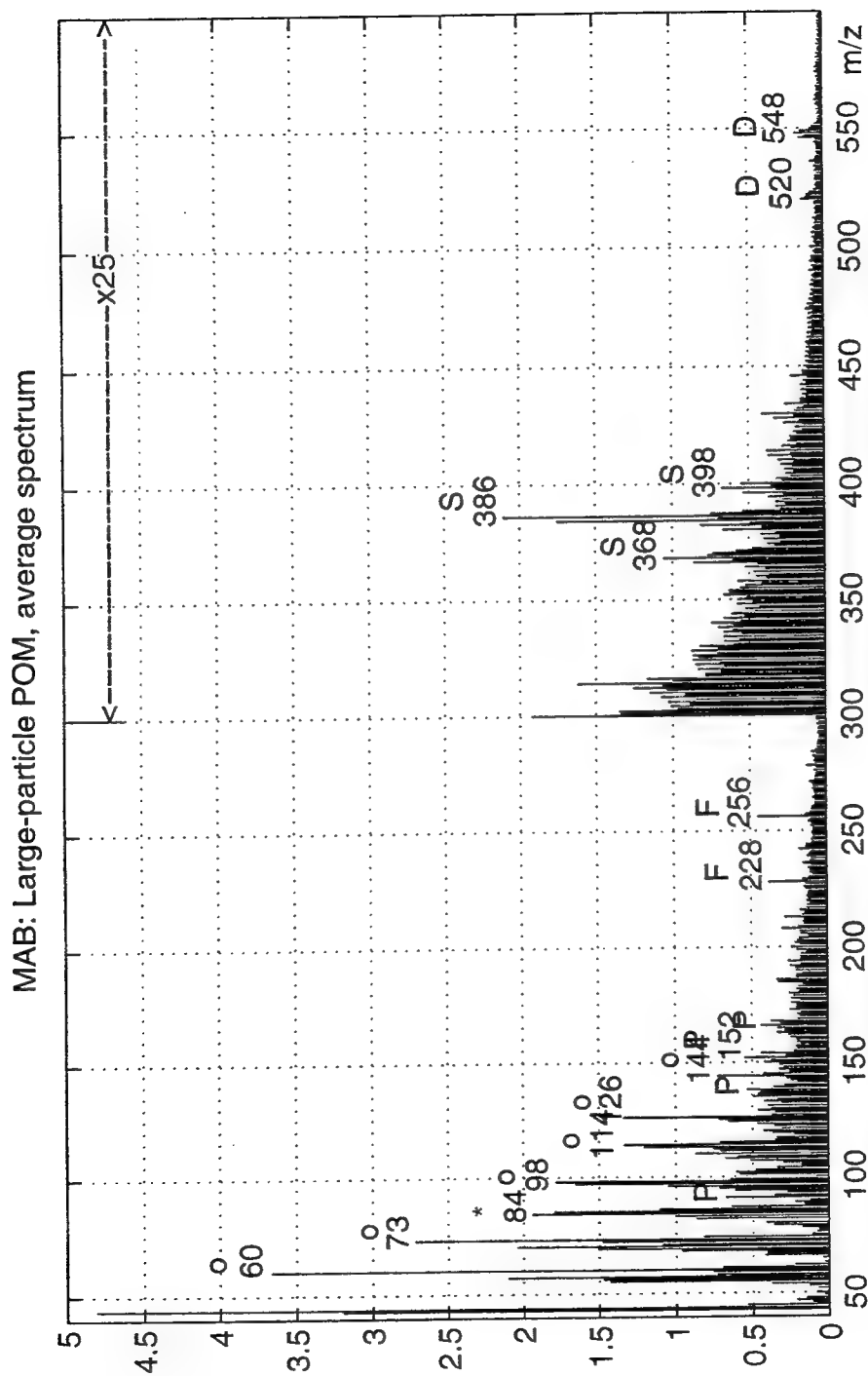


Fig. 4.3a. The average spectrum for large-particle POM from the MAB (generated via Chemometrics, a MATLAB-based program developed at FOM and further modified at WHOI). The latter half of the spectrum (beginning with m/z 300) is magnified 25x for better viewing. Symbols used for all spectra: o=polysaccharide, P=protein, F=fatty acid, S=sterol, D=diglyceride, *=chitin, N=nucleic acid.

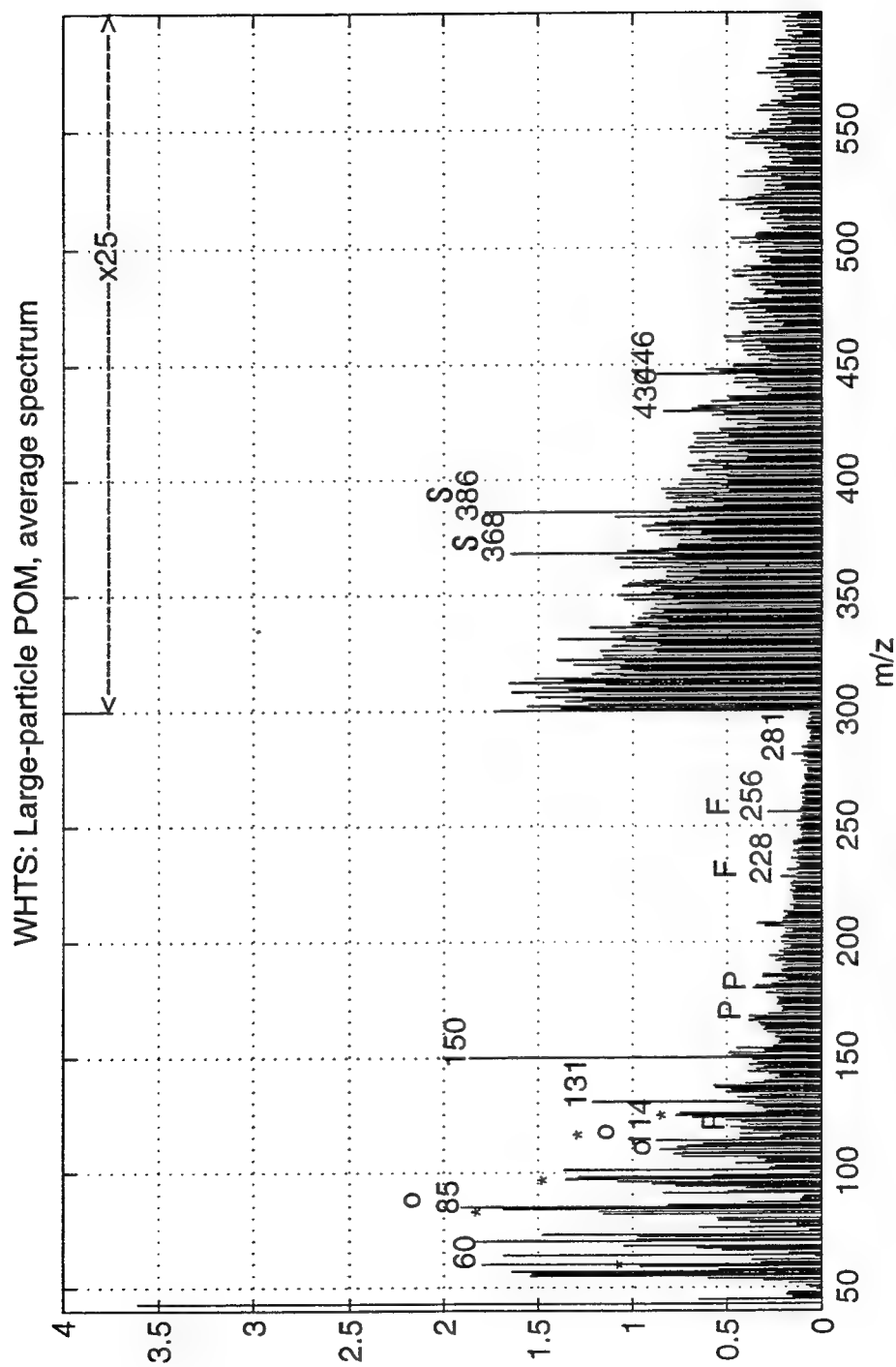


Fig. 4.3b. The average spectrum for large-particle POM from the WHTS.

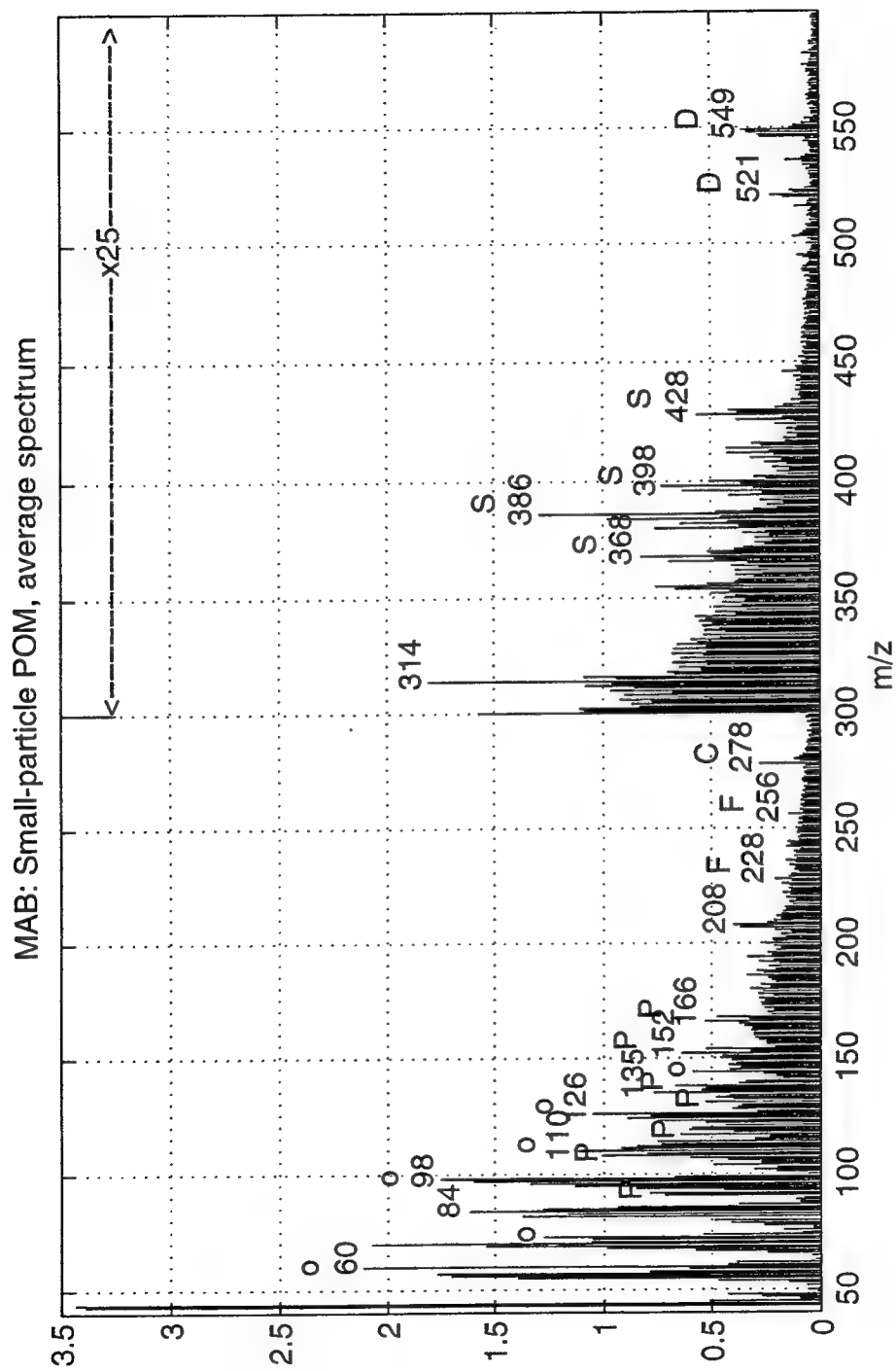


Fig. 4.4a. The average spectrum for small-particle POM from the MAB.

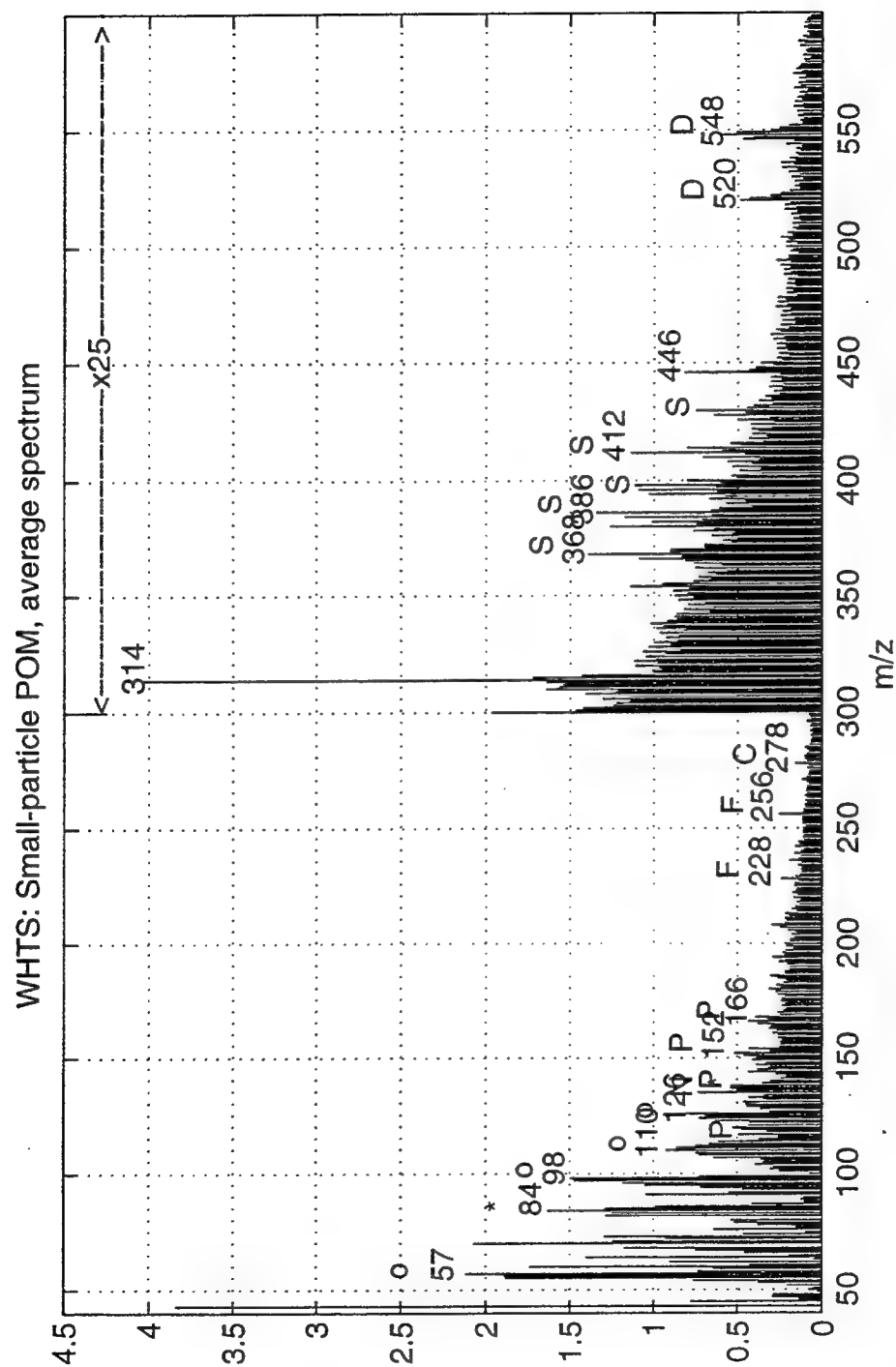


Fig. 4.4b. The average spectrum for small-particle POM from the WHTS.

the number of principle components used in the second stage of the analysis. In this work one quarter of the initial principal components were used for initial discriminant analysis (Hoogerbrugge et al., 1983). Sometimes, within this one quarter there were principal components that explained very little of the variance in the data set; these were removed from consideration as necessary.

Results

The following results and discussion are limited to molecular-level differences among the large-particle, small-particle, "phytoplankton," and "detrital" subclasses of POM. As a result of this focus, the conclusions reached are based on a time-averaged view of POM at the WHTS site and a spatially-averaged view of POM collected from the MAB in March, 1996.

Large-particle and small-particle POM: Average spectra

The zero-point spectra from discriminant analyses of large-particle POM from the MAB and WHTS data sets are shown in Fig 4.3. These spectra can be thought of as average spectra for large-particle POM from the MAB in early spring and from the WHTS station throughout the year.

Saccharides and proteins appear most dominant in both spectra. As polysaccharides and proteins have very low response factors in EI^+ DT-MS relative to the lipids (see Chapter 2), they are actually even more predominant in these samples. Both spectra contain strong saccharide signals (m/z 57, 60, 73, 98, 126, and 144 from fragments of hexose sugars, and 85 and 114 from fragments of pentose sugars) and indicate the presence of amino sugar fragments, probably from chitin (m/z 59, 72, 83, 84, 111, 114, 125, 139). $\text{NH}_3\text{-CI}^+$ DT-MS of representative samples (see Chapter 5) was used to obtain further information about the saccharides. A significant component of the

hexose sugar appears to be polysaccharidic as indicated by ion series for oligomers up to tetrahexose (MAB sample) or trihexose (WHTS sample). The $\text{NH}_3\text{-Cl}^+$ DT-MS spectra also provide further evidence for the presence of chitin in both data sets as the analogous ion series appears in both representative samples; however, it is significantly more prominent in the WHTS sample. The spectra of both sets of large-particle POM also contained m/z values identified as a protein signature, though this is as yet unconfirmed by ancillary analyses.

The average spectra also contains information on the lipid component of large-particle POM. The MAB samples display a more intense fatty acid signature, but both sets of particles contain $\text{C}_{14:0}$ (m/z 228), $\text{C}_{16:0}$ (m/z 256), and $\text{C}_{16:1}$ (present as the molecular ion- H_2O , m/z 236) fatty acids. These mass unit identifications are strengthened by the comparison of DT-MS (16eV EI^+) spectra and GC-MS spectra of transesterified and derivatized (with BSTFA) total lipid extracts from WHTS 5, small-particle POM (see Appendix 2). Both sets contain m/z 278, identified as phytadiene from chlorophyll in the samples (as determined by correlation between m/z values 278, 296, and 300 in, respectively, EI^+ , $\text{NH}_3\text{-Cl}^+$, and $\text{ND}_3\text{-Cl}^+$ mass spectra of the MAB samples 2-S and 9-G, see Chapter 5). The most dominant sterol in both data sets is cholesterol (m/z 386, the molecular ion, and 368, $\text{M-H}_2\text{O}$, identified by analogy to WHTS 5, see Appendix 2), though the MAB data set contains a more complete suite of C_{27-30} sterols (including m/z 380, 384, 396, 398, 400, 414, 428). The MAB particles yield a fairly strong diglyceride signal (m/z 520, probably from a $\text{C}_{14:0}/\text{C}_{16:1}$ diglyceride, and m/z 546 and 548, probably from mono and di-unsaturated $\text{C}_{16}/\text{C}_{16}$ diglycerides; see Chapter 3 for details on diglyceride signatures). These m/z values are present but not prominent in the WHTS data set.

The average small-particle POM spectra from the two data sets (i.e., the zero-point spectra from discriminant analyses) are shown in Fig. 4.4. As in the large-particle spectra, both sets of small-particle POM yield strong polysaccharide signals, including m/z values indicating the presence of chitin. Given the contribution of phytoplankton to

Mid-Atlantic Bight:
Large-particle and Small-particle POM

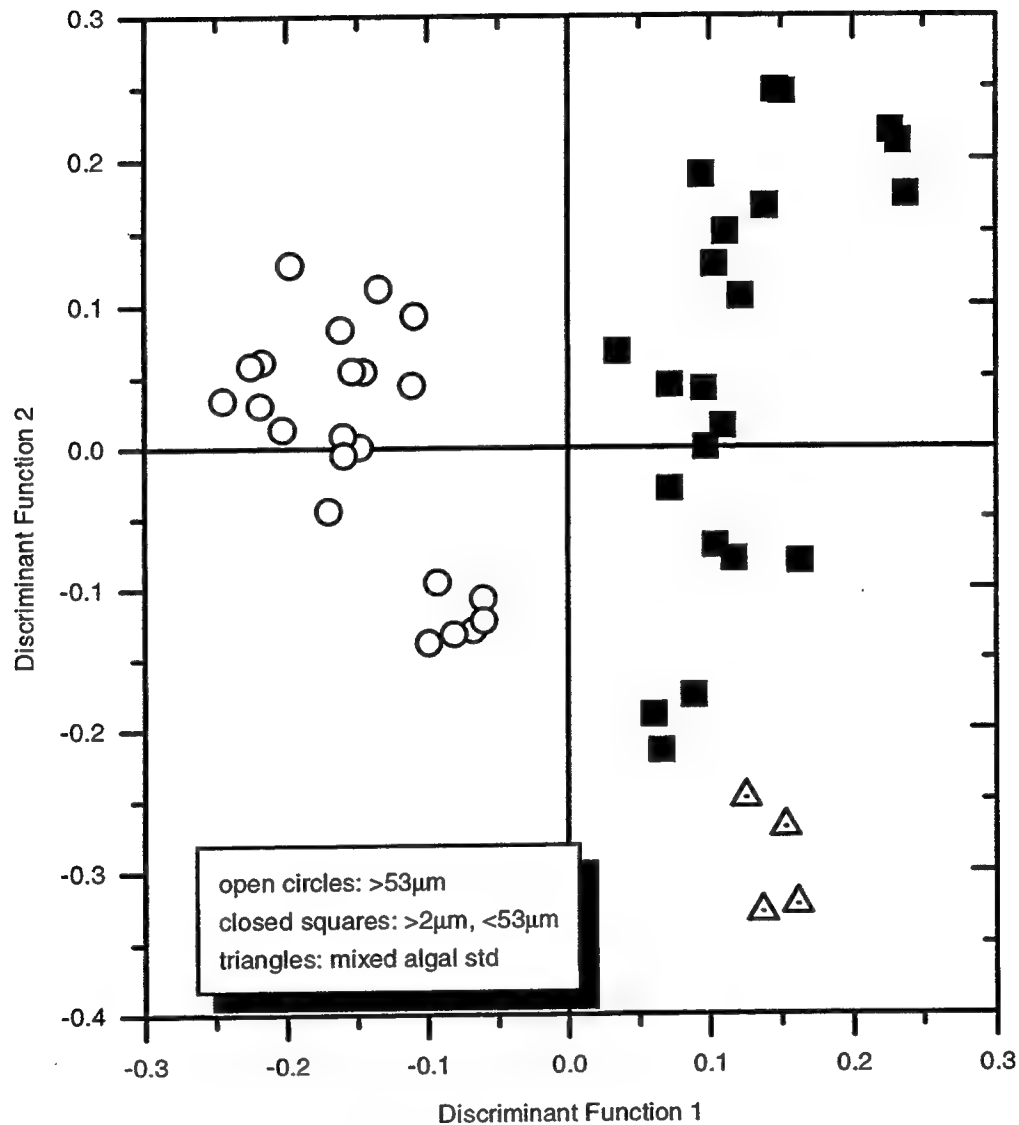


Fig. 4.5a. The score plot from discriminant analysis of large-particle and small-particle POM from the MAB. Discriminant Function 1 (DF1) clearly separates the >53 μm POM from the >2 μm, <53 μm POM, while the smaller particles plot in the same region in DF1 as a mixed algal standard (see Experimental Section).

MAB: Large-particle vs Small-particle POM, DF1

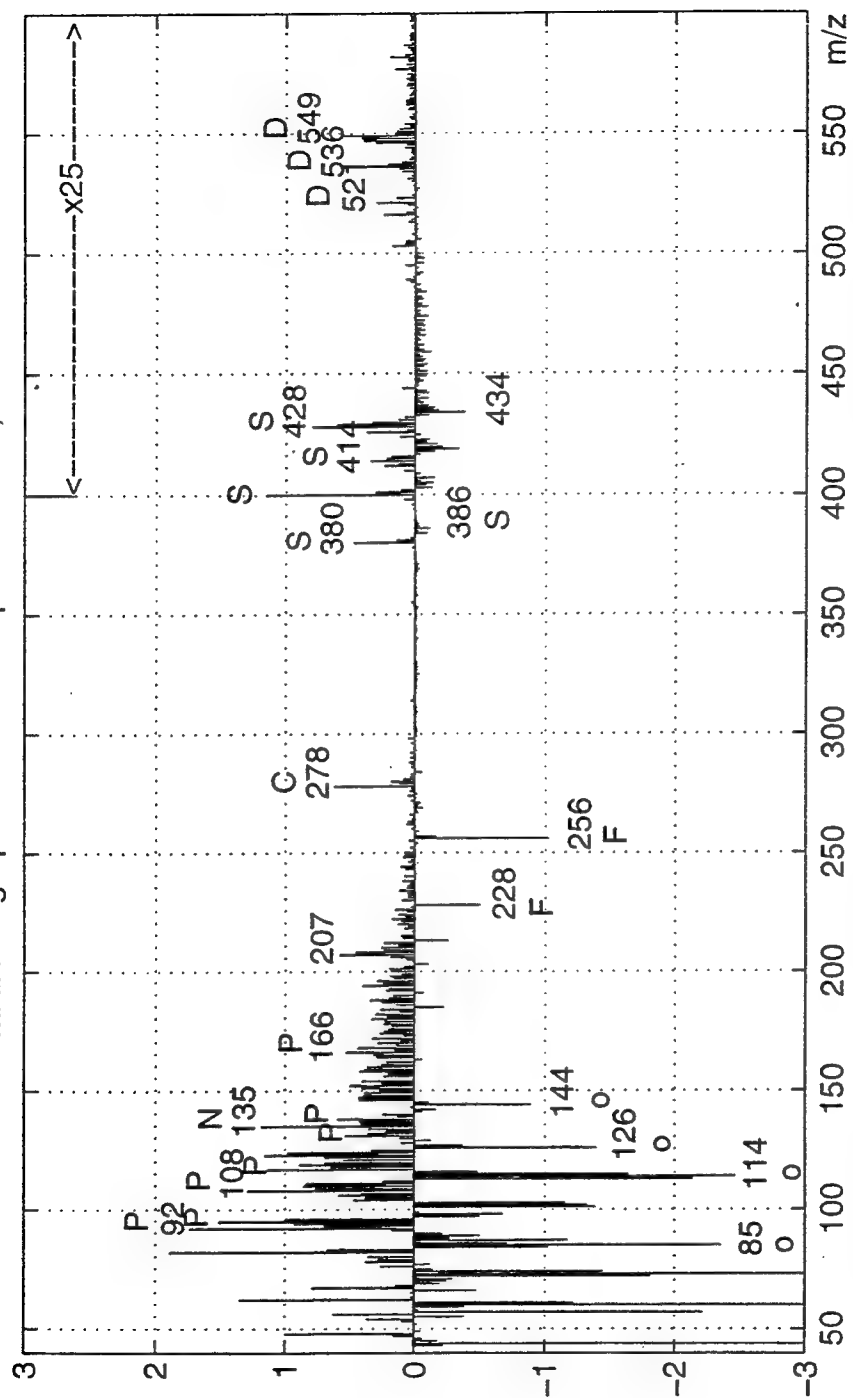


Fig. 4.5b. The reconstructed spectrum for Discriminant Function 1 (see Fig. 3 for the symbol key). DF+, the region the smaller particles and the mixed algal standard plot within, is characterized by enrichment in protein, nucleic acid, chlorophyll, phytosterols, and diglycerides. DF-, in which the larger particles fall, exhibits enrichment in polysaccharides, fatty acids, and cholesterol.

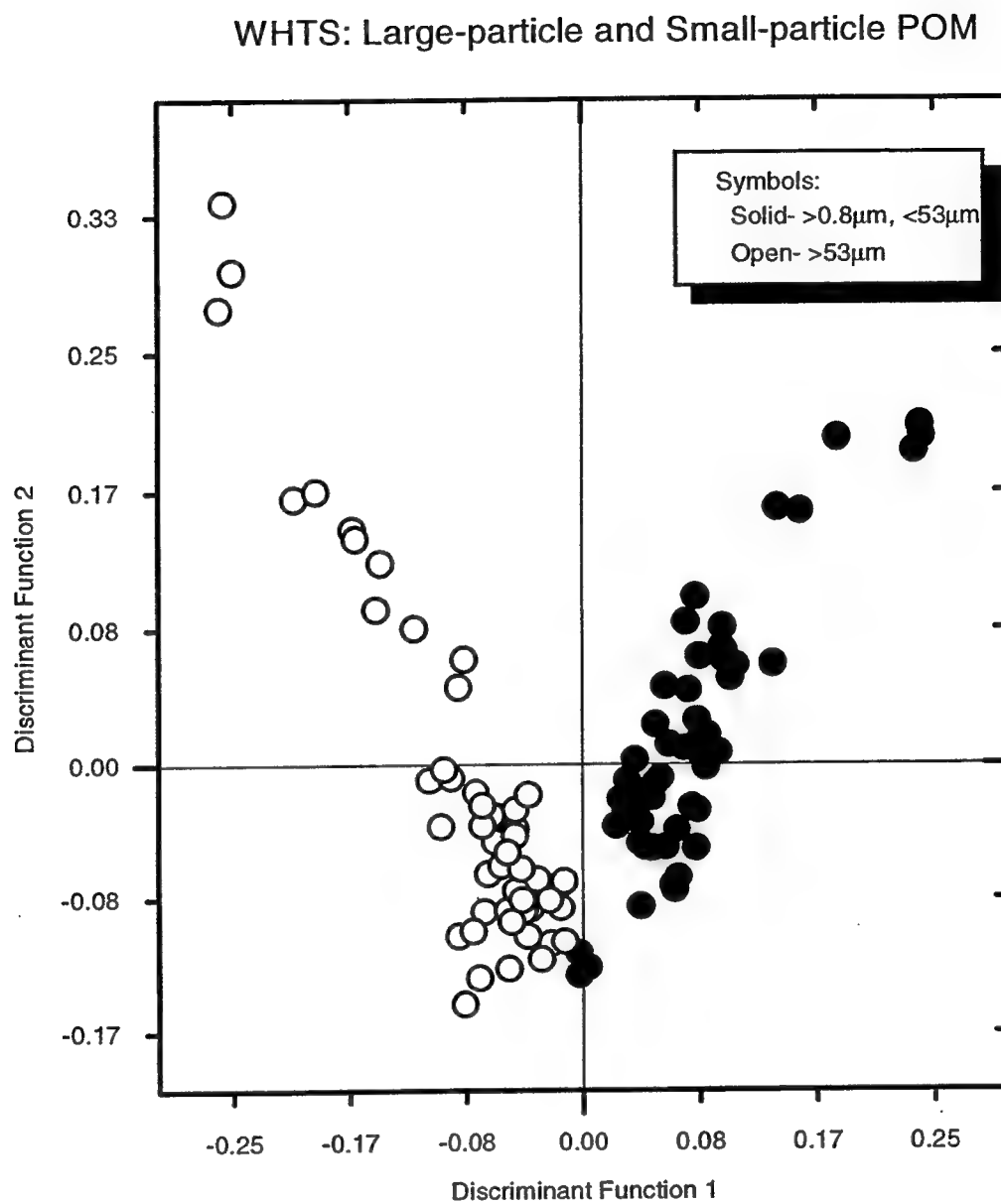


Fig. 4.6a. The score plot from discriminant analysis of large-particle and small-particle POM from the WHTS.

WHTS: Large-particle vs Small-particle POM, DF1

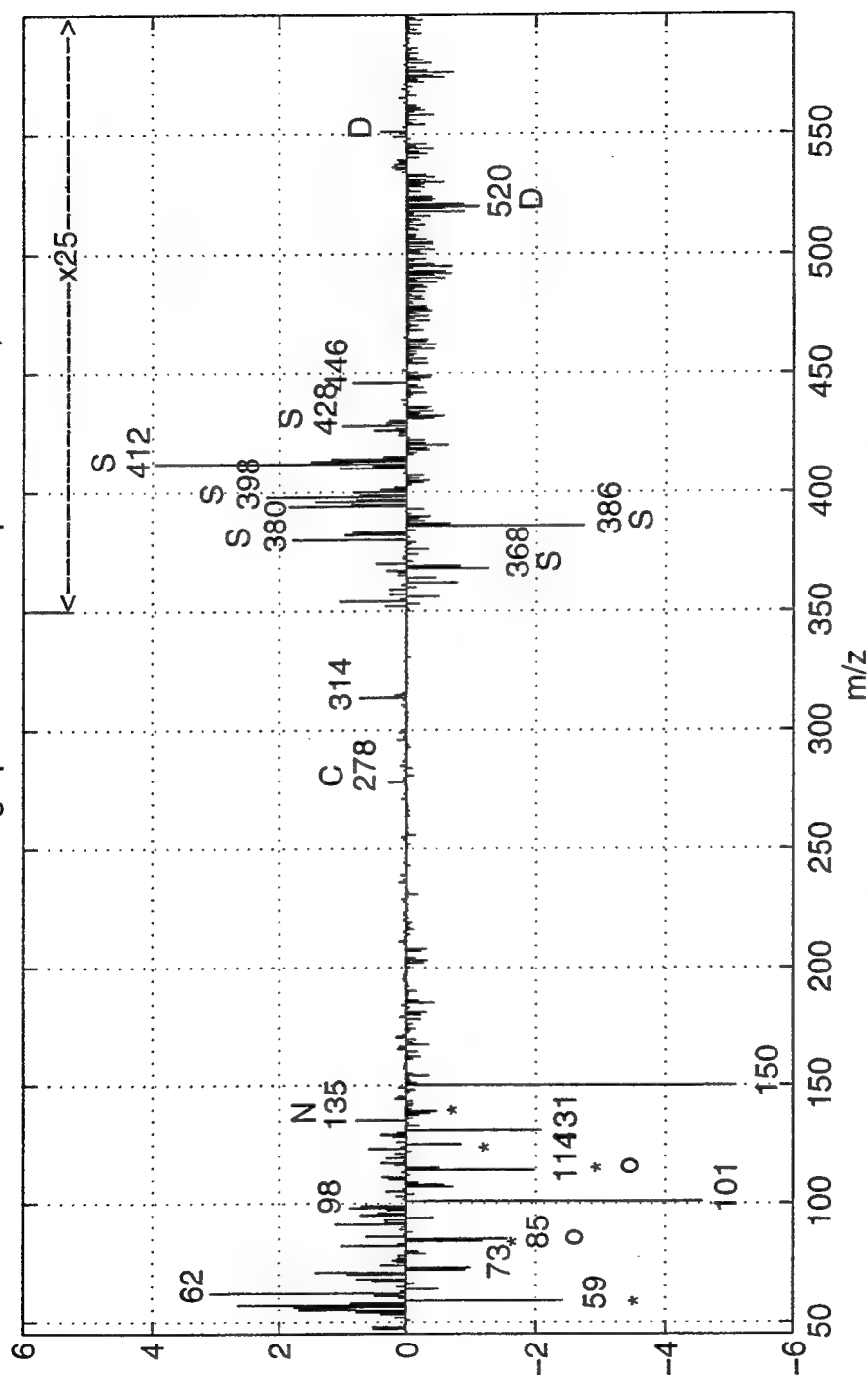


Fig. 4.6b. The reconstructed spectrum for DF1. DF+, in which the small-particle POM plots, is characterized by enrichment in nucleic acid, chlorophyll, phytosterols, and the diglyceride m/z 551. DF-, in which the large-particle POM plots, is enriched in chitin fragments, pentose polysaccharide fragments, cholesterol, and the diglyceride m/z 520.

this particle class, there are also, unsurprisingly, strong protein signals (m/z 92, 94, 108, 117, 120, 124, 125, 138, 152, 166, 180). The $C_{14:0}$, $C_{16:0}$, and $C_{16:1}$ fatty acids are again present. Phytadiene from chlorophyll appears particularly strong. Cholesterol is again a dominant sterol but other sterols (C_{28} , C_{29} , and C_{30} , of varying degrees of unsaturation) are also present in significant quantities (e.g., m/z 380, 396, 398, 412, 414, 428). Diglyceride fragments are present in both sets of small-particle POM, although the MAB diglyceride fragments appear to be from other, larger molecules (possibly triglycerides) as their m/z values are odd, rather than even.

Large-particle vs. small-particle POM: Discriminant analysis

While such average, or zero-point, spectra indicate the average chemical composition of these classes of POM, the focus of discriminant analysis is to highlight chemical differences between samples or groups of samples. Large-particle and small-particle POM from the MAB and WHTS data sets were analyzed via this technique, with discriminant analysis used to reduce variance among replicate DT-MS analyses. In both cases, the first discriminant function, responsible for the largest amount of variance among samples, separated the large-particle POM samples from their small-particle counterparts.

Results from the MAB data set are shown in Fig. 5. The score plot in Fig. 4.5a illustrates the clear separation of $>53\ \mu\text{m}$ and $>2\ \mu\text{m}$, $<53\ \mu\text{m}$ particles along Discriminant Function 1 (responsible for 13% of the variance in the entire data set) and also indicates that the smaller particles were more phytoplanktonic (they fall in the same half of the plot as the mixed algal standard). The loadings plot for Discriminant Function 1 (Fig. 4.5b) shows that the small-particle POM is enriched in protein (m/z 48, 92, 94, 108, 117, 120, 124, 131, 138, 152, 166, 180), chlorophyll (m/z 278), nucleic acids (m/z 135), phytosterols (m/z 380, 398, 428), and diglycerides (m/z 521, 536, 549), while the

larger particles appear enriched in polysaccharides (m/z 57, 60, 73, 85, 98, 114, 126, 144), saturated fatty acids (m/z 228, 256, 284) and cholesterol (m/z 386).

Fig. 4.6 illustrates the results from the WHTS data set. Again Discriminant Function 1 separates large-particle POM ($>53\ \mu\text{m}$) and small-particle ($>0.8\ \mu\text{m}$, $<53\ \mu\text{m}$) POM. It should be mentioned that, in this case, Discriminant Function 1 only explains 5.6% of the variance of the total data set; we believe this is due to the introduction of variance from sample handling (i.e., a low-level hydrocarbon contamination from the Masterflex Pharmed tubing in the peristaltic pump) in the collection of $>53\ \mu\text{m}$ particle samples. The smaller particles from Great Harbor also show enhancement of phytoplankton characteristics, being enriched in phytosterol and chlorophyll fragments as compared to the larger particles. Large-particle POM from this station is enriched in pentose polysaccharide fragments (m/z 85, 114), chitin fragments (m/z 59, 72, 84, 114, 125, 139), $\text{C}_{16:0}$ fatty acid (m/z 256) and cholesterol (m/z 368, 386). The diglyceride signal is split between small-particle POM (m/z 551) and large-particle POM (m/z 520).

The V-pattern within the score plot in Fig. 4.6a appears curious yet so far defies explanation. There appears to be no relationship between the pattern and season, [POC]/[chlorophyll a], seawater chlorophyll a concentration, the ratio of phytoplankton counts to total particle counts (as determined by flow cytometry), or [POC].

“Phytoplankton” and “detritus”: Average spectra

Small-particle POM from both the MAB and the WHTS was further investigated by using flow cytometry to physically separate “phytoplankton” and “detritus” subclasses from this POM size class. In this case, as opposed to the WHTS small-particle samples described above, the POM size-class was defined as $>2.0\ \mu\text{m}$, $<53\ \mu\text{m}$; a smaller size cutoff proved impractical for flow cytometric sorting. “Phytoplankton” was separated on the basis of red (chlorophyll) fluorescence after excitation with a 488 nm laser beam and “detritus” was defined as particles with the same forward angle light scatter (used as a

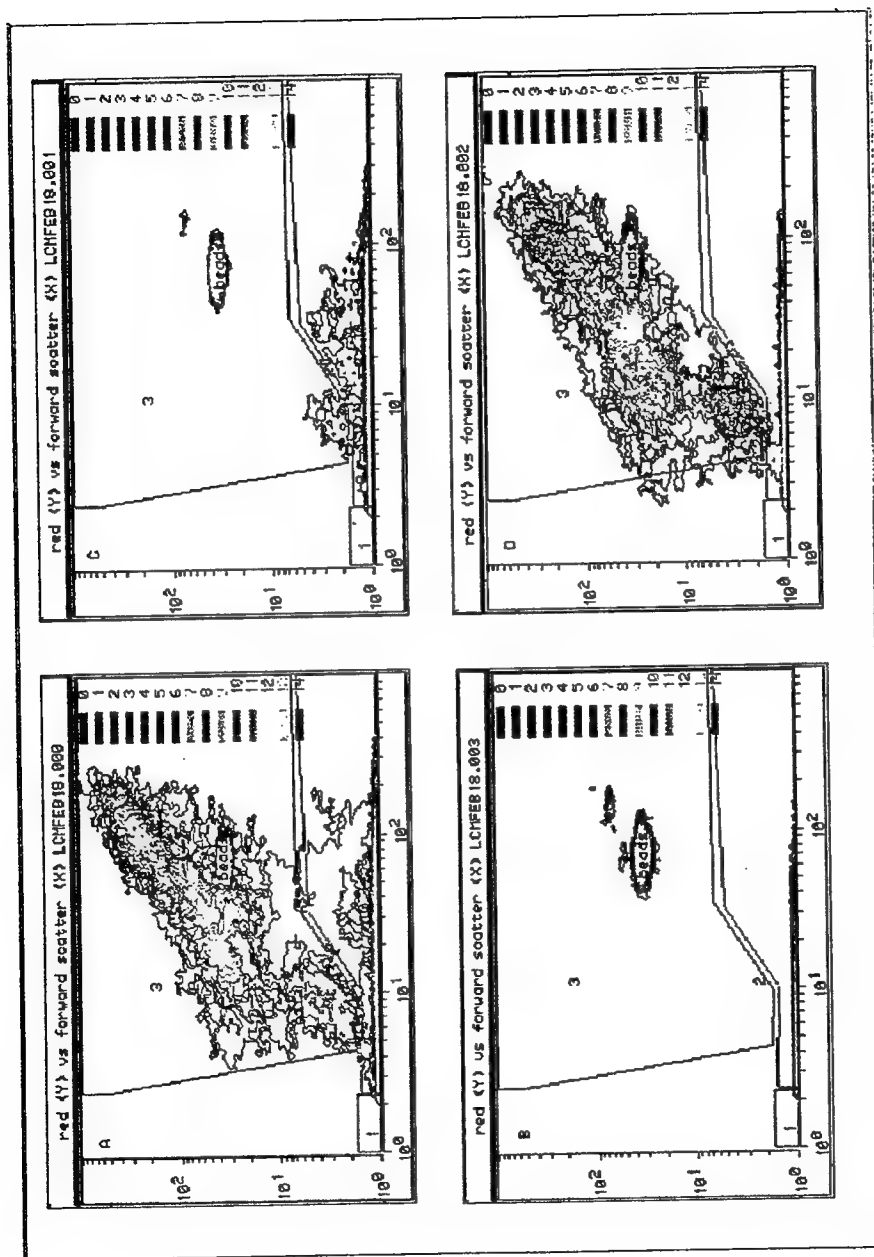


Fig. 4.7. The flow cytometry sort windows for sample WHTS13; region 2 contains "detritus;" region 3, "phytoplankton" and fluorescent beads (as an internal standard). (A) shows the original $>2 \mu\text{m}$, $<53 \mu\text{m}$ POM sample; (B) shows the flow cytometry blank (consisting of sodium chloride solution and fluorescent beads); (C) results from flow cytometric analysis of an aliquot of the "detrital" sort; (D) shows flow cytometric analysis of an aliquot of the "phytoplankton" sort.

**Mid-Atlantic Bight POM:
FCM analysis of total >2 μ m POM, "phytoplankton" and
"detritus"**

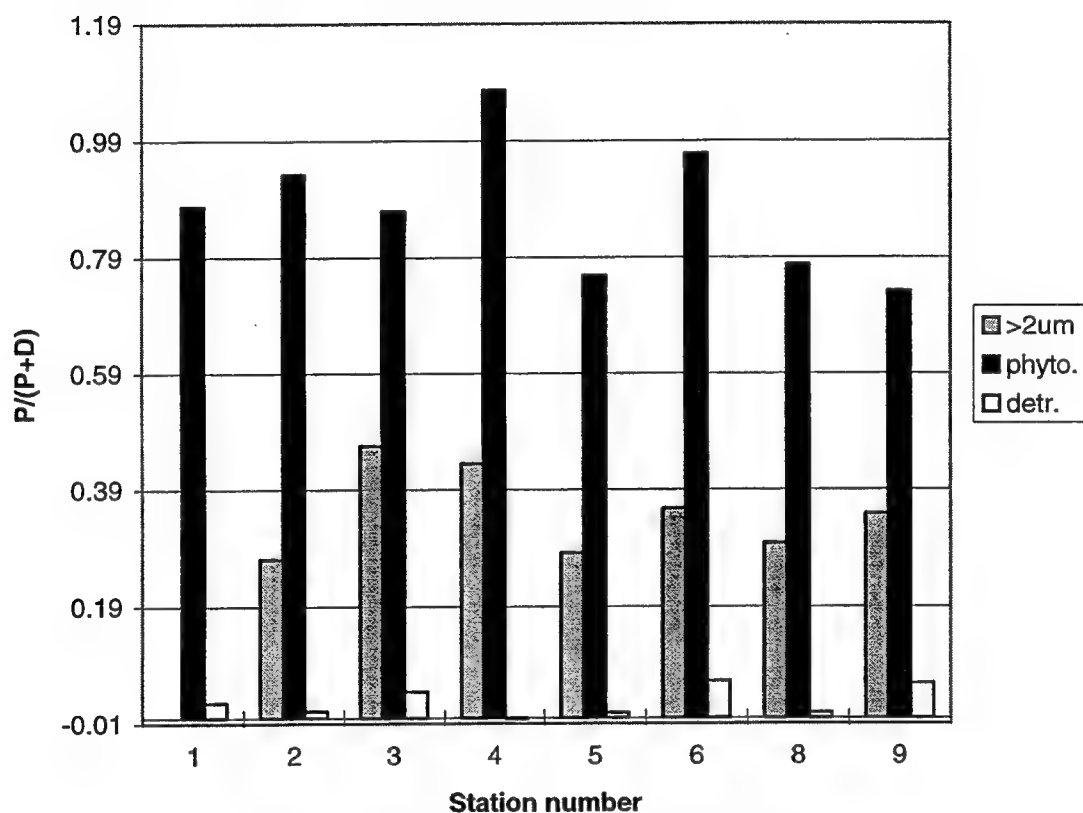
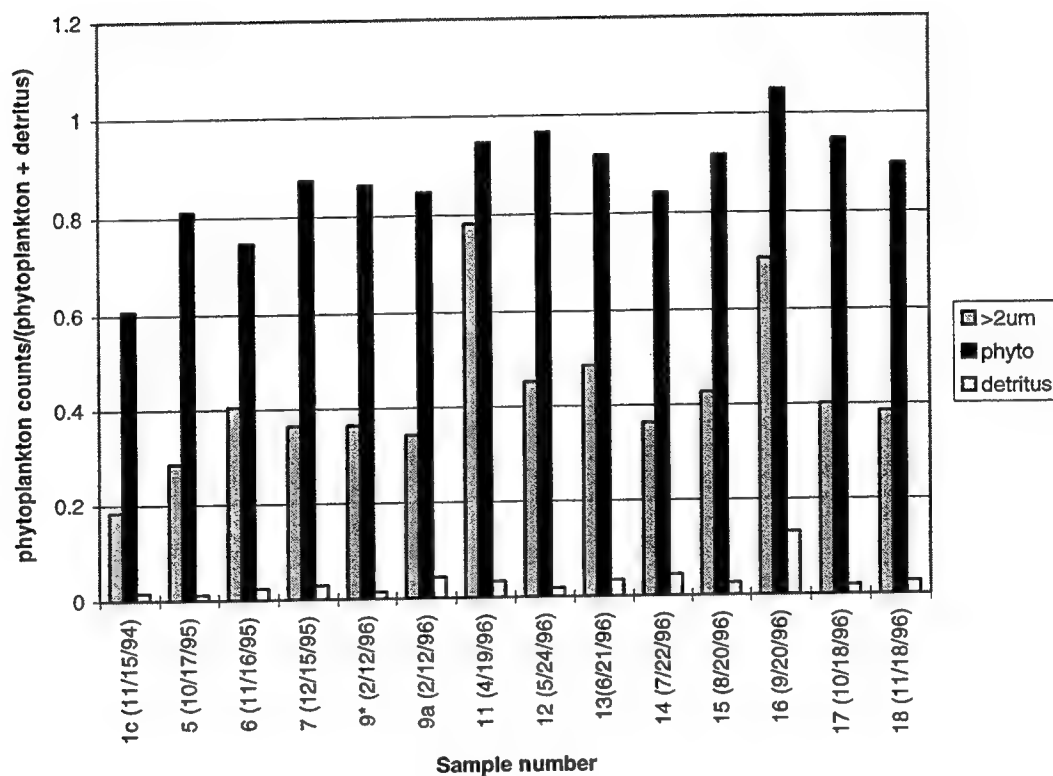


Fig. 4.8a. Flow cytometric analyses of total >2 μ m POM, and "phytoplankton" and "detritus" separated from this >2 μ m POM via FCM sorting. The y-axis is the number of phytoplankton counts divided by the number of phytoplankton and detritus counts. The x-axis lists the MAB station numbers for the samples (see Fig. 4.1).

WHTS POM:
FCM analysis of total >2um POM, "phytoplankton," and "detritus"



* To make an estimate of day-to-day variability in flow cytometer performance, two aliquots of WHTS 9 were processed independently; these are samples 9 and 9a above.

Fig. 4.8b. Same as Fig. 4.8a but for the WHTS sample set. The x-axis indicates sample numbers and sampling dates.

proxy for size) as the "phytoplankton" but exhibiting no measurable red fluorescence (Fig. 4.7). As the physical separation of particle-containing droplets can vary over time due to machine drift, partial clogging of the flow cell tip, and the ratio of particle size to droplet size, it becomes necessary to monitor the sorting process via "purity checks." Therefore, aliquots of the original sample and of the "phytoplankton" and "detrital" subclasses were taken. A fluorescent bead internal standard was added to each aliquot and these were rerun on the flow cytometer. The results of this purity check for both MAB and WHTS samples are shown in Fig. 4.8. All of the "detrital" samples contained very few phytoplankton particles (<15% of the total count). The "phytoplankton" samples were generally between 80 and 100% pure and in all cases showed considerable enrichment in phytoplankton over the unsorted samples.

Average spectra for "phytoplankton" and "detritus" from the MAB and the WHTS site were obtained in the same manner as for average large-particle and small-particle POM. The ion series attributed to protein are predominant in both average "phytoplankton" spectra (Fig. 4.9 a&b). In both cases there is, as expected, a strong phytadiene signal from the pyrolysis of chlorophyll. There is also a distinct sterol signature, which includes ions from both cholesterol (m/z 386, 368) and other sterols and stanols (including m/z 398 and 380 in the WHTS spectrum and m/z 430, 428, 410, 412, 394, 398, and 380 in the MAB data set).

Average "detritus" (Fig. 4.10) from both data sets yields a prominent and distinctive polysaccharide signal (m/z 96, 110, 126) and m/z 104 (possibly styrene). Both data sets also appear to contain a fairly low-intensity protein signal overlaid on this polysaccharide signal and a detectable sterol signature.

A prominent mass unit value of 76, tentatively identified as CS_2 , appears in the average spectra from both the "phytoplankton" and "detritus" sorts. Its identification as CS_2 is strengthened by the fact that m/z 76 and m/z 64 (believed to be from SO_2) have similar mass chromatograms, with both peaks occurring in that portion of a DT-MS run in which inorganic species should appear (Fig. 4.11). The mass unit 76 is also found in

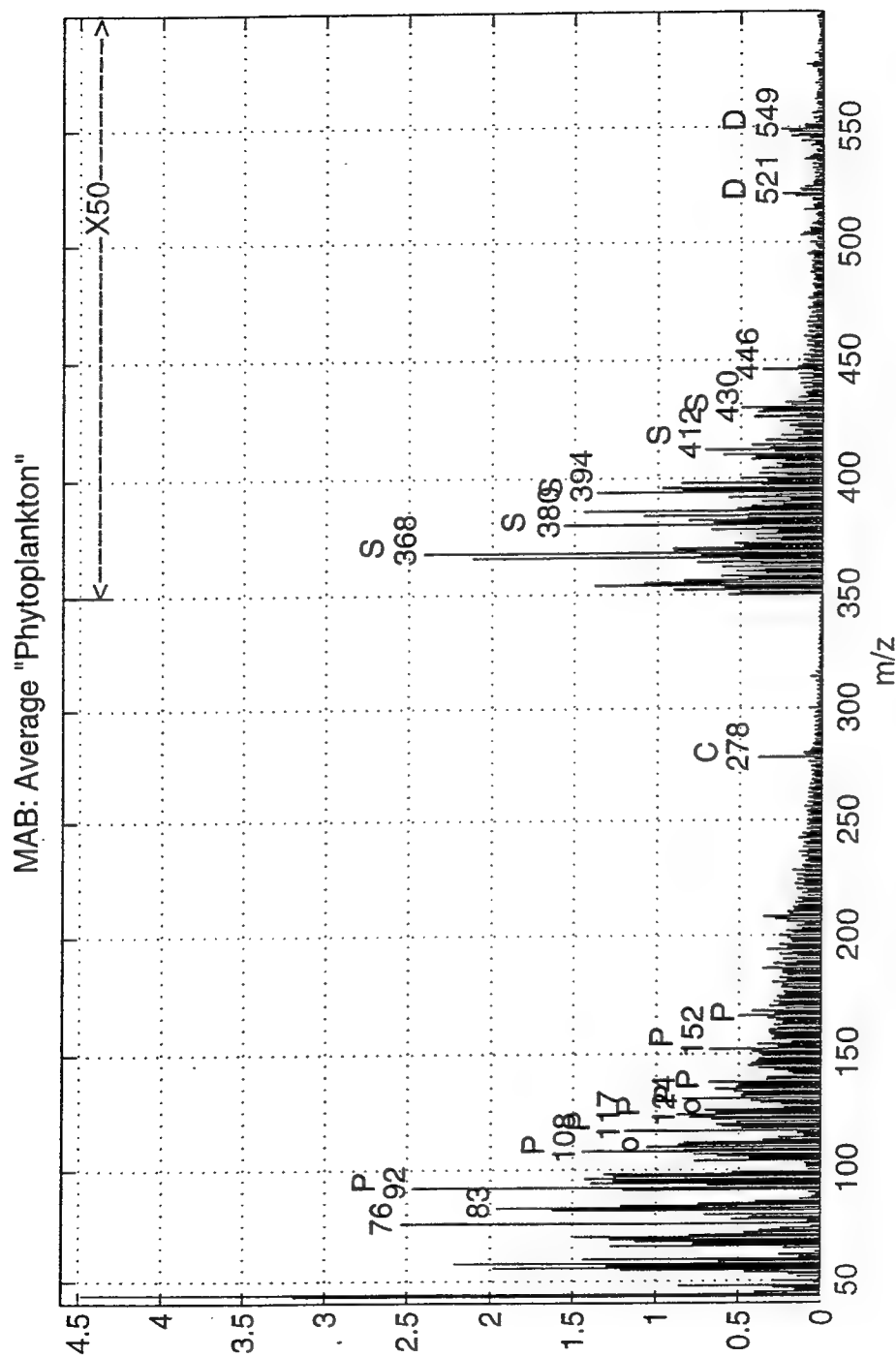


Fig. 4.9a. The average spectrum for "phytoplankton" isolated via flow cytometry from small-particle POM along the MAB.

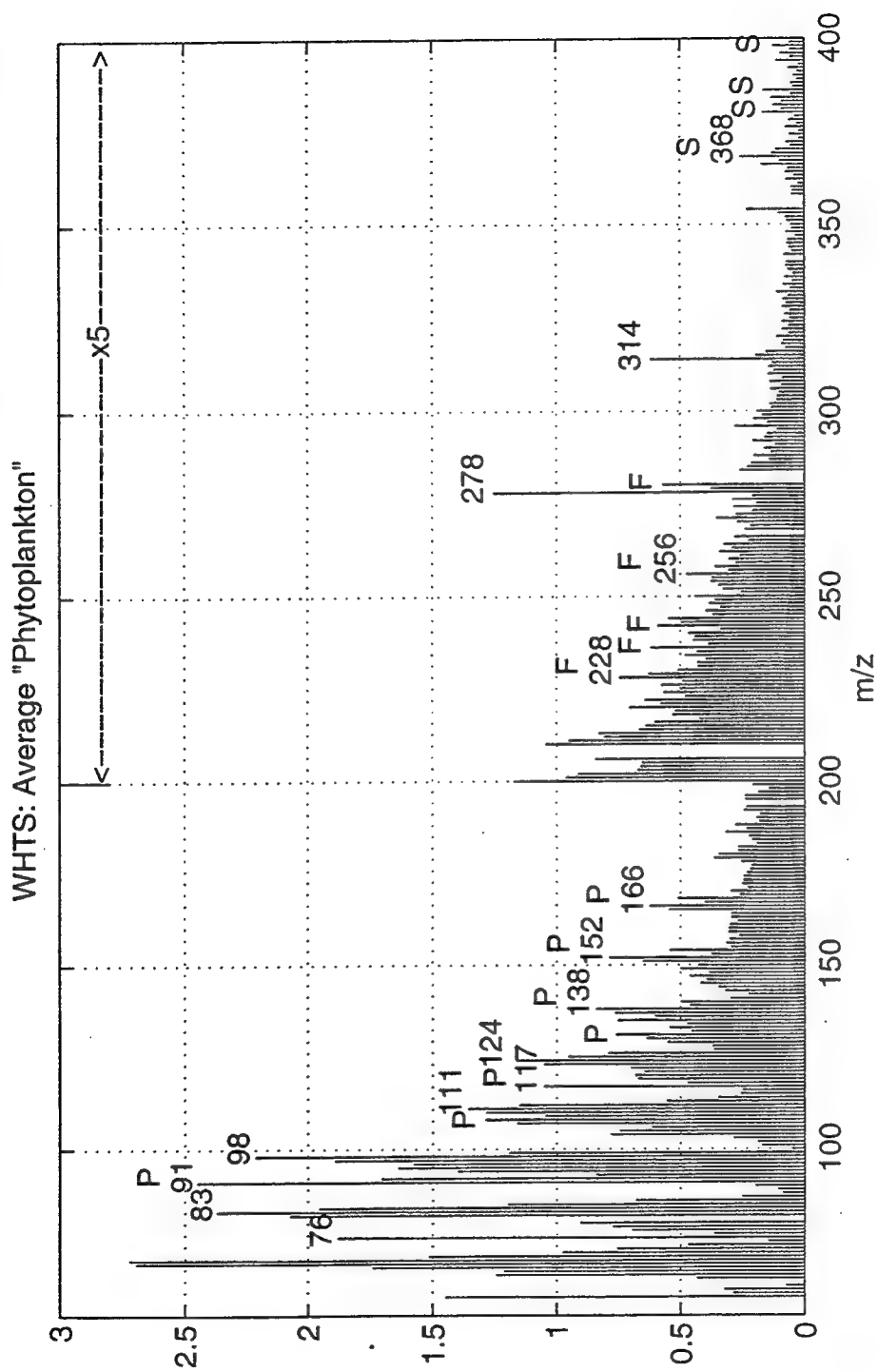


Fig. 4.9b. The average spectrum for "phytoplankton" from the WHTS site.

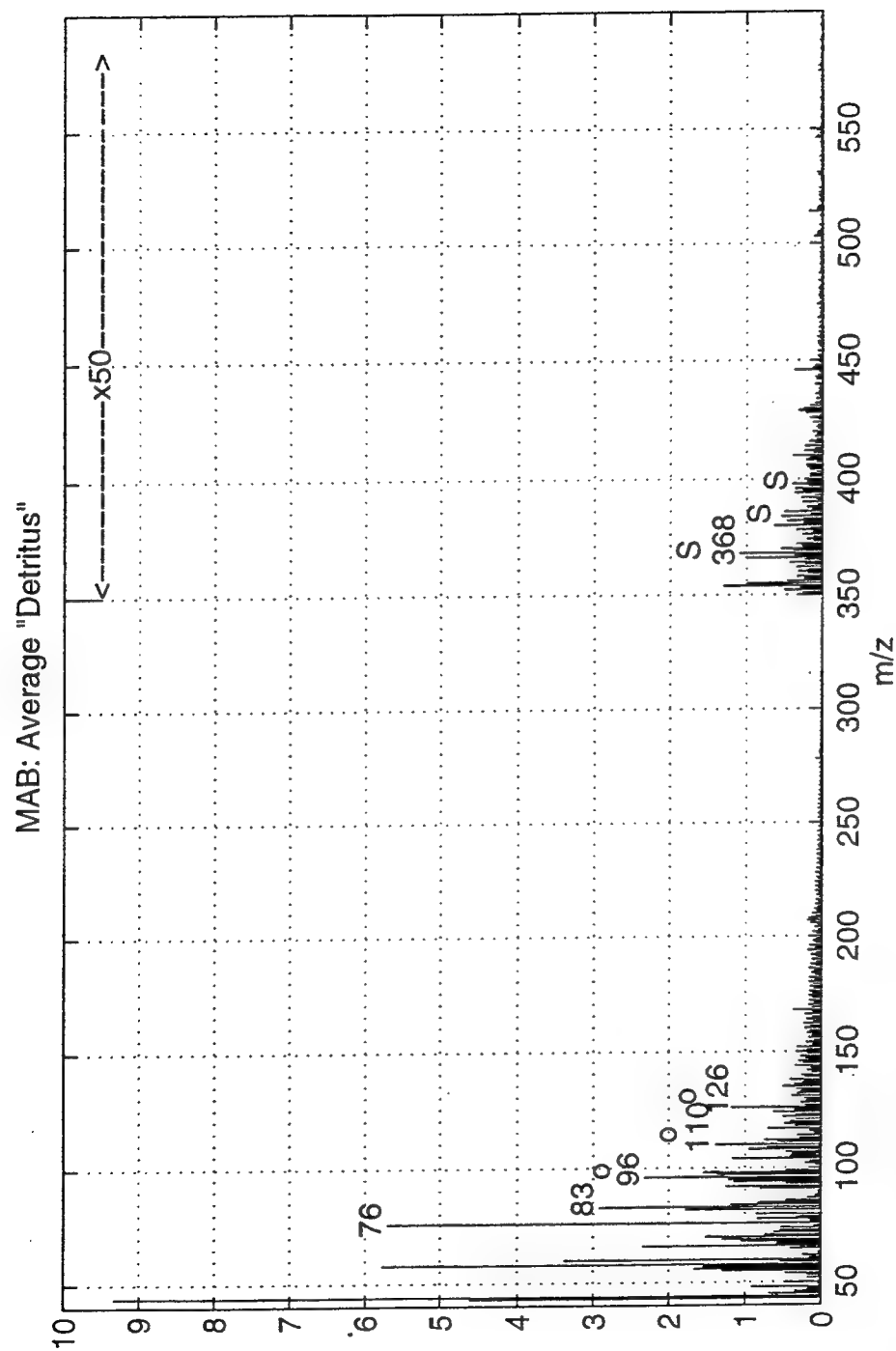


Fig. 4.10a. The average spectrum for "detritus" isolated via flow cytometry from small-particle POM along the MAB.

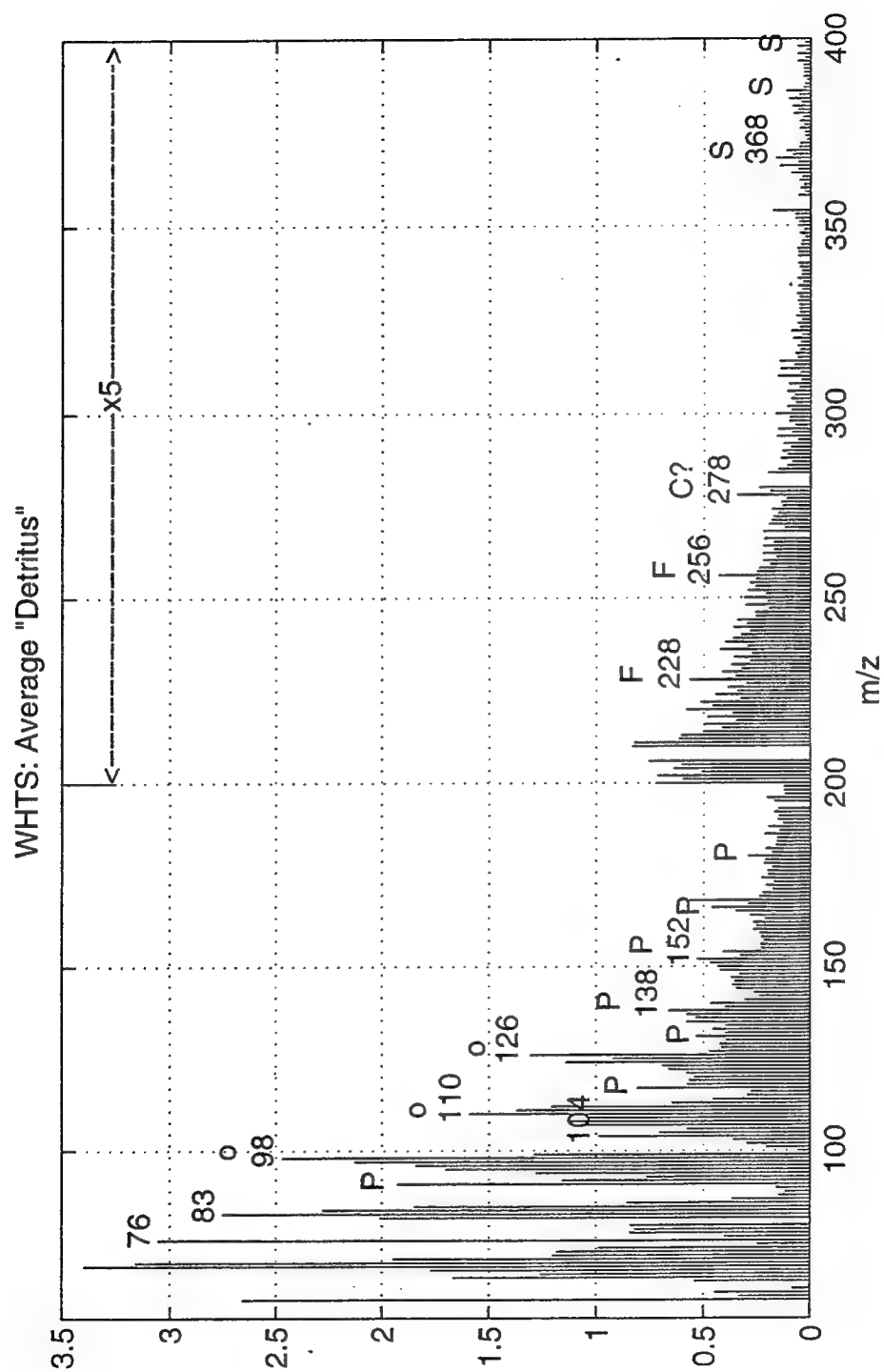


Fig. 4.10b. The average spectrum for "detritus" from the WHTS site.

unsorted material (see Fig. 4.3, 4.4), but is considerably more prominent in the flow cytometric sorts. Thus its prominence may be an artifact of the sorting procedure, though m/z 76 did not appear in flow cytometry sorting blanks collected for DT-MS analysis during method development (Chapter 2).

“Phytoplankton” vs. “detritus”: Discriminant analysis

The results from DT-MS and discriminant analysis of “phytoplankton” and “detritus” from the MAB samples are shown in Fig. 4.12. Discriminant Function 1 was responsible for 36% of the total variance in the data set. The phytoplankton component (plotting in the negative region of Discriminant Function 1) showed enrichment in proteins, chlorophyll, sterols, and diglycerides as compared to the “detrital” component. The “detritus” appeared richer in selected polysaccharide fragments (m/z 96, 98, 110, 126), CO_2 (m/z 44) and m/z 76, tentatively identified as CS_2 , a secondary pyrolysis product indicative of reduced forms of sulfur.

At the WHTS site, Discriminant Function 1 (Fig 4.13), responsible for 20% of the total variance in the data set, again separated “phytoplankton” and “detritus.” As in the MAB data set, the “phytoplankton” was enriched in protein, chlorophyll, and sterols. The “detritus” appeared richer in certain polysaccharide fragments (m/z 60, 85, 96, 98, 110, 114, 126) and CS_2 (m/z 76).

Discussion

As Tables 1 and 2 (which summarize the average compositions of the POM pools from the MAB and the WHTS) and the figures in the previous section illustrate, large-particle POM and small-particle POM from the surface ocean appear chemically similar, having contributions from polysaccharides, protein, $\text{C}_{14:0}$, $\text{C}_{16:0}$, and $\text{C}_{16:1}$ fatty acids, chlorophyll, and cholesterol. They both contain a phytoplankton component as indicated

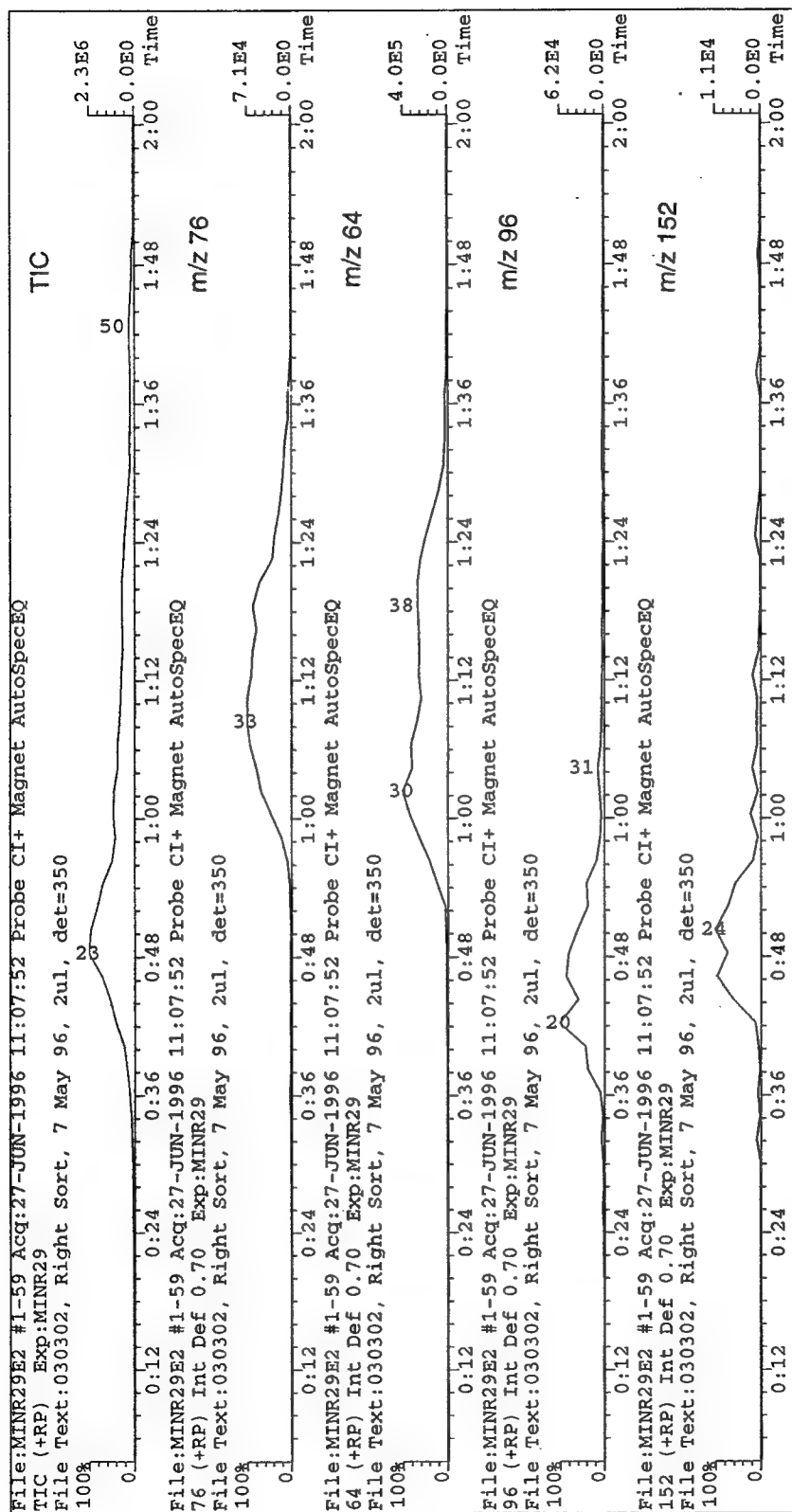


Fig. 4.11. The TIC (Total Ion Chromatogram) and selected mass chromatograms from DT-MS analysis (16eV EI⁺) of a selected "detritus" sample from the MAB. The mass chromatograms shown are for the following mass unit values: 76 (tentatively identified as CS₂), 64 (SO₂), 96 (believed to be from a polysaccharide), 152 (believed to be from a protein. Notice that m/z 76 and 64 appear much later in the course of the analysis, as would be expected for inorganic constituents).

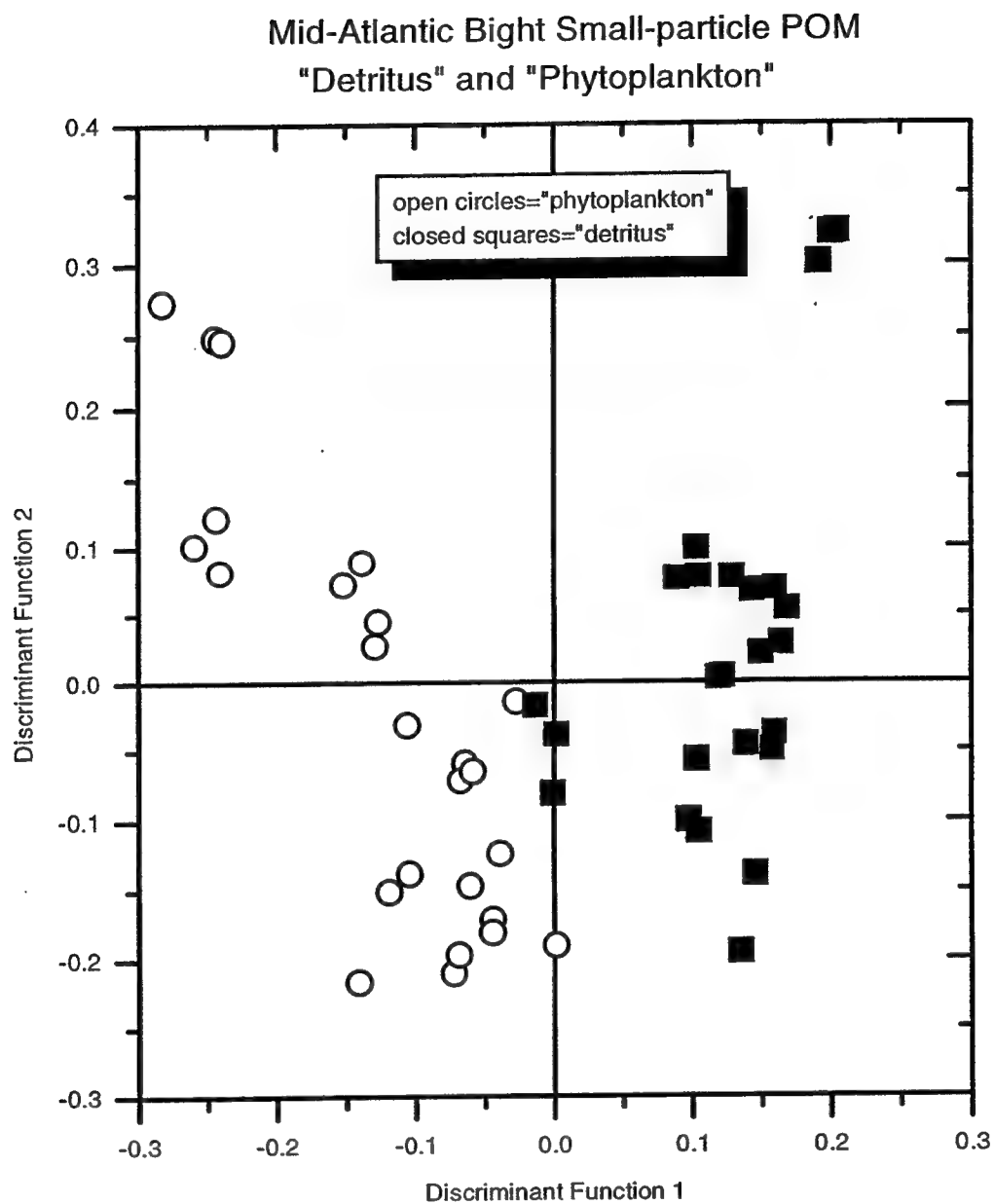


Fig. 4.12a. The score plot from discriminant analysis of MAB "phytoplankton" and "detritus."

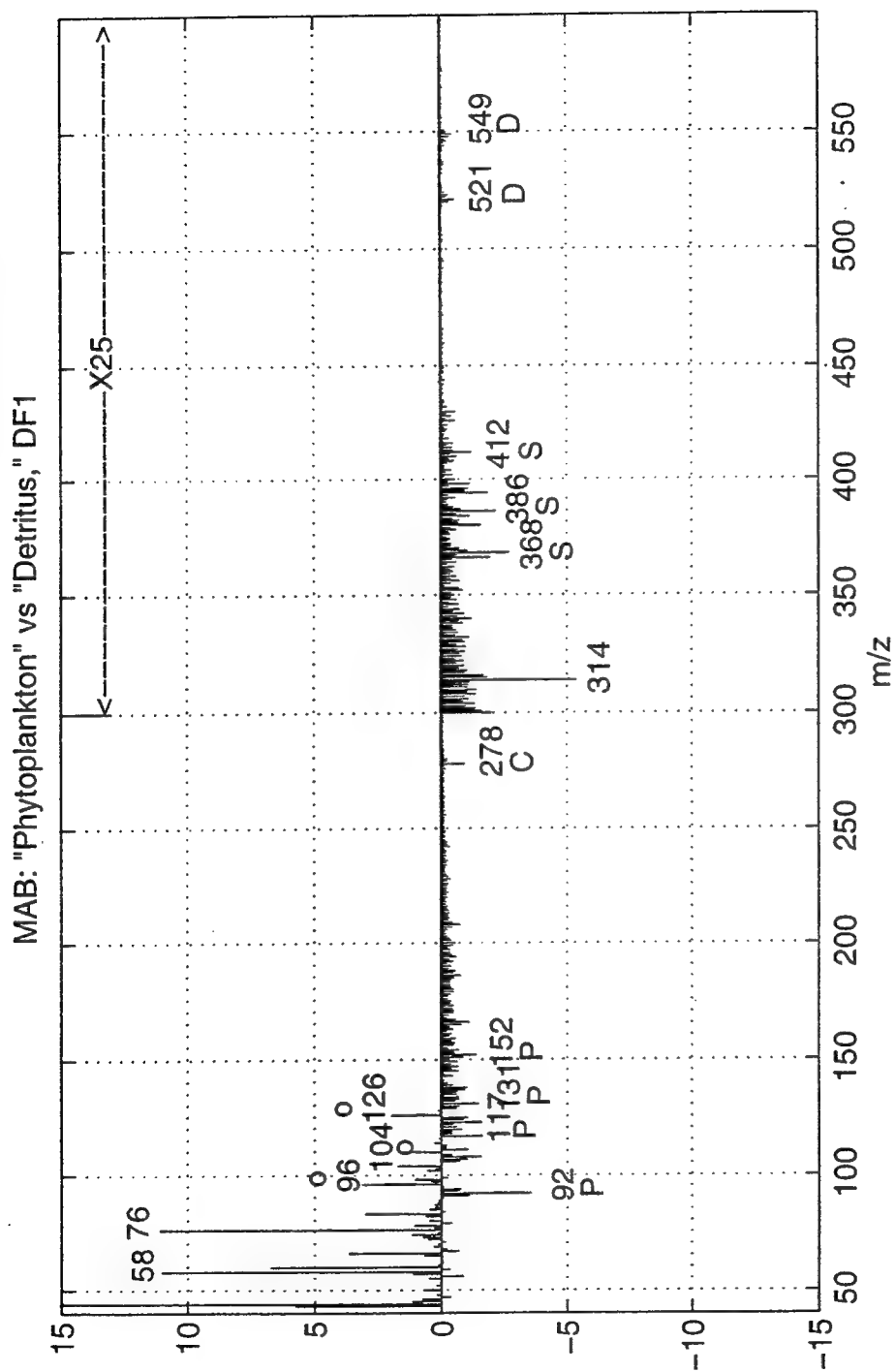


Fig. 4.12b. The reconstructed spectrum for Discriminant Function 1. "Detritus" (DF1+) appears enriched in selected polysaccharide fragments (o). "Phytoplankton" (DF1-) appears enriched in protein (P), chlorophyll (C), sterols (S), and diglycerides (D).

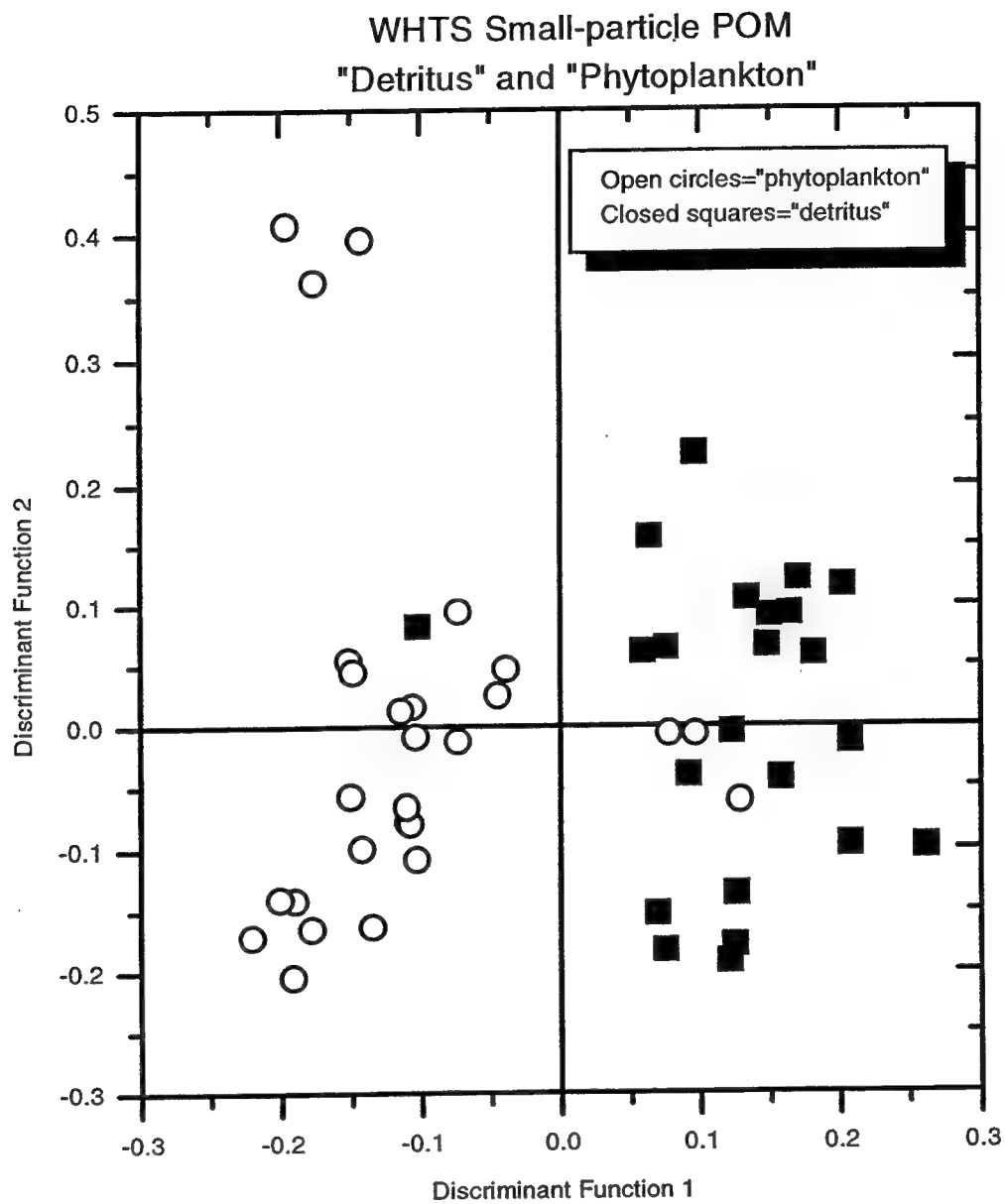


Fig. 4.13a. The score plot from discriminant analysis of WHTS "phytoplankton" and "detritus."

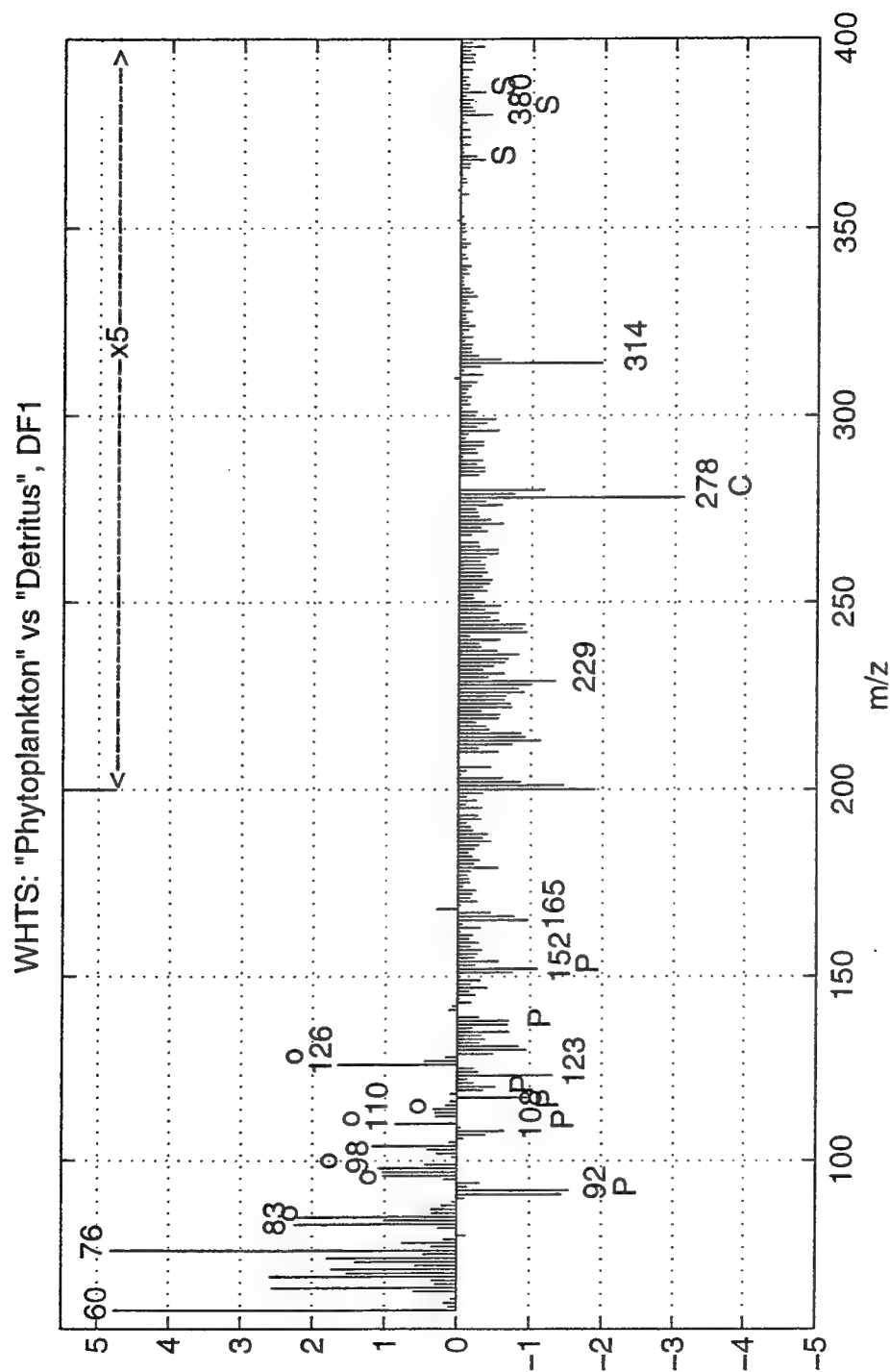


Fig. 4.13b. The reconstructed spectrum for DF1. "Detritus" (DF1+) is enriched in polysaccharides (o). "Phytoplankton" is enriched in protein (P), chlorophyll (C), and sterol (S).

by the presence of chlorophyll and the fatty acid distributions (Wakeham and Canuel, 1988 and sources therein). The presence of chitin in both large and small particles may indicate a grazer population existing in both size classes, though it must be mentioned that chitin also exists in certain phytoplankton (Painter, 1983; Smucker, 1991) and, as chitan, has been found to compose up to 34% of the cell biomass in *Thalassiosira weissflogii* (Smucker, 1991, and references therein). Inspection of the average spectra (Fig. 4.3, 4.4) indicates that small-particle POM are enriched in protein, phytosterols, diglycerides, and chlorophyll and depleted in polysaccharides relative to large-particle POM. "Phytoplankton," isolated from small-particle POM, is enriched in chlorophyll, sterols, diglycerides (MAB data set), and protein and depleted in polysaccharides relative to "detritus."

Discriminant analysis allowed us to explore such variations among particle classes in a more objective manner. In the present study, discriminant analysis indicated that, in general, small-particle POM appears more phytoplanktonic than large-particle POM. As mentioned above, it is enriched in chlorophyll fragments and phytosterols. In both data sets, the larger particles appear to contain higher proportions of pentose polysaccharide fragments, C_{16:0} fatty acid and cholesterol. Previous work on samples from the Peru margin (Eglinton et al., 1996) showed a similar trend between >53 μm particles and >3 μm , <53 μm particles. In the Peruvian data set, small particles also appeared more phytoplanktonic, exhibiting enrichment in proteins, chlorophyll, and C₂₈₋₂₉ sterols. The larger particles were enriched in hexose and pentose polysaccharides, and, unlike the MAB and WHTS large-particle samples, illustrated no enrichment in C_{16:0} fatty acid or cholesterol.

In addition to the trends described above, large-particle POM at the WHTS site (as compared to small-particle POM) is also enriched in chitin fragments, often a component of zooplankton exoskeletons, C_{16:0} fatty acid, which is fairly ubiquitous in living cells, and cholesterol, which, though it is present in phytoplankton as well, is a primary zooplankton sterol (Volkman, 1986 and references therein). Therefore, WHTS

>53 μm POM appears to have a stronger grazer biomass component as compared to smaller particles from the same site. MAB >53 μm POM, on the other hand, is enriched in both pentose and hexose polysaccharide fragments and $\text{C}_{14:0}$ as well as $\text{C}_{16:0}$ fatty acid. While not unambiguous, $\text{C}_{14:0}$ fatty acid can be considered a phytoplankton marker (Wakeham and Canuel, 1988); in conjunction with the polysaccharide signature, its presence indicates that these >53 μm particles contain a larger phytodetritus component as compared to >2 μm , <53 μm POM from the same transects. While viable phytoplankton, either large, single-celled organisms or chains, could be a significant component of the MAB large-particle POM, this appears unlikely due to the low contribution of m/z 278 (chlorophyll) to the corresponding average spectrum (Fig. 4.3a), which suggests that these particles have lost their photosynthetic capacity.

The difference in large-particle POM vs. small-particle POM characteristics in the two data sets may have resulted from the temporal vs. spatial averaging of the chemical composition of the POM subclasses. The WHTS data set contains samples collected throughout the seasons and would include zooplankton blooms; the MAB data set was collected in March when grazer pressure on the phytoplankton population was probably limited and bacterial degradation would have been slowed by low water-column temperatures (Lane et al., 1994). For example, Lane et al. (1994) found that chlorophyll *a* concentrations at their March 1988 study site in the MAB were two to three times higher below 30 m than above 30 m and that most of the grazers were above 20 m; therefore, they concluded that a large portion of late winter/early spring primary productivity sank to the bottom without being grazed. In addition, Flagg et al. (1994) found that zooplankton biomass in the SEEP-II portion of the MAB does not peak until early May.

While DT-MS (with an analysis time of 2 minutes) and multivariate statistical techniques allow rapid exploration of chemical variations within and between size-classes of POM, the most unique aspect of this study is the coupling of flow cytometry and DT-MS. With this coupling, it is possible to chemically characterize phytoplankton and detritus separated from the small-particle size class of surface ocean POM.

Table 4.1. Relative intensities of DT-MS (16 eV, EI⁺) signatures for lipid and biopolymer components in the average spectra of MAB POM subclasses

<i>Constituents:</i>		<i>MAB:</i>			
<i>Lipids</i>	<i>Biopolymers</i>	<i>>53 μm</i>	<i>>2 μm^*</i>	<i>Phyto.</i>	<i>Detritus</i>
Chlorophyll		+	++	++	+
Cholesterol		++	+	++	+
Phytosterols		+	++	++	+
Fatty acids		++	+	++	+
Diglycerides		+	++	++	+
	Proteins	+++	++++	++++	+++
	Polysaccharides(pentose)	++++	+++	+	+
	Polysaccharides(hexose)	++++	+++	+++	++++
	Nucleic acids	++	+++	++	++
	Chitin	++	++	++	++

*Actually >2 μm , <53 μm

Symbols are as follows: "++++" indicates a very strong contribution to the DT-MS spectrum; "+++", a relatively strong contribution; "++," a significant contribution; and "+," presence in the spectrum.

Table 4.2. Same as Table 4.1, but for the WHTS POM subclasses

<i>Constituents:</i>		<i>WHTS:</i>			
<i>Lipids</i>	<i>Biopolymers</i>	<i>>53 μm</i>	<i>>0.8 μm^*</i>	<i>Phyto.</i>	<i>Detritus</i>
Chlorophyll		+	+	++	+
Cholesterol		++	++	++	+
Phytosterols			++	++	+
Fatty acids		+	+	++	+
Diglycerides		+	++	N/A	N/A
	Proteins	++++	++++	++++	+++
	Polysaccharides (pentose)	++++	++	+	+
	Polysaccharides (hexose)	+++	+++	+++	++++
	Nucleic acids	++	+++	++	++
	Chitin	++	++	++	++

* Actually >0.8 μm , <53 μm

Discriminant analysis of "phytoplankton" and "detritus" in the two data sets indicate that "phytoplankton" particles, as expected, are enriched in protein and chlorophyll. Somewhat surprisingly, they are also enriched in lipids, including a distinct sterol signature. In both data sets there are strong signals from cholesterol (m/z 386, 368) and m/z values consistent with 24-methylcholesta-5,22E-dien-3 β -ol (m/z 398, 380), most likely from diatoms (Volkman, 1986). The cholesterol in the "phytoplankton" subclass probably comes from dinoflagellates (Volkman, 1986), known to contribute significantly to algal populations at the WHTS site and in the region of the MAB stations (Wainright and Fry, 1994; Marshall, 1984). This hypothesis is further supported by the presence of m/z 428, tentatively identified as dinosterol, in the reconstructed discriminant spectra for the MAB (Fig. 4.12b), the average "phytoplankton" spectrum for the MAB (Fig. 4.9a) and the average small-particle POM spectra for both the MAB and WHTS data sets (Fig.4.4).

"Detritus" in both data sets is enriched in polysaccharide fragments when compared with "phytoplankton." As flow cytometric separation included all non-red-fluorescing particles as "detritus," further discussion of the potential particulate components of "detritus" is necessary. "Detritus," as defined here, may include dimly fluorescing unhealthy phytoplankton cells, non-red-fluorescing micro-zooplankton, bacteria, fecal pellets, phytodetritus, clay particles, etc. The fact that "phytoplankton" is enriched in lipids over "detritus" indicates that stressed phytoplankton cells cannot form a substantial proportion of "detritus." Phytoplankton lipid concentrations generally increase significantly under nutrient stress (Roessler, 1990 and references therein). In addition, in culture studies (e.g. *Thalassiosira pseudonana*, Brown et al., 1996) total fatty acid concentrations have been shown to increase two- to six-fold and total lipids from 10% to 50% between logarithmic to stationary phase. Zooplankton generally have lower polysaccharide concentrations, higher protein concentrations, and sometimes higher lipid concentrations relative to phytoplankton (Parsons et al., 1984 and references therein). Therefore, "detritus" probably does not contain a significant contribution from

zooplankton biomass (Parsons et al., 1984 and references therein). "Detritus" undoubtedly contains some particle-associated bacteria, though it is difficult to quantify the relative bacterial biomass contribution, which was assumed to be small. The "detrital" pool may contain a significant portion of phytodetritus and fecal pellet material. Indeed, Tanoue et al. (1982), found preferential depletion of amino acids and fatty acids with respect to sugars in fecal pellets collected during feeding experiments with the alga *Dunelliella tertiolecta* and a euphausiid (*Euphausia superba*), a trend quite similar to the comparison of "phytoplankton" and "detrital" particles in our data sets. If Wainright and Fry's (1994) conclusion that POM at the WHTS site is mainly autochthonous can be applied to the "detrital" subclass of POM as well, then "detritus" appears to be mainly phytodetritus and or fecal pellet material.

Summary and Conclusions

1. In the MAB and at the WHTS site, both large-particle ($>53\ \mu\text{m}$) and small-particle POM ($>2\ \mu\text{m}$, $<53\ \mu\text{m}$ or $>0.8\ \mu\text{m}$, $<53\ \mu\text{m}$) contain polysaccharides, protein, $\text{C}_{14:0}$, $\text{C}_{16:0}$, and $\text{C}_{16:1}$ fatty acids, chlorophyll, cholesterol, and chitin. A phytoplankton component appears to exist in both size classes.
2. Small-particle POM, as compared to large-particle POM, is enriched in protein, phytosterols, diglycerides, and chlorophyll and appears more "phytoplanktonic."
3. Large-particle POM, as compared to small-particle POM, is enriched in pentose polysaccharide fragments, $\text{C}_{16:0}$ fatty acid, and cholesterol. WHTS $>53\ \mu\text{m}$ particles are also enriched in chitin fragments, perhaps indicating the presence of a significant grazer biomass component. In the MAB data set, $>53\ \mu\text{m}$ particles are enriched in hexose polysaccharide fragments and $\text{C}_{14:0}$ fatty acid, perhaps indicating the presence of a significant phytodetritus component.

4. "Phytoplankton" is enriched in protein, chlorophyll, and lipids when compared to "detritus."
5. "Detritus" spectra, as compared to "phytoplankton" spectra, show enhancement in selected polysaccharide m/z values and in a mass unit value attributed to CS_2^+ . The comparison of "detritus" and "phytoplankton" spectra indicates that "detritus" probably consists of phytodetritus and/or fecal pellet material and does not contain significant zooplankton or stressed-but-viable phytoplankton components.

The results described above indicate the usefulness of DT-MS and discriminant analysis in obtaining rapid, first-order, molecular-level information on larger sample sets with minimal sample size requirements (a few micrograms of carbon). DT-MS can also provide additional information on the nature of the compounds within the particles as the desorption and pyrolysis regions of the analysis can be studied separately. This work, however, was an initial exploration of surface-ocean POM, so the spectra were summed over the entire temperature-range without separation of biopolymer and lipid components. DT-MS information is particularly valuable as a starting point for more detailed molecular-level analyses, permitting judicious selection of samples and techniques. However, some limitations of the DT-MS method should be taken into consideration. DT-MS sensitivity varies with compound class, and response factors for diagnostic ions are generally one to two orders of magnitude higher for lipids than biopolymers (Chapter 2). In addition, DT-MS is relatively blind to contributions from certain components (e.g., tannins, acidic sugars, chlorophyll pigments) because they are not amenable to desorption or pyrolysis.

This study also indicates the usefulness of flow cytometry as a preparative technique for the separation of selected subclasses from suspended POM. Phytoplankton populations can be isolated from unpreserved, unstained natural particle populations on

the basis of red fluorescence, orange fluorescence (from phycoerythrin), the ratio of right angle light scatter to forward angle light scatter and other criteria (Olson et al., 1989). The addition of appropriate staining techniques could expand the number of subclasses separated from natural POM, allowing the separation of zooplankton and/or bacteria. The linkage of flow cytometry and such chemical measurements as elemental analysis, stable isotopic analysis, and, of course, organic mass spectrometry, could further extensively our understanding of the heterogeneity of suspended POM.

References:

- Biscaye P. E., Flagg C. N., and Falkowski P. G. (1994) The Self Edge Exchange Processes experiment, SEEP-II: an introduction to hypotheses, results, and conclusions. *Deep-Sea Res. II* **41**(2/3), 231-252.
- Bishop J. K. B., and Edmond J. M. (1976) A new large-volume in situ filtration system for sampling oceanic particulate matter. *J.Mar.Res.* **32**, 181-198.
- Boon J. J. (1992) Analytical pyrolysis mass spectrometry: new vistas opened by temperature-resolved in-source PYMS. *Int. J. Mass. Spec. and Ion Process.* **118/119**, 755-787.
- Brown M. R., Dunstan G. A., Norwood S. J., and Miller K. A. (1996) Effects of harvest stage and light on the biochemical composition of the diatom *Thalassiosira pseudonana*. *J. Phycol.* **32**, 64-73.
- Caron D. A., Dam H. G., Kremer P., Lessard E. J., Madin L. P., Malone T. C., Napp J. M., Peele E. R., Roman M. R., Youngbluth M. J. (1995) The contribution of microorganisms to particulate carbon and nitrogen in surface waters of the Sargasso Sea near Bermuda. *Deep-Sea Res. I*, **42**, 943-972.
- Conte M.H. (1989) The biogeochemistry of particulate lipids in warm-core Gulf Stream ring systems, *Ph.D. Thesis*, 584 pp.
- Eglinton T. I., Boon J. J., Minor E. C., and Olson R. J. (1996). Microscale characterization of algal and related particulate organic matter by direct temperature-resolved mass spectrometry. *Mar. Chem.* **52**, 27-54.
- Eglinton T. I., Sinninghe Damste J. S., Pool W., de Leeuw J. W., Eijkel G., Boon J. J. (1992). Organic sulfur in macromolecular sedimentary organic matter-II: Analysis of distributions of organic sulfur pyrolysis products using multivariate techniques. *Geochim. Cosmochim. Acta* **56**, 1545-1560.
- Flagg C. N., Wirick C. D., and Smith S. L. (1994). The interaction of phytoplankton, zooplankton, and currents from 15 months of continuous data in the Mid-Atlantic Bight. *Deep-Sea Res. II*, **41**(2/3), 411-436.
- Gassman G. and Gillbricht M. (1982). Correlations between phytoplankton, organic detritus, and carbon in North Sea waters during the Fladenground Experiment (FLEX '76). *Helgolander Meeresunters* **35**, 253-262.

- Hoogerbrugge R., Willig S. J., and Kistemaker P.G., (1983). Discriminant analysis by double stage principle component analysis. *Anal. Chem.* **55**, 1710-1712.
- Lane P. V. Z., Smith S. L., Urban J. L., and Biscaye P. E., 1994. Carbon flux and recycling associated with zooplanktonic fecal pellets on the shelf of the Middle Atlantic Bight. *Deep-Sea Res. II*, **41**(2/3), 437-458.
- Marshall H. G. (1984). Phytoplankton of the northeastern continental shelf of the United States in relation to abundance, composition, cell volume, seasonal, and regional assemblages. *Rapp. P.-v Reun. Cons. int. Explor. Mer*, **183**, 41-50.
- Meuzelaar H. L. C., Haverkamp J., and Hileman F. D. (1982). *Pyrolysis Mass Spectrometry of Recent and Fossil Biomaterials: Compendium and Atlas*. Elsevier Press, New York, 293 pp.
- Olson R. J., Zettler E. R., and Anderson O. K. (1989). Discrimination of eukaryotic phytoplankton cell types from light scatter and autofluorescence properties measured by flow cytometry. *Cytometry*, **10**, 636-643.
- Painter T. J. (1983). Algal polysaccharides. In Aspinall G. O. (Ed.). *The Polysaccharides*, Vol. 2., Academic Press, New York, pp. 196-275.
- Parsons T. R., Takahashi M., Hargrave B. (1984). *Biological Oceanographic Processes*, 3rd Ed., Pergamon Press, New York, 330 p.
- Passow U., Alldredge A. L., and Logan B. E. (1994). The role of particulate carbon exudates in the flocculation of diatom blooms. *Deep-Sea Res. I*, **42**, 335-262.
- Pomeroy, L. R. (1980). Detritus and its role as a food source. In: Barnes, R.K., Mann, K.H. (eds), *Fundamentals of Aquatic Ecosystems*, Blackwell Sci.Publ., London, pp.84-102.
- Roessler P. G. (1990). Environmental control of glycerolipid metabolism in microalgae: Commercial implications and future research directions. *J. Phycol.* **26**, 393-399.
- Salot A., Ulloa-Guevara A., Viets T. C., de Leeuw J. W., Schenk P. A., Boon J. J. (1984). The application of pyrolysis-mass spectrometry and pyrolysis-gas chromatography-mass spectrometry to the chemical characterization of suspended matter in the ocean. *Org. Geochem.* **6**, 295-304.
- Smucker, R. A. (1991). Chitin primary production. *Biochemical Systematics and Ecology*, **19**(5), 357-369.

- Tanoue E., Handa N., and Sukagawa H. (1982). Difference of the chemical composition of organic matter between fecal pellet of *Euphasia superba* and its feed, *Duneliella tertiolecta*. *Trans. Tokyo Univ. Fish.* **5**, 189-196.
- Verity P. G., Beatty T. M., and Williams S. C. (1996). Visualization and quantification of plankton and detritus using digital confocal microscopy. *Aquatic Microbial Ecology* **10**, 55-67.
- Volkman J. K. (1986). A review of sterol markers for marine and terrigenous organic matter. *Org. Geochem.* **9**(2), 83-99.
- Wainright S. C. and Fry B. (1994). Seasonal variation of the stable isotopic compositions of coastal marine plankton from Woods Hole Massachusetts, USA and Georges Bank. *Estuaries* **17**(3), 552-560.
- Wakeham S. G. and Canuel E. A. (1988). Organic geochemistry of particulate matter in the eastern tropical North Pacific Ocean: Implications for particle dynamics. *J. Mar. Res.* **46**, 183-213.

Chapter 5

Polysaccharides in oceanic POM as determined by chemical ionization DT-MS

Abstract

Positive ammonia chemical ionization direct temperature-resolved mass spectrometry ($\text{NH}_3\text{-Cl}^+$ DT-MS) was applied to selected samples of large-particle ($>53\ \mu\text{m}$), small-particle ($>2\ \mu\text{m}$, $<53\ \mu\text{m}$), "detrital" and "phytoplankton" marine particulate organic matter (POM) collected from the Mid-Atlantic Bight (MAB) and from Great Harbor, Woods Hole, MA. In addition, POM samples from the beginning and end of a laboratory diatom degradation experiment were analyzed in order to determine the applicability of this experiment to processes in coastal and shelf/slope regions. The resulting mass spectra were used to investigate variations in polysaccharide composition among these pools of POM. Principal component analysis was used to explore differences among the mass spectra of large-particle and small-particle marine POM and the diatom degradation experiment samples. The majority of the variance (Principal Component 1) appeared related to the extent of degradation of organic matter. The "fresher" material exhibited enrichment in polyhexoses and possibly chitin, and the "more degraded" material was enriched in methyl-hexose, methyl-deoxysugar, deoxysugar, and selected aminosugar fragments. Comparison with literature data from similar measurements of ultrafiltered DOM (UDOM) indicates that the main difference between POM and UDOM was the presence of a stronger hexose signal in the particles. Otherwise, POM and UDOM appeared compositionally similar with respect to sugars. This suggests that these pools of organic matter may represent different stages of degradation/reactivity.

Introduction

Carbohydrates are the most abundant compound class formed by living organisms (Voet and Voet, 1990). In the oceans carbohydrates comprise 20-40 % of phytoplankton biomass (Parsons et al., 1961). Particulate organic carbon (POC) is found to be 10-30% carbohydrate; after sulfuric acid hydrolysis and MBTH (3-methyl-2-benzothiazolinone hydrazone hydrochloride) analysis, dissolved organic carbon (DOC) is found to be 10-28% carbohydrate (Pakulski and Benner, 1992, and references therein).

Although inputs of carbohydrate into the organic matter cycle are high, studies of the aldose (neutral sugar) components of marine carbohydrates indicate intensive reworking of the carbohydrate pool. In a study of equatorial Pacific POM, aldose primary production is found to be 4 orders of magnitude greater than aldose accumulation rates in the underlying sediment (Hernes et al., 1996). Moreover, much of the total aldose appears to be remineralized in the surface ocean as fluxes measured via sediment trap located just below the euphotic zone (at 105 m depth) in the same region are 2 orders of magnitude lower than the aldose primary productivity estimates (Wakeham et al., 1997, Hernes et al., 1996). The depth-related trend of total seawater aldoses in the equatorial Pacific is similar but less extreme; aldose concentrations decrease three-fold with depth (Skoog and Benner, 1997).

Recently we have found variations in carbohydrate composition when surface-ocean POM samples are separated into size-classes and subclasses (large-particle POM ($>53\ \mu\text{m}$) vs small-particle POM ($>2.0\ \mu\text{m}$, $<53\ \mu\text{m}$), and small-particle phytoplankton vs small-particle detritus) and analyzed via direct temperature-resolved mass spectrometry (DT-MS, 16 eV EI⁺) and discriminant analysis (see Chapter 4). This study indicated that $>53\ \mu\text{m}$ particles, as compared to $>2.0\ \mu\text{m}$, $<53\ \mu\text{m}$ POM, were found to be more enriched in moieties that, upon DT-MS, yielded pentose polysaccharide fragments and either hexoses (along the Mid-Atlantic Bight in March) or aminosugars (in a time-averaged study in Great Harbor, Woods Hole). "Detritus," defined as $2\rightarrow 53\ \mu\text{m}$ particles

lacking chlorophyll fluorescence, was enriched in selected polysaccharide fragments relative to phytoplankton, defined as 2→53 μm particles which red-fluoresce after excitation with a 488 nm laser.

In view of such depth-related and POM class-related and subclass-related variations in this important biological compound class, selected surface-ocean and diatom degradation experiment POM samples were analyzed via ammonia CI^+ DT-MS, a technique that enhances the carbohydrate signature in complex samples and, in addition, can provide oligomer information (Helleur and Guevremont, 1989; Lomax et al., 1991; Arisz and Boon, 1995). Polysaccharide variations among these samples were then explored using principal component analysis.

Experimental

EI^+ DT-MS and discriminant analysis (Chapter 4) was performed on $>53 \mu\text{m}$ and $>2.0 \mu\text{m}$, $<53 \mu\text{m}$ POM samples from the numbered stations in Fig. 5.1 (samples were collected in March 1996, Cruise EN279, see Chapter 4). The following representative samples were chosen for $\text{NH}_3\text{-CI}^+$ DT-MS based on the EI^+ data: 2-G and 2-S, large-particle ($>53 \mu\text{m}$) and small-particle ($>2 \mu\text{m}$, $<53 \mu\text{m}$) POM, respectively, from coastal station 2; and 8-G and 8-S, large-particle and small-particle POM from continental slope station 8. Representative samples of large-particle and small-particle POM (WHTS13-G and WHTS13-S), "phytoplankton" (WHTS13-P), and "detritus" (WHTS13-D) from monthly sampling at Great Harbor, Woods Hole (station WH, Fig. 5.1) were also chosen after perusal of the score plots resulting from DT-MS and discriminant analysis. For comparative purposes, $\text{NH}_3\text{-CI}^+$ MS was also performed on samples ($>2 \mu\text{m}$) from day 0 (DPP0) and day 72 (DPP72) of a diatom degradation experiment (see below).

The sample collection and processing details are described in Chapter 4 but will be summarized briefly here. Roughly 100 L of seawater was collected by diaphragm or peristaltic pump (using primarily TeflonTM tubing and either PharmedTM or silicone tubing

MAB and WHTS Sampling Stations

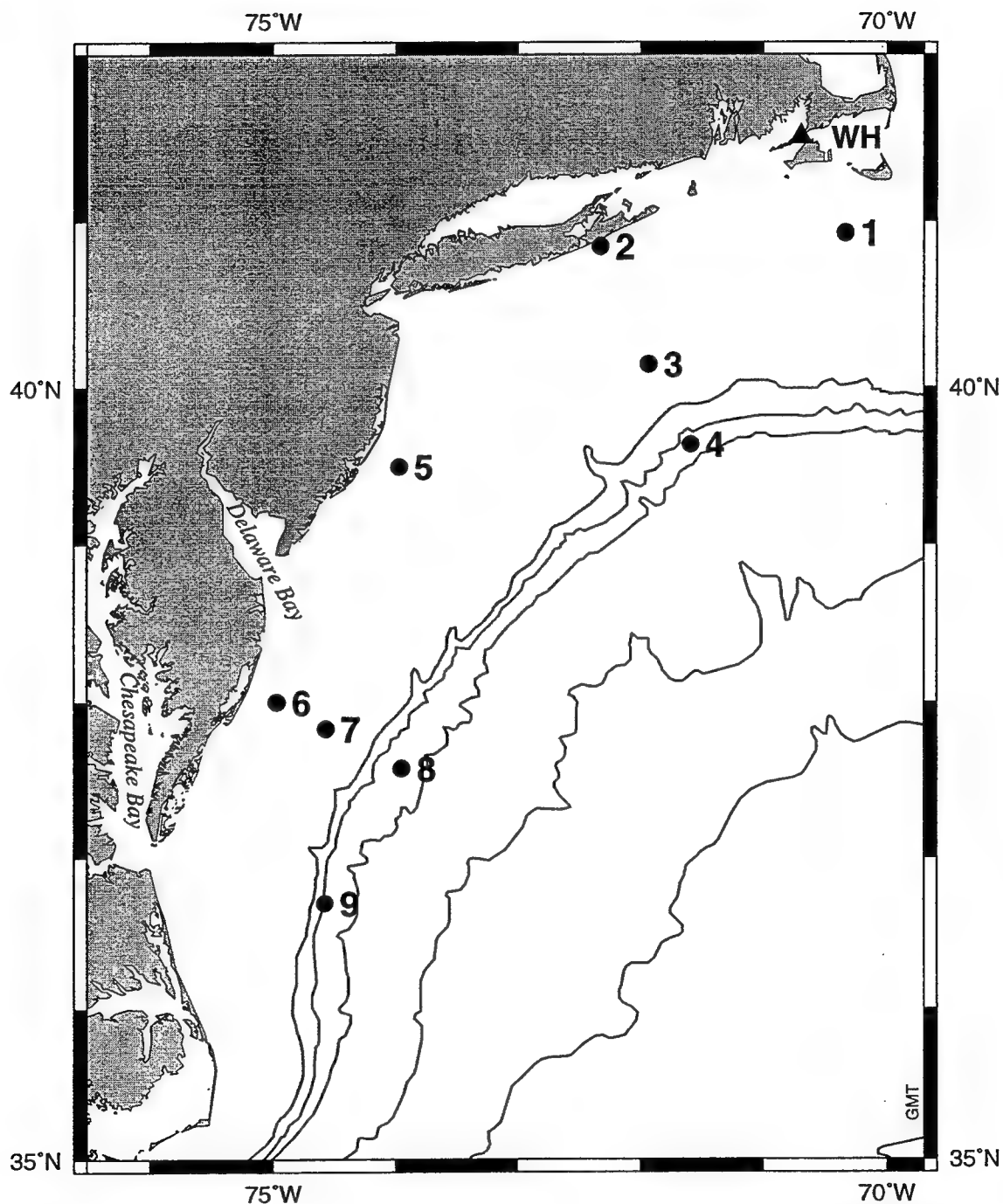


Fig. 5.1. Location of the monthly-sampled WHTS station (WH) and the MAB transects from cruise EN279 (March 1996). Contour levels represent water depth (200 m, 1000 m, 2000 m, 3000 m, 4000 m, and 5000 m).

in the peristaltic pump) and filtered through a 53 μm Nylon screen to recover large-particle POM. The filtrate was further concentrated via cross-flow filtration using a 0.8 μm Filtron Fluoro centrasette and ultrasette (inlet pressure <20 psi) followed by gravity/vacuum (<5 psi) filtration onto a 2 μm polycarbonate filter. Small-particle POM was resuspended off this membrane. Aliquots of this small-particle POM were separated into "phytoplankton" or "detritus" via flow cytometric sorting (on an EPICS V flow cytometer, excitation at 488 nm) using forward angle light scatter as a proxy for size and red (chlorophyll) fluorescence to identify phytoplankton particles. Samples were desalted by centrifugation (4 minutes, 10,000xG, Fisher MicroCentrifuge, Model 59A) with Milli-Q water rinses or centrifugation (same parameters) after flow cytometric sorting using Milli-Q™ water sheath fluid. Large (>53 μm) particles were concentrated in an IEC HN-SII centrifuge (Damon/IEC Division, 10 minutes, ~1800xG) and homogenized with a Teflon™ tissue grinder just prior to desalting.

For comparison with field samples, POM samples were also taken from a diatom degradation experiment conducted at CBL (University of Maryland). In this experiment *Thalassiosira weissflogii* (CCMP 13-36) was grown to late stationary phase in water from Lewes, DE (15 psu) in a 14:10 light:dark cycle at 20°C. The culture was then placed in the dark, and aerobic microbially-mediated degradation was allowed to proceed for 72 days using a flow-through system (2 L/day) with <5 μm Patuxent River water (10 psu). POM samples were collected via centrifugation (18,000xG for 25 minutes) and the resulting pellets were frozen. Prior to analysis the samples were thawed, filtered onto a 2.0 μm polycarbonate filter, resuspended in <0.2 μm seawater, and desalted by centrifugation with milli-Q water rinses. In this study samples from day 0 (DPP0) and day 72 (DPP72) of the experiment were then analyzed by DT-MS. 6.7% of the original carbon remained at Day 72 of the experiment.

$\text{NH}_3\text{-Cl}^+$ DT-MS was performed on a JEOL SX-102 mass spectrometer (direct inlet, mass range 60-1000, cycle time (0.76 + 0.10) seconds, resolution 3000, source temperature 160 to 175°C, total run time 2 minutes) with the sample probe (a 90:10

platinum:rhodium filament) resistively heated at 0.5 A/min. All mass spectra discussed below were summed across scans 60 to 105 in order to maximize the polysaccharide signal and minimize interferences from lipids in the sample. This scan range was chosen after analysis of mass chromatograms for characteristic polysaccharide and lipid m/z values. For principle component analysis, mass spectra summed over these scans were exported to the program FOMPyroMAP and principle component analysis was performed over the m/z range 60-600.

$\text{ND}_3\text{-Cl}^+$ DT-MS was performed on selected samples in order to strengthen molecular assignments of ions observed in the $\text{NH}_3\text{-Cl}^+$ experiments. Mass spectrometry conditions were identical to those for $\text{NH}_3\text{-Cl}^+$ DT-MS with the following exceptions: the lower mass limit was set at m/z 65 and the cycle time was (0.75 ± 0.10) seconds.

POC concentrations and C/N ratios were determined from 1-2 L of seawater filtered through precombusted GF/F filters (24 or 25 mm diam.) using a stainless steel pressure cannister and N_2 gas (<5 psi). The filters were frozen until analysis. Just prior to analysis, they were thawed, placed over fuming HCl for 24 to 48 hours, and dried overnight in an oven at approximately 60°C (Hedges and Stern, 1983). They were weighed and sectioned, and aliquots were then analyzed in replicate on a Fisons EA 1108 Elemental Analyzer.

Chlorophyll *a* concentrations were determined from pigment samples collected in the same manner as the POC samples but stored in liquid nitrogen until analysis. The pigment samples were then thawed and suspended in acetone. An internal standard (zinc pyropheophorbide octadecylester, collection 26-31, Fraction 6, from D. Repeta, WHOI) was added, and the entire sample was ground with a Teflon™ tissue grinder and then centrifuged to remove the filter material. The supernatant from the field samples was injected onto a C-8 reverse-phase column (Rainin "Microsorb 'short one,'" particle size 3 μm , pore size 100 angstroms, column size 4.6x100 mm) in a Waters 600E HPLC system with a photodiode array detector. Solvent A was MeOH: 0.5N NH_4Ac (75:25); solvent B, MeOH; solvent program (minutes, % Solvent A, % Solvent B), (0;100,0), (20;35,65),

Table 5.1. Characteristic carbohydrate m/z values

Compound	EI ⁺ , 16eV char m/z	NH ₃ -CI ⁺ char m/z	ND ₃ -CI ⁺ char m/z [#]
Polyhexoses	57, 60, 73, 98, 126, 144	180, 342, 504, 666 (transglycosylation series) 144, 162 (loss of H ₂ O moieties from 180) 240, 402, 564 (reverse aldolisation series)	187, ?, ?, ? 148/149, 167/168
Polypentoses	85, 114	132, 150, 210, 282, 342, 474	137/138, 156, ?, ?, ?, ?
Methyl-hexose		194	200
Furfural	96	114	
Methylfurfural	110	128	
Deoxyhexoses	128	128, 146, 164, 206	132/133, 151/152, 170, ?
Aminosugars	59, 73, 84, 125, 139		
NAG		204, 221, 186, 119, 102, 203, 126, 143, 222, 239, 77*	207, 227, 189/188, ?, 103, 209/208, ?, ?, 228, 248, 83
NAM		77, 203, 126, 143, 186, 185, 204, 108, 144, 221, 168, 119, 94, 102*	
Chitin		221, 204, 138, 186, 168, 126, 119, 77, 185, 143, 203, 152, 94, 163*	

[#] These values correspond to the NH₃-CI⁺ values to their left.

* Reported in order of decreasing intensity (from Klap, 1997).

(30;25,75), (35;0,100); flow rate, 1.5 mL/min (Goericke and Repeta, 1993; and Repeta, personal communication). The diatom degradation experiment samples were analyzed using a Supelcosil LC-18 column in a Waters 600E HPLC system with an HP1100 Series Diode Array Detector. Solvent A was 0.5N NH₄-acetate:methanol (20:80); solvent B, actone:methanol (20:80); solvent program (0;100,0), (20;0,100); flow rate, 1.5 mL/min.

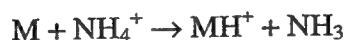
Results

Polysaccharides of POM subclasses

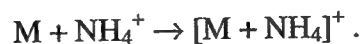
EI⁺ DT-MS coupled with discriminant analysis (Chapter 4) indicated that large-particle POM samples taken along the Mid-Atlantic Bight (MAB) in March 1996 exhibited enhanced pentose and hexose polysaccharide signatures over small-particle POM samples from the same stations. In contrast, near-shore (WHTS) large-particle POM appeared to contain more chitin fragments relative to small-particle POM rather than an enhancement in hexoses (Chapter 4). However, these EI⁺ DT-MS results require further confirmation as they are based on integer-mode data from mass spectrometric analysis with a non-specific ionization method. In other words, multiple ion fragments may contribute to the m/z values considered characteristic for polysaccharides.

As NH₃-Cl⁺ enhances carbohydrate signatures and reduces polysaccharide fragmentation, it is used here to complement and provide further confirmation for the EI⁺ results. There are two main forms of ionization that occur with NH₃-Cl⁺,

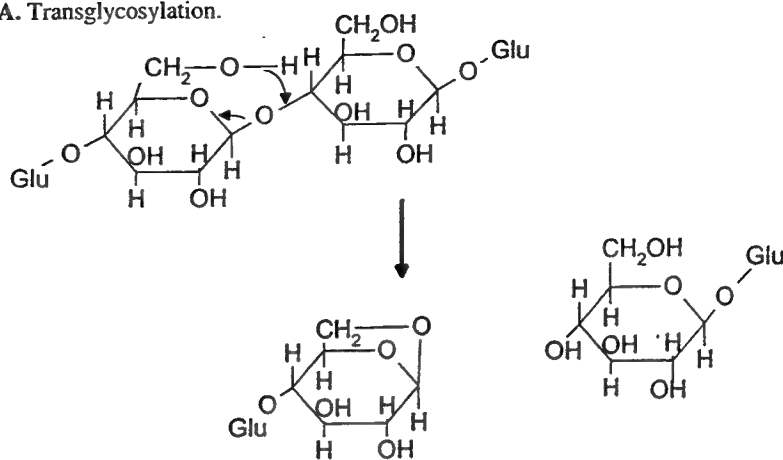
protonation:



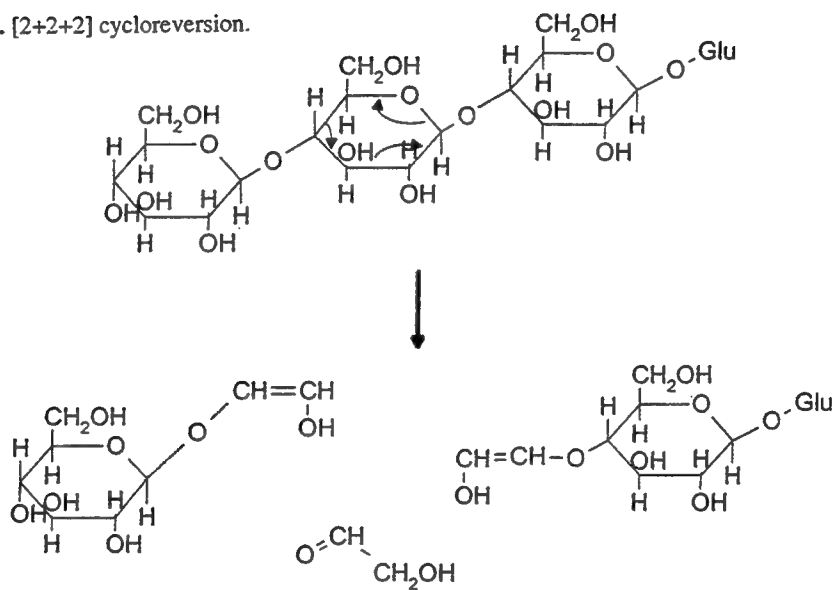
and ammonium adduct formation:



A. Transglycosylation.



B. [2+2+2] cycloreversion.



C. E_i elimination.

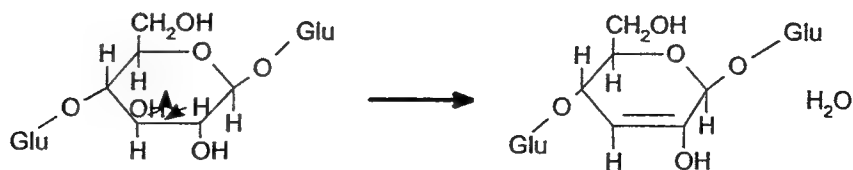


Fig. 5.2. Schematic of the three major forms of polysaccharide dissociation during DT-MS.

The polysaccharide signal is enhanced because labile carbohydrates generally remain fairly intact and can be observed as the ammonium adducts of molecular ions. In addition, pyrolytic dissociation of the polysaccharides occurs mainly through three pathways (Fig. 5.2): transglycosylation, [2+2+2] cycloreversion, and E_i elimination (Lomax et al., 1991; Arisz and Boon, 1995; Klap 1997). In transglycosylation (Fig. 5.2A), anhydrooligomers are formed from the cleavage of glycosidic bonds. In [2+2+2] cycloreversion (Fig. 5.2B), one monomer is cleaved, producing two $\text{CH}=\text{CH}-\text{OH}$ groups, one of which remains attached to each of the cleavage products, and releasing $\text{O}=\text{CH}-\text{CH}_2-\text{OH}$. E_i elimination from unsubstituted polysaccharides (Fig. 5.2C) generally leads to a loss of H_2O . Polysaccharide dissociation through these pathways, coupled with the lack of extensive fragmentation during ionization, leads to easily recognizable and interpretable ion series.

While $\text{NH}_3\text{-Cl}^+$ DT-MS of polysaccharides yields easily recognizable ion series, it provides little information to distinguish among isomeric saccharides. $\text{ND}_3\text{-Cl}^+$ can often be used to provide further structural information as free hydroxyl groups will readily undergo proton exchange with deuterium (see above). Thus the ammonium adduct of a saccharide will be 4 units higher due to ND_4^+ plus an additional mass unit for each exchangeable hydroxyl proton in its structure (see Table 5.1).

$\text{NH}_3\text{-Cl}^+$ DT-MS analyses of $>2\ \mu\text{m}$, $<53\ \mu\text{m}$ POM and $>53\ \mu\text{m}$ POM from station 8 (continental slope, Fig. 5.3a, b) and the same size-classes of POM from Great Harbor (Fig. 5.4a, b) are consistent with the EI^+ DT-MS data (see Table 5.1 for EI^+ , $\text{NH}_3\text{-Cl}^+$ and $\text{ND}_3\text{-Cl}^+$ mass spectral assignments for various polysaccharide components). The small-particle POM sample 8-S (Fig. 5.3a) is dominated by ammonia-adducts of anhydrohexoses (m/z 180, identification consistent with the presence of m/z 187 in the corresponding $\text{ND}_3\text{-Cl}^+$ mass spectrum) and anhydro-oligo-hexoses (m/z 342, 504, 666) from transglycosylation of polyhexoses. Also showing a distinct presence are ammonia-adducts from a reverse aldolisation cleavage of polyhexoses (m/z 240, 402, 564) and m/z values reflecting a loss of water (-18 mass units) from fragments in these two ion series

Figure 3

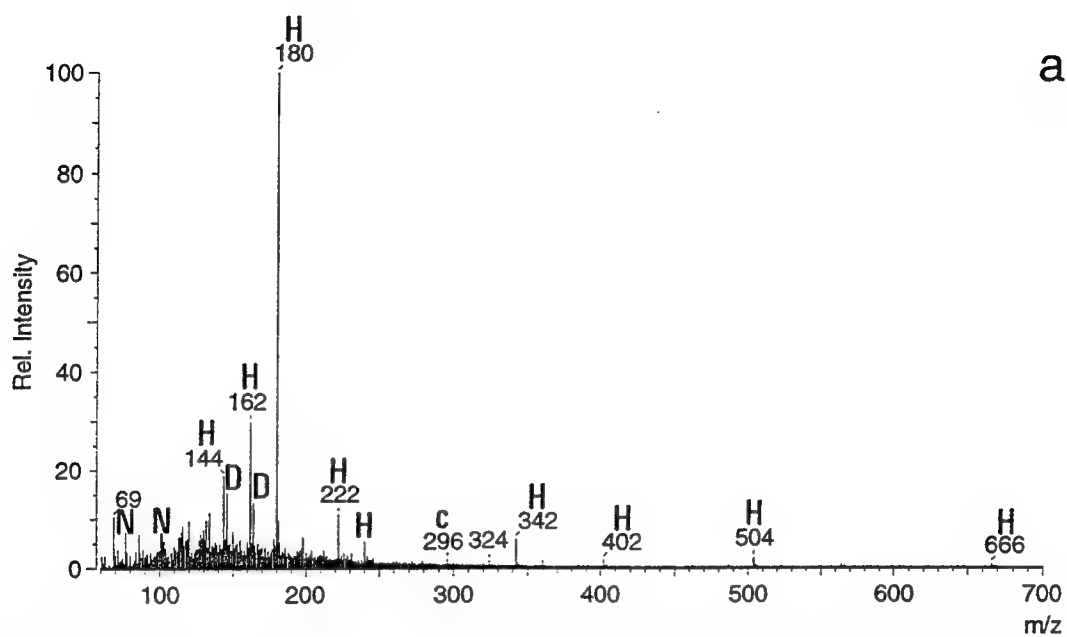


Fig. 5.3. a. $\text{NH}_3\text{-Cl}^+$ mass spectrum for sample 8-S. Symbols for Fig. 5.3: **N**, aminosugar; **H**, hexose; **D**, deoxyhexose; **c**, chlorophyll.

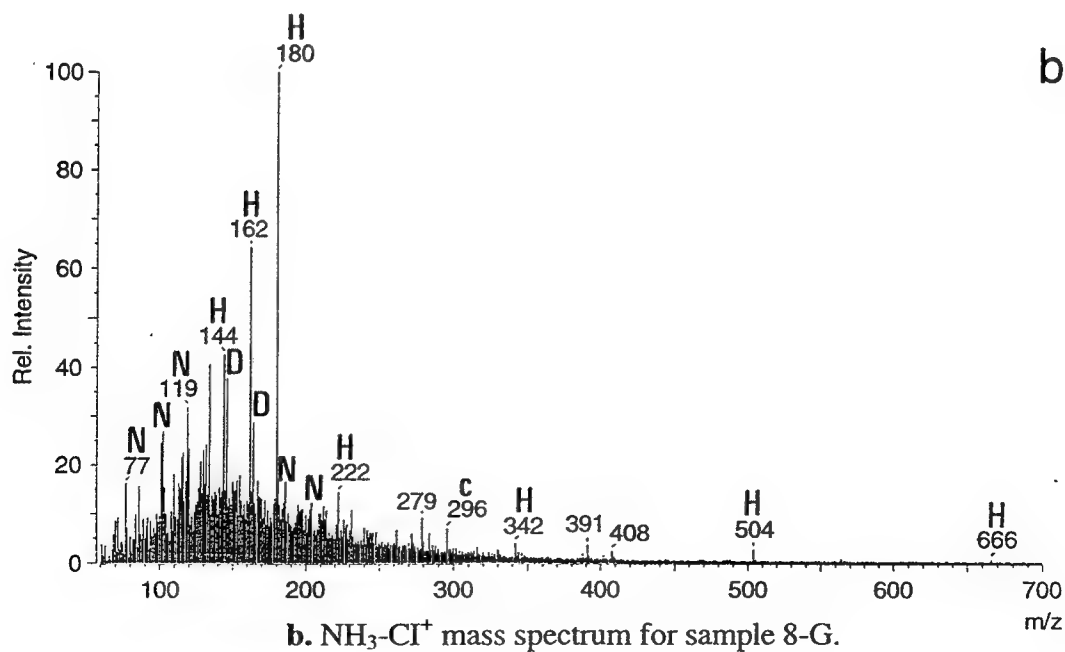


Figure 4

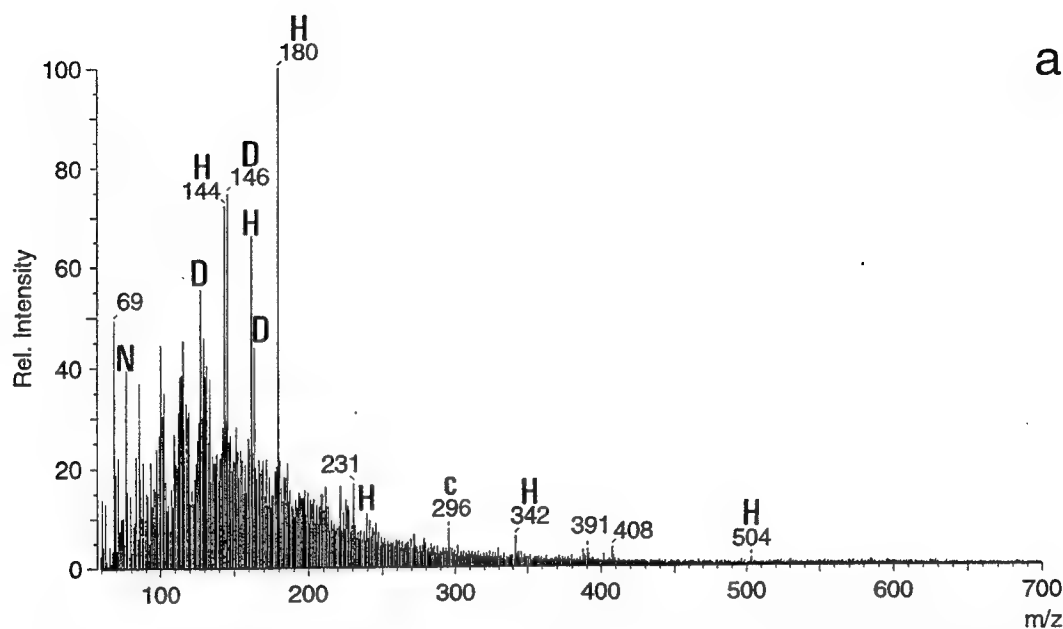
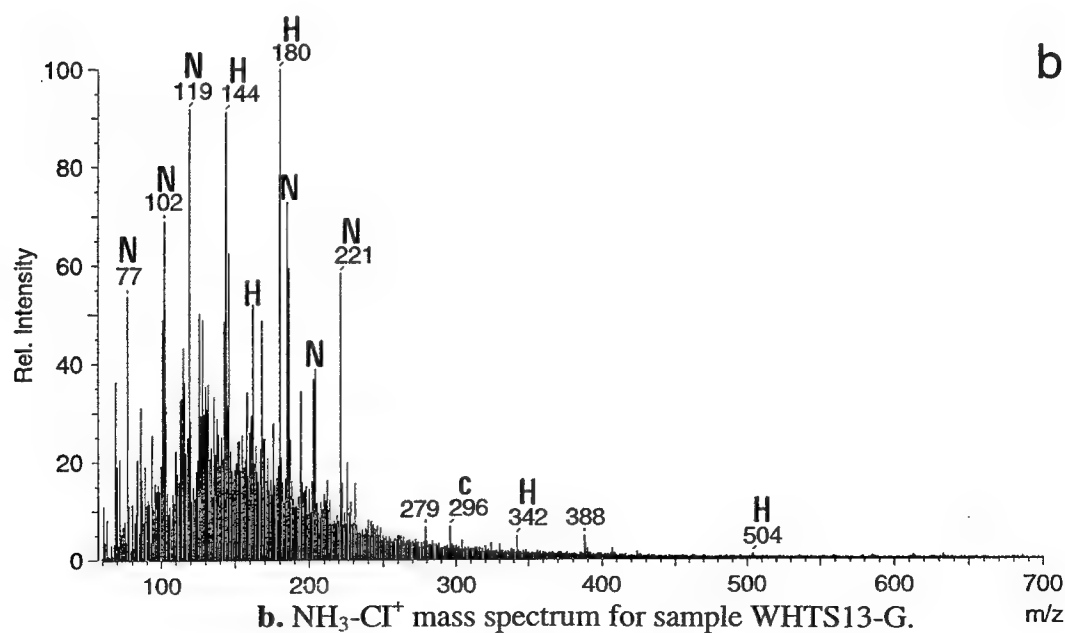


Fig. 5.4. a. $\text{NH}_3\text{-Cl}^+$ mass spectrum for sample WHTS13-S. Symbols for Fig. 5.4: **N**, aminosugar; **H** hexose; **D**, deoxyhexose; **c**, chlorophyll.



b. $\text{NH}_3\text{-Cl}^+$ mass spectrum for sample WHTS13-G.

(Lomax et al., 1991, Arisz and Boon, 1995, Klap, 1997). There is some evidence for the presence of deoxysugars (m/z 146, 164) but no discernible ion series for pentoses or aminosugars. The corresponding large-particle POM sample (8-G, Fig. 5.3b) has a more complex mass spectrum in which several carbohydrate ion series are superimposed on an "envelope" of non-specific m/z values. The polyhexose pattern seen in Fig. 5.3a is again evident. In addition, there appears to be a minor contribution from aminosugars (m/z 77, 102, 119, 143, 203, 221) as identified by comparison with $\text{NH}_3\text{-Cl}^+$ DT-MS of standards (de Nobel et al., 1993, Klap 1997). This identification is strengthened by analogy to 2-G, whose $\text{ND}_3\text{-Cl}^+$ mass spectrum contains m/z 228, 209, and 82/83 (corresponding to m/z 221, 209, and 77 in $\text{NH}_3\text{-Cl}^+$, Boon et al. 1998). The 8-G sample also appears to contain a trace contribution from polypentose fragments (m/z 150, 210, 282, 342, 474, Lomax et al. 1991). The presence of heteropolysaccharides in these samples is not excluded as they would appear as a suite of monomeric fragments with few oligomers (Boon, personal communication). For both samples from station 8, polyhexoses, appear predominant. While the mass spectra from 8-S and 8-G look fairly similar, there are distinct differences in the WHTS13-S and WHTS13-G (Fig. 4a, b) spectra. Notably, the ion series for aminosugars in WHTS13 large-particle POM rivals the intensity of the ion series for polyhexoses. Thus, the EI^+ data is corroborated, though pentose enrichment in large-particle POM appears weak in the $\text{NH}_3\text{-Cl}^+$ mass spectra.

Polysaccharides in small-particle POM from WHTS13 were further explored after separation of WHTS13-S into "phytoplankton" and "detritus" via flow cytometry. EI^+ MS data indicated that "detritus" was enriched in polysaccharide fragments (including m/z 96, 110, and 126, tentatively identified as furfural, methylfurfural, and tri-anhydrohexose) as compared to "phytoplankton." $\text{NH}_3\text{-Cl}^+$ DT-MS of these two subclasses (Fig 5.5a, b) is consistent with these identifications although, in both samples, an ion series from chloride clusters overwhelms the other series in later scans (not shown). This chloride cluster series probably stems from incomplete desalting of the flow cytometry samples and indicates that in the future, multiple Milli-Q™ water rinses

Figure 5

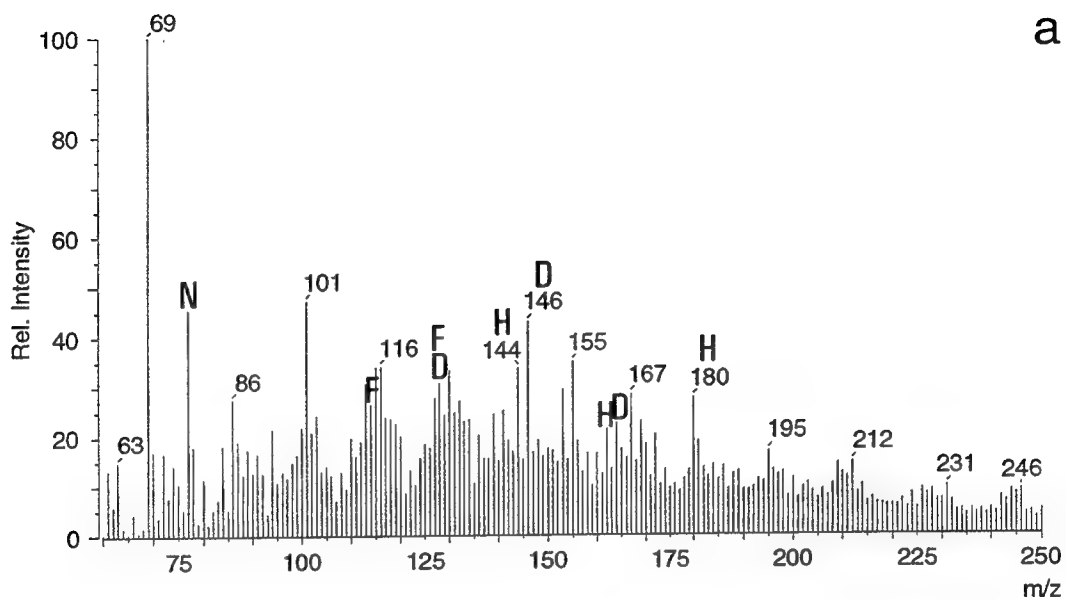
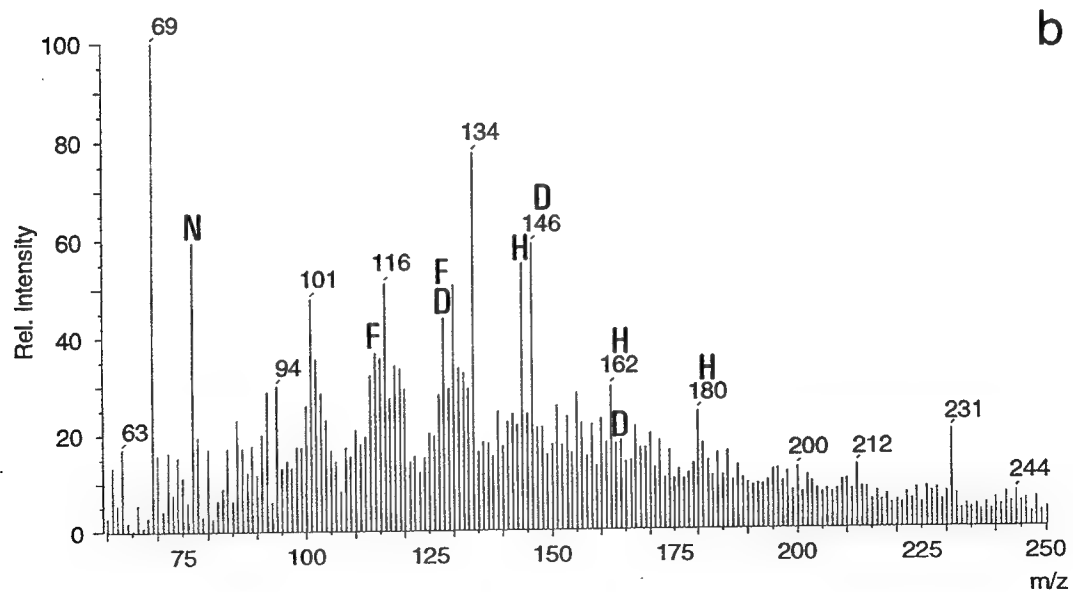


Fig. 5.5. a. $\text{NH}_3\text{-Cl}^+$ mass spectrum for sample WHTS13-P. Symbols for Fig. 5.5: **N**, aminosugar; **H** hexose; **D**, deoxyhexose; **F**, furfural; **c**, chlorophyll.



b. $\text{NH}_3\text{-Cl}^+$ mass spectrum for sample WHTS13-D.

should be used rather than reliance on dilution by Milli-Q™ sheath water during the sorting procedure. Under $\text{NH}_3\text{-Cl}^+$ conditions, both the “phytoplankton” and “detritus” spectra (Fig. 5.5a and b) contain ions attributed to: acetamide from aminosugars (m/z 77); tri-anhydrohexose, di-anhydrohexose and anhydrohexose from hexoses (m/z 144, 162, 180, respectively); dianhydrodeoxyhexose from deoxyhexose (m/z 146); and furfural and methylfurfural (m/z 114 and 128, respectively). In “phytoplankton” as compared to “detritus,” the relative intensity of anhydrohexose is higher as compared to the other sugars. The other sugar signatures, especially dianhydrodeoxyhexose, tri-anhydrohexose, methylfurfural, and acetamide have higher intensities (relative to the base peak) in “detritus” than in “phytoplankton.” Both “phytoplankton” and “detritus” lack oligomer information. This may also be due to the presence of seasalt through a mechanism analogous to that described for alkali metals and amylose (Scheijen and Boon, 1989). Chloride may also react with available protons in the sample to release HCl, leaving the rest of the sample more basic and thus shifting polysaccharide pyrolysis toward more reverse aldol condensation relative to transglycosylation (van der Kaaden et al., 1983). This could also explain the lack of intensity of m/z 180, the major ion resulting from transglycosylation of polyhexoses.

Principal component analysis (PCA)

To obtain an overview of polysaccharide variation in surface-ocean POM, $\text{NH}_3\text{-Cl}^+$ data from the six large-particle and small-particle POM field samples (see experimental) and two diatom degradation experiment samples were analyzed via principal component analysis (PCA). WHTS13-P and WHTS13-D, the two flow cytometry samples, were not included because of the salt interferences described above.

DPP0, from the beginning of the diatom degradation experiment, and DPP72, from day 72 of the experiment, bracket the field samples in the score plot of Principal Component 1 (PC1, shown in Fig. 5.6), responsible for 51.7% of the variance in the data

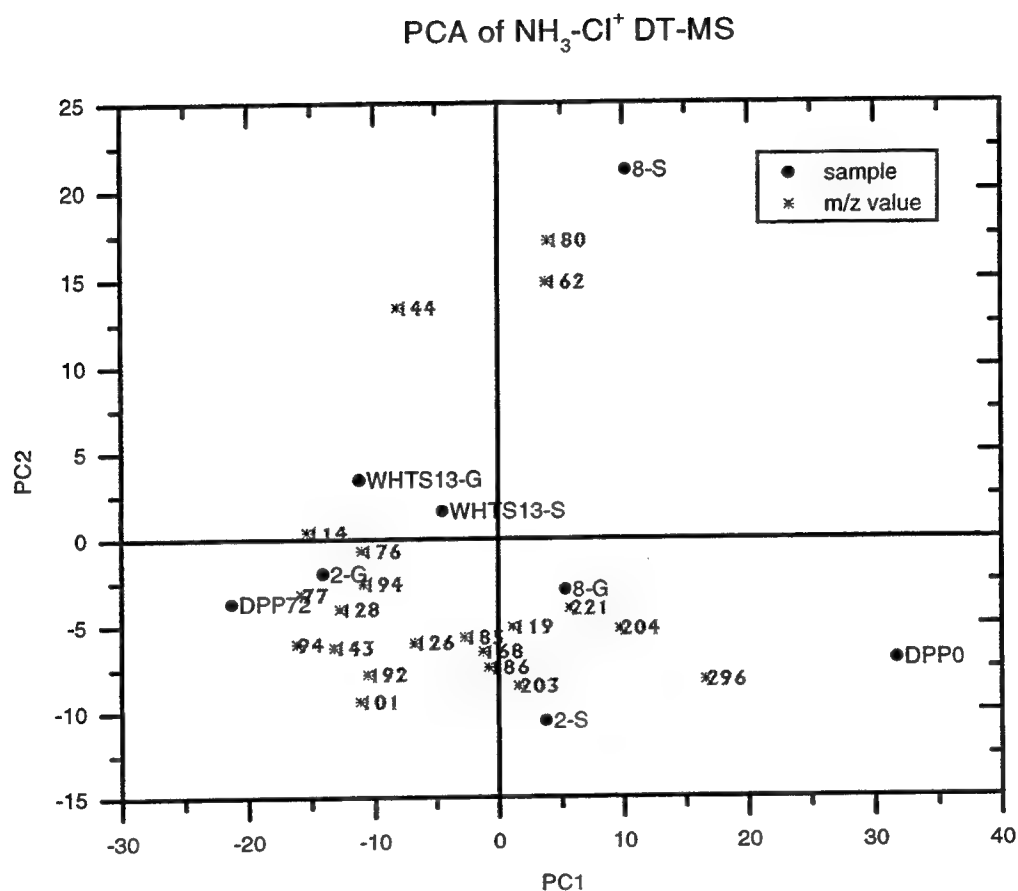


Fig. 5.6. Score plot for principal component analysis of $\text{NH}_3\text{-Cl}^+$ mass spectra of large-particle POM (WHTS13-G, 2-G, 8-G) and small-particle POM (WHTS13-S, 2-S, 8-S) and diatom degradation experiment (DPP0, DPP72) samples. The loadings for selected m/z values are superimposed upon the score plot to indicate the relative contribution of these values to the samples. In other words, m/z values falling in the same direction from the origin as the samples are important contributors to the samples; the relative distance of the m/z values from the origin is a measure of the strength of their contribution.

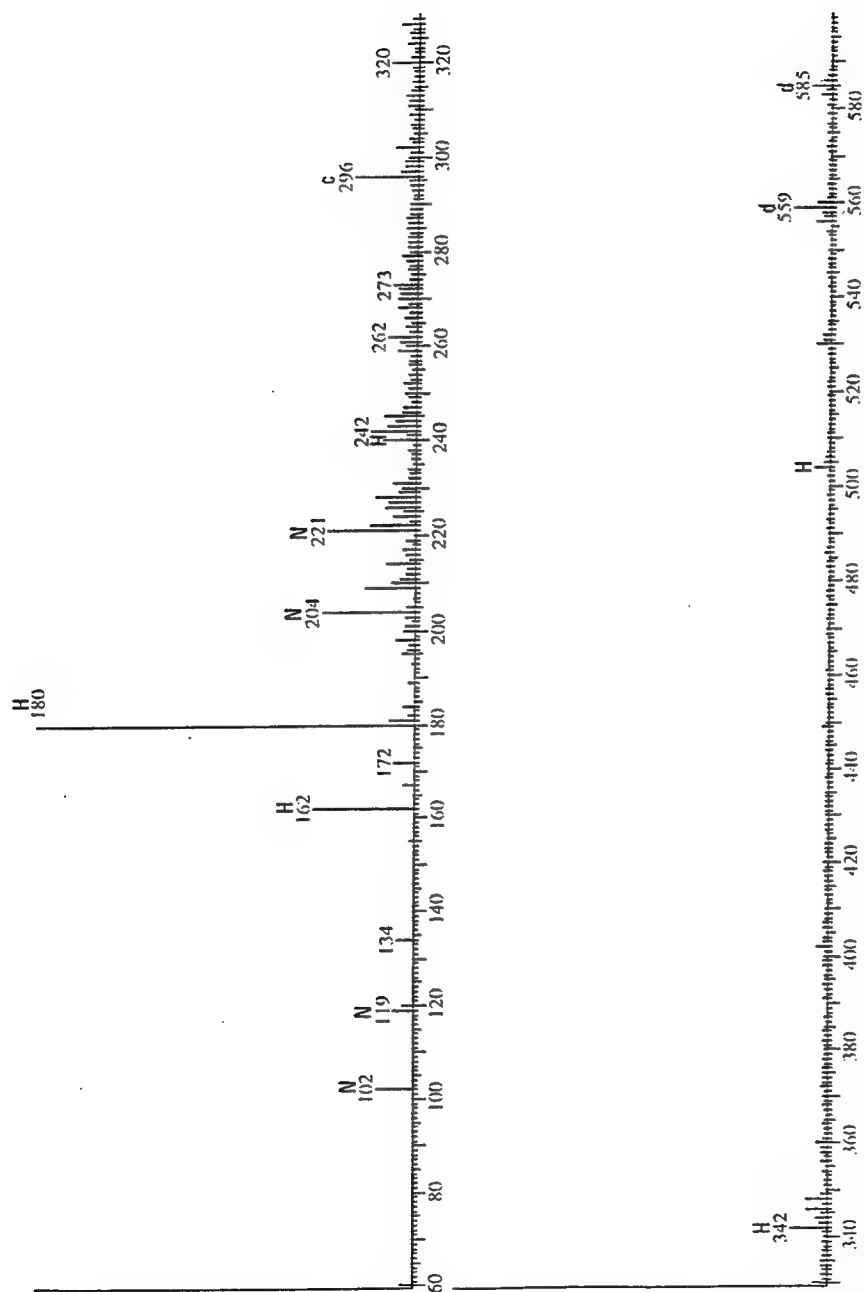
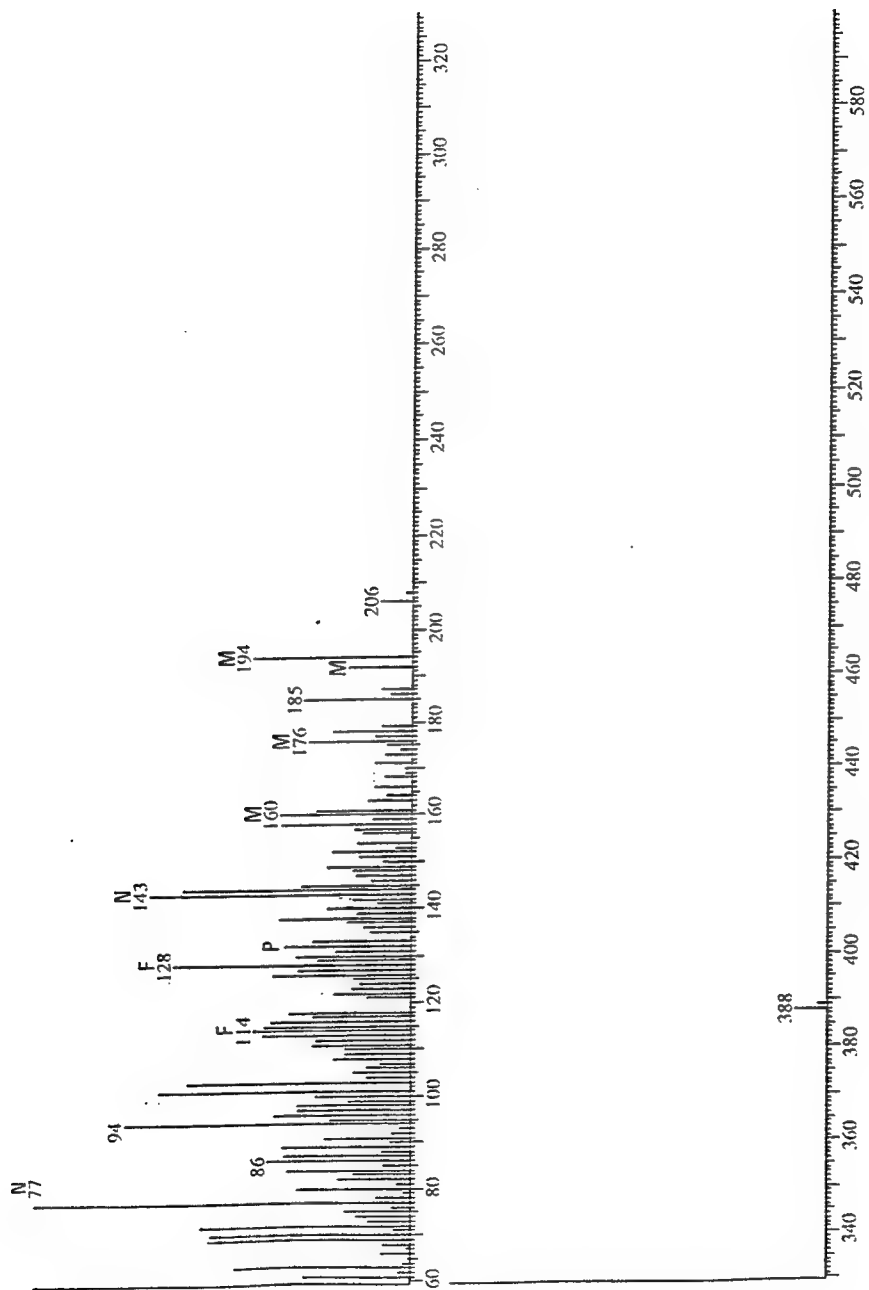


Fig. 5.7. a. Reconstructed spectrum for Principal Component +1, in which the "fresher" organic matter appears, illustrating the m/z values responsible for the relationship among samples shown in the score plot in Fig. 5.5.

Symbols for Fig. 5.7 are as follows: **N**, aminosugar; **H**, hexose; **P**, pentose; **F**, furfural or methylfurfural; **M**, methyl hexose or methyl deoxyhexose; **C**, phytadiene; **d**, diglyceride. Capital letters indicate carbohydrates; lower case letters, lipids.



b. Loadings plot for Principal Component -1, in which the "more degraded" organic matter appears.

set. This bracketing of the samples might indicate that PC1 could be considered an indicator of the extent/degree of degradation of the organic matter. However, it could also mean that PC1 is mainly determined by the chemical signatures of these two samples. To check this, the diatom degradation experiment samples were removed from the sample set and PCA was performed as before. The samples plotted in the same order in the same regions of PC1, with PC+1 loadings, as before, characterized by polyhexose and PC-1 exhibiting a similar signal to the previous PC-1 (see below), though containing a more intense aminosugar signal.

In order to constrain potential terrestrial inputs and organic matter "freshness" levels in the samples, the ratio of POC/chlorophyll *a* ([POC]/[chl *a*] in terms of $\mu\text{g/L}/[\mu\text{g/L}]$) and the atomic C/N ratio were measured. These parameters have been used to indicate reworking of organic matter and/or terrestrial inputs of organic matter to marine systems (Cifuentes et al., 1996, and references therein). Like all bulk measurements, however, they should be used with caution; for example, there is some indication that high bacterial biomass levels and bacterially-mediated humification processes can significantly lower C/N ratios, thus making them unreliable for determinations of terrestrial input (Cifuentes et al., 1996). No significant terrestrial inputs are present in the diatom degradation experiment samples (DPP0 and DPP72). Therefore, the extremely high [POC]/[chl *a*] ratio (2700) in DPP72 indicates a strong degree of organic matter degradation. Significant terrestrial inputs in the field samples appear unlikely for two reasons: atomic C/N ratios (Table 5.2) are lower than the "average marine phytoplankton" value of 6.6 proposed by Redfield et al. (1963), and [POC]/[chl *a*] values are similar to those reported for a seawater phytoplankton consortium isolated within a plastic sphere and monitored over time (25 to 60, Parsons et al., 1984). If there were considerable terrestrial inputs (and bacterial effects on C/N were minimal), C/N and [POC]/[chl *a*] ratios should both be considerably higher. If the

Table 2- The ratio of POC concentration and chlorophyll *a* concentration and the atomic C/N ratio for POM samples (see text for details).

Sample	[POC]/[chl <i>a</i>] ($\mu\text{g/L}$)/($\mu\text{g/L}$)	(C/N) _a
DPP72*	2700	6.24
WHTS13	90	3.6
2	50	4.7
8	50	5.1
DPP0*	40	7.45

* [POC] and (C/N)_a from R. T. Nguyen and H. R. Harvey; procedure described in Nguyen and Harvey, 1997.

assumption is made that, in the field samples, total POM consists mainly of small-particle POM, then the trend in [POC]/[chl *a*], which was measured on POM >0.8 μm for both degradation experiment and field samples, is consistent with the hypothesis that PC1 is a “freshness” indicator. In other words, the samples with lower [POC]/[chl *a*] ratios plot farther into PC+1, while those with higher ratios plot farther into PC-1 (Fig. 5.6).

The reconstructed mass spectra from PC1 loadings (Fig.5.7a, b) indicate the *m/z* values responsible for the separation of samples in Fig. 5.6 (selected *m/z* values are also superimposed onto Fig. 5.6 for ease in viewing the relative contributions of these values to PC1 and PC2). The “freshest” organic material falls within PC+1, whose loadings indicate enrichment in polyhexose polymers (both the transglycosylation ion series and the reverse aldolisation ion series appear), chlorophyll (*m/z* 296 from the ammonia-adduct of phytadiene), and aminosugars (*m/z* 102, 119, 204, 221). The “more degraded” organic material, PC-1, shows no enrichment in oligomer fragments. It appears enriched in *m/z* 114, 128 (identified as furfural and methylfurfural, respectively) and 144 (tri-anhydrohexose?). There also appears to be significant enrichment in methyl-deoxyhexoses (*m/z* 160, 176, and 192), methyl-hexose (*m/z* 194), and the aminosugar fragments, acetamide (*m/z* 77) and trianhydrohexoseamine (*m/z* 143).

Mass unit values consistent with deoxyhexoses (m/z 128, 146, 164, and 206) appear in this reconstructed spectrum but at lower intensities.

The identifications of m/z values in PC+1 and PC-1 are strengthened by comparison of $\text{NH}_3\text{-Cl}^+$ and $\text{ND}_3\text{-Cl}^+$ mass spectra of 8-S and 2-S. Further evidence for a polyhexose signature in PC+1 is given by $\text{ND}_3\text{-Cl}^+$ MS of 8-S. The resulting spectrum contains m/z 187, 168, and 149 (corresponding to 180, 162, and 144 in $\text{NH}_3\text{-Cl}^+$ MS). The identification of the methyl hexose signal (m/z 194) for PC-1 is also strengthened by comparing $\text{ND}_3\text{-Cl}^+$ and $\text{NH}_3\text{-Cl}^+$ analyses of 2-S, which yield corresponding ions at m/z 200 and m/z 194 respectively. Although the sample 2-S falls within PC+1, it was chosen because it has the most distinct m/z 194 of any of the samples analyzed via $\text{ND}_3\text{-Cl}^+$ MS.

PC2 is responsible for 17.2% of the variance in the data set. PC+2 consists mainly of hexose ions (m/z 180 and 162), while PC-2 consists of aminosugar ions (m/z 77, 94, 119, 126, 143, 168, 185, 186, 203, 204, 221). The relative contribution of these ion series to PC1 and PC2 is shown in Fig. 5.6.

Discussion

To summarize the above results, $\text{NH}_3\text{-Cl}^+$ DT-MS has confirmed polysaccharide trends from discriminant analysis of EI^+ DT-MS data and has provided new information on polysaccharide variations among POM subclasses.

In our ammonia- Cl^+ analyses of suspended POM, the main polysaccharide signal is from polyhexoses. The prevalence of polyhexoses is consistent with neutral aldose studies indicating that glucose is the most common aldose in POM (Tanoue and Handa, 1987; Hernes et al., 1996; Skoog and Benner, 1997). Glucose, a hexose, is the monomeric unit for several storage polysaccharides (e.g., starch, laminaran) and structural polysaccharides (including cellulose) and is probably the monomeric unit for the majority of our polyhexose signal.

As station WH is coastal and station 8 is on the continental margin, the strong polyhexose signature present in our small-particle POM samples could result from allochthonous sources of organic matter; land plants contain a very strong polysaccharide (mainly cellulose) component. However, C/N and POC/chl *a* ratios indicate that the organic matter present in this small-particle POM is primarily marine; therefore, it is unlikely that cellulose ($\beta 1 \rightarrow 4$ glucan) from land plants could be responsible for the polyhexose signal.

Aldose studies of phytoplankton cultures and field samples (Hecky et al., 1973; Cowie and Hedges, 1984; Cowie, 1990; Cowie et al., 1992; Hamilton and Hedges, 1988; Tanoue and Handa, 1987), like the POM studies, generally find glucose to be the most common monomer. This trend is attributed by Arnosti (1993) to the prevalence of glucose-based storage polysaccharides in phytoplankton. Glucose has also been found to be quite prevalent in phytoplankton structural polysaccharides. In fact, Biersmith and Benner (1998) found glucose to be a much higher mole percentage of total aldoses in cell structural organic matter (CSOM) as compared to cell lysate organic matter (CLOM) in the prymnesiophytes *Phaeocystis* sp. and *Emiliana huxleyi*. In the cyanophyte *Synechococcus bacillaris*, glucose represented greater than 50 mole % of the total aldoses in both CSOM and CLOM. In the diatom *Skeletonema costatum*, however, the contribution of glucose to total aldoses in CSOM was much lower than for the other algae and was similar to the glucose contribution to CLOM aldoses (~30 mole %). The prevalence of glucose in structural polysaccharides reported by Biersmith and Benner (1998) contradicts previous studies such as Cowie and Hedges (1996). In this earlier study, whole cells of the diatom *Thalassiosira weissflogii* were found to be considerably enriched in glucose relative to cell wall material. The difference was attributed to glucan storage polymers in cell sap. The results of Biersmith and Benner (1998) may be due to species-specific polysaccharide variations or to their analytical protocol. They separated CSOM and CLOM by centrifugation; as a result, their CSOM contained whole cells as well as cell structural material and their CLOM may have included extracellular material.

Pigment analyses indicate that diatoms are the dominant phytoplankton in our samples; fucoxanthin and chlorophyll *a* are the only identifiable pigments at Station 8 and fucoxanthin concentrations are second only to chlorophyll *a* in the WHTS 13 pigment sample (Minor, Appendix 3). Both Cowie and Hedges (1996) and Biersmith and Benner (1998) indicate that, in diatoms, a considerable portion of cell glucose is found in cell sap. Therefore, it appears probable that, in these samples, most of the polyhexose signal results from laminaran, the storage sugar in diatoms (Painter, 1983).

Large-particle POM from Station 8 has a more complex sugar pattern which, while still dominated by polyhexoses, includes a distinct signature from aminosugars, probably chitin from either zooplankton (e.g. Ittekkot et al., 1984) or diatoms (Painter 1983). Sample WHTS13-G has an aminosugar signal equal in intensity to the polyhexose ion series. This information, coupled with EI⁺ DT-MS data showing that large-particle POM from Station WH is strongly enriched in cholesterol relative to small-particle POM from the same station (Chapter 4), indicates a significant zooplankton presence.

NH₃-CI⁺ DT-MS of "phytoplankton" and "detritus" from flow cytometric sorting of WHTS13-S agrees with EI⁺ DT-MS in that "detritus" is richer in selected sugars (methylfurfural, tri-anhydrohexose, dianhydrodeoxyhexose) than "phytoplankton." "Phytoplankton" particles are slightly enriched in anhydrohexose, a major pyrolysis product of hexoses (Lomax et al., 1991; and Klap, 1997). Unfortunately, a salt signal from incomplete desalting of these samples dominates the mass spectra and appears to have obscured any oligomer information, including any evidence of polyhexose enrichment in "phytoplankton."

PCA of NH₃-CI⁺ mass spectra from >53 μm and >2 μm, <53 μm POM field samples and two diatom degradation samples indicates that the most variance in polysaccharide composition appears to be related to the degree of degradation of the organic matter. The "freshest" samples (found in PC+1) are enriched in polyhexoses, probably from storage sugars, and selected aminosugar fragments, perhaps from chitin. The "more degraded" samples (PC-1) are enriched in furfural, methylfurfural, m/z 144

(tentatively identified as trianhydrohexose), methyl-hexose, methyl-deoxyhexose, acetamide, trianhydrohexoseamine, and, to a minor extent, deoxyhexoses.

The separation of aminosugar fragments between PC+1 and PC-1 is somewhat puzzling at first. It could result from incomplete rotation of the aminosugar signal in the principal component analysis. However, the separation among aminosugar fragments in the plot of PC1 and PC2 (Fig. 5.6) indicates the possibility that there are two sources of aminosugar whose ion series vary in intensity. Chitin (poly-[1→4]-β-N-acetyl-D-glucosamine), from zooplankton and/or diatoms could be the source of aminosugar in the “fresher” region; while bacterial cell wall material, probably consisting of peptidoglycans with equal amounts of N-acetylglucosamine (NAG) and N-acetylmuramic acid (NAM) (Voet and Voet, 1990) may be the source in the “more degraded” region. This interpretation is strengthened by comparison with NH₃-CI⁺ DT-MS analyses of chitin, NAG, and NAM standards (Klap, 1997). In the mass spectra of chitin and N-acetylglucosamine, m/z 77 is relatively low in intensity (48% and 8% (relative to the base peak) respectively), while for N-acetylmuramic acid, m/z 77 is the base peak (Klap, 1997). A similar argument can be made for m/z 143 in PC-1; this mass unit is 59% of the base peak in NAM, 24% in NAG and 30% in chitin. Comparison of the locations in which m/z 77 and m/z 143 fall in the plot of PC1 vs. PC2, indicate that these m/z values may be related. The two largest aminosugar mass unit values in PC+1 are m/z 204 and 221, which are also the two most dominant values in the chitin standard (Klap, 1997). In Fig. 5.6, these m/z values appear related to each other (as they fall along the same line from the origin), but relatively unrelated to m/z 77 and m/z 143. Mass unit values sharing similar intensities in chitin, NAG, and NAM fall within the arc defined by m/z 77 and m/z values 221 and 204. Based on this information we infer that there is more than one aminosugar component in these POM samples and we suggest that one of these is a bacterial cell wall component and that the other may be chitin, from either phytoplankton or zooplankton.

The molecular-level characteristics of "degraded" organic matter (PC-1) appear to result from both polysaccharide degradation and enrichment in bacterial biomass. Evidence for polysaccharide degradation includes the depletion in storage sugars relative to "fresher" organic matter and the presence of the polysaccharide ion series, m/z 114, 128, and 144. Klap (1997) found this ion series to be present at greater intensities in floodtide winter seston relative to floodtide summer seston in Saeftinghe salt marsh, The Netherlands. The presence of furfural (m/z 114) and methylfurfural (m/z 128) has also been noticed in suspended POM from the Rhone River; where it was attributed by Sicre et al. (1994) to "partially transformed polysaccharides" that may result from degraded plant lignocellulose. Whether or not this "degraded" polysaccharide signature is from allochthonous material, it appears to be enhanced in samples characterized by a lack of fresh autochthonous organic matter. The presence of bacterial biomass in the "more degraded" organic matter is indicated by the aminosugar signature described above and by the presence of the methyl-hexose and methyl-deoxyhexose signatures in the PC-1 reconstructed spectrum. Methylated sugars have been found in lipopolysaccharides from bacterial cell envelopes (Weckesser et al., 1979; Klok et al., 1984b, and references therein) and in a high molecular-weight material from marine sediments believed to be lipopolysaccharide (Klok et al., 1984a; Klok et al., 1984b). Therefore, they are inferred to be bacterial biomass indicators (Boon et al., 1998; Moers, 1989; and Klok et al., 1984a; Klok et al., 1984b). The possibility that a considerable portion of the POM pool may consist of bacterial biomass has been explored in algal degradation experiments (Harvey and Macko, 1997); during oxic degradation up to 21.4% of POC could be accounted for by bacterial carbon. Therefore, it is quite probable that some of our POM samples contain a considerable bacterial biomass component.

The depletion in storage polysaccharides between "fresher" organic matter and "degraded" organic matter is consistent with the observation that intracellular polysaccharides, and indeed intracellular polymers in general, are preferentially digested in feeding experiments with the diatom *Thalassiosira weissflogii* and the herbivore

Calanus pacificus (Cowie and Hedges, 1996). It is also consistent with depth profiles of aldoses collected via sediment trap in the equatorial Pacific (Hernes et al., 1996) if one assumes depth and increased degradation to be correlated. Puzzlingly, however, Skoog and Benner (1997) find that in suspended POM (0.1→60 μm) from the equatorial Pacific, the mole % of glucose increases, rather than decreases, with depth, indicating that glucose is a relatively refractory aldose. However, in their study, only 7 to 20 % of the total carbohydrate pool could be accounted for as neutral aldoses. DT-MS may measure a different portion of the carbohydrate pool, thus leading to the polyhexose trend in PC1. It is also possible that our POM size fractions (2→53 μm , >53 μm) contain a very different neutral aldose composition than equatorial Pacific particles ranging between 0.1 and 60 μm .

Finally, it is of interest to compare DPP72, the most “degraded” POM sample according to PC-1, with colloidal dissolved organic matter (DOM, >1kD) that can be recovered via ultrafiltration and analyzed by the same technique. NMR analysis (Aluwihare et al., 1997) and monosaccharide analysis (McCarthy et al., 1996; Aluwihare et al., 1997) indicate that ultrafiltered DOM (UDOM) is remarkably constant in composition throughout the world’s oceans. Therefore, the spectrum in Fig. 5.8a, which shows the results of $\text{NH}_3\text{-Cl}^+$ DT-MS of UDOM from Georges Bank (Boon et al., 1998) can be considered a valid approximation for “oceanic UDOM” and compared with the spectrum for DPP72 (Fig. 5.8b), POM collected from Day 72 of the diatom degradation experiment. All the dominant m/z values in the UDOM spectrum are clearly present in DPP72 (and in the field sample 2-S, spectrum not shown). The main difference between the two spectra is that DPP72 (Fig. 5.8b) contains strong hexose and deoxyhexose signals.

The UDOM spectrum thus appears to be an attenuated POM spectrum, where the POM already shows substantial signs of degradation and incorporation of bacterial biomass. This indicates that UDOM is either the product of further degradation of the main components of POM or related to a subclass (perhaps refractory) of POM. UDOM

Figure 8

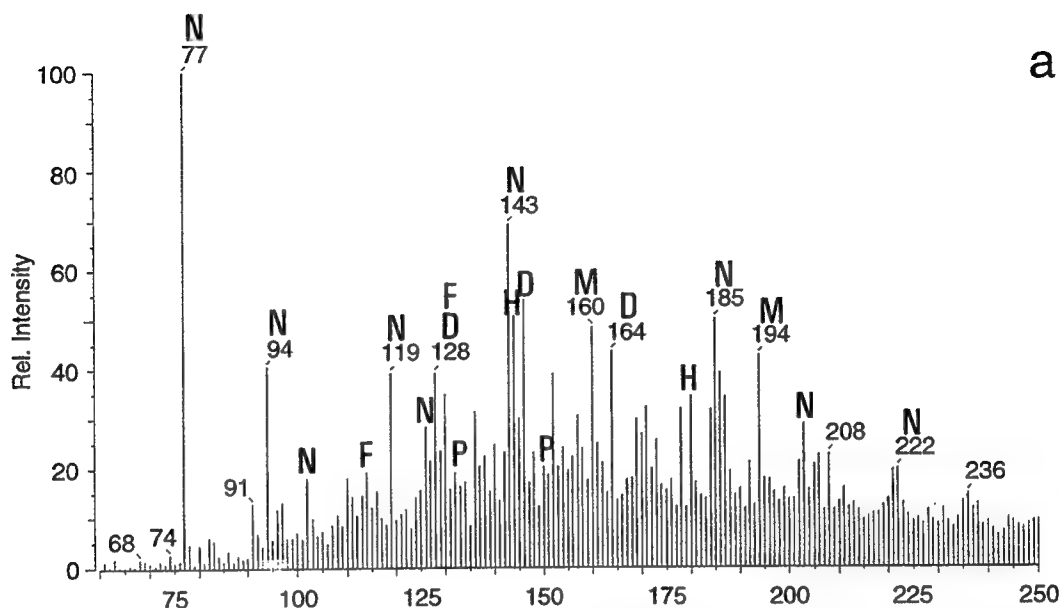
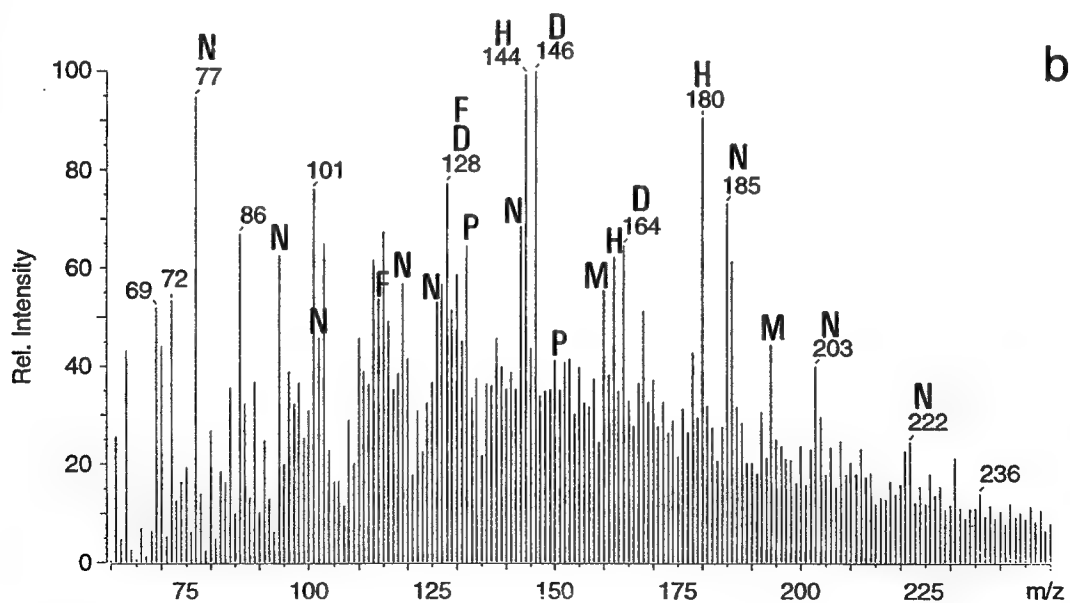


Fig. 5.8. a. $\text{NH}_3\text{-Cl}^+$ DT-MS of UDOM from Georges Bank. From Boon et al., 1998. Symbols for Fig. 5.8: **N**, aminosugar; **H**, hexose; **D**, deoxyhexose; **P**, pentose; **F**, furfural or methylfurfural; **M**, methyl hexose or methyl deoxyhexose; **c**, phytadiene; **d**, diglyceride.



b. $\text{NH}_3\text{-Cl}^+$ spectrum of DPP72, a POM sample collected from day 72 of a diatom degradation experiment (see text).

could result from selective preservation of particular components of the POM such as bacterial and /or phytoplankton cell wall or membrane material. The aminosugar, methylhexose, and methyl-deoxyhexose presence in UDOM would be consistent with selective preservation of bacterial cell wall and membrane material. An additional hypothesis is that UDOM carbohydrate consists mainly of exopolymer secretions (EPS) from bacteria and phytoplankton, which would be likely to increase at the end of a bloom (Decho, 1990 and references therein), and which would also be likely to appear in more "degraded," in other words, less phytoplanktonic, POM. The apparent lack of oligomer fragments in the more "degraded" samples (and UDOM) and the increase in intensity of a mixture of monosaccharide components indicates that there is a shift away from homopolysaccharidic constituents to heteropolysaccharidic constituents (Boon, personal communication). Such a shift would be consistent with an increasing proportion of EPS in the samples since both diatom exopolymer secretions and many marine bacterial EPS are known to contain a large heteropolysaccharide component (Decho, 1990). The above hypotheses assume that UDOM results from a process or processes acting upon particulate organic matter. Chin et al. (1998) provide interesting evidence that DOM may aggregate to form POM through the formation and annealing of exopolymer gels. These workers found that POM forms abiotically in $<0.22\ \mu\text{m}$ filtered seawaters samples following formation times and size and concentration functions consistent with polymer gel theory.

Regardless of the actual processes relating POM and UDOM, the fact that POM appears "fresher" than UDOM is consistent with the "size-reactivity continuum model" proposed by Amon and Benner (1996). This model, which states that larger organic matter size classes are generally more bioreactive than smaller organic matter size classes, appears to hold if POM is considered one large OM size class. However, $>53\ \mu\text{m}$ POM in this study appears less "fresh" than the corresponding $2\rightarrow 53\ \mu\text{m}$ POM, indicating that, in the surface ocean, for particles larger than or equal in size to the primary producers, the model no longer applies.

Conclusions

1. $\text{NH}_3\text{-Cl}^+$ DT-MS indicates that surface-ocean small-particle ($2\rightarrow 53\text{ }\mu\text{m}$) POM is enriched in storage polysaccharides relative to large-particle ($>53\text{ }\mu\text{m}$) POM. Large-particle POM shows varying levels of enrichment in aminosugars (probably chitin).
2. When principle component analysis is performed on $\text{NH}_3\text{-Cl}^+$ mass spectra of POM from a diatom degradation experiment and field large-particle and small-particle POM samples, the most variance in the data set appears related to the degree of degradation of the organic matter. The "fresher" organic matter is enriched in "storage" polysaccharides while the "degraded" organic matter indicates both polysaccharide degradation and the presence of bacterial sugars.
3. "Degraded" POM from this study and UDOM from Georges Bank appear remarkably similar, distinguished mainly by the presence of hexoses (perhaps as yet undegraded storage sugars?) in the "degraded" POM. UDOM, therefore, appears more extensively modified than "degraded" POM, which is consistent with the "size-reactivity continuum model" proposed by Amon and Benner (1996). In contrast, $>53\text{ }\mu\text{m}$ POM in this study appears less "fresh" than $2.0\rightarrow 53\text{ }\mu\text{m}$ POM, indicating that, in the surface ocean, the model does not apply to particles larger than or equal in size to the majority of the primary producers.
4. $\text{NH}_3\text{-Cl}^+$ DT-MS appears to be a sensitive technique for probing variations in polysaccharide composition in marine samples. It should prove a useful complement to existing sugar analysis methods as it can simultaneously measure multiple categories of underivatized sugar (neutral sugars, aminosugars, methylated sugars, and, perhaps, acidic sugars (Boon et al., 1998)) and can provide oligomer information as well (Lomax et al., 1991; Klap, 1997). It is not able to discriminate among carbohydrate isomers although

applying collision-induced dissociation could provide further information in this regard (Helleur and Guevremont, 1989). At present it is only semiquantitative, but it could easily be used in conjunction with a more quantitative technique as it only requires microgram quantities of sample.

References:

- Aluwihari L. I., Repeta D. J., and Chen R. F. (1997). A major biopolymeric component to dissolved organic carbon in surface seawater. *Nature* **387**, 166-169.
- Amon R.M.W. and Benner R. (1996) Bacterial utilization of different size classes of dissolved organic matter. *Limnol. Oceanogr.*, **41**(1), 41-51.
- Arisz P. W. and Boon J. J. (1995). Pyrolysis chemical ionization mass spectrometry of cellulose ethers. *J. of Polymer Science: Part A: Polymer Chemistry*, **33**, 2855-2864.
- Arnosti C. (1993). Structural characterization and bacterial degradation of marine carbohydrates. Ph.D. Thesis, MIT/WHOI Joint Program, 239 pp.
- Biersmith A. and Benner R. (1998). Carbohydrates in phytoplankton and freshly-produced dissolved organic matter, *Mar. Chem.*, submitted.
- Boon J.J., Klap V., and Eglinton T. (1998) Molecular characterization of microgram amounts of colloidal dissolved organic matter (UDOM) in ocean water samples by direct temperature resolved ammonia chemical ionization mass spectrometry. *Org. Geochem.*, submitted.
- Chin W-C., Orellana M.V., Verdugo P. (1998). Spontaneous assembly of marine dissolved organic matter into polymer gels. *Nature*, **391**, 568-572.
- Cifuentes L.A., Coffin R. B., Solorzano L., Cardenas W., Espinoza J., and Twilley R.R. (1996) Isotopic and elemental variations of carbon and nitrogen in a mangrove estuary. *Estuarine, Coastal and Shelf Science*, **43**, 781-800.
- Cowie G. L. (1990). Marine organic diagenesis: A comparative study of amino acids, neutral sugars, and lignin, U. of Washington, 189 pp.
- Cowie G. L. and Hedges J. I. (1996). Digestion and alteration of the biochemical constituents of a diatom (*Thalassiosira weissflogii*) ingested by an herbivorous zooplankton (*Calanus pacificus*). *Limnol. Oceanogr.*, **41**(4), 581-594.
- Cowie G. L. and Hedges J. I. (1984). Carbohydrate sources in a coastal marine environment. *Geochim. Cosmochim. Acta*, **48**, 2075-2087.
- Cowie G. L., Hedges J. I., and Calvert S. E. (1992). Sources and reactivities of amino acids, neutral sugars, and lignin in an intermittently anoxic marine environment. *Geochim. Cosmochim. Acta*, **56**, 1963-1978.

Decho A. W. (1990). Microbial exopolymer secretions in ocean environments: Their role(s) in food webs and marine processes. *Oceanogr. Mar. Biol. Annu. Rev.*, **28**, 73-153.

Goericke R. and Repeta D.J. (1993) Chlorophylls *a* and *b* and divinyl chlorophylls *a* and *b* in the open subtropical North Atlantic Ocean. *Mar. Ecol. Prog. Ser.*, **101**, 307-313.

Hamilton S. E. and Hedges J. I. (1988). The comparative chemistries of lignins and carbohydrates in an anoxic fjord. *Geochim. Cosmochim. Acta*, **52**, 129-152.

Harvey H. R. and Macko S. A. (1997). Catalysts or contributors? Tracking the bacterial mediation of early diagenesis in the marine water column. *Org. Geochem.*, **26**(9/10), 531-544.

Hecky R.E., Mopper K., Kilham P., and Degens E.T. (1973). The amino acid and sugar composition of diatom cell-walls. *Mar Biol.*, **19**, 323-331.

Hedges J.I. and Stern J.H. (1984) Carbon and nitrogen determinations of carbonate-containing solids. *Limnol. Oceanogr.*, **29**(3), 657-663.

Helleur R.J. and Guevremont R. (1989) Initial application of desorption chemical ionization-pyrolysis-tandem mass spectrometry to structural analysis of carbohydrates. *J. Anal. Appl. Pyrol.*, **15**, 85-95.

Hernes P.J., Hedges J.I., Peterson M.L., Wakeham S.G., and Lee C. (1996) Neutral carbohydrate geochemistry of particulate material in the central Equatorial Pacific. *Deep Sea Res. II*, **43**, 1181-1204.

Ittekkot V., Degens E.T. and Honjo S. (1984) Seasonality in the fluxes of sugars, amino acids, and aminosugars to the deep ocean: Panama Basin. *Deep-Sea Res.*, **31**(9), 1071-1083.

van der Kaaden A., Haverkamp J., Boon J.J., de Leeuw J.W. (1983) Analytical pyrolysis of carbohydrates, 1. Chemical interpretation of matrix influences on pyrolysis-mass spectra of amylose using pyrolysis-gas chromatography-mass spectrometry. *J. Anal. Appl. Pyrol.*, **5**, 199-220.

Klap V A (1997). Biogeochemical aspects of salt marsh exchange processes in the SW Netherlands, Ph.D. Thesis, NIOO/CEMO, 170 p.

Klok J., Baas M., Cox H. C., de Leeuw J.W., Rijpstra W. I. C., and Schenk P. A. (1984a). Qualitative and quantitative characterization of the total organic matter in a recent marine sediment (Part II). *Org. Geochem.*, **6**, 265-278.

Klok J., Cox H. C., Baas M., Schuyt P. J. W., de Leeuw J. W., and Schenk P. A. (1984b). Carbohydrates in recent marine sediments--I. Origin and significance of deoxy- and O-methyl-monosaccharides. *Org. Geochem.*, **7**, 73-84.

Lomax J A, Boon J.J., and Hoffmann R.A. (1991) Characterisation of polysaccharides by in-source pyrolysis positive- and negative-ion direct chemical ionisation-mass spectrometry. *Carbohydrate Research*, **221**, 219-233.

McCarthy, M., J. Hedges, R. Benner (1996). Major biochemical composition of dissolved high molecular weight organic matter in seawater. *Mar. Chem.* **55**: 281-297.

Moers M. E. C. (1989). Occurrence and fate of carbohydrates in recent and ancient sediments from different deposition environments. Ph.D. Thesis. Technical University of Delft. 195 pp.

Nguyen R. T. and Harvey H. R. (1997). Protein and amino acid cycling during phytoplankton decomposition in oxic and anoxic waters. *Org. Geochem.*, **27**, 115-128.

Painter T.J. (1983) Algal polysaccharides. In: Aspinall G.O. (ed.) *The Polysaccharides*, Vol.2, Academic Press, New York, NY, pp. 196-275.

Pakulski J.D. and Benner R. (1992) An improved method for the hydrolysis and MBTH analysis of dissolved and particulate carbohydrates in seawater. *Mar. Chem.*, **40**, 143-160.

Parsons T. R., Takahashi M., Hargrave B. (1984). *Biological Oceanographic Processes*, 3rd Ed., Pergamon Press, New York, 330 p.

Parsons T. R., Stephens K., and Strickland J. D. H. (1961). On the chemical composition of eleven species of marine phytoplankton. *J. Fish. Res. Bd. Canada*, **18**(6): 1001-1016.

Redfield A. C., Ketchum, B. H., and F. A. Richards (1963). The influence of organisms on the composition of seawater. In: Hill M. N. (Ed), *The Sea*, Vol. 2., Interscience, pp.26-77.

Scheijen M.A. and Boon J.J. (1989) Loss of oligomer information in pyrolysis-desorption/chemical-ionisation mass spectrometry of amylose, due to the influence of potassium hydroxide. *Rapid Communications in Mass Spectrometry*, **3**(7), 238-240.

Sicre M-A, Peulve S., Saliot A., de Leeuw J.W., and Baas M. (1994). Molecular characterization of the organic fraction of suspended matter in the surface waters and bottom nepheloid layer of the Rhone delta using analytical pyrolysis. *Org. Geochem.* **21**(1), 11-26.

Skoog A. and Benner R. (1997). Aldoses in various size fractions of marine organic matter: Implications for carbon cycling. *Limnol. Oceanogr.*, in press.

Tanoue E. and Handa N. (1987). Monosaccharide composition of marine particles and sediments from the Bering sea and northern North Pacific. *Oceanol. Acta*, **10**(1): 91-99.

Voet D and Voet J.G. (1990). *Biochemistry*. John Wiley & Sons, New York, 1223 p.

Wakeham S.G., Lee C., and Hedges J. I. (1997). Fluxes of major biochemicals in the equatorial Pacific Ocean. *Biogeochemistry of Marine Organic Matter*, submitted.

Weckesser J., Drews G., and Mayer H. (1979). Lipopolysaccharides of photosynthetic prokaryotes. *Ann. Rev. Microbiol.*, **33**, 215-239.

Chapter 6

Molecular-level variations in POM subclasses along the Mid-Atlantic Bight

Abstract

A significant portion of oceanic primary productivity occurs on continental margins. As the fate of this primary production has not been clearly determined, continental margins have been the subject of an increased research focus over the past ten to twenty years. In this chapter molecular-level characteristics of particulate organic matter (POM) subclasses from the Mid-Atlantic Bight (collected as part of the DOE-Ocean Margins Project) are explored in an attempt to further our understanding of organic matter cycling on the continental shelf and slope.

Small-particle POM ($>2\ \mu\text{m}$, $<53\ \mu\text{m}$), large-particle POM ($>53\ \mu\text{m}$), "phytoplankton" ($>2\ \mu\text{m}$, $<53\ \mu\text{m}$) and "detritus" ($>2\ \mu\text{m}$, $<53\ \mu\text{m}$) were isolated from surface waters collected from different regimes along the Mid-Atlantic Bight (MAB) in March 1996. Broad-band molecular-level variations within these subclasses were explored using direct temperature-resolved mass spectrometry (DT-MS) and multivariate analysis techniques. Correlations between molecular-level compositional differences and external environmental and biological variables such as salinity, temperature, and chlorophyll *a* concentrations were also examined.

Both large-particle and small-particle POM exhibited molecular-level variations related to regime. Large-particle POM from the continental shelf appeared to contain a greater zooplankton biomass component, characterized by an enhanced chitin, protein, and cholesterol signature. Large-particle POM from slope waters appeared to contain a greater phytodretital component, as indicated by enrichment in molecular-level characteristics similar to those of phytoplankton. A higher relative proportion of phytoplankton biomass was present in small-particle POM from the shelf-edge than from the mid-shelf or the slope. In addition, there was also an alongshelf (roughly north-south)

trend in the composition of $>2 \mu\text{m}$, $<53 \mu\text{m}$ POM, with samples farther along the shelf (i.e., farther south) appearing more enriched in polysaccharides, fatty acids, chlorophyll, and diglycerides (which may result from triglycerides, phospholipids, or diglycerides within the samples). The molecular-level composition of "phytoplankton" also appeared to vary as a function of location, while the composition of "detritus" illustrated no easily interpretable variations with either location or external variables.

Introduction

Although continental margins comprise a very small portion of the total area of the world oceans, they play a significant role in oceanic primary productivity and organic matter burial. These regions of the world ocean are also the most impacted by anthropogenic activities. Coastal zones are responsible for roughly 20% of total oceanic primary production (Walsh, 1988). They generally contain significantly greater standing stocks of phytoplankton ($\sim 10\times$ more) than are found in pelagic waters (Walsh 1988). In addition to, and partly because of, their major ecological role, they also play a significant role in the global carbon cycle. Continental margin sediments are responsible for 80% of the organic matter burial in oceanic sediments; they may also be a key repository for terrestrial organic matter (Hedges, 1992).

In the past decade, several major research programs have focused on one continental margin, the Mid-Atlantic Bight (MAB), in an attempt to further understand carbon cycling in coastal regions. In SEEP-I, which focused primarily on the northern MAB, and SEEP-II, which focused primarily on the southern MAB, the main emphasis was to test the hypothesis that the decoupling of primary production and zooplankton grazing during the spring bloom allows a large portion of phytoplankton carbon to be exported from the shelf and, possibly, sequestered in the deep ocean (Walsh et al., 1981). SEEP-I led to a wide variation of opinion as to the validity of Walsh's hypothesis. SEEP-II, which, like SEEP-I, was a particulate-carbon-based study, indicated that that less than

25% (probably ~10%) of shelf production is exported (Biscaye et al., 1994). However, dissolved organic carbon (DOC) was not included in these programs and suspended particulate organic matter (POM) only received cursory attention. In addition, molecular-level studies that would aid in the identification of sources and transformations of organic matter in the MAB were not included. A third study of the Mid-Atlantic Bight (the DOE-OMP) is presently underway and includes a more comprehensive field and analysis program in an attempt to further constrain organic matter cycling on the shelf.

In this chapter variations within and between POM size-classes and subclasses (small-particle POM, large-particle POM, and "detritus" and "phytoplankton" isolated from small-particle POM) are explored in an attempt to further understand particulate organic matter composition and cycling in a shelf-slope environment. The data set used in this study is the MAB POM set from Chapter 4. Direct temperature-resolved mass spectrometry (DT-MS, 16 eV EI⁺) is used to provide broad-band molecular-level characterization of POM samples; the resulting DT-MS spectra are subjected to discriminant analysis in order to explore variations among the samples. While Chapter 4 focuses upon variations among POM classes and subclasses, this chapter discusses variations within large-particle POM, small-particle POM, "phytoplankton," and "detritus" in order to provide potential insights into how these OM pools behave and interact with each other in a continental margin system.

Experimental

Surface water (from approximately 3 m depth) was collected by diaphragm pump from the MAB on multiple transects across the shelf (Cruise EN279, March 1996, see Fig. 6.1). Aliquots were sampled for the determination of nutrient concentrations and concentrations, atomic C/N ratios, pigment concentrations and flow cytometry. Large-volume samples were collected and processed for molecular-level analyses via direct temperature-resolved mass spectrometry (DT-MS) and for flow cytometry (FCM)

MAB Sampling Stations

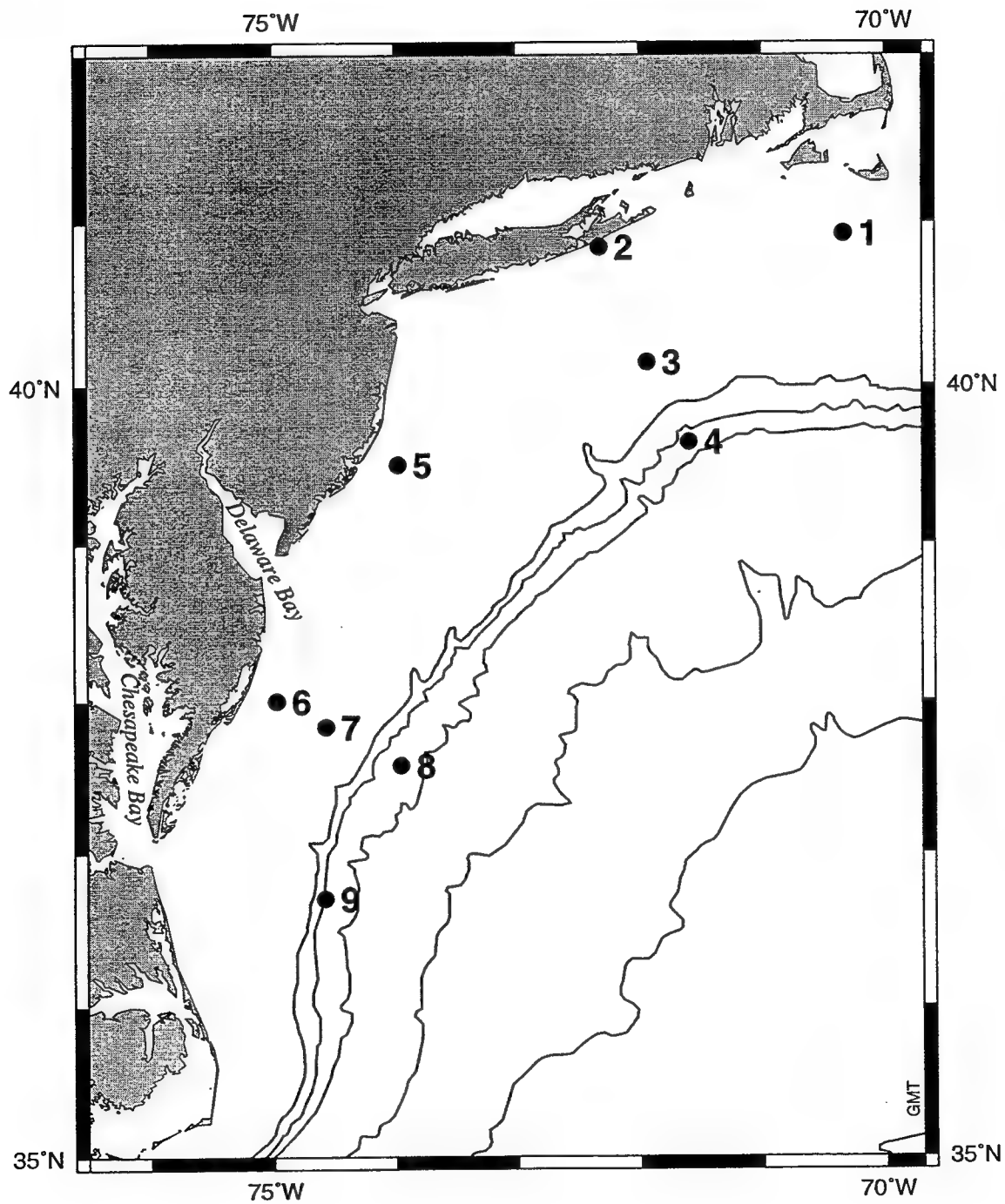


Fig. 6.1. Map showing station locations. Contour lines represent water depth (200 m, 1000 m, 2000 m, 3000m, 4000 m, and 5000 m).

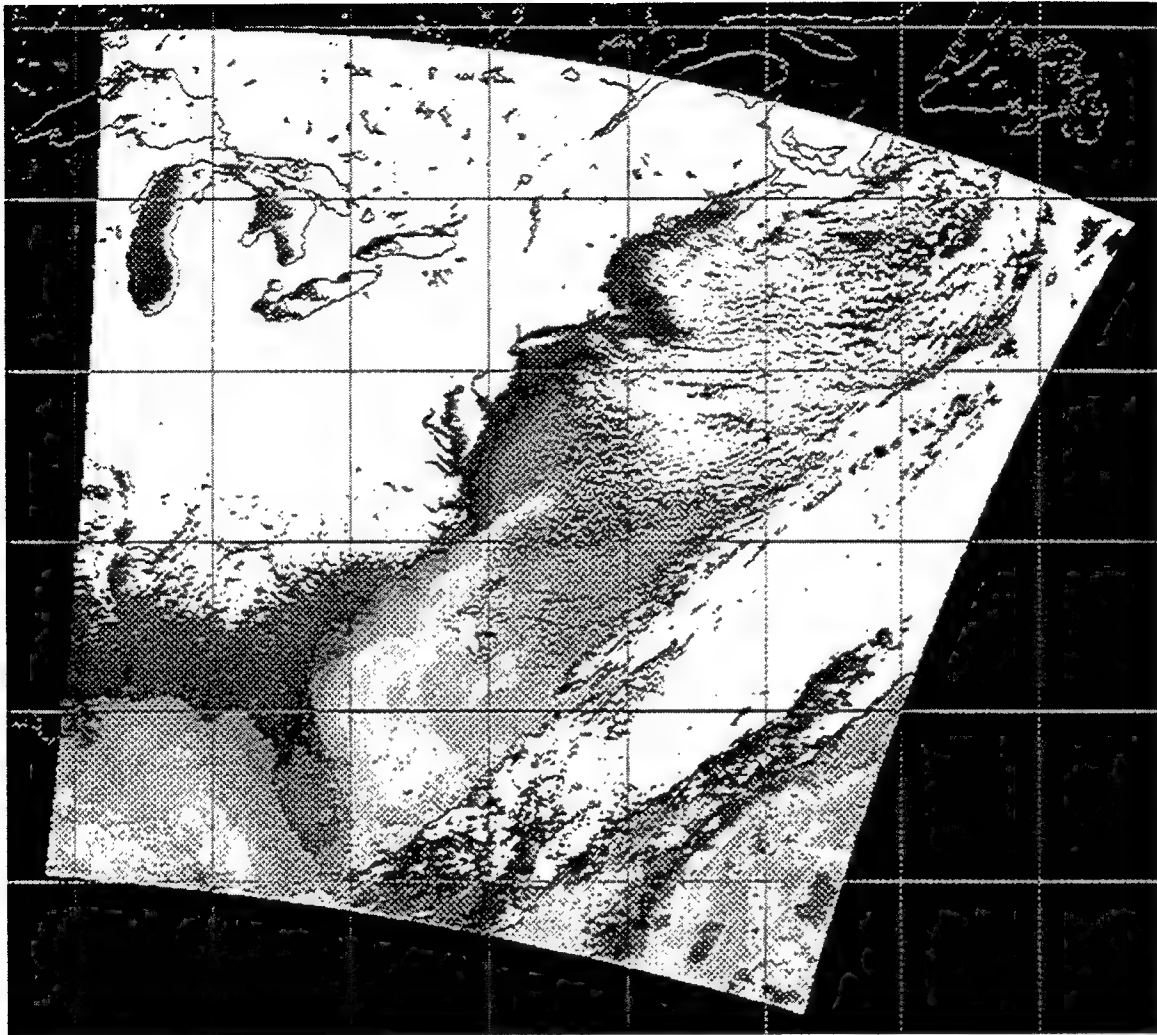


Fig. 6.2. AVHRR image from March 4, 1996 (12:08:49 GMT) illustrating the shelf/slope front in the MAB.

coupled with DT-MS. Temperature, salinity, and location were continuously monitored using the shipboard SAIL system.

Region of Interest

A summary of studies of hydrography in the Mid-Atlantic Bight (e.g., Beardsley et al., 1976, Beardsley and Boicourt, 1981) is provided in Biscaye et al., 1994. The alongshore movement of water in the MAB originates with the upwelling of Gulf of Maine water and Labrador Sea Water onto Georges Bank and the subsequent transfer of Georges Bank water across Nantucket Shoals and onto the shelf. Water on the shelf drifts southeastward following the coastline. Exchange of water along the shelf is limited by a permanent thermohaline front at the shelf-break, though it is estimated that roughly half of the alongshore transport of water exits the shelf between Cape Cod and Cape Hatteras (Biscaye et al., 1994). Oxygen isotope studies indicate a 50% dilution of shelf water by slope water between Georges Bank and the region of the Delaware and Chesapeake Bays (Fairbanks, 1982, discussed in Biscaye et al., 1994). Therefore, Biscaye et al. (1994) estimate that three quarters of the original Georges Bank water is lost to the slope during transport to the southern MAB. In the southern Mid-Atlantic Bight there is substantial impact from the fresh-water outflows of the Hudson River, the Delaware Bay, and the Chesapeake Bay (see Fig. 6.1).

In the winter and early spring, mixing on the shelf from cooling and storm events reduces across-shelf gradients and results in a vertically mixed water column. The thermohaline front at the shelf break separates colder, fresher inshore waters from warmer, saltier slope waters (as in Fig. 6.2). In the late spring a seasonal thermocline develops at about 20 m depth, isolating remnant winter water, "the cold pool," in the deep waters of the outer shelf (Houghton et al., 1982). This thermocline also decreases the intensity of the shelf/slope front in surface waters (Biscaye et al., 1994).

A final hydrographic point is that the Gulf Stream and MAB water interact via frontal instabilities, eddies, and displacement of the entire Gulf Stream (Biscaye et al, 1994, and references therein).

During our spring transects in the MAB region (EN279, March 1996), nitrate varied from less than 0.1 $\mu\text{M/L}$ to 5.3 $\mu\text{M/L}$; phosphate from 0.15 to 0.56 $\mu\text{M/L}$. Salinity and temperature (as determined by an on-board SAIL system) varied between 32.27 and 35.25 psu and 2.67 and 9.68°C, respectively, and were comparable to literature values for early spring in the SEEP-II study region of the MAB. As in Biscaye et al. (1994), the inner shelf waters were colder and fresher (2.67 to 4.5°C and 32.27 to 32.59 psu), while those stations off the shelf break were warmer and more saline (8.03 to 9.68°C and 33.24 to 35.25 psu). The distinction between shelf and slope waters is particularly evident in Fig. 6.2, showing AVHRR data for March 4, 1996 (12:08:49 GMT).

Sampling method for molecular-level analyses

The analytical method for the large-volume samples (Fig. 6.3) is described in Chapter 4 (see Chapter 2 for details of the development and evaluation of this method) and will be summarized here. Seawater was prefiltered through a nylon 53 μm screen to separate large-particle from small-particle POM (as in Bishop and Edmond, 1976). Tangential flow filtration or TFF (0.8 μm Fluoro centrase and ultrasette, Filtron, driven by Masterflex peristaltic pumps) was used to concentrate small particles from seawater. Large particles were resuspended off the nylon screen, concentrated by centrifugation (10 minutes at $\sim 1800\times\text{G}$ on an IEC HN-SII centrifuge, Damon/IEC Division), homogenized via Teflon tissue grinder, and then desalted by centrifugation (4 minutes at $10,500\times\text{G}$ on a Fisher Micro-Centrifuge, Model 59A) with Milli-Q™ water rinses. Samples were stored in liquid nitrogen after tangential flow filtration and/or after centrifugation as necessary.

For flow cytometric sorting of small-particle POM, two further filtration steps were necessary. The $>0.8 \mu\text{m}$ retentate was filtered onto a 2 μm polycarbonate membrane

ANALYTICAL SCHEME

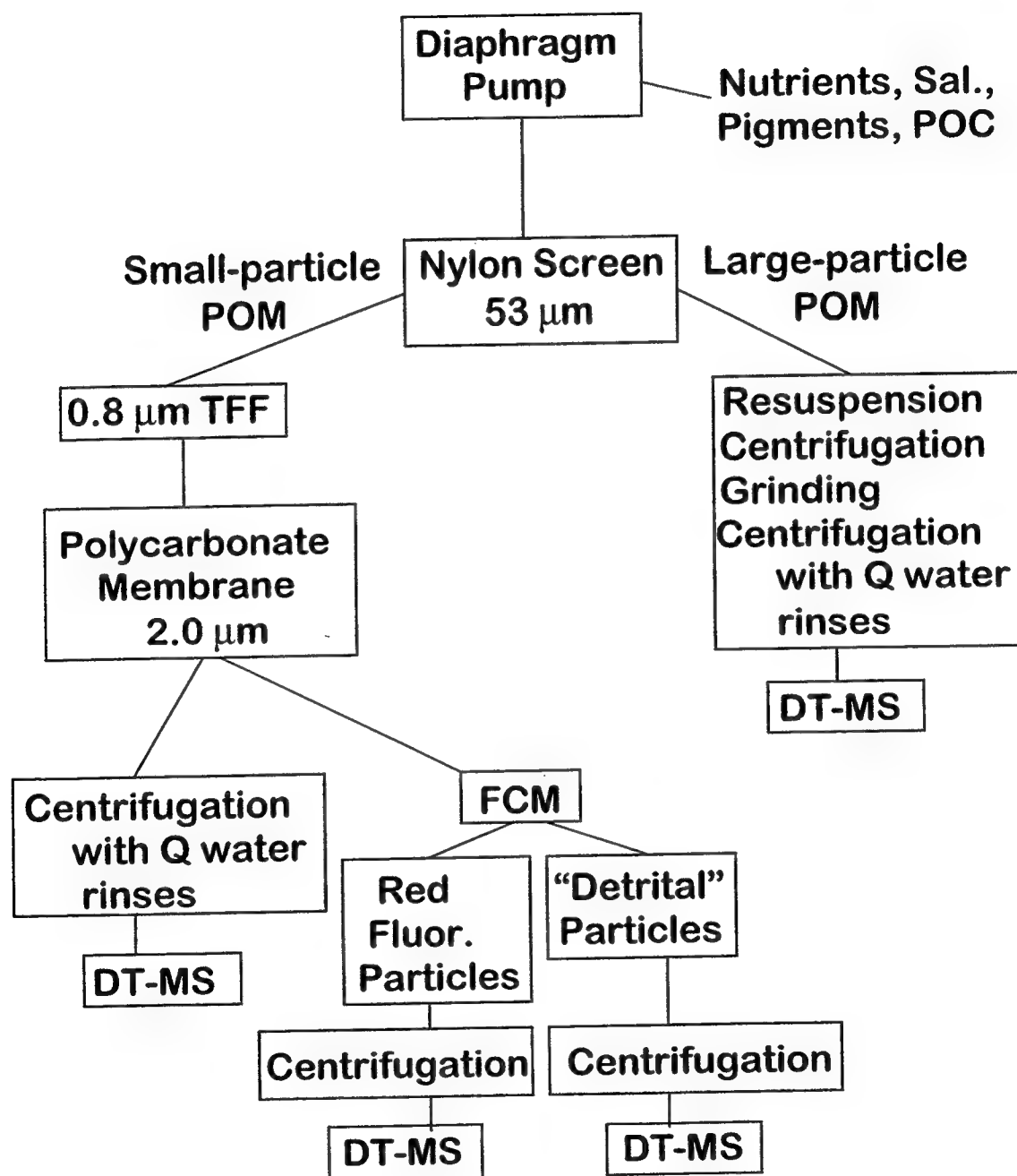


Fig. 3. Analytical scheme for large-volume POM samples.

filter (Poretics) using a slight vacuum (<5 psi); the sample was rinsed with and resuspended in <0.2 μm syringe-filtered seawater and then placed in liquid nitrogen to await flow cytometry. Just prior to sorting, the sample was thawed and syringe-filtered through a 53 μm nylon screen to remove any aggregates that might otherwise clog the flow cell tip. For better comparison with the flow cytometrically sorted samples, additional aliquots of >2 μm POM were further concentrated by centrifugation (4 minutes at 10,500xG on a Fisher Micro-Centrifuge, Model 59A) and desalted by centrifugation with Milli-Q™ water rinses. These are the small-particle POM samples discussed in this chapter.

Flow cytometry

Flow cytometry was performed on an EPICS V flow cytometer (Coulter, Inc.) using a Cicero data acquisition system (Cytomation, Inc.), a standard lens assembly, a 100 μm jet-in-air flow cell, excitation at 488 nm with a 130 mW laser beam and detector settings optimized for eukaryotic phytoplankton. Small-particle POM (<53 μm , >2 μm) was separated into “phytoplankton” and “detritus” based on forward angle light scatter and red fluorescence measurements. Desalting of sorted samples was done during flow cytometric sorting by using Milli-Q™ water sheath fluid, centrifuging the resulting samples and discarding the supernatant.

Flow cytometric analysis (without sorting) was performed on both unfiltered seawater and filtered seawater (<53 μm , >2 μm) POM in order to determine the proportions of phytoplankton and detritus in samples from each station.

DT-MS and multivariate analysis

Low voltage electron impact ionization (EI^+) DT-MS (a form of PyMS, Boon, 1992) was used to provide molecular-level information on 2→53 μm POM, >53 μm

POM, “phytoplankton,” and “detritus.” This mass spectrometry technique was chosen as it provides broadband information (i.e., information on polysaccharides, proteins, lipids, etc.) and requires only microgram quantities of sample.

Sample pellets, resuspended in a small quantity of Milli-Q™ water, were analyzed in triplicate via DT-MS on a VG AutospecQ magnetic sector instrument (16 eV EI⁺, acceleration voltage 8.0 kV, direct inlet, mass range 41-795, scan speed 2 s, resolution 1000) with the sample probe (a platinum/rhodium (87/13) wire, 0.125 mm diam.) resistively heated to just below the melting point of the wire. Spectra were then exported to a multivariate statistics program and molecular-level differences among the spectra were investigated using principal component and discriminant analyses (as in Saliot et al., 1984; Eglinton et al., 1992, and others, for further discussion of DT-MS applications in marine organic geochemistry, see Eglinton et al., 1996; Klap 1997; Boon et al., 1998). In this case, mass spectra for each run were summed over the entire region of the total ion chromatogram (TIC), averaged to the nearest integer value (using a mass defect of 0.75), and exported to Chemometricks (a MATLAB-based program developed at FOM-AMOLF and further modified at WHOI). Overloaded spectra, *m/z* values related to salt contamination and one outlier sample resulting from poor sample preparation were removed from the data sets prior to analysis.

Potential correlations between molecular-level variations (discriminant scores) and external variables (salinity, temperature, atomic C/N ratios, etc.) were explored using correlation matrices calculated with Statistica.

Ancillary data

POC concentrations and C/N ratios were determined from 1 to 2 L samples collected onto precombusted GF/F filters (24 or 25 mm diam.) using a pressure canister and N₂ gas (<5 psi); these samples were stored in a conventional freezer until analysis. Just prior to analysis, the filters were thawed, placed over fuming HCl for 24 to 48 hours,

and dried overnight in an oven at approximately 60°C (Hedges and Stern, 1984). The filters were weighed and cut into pieces, which were then analyzed on a Fisons EA 1108 Elemental Analyzer.

Pigment samples were collected in the same manner as POC samples, but were stored in liquid nitrogen until analysis. These samples were thawed and suspended in acetone and an internal standard (zinc pyropheophorbide octadecylester collection 26-31, Fraction 6, from D. Repeta, WHOI) was added. The entire sample was ground with a Teflon tissue grinder and then centrifuged to remove the filter pieces. Supernatant was injected onto a C-8 column (Rainin "Microsorb 'short-one,'" particle size 3 μm , pore size 100 angstroms, column size 4.6x100 mm) in a Waters 600E HPLC system with a photodiode array detector. Solvent A was MeOH: 0.5N NH_4Ac (75:25); Solvent B, MeOH; solvent program (minutes, % Solvent A, % Solvent B), (0;100,0), (20;35,65), (30; 25,75), (35; 0,100); flow rate, 1.0 mL/min (Goericke and Repeta, 1993).

Nutrient data was kindly provided by R. Wilke (Brookhaven National Laboratory).

Results

Chlorophyll a concentrations and phytoplankton/(phytoplankton+detritus) ratios

Both the chlorophyll *a* concentration and the unfiltered seawater phytoplankton/(phytoplankton + detritus) ($P/(P+D)$) ratio can be considered indicators of the importance of primary producers at a sampling site. The measurements are complementary as one gives a concentration and the other may indicate the contribution of phytoplankton to the total particle pool. A better ratio than $P/(P+D)$, which is based on particle counts, would be a measure of the biomass ratio of phytoplankton to total particles. Unfortunately, this determination, while possible, was beyond the scope of this

Table 6.1. Ancillary data for MAB samples

station #	1	2	3	4	5	6	7	8	9
lat. (deg. min. N)	40 56	40 51	40 08	39 38	39 30	38 00	37 50	37 35	36 42
long. (deg. min. W)	70 20	72 19	71 56	71 35	73 58	74 58	74 34	73 57	74 35
salinity (psu)	32.53	32.59	32.92	34.06	32.27	32.45	32.76	35.25	33.24
temp. (°C)	2.7	3.2	4.9	8.0	3.0	4.5	6.8	9.7	9.2
POC conc. (µg/L)	170	210	110		670	240	90	140	80
chl <i>a</i> conc (µg/L)	13	4.5	8.3	4.0	13		12	2.8	2.0
POC/ chl <i>a</i>	13	46	13		51		7.4	50	40
fuco-xanthin conc. (µg/L)	12	5.5	9.5	1.9	12		11	1.2	1.7
diadino xanthin conc. (µg/L)	2.45	1.6	1.6	1.2	3.3		3.4	0	0.47
(C/N) _a	3.8	4.7	4.3		8.9	6.5	3.4	5.1	4.1
USW P/(P+D) counts/ counts		0.0313	0.310	0.488	0.125	0.169			0.283
>2 µm P/(P+D) counts/ counts		0.271	0.464	0.434	0.282	0.358			0.348
PO ₄ conc. (µM)	0.243	0.558	0.493	0.438	0.167	0.051		0.341	0.225
NO ₃ conc. (µM)	0.088	2.214	5.258	5.698	0.060	0.065		5.113	1.776

Note: P/(P+D) is the ratio of phytoplankton counts to phytoplankton plus detritus counts as determined by flow cytometry for unfiltered seawater (USW) and >2 µm POM samples.

thesis. Therefore, the chlorophyll *a* concentration and P/(P+D) ratio are reported in Table 6.1 and presented here.

The chlorophyll *a* concentration was high (between 5 and 13 $\mu\text{g/L}$) on the shelf and shelf-edge and considerably lower (between 2 and 4 $\mu\text{g/L}$) on the slope. There is some indication that the shelf-edge has higher chlorophyll concentrations than the mid-shelf. The P/(P+D) ratio shows a different trend. It is lowest at the stations nearest shore and increases across the shelf into slope waters. The P/(P+D) ratio of the nearshore stations also appears to increase downshelf (from N to S).

Table 6.2. Variables used in correlation matrices.

Variables	Units
DF1 score	
DF2 score	
Salinity	psu
Seawater temperature	$^{\circ}\text{C}$
POC concentration	$\mu\text{g/L}$ seawater
(C/N) _a	atom/atom
[POC]/[chlorophyll <i>a</i>]	weight/weight
chlorophyll concentration	$\mu\text{g/L}$ seawater
fucoxanthin concentration	$\mu\text{g/L}$ seawater
diadinoxanthin concentration	$\mu\text{g/L}$ seawater
unfiltered SW phyto/(phyto + detritus)	FCM counts/FCM counts
>2 μm , <53 μm phyto/(phyto + detritus)	FCM counts/FCM counts
"phyto" phyto/(phyto + detritus)*	FCM counts/FCM counts
"detritus" phyto/(phyto + detritus) [#]	FCM counts/FCM counts
PO ₄	μM
NO ₃	μM

* used only with DF scores from the "phytoplankton" data set.

[#]used only with DF scores from the "detritus" data set.

Large-particle POM

The DT-MS mass spectrum of average large-particle POM in the MAB (see Chapter 4, Fig. 4.3a) is characterized by a strong polysaccharide signal, a weaker but significant protein signal, C_{14:0} and C_{16:0} fatty acids, and a sterol signature in which cholesterol is dominant (see Chapter 4 and Appendix 1 for m/z assignments). It is important to note that ion intensities are a function of precursor abundance, the mode of volatilization (pyrolysis vs. desorption), and ionization efficiency. As a result signal strength cannot be directly related to absolute abundance. However, knowledge of the response factors of different compound classes (as determined in Chapter 2) can make DT-MS semi-quantitative. For example, polysaccharides and proteins (under these DT-MS conditions) have much lower response factors than fatty acids and sterols and are therefore even more abundant than the relative intensity of their ion series indicates.

Comparisons among samples can indicate changes in the relative abundances of specific compounds or compound classes in the samples. Therefore, while average spectra are very informative, exploring variations within POM classes and subclasses can provide further useful information, especially if the variations are correlated with additional external variables. Applying discriminant analysis, in this case a two stage principal component analysis (Hoogerbrugge et al., 1983), to mass spectra allows the researcher to explore variations among samples by maximizing intersample differences and minimizing intrasample differences (i.e., variation within replicate DT-MS analyses due to sample heterogeneity, instrument drift, subtle changes in pyrolysis or ionization conditions, etc.).

In analysis of MAB large-particle POM, Discriminant Function 1 (DF1) explains 26% of the total variance in the data set and has a between-to-within-sample variance ratio (B/W) of 81.5. The score plot in Fig. 6.4 indicates the relationship among samples as a function of the m/z values in the reconstructed spectra of DF1 (Fig. 6.5). Large (>53 µm) particles in the MAB appear to be divided by DF1 into colder, less saline shelf



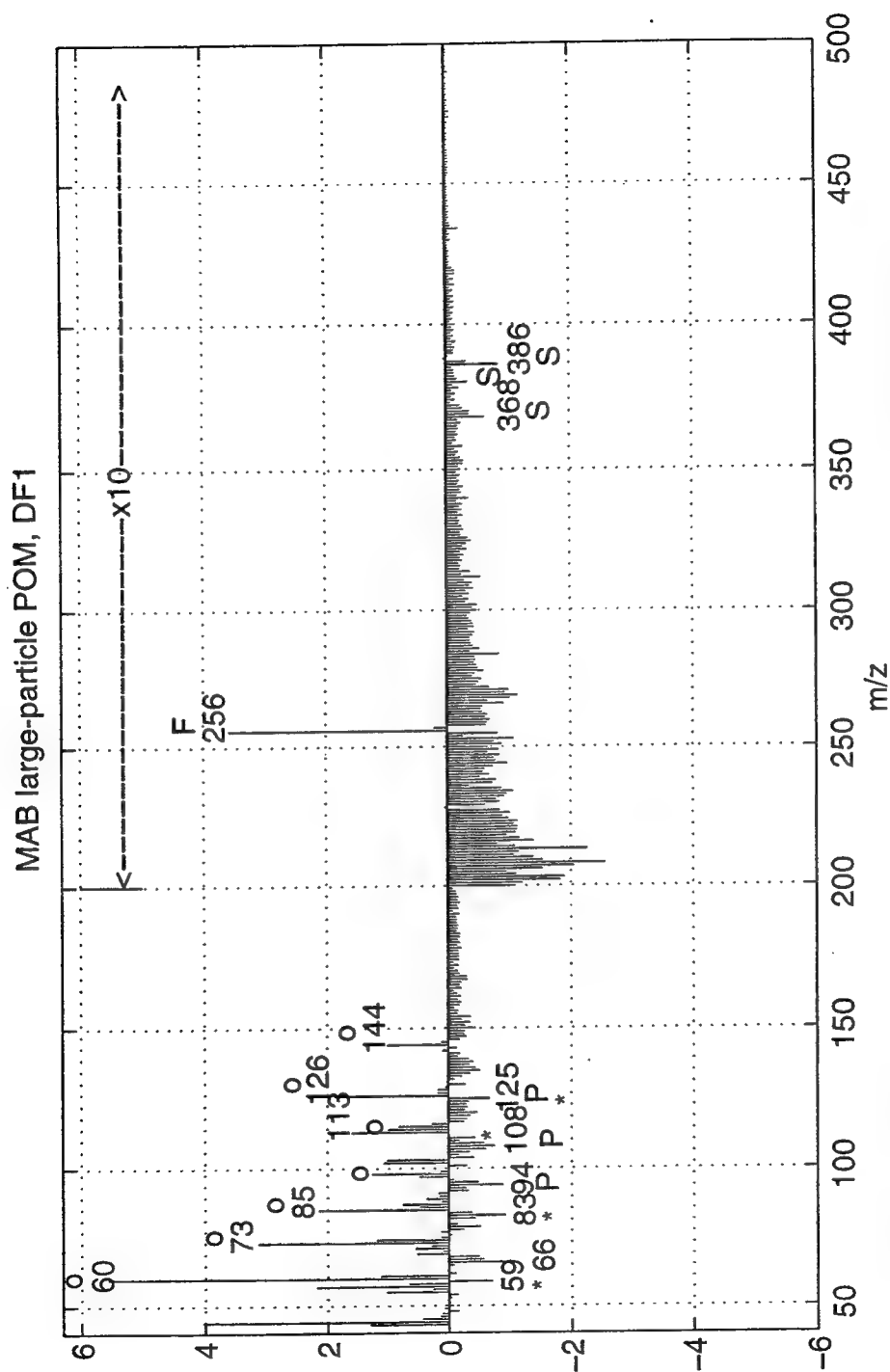
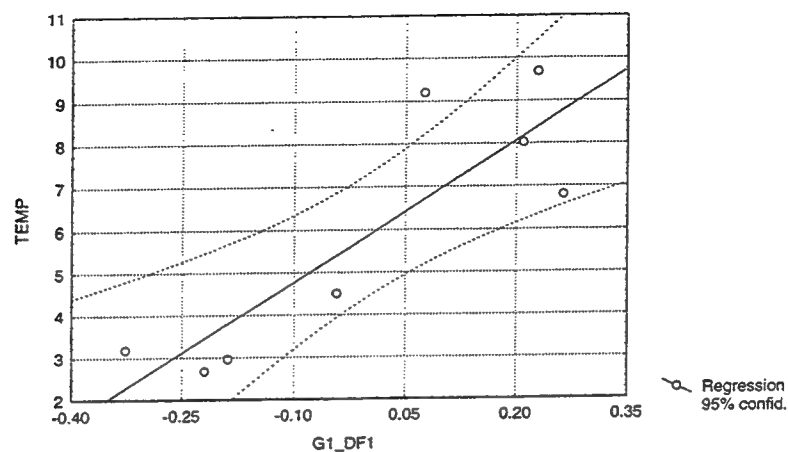
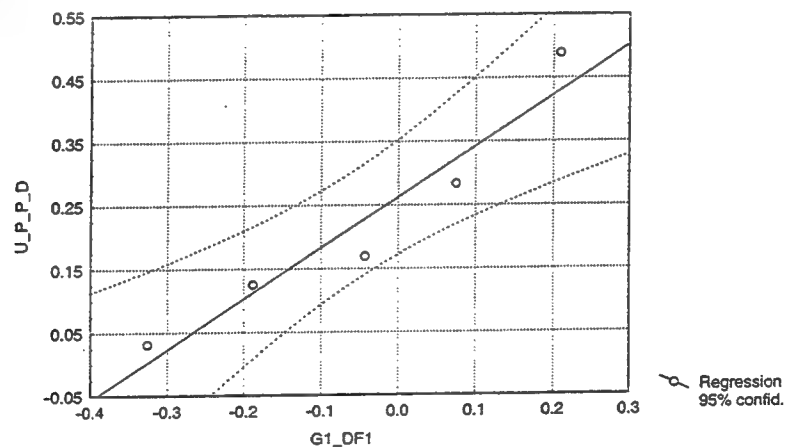


Fig. 6.5. Reconstructed mass spectrum of DF1 from analysis of MAB large-particle POM. The negative portion of the spectrum corresponds to DF-1 in Fig. 6.4; the positive portion of the spectrum to DF+1. Symbols: **o** polysaccharide; **P** protein, ***** aminosugar, **F** fatty acid, **S** sterol.

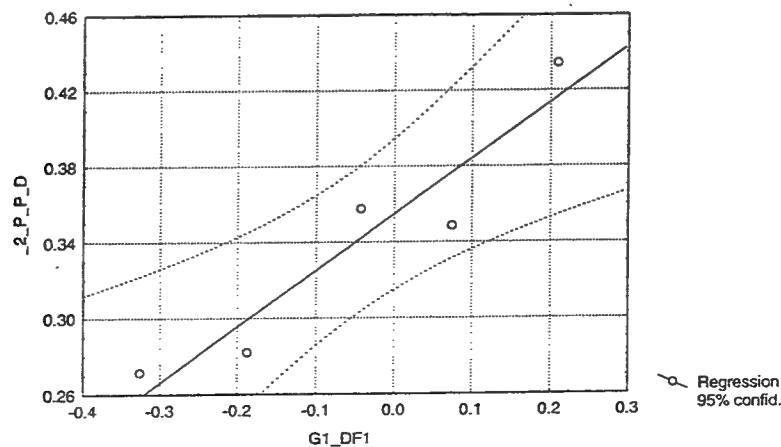
Fig. 6.6a. Plot of DF1 scores (see Fig. 6.4) vs seawater temperature.



6b. Plot of DF1 scores (see Fig. 6.4) vs unfiltered seawater ratios of phytoplankton/total analyzed particles (determined via flow cytometry).



6c. Plot of DF1 vs phytoplankton/total analyzed particles ratios in filtered (<53 μm , >2.0 μm) POM.



samples, which fall in the negative portion of DF1, and warmer, more saline slope samples, which plot in DF+1 (see Fig. 6.4). The chemical characteristics responsible for this separation are shown in Fig. 6.5. The slope samples (DF+1) are enriched in polysaccharides (mainly ion series from pentoses, m/z 85, 114, and hexoses, m/z 60, 73, 98, 126, 144) and $C_{16:0}$ fatty acid. The shelf samples (DF-1) are enriched in ion series believed to result from chitin (m/z 59, 84, 111, 125, 139) and protein (m/z 92, 94, 108, 117, 124, 125, 138, 152, 166, 180). The inner shelf samples are also more enriched in sterols, in particular, cholesterol (m/z 386, the molecular ion, and 368, $M-H_2O$).

The discriminant scores from DF1 were imported into Statistica along with external environmental variables (see Table 6.2); correlation matrices were calculated for DF1 and these external variables. The resulting correlations are considered statistically significant when $p < 0.05$, i.e., when there is a 5% chance that the variables are actually independent (see Davis, 1986, for a further description of the test of correlation). DF1 is positively correlated with temperature and with the ratio of phytoplankton to total analyzed particles (FCM analysis) from both unfiltered seawater samples and filtered ($>2 \mu m$) seawater samples (Fig. 6.6).

DF2 (responsible for 11% of the total variance in the data set with a B/W of 17) exhibits no clear-cut trends with location and no statistically significant correlations with the external variables listed in Table 6.2.

Small-particle POM

Average small-particle ($>2 \mu m$, $<53 \mu m$) POM in the MAB, like large-particle ($>53 \mu m$) POM, contains strong polysaccharide and protein signatures (see Chapter 4, Fig. 4.4a). However, for small-particle POM, the protein signature is slightly more intense and the polysaccharide signature includes stronger contributions from m/z 96, 110, 126. The m/z value identified as phytadiene (m/z 278) is also considerably more prominent in $>2 \mu m$, $<53 \mu m$ POM, as are the values identified as diglyceride fragments

(m/z 521, 549). The sterol signature includes mass unit values associated with diatomsterol (m/z 398, 380), Volkman et al., 1997, and dinosterol (m/z 428, 410).

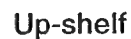
Applying discriminant analysis to MAB small-particle POM leads to a clustering of samples based on location on the shelf (see Fig. 6.7). The score plot for DF1 (13.8% of the total variance in the data set, B/W of 45.5) vs DF2 (11.4 % of the total variance, B/W of 9) shows samples falling along DF1 in a roughly northwest to southeast, or along-shelf, direction. DF2 separates the samples into those collected from the shelf-edge (falling within DF+2), the slope (plotting along the origin), and the mid-shelf (falling within DF-2).

The reconstructed spectra for DF1 (Fig. 6.8) indicate that particles towards the southern end of the Bight are more enriched in polysaccharides (as ion series from both hexose and pentose fragments appear in DF-1), $C_{14:0}$ and $C_{16:0}$ fatty acid (m/z 228 and 256, respectively), and chlorophyll (m/z 278, identified as phytadiene, a chlorophyll pyrolysis product). The sterol signature appears oddly split between DF-1 and DF+1, but the diglycerides appear mainly in DF-1.

The reconstructed spectra for DF2 (Fig. 6.9) indicate that the shelf break samples (falling in DF+2) are enriched in protein, $C_{14:0}$, $C_{16:1}$, $C_{15:0}$, and $C_{16:0}$ fatty acids (m/z 228, 236 (from M- H_2O), 242, and 256 respectively), and chlorophyll (m/z 278). The mid-shelf samples are enriched in polysaccharides. The sterol signature and the diglyceride signature also fall primarily in DF-2, indicating that the shelf samples are enriched in these components as well.

Correlation matrices for the scores from DF1 and DF2 and external variables indicate a positive correlation between DF1 and PO_4 concentration and a negative correlation between DF2 and the ratio of POC to chlorophyll *a* (Fig. 6.10).

Down-shelf



220

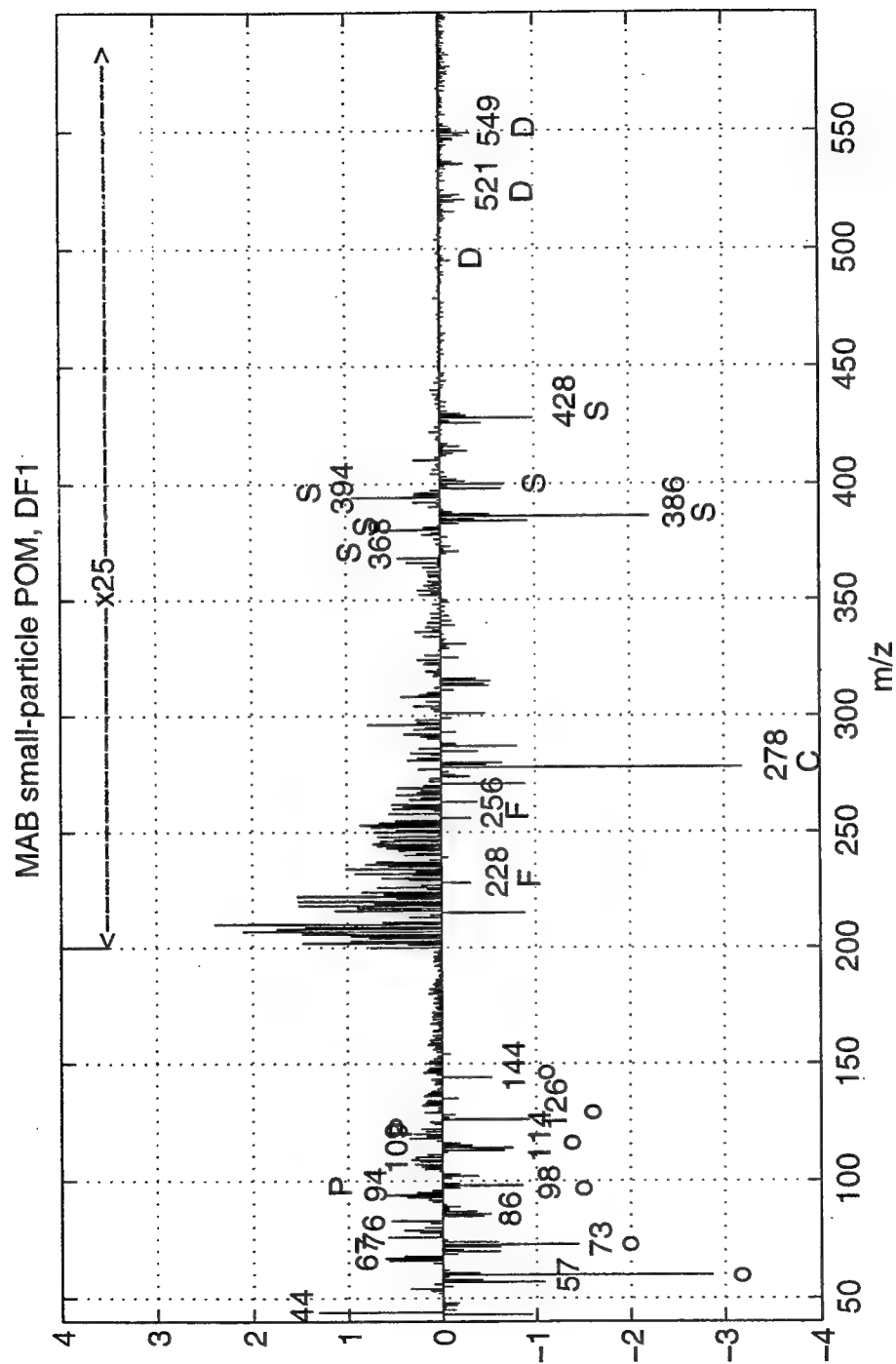


Fig. 6.8. Reconstructed spectrum for DF1 from Fig. 6.7. Symbols as in Fig. 6.5.

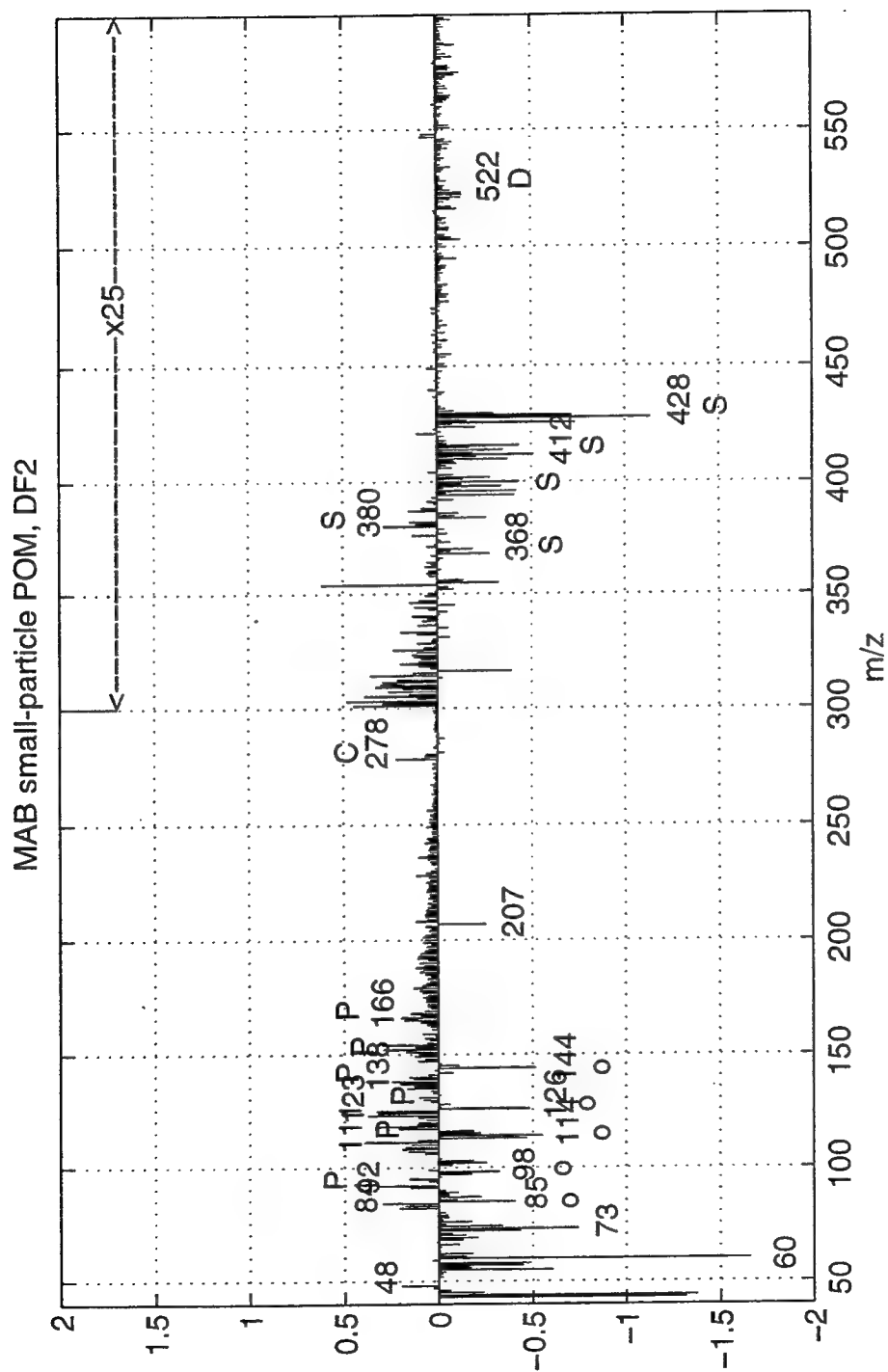


Fig. 6.9. Reconstructed spectrum for DF2 from Fig. 6.7. See Fig. 6.5 for symbols.

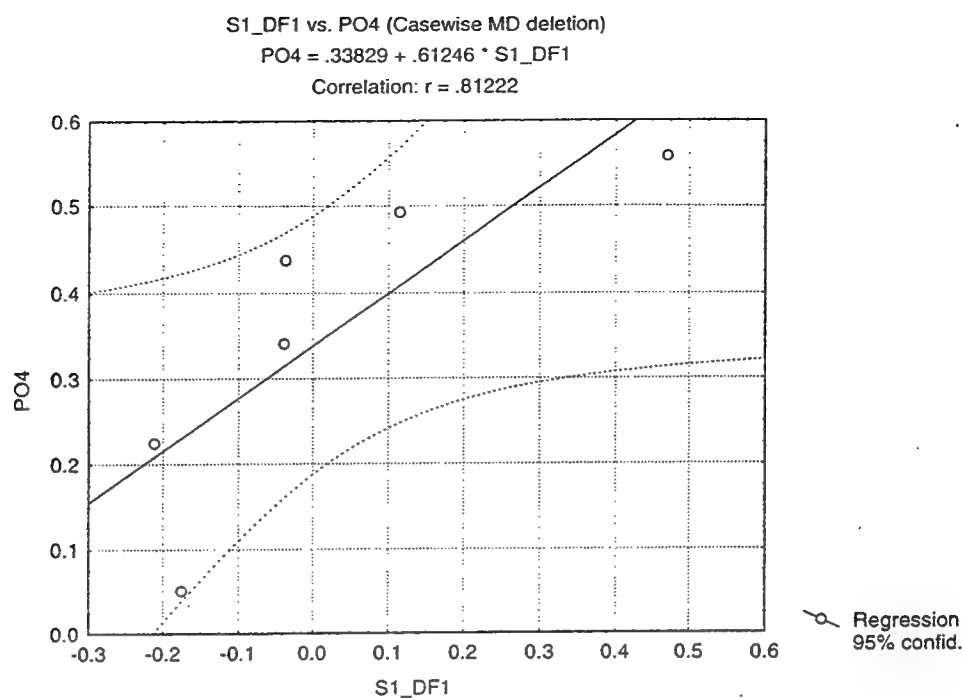
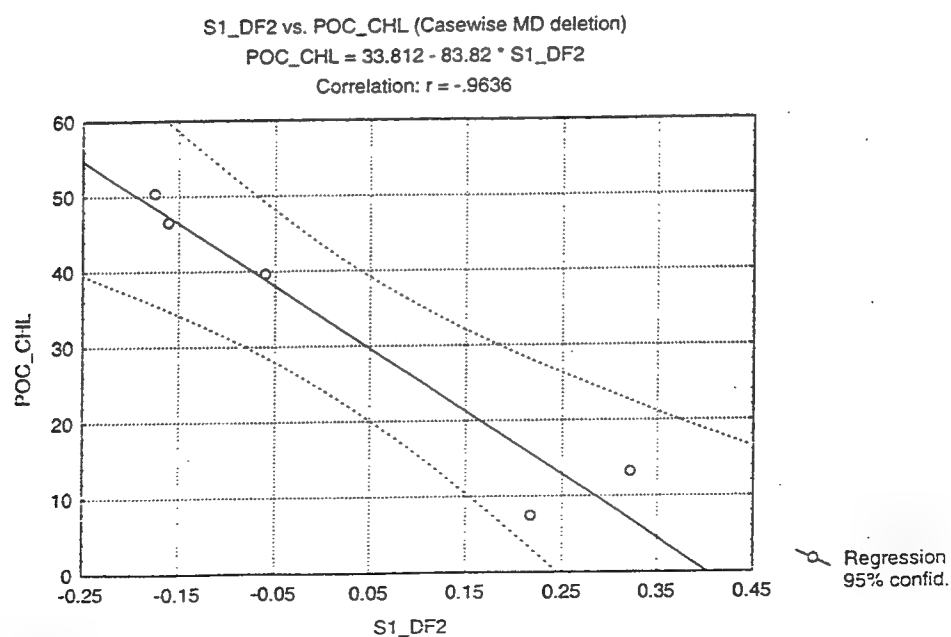


Fig. 6.10a. Plot of DF1 scores (see Fig. 6.7) from analysis of small-particle POM vs. PO_4 concentration.



10b. Plot of DF2 scores (see Fig. 6.7) from analysis of small-particle POM vs. $[POC]/[chlorophyll\ a]$.

"Phytoplankton"

In the MAB average "phytoplankton" mass spectrum (Chapter 4, Fig. 4.9a) the ion series attributed to protein predominates. The polysaccharide and chlorophyll signals are also strong. The sterol signature contains a range of ions (m/z 366, 368, 380, 384, 386, 394, 412, 430) with m/z 368, attributed to cholesterol ($M-H_2O$) as the most intense ion in the series.

In discriminant analysis of MAB "phytoplankton," DF1 is responsible for 23% of the total variance in the data set and has a B/W of 23. The DF1 score plot (Fig. 6.11) indicates that DF+1 contains mid-shelf samples, the region around the origin contains two slope and two mid-shelf samples, and DF-1 contains one slope and two shelf-edge samples. The main m/z values in DF+1 (Fig. 6.12) are identified as partial protein (m/z 124, 138, 152, 153, 166, 180) and polysaccharide (m/z 85, 110, 114, 126, 128) signatures, $C_{14:0}$ and $C_{15:0}$ fatty acids and sterols and stanols (m/z 386, 394, 398, 412, 430). Diglycerides are also more prevalent in DF+1. DF-1 is characterized by ions identified as a partial protein signature (m/z 91, 92, 94, 106, 108, 117, 131) and a chlorophyll signature (m/z 278).

Correlation matrices indicate that there is a statistically significant positive correlation (Fig. 6.13a) between DF1 score and the POC/chlorophyll *a* ratio and a significant negative correlation (Fig. 6.13b) between DF1 and the phytoplankton/(phytoplankton + detritus) ratio in filtered seawater POM ($>2 \mu m$, $<53 \mu m$).

MAB small-particle "phytoplankton:" Discriminant Function 1

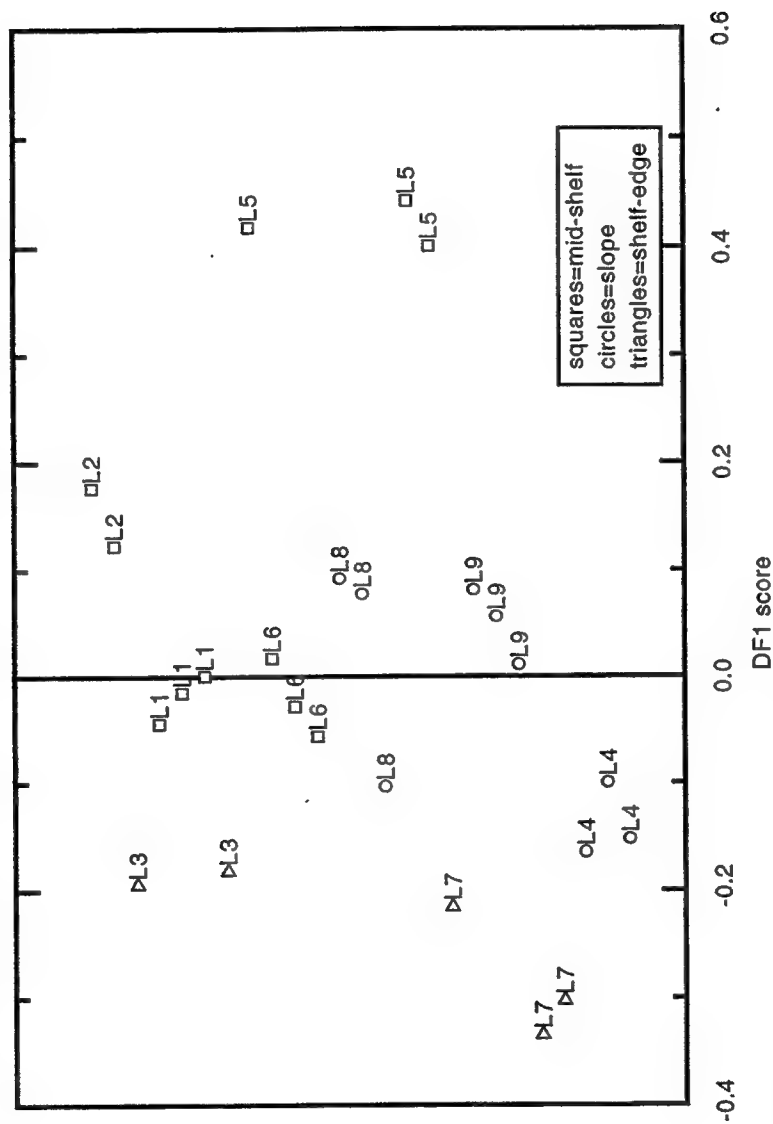


Fig. 6.11. Score plot for discriminant analysis of MAB "phytoplankton" (>2 μm, <53 μm)

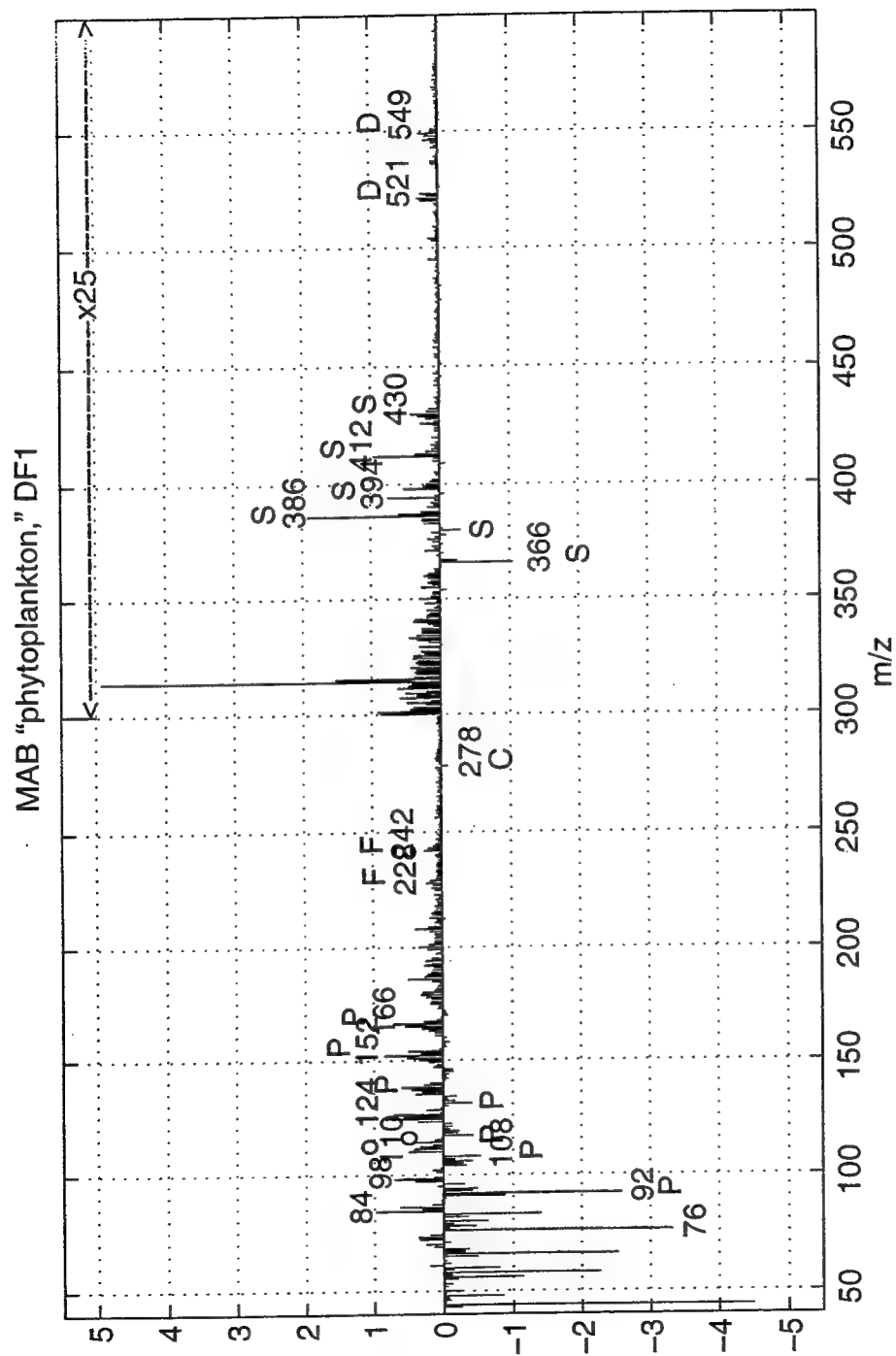


Fig. 6.12. Reconstructed spectrum for DF1 from Fig. 6.11. Symbols as in Fig. 6.5.

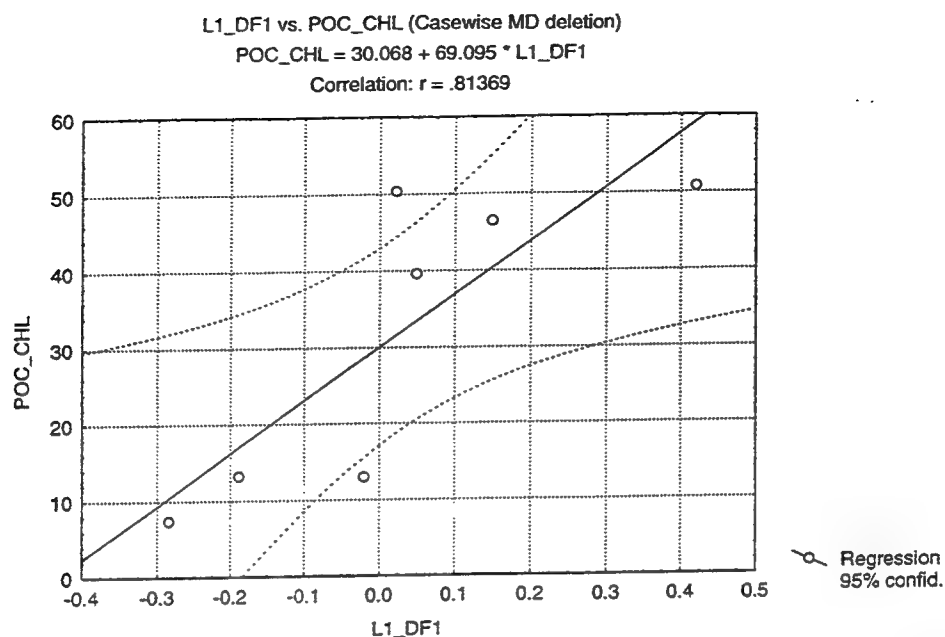
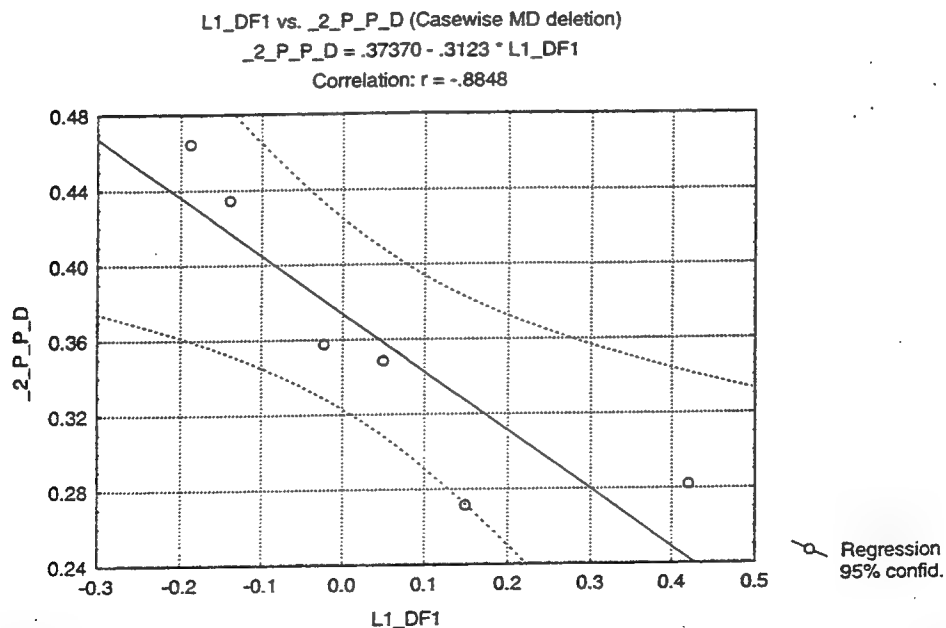


Fig. 6.13.a. Plot of DF1 scores (see Fig. 6.11) from analysis of MAB “phytoplankton” vs [POC]/[chlorophyll *a*].



13b. Plot of DF1 vs the ratio of phytoplankton/total analyzed particles in filtered (<53 μm , >2.0 μm) POM samples.

"Detritus"

The average DT-MS spectrum for MAB "detritus" (Chapter 4, Fig. 4.10a) contains a strong polysaccharide signature (m/z 96, 110, 126), a less intense protein signature, m/z 76 (tentatively identified as CS_2) and m/z 104 (possibly styrene).

Discriminant analysis (score plot, Fig. 6.14) shows no obvious locational trend related to DF1 (22.4% of total variance, B/W of 38) or DF2 (9.8% of total variance, B/W of 20). DF-1 is characterized mainly by an enrichment in polysaccharides, DF+1 indicates enrichment in proteins (Fig. 6.14). Lipids appear to fall mainly in DF+1 as well.

There were no obvious correlations between DF1 or DF2 and the external variables in Table 6.2.

Discussion

The sensitivity of DT-MS (16 eV, El^+) over a broad range of compound classes allows distinctions within POM subclasses to be viewed in a new context. Molecular-level variations can be explored using multivariate analysis of DT-MS "fingerprints" of individual samples rather than from combinations of multiple, compound-class specific analyses (e.g., Wakeham et al., 1997). This facilitates the comparison of variations in broad-band molecular-level characteristics of OM samples with variations in external variables such as seawater temperature and salinity. This chapter presents one of the first attempts to compare the specific biochemical composition of POM with water-column physical and biological parameters.

Statistical (discriminant) analysis indicates that both large-particle and small-particle POM vary in molecular-level composition as a function of location in the MAB.

The chemical characteristics of large-particle POM vary as a function of cross-shelf location, with shelf samples exhibiting an enrichment in chitin, protein, and sterols, particularly cholesterol, and slope samples appearing enriched in polysaccharides and

MAB small-particle "detritus:" DF1 vs DF2

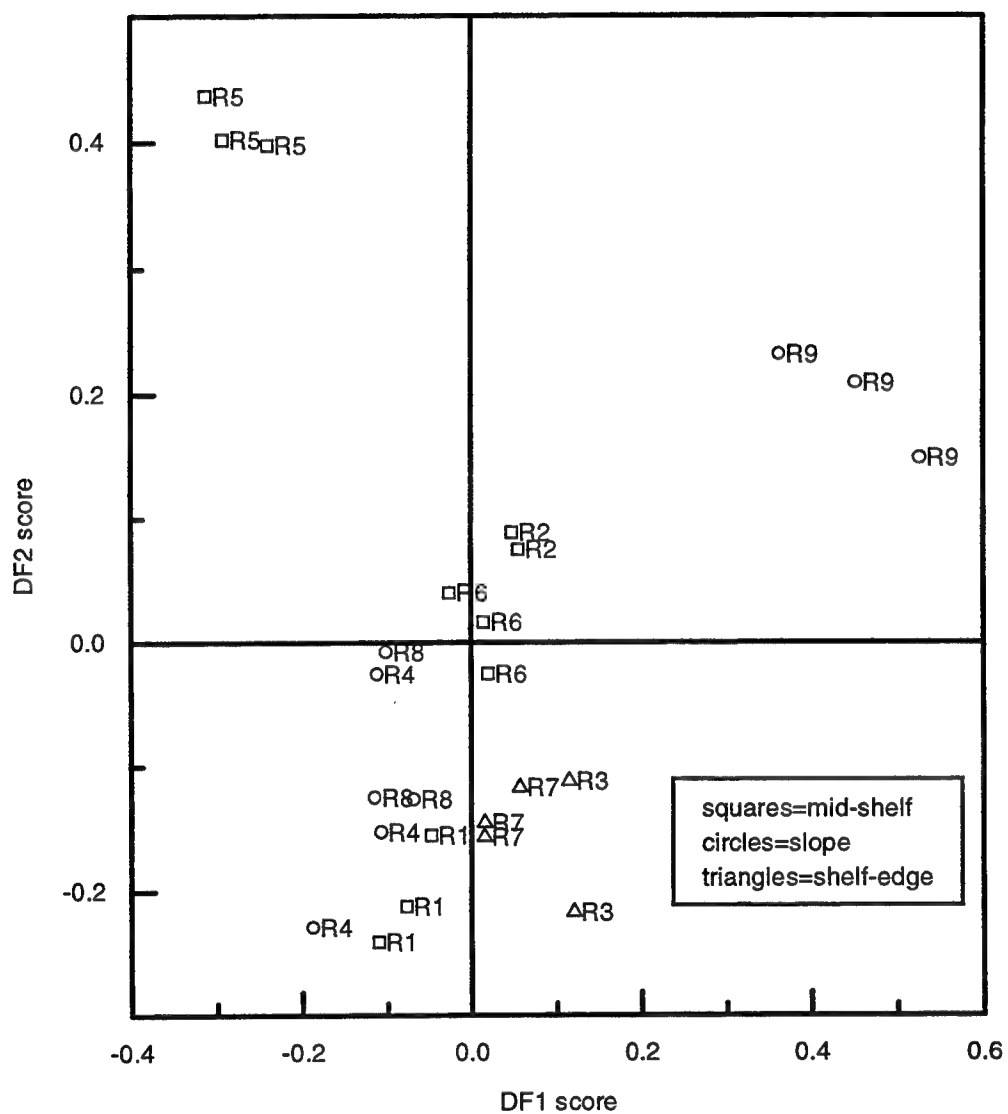


Fig. 14. Score plot showing DF1 vs DF2 from analysis of MAB "detritus" (>2 μm , <53 μm).

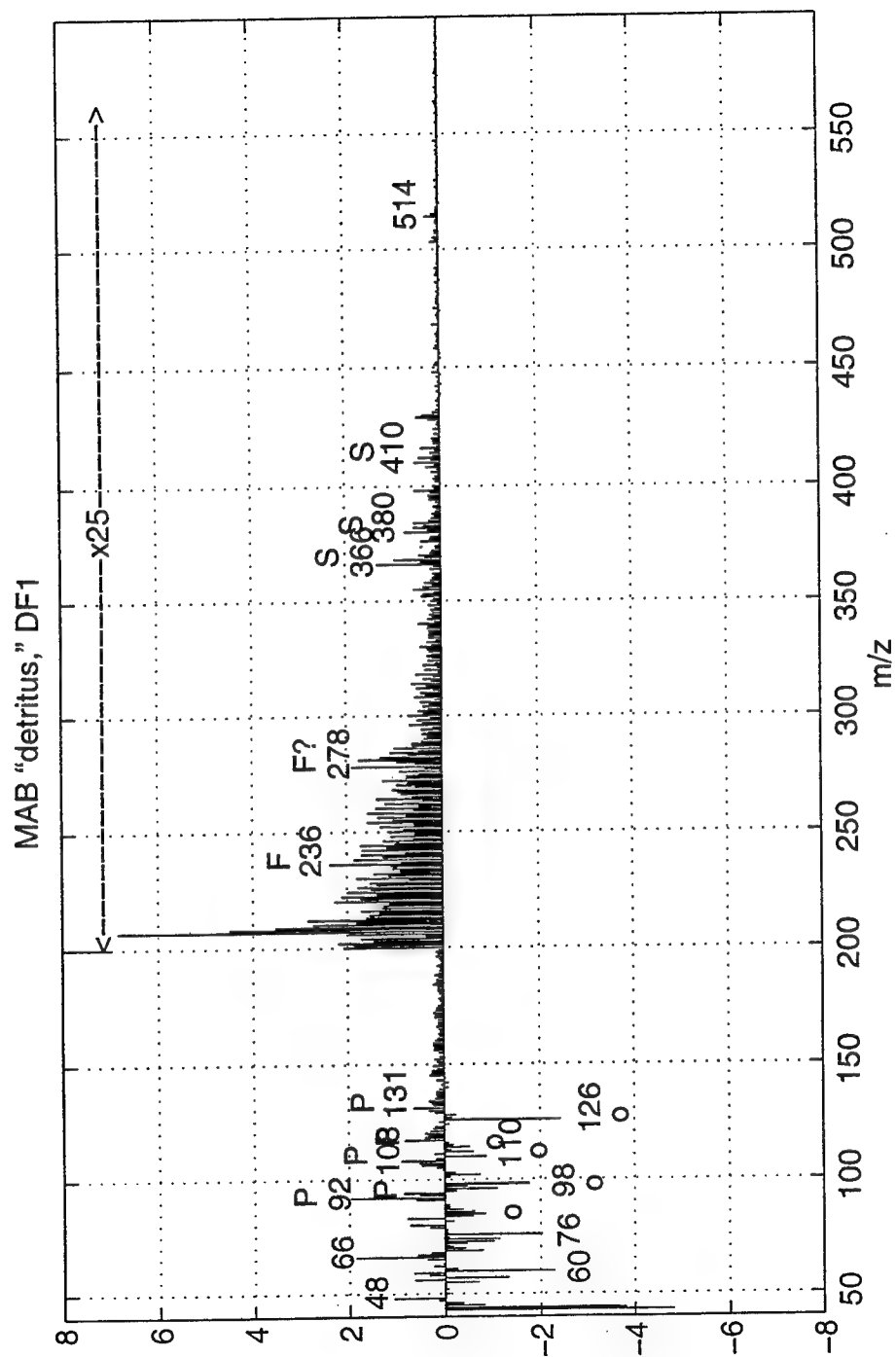


Fig. 6.15. Reconstructed spectrum from DF1 in Fig. 6.14. Symbols as in Fig. 6.5.

C_{16:0} fatty acid. Zooplankton cuticles and exoskeletons often contain chitin (Jeuniaux and Voss-Foucart, 1991; Baas et al., 1995; Stankiewicz et al., 1996, and others), and zooplankton are generally enriched in proteins and depleted in polysaccharides relative to phytoplankton (Parsons et al., 1984 and references therein). Cholesterol, though biosynthesized by phytoplankton, is a primary zooplankton sterol (Volkman 1986). Based on these observations, we infer that large-particle POM from the shelf is enriched in zooplankton biomass, while large-particle POM from the slope contains a greater phytoplankton or phytodetritus component. This hypothesis is reinforced as DF1 (the function separating shelf and slope samples as described above) is positively correlated with the ratio of phytoplankton to total particles. DF+1, in which the slope samples fall, is the region of higher phytoplankton ratios, and the molecular-level characteristics there appear more "phytoplanktonic."

Small-particle POM in the MAB appears to vary as both a function of along-shelf location (DF1) and cross-shelf location (DF2). Particles farther south along the shelf are more enriched in polysaccharides, C_{14:0} and C_{16:0} fatty acids, chlorophyll, and diglycerides (which may actually be present in the particles as triglycerides, phospholipids, or diglycerides, see Chapter 3). Phytoplankton culture studies have shown an increase in the percentage (wt %) of organic carbon present as carbohydrates and lipids as cultures enter stationary phase (e.g. Brown et al., 1996). Therefore, our along-shelf trend could be explained by the presence of a more established bloom in the more southern, down-shelf waters. This interpretation is consistent with the correlation between DF1 and phosphate concentration as the most depleted phosphate levels are found in the more southern waters; an older, established bloom would be expected to have lowered nutrient levels.

In the cross-shelf direction, small-particle POM samples from the shelf-break appear enriched in protein, C_{14:0}, C_{15:0}, C_{16:1}, and C_{16:0} fatty acids, and chlorophyll as compared to slope or mid-shelf samples. The mid-shelf samples contain stronger polysaccharide, sterol, and diglyceride signatures. The trend of reduced polysaccharide

signature with distance offshore has also been seen in suspended POM from the Rhone delta (Sicre et al., 1994), and was attributed by these authors to dilution of river waters containing polysaccharides and/or consumption by biota. The polysaccharide signature of small-particle POM from the MAB differs from the suspended POM in the Rhone delta, however, as the former contains anhydrohexoses and a much less pronounced furfural and methylfurfural component. This difference may be due partly to analytical differences as Sicre et al. (1994) applied Curie point Py-GC and Py-GC-MS to undesalted samples while this study applied DT-MS to desalted samples (see van der Kaaden and Haverkamp, 1983, for a discussion of matrix effects in analytical pyrolysis). However, if real, it may indicate that the polysaccharide signal in the MAB is less diagenetically altered (see also Chapter 5).

It is difficult to tell if the polysaccharide variations in the MAB are a general offshore trend or a riverine outflow trend as the data set is small. However, in an attempt to see if the decrease in polysaccharides could be extended from the shelf break to slope waters, the mass spectra from stations 3 and 4 and 7 and 8 were compared by eye (see Fig. 6.1 for station locations). In this rather subjective approach, no significant difference in the relative intensity of polysaccharides could be seen in the spectra of stations 3 and 4, but station 7 (shelf-break) had a more intense signature than station 8 (slope). This could indicate that the polysaccharide variations are related to riverine inputs to the shelf as stations 7 and 8 are down-shelf from the mouth of the Delaware Bay. Additional evidence in favor of the river trend can be found in Fig. 6.6, where the relative positions of S6, S9 and m/z 126, 114, 85, and 144 indicate that polysaccharides are distinguishing features of the downshelf stations S6 and S9. However, it is difficult to determine whether this river trend is due to the input of allochthonous organic matter or due to riverine effects on nearshore primary and secondary production (as the result of nutrient inputs or changes in hydrography).

The fact that large-particle POM from the slope is enriched in phytoplankton biochemicals relative to shelf large-particle POM and that slope small-particle POM

appears less phytoplankton-rich than shelf-break small-particle POM could indicate that larger phytoplankton are a more important component of slope plankton populations. However, discriminant analysis of MAB $>53\text{ }\mu\text{m}$ and $>2\text{ }\mu\text{m}$, $<53\text{ }\mu\text{m}$ POM indicates that everywhere in the MAB, $>2\text{ }\mu\text{m}$, $<53\text{ }\mu\text{m}$ POM has a stronger phytoplankton biochemical component than $>53\text{ }\mu\text{m}$ POM (Chapter 4, Fig. 4.5, DF1). There is no evidence in the scoreplot of DF1 (Chapter 4, Fig. 4.5, DF1, and the same plot including station locations (unpublished)) that large-particle POM from the slope plots closer to either the phytoplankton standard or to the more "phytoplanktonic" small-particle POM than large-particle POM from shelf stations. This is consistent with a microscopy-based plankton study in the MAB which indicates that the importance of large phytoplankton decreases with increasing distance offshore (Verity et al., 1996).

In contrast to bulk large-particle and small-particle POM, the two subclasses of POM isolated from small-particle POM do not appear to exhibit strong spatial variations. "Phytoplankton" ($>2\text{ }\mu\text{m}$, $<53\text{ }\mu\text{m}$) may exhibit some variation with cross-shelf distance (DF1), with shelf samples being more enriched in lipids and selected polysaccharides and shelf-break samples more enriched in a partial protein signature and chlorophyll. This spatial distribution is not clear, however, as both slope and shelf samples plot near the origin in DF1. Nevertheless, the spatial trends in "phytoplankton" composition, if valid, are consistent with the spatial and molecular-level variations in small-particle POM (DF2). If correct, this would indicate that changes in the phytoplankton population may be responsible for cross-shelf variations in small-particle POM in early spring. Correlating "detritus" ($>2\text{ }\mu\text{m}$, $<53\text{ }\mu\text{m}$) variations with location is more difficult. In addition, there are no obvious correlations between discriminant scores and external variables (listed in Table 6.2). Taken together these observations suggest that this component of detrital OM is relatively invariant. Indeed, viewing individual spectra for "detritus" indicates that this pool always contains a strong and characteristic polysaccharide signature (m/z 96, 110, and 126) and a mass unit value tentatively identified as styrene (m/z 104) from either an anthropogenic source (e.g., de Koster and

Boon) or natural marine source (as in Stankiewicz et al., 1996). "Detritus" varies mainly in the intensity of these peaks vs. an underlying signature tentatively identified as a combination of nucleic acids and protein and/or lignin.

The lack of compositional trends in "phytoplankton" and "detritus" as compared to total small-particle POM is, at a first glance, disconcerting. It could indicate that there are additional POM subclasses invisible to the flow cytometer (i.e., below the forward angle light scatter detection limit) or otherwise lost during flow cytometric sorting (as >80% of the particles seen via flow cytometry are separated into the "phytoplankton" and "detritus" subclasses). However, it is also quite likely that the biochemical composition of total small-particle POM is affected by the ratio of phytoplankton biomass to detritus "biomass." While not a measure of biomass variations, the P/(P+D) ratio does vary in across-shelf and along-shelf directions (See Table 6.1 and Figure 6.1).

The observed variations with location in small-particle and large-particle POM compositions are consistent with findings by other workers in the MAB. For example, Wirick (1994) finds the highest stocks of phytoplankton along the shelf-slope front; discriminant analysis of suspended POM indicates that the strongest phytoplanktonic signature appears in shelf-edge samples. Falkowski et al. (1988) find that surface shelf waters, as compared to surface slope waters, contain almost an order of magnitude more organisms. These workers also compared abundances of dominant shelf herbivorous zooplankton in shelf and slope waters. The zooplankton were considerably more abundant in shelf waters, leading to estimated ingestion rates six times higher on the shelf than on the slope. These findings are consistent with the DT-MS analyses of large-particle POM, which indicate a greater contribution of zooplankton biomass to larger particles on the shelf than on the slope. The strong cross-shelf trends in small-particle and large-particle POM indicate that, as has been found by other workers, exchange of particles across the shelf-slope front is small (Biscaye et al., 1994 and references therein) and that there is significant grazing of the zooplankton bloom on the shelf (Falkowski et al., 1988).

Similarities in the composition of "detrital" components of small-particle POM irrespective of location indicate that suspended "detritus" should perhaps be considered an additional sink for phytoplankton carbon, along with grazing, burial in the sediments, contribution to the DOC pool, and export from the region. The lack of variation within "detritus" also indicates that the source of this POM pool may be autochthonous; allochthonous inputs from the Chesapeake and Delaware Bays would cause a north-south trend in "detrital" composition. Work by Verity et al. (1996) is consistent with these hypotheses; it indicates that in the MAB there is an active community of smaller grazers, especially protozoans and small copepods, whose fecal pellets would remain in suspension and would be exported along with shelf water during transport along the shelf and entrainment at Cape Hatteras.

Conclusions

1. Based on DT-MS analysis of particle subpopulations in MAB surface waters, large-particle ($>53\ \mu\text{m}$) POM on the shelf appears to contain a larger proportion of zooplankton biomass (compared to $>53\ \mu\text{m}$ POM on the slope) as indicated by enrichment in chitin, protein, and sterols, particularly cholesterol. Large-particle POM from the slope is enriched in polysaccharides and $\text{C}_{16:0}$ fatty acid. The polysaccharide enrichment indicates that this POM is probably more phytodetrital in origin, though it may include fecal pellets as well. The trend in large-particle POM composition is consistent with previous work in the MAB indicating enhanced grazing in shelf waters.
2. The polysaccharide component of small-particle ($>2\ \mu\text{m}$, $<53\ \mu\text{m}$) POM increases with alongshelf distance and decreases with cross-shelf distance. This may be due to input from the Chesapeake and Delaware Bays (either directly as allochthonous OM or indirectly as the result of nutrient and freshwater input).

Small-particle POM at the shelf-break (compared to other MAB $>2\ \mu\text{m}$, $<53\ \mu\text{m}$ POM) appears to contain a greater phytoplankton component as it is enriched in protein, $\text{C}_{14:0}$, $\text{C}_{16:1}$, and $\text{C}_{16:0}$ fatty acids, and chlorophyll. Enrichment in $\text{C}_{15:0}$ fatty acid may also indicate an increased bacterial presence. The fact that shelf-break small-particle POM appears more phytoplanktonic is consistent with the study of Wirick (1994), which reports the highest stocks of phytoplankton along the shelf/slope front.

3. "Phytoplankton" (isolated from small-particle POM) exhibits less clear-cut spatial variations. Shelf-break samples appear enriched in a partial protein signal and chlorophyll while shelf samples appear enriched in lipids, a partial protein signal, and selected polysaccharides (pentose, deoxyhexose and m/z 110, 126).

The variation in "phytoplankton" composition may be responsible for a significant proportion of the cross-shelf variation in small-particle POM. The relative contribution of small-particle POM subclasses may also contribute to the biochemical variation of this POM pool.

4. The composition of "detritus" (isolated from small-particle POM) appears relatively invariant with location. It may act as an additional sink for phytoplankton carbon, thus contributing to organic matter export from the shelf in a manner similar to that proposed for dissolved organic carbon.

The coupling of DT-MS and multivariate statistics, as shown here, provides information on variations in molecular-level composition among samples from multiple POM subclasses. The ability of this technique to reduce the dimensionality of the molecular-level data facilitates the search for correlations between POM compositional differences and environmental and biological variables. Unfortunately, the semi-quantitative nature of DT-MS at present limits our understanding of variations in POM composition to a change in molecular-level "fingerprints." It is hoped that with future

methods development DT-MS could provide quantitative information concerning the compounds in oceanic organic matter.

References:

- Baas M., Briggs D. E. G., van Heemst J. D. H., Kear A. J., de Leeuw J. W. (1995). Selective preservation of chitin during the decay of shrimp. *Geochim. Cosmochim. Acta*, **59**(5), 945-951.
- Beardsley R. C., and Boicourt W. C. (1981). On estuarine and continental shelf circulation in the Middle Atlantic Bight. In: Warren B. A. and Wunsch C. (Ed.), *Evolution of Physical Oceanography*, The MIT Press, Cambridge, MA, pp. 198-233.
- Beardsley R. C., Boicourt W. C., and Hansen D. H. (1976). Physical oceanography of the Middle Atlantic Bight. In: Gross M. G. (Ed.), *Middle Atlantic continental shelf and New York Bight*, American Society of Limnology and Oceanography, special Symposia, Vol. 2, pp. 20-34.
- Biscaye P. E., Flagg C. N., and Falkowski P. G. (1994). The Shelf Edge Exchange Processes experiment, SEEP-II: an introduction to hypotheses, results, and conclusions. *Deep-Sea Res. II*, **41**(2/3), 231-252.
- Bishop, J. K. B. and Edmond, J. M., 1976. A new large-volume *in situ* filtration system for sampling oceanic particulate matter. *J. Mar. Res.*, **32**:181-198.
- Boon J. J. (1992). Analytical pyrolysis mass spectrometry: new vistas opened by temperature-resolved in-source PYMS. *Int. J. Mass. Spec and Ion Process.*, **118/119**, 755-787.
- Boon J. J., Klap V., and Eglinton T. (1998) Molecular characterization of microgram amounts of colloidal dissolved organic matter (UDOM) in ocean water samples by direct temperature resolved ammonia chemical ionization mass spectrometry. *Org. Geochem.*, submitted.
- Brown M. R., Dunstan G. A., Norwood S. J., and Miller K. A. (1996). Effects of harvest stage and light on the biochemical composition of the diatom *Thalassiosira pseudonana*. *J. Phycol.* **32**, 64-73.
- Davis J. C. (1986). *Statistics and data analysis in geology*. New York, John Wiley and Sons, 646 pp.
- Eglinton T. I., Boon J. J., Minor E. C., and Olson R. J. (1996). Microscale characterization of algal and related particulate organic matter by direct temperature-resolved mass spectrometry. *Mar. Chem.* **52**, 27-54.

- Eglinton T. I., Sinninghe Damste J. S., Pool W., de Leeuw J. W., Eijkel G., Boon J. J. (1992). Organic sulfur in macromolecular sedimentary organic matter-II: Analysis of distributions of organic sulfur pyrolysis products using multivariate techniques. *Geochim. Cosmochim. Acta* **56**, 1545-1560.
- Falkowski P. G., Flagg C. N., Rowe G. T., Smith S. L., Whitledge T. E., and Wirick C. D. (1988). The fate of a spring phytoplankton bloom: export or oxidation? *Continental Shelf Res.* **8**(5-7), 457-484.
- Fairbanks R. G. (1982). The origin of continental shelf and slope water in the New York Bight and Gulf of Maine: evidence from H₂1802/H₂1602 ratio measurements. *J. Geophys. Res.*, **87**, 5796-5808.
- Goericke R. and Repeta D. J. (1993). Chlorophylls *a* and *b* and divinyl chlorophylls *a* and *b* in the open subtropical North Atlantic Ocean. *Mar. Ecol. Prog. Ser.*, **101**, 307-313.
- Hedges J. I. (1992). Global biogeochemical cycles: progress and problems. *Mar. Chem.* **39**, 67-93.
- Hedges J. I. and Stern J. H. (1984). Carbon and nitrogen determinations of carbonate-containing solids. *Limnol. Oceanogr.* **29**(3), 657-663.
- Hoogerbrugge R., Willig S. J., and Kistemaker P. G., (1983). Discriminant analysis by double stage principle component analysis. *Anal. Chem.* **55**, 1710-1712.
- Houghton R. W., R. Schiltz, Beardsley R. C., Butman B., and Chmberlin J. L. (1982). Middle Atlantic cold pool: evolution of the temperature structure during summer 1979. *J. Phys. Oceanogr.*, **12**, 1019-1029.
- Jeuniaux C. and Voss-Foucart M. F. (1991). Chitin biomass and production in the marine environment. *Biochemical Systematics and Ecology*, **19**(5), 347-356.
- van der Kaaden A., Haverkamp J., Boon J. J., de Leeuw J. W. (1983). Analytical pyrolysis of carbohydrates: I. Chemical interpretation of matrix influences on pyrolysis-mass spectra of amylose using pyrolysis-gas chromatography-mass spectrometry. *J. An. Appl. Pyrol.* **5**, 199-220.
- Klap V. A. (1997). Biogeochemical aspects of salt marsh exchange processes in the SW Netherlands, Ph.D. Thesis, NIOO/CEMO, 170 p.
- de Koster C. G. and Boon J. J. (1994?). Qualitative and quantitative analysis of fire retardants in complex polymer matrices by direct temperature resolved mass

spectrometry. FOM Institute (at the request of the Consumentenbond, 's-Gravenhage, The Netherlands), Amsterdam, The Netherlands, 149 pp.

Parsons T. R., Takahashi M., Hargrave B. (1984). *Biological Oceanographic Processes*, 3rd Ed., Pergamon Press, New York, 330 p.

Saliot A., Ulloa-Guevara A., Viets T. C., de Leeuw J. W., Schenk P. A., Boon J. J. (1984). The application of pyrolysis-mass spectrometry and pyrolysis-gas chromatography-mass spectrometry to the chemical characterization of suspended matter in the ocean. *Org. Geochem.* **6**, 295-304.

Sicre M-A, Peulve S., Saliot A., de Leeuw J. W., and Baas M. (1994). Molecular characterization of the organic fraction of suspended matter in the surface waters and bottom nepheloid layer of the Rhone delta using analytical pyrolysis. *Org. Geochem.* **21**(1), 11-26.

Stankiewicz B. A., van Bergen P. F., Duncan I. J., Carter J. F., Briggs D. E. G., and Evershed R. P. (1996). Recognition of chitin and proteins in invertebrate cuticles using analytical pyrolysis/gas chromatography and pyrolysis/gas chromatography/mass spectrometry. *Rapid Communications in Mass Spectrometry*, **10**, 1747-2757.

Verity P. G., Paffenhofer G.-A., Wallace D., Sherr E. and Sherr B. (1996). Composition and biomass of plankton in spring on the Cape Hatteras shelf, with implications for carbon flux. *Continental Shelf Research*, **16**(8), 1087-1116.

Volkman J. K. (1986). A review of sterol markers for marine and terrigenous organic matter. *Org. Geochem.* **9**(2), 83-99.

Wakeham S. G., Lee C., and Hedges J. I. (1997). Fluxes of major biochemicals in the equatorial Pacific Ocean. *Biogeochemistry of Marine Organic Matter*, submitted.

Walsh J. J. (1988). *On the nature of continental shelves*, Academic Press, New York, 520 pp.

Walsh J. J., Rowe G. T., Iverson R. L. and McRoy C. P. (1981). Biological export of shelf carbon is a sink of the global CO₂ cycle. *Nature* **291**, 196-201.

Wirick C. D. (1994). Exchange of phytoplankton across the continental shelf-slope boundary of the Middle Atlantic Bight during spring 1988. *Deep-Sea Res. II*, **41**(2/3), 391-410.

Chapter 7

Synthesis, conclusions, and future work

General

In this thesis, applications of DT-MS (direct temperature-resolved mass spectrometry) to the study of oceanic particulate organic matter (POM) were explored. DT-MS with low voltage electron impact ionization was used as a rapid molecular-level screening technique yielding information on a wide range of biochemicals. Thus DT-MS served to fill the gap between bulk measurements and detailed but time-consuming molecular-level analyses (Eglinton et al., 1996). Representative samples, as determined by EI^+ DT-MS, were further analyzed by ammonia chemical ionization DT-MS and/or GC-MS (Chapters 3, 5, Appendix 2). In addition, the sensitivity of DT-MS made it an appropriate technique for the novel approach of coupling analytical chemistry with flow cytometric sorting. This, for the first time, enabled the molecular-level characterization of "phytoplankton" and "detritus" separated from natural samples of surface ocean water. Chemical characteristics of primary producers from field samples could then be compared with those of small-particle POM, large-particle POM and non-phytoplankton small particles taken from the same stations (see Chapters 4, 6).

Chapter 1 explains the available methods of viewing early diagenesis of marine organic matter in the water column, raises key issues concerning the cycling of POM in the water column, and places the present study in context. With the coupling of flow cytometry and mass spectrometry, primary producer organic matter can be more directly compared with other POM (and DOM, dissolved organic matter) pools. Chapter 1 also introduces the analytical techniques (cross-flow filtration, DT-MS, flow cytometry, and multivariate analysis) used in this thesis.

The protocol for sample collection and analysis is presented and tested in Chapter 2. Since both DT-MS and flow cytometry require samples suspended in a fluid, traditional filtration and extraction techniques could not be used. Therefore, cross-flow filtration, centrifugation as a desalting technique, homogenization of large particles, and

flow cytometric recognition of phytoplankton were evaluated. To the best of our knowledge the protocol presented in Chapter 2 yields representative and reproducible results, though it could be improved by changing the pump style used in cross-flow filtration and by more efficiently desalting flow cytometric sorts.

Chapter 3 provides an example of the potential applications of DT-MS. A set of suspended POM samples collected on a transect from the mouth of the Delaware Bay to the Sargasso Sea was screened at the molecular level via EI^+ DT-MS and discriminant analysis. The results indicated that diglyceride moieties were key variables distinguishing the POM samples. Representative samples were selected for further DT-MS analysis using ammonia and deuterated ammonia chemical ionization (CI). The origin of the diglyceride moieties appeared to be triglycerides and diglycerides, with the amount of each compound class varying with sample. However, the inability to further constrain the origins of variability in the triglyceride and diglyceride pool illustrates the need for preparative flow cytometry coupled with DT-MS.

In Chapter 4 flow cytometry was coupled with DT-MS to provide a description of the average chemical composition of small-particle "phytoplankton," small-particle detritus," large-particle ($>53\ \mu\text{m}$) POM, and small-particle (either $>2\ \mu\text{m}$, $<53\ \mu\text{m}$ or $>0.8\ \mu\text{m}$, $<53\ \mu\text{m}$) POM isolated from total POM at stations along the Mid-Atlantic Bight (MAB) in March 1996 and from monthly samplings in Great Harbor, Woods Hole, MA. Based on these studies it was found that large-particle POM along the MAB was enriched in polysaccharides composed of both pentose and hexose units and $C_{14:0}$ and $C_{16:0}$ fatty acids compared to small-particle POM. These chemical characteristics indicate that this large-particle POM contained a significant phytodetritus component. Large-particle POM from Great Harbor, on the other hand, appeared to contain a significant zooplankton biomass component as indicated by enrichment in chitin, cholesterol and $C_{16:0}$ fatty acid. "Phytoplankton" isolated from $>2\ \mu\text{m}$, $<53\ \mu\text{m}$ POM in both sample sets was enriched in protein, chlorophyll, and lipids (fatty acids, sterols, and, when measured, diglycerides)

compared to "detritus" isolated from the same size-class of POM. "Detritus" was enriched in specific polysaccharide fragments.

Because polysaccharides represented a quantitatively significant and variable component of the different POM pools, they were selected for further study. In Chapter 5, ammonia and deuterated ammonia CI^+ DT-MS was applied to selected samples from Chapter 4 in order to provide supplementary information on their polysaccharide contents. In addition, results from ammonia CI^+ of these samples and samples from a diatom degradation experiment were explored via principal component analysis. The most variance in the data set was explained by a principal component that appeared related to the extent of organic matter degradation in the samples. The "fresher" material exhibited enrichment in polyhexoses and possibly chitin and the "more degraded" material was enriched in methyl-hexose, methyl-deoxyhexose, deoxysugar, and selected aminosugar fragments. Interestingly, the polysaccharide component of the most degraded particulate material shared several characteristics with colloidal DOM polysaccharides, suggesting that degraded POM and colloidal DOM may share a common source.

In Chapter 6 the molecular-level variations within POM subclasses in surface waters along the MAB were explored. While large-particle POM from slope waters contained a greater proportion of phytoplankton biomass, large-particle POM from the continental shelf was characterized by an increased chitin, protein, and cholesterol signature, indicating greater zooplanktonic inputs. Small-particle POM from the shelf edge contained a larger phytoplankton component than mid-shelf or slope small-particle POM. Small particles farther south along the shelf (i.e., closer to Cape Hatteras) were more enriched in polysaccharides, fatty acids, chlorophyll, and diglycerides. The molecular-level composition of "phytoplankton" also appeared to vary with location. "Detritus," however, showed no easily interpretable variations with location or external variables (such as salinity, temperature, or chlorophyll *a* concentration). Small-particle "detritus," as a potential sink for phytoplankton carbon, should be further explored in

studies of continental margins, as it, like DOM, could be passively transported by shelf water and exported as this water exits the shelf.

The data described in Chapters 4, 5, and 6 can also be interpreted in a more general sense to propose a descriptive model for organic matter cycling in the upper ocean. This model, which builds upon existing concepts of organic matter source, composition, and reactivity, is described in the next section.

A modified size-reactivity continuum model

There are two prevailing methods of viewing the pattern of organic matter degradation in the ocean: by depth and by size.

The classical method is to assume that fresher organic matter occurs in the surface ocean (the region of primary productivity) and that particles found at greater depths are more degraded. For organic matter within a particular size class (e.g., sediment trap samples or ultrafiltered dissolved organic matter (UDOM)), this view appears correct and has yielded valuable insights into the relative lability of different compound classes (e.g., Wakeham et al., 1984; Hedges et al., 1988; Wakeham et al., 1997). However, this view begins to change when one looks across the spectrum of organic matter size classes at a particular depth, as shown by Amon and Benner (1996).

It is widely accepted that zooplankton grazing and/or bacterial degradation are the most likely fate for organic matter created by oceanic primary producers. Therefore, Amon and Benner (1996) took a direct approach in determining the biolability of high molecular weight dissolved OM (HMW DOM, >1kDa) and low molecular weight DOM (LMW DOM, <1 kDa). They fed both size classes, isolated from various marine regimes, to bacterial cultures. Though they found bacterial growth efficiencies (determined from bacterial carbon production and bacterial respiration with a respiratory quotient of one) to be higher for the LMW samples, HMW DOM supported higher growth rates (determined by both leucine incorporation and bacterial abundance measurements) and respiration

rates (determined from initial oxygen levels, oxygen levels when bacterial abundance peaked, and incubation times). In addition, a larger percentage of HMW DOC was used per day. These results, along with the amount of characterizable organic carbon in field samples of different size classes, and results from an Amazon River study of coarse POM, fine POM, and UDOM (Hedges et al., 1994) are used as evidence for a new model of organic matter reactivity. The "size-reactivity continuum model" (Amon and Benner, 1996) states that there is a general diagenetic trend from larger size classes of organic matter (more reactive, less degraded) to smaller size classes (less reactive, more degraded).

The "size-reactivity continuum model" seems valid as long as the particle size involved is equal to or smaller than the size class of the majority of the primary producers within the particular marine regime (e.g., the Amazon study in Hedges et al., 1994; the continental shelf study in Chapter 5). In $\text{NH}_3\text{-Cl}^+$ DT-MS analyses (Chapter 5), the major chemical characteristic responsible for differences among POM samples appears to be a polysaccharide signal related to the "freshness" of the organic matter. As the OM moves down the diagenetic pathway from fresh algal culture to residue from a degradation experiment, it loses polyhexoses (probably from storage sugars) and gains (in relative terms) in methyl-hexose, methyldeoxysugar, deoxysugar, and selected aminosugar fragments. UDOM analyzed in the same manner (Boon et al., 1998) seems to fall even further along the diagenetic scale. Indeed, all the mass unit values present in the $\text{NH}_3\text{-Cl}^+$ DT-MS spectrum of Georges Bank UDOM are also present in the most degraded POM sample. The major difference between the two is that, in the UDOM sample, the polyhexose signal is completely absent.

Chapter 5 also indicates, however, that the "size-reactivity continuum" does not hold when POM is split into $>53\ \mu\text{m}$ and $<53\ \mu\text{m}$ POM. In the score plot of Principal Component 1 (Chapter 5, Fig. 5.6), large-particle POM samples always plot to the left (i.e., in the direction of increased degradation) of concurrently-collected small-particle POM. Both Chapter 4 and Chapter 5 indicate that small-particle POM appears more

Phytoplankton (L) and >53 μm POM (G) from the MAB

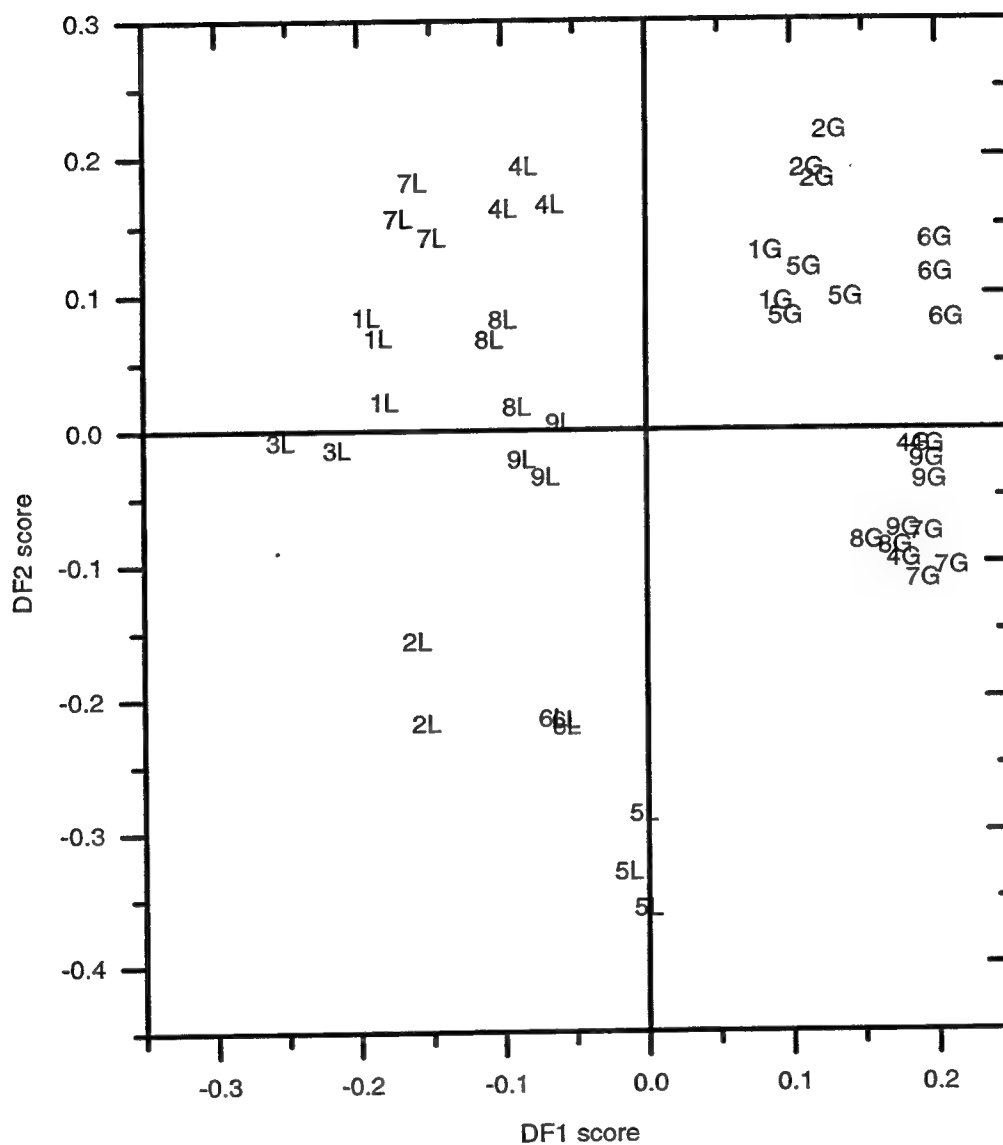


Fig. 7.1. Score plot of discriminant analysis of large-particle (>53 μm) POM and “phytoplankton” isolated from small-particle POM. Sample numbers indicate Mid-Atlantic Bight station numbers (see Chapter 4 for sampling and analytical details).

MAB: "Phytoplankton" vs >53 μm POM, DF1

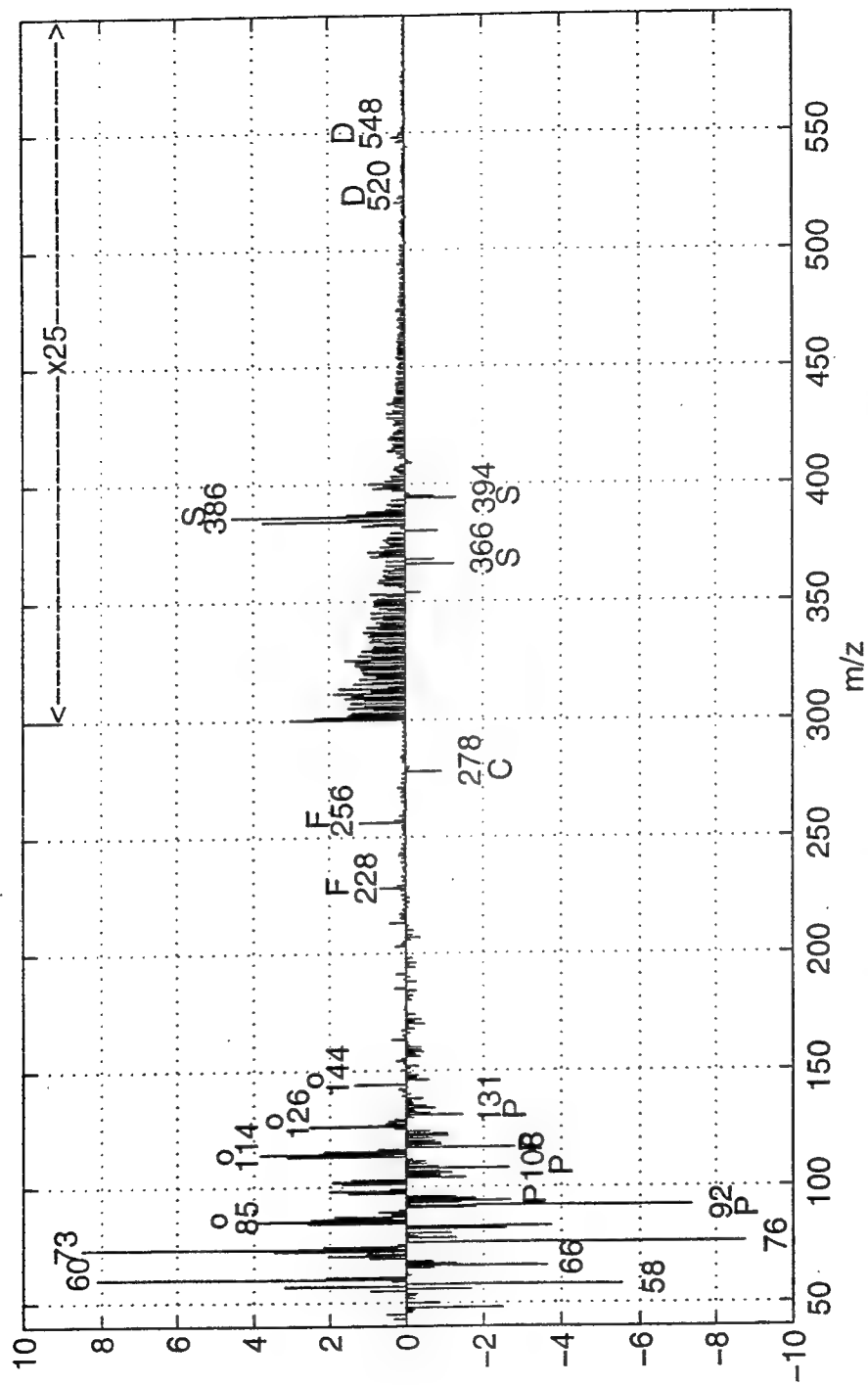


Fig. 7.2. Reconstructed mass spectrum for DF1 from Fig. 7.1. Symbols: **O** polysaccharide, **P** protein, **F** fatty acid, **S** sterol, **D** diglyceride, **C** chlorophyll.

“phytoplanktonic” than large-particle POM along the Mid-Atlantic Bight (MAB) and in Great Harbor, Woods Hole, MA. This also indicates that $>53\ \mu\text{m}$ POM is less “fresh” than $<53\ \mu\text{m}$ POM.

As a further test of the “freshness” of large-particle POM, discriminant analysis was performed upon large-particle POM and “phytoplankton” from the MAB. The first discriminant function (DF1, responsible for 26% of the total variance in the data set, with an intersample to intrasample variance ratio of 237) separates “phytoplankton” from large-particle POM (score plot, Fig. 7.1). The reconstructed spectrum of DF1 (Fig. 7.2) indicates that large-particle POM is enriched in hexose and pentose polysaccharide fragments (m/z 57, 60, 73, 85, 98, 114, 126, 144), $\text{C}_{14:0}$ fatty acid (m/z 228), and $\text{C}_{16:0}$ fatty acid (m/z 256). The “phytoplankton” is enriched in selected protein fragments (m/z 91, 92, 94, 106, 108, 117, 131) and phytadiene from chlorophyll (m/z 278). That “phytoplankton” is enriched in chlorophyll and protein and large-particle POM is enriched in carbohydrates is consistent with the hypothesis that large-particle POM is diagenetically altered from primary producer organic matter. For example, in a sediment trap study in the equatorial Pacific (Wakeham et al., 1997) the following diagenetic sequence was found: “pigments>>lipids>amino acids>carbohydrates.” However, the fact that large-particle POM is enriched in fatty acids does not fit the above diagenetic sequence. This could be explained by variance in the placement of lipids within the sequence as a function of study site. Sediment trap work in the Sargasso Sea, the equatorial Atlantic, the north Pacific, the California current, and the Peruvian upwelling region led to a somewhat different sequence: “hydrolyzable amino acids>total fatty acids>lipids>POC>total particulate organic matter” (Wakeham et al., 1984). Such variation in the determination of the relative lability of lipids is also, undoubtedly, due in part to the extremely varied nature of the compounds described as “lipids.”

The results from the discriminant analysis described above could be affected by differences in sample-handling procedures for “phytoplankton” samples and $>53\ \mu\text{m}$ particles (see Chapter 2). The homogenization procedure for large-particle samples could

have led to additional losses of hydrophilic material and/or increased enzyme activity, although initial comparison of early samples processed unhomogenized vs homogenized (with a mortar and pestle) showed relatively similar DT-MS signatures with prominent protein, polysaccharide, and lipid mass unit values. However, within these compound class signatures, it was difficult to separate sample inhomogeneity effects from sample processing effects. An additional complicating factor for discriminant analysis is that the "phytoplankton" samples were less efficiently desalted than the $>53\ \mu\text{m}$ particles (see Chapters 2 & 5). The desalting issue does not appear significant, however, as indicated by the comparison of "phytoplankton" vs $>53\ \mu\text{m}$ POM results and large-particle vs small-particle POM results (Chapter 4). Both $>53\ \mu\text{m}$ and $<53\ \mu\text{m}$ samples underwent the same desalting procedure; therefore, the comparison of these two pools should not be affected by sample salinities. The EI^+ and $\text{NH}_3\text{-Cl}^+$ spectra of large and small particles indicates that small-particle POM is less degraded (Chapter 5) and more "phytoplanktonic" (Chapter 4) than large-particle POM. These results and the discriminant analysis in this chapter are therefore complimentary and indicate alteration of the primary producer signal in large-particle POM.

Building upon the results from Chapter 5, coupled with the results described above, the following modification (see Fig. 7.3) to the "size-reactivity continuum model" is proposed: Amon and Benner's (1996) model holds for size classes smaller than or equal to the primary producer pool. However, in the surface ocean, particles larger than the majority of the primary producers are generally a modification of primary producer organic matter (e.g., grazer biomass, fecal pellets, or aggregates) and are therefore less "fresh" (or phytoplanktonic). At depth, exchange between the various size classes of organic matter can further complicate views of diagenesis. For example, disaggregation of marine snow aggregates can release fresher organic matter into the suspended pool at depth (as proposed by Wakeham and Canuel, 1988). However, below the size of the primary producer, the size continuum model should still apply as increased degradation leads to smaller and smaller units of organic matter.

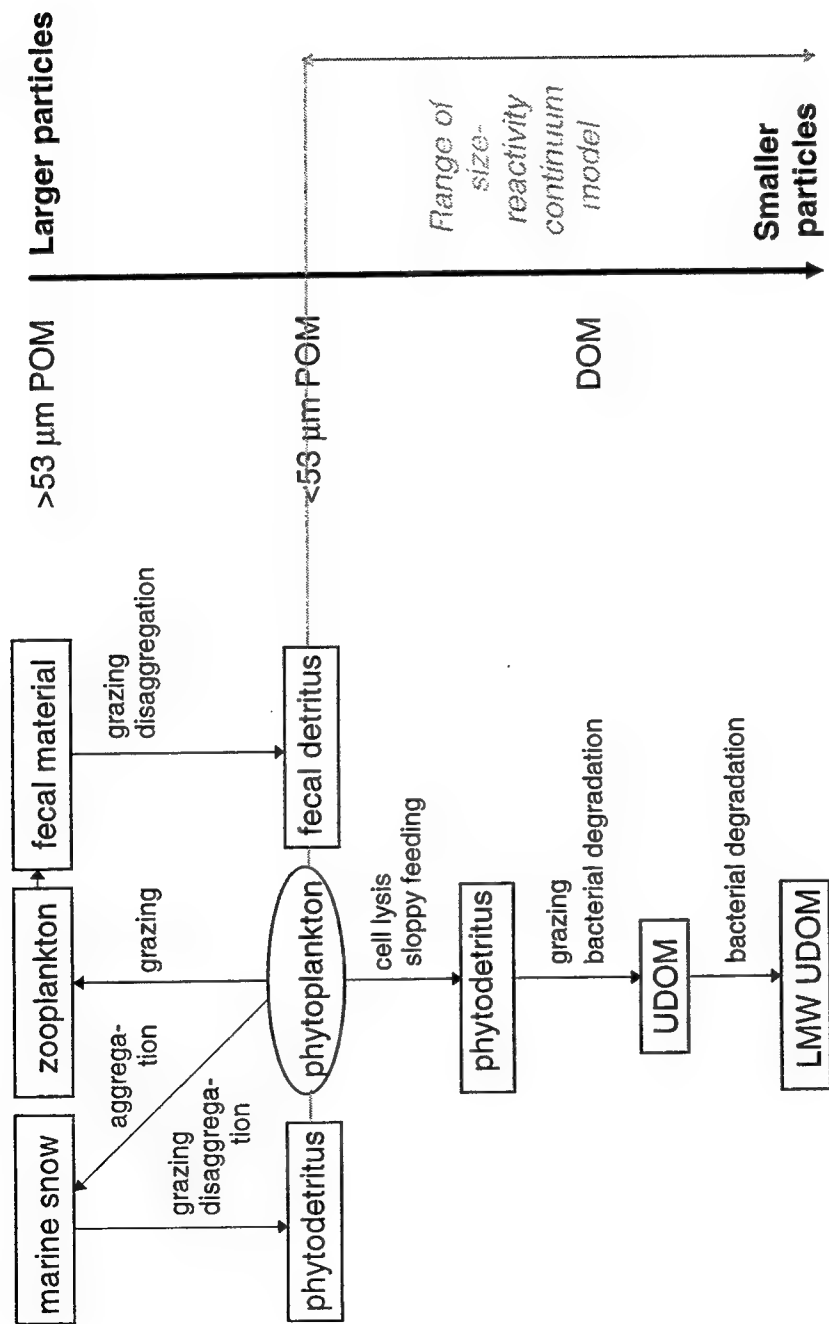


Fig. 7.3. The modified size-reactivity continuum model. See text for discussion. DOM=dissolved organic matter; LMW DOM=low molecular weight DOM; UDOM=ultrafiltered (or colloidal) DOM.

Future work

Organic matter cycling: Unresolved issues from this thesis

This thesis offers preliminary applications of DT-MS, multivariate statistics, and preparative flow cytometry to the subject of organic matter cycling in the surface ocean. As a result each of the main chapters suggests many areas for further research. Some of the more obvious of these will be discussed here.

The nature of the "diglyceride" signal in Chapter 3 was never fully resolved. Preparative flow cytometry, pigment analyses, and measurements of environmental and biological variables (as in Chapter 6) would be necessary in order to determine if the triglyceride and diglyceride variations in suspended POM were due to phytoplankton or zooplankton species variations and/or environmental stresses on the phytoplankton population. In addition, given the strength of the fatty acid signals in the POM samples, the role of phospholipids, which should have been present at significant levels, bears further investigating.

Chapter 4 discusses broad-band molecular-level differences among subclasses of POM collected from the surface waters of the Mid-Atlantic Bight and Great Harbor, Woods Hole. However, both sample sets came from the continental margin of the western North Atlantic. Other oceanographic regimes such as oligotrophic waters, equatorial upwelling regimes, and regions of intense coastal upwelling should also be investigated; they may show different relationships among small-particle POM, large-particle POM, small-particle "phytoplankton" and small-particle "detritus." In addition, the changes in POM subclasses (as determined by flow cytometry and DT-MS) should be explored throughout the water column. Such work would provide a useful complement to sediment trap and filtration studies (see Chapter 1) of variations in POM composition with depth.

The trend in polysaccharide composition with the level of organic matter degradation (Chapter 5) should be further explored with a data set containing a wider range of POM samples. Large-particle and small-particle POM from several oceanographic regimes and from several timepoints in multiple algal degradation experiments should be analyzed as should POM samples from several water column depths. In addition, $\text{NH}_3\text{-Cl}^+$ DT-MS should be applied to additional samples of "phytoplankton" and "detritus" which have been sufficiently desalted so that potential oligosaccharide components can be identified. The "degraded" polysaccharide signal (Klap 1997) appearing in "detritus" should be further characterized by PyGC-MS (if sufficient material can be isolated via flow cytometry) in order to determine if it is analogous to that found by Sicre et al. (1994) in the Rhone delta.

Variability within the small-particle and large-particle POM pools in the Mid-Atlantic Bight (Chapter 6) should be further explored. For comparison with biochemical variations in small-particle POM, it would be useful to have biomass ratios of "phytoplankton" and "detritus" (rather than simply particle counts) from each station. Systematic visual inspection of large-particle POM from the shelf and slope would further constrain the zooplankton biomass contribution to this organic matter pool. In addition, year-round studies of the molecular-level composition of large-particle and small-particle POM on the shelf and slope would indicate the potential level of export of POM and the quality (i.e., biological lability) of the exported POM.

The role of "detritus" in the MAB could be further explored using carbon isotope analyses. The $\delta^{13}\text{C}$ value of "detritus" along the shelf could indicate if its source is primarily terrestrial or marine or changes with location on the shelf. Comparisons of isotope ratios and DT-MS spectra from "detritus" and UDOM could be used in an attempt to constrain the relationship between these two pools of OM.

Further evidence is needed to test the applicability of the theoretical model of organic matter cycling proposed in the previous section of this chapter. The systematic DT-MS analysis of colloidal DOM and various sizes of POM from multiple oceanic

regimes could provide support for this model. In addition it could provide further information on the relative lability of organic compounds in marine environments.

Additional areas for future research

DT-MS used with low voltage electron impact ionization and principal component/discriminant analysis has been shown (Eglinton et al., 1996, this thesis) to be a rapid molecular-level screening technique for marine organic matter samples. It can therefore be used to improve the statistical significance of organic matter characterizations by allowing representative samples to be chosen from large data sets for more time-consuming and more extensive molecular-level analyses. It has also been proposed (Eglinton et al., 1996) that EI^+ DT-MS be used to provide information for molecular-level mapping of POM in ocean waters as marine organic geochemistry falls far behind physical oceanography in the mapping of variables of interest.

In addition to its rapidity, DT-MS is a fairly sensitive technique, requiring only micrograms of sample. This thesis took advantage of DT-MS sensitivity by coupling DT-MS characterization to preparative flow cytometric sorting (Chapters 4, 5, and 6). As sensitivity issues are one of the main limiting factors in the characterization of DOM, DT-MS and other mass spectrometry techniques could provide significant new information on DOM composition (see Boon et al., 1998 for preliminary work in this area), expanding both the number of samples analyzed and the size range of DOM characterized at the molecular level.

While its rapidity and sensitivity allow DT-MS to fill the niche between bulk analyses and detailed molecular-level analyses in chemical oceanography, its semi-quantitative nature remains a major drawback. Much more work needs to be done in order to quantify the relative response factors of compound classes and specific compounds within each class. Understanding how these response factors vary as a result of matrix effects within samples is a difficult but crucial step if DT-MS is to realize its

full potential as an oceanographic tool. However, even in its semi-quantitative state, the ability of DT-MS to provide rapid molecular-level analysis of large sample sets enables chemical oceanographers to move beyond the snapshot approach of understanding POM and DOM composition and to place detailed analyses in an oceanographic context.

As chemical oceanography data sets become larger and provide a more statistically significant view of the world ocean, the need for multivariate analysis techniques such as principal component analysis and discriminant analysis will become more acute. Importing and adapting suitable statistical techniques from other disciplines is a fertile area for further research.

The potential of flow cytometric sorting as a preparative technique has barely been tapped. The use of natural particle characteristics such as autofluorescence, the ratio of forward to right angle light scatter, and polarization of forward angle light scatter can be used to separate specific phytoplankton populations (such as diatoms and coccolithophores) from natural samples (Olson et al., 1989). The C/N ratios and isotopic composition of these phytoplankton could then be analyzed to provide further information on nutrient dynamics. Stable carbon isotope ratios of "phytoplankton" and "detritus" as separated in Chapters 4, 5, and 6 could be used to provide a true marine endpoint for determinations of allochthonous input into coastal ecosystems. "Phytoplankton" $\delta^{13}\text{C}$ values could also be used to examine isotope effects associated with autotrophic carbon fixation, perhaps providing field confirmation for effects proposed from phytoplankton culture experiments (e.g., Laws et al., 1995; Hinga et al., 1994). With the use of appropriate staining protocols the contribution of zooplankton and bacteria to "detritus" could be further explored, and perhaps quantified by elemental analysis.

The coupling of flow cytometry and DT-MS described in this thesis can also be used for the analysis of anthropogenic compounds such as PCBs and PAHs. The influence of such compounds on coastal ecosystems is of considerable interest as they may seriously affect fisheries, shipping (via dredging restrictions), recreation, etc. The partitioning of hydrophobic contaminants between different dissolved and particulate

pools (both living and non-living) will help to further understanding of their cycling and fate in the marine environment.

References:

- Amon R. M. W. and Benner R. (1996) Bacterial utilization of different size classes of dissolved organic matter. *Limnol. Oceanogr.*, **41**(1), 41-51.
- Boon J. J., Klap V., and Eglinton T. (1998) Molecular characterization of microgram amounts of colloidal dissolved organic matter (UDOM) in ocean water samples by direct temperature resolved ammonia chemical ionization mass spectrometry. *Org. Geochem.*, submitted.
- Eglinton T. I., Boon J. J., Minor E. C., and Olson R. J. (1996). Microscale characterization of algal and related particulate organic matter by direct temperature-resolved mass spectrometry. *Mar. Chem.*, **52**, 27-54.
- Hedges J. I., Cowie G. L., Richey J. E., Quay P. D., Benner R., Strom M., and Forsberg B. R. (1994). Origins and processing of organic matter in the Amazon river as indicated by carbohydrates and amino acids. *Limnol. Oceanogr.*, **39**, 743-761.
- Hedges J. I., Clark W. A., and Cowie G. L. (1988). Fluxes and reactivities of organic matter in a coastal marine bay. *Limnol. Oceanogr.*, **33**(5), 1137-1152.
- Hinga K. R., Arthur M. A., Pilson M E. Q., and Whitaker D. (1994). Carbon isotope fractionation by marine phytoplankton in culture: The effects of CO₂ concentration, pH, temperature, and species. *Global Biogeochemical Cycles*, **8**(1), 91-102.
- Laws E.A., Popp B. N., Bidigare R. R., Kennicutt M. C., and Macko S. A. (1995). Dependence of phytoplankton carbon isotopic composition on growth rate and [CO₂]_{aq}: Theoretical considerations and experimental results. *Geochim. Cosmochim. Acta*, **59**(6), 1131-1138.
- Klap V. A. (1997). Biogeochemical aspects of salt marsh exchange processes in the SW Netherlands, Ph.D. Thesis, NIOO/CEMO, 170 p.
- Olson R. J., Zettler E. R., and Anderson O. K. (1989). Discrimination of eukaryotic phytoplankton cell types from light scatter and autofluorescence properties measured by flow cytometry. *Cytometry*, **10**, 636-643.
- Sicre M-A, Peulve S., Saliot A., de Leeuw J. W., and Baas M. (1994). Molecular characterization of the organic fraction of suspended matter in the surface waters and bottom nepheloid layer of the Rhone delta using analytical pyrolysis. *Org. Geochem.* **21**(1), 11-26.

Wakeham S. G. and Canuel E. A. (1988). Organic geochemistry of particulate matter in the eastern tropical North Pacific Ocean: Implications for particle dynamics. *J. Mar. Res.*, **46**, 183-213.

Wakeham S. G., Lee C., and Hedges J. I. (1997). Fluxes of major biochemicals in the equatorial Pacific Ocean. *Biogeochemistry of Marine Organic Matter*, submitted.

Wakeham, S.G., Lee C., Farrington J. W., and Gagosian R. B. (1984). Biogeochemistry of particulate organic matter in the oceans: results from sediment trap experiments. *Deep-Sea Res.*, **31**(5), 509-528.

Appendix 1
Characteristic ions in DT-MS

Table A1.1: Characteristic ions in DT-MS

Compound	characteristic m/z (EI ⁺ , 16eV)	characteristic m/z (NH ₃ -CI ⁺)	pyrolysis or desorption
Sterols ^a	386, 368 (C27:1); 384, 366 (C27:2); 400, 382 (C28:1); 398, 380 (C28:2); 396, 378 (C28:3); 414, 396 (C29:1); 412, 394 (C29:2); 410, 392 (C29:3); 428, 410 (C30:1);		desorption
Fatty acids (free)*	228 (C14:0) ^a 256 (C16:0) ^a 254, 236 (C16:1) ^a 284 (C18:0) ^a 282, 264 (C18:1) ^a 312 (C20:0) ^a 310, 292 (C20:1) ^a 326 (C22:0) ^a	246 274 272 302 300 330 328 344	desorption
Fatty acids (acyl-bound) ^a	211 (C14:0) 239 (C16:0) 265 (C18:0) 293 (C20:0) 321 (C22:0)		pyrolysis
Monoglycerides	302 (C14:0) 330 (C16:0) 358 (C18:0)		desorption
Diglycerides	494 (C14:0+C14:0) ^a 522 (C16:0+C14:0) ^a 550 (C16:0+C16:0) ^a 578 (C16:0+C18:0) ^a 606 (C18:0+C18:0) ^a note: results from a loss of H ₂ O (M-18) in free diglycerides a, b	ammonia adducts of M???	desorption

* There is some indication that bound fatty acids can also yield these ions.

Compound	characteristic m/z (EI+, 16eV)	characteristic m/z (NH ₃ -CI)	pyrolysis or desorption
Triglycerides	722/495 (14/14/14:0) ^a 806/551 (16/16/16:0) ^a 890/607 (18/18/18:0) ^a Note: Loss of water does not always occur in the formation of diglyceride fragments ^b .	740 ^b 824 ^b 908 ^b	desorption/ pyrolysis
Tocopherols ^a	430 (α-tocopherol) 416 (β-tocopherol) 402 (γ-tocopherol)		desorption
Alkylphenols ^c (unknown precursor)	94 (phenol) 108 (methylphenol) 122 (ethylphenol)		pyrolysis
Lignin (guaiacyl) ^d	180, 178, 166, 164, 152, 137, 124		pyrolysis
Lignin (mixed guaiacyl-syringyl) ^d	210, 208, 196, 194, 182, 167, 154		pyrolysis
Polysaccharides (hexoses)	144, 126, 98, 73, 60, 57 ^a	666, 504, 342, 180 (transglycolisation series) ^{e,f,g} 564, 402, 240 (reverse aldolisation series) ^{e,f,g}	pyrolysis
Polysaccharides (pentoses)	114, 85 ^a	474, 342, 282, 210, 150 ^e	pyrolysis
Polysaccharides (deoxyhexoses)	128 ^a	146, 164	pyrolysis
Polysaccharides (aminosugars)	204, 185, 167, 153, 139, 125, 114, 111, 109, 97, 84, 83, 72, 59 ^{h,i}	221, 203, 143, 119, 102, 77 ^j	pyrolysis

Compound	characteristic m/z (EI+, 16eV)	characteristic m/z (NH ₃ -CI)	pyrolysis or desorption
Proteins/peptides ^{k, l}	94/108/120 (tyrosine) 91/92/106 (phenylalanine) 117/131 (tryptophan) 47, 48, 61 (methionine) 125 (alanine dimer) 209/166/124/98/56 (leucine dimer) 195/153/138 (leucine/valine dimer) 180/166/152 (aliphatic amino acid markers)		pyrolysis
Nucleic acids ^a	98, 112 135 (adenine) 126 (cytosine)		pyrolysis
Phytadiene	278 (C20:2) ^a	296 ^g	pyrolysis
Carotene ^a	536 (C40)		desorption
alkenones ^a	530 (C37:2) 528 (C37:3) 544 (C38:2) 542 (C38:3) 558 (C39:2) 556 (C39:3)		desorption
n-alkanes ⁱ	240 (C17) 380 (C27), etc.		desorption
n-alkenes ⁱ	238 (C17:1) 378 (C27:1), etc.		desorption

References:

- ^a Eglinton T. I., Boon J. J., Minor E. C., and Olson R. J. (1996). Microscale characterization of algal and related particulate organic matter by direct temperature-resolved mass spectrometry. *Mar. Chem.*, **52**, 27-54.
- ^b Chapter 3 of this thesis and references therein.
- ^c van Heemst J. D. H., Peulve S., and de Leeuw J. W. (1996). Novel algal polyphenolic biomacromolecules as significant contributors to resistant fractions of marine dissolved and particulate organic matter. *Org. Geochem.*, **24**(6/7): 629-640.
- ^d Saiz-Jiminez C., Boon J. J., Hedges J. I., Hessels J. K. C. and de Leeuw J. W. (1987). Chemical characterization of recent and buried woods by analytical pyrolysis: Comparison of pyrolysis data with ¹³C NMR and wet chemical data. *J. Anal. Appl. Pyr.*, **11**, 437-450.
- ^e Lomax J. A., Boon J. J., and Hoffmann R. A. (1991) Characterisation of polysaccharides by in-source pyrolysis positive- and negative-ion direct chemical ionisation-mass spectrometry. *Carbohydrate Research*, **221**, 219-233.
- ^f Arisz P. W. and Boon J. J. (1995). Pyrolysis chemical ionization mass spectrometry of cellulose ethers. *J. of Polymer Science: Part A: Polymer Chemistry*, **33**, 2855-2864.
- ^g Klap V. A. (1997). Biogeochemical aspects of salt marsh exchange processes in the SW Netherlands, Ph.D. Thesis, NIOO/CEMO, 170 p.
- ^h Minor E. C. (1998), unpublished.
- ⁱ Stankiewicz B. A., van Bergen P. F., Duncan I. J., Carter J. F., Briggs D. E. G., and Evershed R. P. (1996). Recognition of chitin and proteins in invertebrate cuticles using analytical pyrolysis/gas chromatography and pyrolysis/gas chromatography/mass spectrometry. *Rapid Communications in Mass Spectrometry*, **10**, 1747-2757.
- ^j Boon J. J., Klap V., and Eglinton T. (1998) Molecular characterization of microgram amounts of colloidal dissolved organic matter (UDOM) in ocean water samples by direct temperature resolved ammonia chemical ionization mass spectrometry. *Org. Geochem.*, submitted.
- ^k Boon J. J. and de Leeuw J. W. (1987). Amino acid sequence information in proteins and complex proteinaceous material revealed by pyrolysis-capillary gas

chromatography-low and high resolution mass spectrometry. *J. Anal. and Appl. Pyr.*, **11**, 313-327.

¹Meuzelaar H. L. C., Haverkamp J., and Hileman F. D. (1982). *Pyrolysis Mass Spectrometry of Recent and Fossil Biomaterials: Compendium and Atlas*. Elsevier Press, New York, 293 pp.

Appendix 2

GC-MS of selected samples

To help confirm DT-MS (16 eV, EI⁺) identifications of lipids in POM samples, selected samples were extracted and analyzed via GC-MS. The samples analyzed were: ISO, an *Isochrysis galbana* culture sample from Bob Nelson; 7B, a suspended POM sample (>0.8 μm , <53 μm) collected from the continental shelf just off the mouth of the Delaware Bay; WHTS 5, a suspended POM sample (>0.8 μm , <53 μm) from Great Harbor, Woods Hole; and PMP 141, a >3.0 μm POM sample collected from a depth of 6 m in the Peruvian upwelling region.

Extraction procedure

The samples were removed from liquid nitrogen storage dewars and allowed to thaw. They were then brought to roughly equal volume by addition of Milli-Q water and centrifuged at ~1800xG for 20 min (using an IEC HN-SII centrifuge with a swinging bucket rotor). The supernatant from each sample was transferred to a separatory funnel. The samples were then sequentially extracted with equal volumes of methanol, methanol:dichloromethane (1:1), methanol:dichloromethane (1:4) and hexane:dichloromethane (1:4). The extraction procedure was as follows: solvent was added to each sample; the sample was sonicated for twenty minutes and then centrifuged as above; the supernatant was transferred to the appropriate separatory funnel (mentioned above). The samples were back extracted and the organic fractions were dried overnight with Na₂SO₄.

After syringe-filtering to remove the Na₂SO₄, the samples were brought to equal volumes and heneicosanoic acid was added as an internal standard. The samples were transesterified overnight at ~70°C in MeOH:HCl (95:5) under a helium headspace. They were then back-extracted with hexane and dried under N₂. A fatty alcohol standard (1-

Table A2.1. Compounds identified in GC-MS analysis of WHTS#5

letter code (Fig. 1)	compound	characteristic m/z values
a	tetradecanoic acid ME	242, 199, 143
b	hexadecenoic acid ME	268, 236, 194, 152, 123
c	hexadecanoic acid ME	270, 227, 143
d	alkane	
e	alkane	
f	???	
g	octadecenoic acid ME	296, 264, 222, 180
h	octadecanoic acid ME	298, 255, 143
i	???	327
j	alkane	
k	nonadecanoic acid ME	312, 269
l	C _{20:5} fatty acid ME	
m	octadecanoic acid TMS	341
n	1-nonadecanoic acid TMS*	341
o	heneicosanoic acid ME*	340, 297
p	cholesterol TMS	458, 368, 329

*internal standard

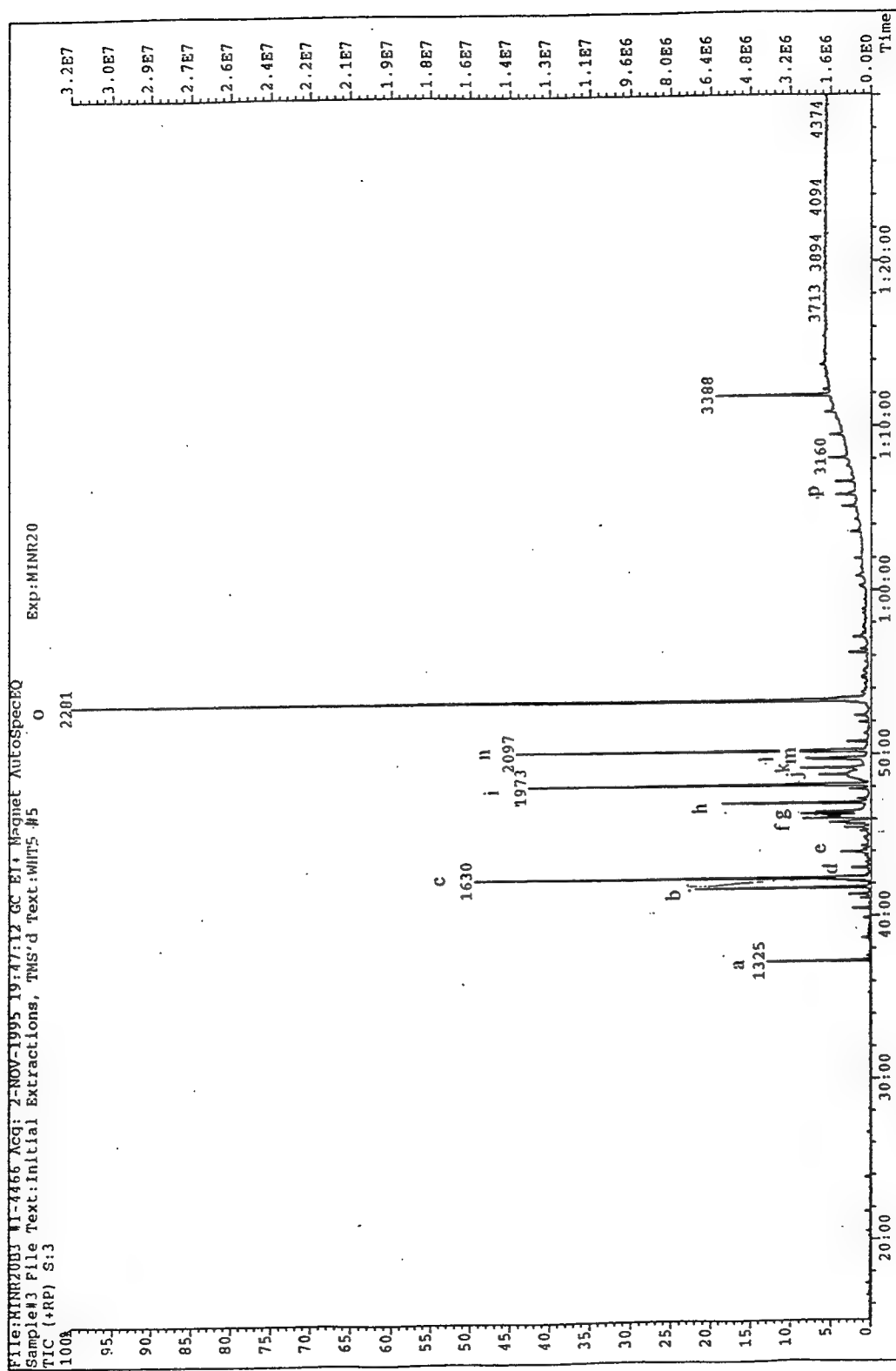


Fig. A2.1. GC-MS of WHTS#5. See Table 1 for peak identifications.

nonadecanol) was added and the samples were derivatized (at 60°C for 15 min.) with BSTFA (bis(trimethylsilyl)trifluoroacetamide) and ethyl acetate.

The samples were then analyzed by GC and GC-MS. As we were interested mainly in compound identification rather than quantification, only GC-MS will be discussed here. GC-MS was performed with a DB-5 column on an HP 5890A, Series II gas chromatograph attached to a VG AutospecQ mass spectrometer. GC conditions were as follows: 5 min. hold at injection temperature (55°C), temperature ramp 4°/min, 20 min. hold at the final temperature (320°C).

Results

The total ion chromatogram from analysis of WHTS5 is shown in Fig.1 (peak identifications are in Table 1). The main fatty acids in the sample (analyzed as fatty acid methyl esters) are C_{14:0}, C_{16:1}, and C_{16:0}, and C_{18:0}. The only detectable sterol (analyzed as the TMS ether) is cholesterol.

The main fatty acids in ISO (data not shown) were C_{14:0}, C_{16:0}, and C_{18:0}. The major sterol was C_{28:2}, and there was a strong C_{18:0} fatty alcohol peak as well.

In PMP 141 (data not shown) the only identifiable sterol was cholesterol. The main fatty acids were C_{14:0}, C_{16:1}, C_{16:0}, C_{18:0}, and C_{18:1}.

There were no distinguishable sterols in 7B (data not shown). The main fatty acids were C_{14:0}, C_{16:1}, C_{16:0}, and C_{18:0}. The main fatty alcohol was C_{18:0}.

Appendix 3

Ancillary data and EI⁺ DT-MS spectra from the MAB and WHTS data sets

For both the MAB stations (see Chapters 4 and 6) and the WHTS samplings (Chapter 4), a great deal of ancillary data was obtained. As this data does not always figure prominently within the thesis chapters, it is included here in Tables 1-3. A DT-MS (EI⁺, 16 eV) spectrum for each POM sample (large-particle, small-particle, "phytoplankton" and "detritus") in the MAB and WHTS data sets is also included in this appendix. For the interested reader, these spectra (catalogued in Table 4) should prove a useful complement to the average spectra and difference spectra resulting from principal component analysis or discriminant analysis of the DT-MS data (Chapters 4 and 6).

Experimental

For the MAB stations, salinity and temperature were obtained via shipboard SAIL system. For the WHTS samples, salinity was obtained by salinometer and temperature by using a bucket and a laboratory thermometer.

Particulate organic carbon (POC) samples in both data sets were obtained by filtering seawater through GF/F filters using a stainless steel pressure cannister and nitrogen gas (<5 psi). The filters were stored frozen. Just prior to analysis they were thawed, placed over fuming HCl for 24 to 48 hours and dried overnight in an oven at approximately 60°C (Hedges and Stern, 1983). They were weighed and sectioned; and aliquots were then analyzed on a Fisons EA 1108 Elemental Analyzer in order to determine POC concentrations and C/N ratios.

Pigment samples were collected onto GF/F filters in the same manner as the POC samples. The filters were stored in liquid nitrogen. Just prior to analysis via HPLC, the samples were thawed and extracted in acetone. The extracts were then analyzed using a Waters 600E HPLC system and either a C-8 reverse phase column or a C-18 column.

Peaks were detected using a photodiode array detector (see Chapter 5 for chromatography parameters).

The ratio of “phytoplankton” counts to total “phytoplankton” + “detritus” counts was determined for both unfiltered seawater samples and filtered $>2.0\ \mu\text{m}$ POM samples (see Chapters 4 and 6) that were stored in liquid nitrogen until flow cytometric analysis. Flow cytometry (see Chapter 4 for details) was performed on an EPICS V flow cytometer (Coulter, Inc.) using a Cicero data acquisition system (Cytomation, Inc.).

For the MAB data set, nutrient data was provided by R. Wilke (Brookhaven National Laboratory).

DT-MS was performed on a VG Autospec Q magnetic sector mass spectrometer (see Chapter 4 for details).

Table A3.1. MAB ancillary data

station #	lat. (deg. min N)	long. (deg. min. W)	salinity (psu)	temp. (°C)	POC conc. (µg/L)	(C/N) atomic	chl <i>a</i> conc. (µg/L)	POC/ chl <i>a</i>	>2 µm P/(P+D) counts/ counts	USW P/(P+D) counts/ counts	PO ₄ conc. (µM)	NO ₃ conc. (µM)
1	40 56	70 20	32.53	2.7	170	3.8	13	13			0.243	0.088
2	40 51	72 19	32.59	3.2	210	4.7	4.5	46	0.271	0.0313	0.558	2.214
3	40 08	71 56	32.92	4.9	110	4.3	8.3	13	0.464	0.310	0.493	5.258
4	39 38	71 35	34.06	8.0			4.0		0.434	0.488	0.438	5.698
5	39 30	73 58	32.27	3.0	670	8.9	13	51	0.282	0.125	0.167	0.060
6	38 00	74 58	32.45	4.5	240	6.5			0.358	0.169	0.051	0.065
7	37 50	74 34	32.76	6.8	90	3.4	12	7.4				
8	37 35	73 57	35.25	9.7	140	5.1	2.8	50			0.341	5.113
9	36 42	74 35	33.24	9.2	80	4.1	2.0	40	0.348	0.283	0.225	1.776

Note: P/(P+D) is the ratio of phytoplankton counts to phytoplankton plus detritus counts as determined by flow cytometry for unfiltered seawater (USW) and >2 µm POM samples.

Table A3.2. WHTS Ancillary data

sample	sampling date	sal. (psu)	water temp. (°C)	POC (µg/L)	(C/N) atomic	chl <i>a</i> conc (µg/L)	POC/ chl <i>a</i>	>2 µm p/(p+d) counts/counts	USW: p/(p+d) counts/counts
whts1	11/15/94	32.26	12.3	250	4.7	0.94**	270	0.184	
whts2	12/13/94	31.96	6.5	170	4.2				
whts5	10/17/95	31.90	17	220	5.9	3.0	73	0.286	0.11
whts6	11/16/95	29.63	9	227	5.8			0.405	0.0772
whts7	12/15/95	31.61	2.3	122	3.0			0.364	0.0396
whts8	1/16/96	31.36	1	190	4.3	2.4	81		
whts9	2/12/96	31.00	2	200	6.0	2.0	100	0.353	0.062
whts10	3/22/96	31.02	4			0.85			
whts11	4/19/96	30.99	8	165	5.5	1.25	130	0.782	0.107
whts12	5/24/96	30.92	16.5	160	3.8	2.1	77	0.452	0.191
whts13	6/21/96	31.14	17	191	3.6	2.2	86	0.485	0.107
whts14	7/22/96	31.22	21.5	257	5.1	3.9	65	0.363	
whts15	8/20/96	31.14	22	150	4.9	2.5	59	0.427	0.151
whts16	9/20/96	29.53	19.5	230	5.7			0.706	
whts17	10/18/96	30.58	16	150	5.0			0.401	0.0751
whts18	11/18/96	30.18	9	116	4.5			0.384	0.0925
whts19	2/27/97	30.49	6	85	6.2				

**different HPLC column, some possibility of internal standard mix-up.

Table A3.3. Pigment results from HPLC analysis of WHTS and MAB samples.

sample	chl <i>c</i>	fuco-xanthin	19'-hexanoyl-oxy-fucoxanthin*	diadinoxanthin	diatoxanthin*	alloxanthin*	zeaxanthin*	chl <i>b</i>	chl <i>a</i> + allomer of chl <i>a</i>	α,β -carotene
whts1 [#]	0.45	0.43				0.16		0.17	0.94	
whts5		1.8							3.0	
whts8		2.7		0.88					2.4	
whts9		1.5		0.63					2.0	
whts10		0.85							0.85	
whts11		1.7		0.52					1.3	
whts12		1.5		0.59	0.42				2.07	0.68
whts13		1.7			0.89			0.55	2.21	0.47
whts14	0.97	3.3		1.9	0.98		0.42	0.57	3.9	0.88
whts15	0.57	0.76		0.70	0.38		0.17	0.44	2.53	0.50
st 1	8.8	12.2		2.5	1.2				13.97	0.80
st 2		5.5		1.6					4.5	
st 3	3.9	9.5		1.6					8.82	0.46
st 4	0.52	1.9		1.2		1.2			4.0	
st 5	5.3	11.8		3.3					15.4	
st 7	2.6	10.9		3.4					12.9	0.83
st 8	2.8	1.2	1.1						2.8	
st 9		1.7	0.28	0.47		1.0			2.0	

Units: $\mu\text{g/L}$ seawater

* tentative identification as there was not enough material to yield a good spectrum.

[#]run on a C-18 column

DT-MS (16 eV, EI⁺) spectra

Table A3.4a. List of EI⁺ DT-MS spectra (MAB data set) included in Appendix 3

Cruise sample name	Station # (used in thesis chapters)	Particle type	Mass spectrometry file name
030104 Left Sort	1	"phytoplankton"	MINR29F13
030104 Right Sort	1	"detritus"	MINR29F14
030104 Desalted	1	>2.0 µm	MINR29F9
030302 Left Sort	2	"phytoplankton"	MINR29E8
030302 Right Sort	2	"detritus"	MINR29E7
030302 Desalted	2	>2.0 µm	MINR29E13
030404 Left Sort	3	"phytoplankton"	MINR29F7
030404 Right Sort	3	"detritus"	MINR29F5
030404 Desalted	3	>2.0 µm	MINR29K15
030410 Left Sort	4	"phytoplankton"	MINR29K10
030410 Right Sort	4	"detritus"	MINR29K4
030410 Desalted	4	>2.0 µm	MINR29K7
030502 Left Sort	5	"phytoplankton"	MINR29H9
030502 Right Sort	5	"detritus"	MINR29H7
030502 Desalted	5	>2.0 µm	MINR29H11
030610 Left Sort	6	"phytoplankton"	MINR29H15
030610 Right Sort	6	"detritus"	MINR29H17
030610 Desalted	6	>2.0 µm	MINR29H24
030705 Left Sort	7	"phytoplankton"	MINR29J4
030705 Right Sort	7	"detritus"	MINR29J11
030705 Desalted	7	>2.0 µm	MINR29J9
030714 Left Sort	8	"phytoplankton"	MINR29H25
030714 Right Sort	8	"detritus"	MINR29H32
030714 Desalted	8	>2.0 µm	MINR29H30
030802 Left Sort	9	"phytoplankton"	MINR29J16
030802 Right Sort	9	"detritus"	MINR29J14
030802 Desalted	9	>2.0 µm	MINR29J18
030104 gt53um	1	>53 µm	MINR29K20
030302 gt53um	2	>53 µm	MINR29K21
030410 gt53um	4	>53 µm	MINR29K16
030502 gt53um	5	>53 µm	MINR29E15
030610 gt53um	6	>53 µm	MINR29E18
030705 gt53um	7	>53 µm	MINR29E28
030714 gt53um	8	>53 µm	MINR29F21
030802 gt53um	9	>53 µm	MINR29E19

Table A3.4b. List of EI⁺ DT-MS spectra (WHTS data set) included in Appendix 3

WHTS #	Date sampled	Particle type	Mass spectrometry file name
1 gt 0.8	11/15/94	>0.8 μm	MINR31G38
2 gt 0.8	12/13/94	>0.8 μm	MINR31G21
5 gt 0.8	10/17/95	>0.8 μm	MINR31H31
6 gt 0.8	11/16/95	>0.8 μm	MINR31J30
7 gt 0.8	12/15/95	>0.8 μm	MINR31G13
8 gt 0.8	1/16/96	>0.8 μm	MINR31G15
9 gt 0.8	2/12/96	>0.8 μm	MINR31G14
10 gt 0.8	3/22/96	>0.8 μm	MINR31H36
11 gt 0.8	4/19/96	>0.8 μm	MINR31H29
12 gt 0.8	5/24/96	>0.8 μm	MINR31G12
13 gt 0.8	6/21/96	>0.8 μm	MINR31H6
14 gt 0.8	7/22/96	>0.8 μm	MINR31H30
15 gt 0.8	8/20/96	>0.8 μm	MINR31K22
16 gt 0.8	9/20/96	>0.8 μm	MINR31K17
17 gt 0.8	10/18/96	>0.8 μm	MINR31J25
18 gt 0.8	11/18/96	>0.8 μm	MINR31G23
19 gt 0.8	2/27/97	>0.8 μm	MINR31G24
1a gt53	11/15/94	>53 μm	MINR31J27
2 gt53	12/13/94	>53 μm	MINR31K24
5 gt53	10/17/95	>53 μm	MINR31G35
6 gt53	11/16/95	>53 μm	MINR31J23
8 gt53	1/16/96	>53 μm	MINR31K25 ¹
9 gt 53	2/12/96	>53 μm	MINR31K27
10 gt53	3/22/96	>53 μm	MINR31J22 ²
11 gt53	4/19/96	>53 μm	MINR31J29 ³
12 gt53	5/24/96	>53 μm	MINR31H13 ¹
13 gt53	6/21/96	>53 μm	MINR31K21 ⁴
14 gt53	7/22/96	>53 μm	MINR31G28
15 gt53	8/20/96	>53 μm	MINR31H25 ³
16 gt53	9/20/96	>53 μm	MINR31G25
17 gt53	10/18/96	>53 μm	MINR31H14 ³
18 gt53	11/18/96	>53 μm	MINR31H12 ¹
19 gt 53	2/27/97	>53 μm	MINR31G42
2 Left	12/13/94	"phytoplankton"	MINR30L16
2 Right	12/13/94	"detritus"	MINR30L17
2 gt2um	12/13/94	>2.0 μm	MINR30L15

Table A3.4b (cont'd)

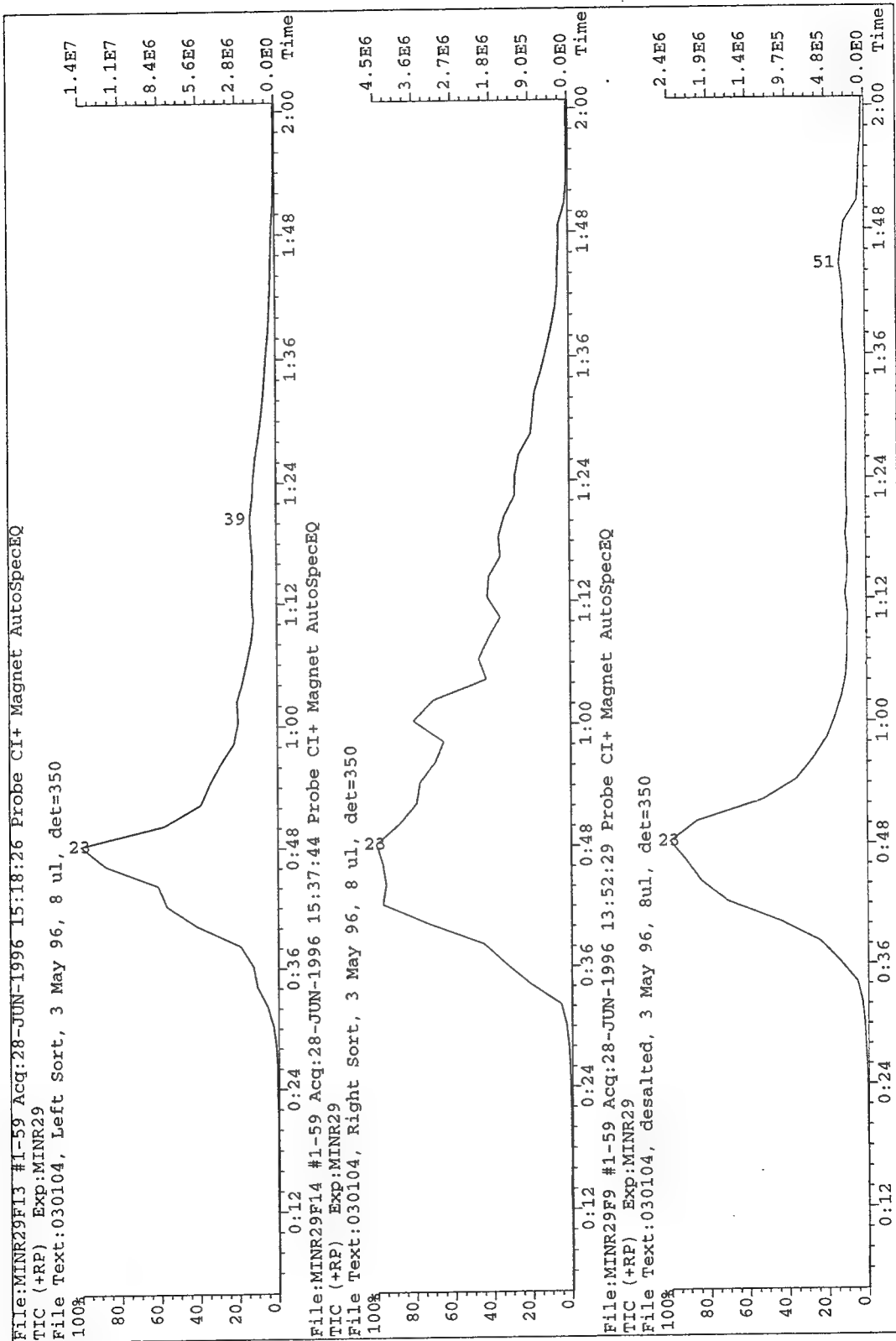
WHTS #	Date sampled	Particle type	Mass spectrometry file name
5 Left	10/17/95	"phytoplankton"	MINR30M11
5 Right	10/17/95	"detritus"	MINR30M6
5 gt2um	10/17/95	>2.0 μm	MINR30M15
9 L	2/12/96	"phytoplankton"	MINR30H9
9 R	2/12/96	"detritus"	MINR30H6
9 gt2um	2/12/96	>2.0 μm	MINR30H10
11 L2	4/19/96	"phytoplankton"	MINR30K15
11 Right	4/19/96	"detritus"	MINR30K12
11 gt2um	4/19/96	>2.0 μm	MINR30K16
12 L	5/24/96	"phytoplankton"	MINR30H12
12 R	5/24/96	"detritus"	MINR30H24
12 gt2um	5/24/96	>2.0 μm	MINR30H26
13 Left	6/21/96	"phytoplankton"	MINR30N21
13 Right	6/21/96	"detritus"	MINR30N22
13 gt2um	6/21/96	>2.0 μm	MINR30N23
14 L	7/22/96	"phytoplankton"	MINR30G12
14 R	7/22/96	"detritus"	MINR30G23
14 gt2um	7/22/96	>2.0 μm	MINR30G28
15 Left	8/20/96	"phytoplankton"	MINR30N13
15 Right	8/20/96	"detritus"	MINR30N14
15 gt2um	8/20/96	>2.0 μm	MINR30N15
18 Left	11/18/96	"phytoplankton"	MINR30N17
18 Right	11/18/96	"detritus"	MINR30N18
18 gt2um	11/18/96	>2.0 μm	MINR30N9

¹m/z 100 overloaded

²m/z 60, 100 overloaded

³m/z 81, 100 overloaded

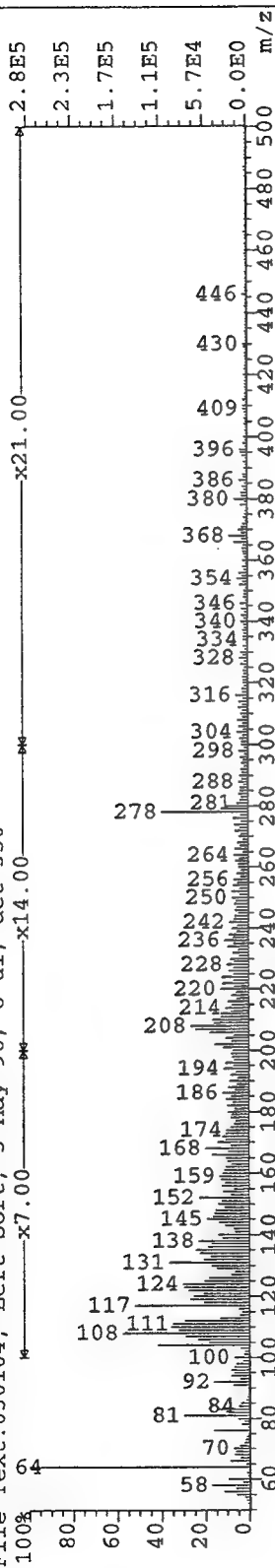
⁴m/z 44, 81, 100 overloaded



File:MINR29F13 Ident:1_59 Int Def 0.70 Acq:28-JUN-1996 15:18:26 +1:02 Cal:MINR29A2

AutoSpecEQ CI+ Magnet BpM:64 BpI:284799 TIC:1926377 Flags:HALI

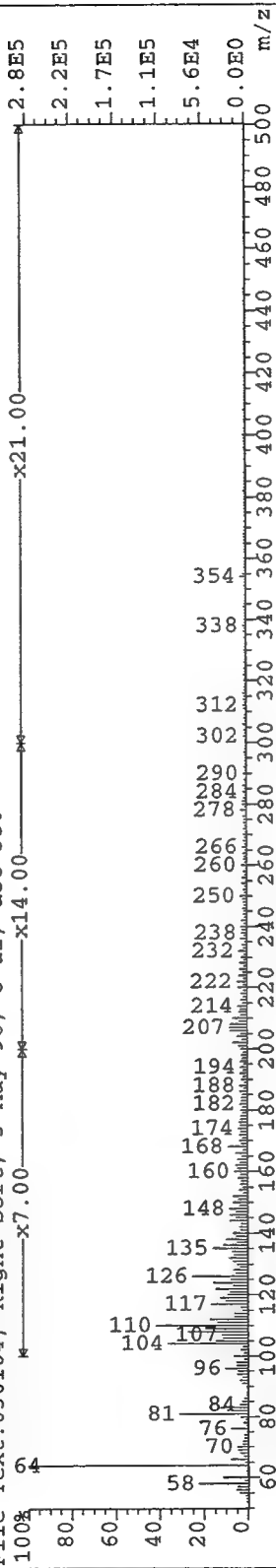
File Text:030104, Left Sort, 3 May 96, 8 ul, det=350



File:MINR29F14 Ident:1_59 Int Def 0.70 Acq:28-JUN-1996 15:37:44 +1:02 Cal:MINR29A2

AutoSpecEQ CI+ Magnet BpM:64 BpI:280990 TIC:1259525 Flags:HALI

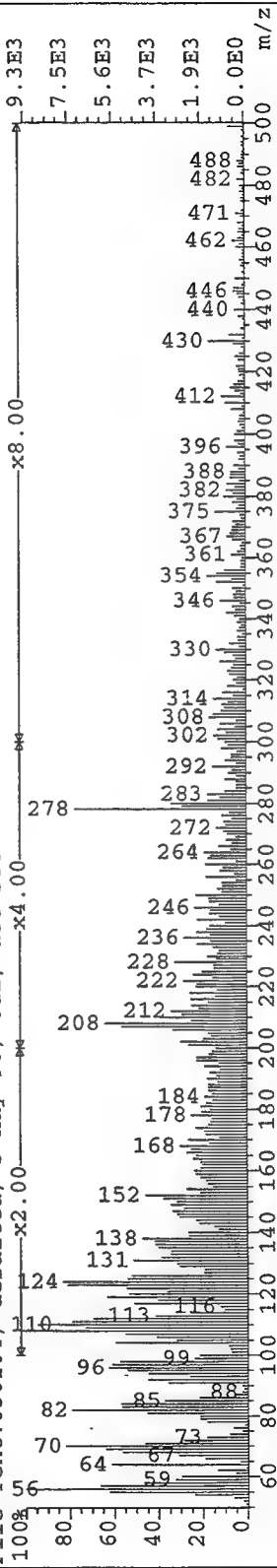
File Text:030104, Right Sort, 3 May 96, 8 ul, det=350

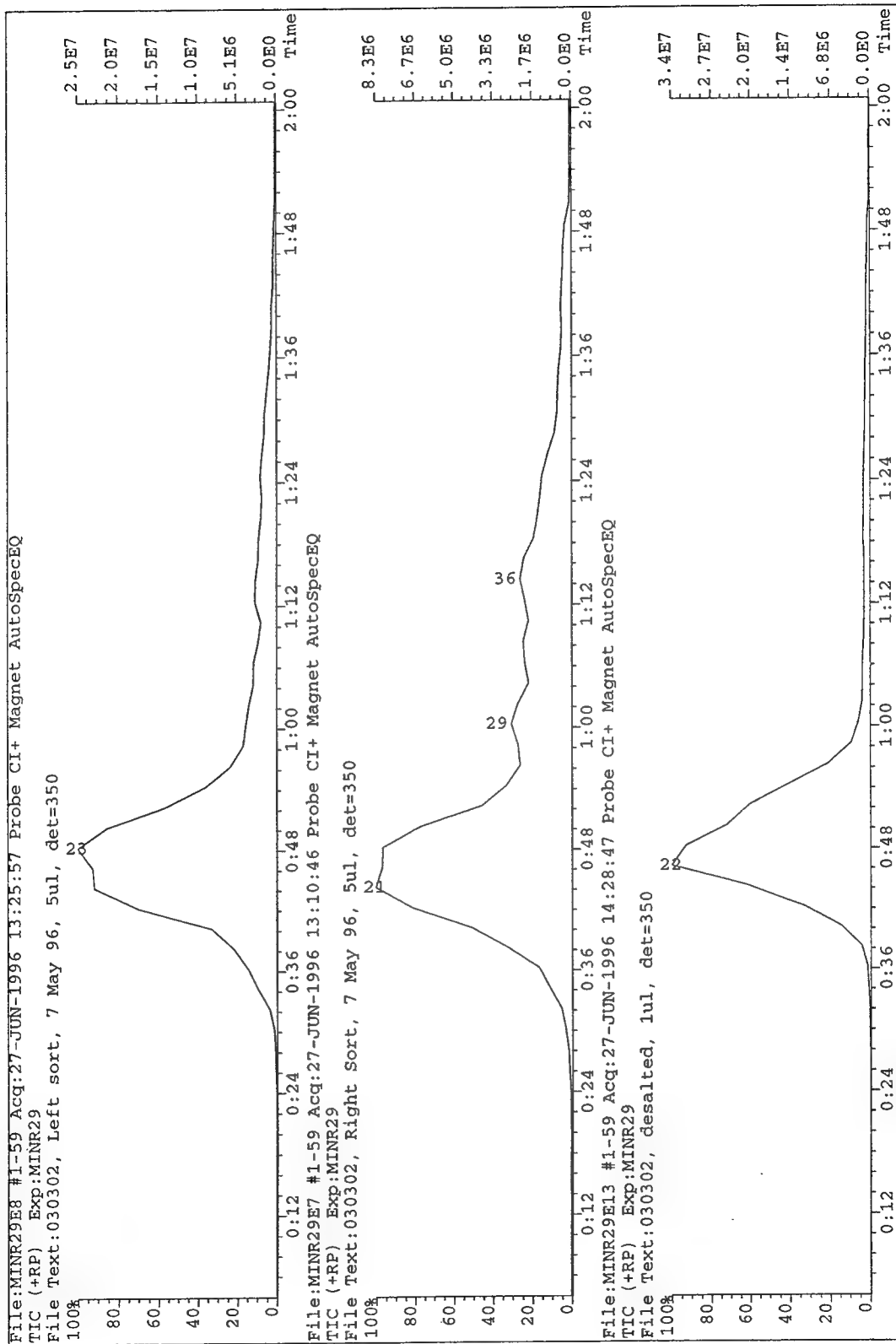


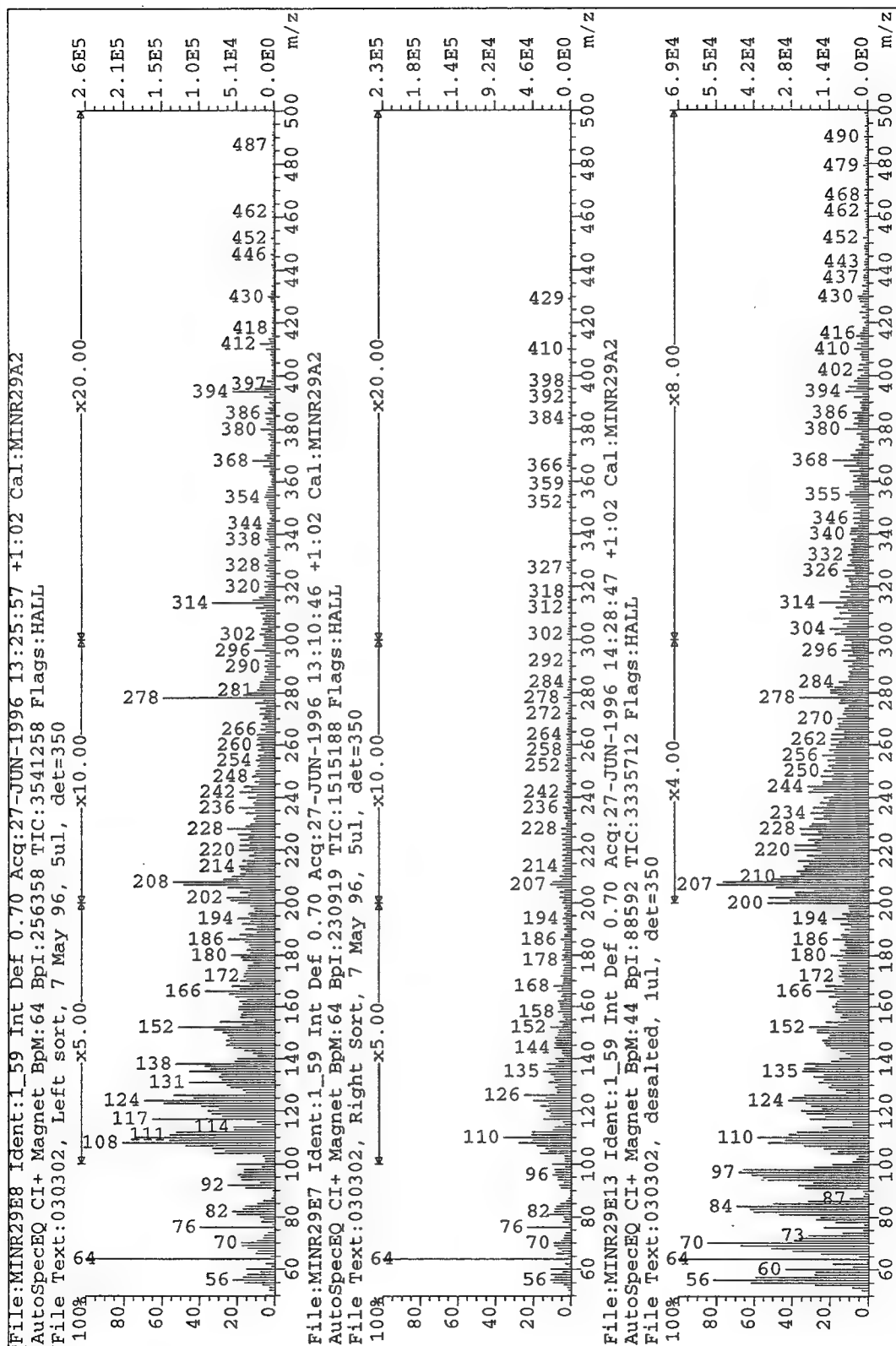
File:MINR29F9 Ident:1_59 Int Def 0.70 Acq:28-JUN-1996 13:52:29 +1:02 Cal:MINR29A2

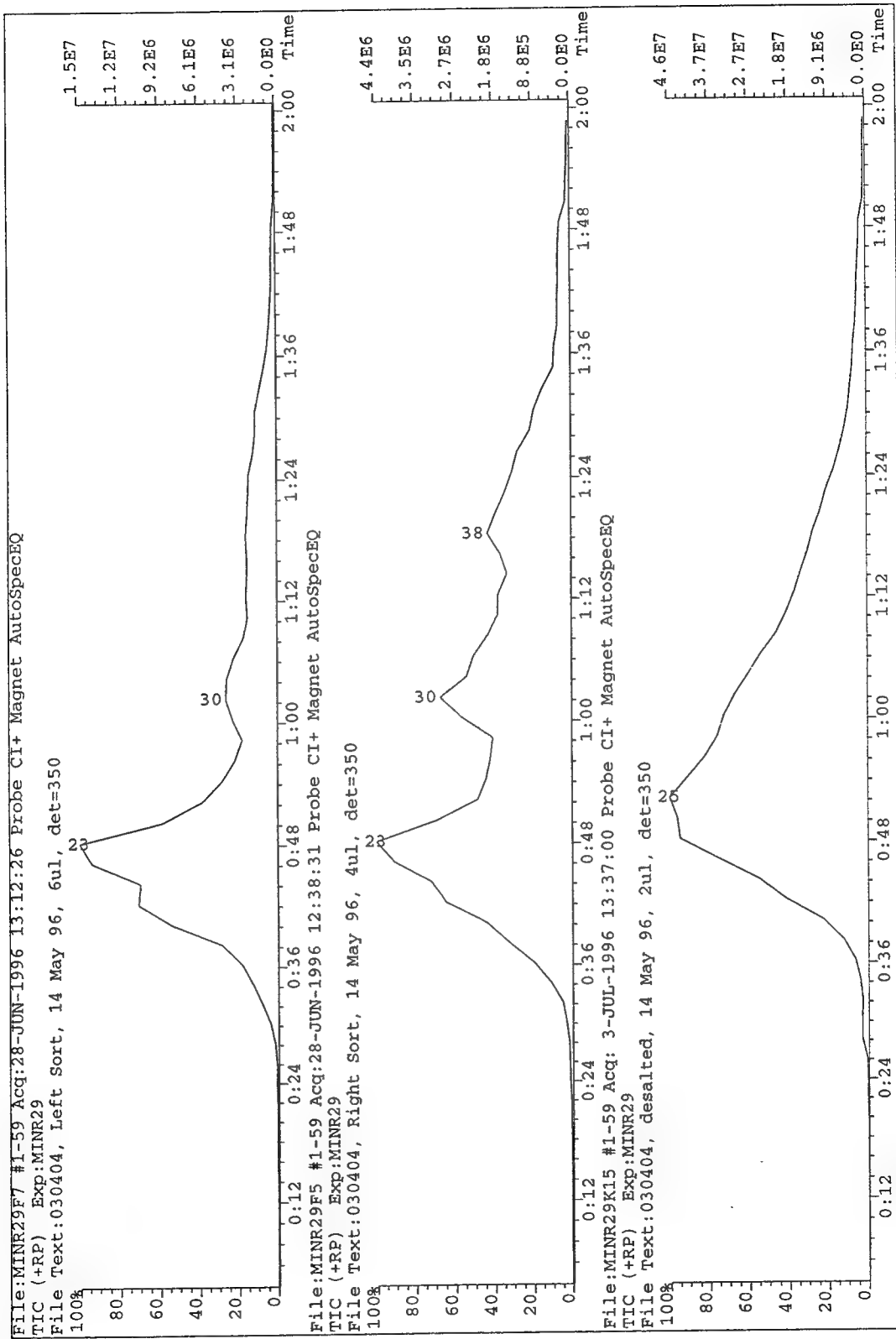
AutoSpecEQ CI+ Magnet BpM:44 BpI:21585 TIC:382863 Flags:HALI

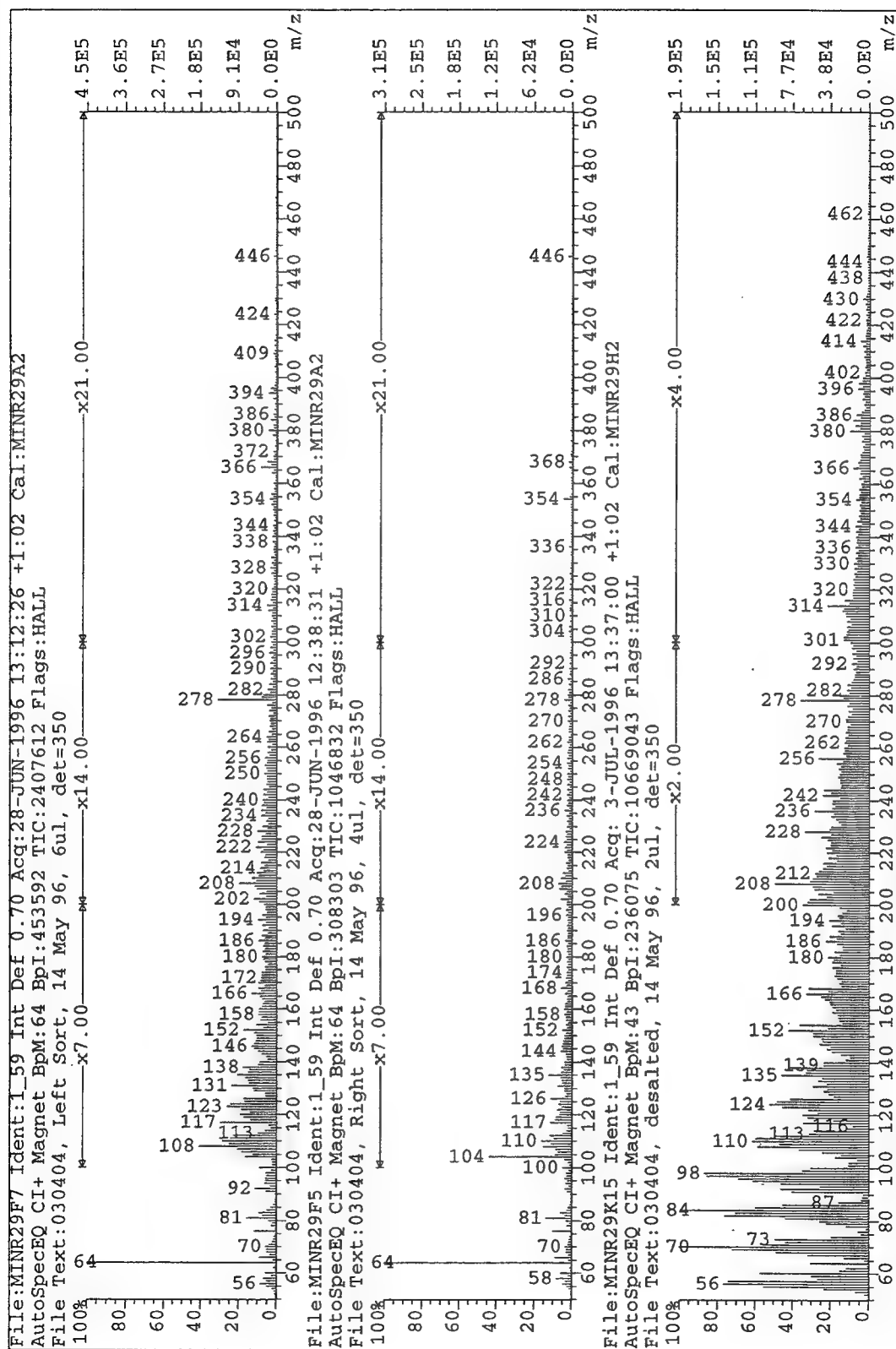
File Text:030104, desalted, 3 May 96, 8ul, det=350

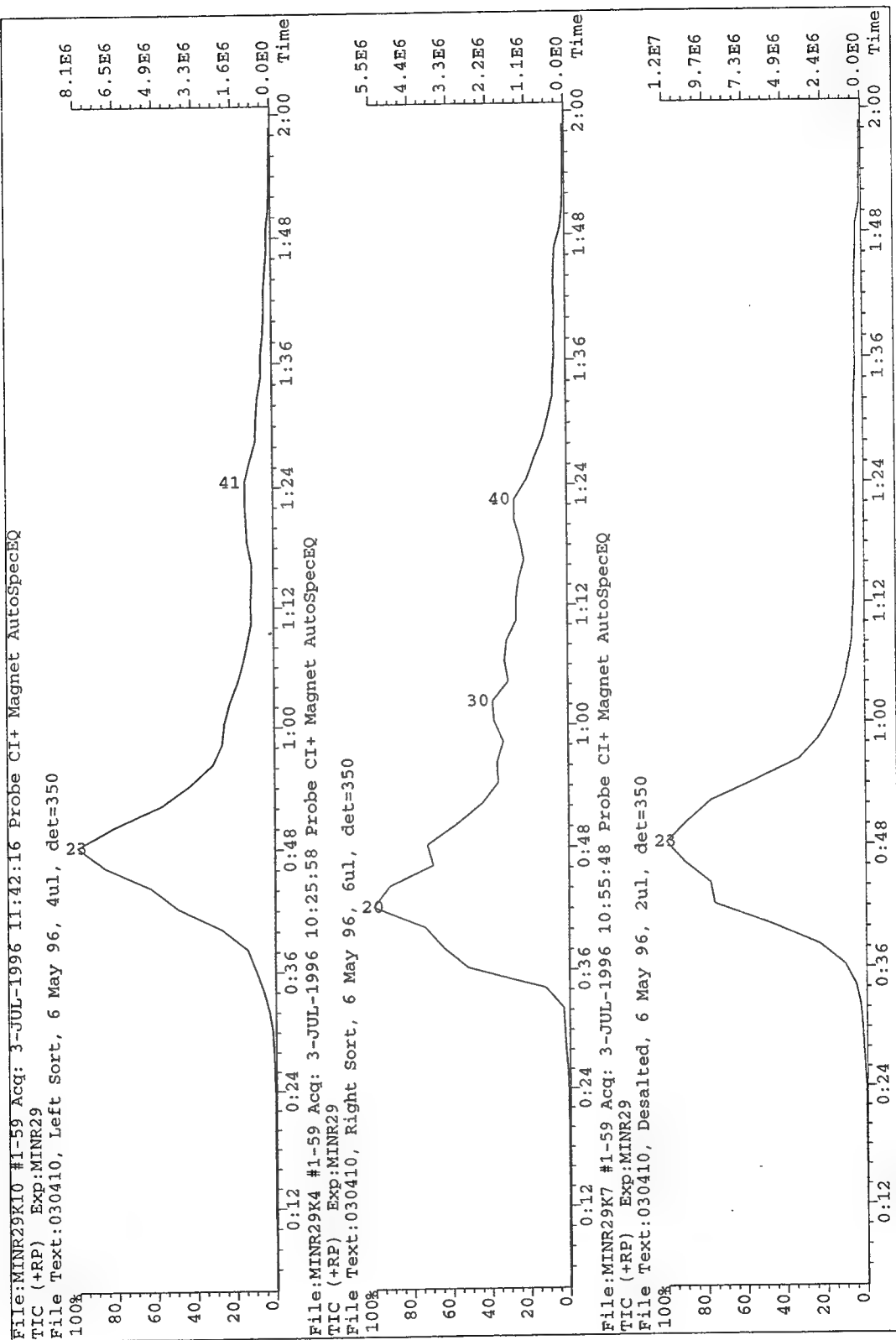


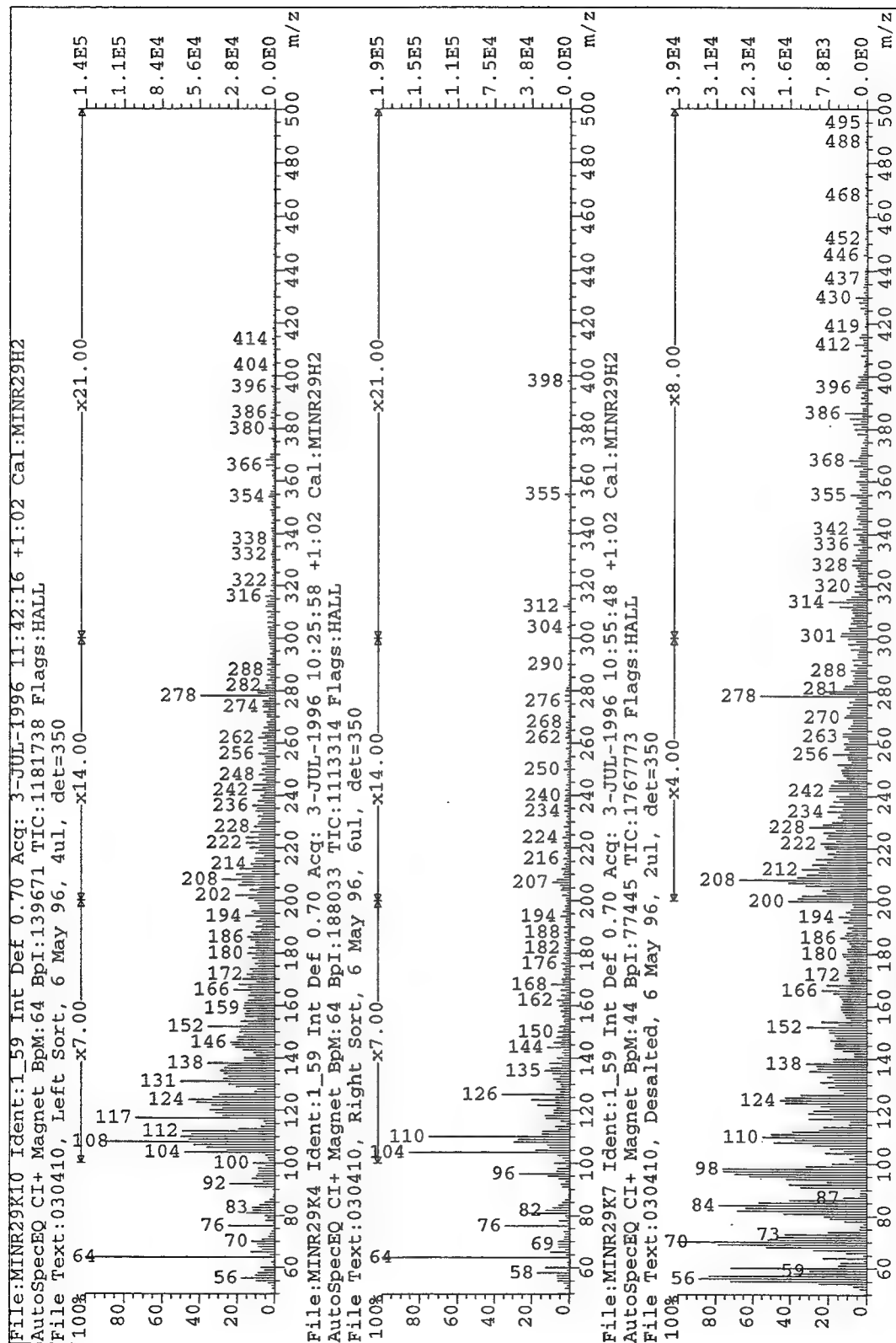


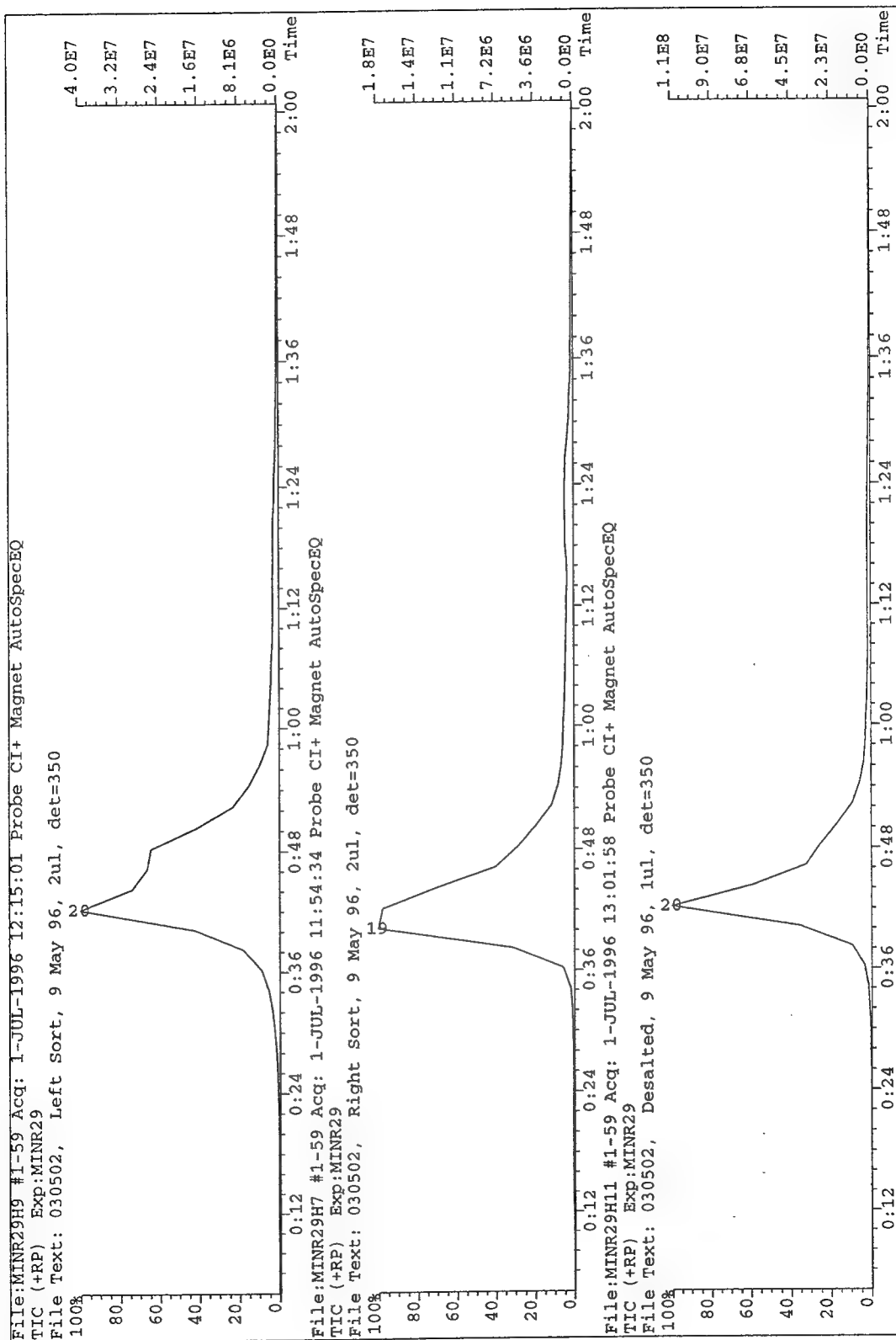


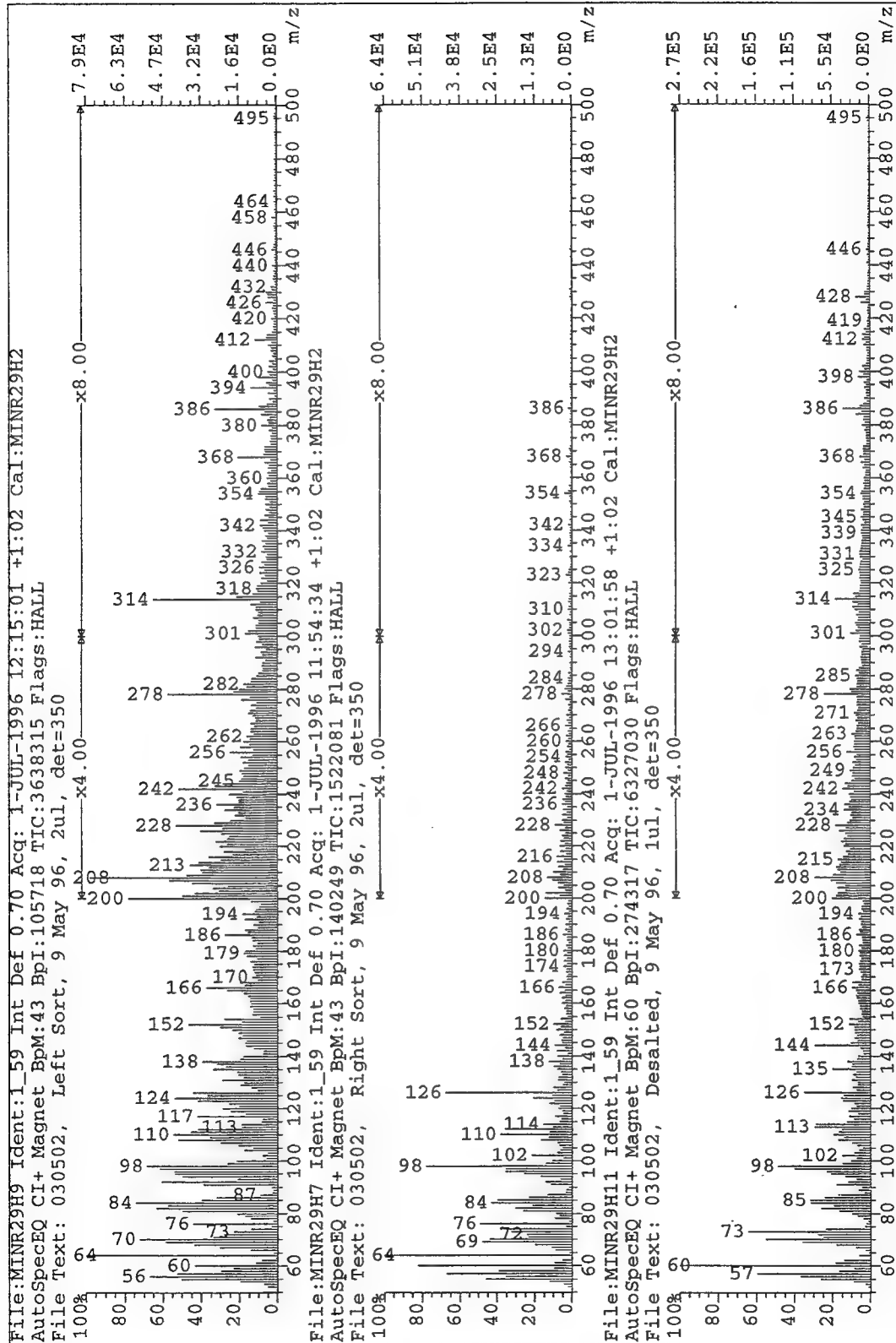


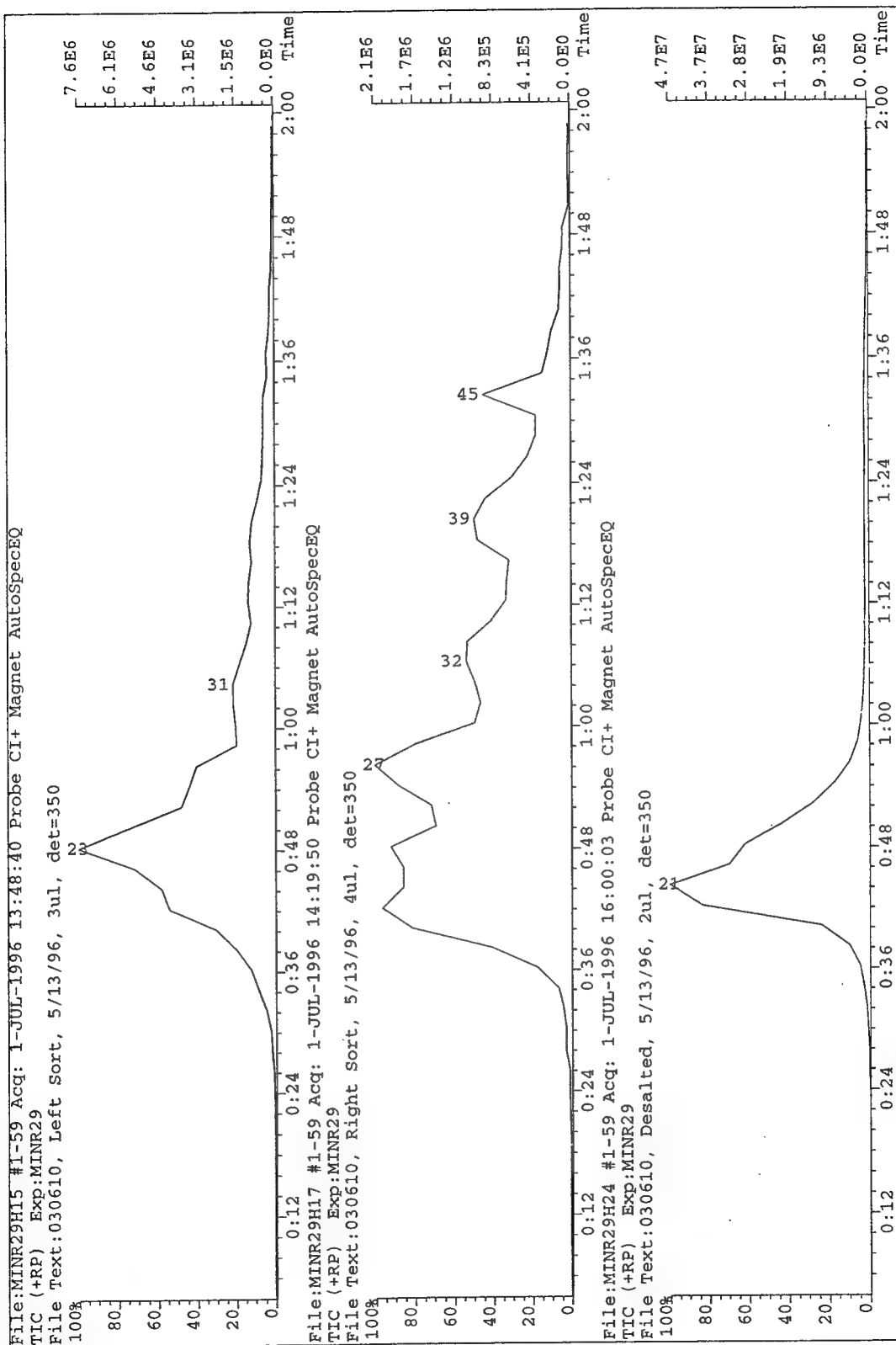








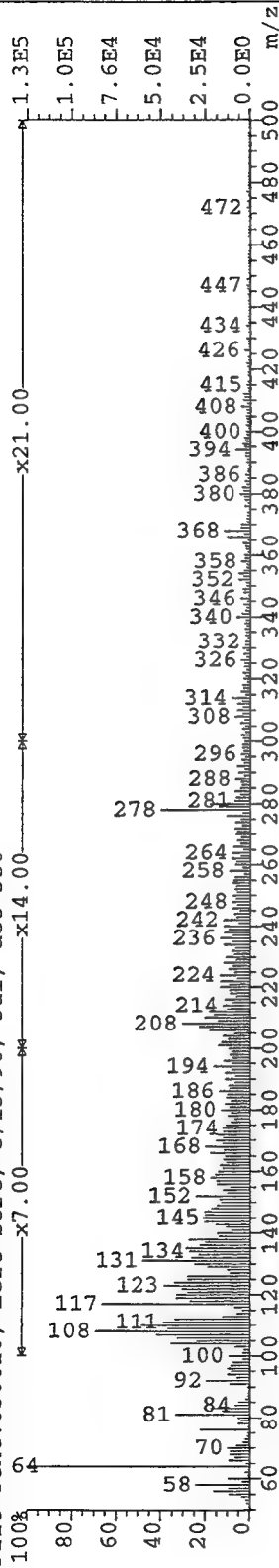




File:MINR29H15 Ident:1.59 Int Def 0.70 Acq: 1-JUL-1996 13:48:40 +1:02 Cal:MINR29H2

AutoSpecEQ CI+ Magnet BpM:64 BpI:126233 TIC:1052588 Flags:HALL

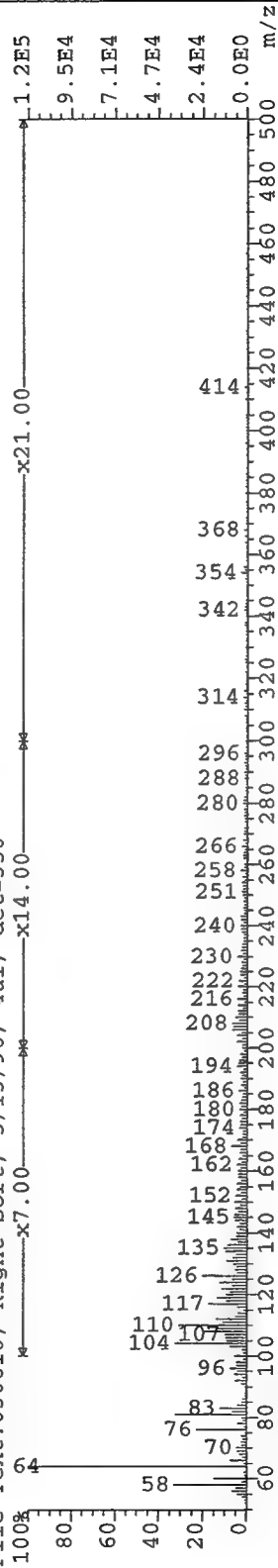
File Text:030610, Left Sort, 5/13/96, 3ul, det=350



File:MINR29H17 Ident:1.59 Int Def 0.70 Acq: 1-JUL-1996 14:19:50 +1:02 Cal:MINR29H2

AutoSpecEQ CI+ Magnet BpM:64 BpI:118290 TIC:579601 Flags:HALL

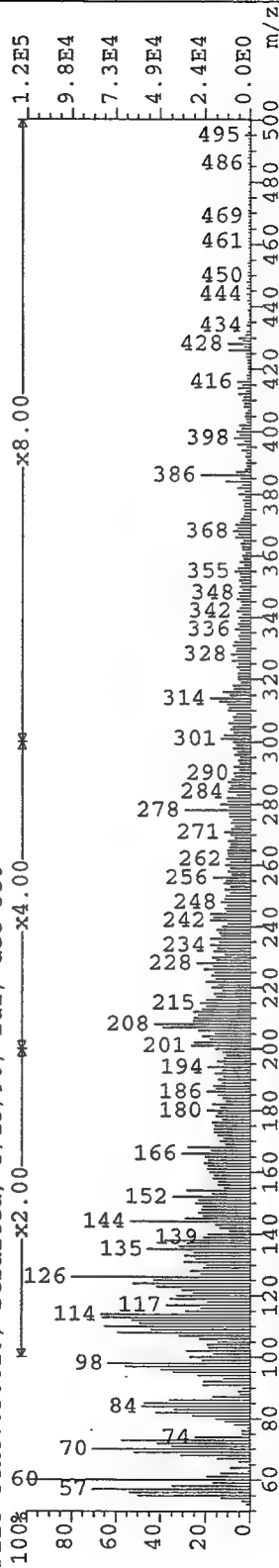
File Text:030610, Right Sort, 5/13/96, 4ul, det=350

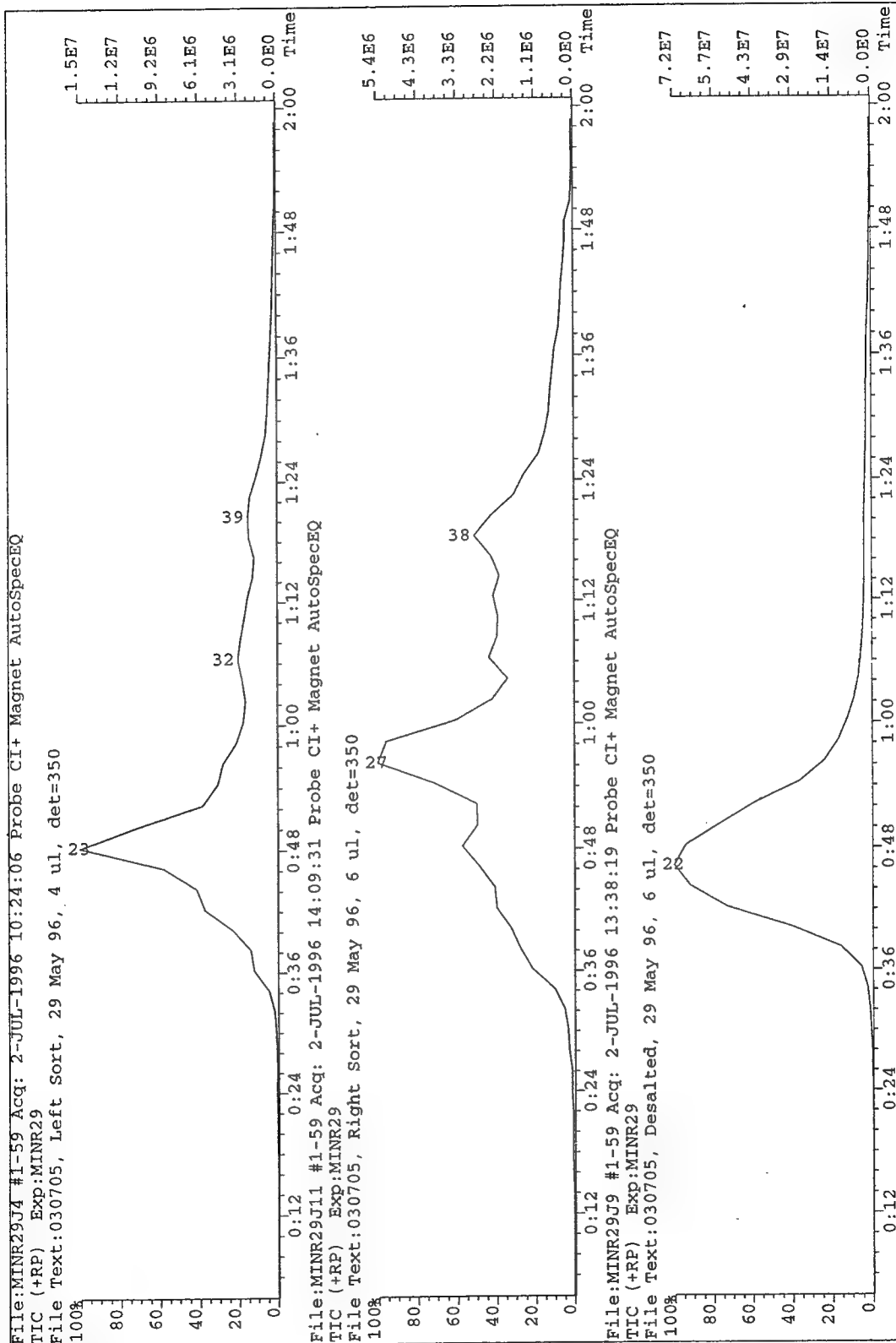


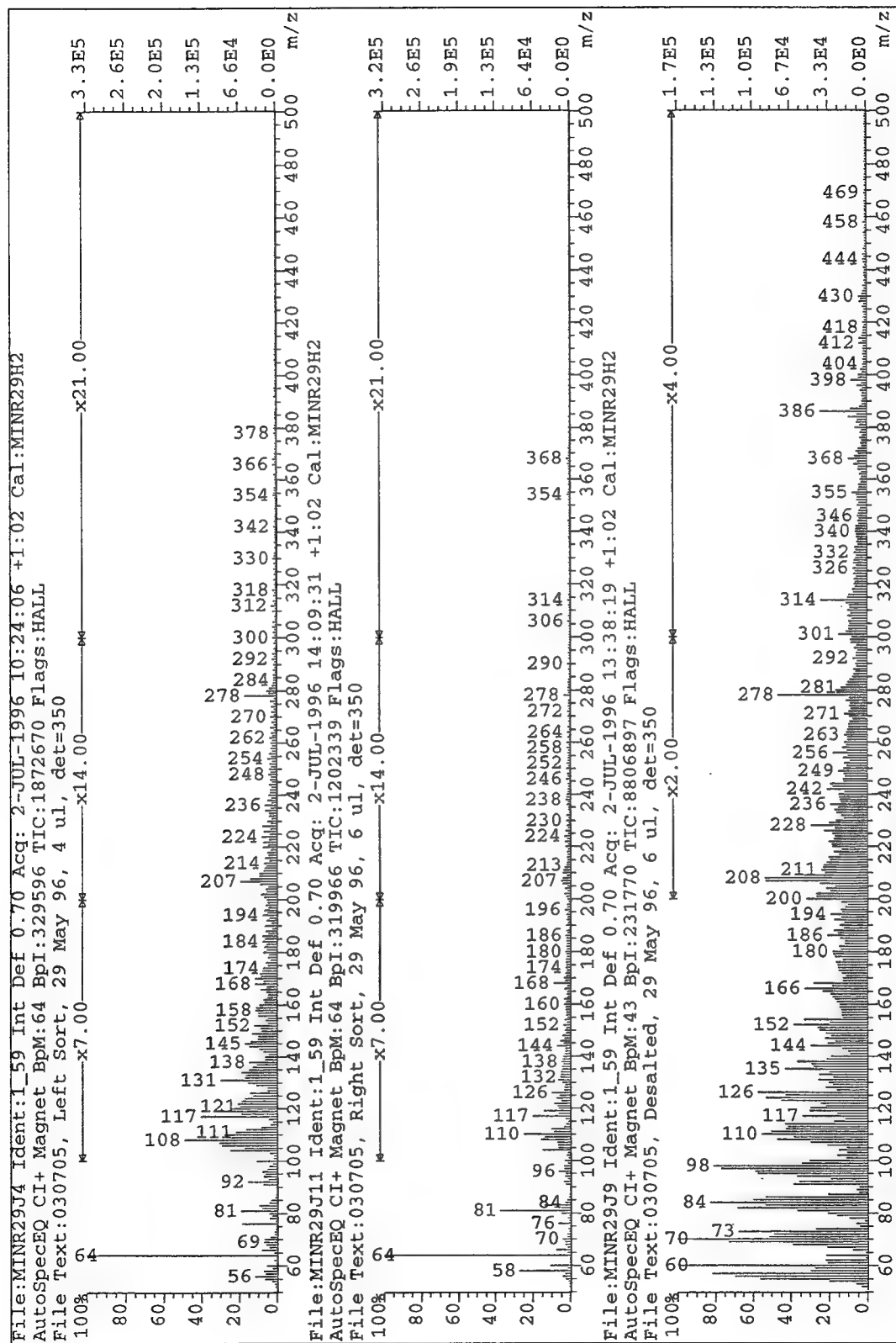
File:MINR29H24 Ident:1.59 Int Def 0.70 Acq: 1-JUL-1996 16:00:03 +1:02 Cal:MINR29H2

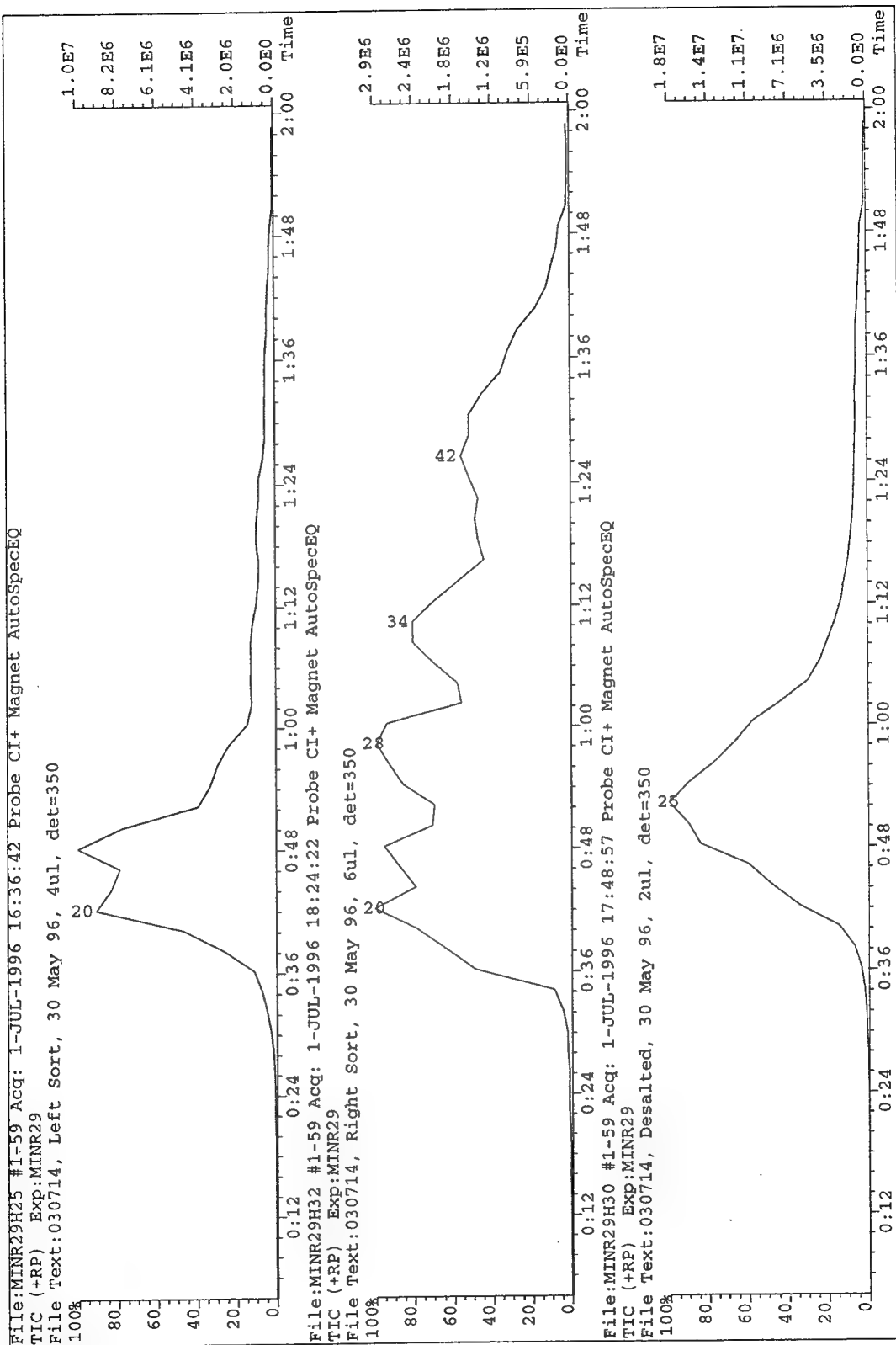
AutoSpecEQ CI+ Magnet BpM:43 BpI:150773 TIC:4006163 Flags:HALL

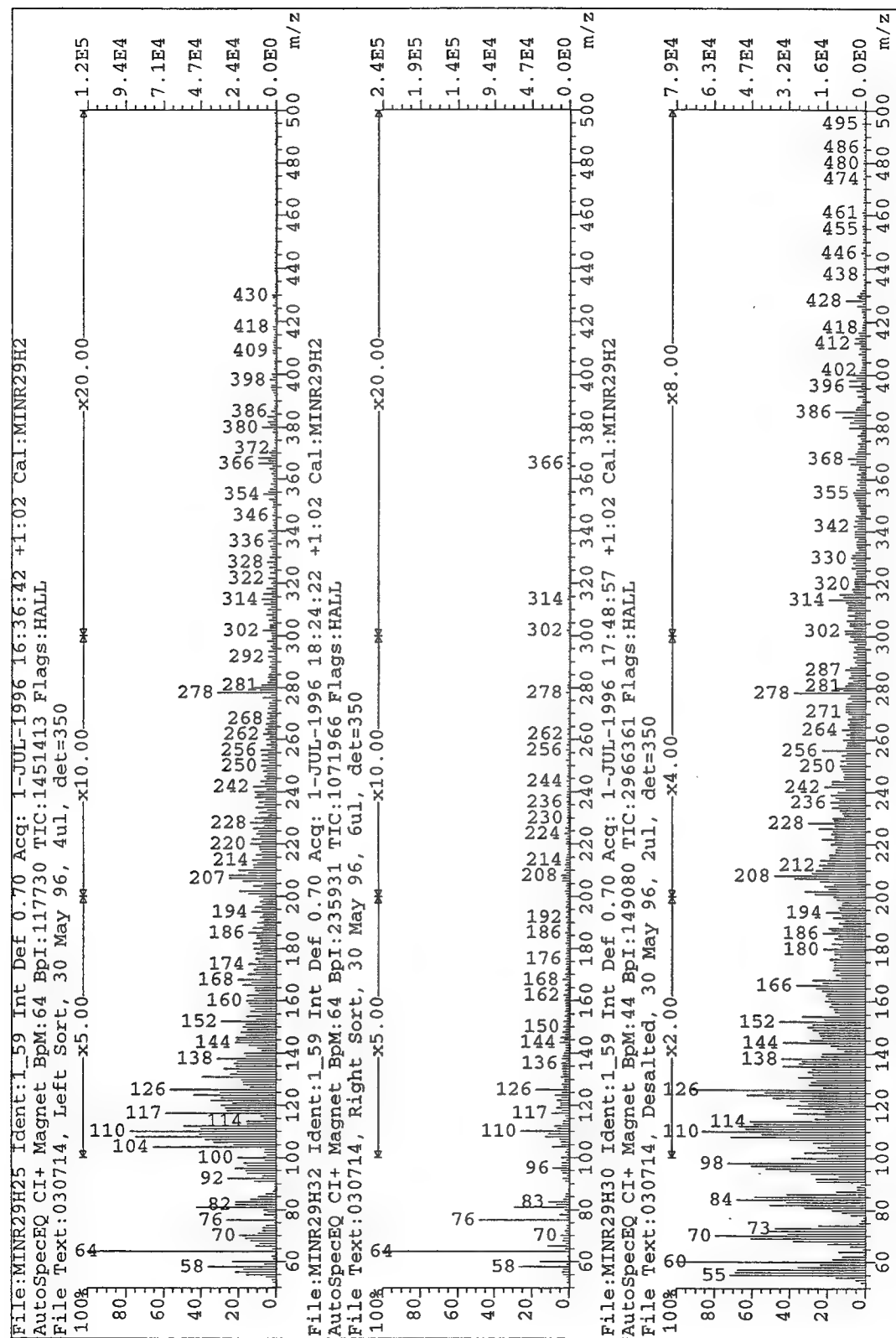
File Text:030610, Desalted, 5/13/96, 2ul, det=350

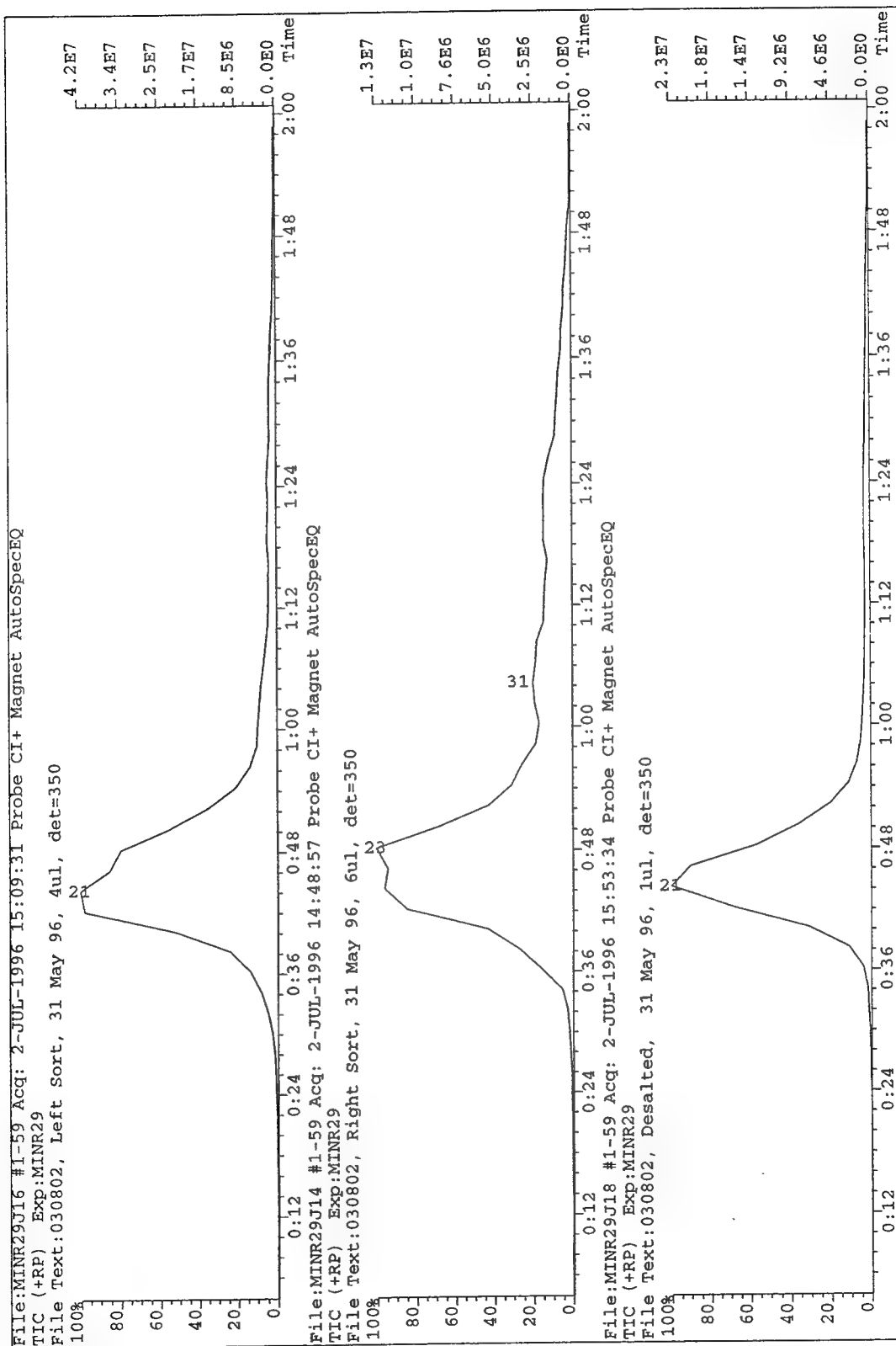








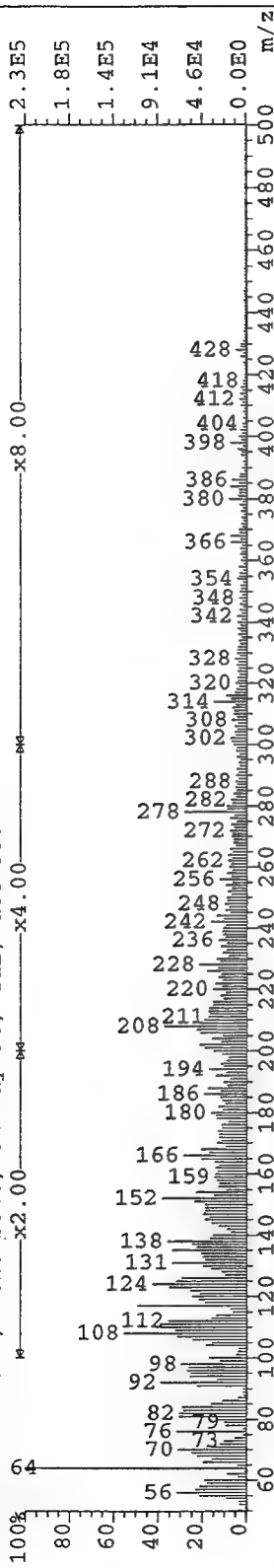




File:MINR29J16 Ident:1.59 Int Def 0.70 Acq: 2-JUL-1996 15:09:31 +1:02 Cal:MINR29H2

AutoSpecEQ CI+ Magnet BpM:64 BpI:227844 TIC:5033438 Flags:HALL

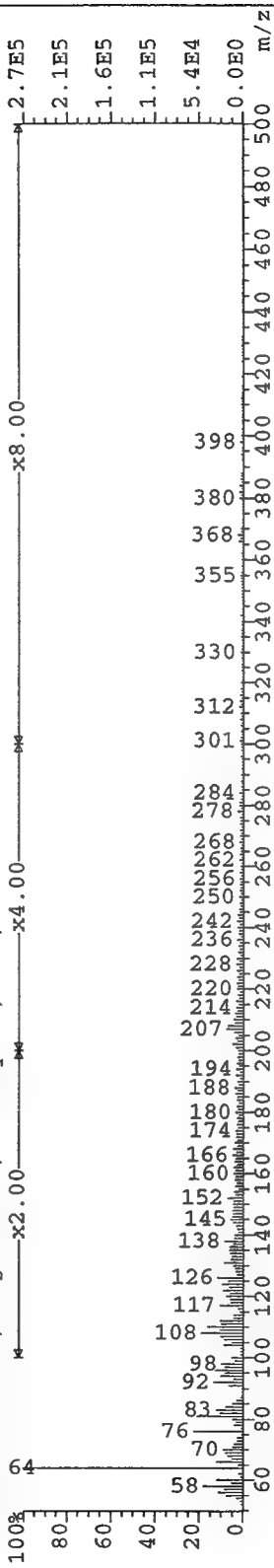
File Text:030802, Left Sort, 31 May 96, 4ul, det=350



File:MINR29J14 Ident:1.59 Int Def 0.70 Acq: 2-JUL-1996 14:48:57 +1:02 Cal:MINR29H2

AutoSpecEQ CI+ Magnet BpM:64 BpI:267524 TIC:1982411 Flags:HALL

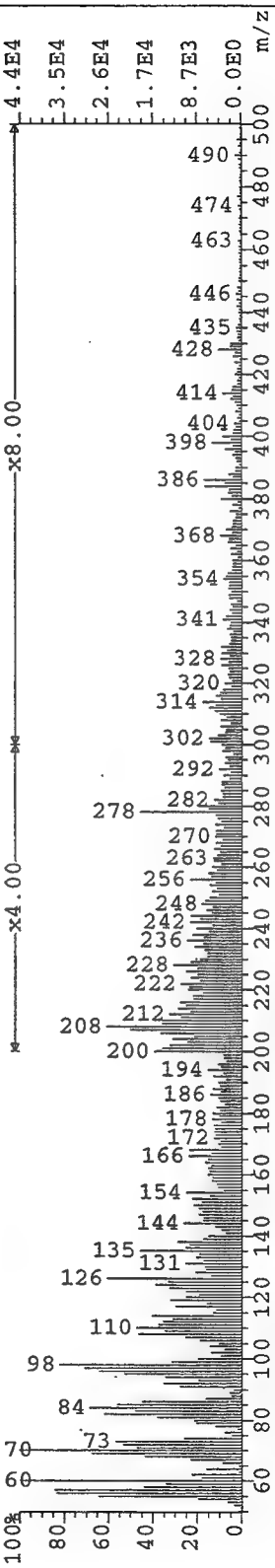
File Text:030802, Right Sort, 31 May 96, 6ul, det=350

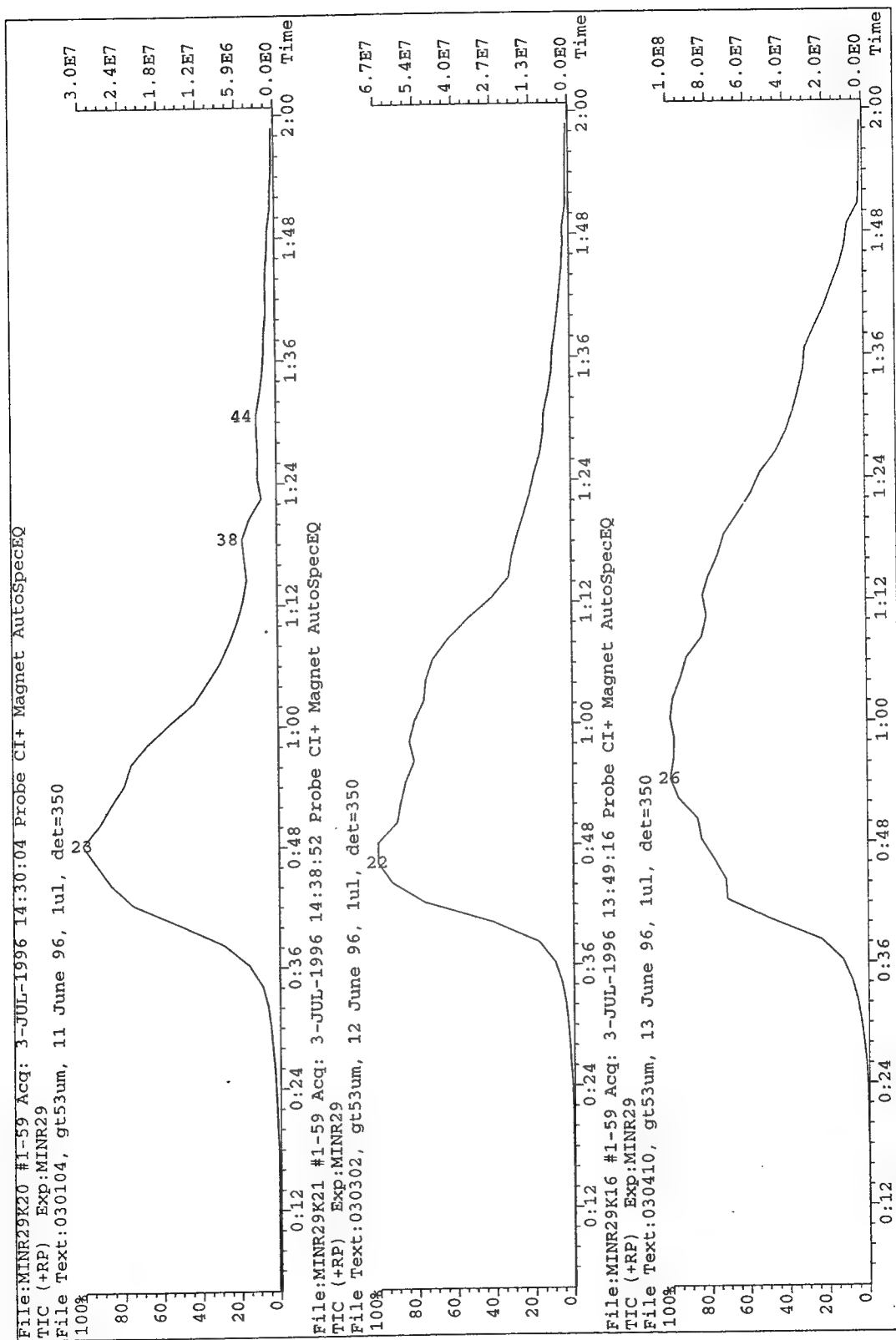


File:MINR29J18 Ident:1.59 Int Def 0.70 Acq: 2-JUL-1996 15:53:34 +1:02 Cal:MINR29H2

AutoSpecEQ CI+ Magnet BpM:43 BpI:73632 TIC:1964115 Flags:HALL

File Text:030802, Desalted, 31 May 96, 1ul, det=350

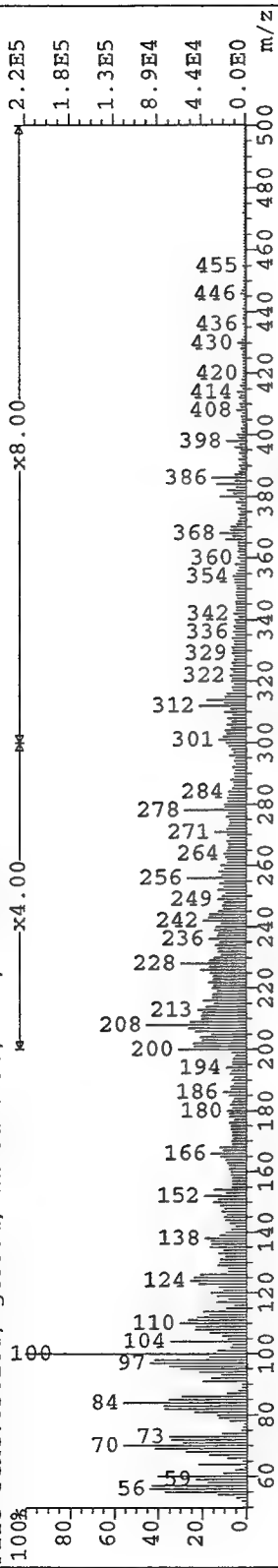




File:MINR29K20 Ident:1_59 Int Def 0.70 Acq: 3-JUL-1996 14:30:04 +1:02 Cal:MINR29H2

AutoSpecEQ CI+ Magnet BpM:44 BpI:285989 TIC:6345090 Flags:HALL

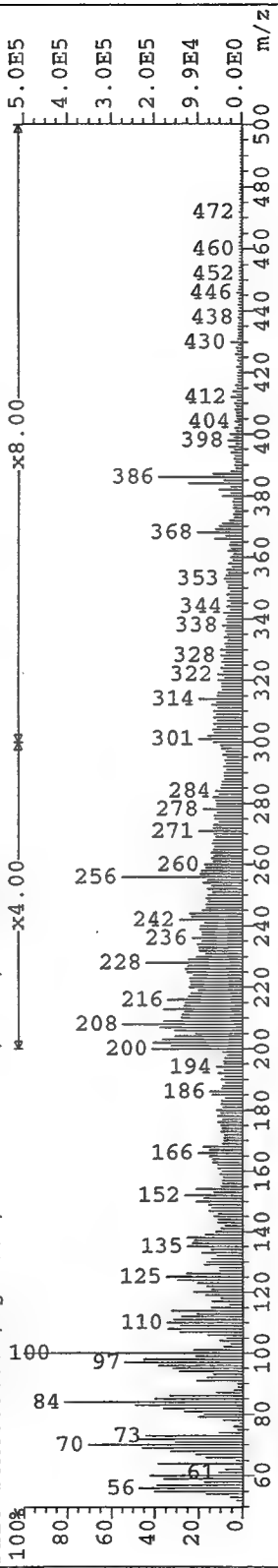
File Text:030104, gt53um, 11 June 96, 1ul, det=350



File:MINR29K21 Ident:1_59 Int Def 0.70 Acq: 3-JUL-1996 14:38:52 +1:02 Cal:MINR29H2

AutoSpecEQ CI+ Magnet BpM:44 BpI:767743 TIC:18260740 Flags:HALL

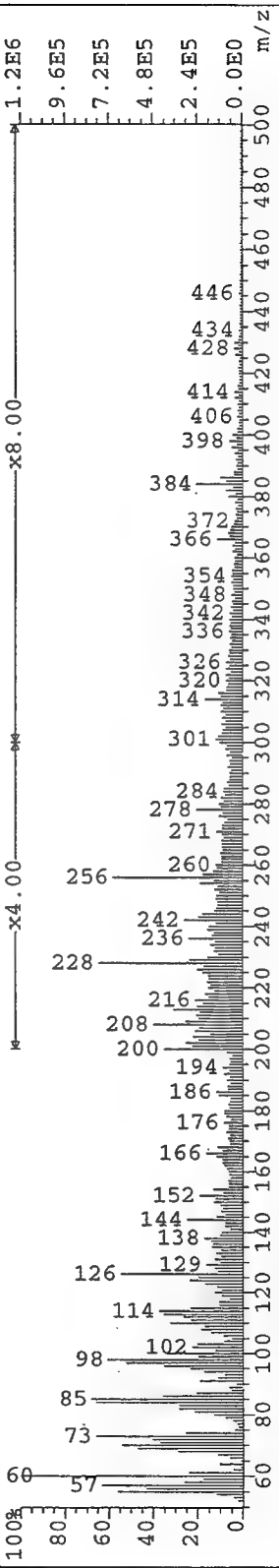
File Text:030302, gt53um, 12 June 96, 1ul, det=350

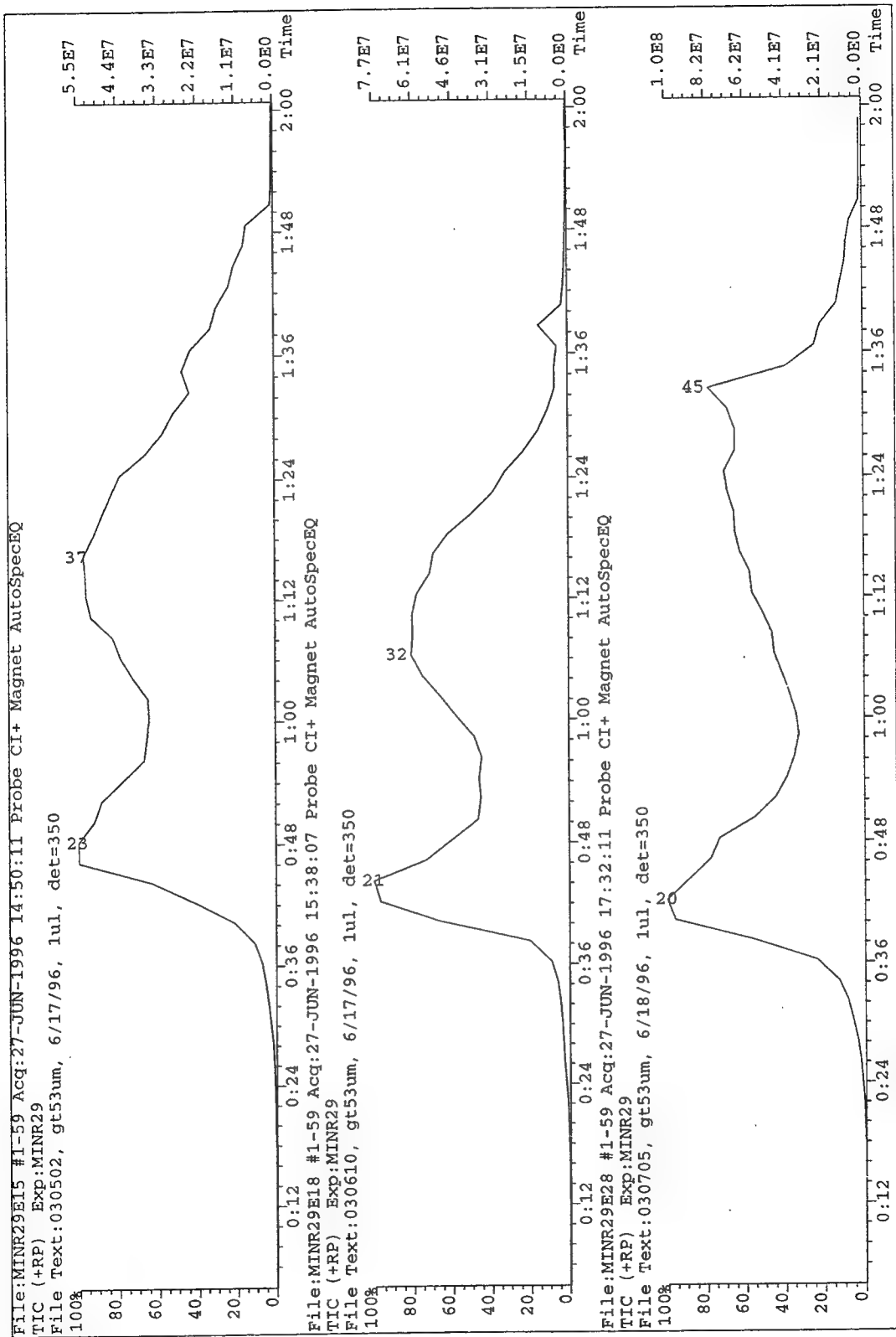


File:MINR29K16 Ident:1_59 Int Def 0.70 Acq: 3-JUL-1996 13:49:16 +1:02 Cal:MINR29H2

AutoSpecEQ CI+ Magnet BpM:44 BpI:1850999 TIC:3791396 Flags:HALL

File Text:030410, gt53um, 13 June 96, 1ul, det=350

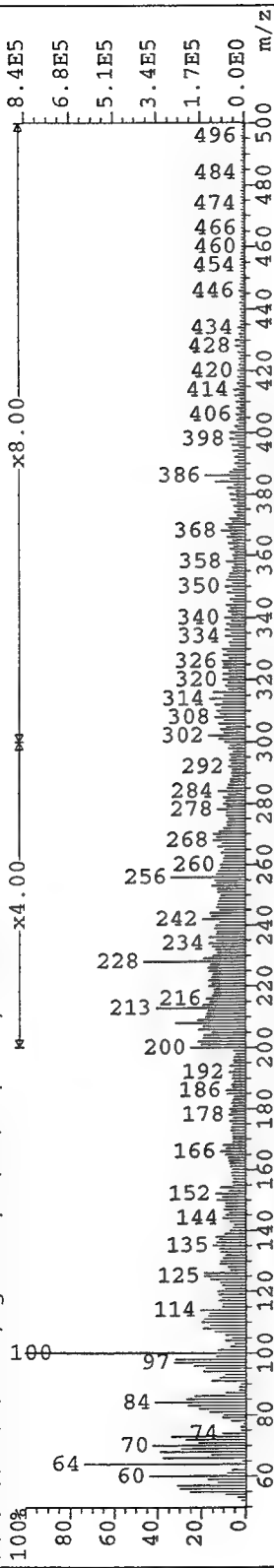




File:MINR29E15 Ident:1_59 Int Def 0.70 Acq:27-JUN-1996 14:50:11 +1:02 Cal:MINR29A2

AutoSpecEQ CI+ Magnet BpM:100 BpI:844599 TIC:21177282 Flags:HALL

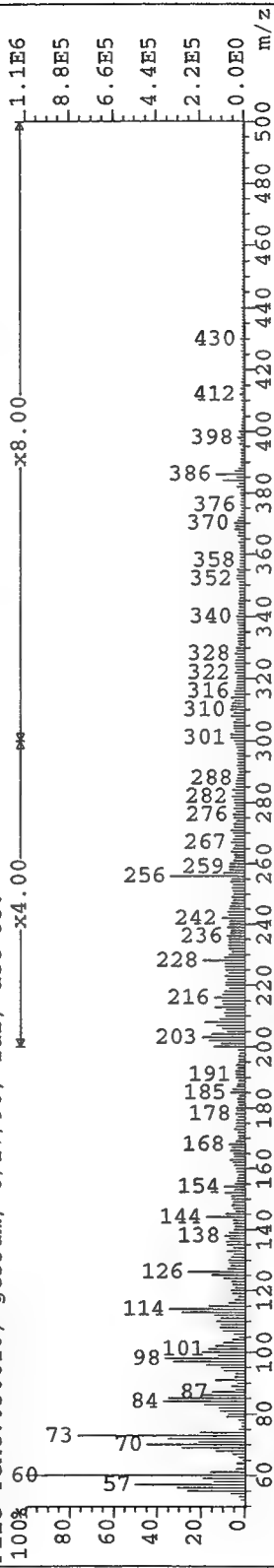
File Text:030502, gt53um, 6/17/96, 1ul, det=350



File:MINR29E18 Ident:1_59 Int Def 0.70 Acq:27-JUN-1996 15:38:07 +1:02 Cal:MINR29A2

AutoSpecEQ CI+ Magnet BpM:60 BpI:109931 TIC:20904714 Flags:HALL

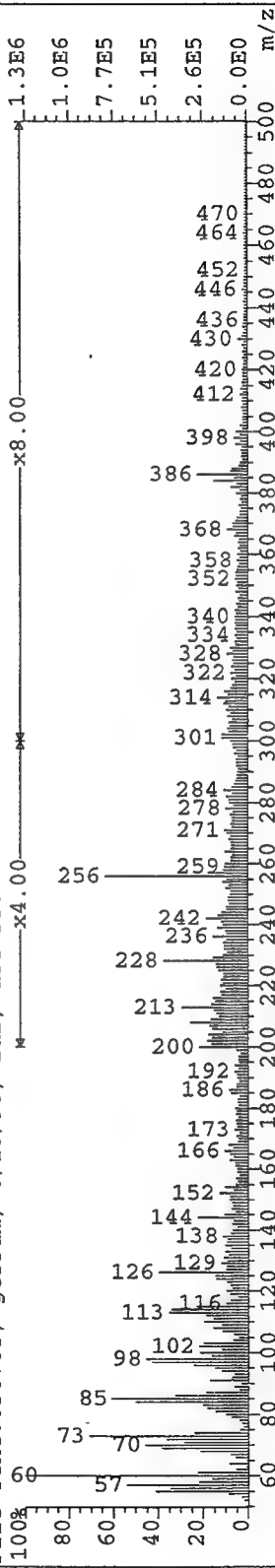
File Text:030610, gt53um, 6/17/96, 1ul, det=350

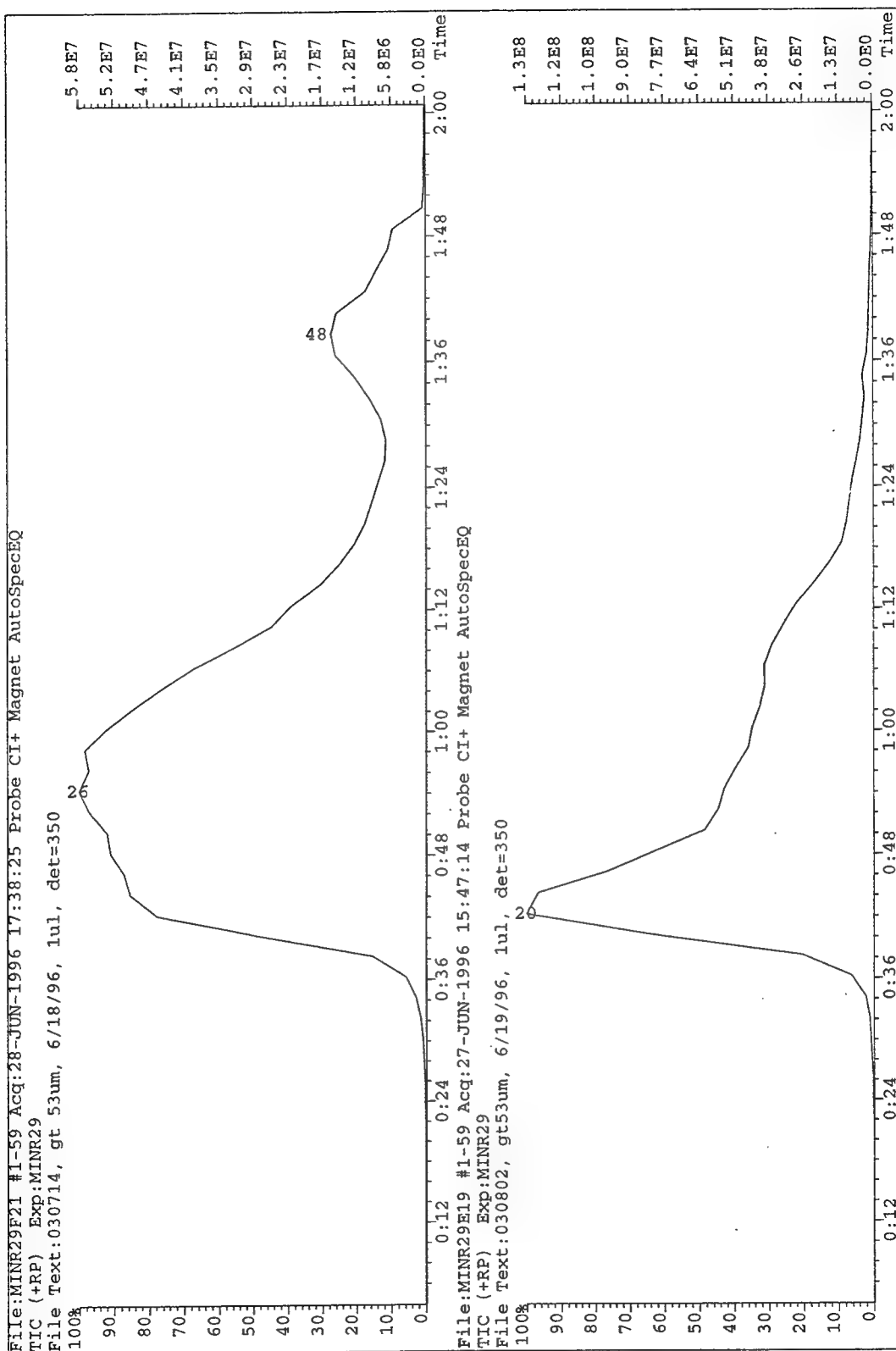


File:MINR29E28 Ident:1_59 Int Def 0.70 Acq:27-JUN-1996 17:32:11 +1:02 Cal:MINR29A2

AutoSpecEQ CI+ Magnet BpM:44 BpI:1369683 TIC:32506854 Flags:HALL

File Text:030705, gt53um, 6/18/96, 1ul, det=350

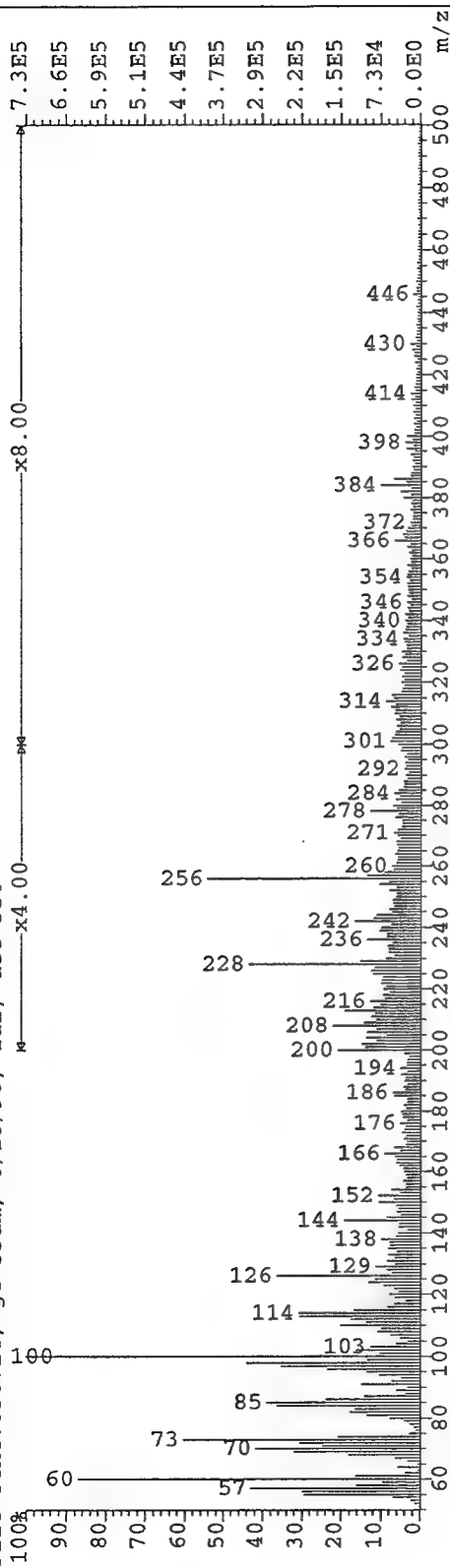




File: MINR29F21 Ident: 159 Int Def 0.70 Acq: 28-JUN-1996 17:38:25 +1:02 Cal: MINR29A2

AutoSpecEQ CI+ Magnet BpM: 44 BpI: 1664067 TIC: 16626733 Flags: HALL

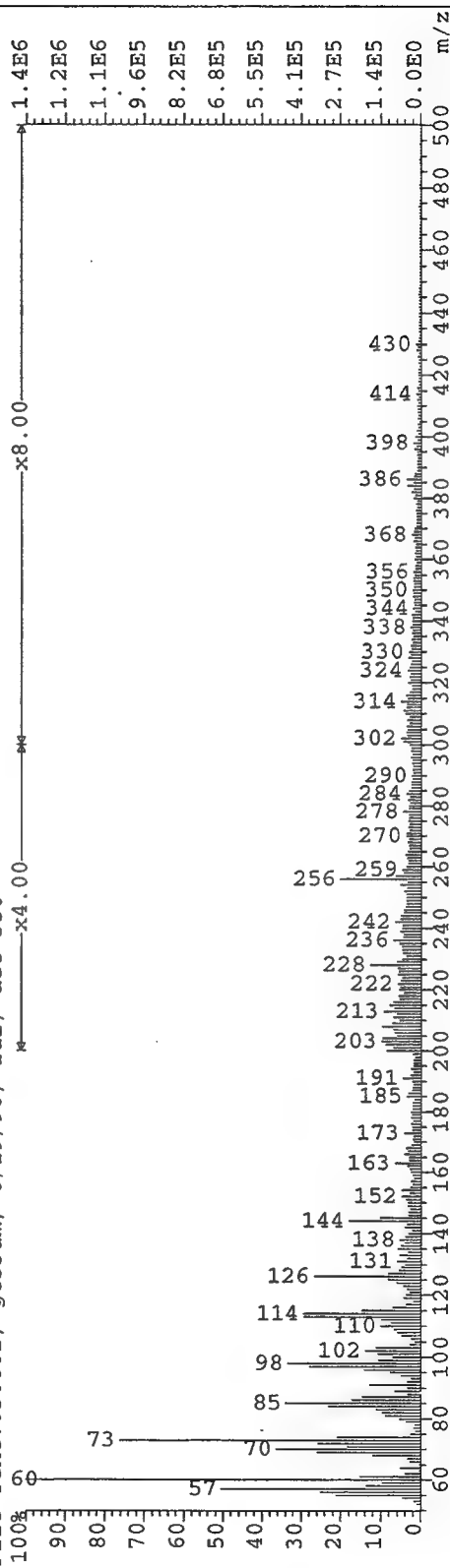
File Text: 030714, gt 53um, 6/18/96, lul, det=350

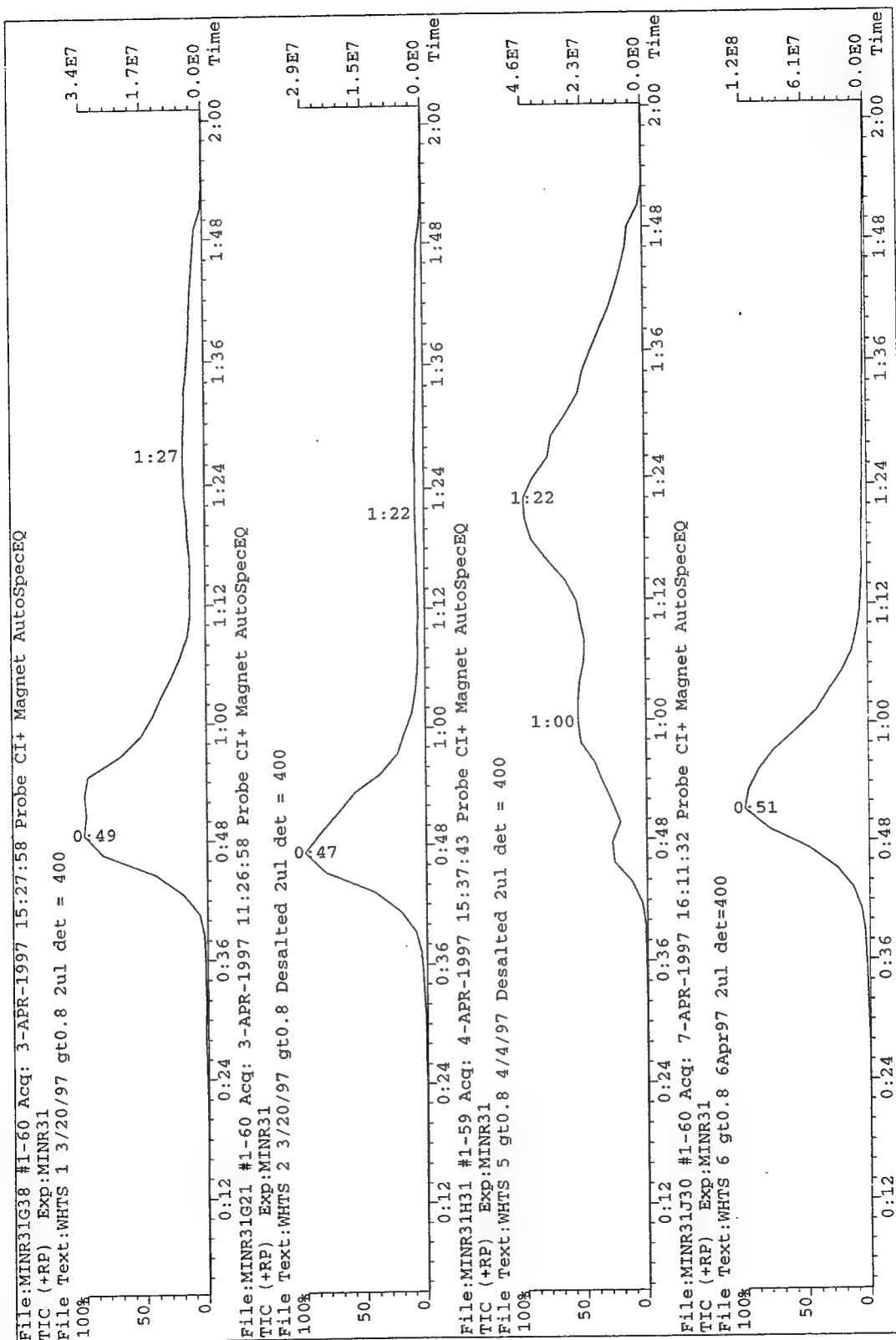


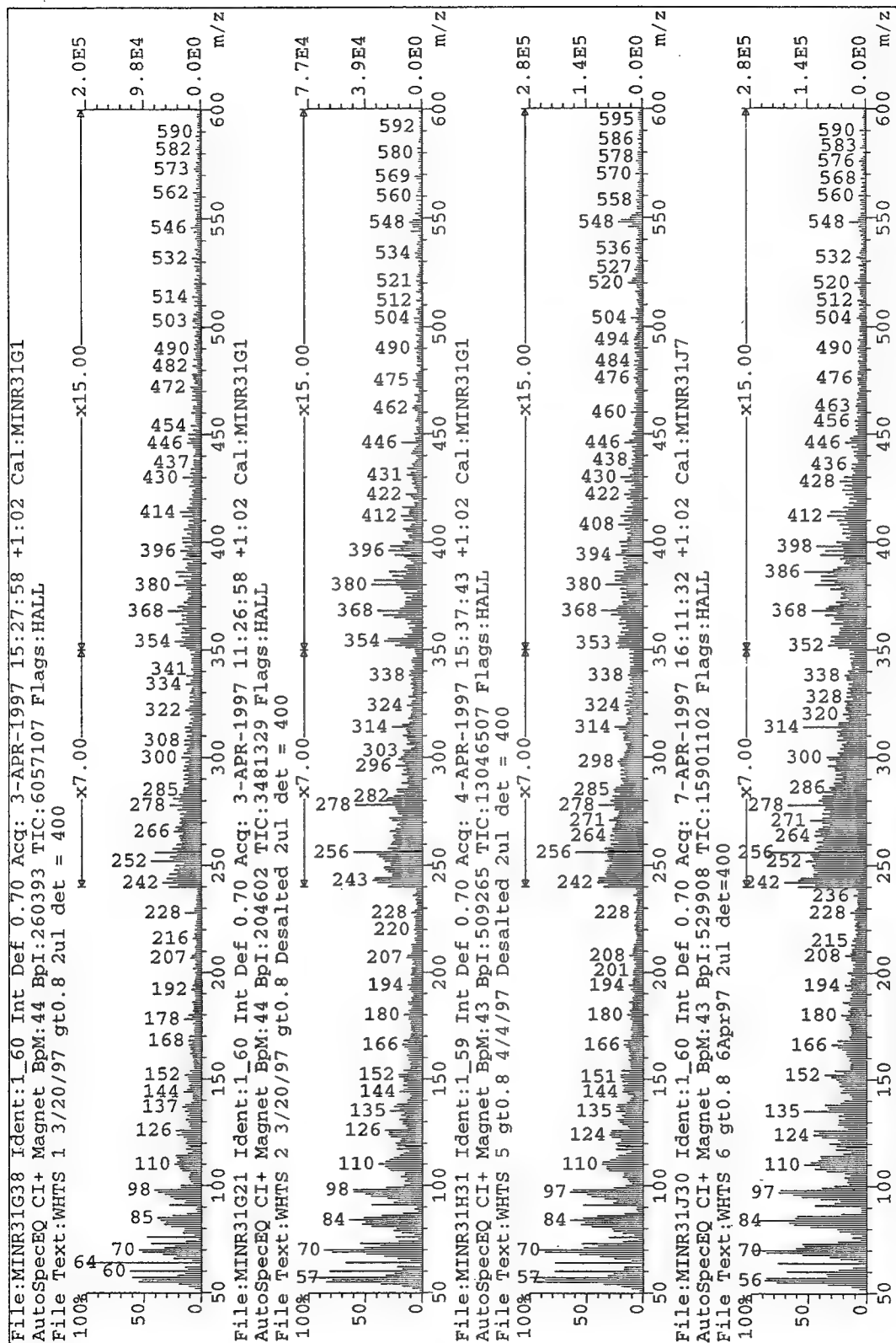
File: MINR29E19 Ident: 159 Int Def 0.70 Acq: 27-JUN-1996 15:47:14 +1:02 Cal: MINR29A2

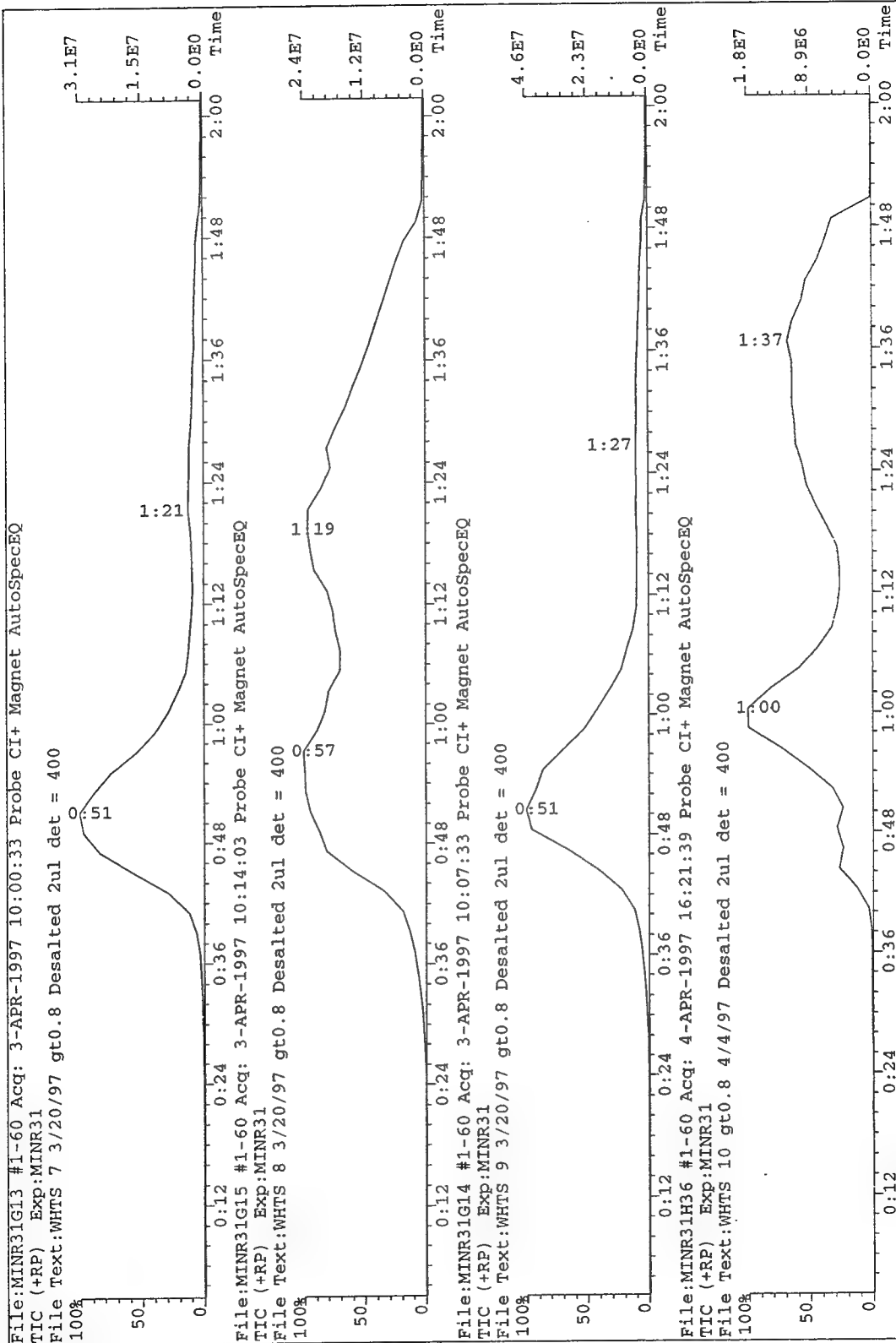
AutoSpecEQ CI+ Magnet BpM: 60 BpI: 1365965 TIC: 20189226 Flags: HALL

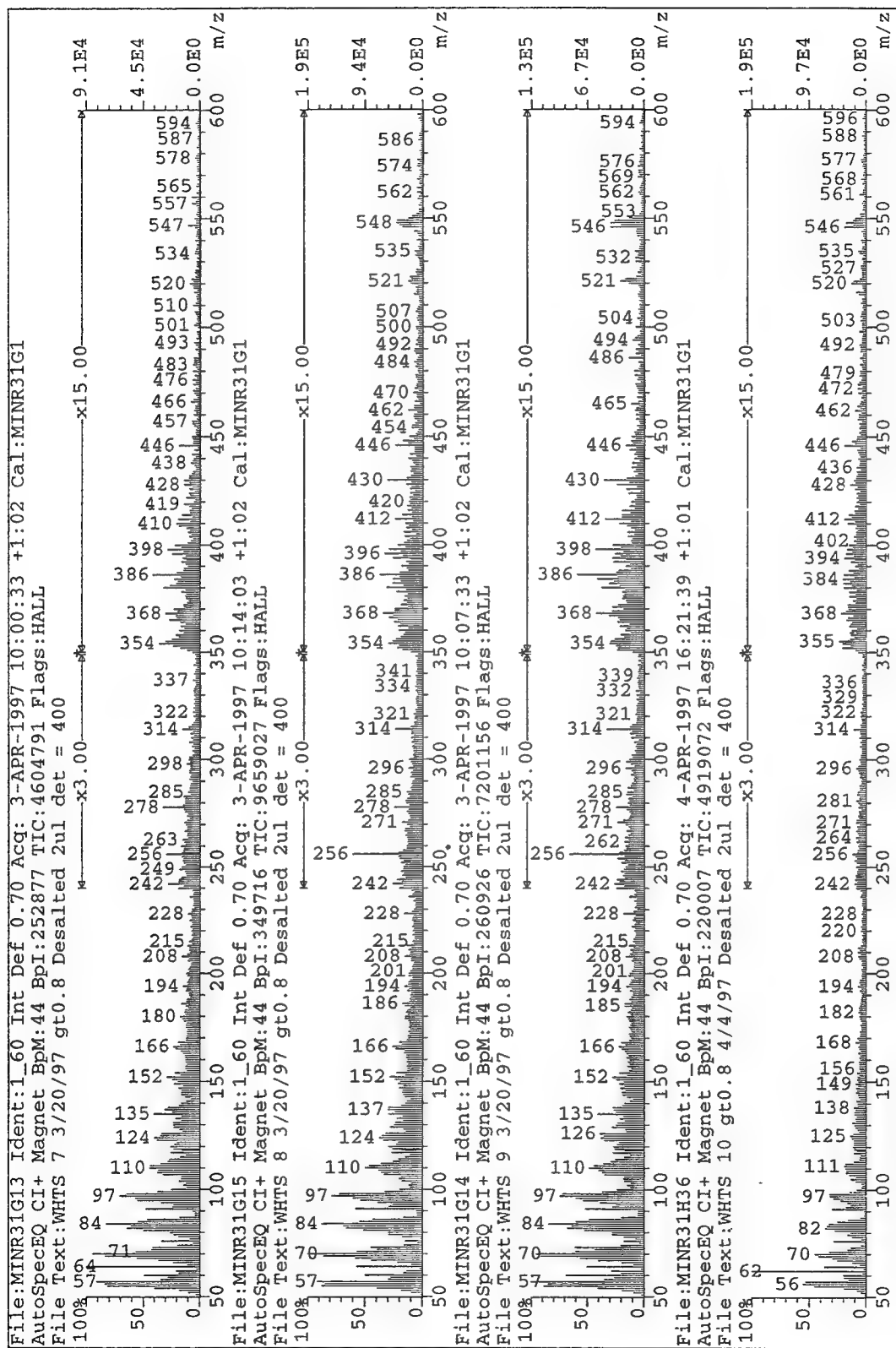
File Text: 030802, gt 53um, 6/19/96, lul, det=350

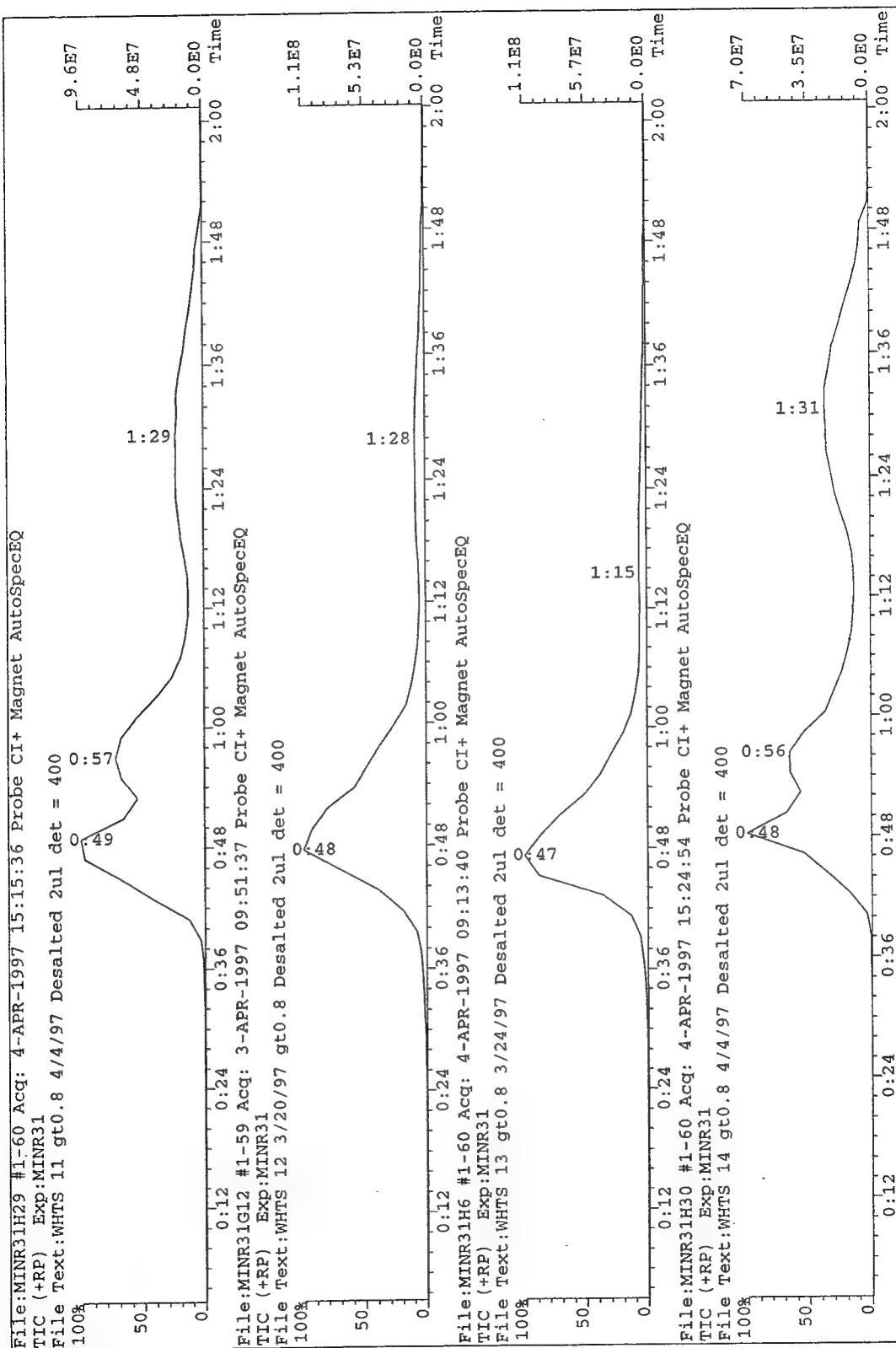


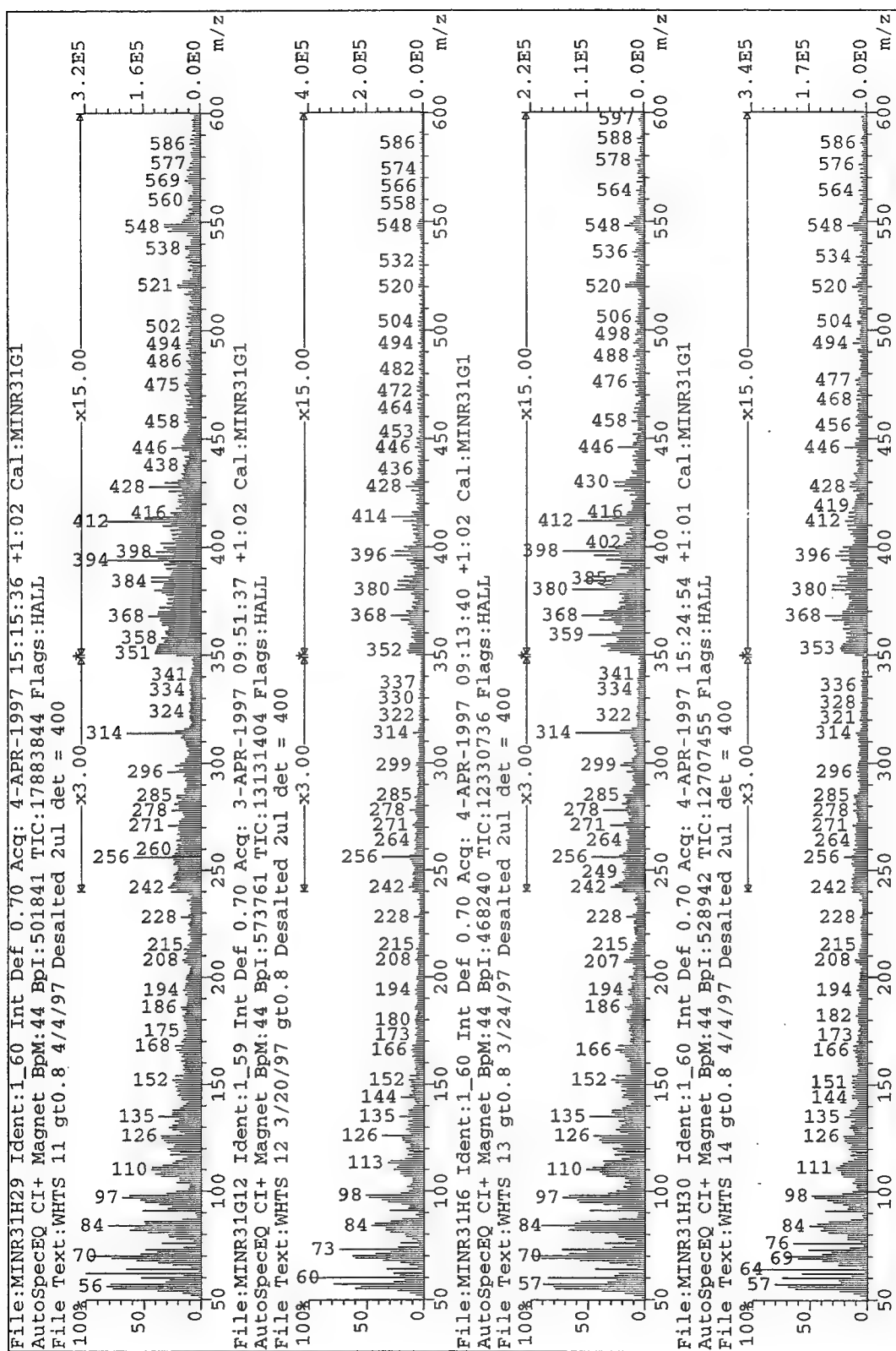


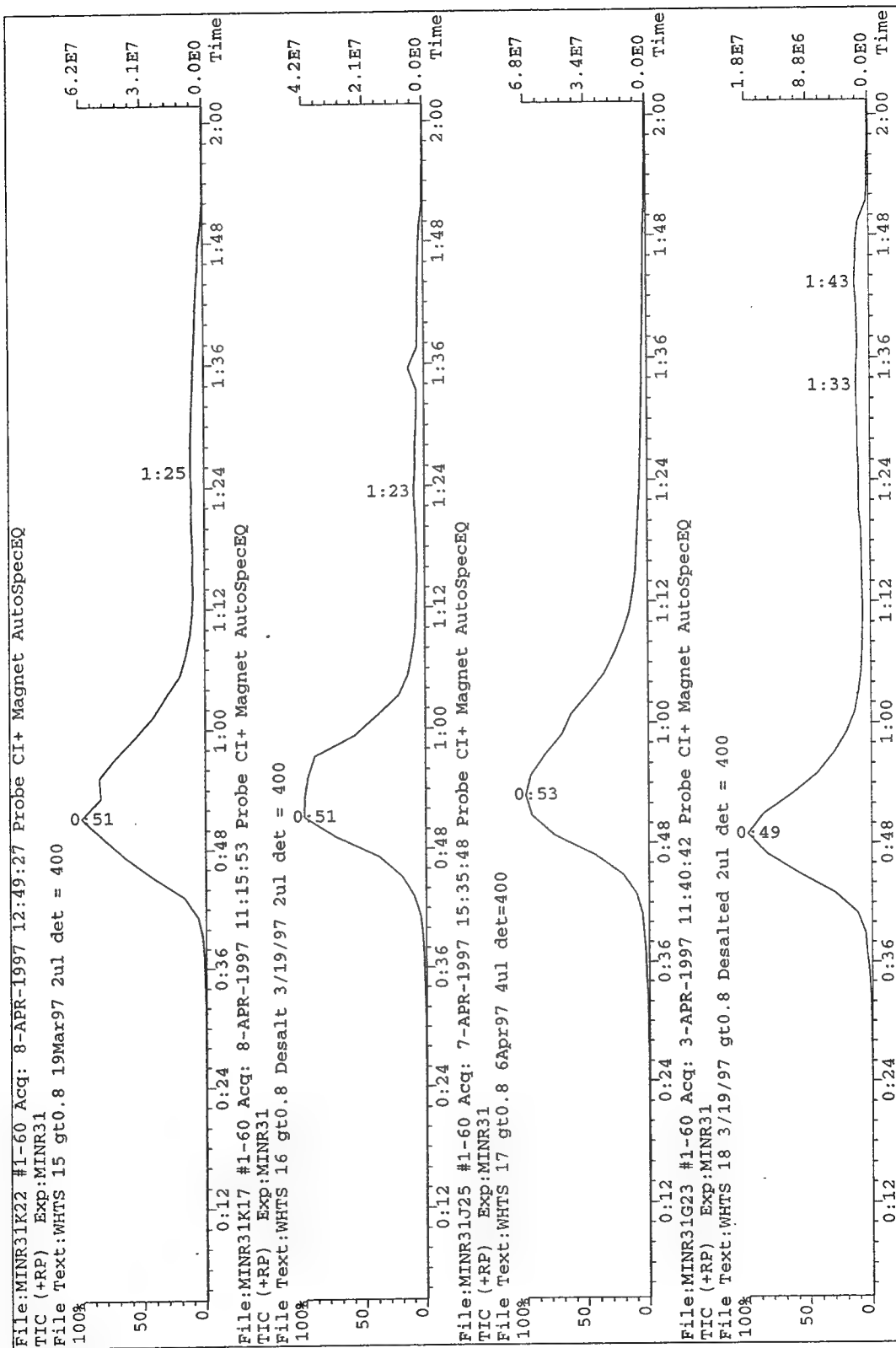


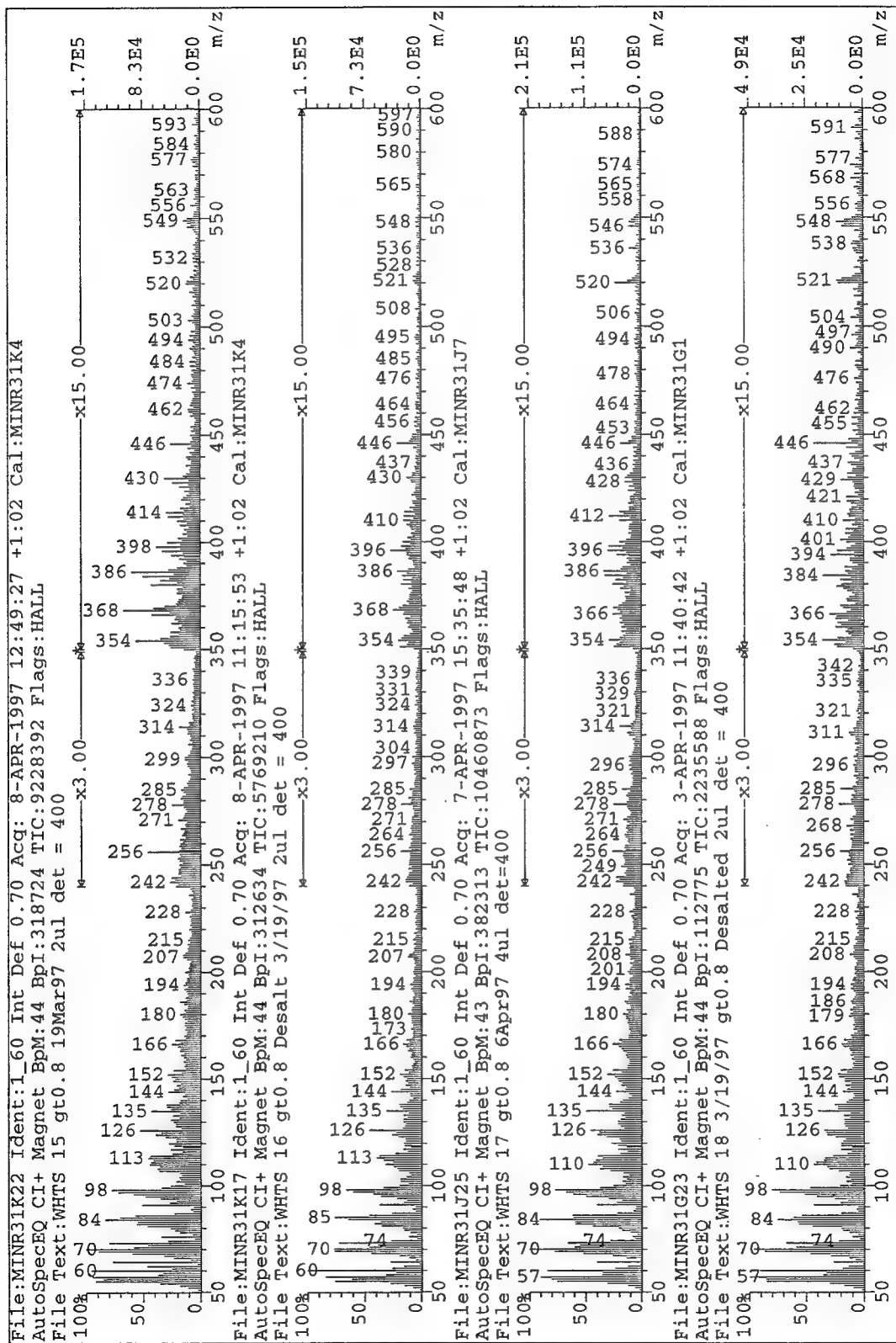


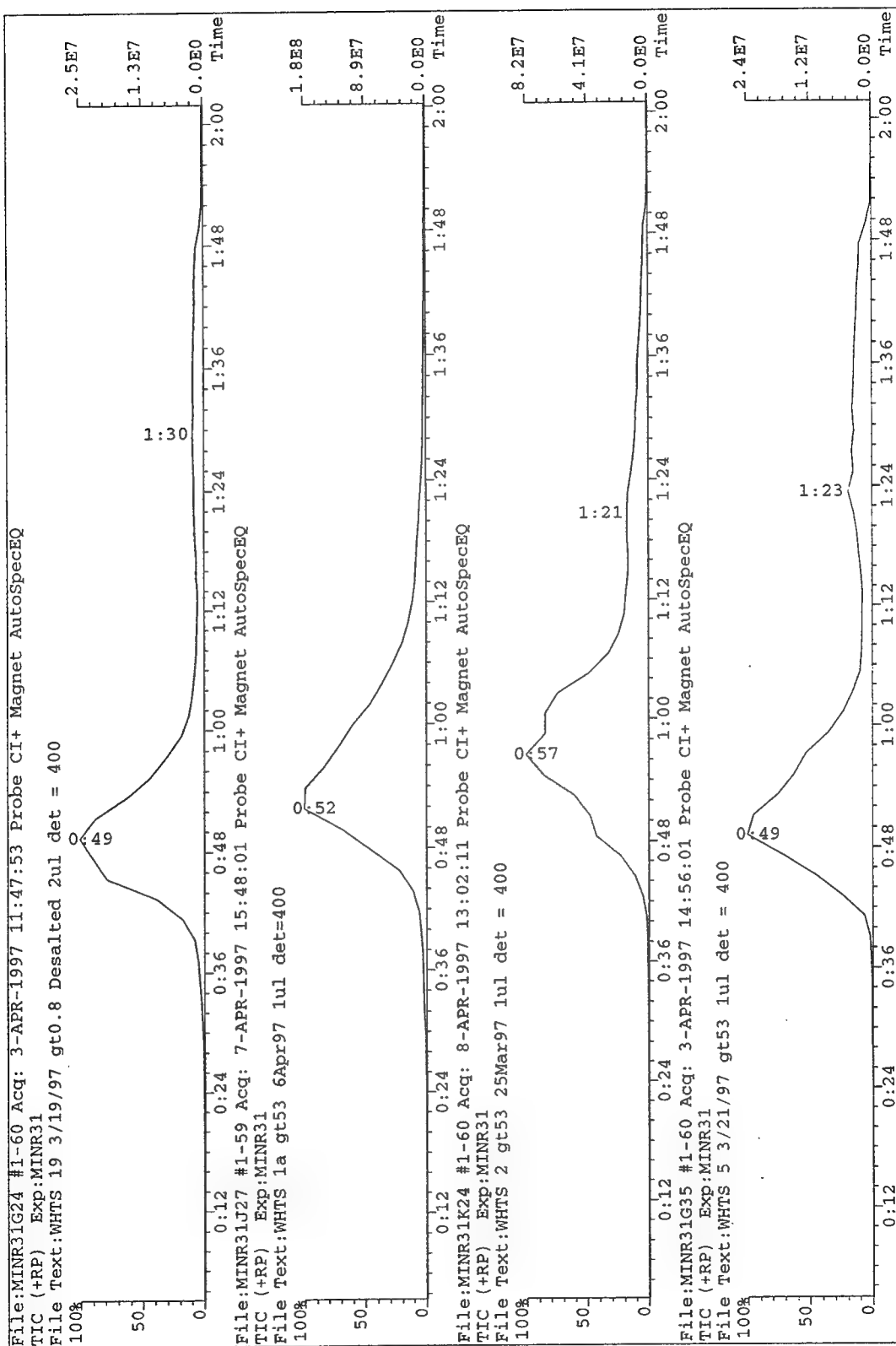


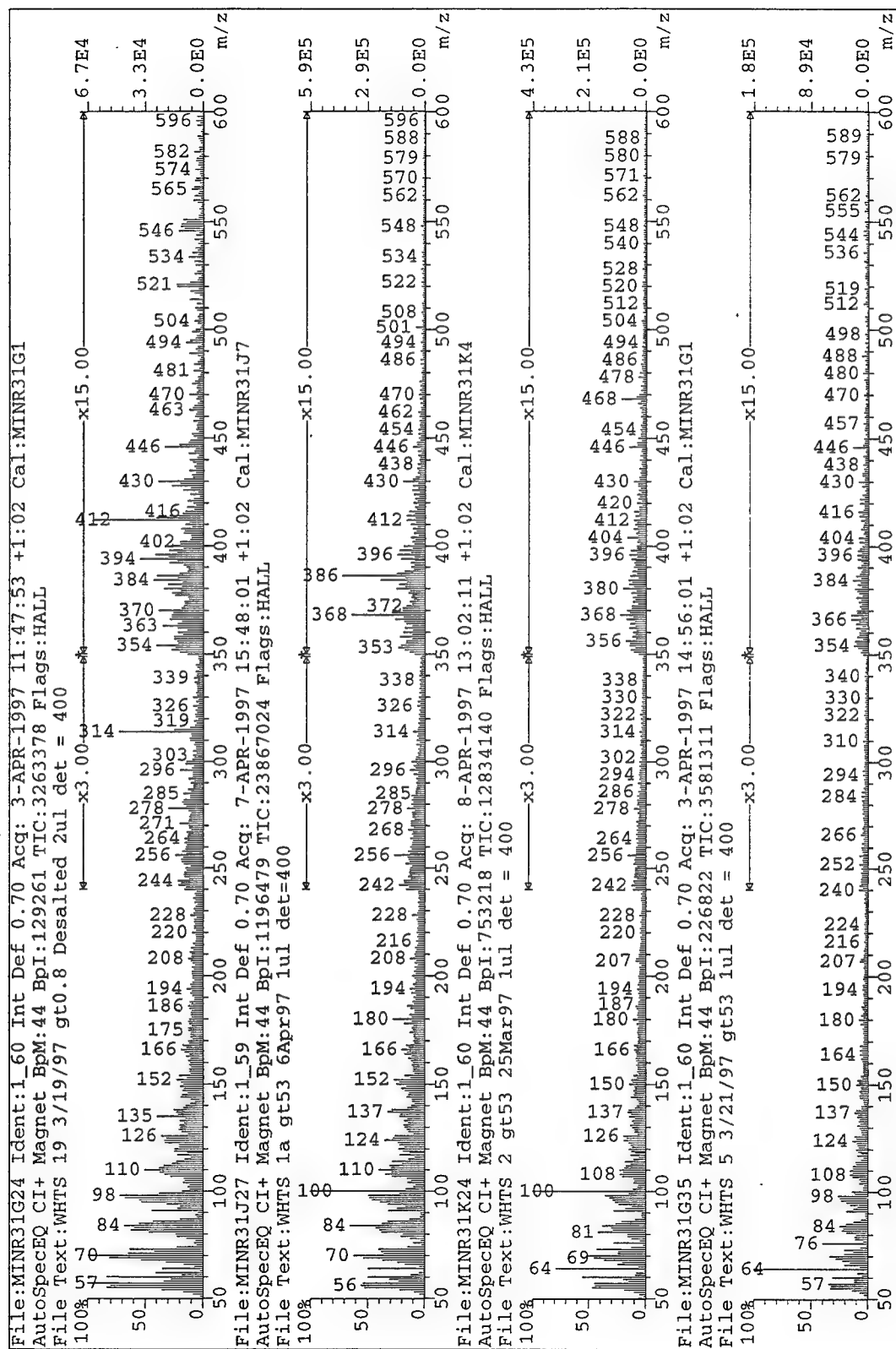


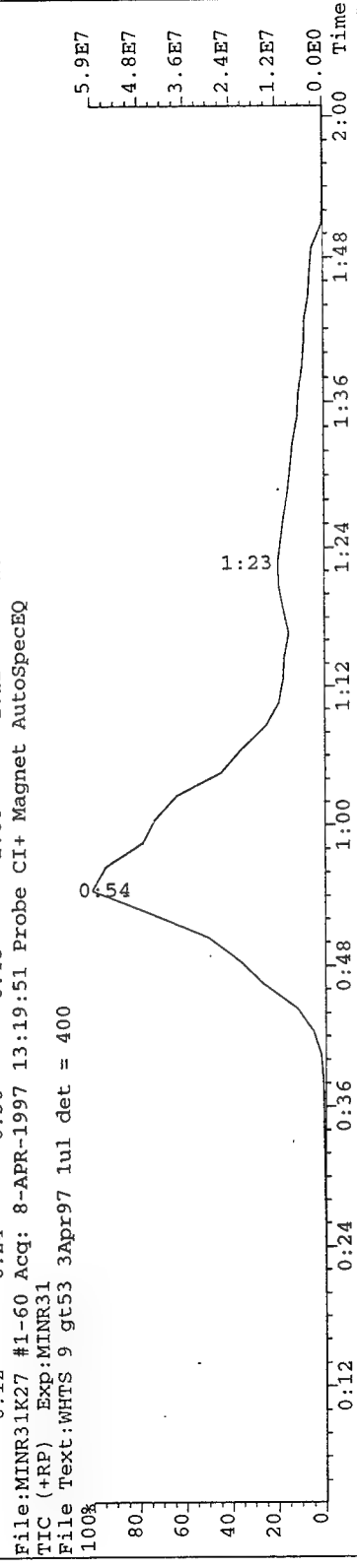
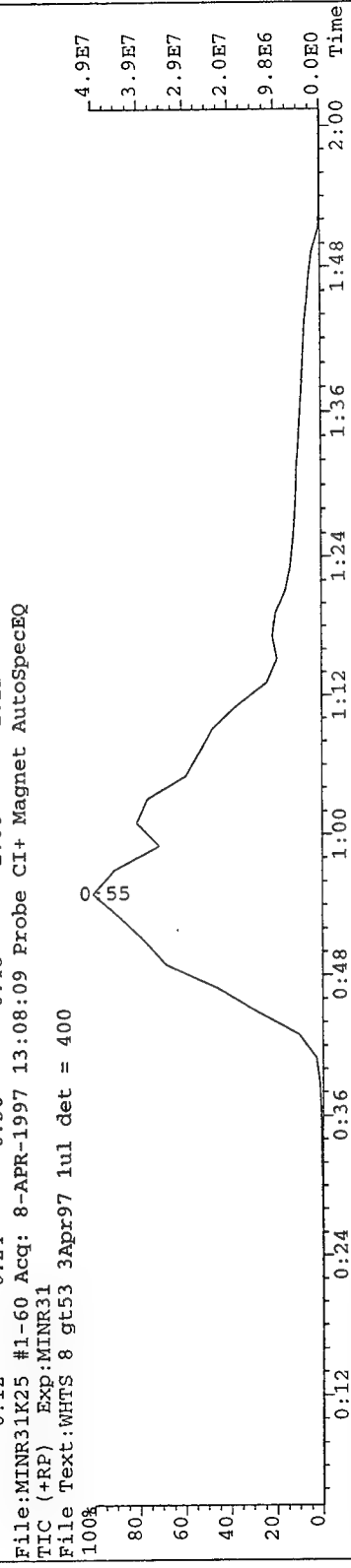
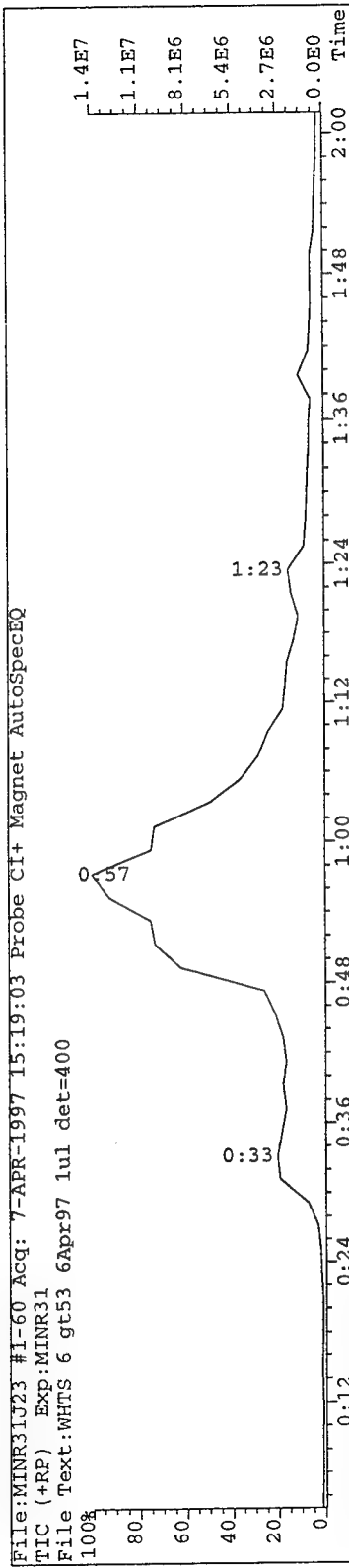








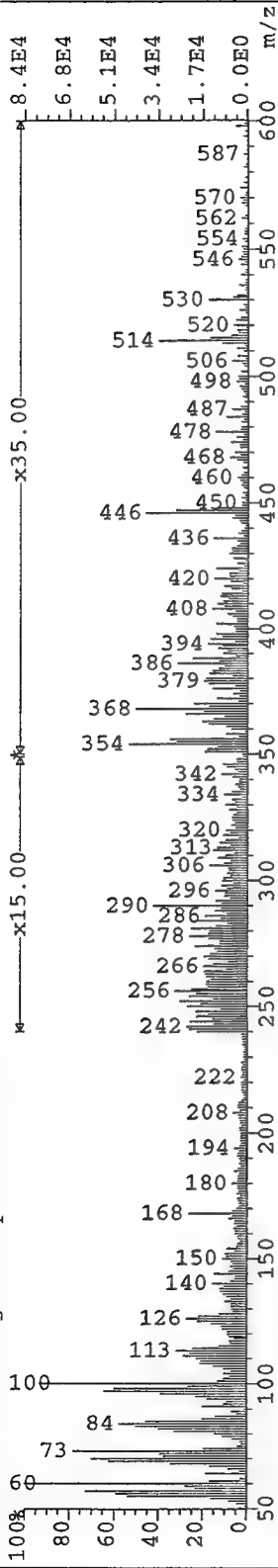




File:MINR31J23 Ident:1_60 Int Def 0.70 Acq: 7-APR-1997 15:19:03 +1:02 Cal:MINR31J7

AutoSpecEQ CI+ Magnet BpM:44 BpI:168941 TIC:2465234 Flags:HALL

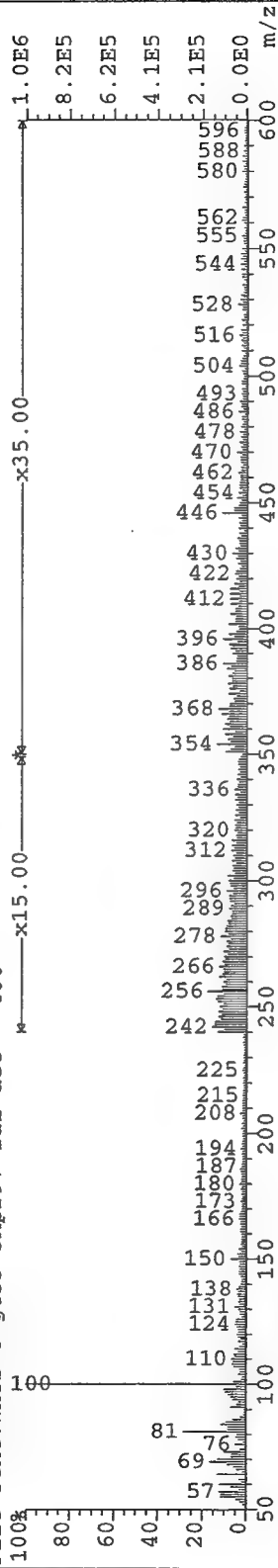
File Text:WHTS 6 gt53 6Apr97 1ul det=400



File:MINR31K25 Ident:1_60 Int Def 0.70 Acq: 8-APR-1997 13:08:09 +1:02 Cal:MINR31K4

AutoSpecEQ CI+ Magnet BpM:100 BpI:1030195 TIC:9411149 Flags:HALL

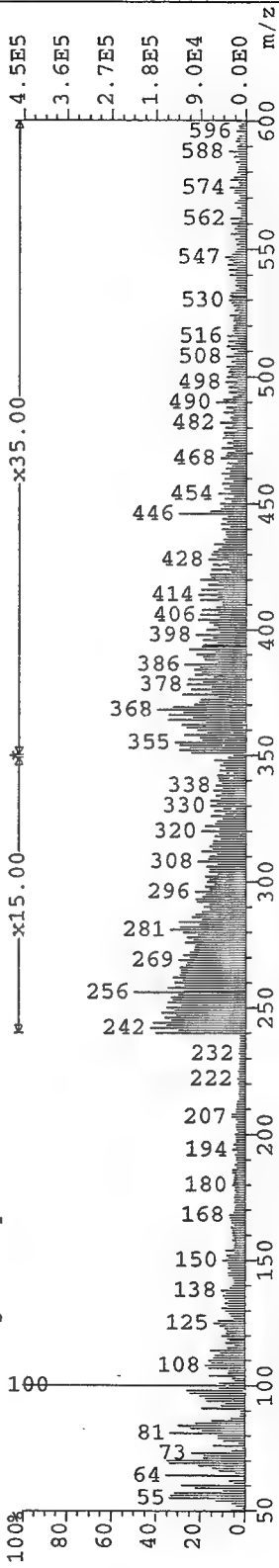
File Text:WHTS 8 gt53 3Apr97 1ul det = 400

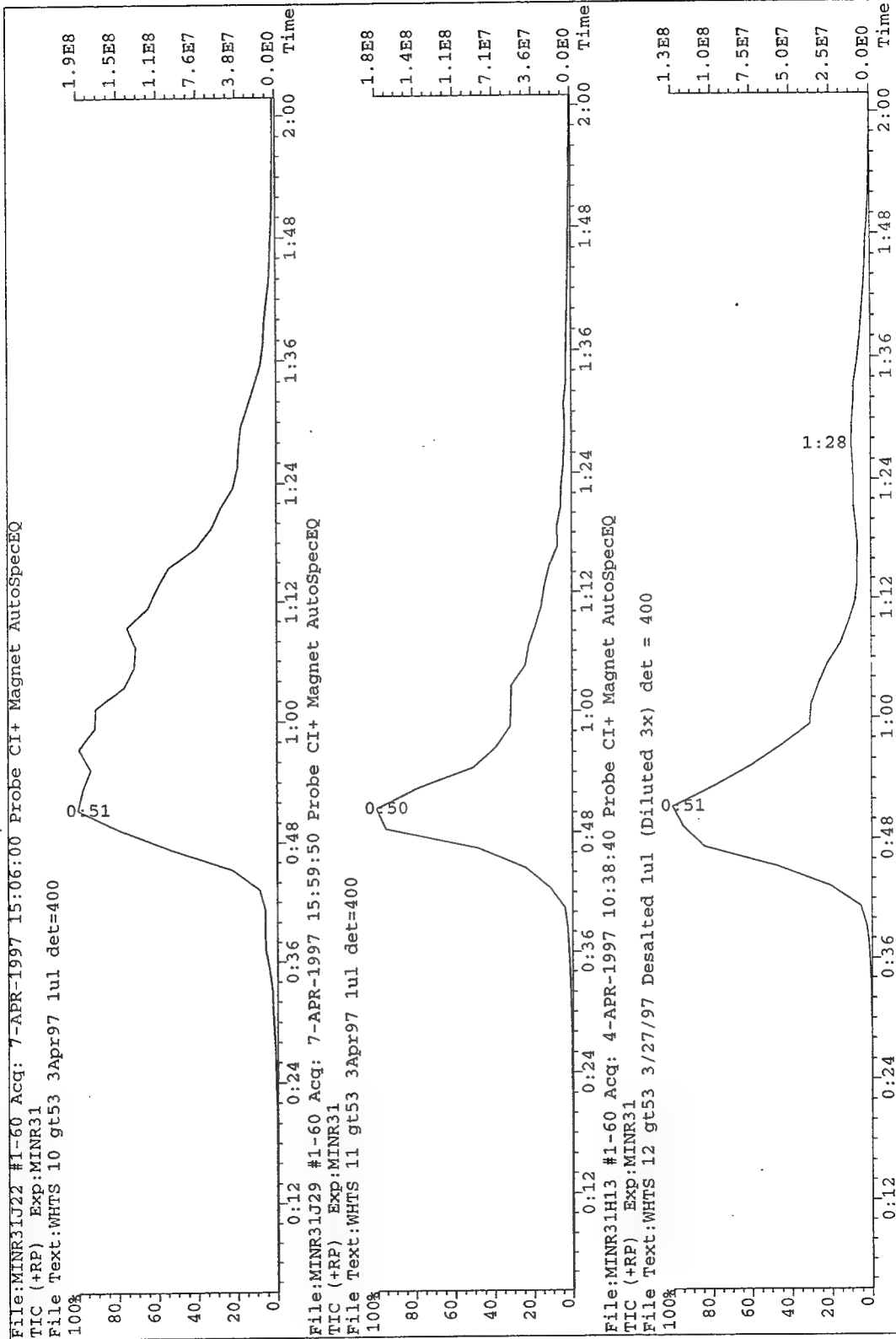


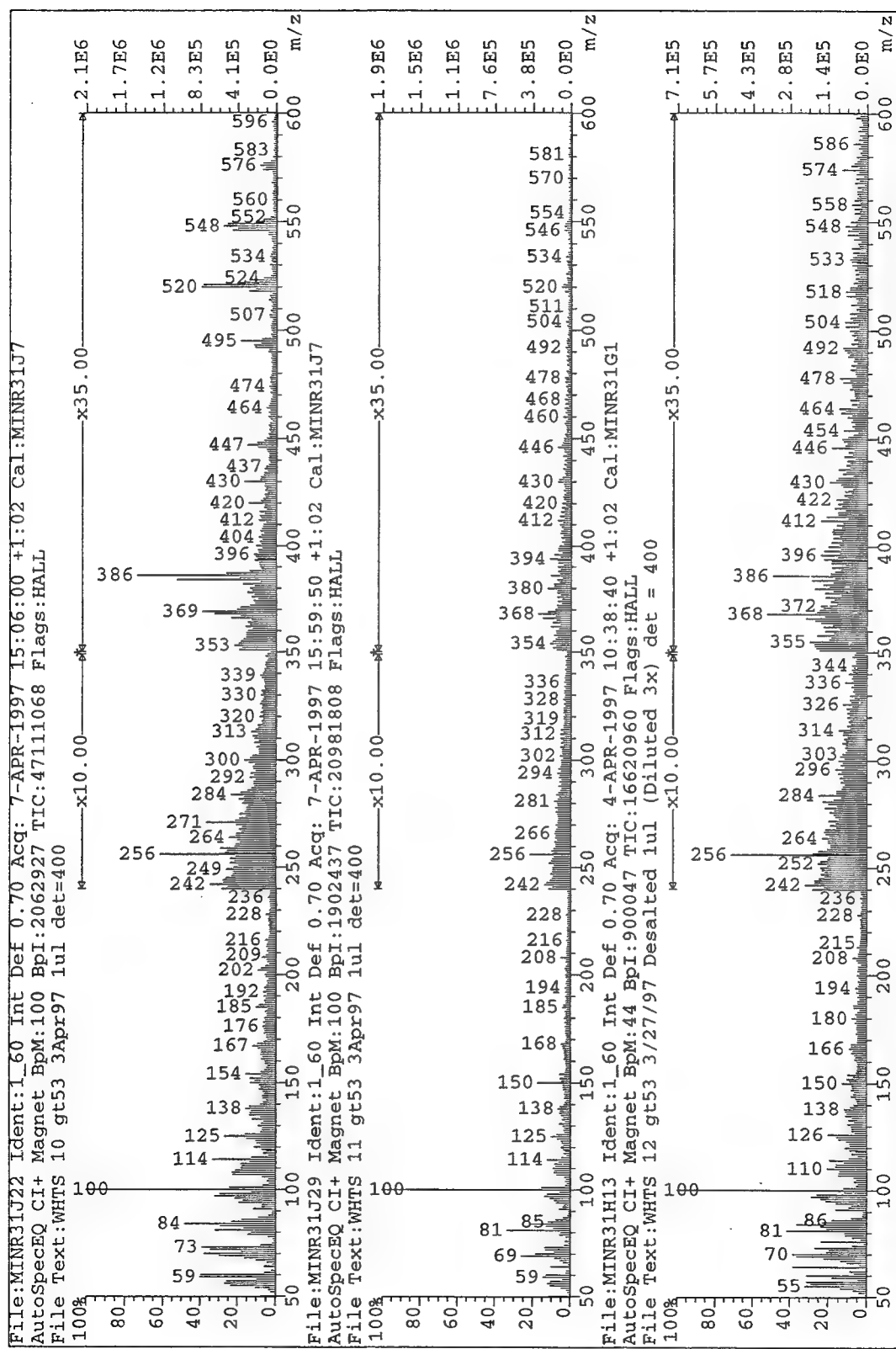
File:MINR31K27 Ident:1_60 Int Def 0.70 Acq: 8-APR-1997 13:19:51 +1:02 Cal:MINR31K4

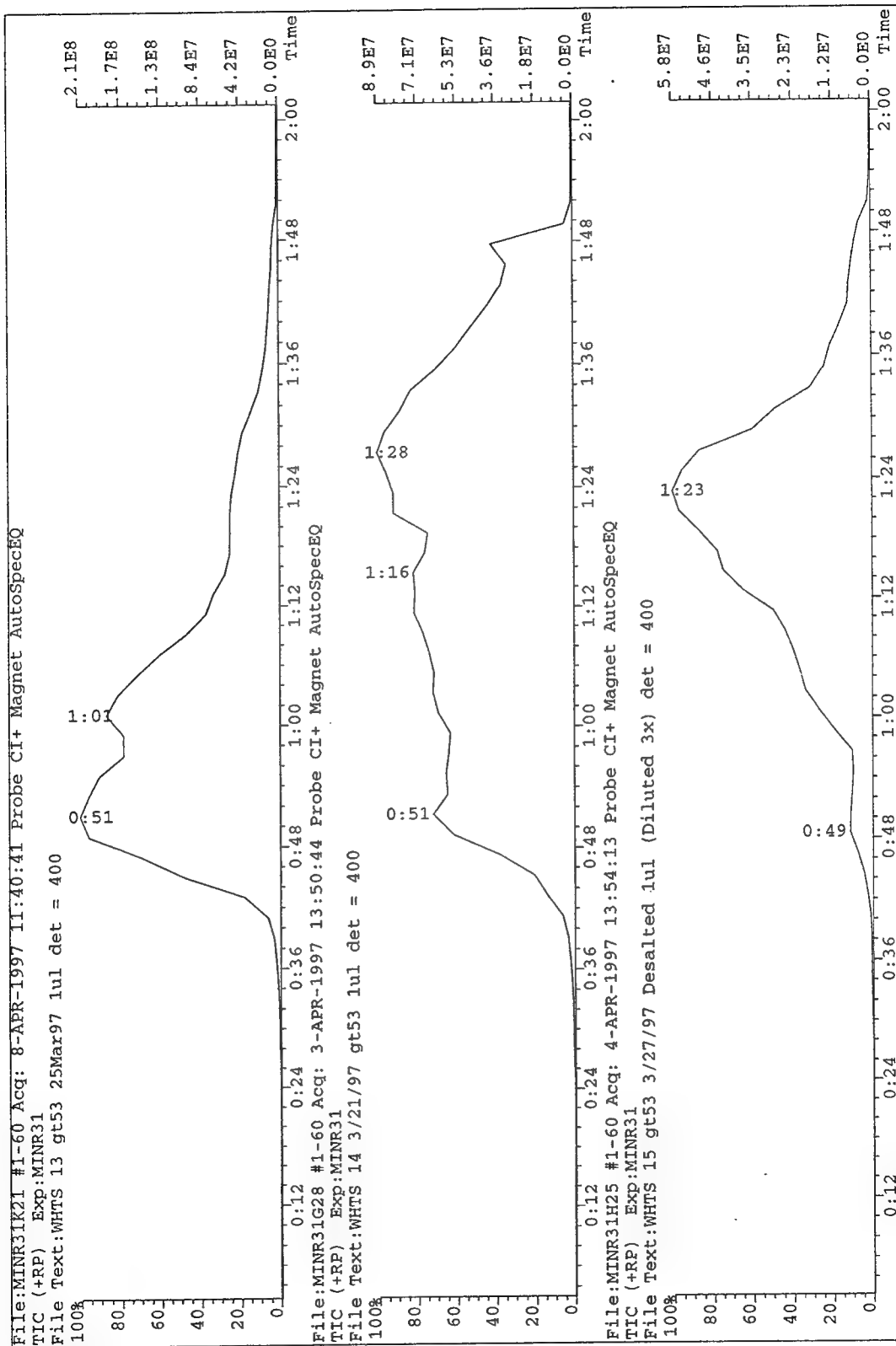
AutoSpecEQ CI+ Magnet BpM:44 BpI:480479 TIC:9752122 Flags:HALL

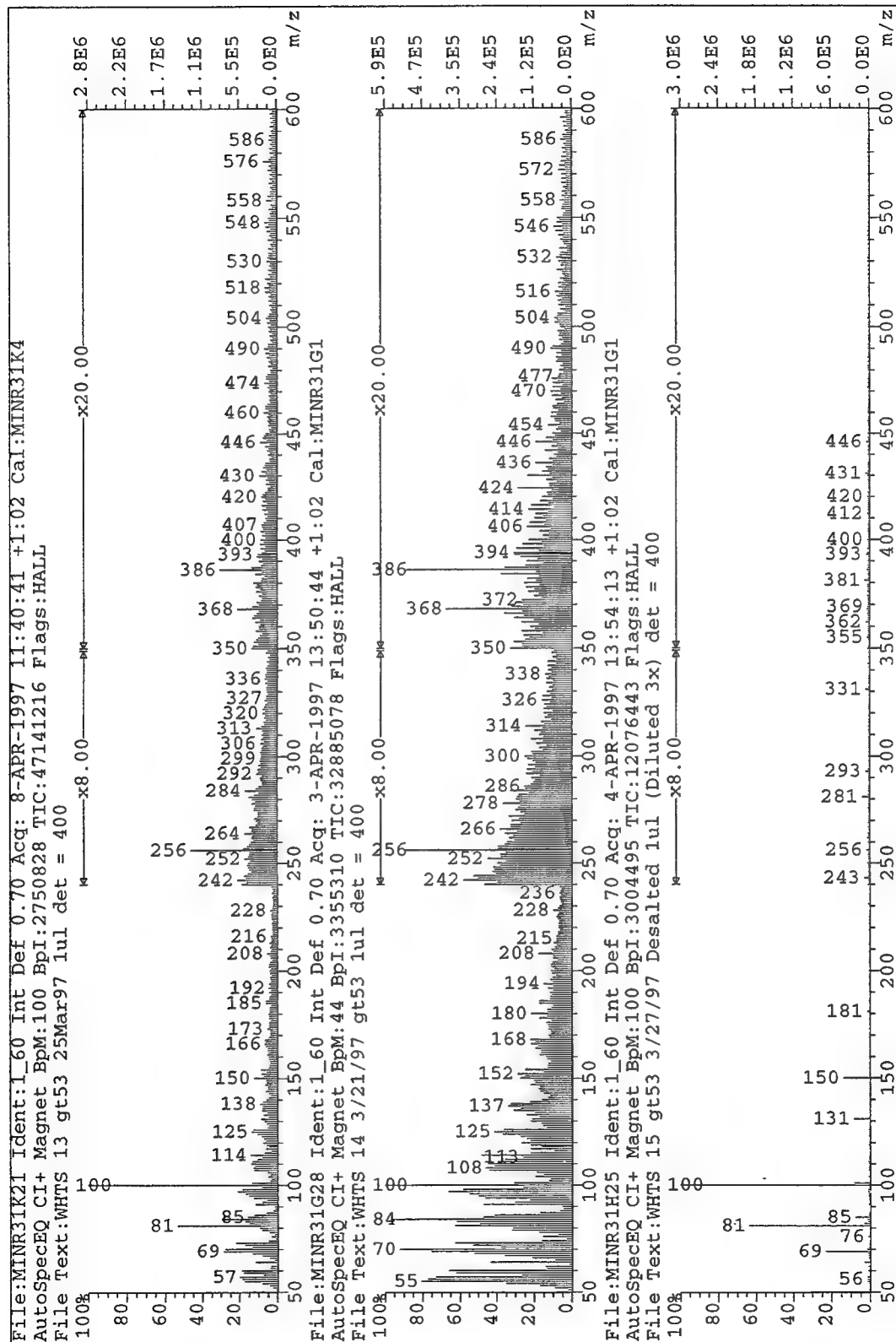
File Text:WHTS 9 gt53 3Apr97 1ul det = 400

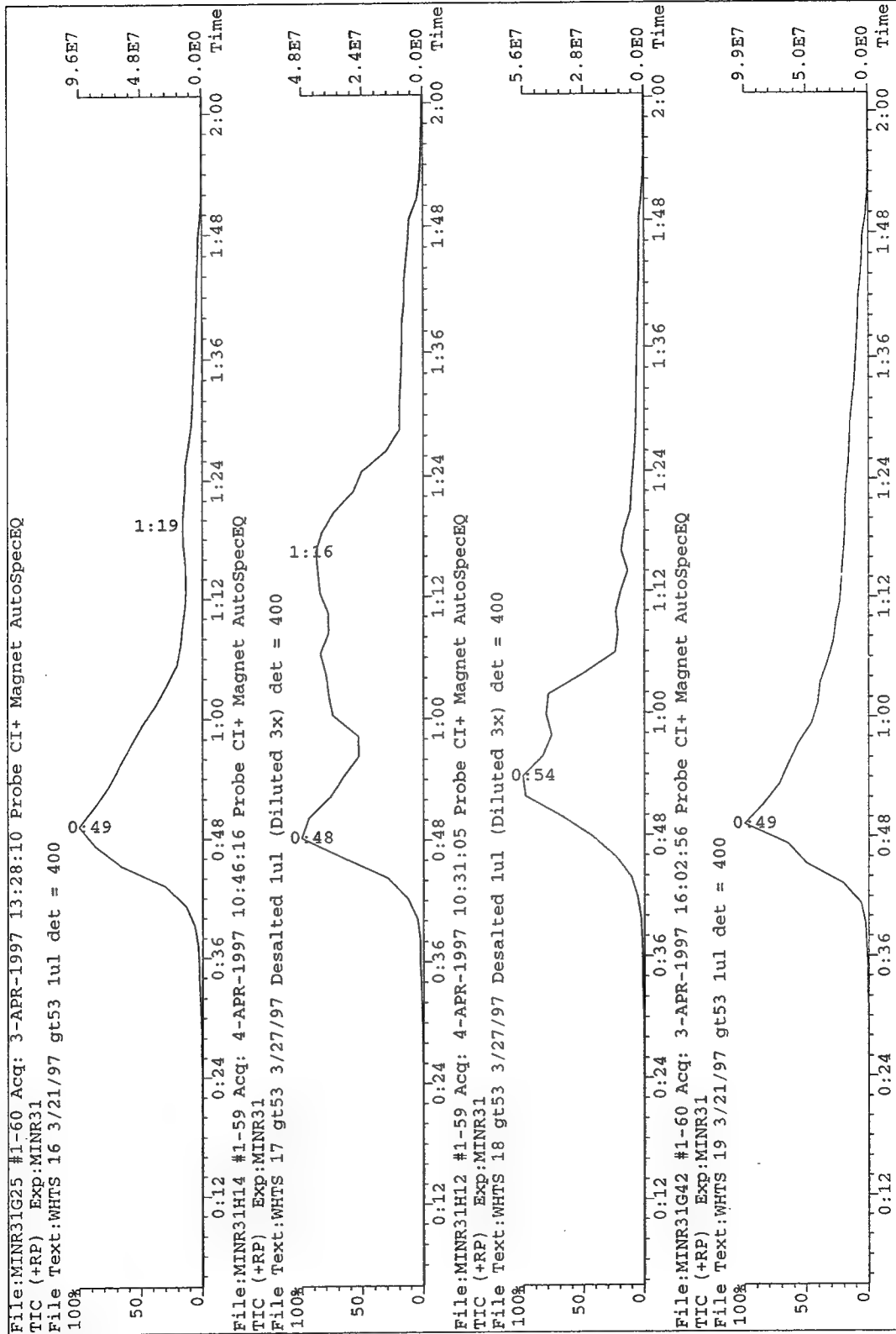


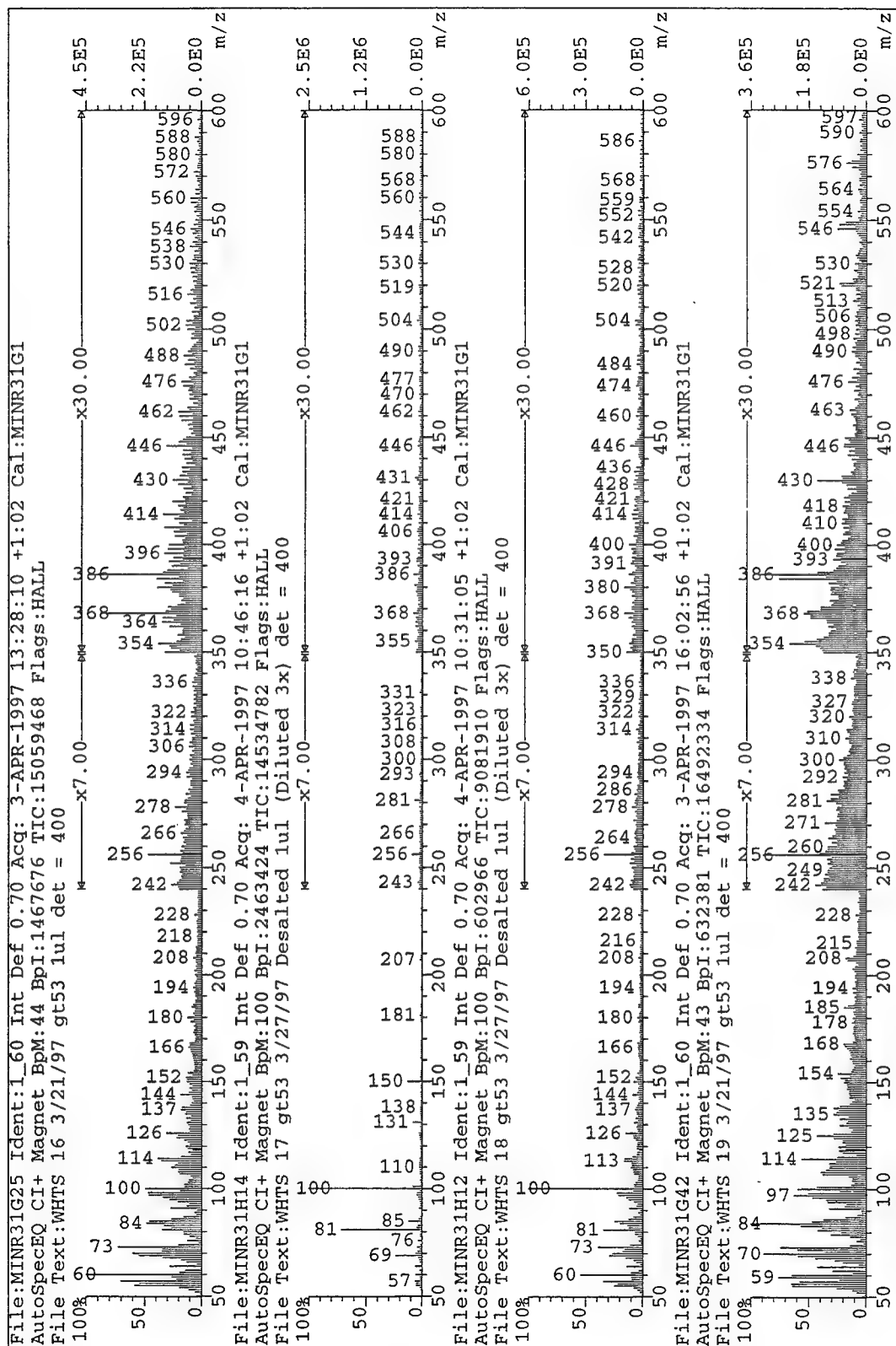


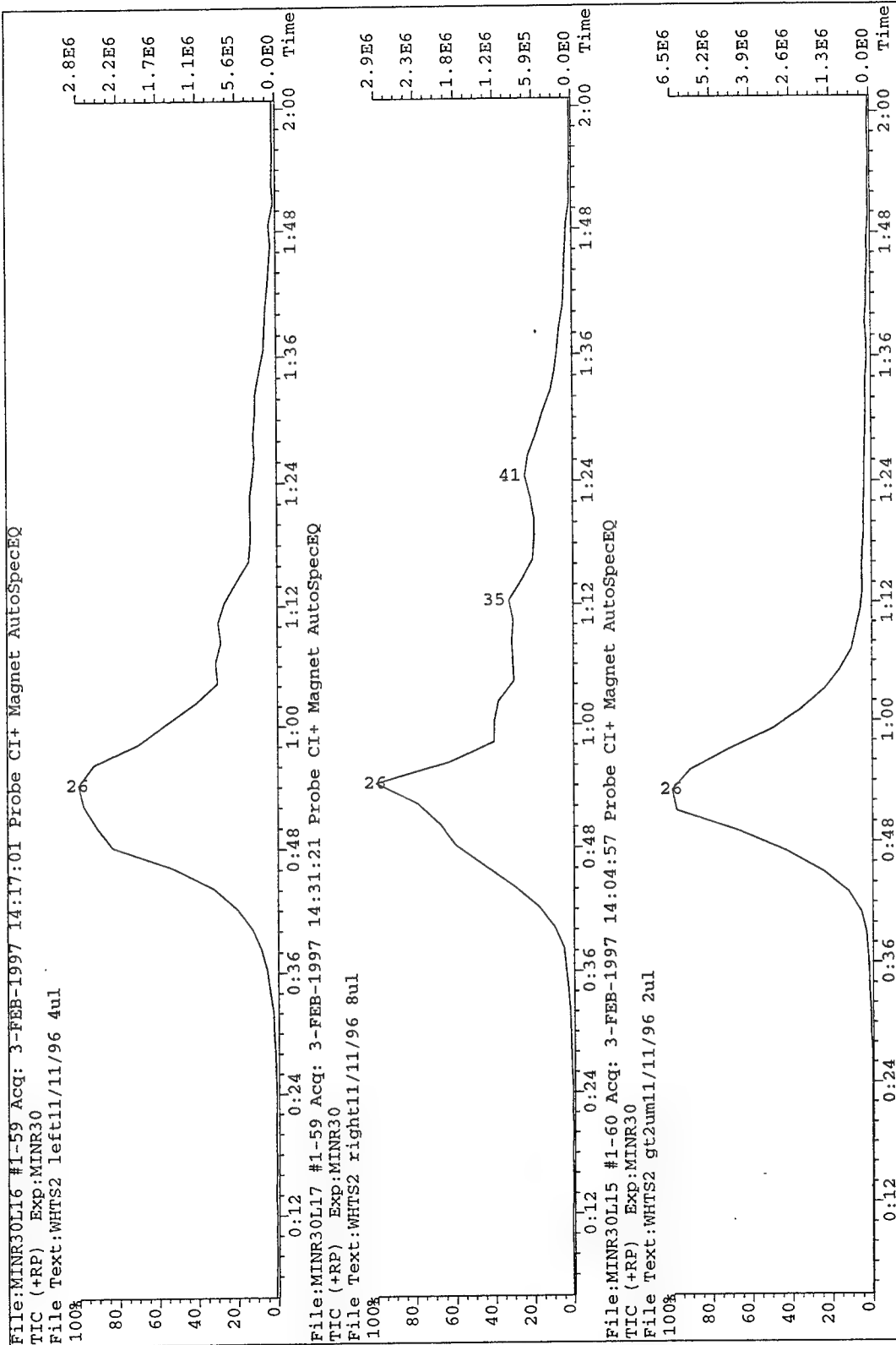


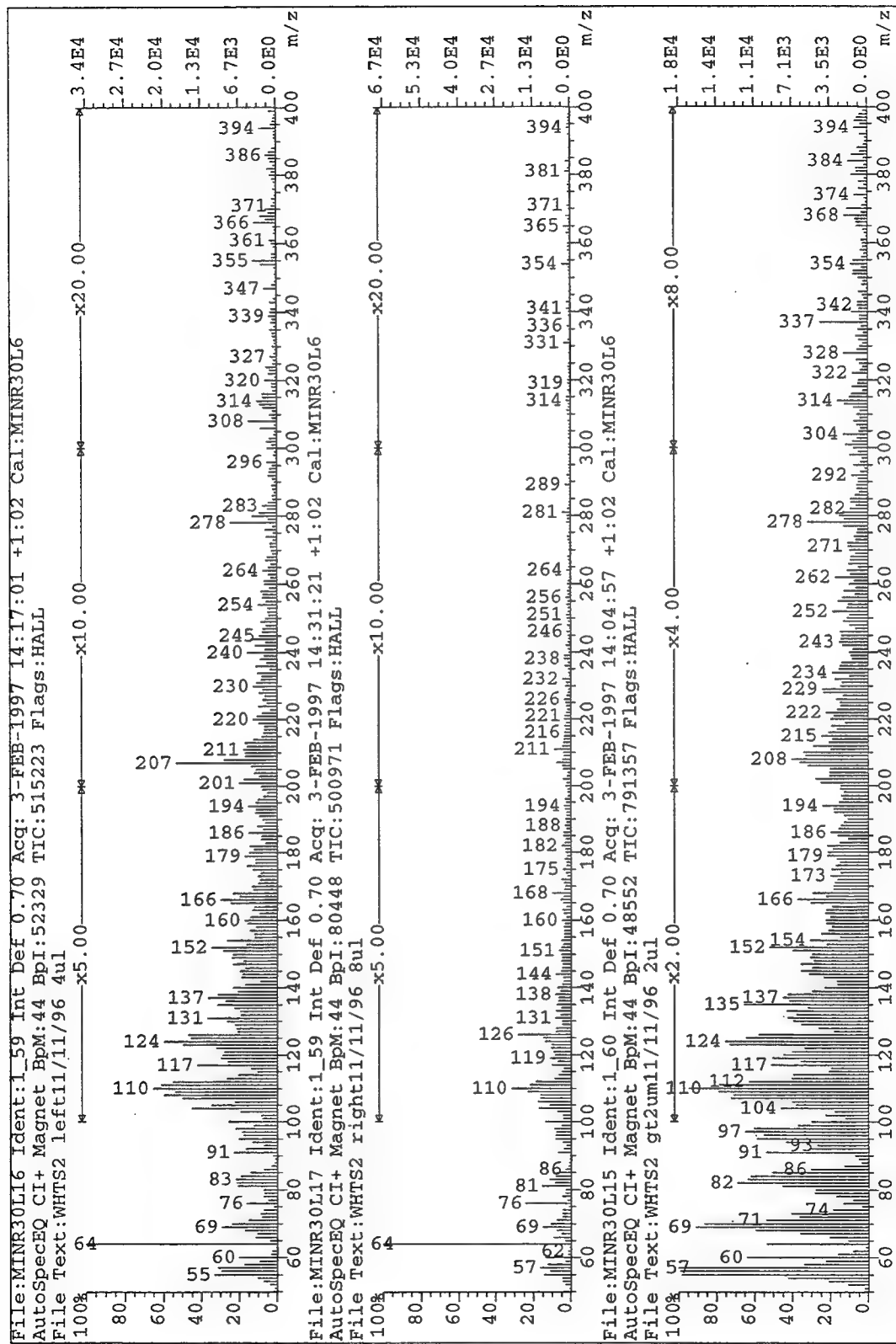








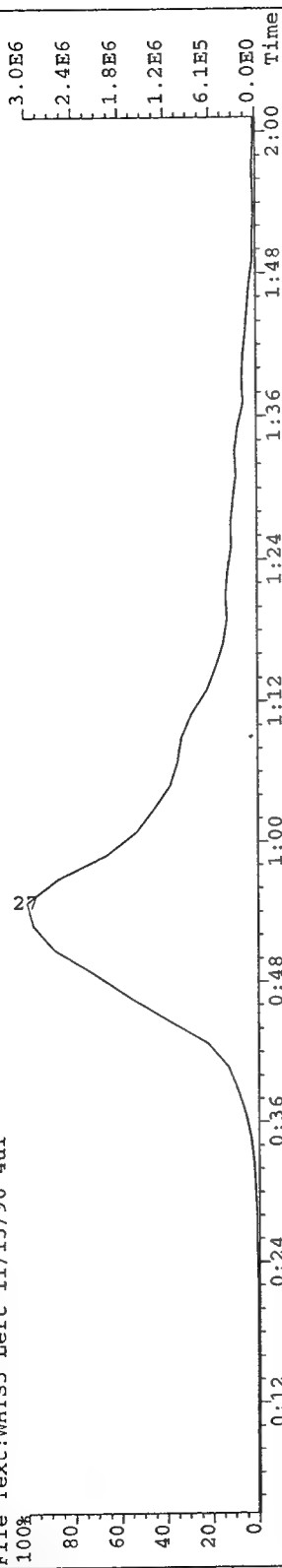




File:MINR30M11 #1-60 Acq: 4-FEB-1997 13:08:07 Probe CI+ Magnet AutoSpecEQ

TIC (+RP) Exp:MINR30

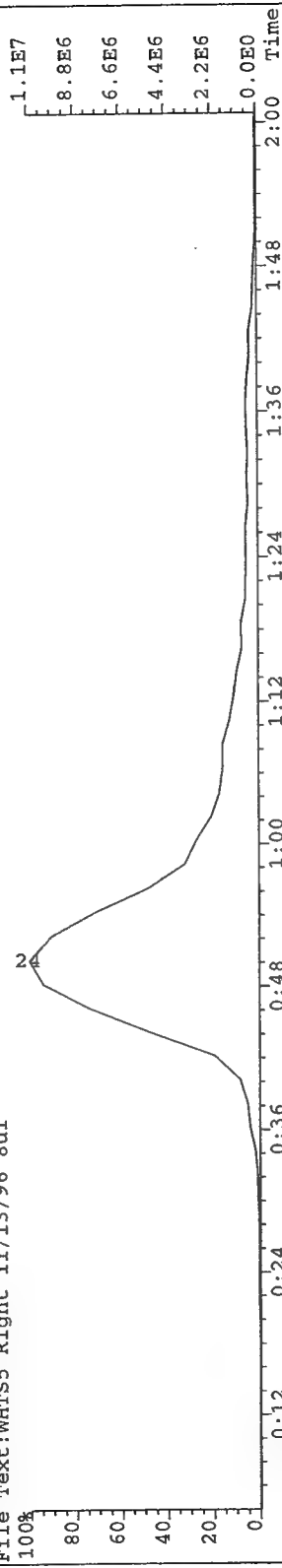
File Text:WHTS5 Left 11/13/96 4ul



File:MINR30M6 #1-59 Acq: 4-FEB-1997 10:59:07 Probe CI+ Magnet AutoSpecEQ

TIC (+RP) Exp:MINR30

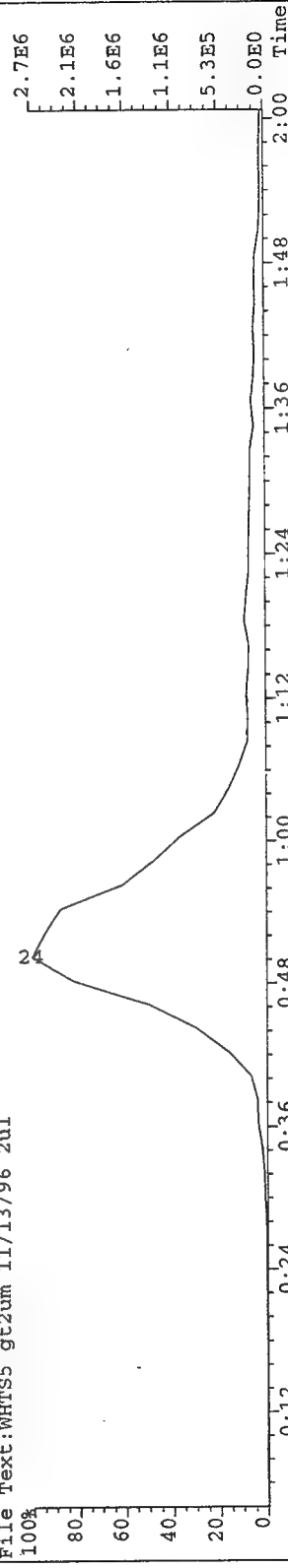
File Text:WHTS5 Right 11/13/96 8ul

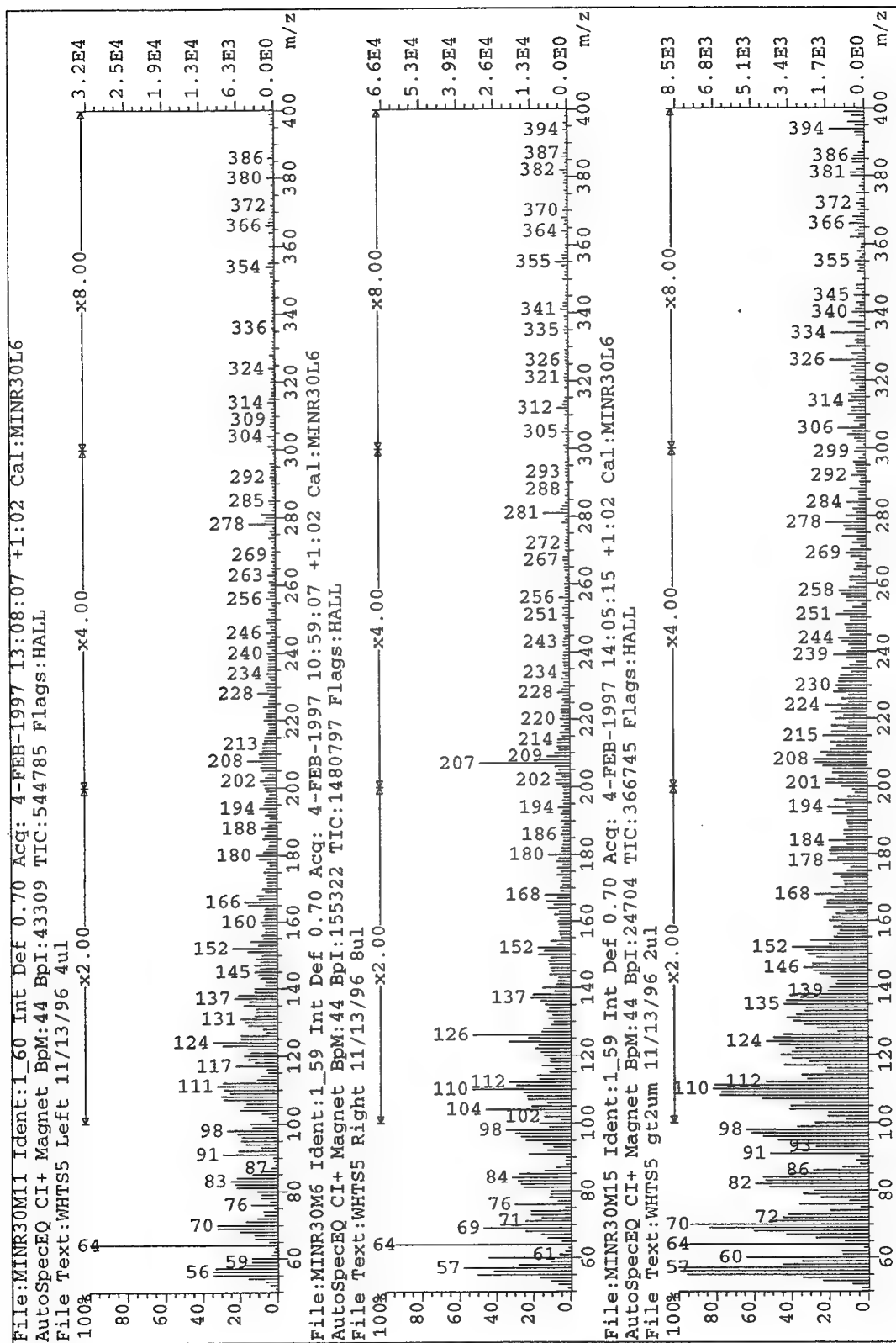


File:MINR30M15 #1-59 Acq: 4-FEB-1997 14:05:15 Probe CI+ Magnet AutoSpecEQ

TIC (+RP) Exp:MINR30

File Text:WHTS5 gt2um 11/13/96 2ul

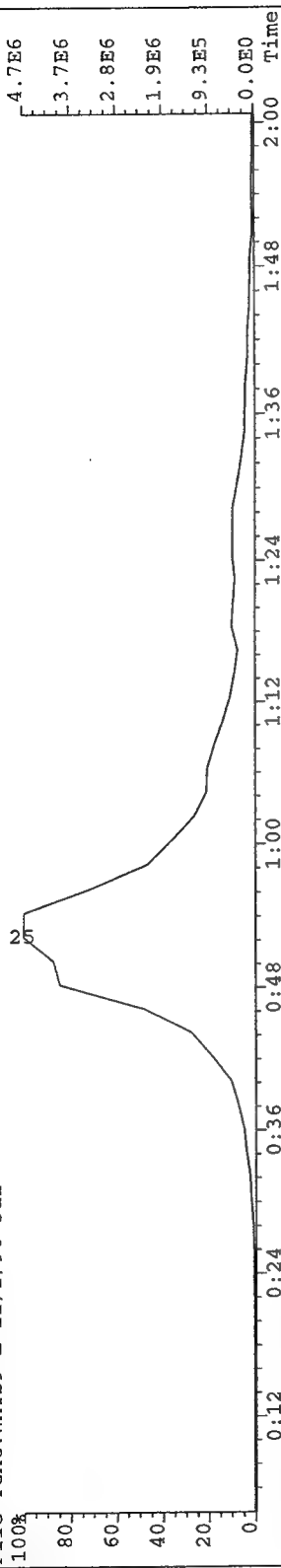




File: MINR30H9 #1-59 Acq: 29-JAN-1997 13:26:01 Probe CI+ Magnet AutoSpecEQ

TIC (+RP) Exp: MINR30

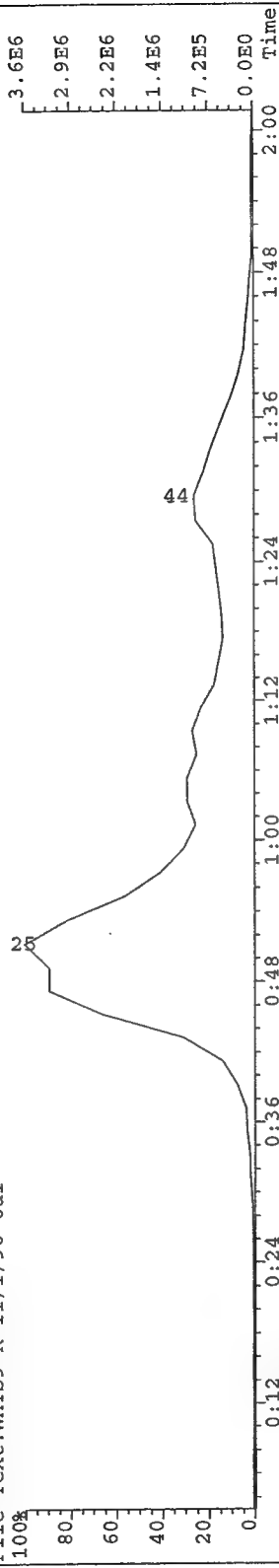
File Text: WHTS9 L 11/1/96 3ul



File: MINR30H6 #1-60 Acq: 29-JAN-1997 11:37:15 Probe CI+ Magnet AutoSpecEQ

TIC (+RP) Exp: MINR30

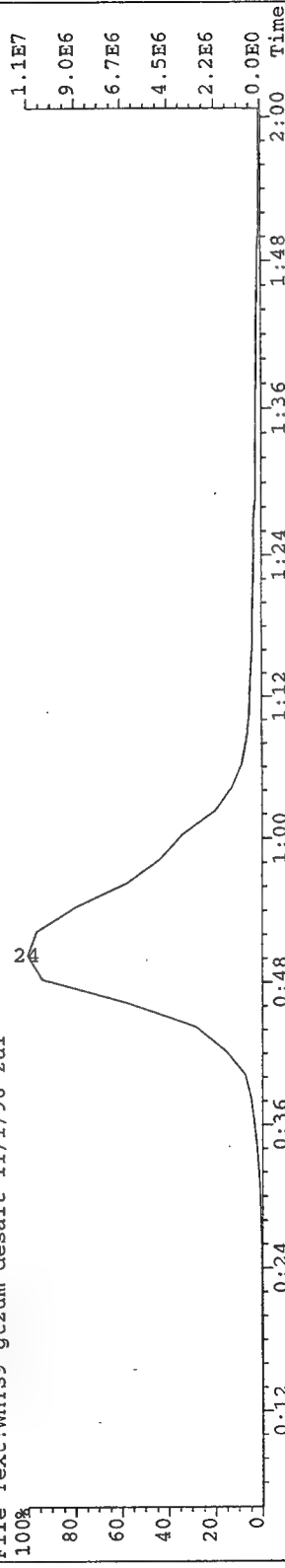
File Text: WHTS9 R 11/1/96 6ul

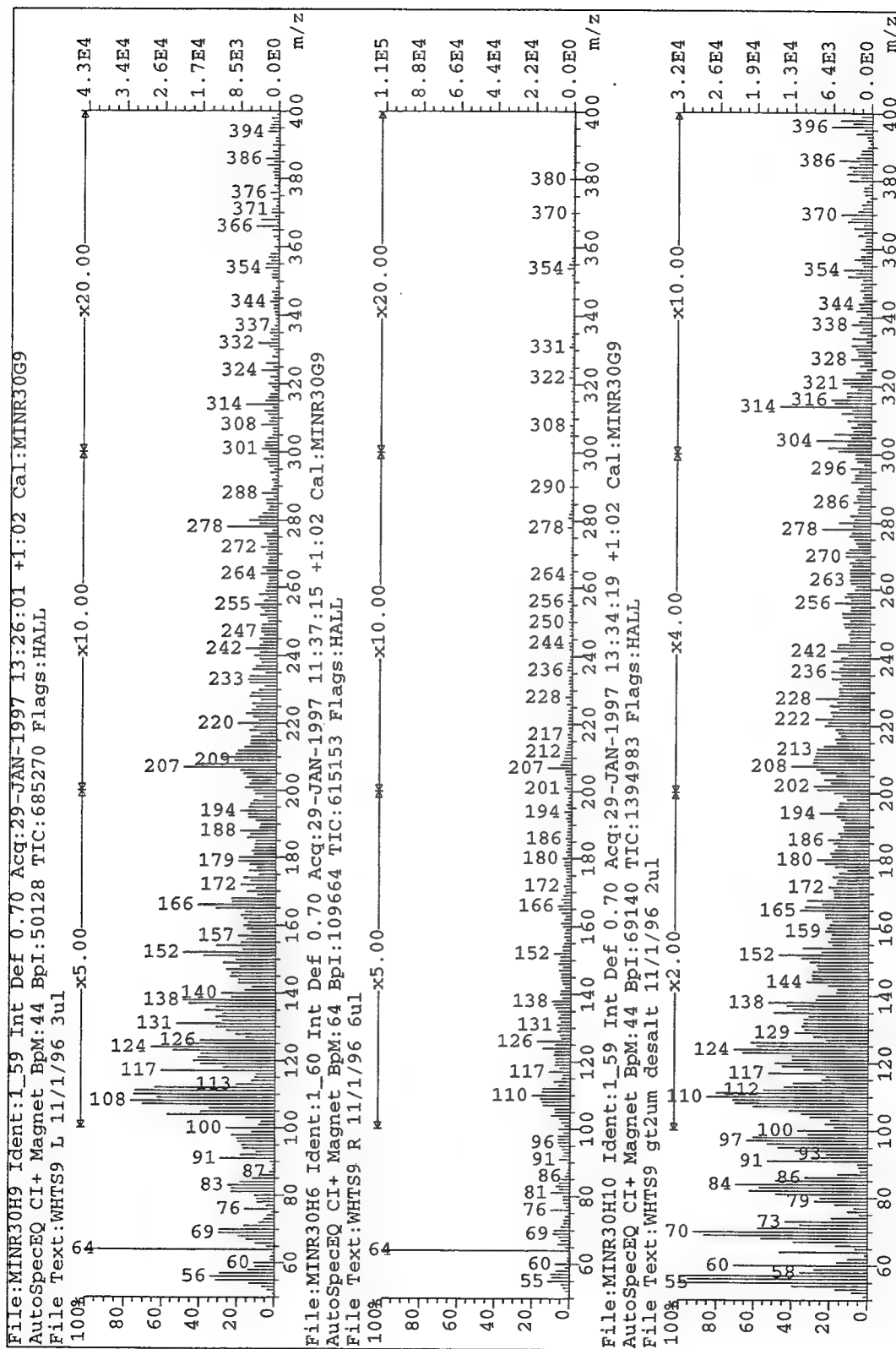


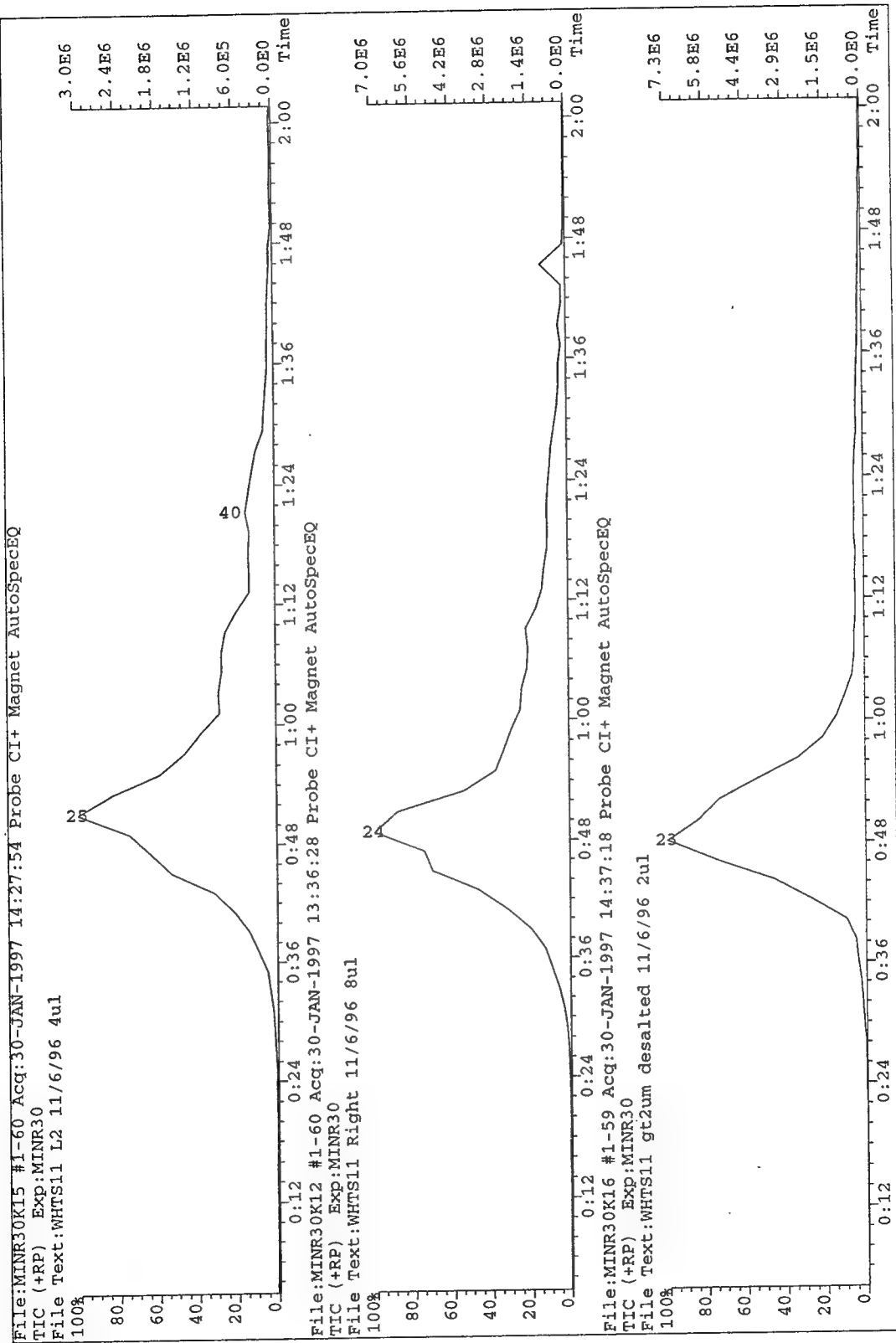
File: MINR30H10 #1-59 Acq: 29-JAN-1997 13:34:19 Probe CI+ Magnet AutoSpecEQ

TIC (+RP) Exp: MINR30

File Text: WHTS9 gt2um desalt 11/1/96 2ul



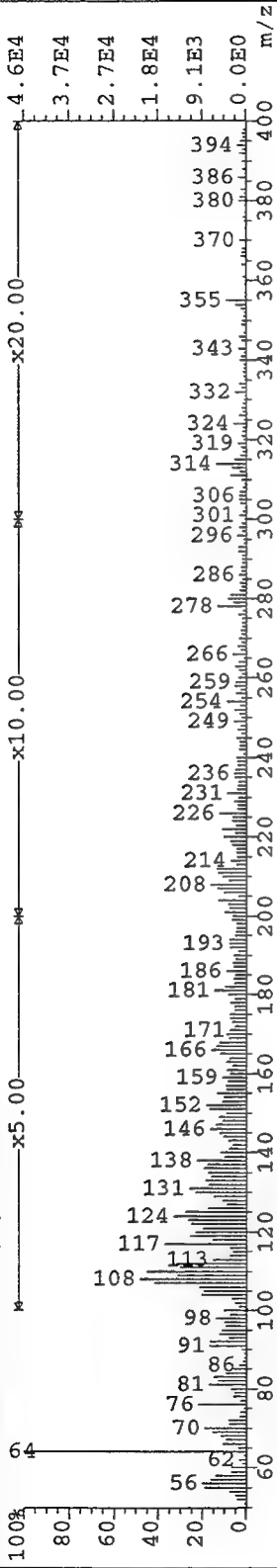




File:MINR30K15 Ident:1_60 Int Def 0.70 Acq:30-JAN-1997 14:27:54 +1:02 Cal:MINR30G9

AutoSpecEQ CI+ Magnet BpM:64 BpI:45662 TIC:449571 Flags:HALL

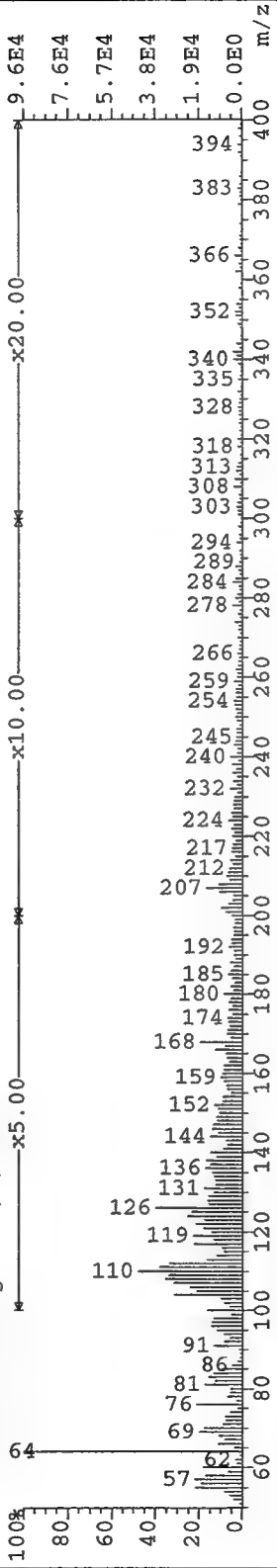
File Text:WHTS11 L2 11/6/96 4ul



File:MINR30K12 Ident:1_60 Int Def 0.70 Acq:30-JAN-1997 13:36:28 +1:02 Cal:MINR30G9

AutoSpecEQ CI+ Magnet BpM:44 BpI:132147 TIC:1016070 Flags:HALL

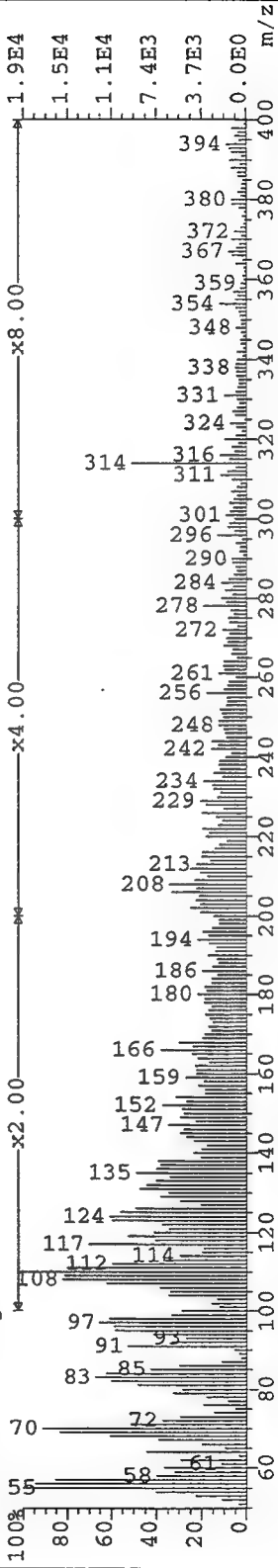
File Text:WHTS11 Right 11/6/96 8ul

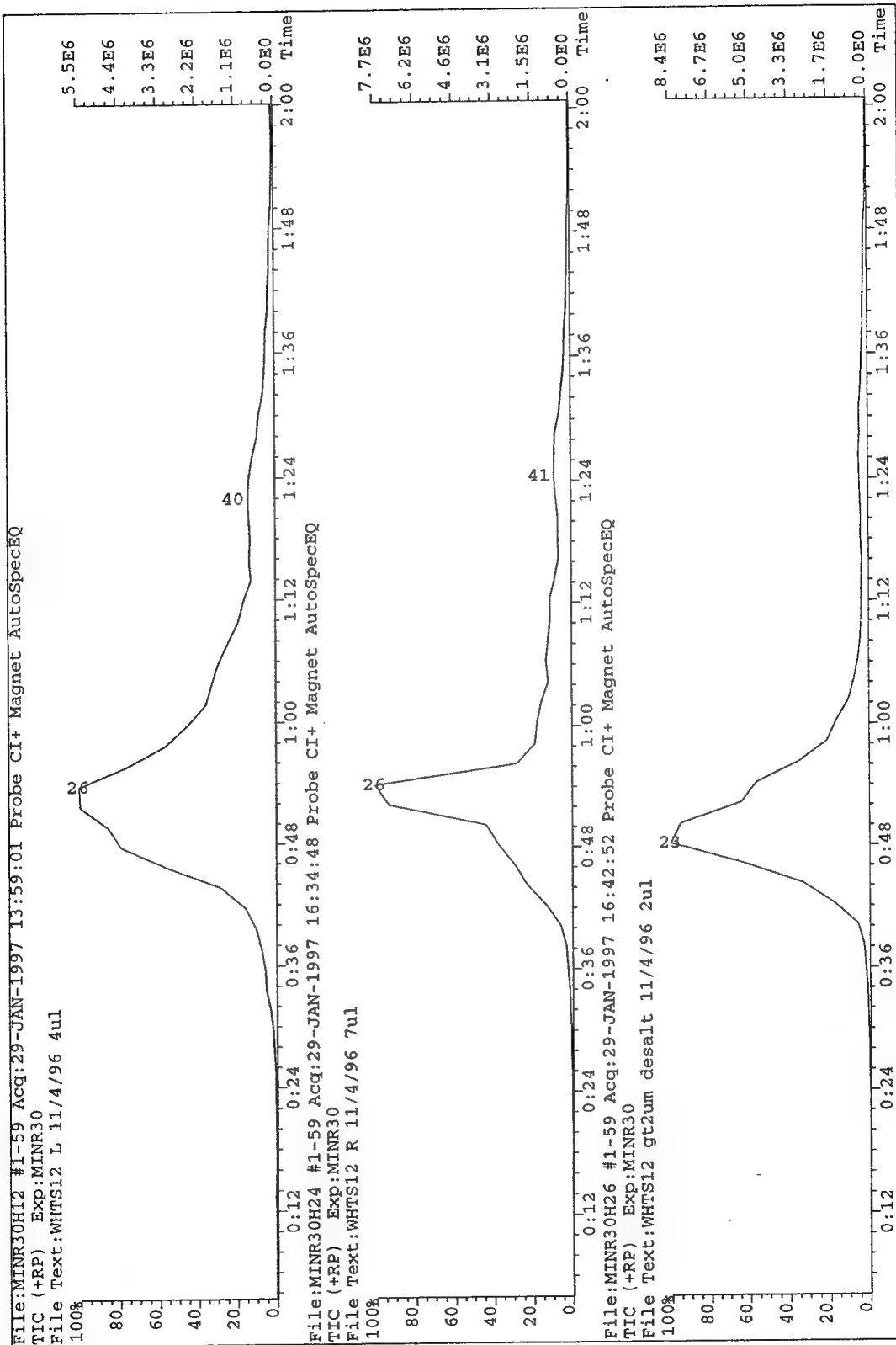


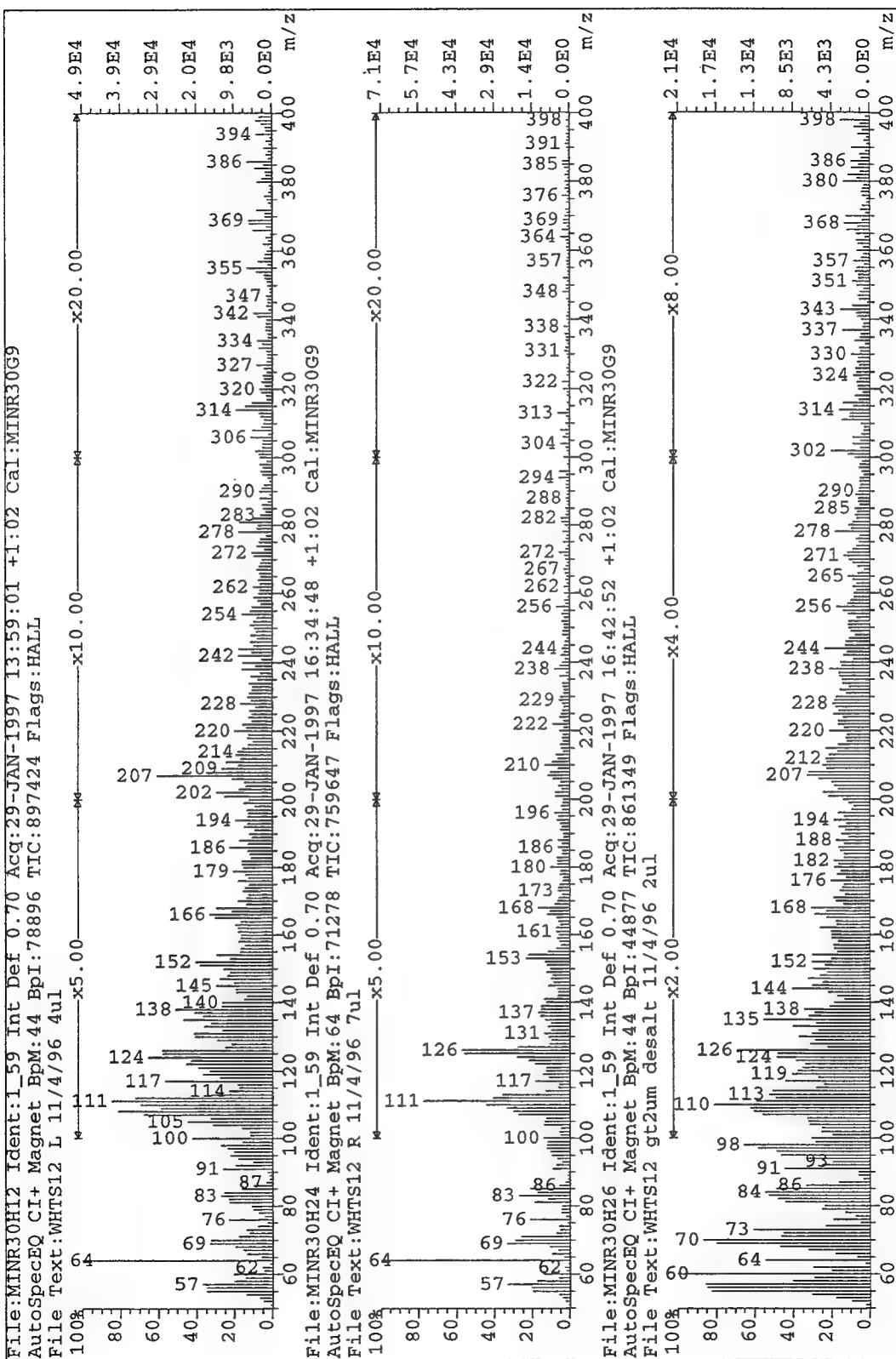
File:MINR30K16 Ident:1_59 Int Def 0.70 Acq:30-JAN-1997 14:37:18 +1:02 Cal:MINR30G9

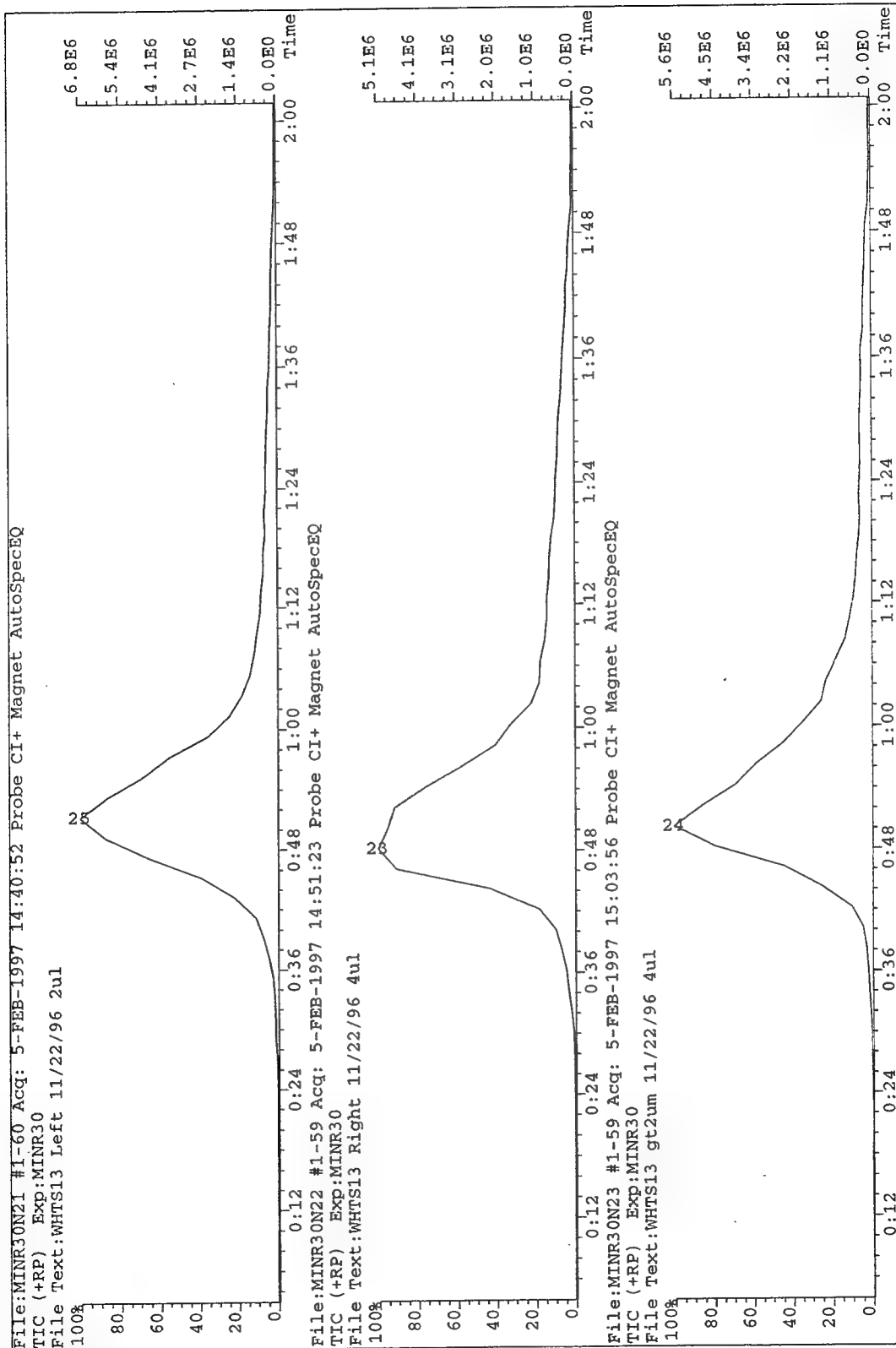
AutoSpecEQ CI+ Magnet BpM:44 BpI:43461 TIC:793586 Flags:HALL

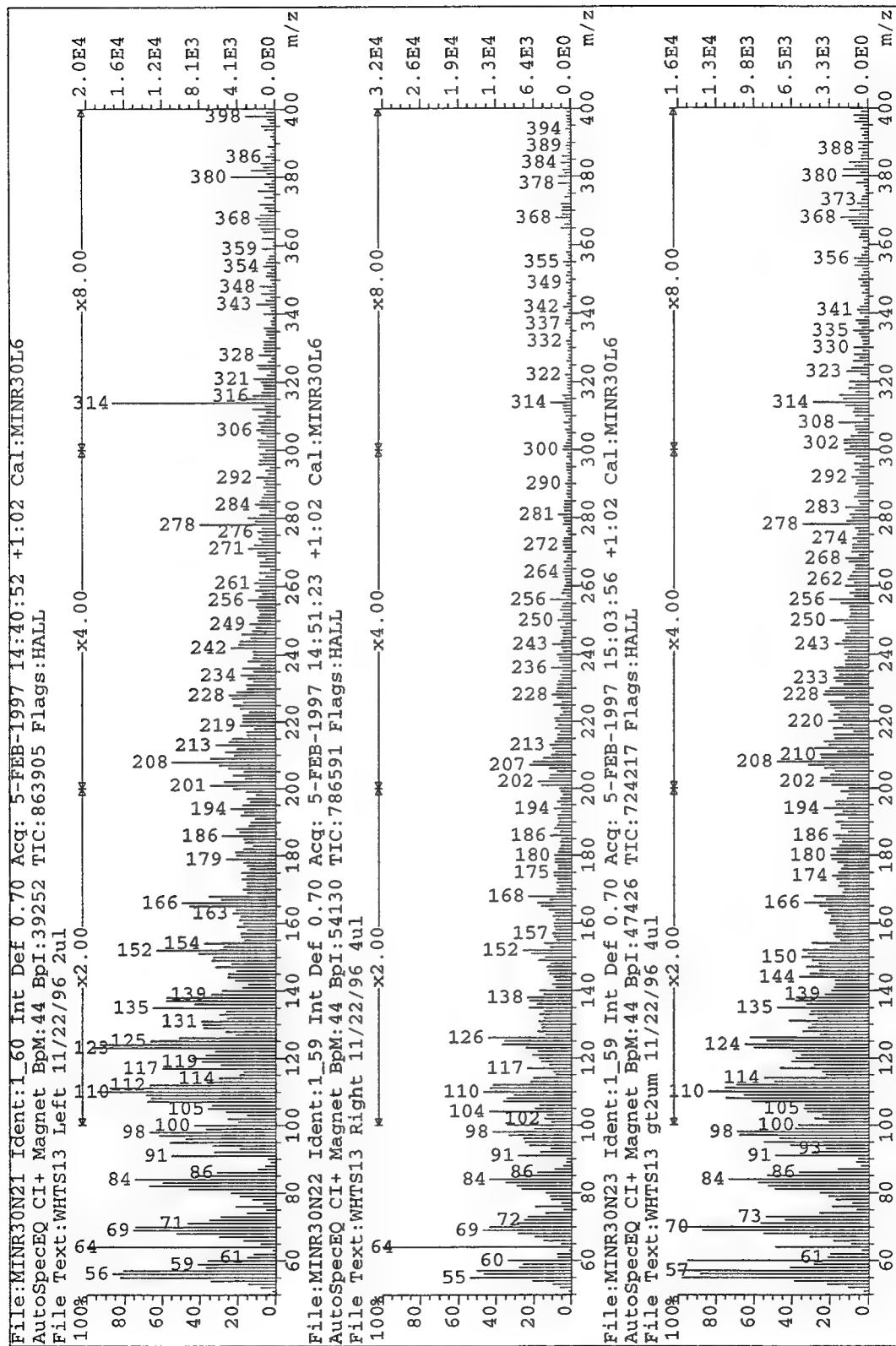
File Text:WHTS11 gt2um desalted 11/6/96 2ul

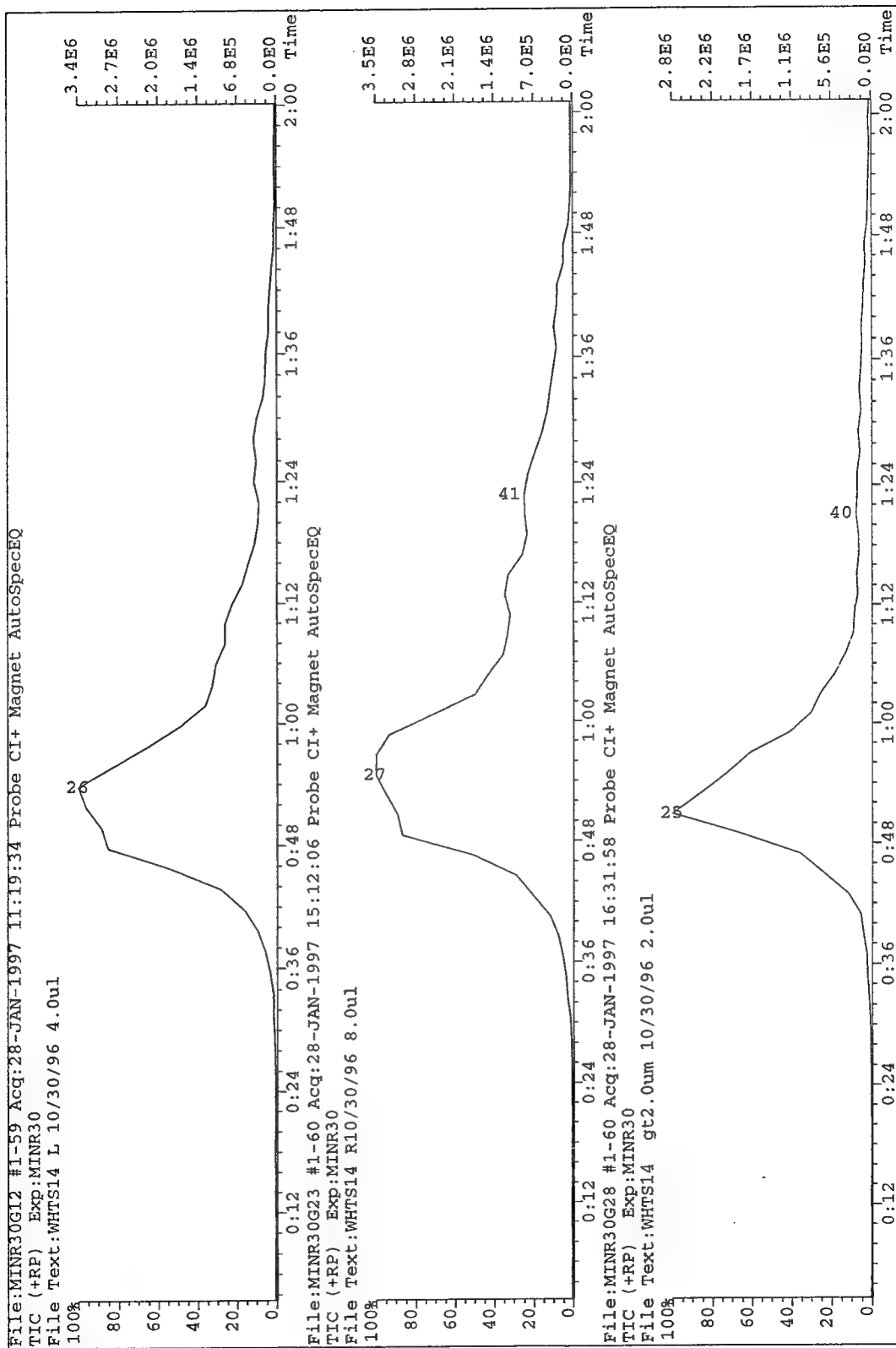


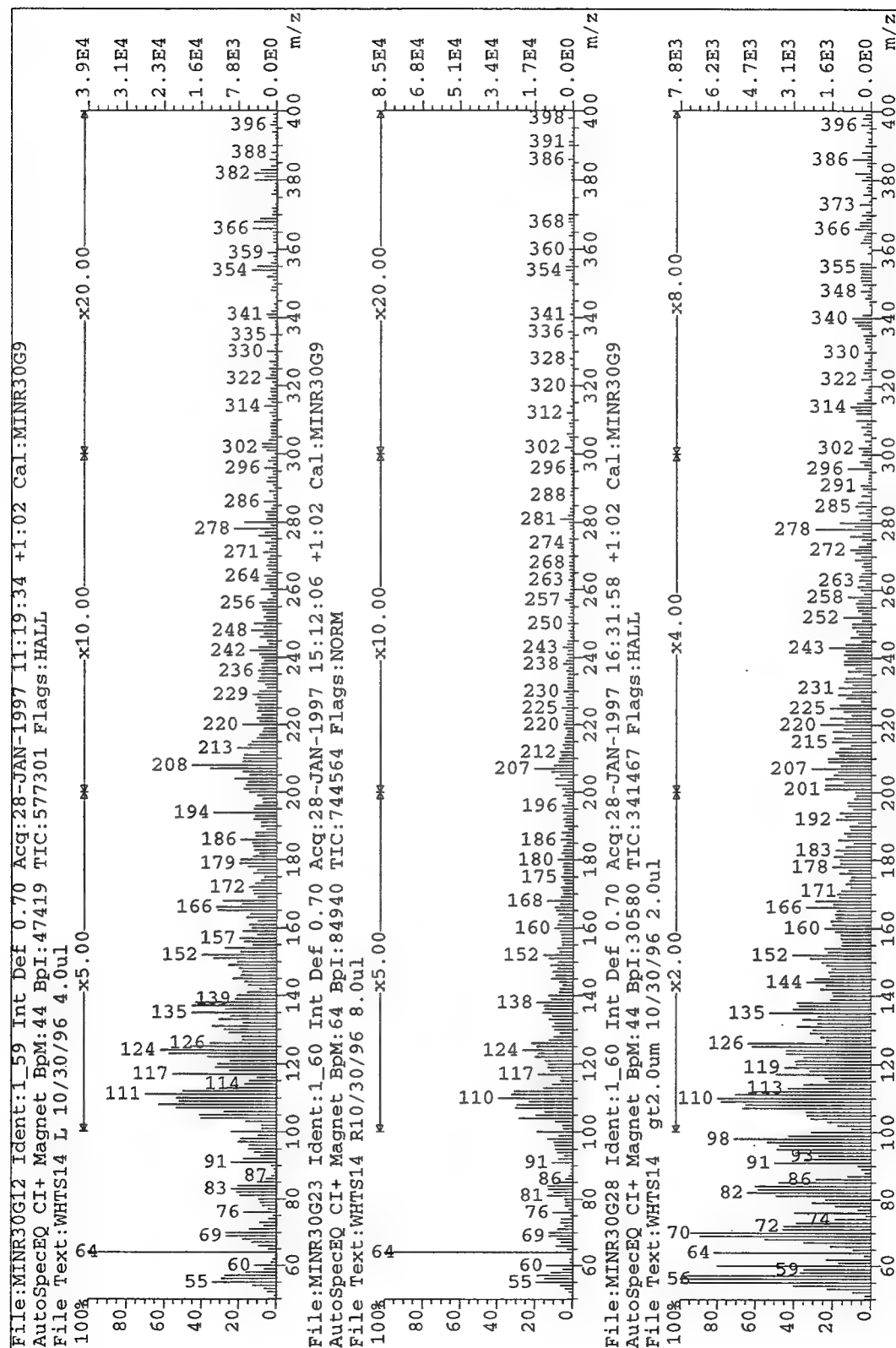








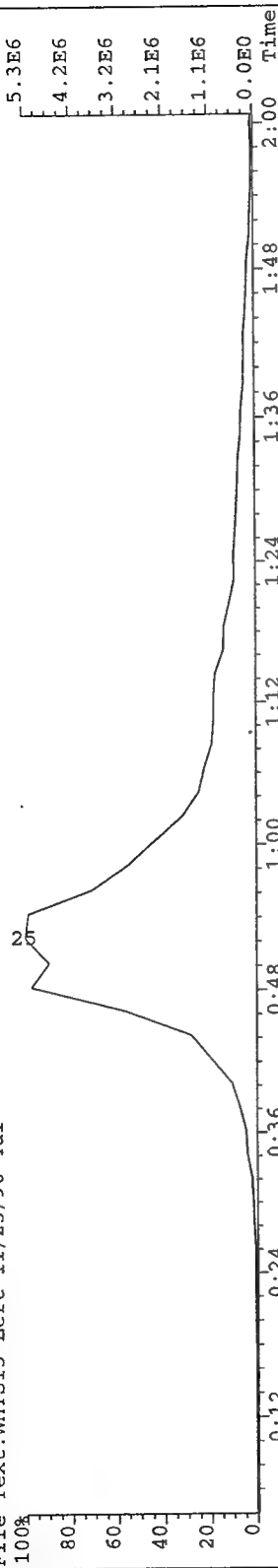




File:MINR30N13 #1-59 Acq: 5-FEB-1997 13:28:19 Probe CI+ Magnet AutoSpecEQ

TIC (+RP) Exp:MINR30

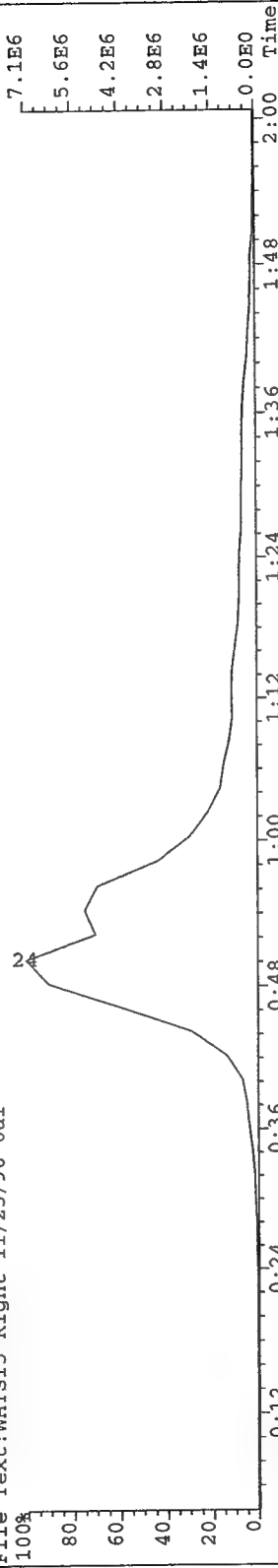
File Text:WHTS15 Left 11/25/96 4ul



File:MINR30N14 #1-59 Acq: 5-FEB-1997 13:42:16 Probe CI+ Magnet AutoSpecEQ

TIC (+RP) Exp:MINR30

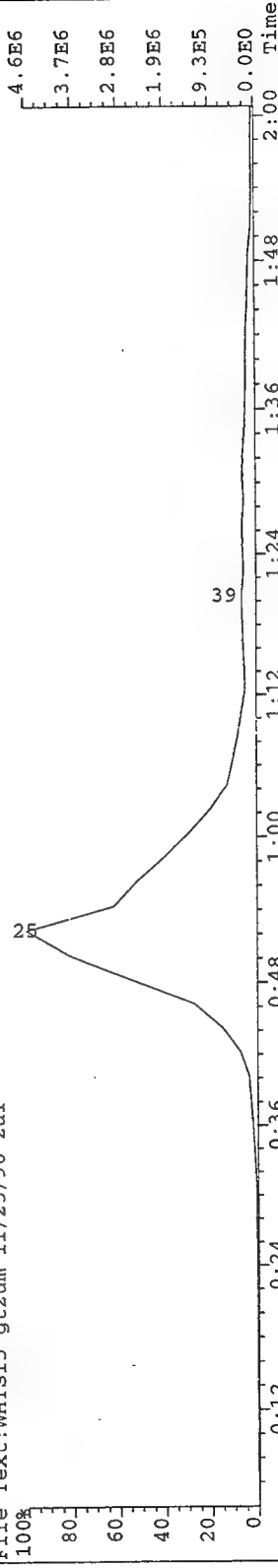
File Text:WHTS15 Right 11/25/96 6ul

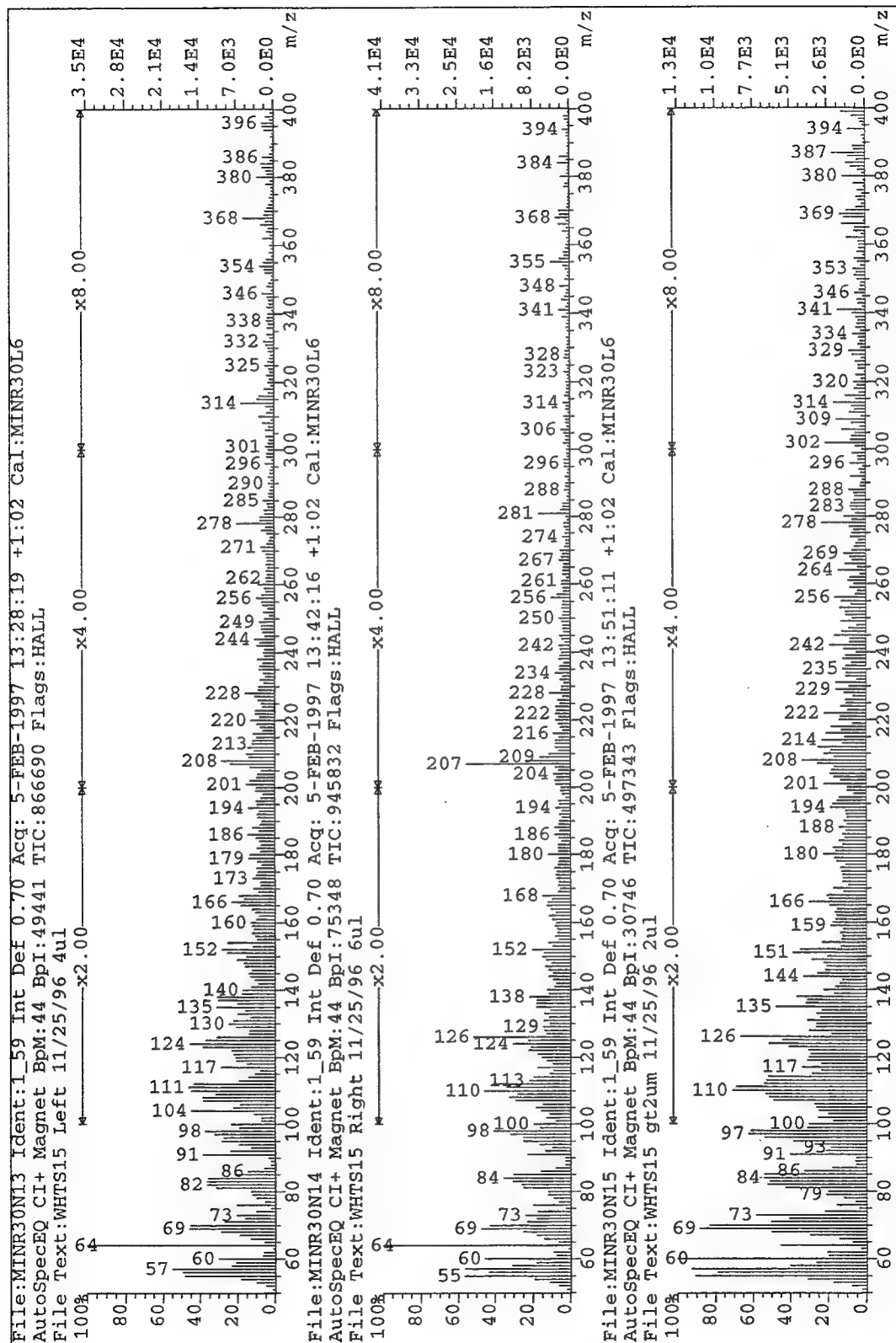


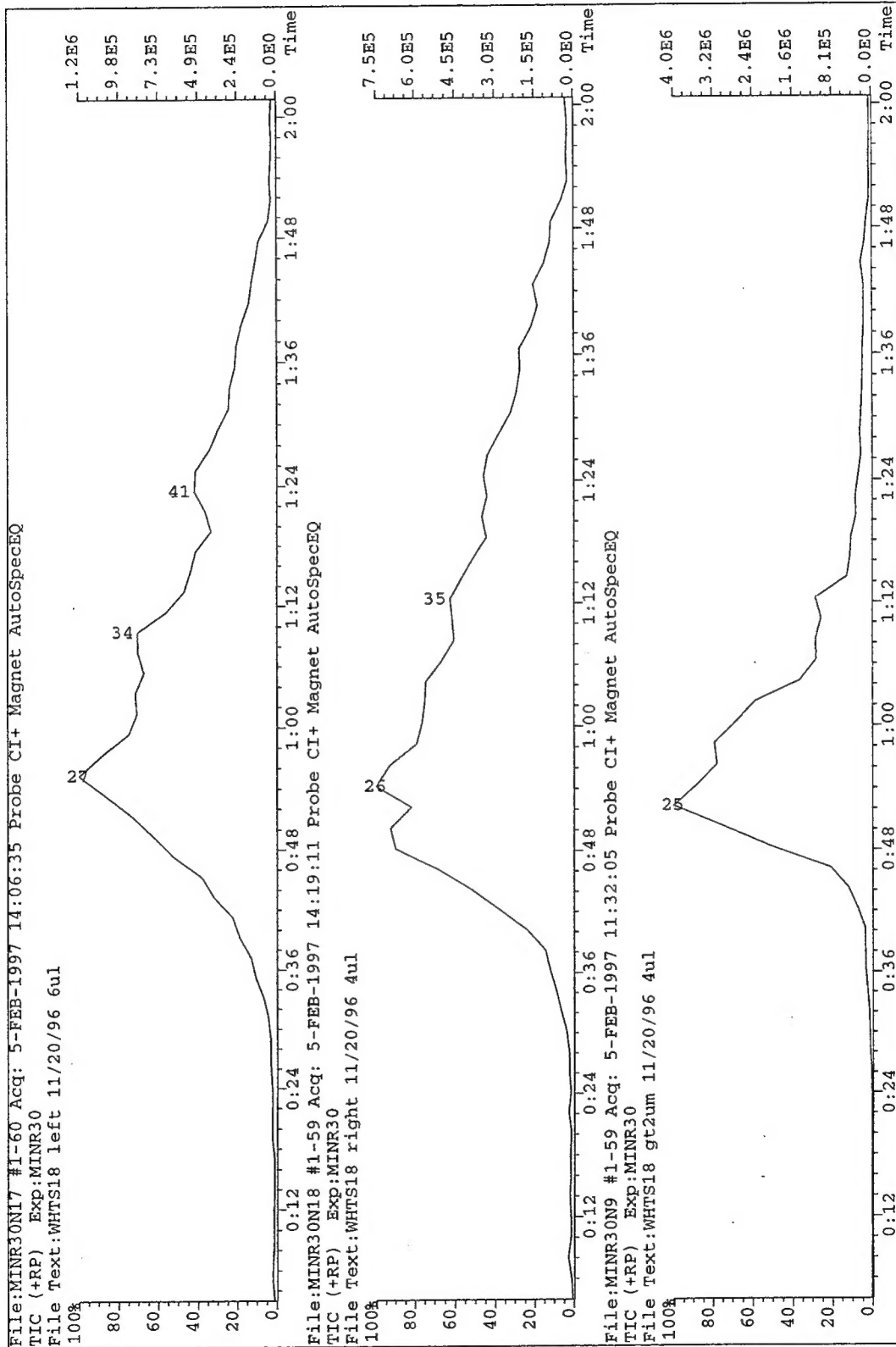
File:MINR30N15 #1-59 Acq: 5-FEB-1997 13:51:11 Probe CI+ Magnet AutoSpecEQ

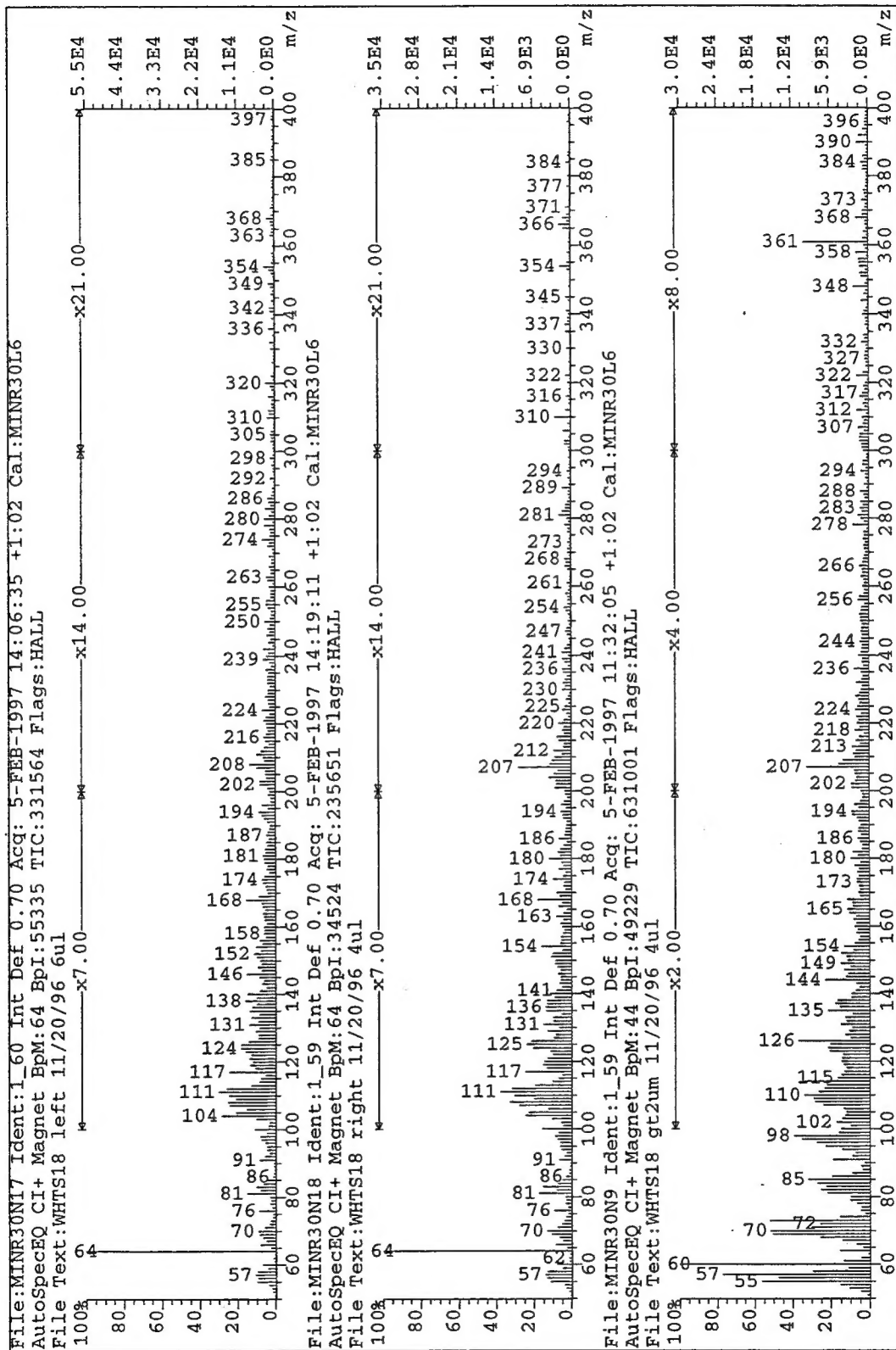
TIC (+RP) Exp:MINR30

File Text:WHTS15 gt2um 11/25/96 2ul









DOCUMENT LIBRARY

Distribution List for Technical Report Exchange – February 1996

University of California, San Diego
SIO Library 0175C
9500 Gilman Drive
La Jolla, CA 92093-0175

Hancock Library of Biology & Oceanography
Alan Hancock Laboratory
University of Southern California
University Park
Los Angeles, CA 90089-0371

Gifts & Exchanges
Library
Bedford Institute of Oceanography
P.O. Box 1006
Dartmouth, NS, B2Y 4A2, CANADA

NOAA/EDIS Miami Library Center
4301 Rickenbacker Causeway
Miami, FL 33149

Research Library
U.S. Army Corps of Engineers
Waterways Experiment Station
3909 Halls Ferry Road
Vicksburg, MS 39180-6199

Institute of Geophysics
University of Hawaii
Library Room 252
2525 Correa Road
Honolulu, HI 96822

Marine Resources Information Center
Building E38-320
MIT
Cambridge, MA 02139

Library
Lamont-Doherty Geological Observatory
Columbia University
Palisades, NY 10964

Library
Serials Department
Oregon State University
Corvallis, OR 97331

Pell Marine Science Library
University of Rhode Island
Narragansett Bay Campus
Narragansett, RI 02882

Working Collection
Texas A&M University
Dept. of Oceanography
College Station, TX 77843

Fisheries-Oceanography Library
151 Oceanography Teaching Bldg.
University of Washington
Seattle, WA 98195

Library
R.S.M.A.S.
University of Miami
4600 Rickenbacker Causeway
Miami, FL 33149

Maury Oceanographic Library
Naval Oceanographic Office
Building 1003 South
1002 Balch Blvd.
Stennis Space Center, MS, 39522-5001

Library
Institute of Ocean Sciences
P.O. Box 6000
Sidney, B.C. V8L 4B2
CANADA

National Oceanographic Library
Southampton Oceanography Centre
European Way
Southampton SO14 3ZH
UK

The Librarian
CSIRO Marine Laboratories
G.P.O. Box 1538
Hobart, Tasmania
AUSTRALIA 7001

Library
Proudman Oceanographic Laboratory
Bidston Observatory
Birkenhead
Merseyside L43 7 RA
UNITED KINGDOM

IFREMER
Centre de Brest
Service Documentation - Publications
BP 70 29280 PLOUZANE
FRANCE

REPORT DOCUMENTATION PAGE	1. REPORT NO. MIT/WHOI 98-08	2.	3. Recipient's Accession No.
4. Title and Subtitle Compositional Heterogeneity Within Oceanic POM: A Study Using Flow Cytometry and Mass Spectrometry			5. Report Date June 1998
7. Author(s) Elizabeth C. Minor			6.
9. Performing Organization Name and Address MIT/WHOI Joint Program in Oceanography/Applied Ocean Science & Engineering			8. Performing Organization Rept. No.
12. Sponsoring Organization Name and Address National Science Foundation, Department of Energy and Dutch Organization of Scientific Research			10. Project/Task/Work Unit No. MIT/WHOI 98-08
			11. Contract(C) or Grant(G) No. (C) OCE-9503455; (G) DE-FG02-92ER61428
15. Supplementary Notes This thesis should be cited as: Elizabeth C. Minor, 1998. Compositional Heterogeneity Within Oceanic POM: A Study Using Flow Cytometry and Mass Spectrometry. Ph.D. Thesis. MIT/WHOI, 98-08.			13. Type of Report & Period Covered Ph.D. Thesis
			14.
16. Abstract (Limit: 200 words) <p>This thesis applied direct temperature-resolved mass spectrometry (DT-MS), flow cytometry, and multivariate statistics to the study of marine particulate organic matter (POM) collected from the North Atlantic.</p> <p>DT-MS is a rapid and sensitive molecular-level analytical technique. The fact that DT-MS only requires microgram quantities of sample permits the coupling of DT-MS and preparative flow cytometry. Flow cytometry was used here to isolate "phytoplankton" and "detritus" in 2→53 μm POM. The molecular-level differences between and within small-particle POM (<53 μm), large-particle POM (>53 μm), "phytoplankton" and "detritus" were explored using DT-MS and discriminant analysis.</p> <p>As the polysaccharide composition of POM subclasses was a major source of variation, polysaccharides in selected samples were further studied using ammonia CI⁺ DT-MS. Principal component analysis of the resulting NH₃-CI⁺ spectra indicated that the majority of polysaccharide variation in the selected samples could be explained by a component related to the degree of degradation of the organic matter.</p> <p>The results from this thesis, coupled with existing work on marine organic matter, were used to support a modified "size-reactivity continuum model" of organic matter cycling.</p>			
17. Document Analysis a. Descriptors particulate organic matter flow cytometry mass spectrometry b. Identifiers/Open-Ended Terms c. COSATI Field/Group			
18. Availability Statement Approved for publication; distribution unlimited.		19. Security Class (This Report) UNCLASSIFIED	21. No. of Pages 343
		20. Security Class (This Page)	22. Price